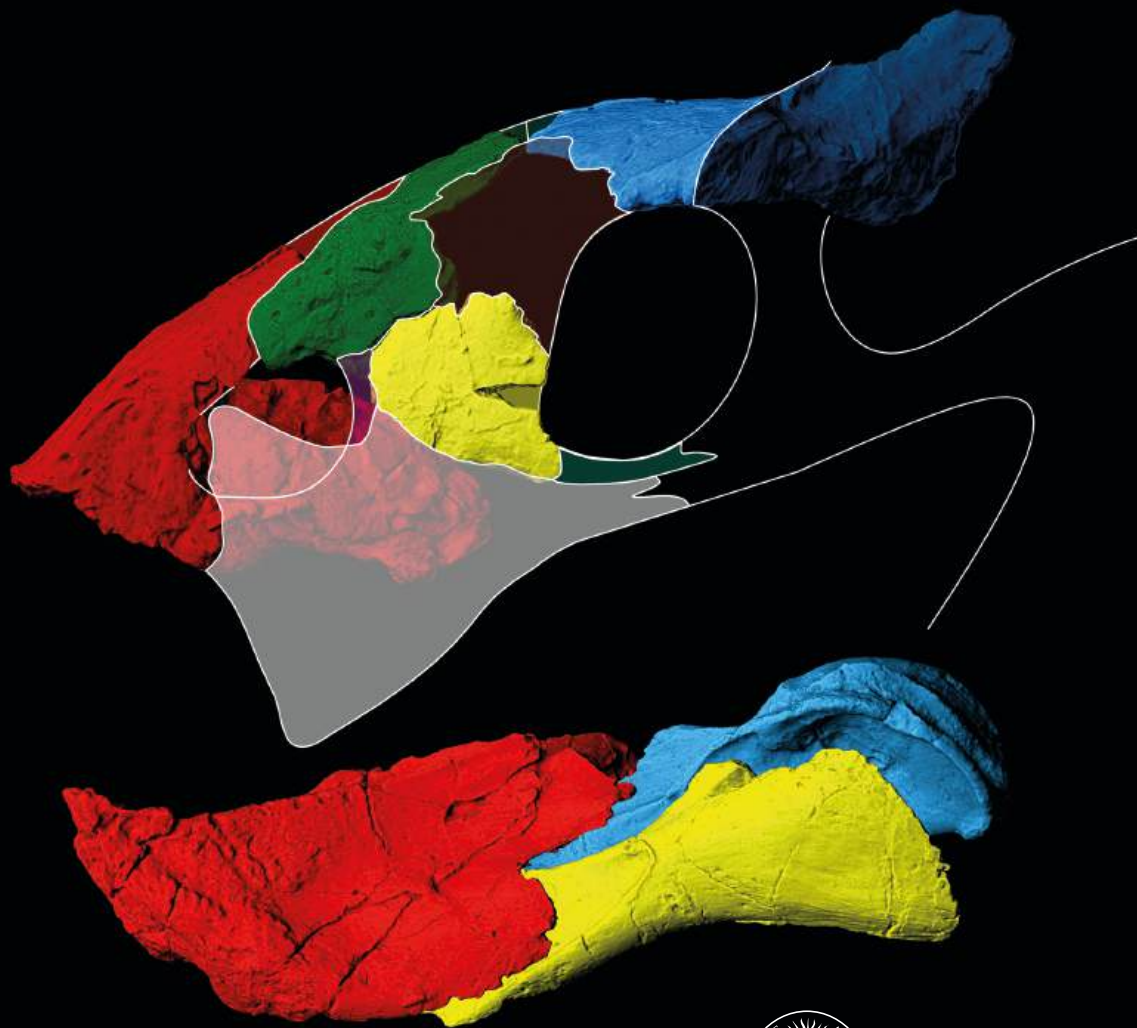


Woznikella triradiata n. gen., n. sp.
– a new kannemeyeriiform dicynodont
from the Late Triassic of northern Pangea
and the global distribution of Triassic dicynodonts

Tomasz SZCZYGIELSKI & Tomasz SULEJ



art. 22 (16) — Published on 16 May 2023
www.cr-palevol.fr



PUBLICATIONS
SCIENTIFIQUES



DIRECTEURS DE LA PUBLICATION / *PUBLICATION DIRECTORS*:

Bruno David, Président du Muséum national d'Histoire naturelle
Étienne Ghys, Secrétaire perpétuel de l'Académie des sciences

RÉDACTEURS EN CHEF / *EDITORS-IN-CHIEF*: Michel Laurin (CNRS), Philippe Taquet (Académie des sciences)

ASSISTANTE DE RÉDACTION / *ASSISTANT EDITOR*: Adenise Lopes (Académie des sciences; cr-palevol@academie-sciences.fr)

MISE EN PAGE / *PAGE LAYOUT*: Audrina Neveu (Muséum national d'Histoire naturelle; audrina.neveu@mnhn.fr)

RÉVISIONS LINGUISTIQUES DES TEXTES ANGLAIS / *ENGLISH LANGUAGE REVISIONS*: Kevin Padian (University of California at Berkeley)

RÉDACTEURS ASSOCIÉS / *ASSOCIATE EDITORS* (*, took charge of the editorial process of the article/a pris en charge le suivi éditorial de l'article):

Micropaléontologie/*Micropalaeontology*

Maria Rose Petrizzo (Università di Milano, Milano)

Paléobotanique/*Palaeobotany*

Cyrille Prestianni (Royal Belgian Institute of Natural Sciences, Brussels)

Métazoaires/*Metazoa*

Annalisa Ferretti (Università di Modena e Reggio Emilia, Modena)

Paléoichthyologie/*Palaeoichthyology*

Philippe Janvier (Muséum national d'Histoire naturelle, Académie des sciences, Paris)

Amniotes du Mésozoïque/*Mesozoic amniotes*

Hans-Dieter Sues* (Smithsonian National Museum of Natural History, Washington)

Tortues/*Turtles*

Walter Joyce (Universität Freiburg, Switzerland)

Lépidosauromorphes/*Lepidosauromorphs*

Hussam Zaher (Universidade de São Paulo)

Oiseaux/*Birds*

Eric Buffetaut (CNRS, École Normale Supérieure, Paris)

Paléomammalogie (mammifères de moyenne et grande taille)/*Palaeomammalogy (large and mid-sized mammals)*

Lorenzo Rook (Università degli Studi di Firenze, Firenze)

Paléomammalogie (petits mammifères sauf Euarchontoglires)/*Palaeomammalogy (small mammals except for Euarchontoglires)*

Robert Asher (Cambridge University, Cambridge)

Paléomammalogie (Euarchontoglires)/*Palaeomammalogy (Euarchontoglires)*

K. Christopher Beard (University of Kansas, Lawrence)

Paléoanthropologie/*Palaeoanthropology*

Aurélien Mounier (CNRS/Muséum national d'Histoire naturelle, Paris)

Archéologie préhistorique (Paléolithique et Mésolithique)/*Prehistoric archaeology (Palaeolithic and Mesolithic)*

Nicolas Teyssandier (CNRS/Université de Toulouse, Toulouse)

Archéologie préhistorique (Néolithique et âge du bronze)/*Prehistoric archaeology (Neolithic and Bronze Age)*

Marc Vander Linden (Bournemouth University, Bournemouth)

RÉFÉRÉS / *REVIEWERS*: <https://sciencepress.mnhn.fr/fr/periodiques/comptes-rendus-palevol/referes-du-journal>

COUVERTURE / *COVER*:

Woznikella tirradiata n. gen., n. sp., ZPAL V. 34/1: reconstruction of the skull and mandible in lateral left view.

Comptes Rendus Palevol est indexé dans / *Comptes Rendus Palevol* is indexed by:

- Cambridge Scientific Abstracts
- Current Contents® Physical
- Chemical, and Earth Sciences®
- ISI Alerting Services®
- Geoabstracts, Geobase, Georef, Inspec, Pascal
- Science Citation Index®, Science Citation Index Expanded®
- Scopus®.

Les articles ainsi que les nouveautés nomenclaturales publiés dans *Comptes Rendus Palevol* sont référencés par /
Articles and nomenclatural novelties published in Comptes Rendus Palevol are registered on:

- ZooBank® (<http://zoobank.org>)

Comptes Rendus Palevol est une revue en flux continu publiée par les Publications scientifiques du Muséum, Paris et l'Académie des sciences, Paris
Comptes Rendus Palevol is a fast track journal published by the Museum Science Press, Paris and the Académie des sciences, Paris

Les Publications scientifiques du Muséum publient aussi / The Museum Science Press also publish:

Adansonia, *Geodiversitas*, *Zoosystema*, *Anthropozoologica*, *European Journal of Taxonomy*, *Naturae*, *Cryptogamie* sous-sections *Algologie*, *Bryologie*, *Mycologie*.

L'Académie des sciences publie aussi / The Académie des sciences also publishes:

Comptes Rendus Mathématique, *Comptes Rendus Physique*, *Comptes Rendus Mécanique*, *Comptes Rendus Chimie*, *Comptes Rendus Géoscience*, *Comptes Rendus Biologies*.

Diffusion – Publications scientifiques Muséum national d'Histoire naturelle

CP 41 – 57 rue Cuvier F-75231 Paris cedex 05 (France)

Tél.: 33 (0)1 40 79 48 05 / Fax: 33 (0)1 40 79 38 40

diff.pub@mnhn.fr / <https://sciencepress.mnhn.fr>

Académie des sciences, Institut de France, 23 quai de Conti, 75006 Paris.

***Woznikella triradiata* n. gen., n. sp. – a new kannemeyeriiform dicynodont from the Late Triassic of northern Pangea and the global distribution of Triassic dicynodonts**

**Tomasz SZCZYGIELSKI
Tomasz SULEJ**

Institute of Paleobiology, Polish Academy of sciences, Twarda 51/55, 00-818 Warsaw (Poland)

t.szczygielski@twarda.pan.pl
sulej@twarda.pan.pl

Submitted on 6 October 2021 | Accepted on 22 February 2022 | Published on 16 May 2023

[urn:lsid:zoobank.org:pub:5BEBCC73-819E-47AE-9610-1E50B1AD6B60](https://doi.org/10.5852/cr-palevol2023v22a16)

Szczygielski T. & Sulej T. 2023. — *Woznikella triradiata* n. gen., n. sp. – a new kannemeyeriiform dicynodont from the Late Triassic of northern Pangea and the global distribution of Triassic dicynodonts. *Comptes Rendus Palevol* 22 (16): 279-406. <https://doi.org/10.5852/cr-palevol2023v22a16>

ABSTRACT

Despite nearly two centuries of intensive research of dicynodont diversity and distribution, the progress of the last two decades makes the early 21st century a dicynodont renaissance. Here we introduce *Woznikella triradiata* n. gen., n. sp., a Late Triassic European kannemeyeriiform with stahleckeriid affinities that may represent an early diverging lineage of that family, preceding its split into *Placeriinae* King, 1988 and *Stahleckeriinae* Lehman, 1961. *Woznikella triradiata* n. gen., n. sp. is distinguished from other dicynodonts by its autapomorphic, slender scapula with distinctly expanded dorsal and ventral parts, acromion directed anterodorsally, and inconspicuous scapular spine. Furthermore, we review reported global occurrences of Triassic dicynodonts, including fragmentary, indeterminate finds that may capture cryptic diversity, and analyze the biogeography of the Permian and Triassic Dicynodontia. According to our results, the region of southeastern Africa (Malawi, Mozambique, Namibia, South Africa, Tanzania, Zambia) throughout the Permian and Triassic served as a hotspot of dicynodont diversity and origin point for lineages migrating north and west. Multiple taxa independently migrated to the Americas and Eurasia, indicating open passages between the regions of Southern and Northern Hemisphere. Southern migrations from the Northern Hemisphere appear to be very rare, however.

RÉSUMÉ

Woznikella triradiata n. gen., n. sp. – un nouveau dicynodonte kannemeyeriiforme du Trias supérieur du nord de la Pangée et la répartition mondiale des dicynodontes du Trias.

Malgré près de deux siècles de recherches intensives sur la diversité et la distribution des dicynodontes, les progrès des deux dernières décennies font du début du 21^e siècle une renaissance des dicynodontes. Nous présentons ici *Woznikella triradiata* n. gen., n. sp., un kannemeyeriiforme européen du Trias supérieur apparenté aux stahleckeriidés, qui pourrait représenter une lignée divergente précoce de cette famille, précédant sa scission en *Placeriinae* King, 1988 et *Stahleckeriinae* Lehman, 1961. *Woznikella*

KEY WORDS
Synapsida,
Anomodontia,
Dicynodontia,
Kannemeyeriiformes,
Stahleckeriidae,
Triassic,
Europe,
Pangea,
biogeography,
distribution.

MOTS CLÉS
 Synapsida,
 Anomodontia,
 Dicynodontia,
 Kannemeyeriiformes,
 Stahleckeriidae,
 Trias,
 Europe,
 Pangée,
 biogéographie,
 distribution.

triradiata n. gen., n. sp. se distingue des autres dicynodontes par sa scapula mince et autapomorphique, avec des parties dorsale et ventrale nettement élargies, un acromion dirigé antérodorsalement et une épine scapulaire peu visible. En outre, nous passons en revue les occurrences mondiales signalées de dicynodontes du Trias, y compris les découvertes fragmentaires et indéterminées qui peuvent capturer la diversité cryptique de ce groupe, et analysons la biogéographie des dicynodontes du Permien et du Trias. Selon nos résultats, la région du sud-est de l'Afrique (Malawi, Mozambique, Namibie, Afrique du Sud, Tanzanie, Zambie), à travers le Permien et le Trias, a servi de point chaud de diversité de dicynodontes et de point d'origine pour les lignées migrant vers le nord et l'ouest. Plusieurs lignées ont migré indépendamment vers les Amériques et l'Eurasie, indiquant des passages ouverts entre les régions de l'hémisphère sud et nord. Les migrations vers le sud depuis l'hémisphère nord semblent cependant très rares.

INTRODUCTION

Dicynodonts were an important clade of herbivorous therapsids, which originated in the Permian and vanished in the latest Triassic. During their roughly 60 million years of existence, they were an unquestionable evolutionary success, as expressed by their global geographical range, generic and specific diversity, and (locally) exceptionally high relative abundance – not once, but twice: first in the Permian, and then, after a major faunistic turnover, in the Triassic (King 1988, 1990a, b; Fröbisch 2008, 2009). In the Triassic, this clade ranged from minuscule animals less than half a meter long (e.g., Cluver 1974; Hotton 1974; Hammer & Cosgriff 1981; Fröbisch 2007) to massive species comparable in size to the largest extant terrestrial mammals (e.g., von Huene 1935; Romer & Price 1944; Vjuschkov 1969; Sulej & Niedźwiedzki 2019; Romano & Manucci 2021). The diversity, evolutionary trends, and geographic and temporal distribution of Triassic dicynodonts have been the subject of extensive research (Camp 1956; Sun 1963; Cox 1965, 1968, 1969; Elliot *et al.* 1970; Colbert 1971a; Keyser 1974; Anderson & Cruickshank 1978; Keyser & Cruickshank 1979; Cooper 1980; Colbert 1982; Cruickshank 1986a; King 1990a, b; Cox 1991; Lucas & Harris 1996; Fröbisch 2009; Hancox *et al.* 2013). However, due to dynamic progress in the understanding of dicynodont phylogeny and biostratigraphy, as well as numerous new discoveries and taxonomic revisions performed in recent years, many of these studies are now outdated. The largest and most recent systematic attempts to review global dicynodont paleobiogeography and diversity, made by Fröbisch (2008, 2009), remain a valuable and useful source of information, but are now over a decade old and require updating to reflect the many recent additions to the dicynodont literature. Furthermore, this provides an opportunity to employ methods of biogeographic reconstruction (Matzke 2013, 2014) developed after their publication.

Recently, numerous new localities bearing Late Triassic terrestrial vertebrates have been discovered in Poland (Dzik 2001; Szulc *et al.* 2006; Dzik *et al.* 2008a; Sulej *et al.* 2011, 2012). Among these sites, dicynodont fossils are known from Lisowice (Dzik *et al.* 2008a; Sulej & Niedźwiedzki

2019), Woźniki (Sulej *et al.* 2011), Zawiercie-Marciszów (Budziszewska-Karwowska *et al.* 2010), and Myszków (Sulej *et al.* 2019), and their possible coprolites have been described from Poręba (Bajdek *et al.* 2019). It seems that they comprised the main group of large herbivores in the Late Triassic of Poland. No unambiguous body fossils of sauropodomorph dinosaurs have been found in any of the Polish Triassic localities (Skawiński *et al.* 2016), in stark contrast to, e.g., Germany or Greenland, where sauropodomorphs are abundant and dicynodonts virtually absent (e.g., Deutsche Stratigraphische Kommission 2005; Schoch 2012; Marzola *et al.* 2018). The ichnological record, however, does indicate that at least some sauropodomorphs were present in the Late Triassic of Poland (Gierliński 2009; Niedźwiedzki 2011). Unlike in the Americas and Africa (e.g., Ellenberger 1970; Lockley & Hunt 1995; Citton *et al.* 2018a; Kammerer 2018; and references therein), no Late Triassic tracks referable to dicynodonts are known from Europe, with the exception of two specimens from Woźniki (Sulej *et al.* 2011), two or three specimens from Zawiercie (Sadlok & Wawrzyniak 2013), Poland, and some putative therapsid tracks from France (Courel *et al.* 1968).

The aim of this work is to place the Central European Late Triassic dicynodonts in a broad phylogenetic and paleobiogeographic context. To that end, we also present an up-to-date global review of Triassic dicynodont occurrences. This record is, furthermore, supplemented by a new genus and species of dicynodont from Poland.

ABBREVIATIONS

Institutions

AM	Albany Museum, Grahamstown;
AMNH	American Museum of Natural History, New York;
BP	Evolutionary Studies Institute (former Bernard Price Institute for Palaeontological Research), University of the Witwatersrand, Johannesburg;
CRILAR-Pv	Centro Regional de Investigaciones y Transferencia, Tecnológica de La Rioja, Paleontología de Vertebrados, Anillaco, La Rioja;
DGM	Divisão de Geologia e Mineralogia, Ministerio das Minas e Energia, Rio de Janeiro;
GPIT	Institut und Museum für Geologie und Paläontologie, Eberhard-Karls-Universität Tübingen, Tübingen;
GSM	Institute of Geological Sciences, London;

ISI	Indian Statistical Institute, Kolkata;
IVPP	Institute of Vertebrate Paleontology and Paleoanthropology, Chinese Academy of Sciences, Beijing;
LAR-Ic	Ichnological Collection, Agencia de Cultura de La Rioja, La Rioja;
MCN-PIC	Paleoichnological Collection, Museu de Ciências Naturais, Porto Alegre;
MCN PV	Vertebrate Paleontology Collection, Museu de Ciências Naturais, Porto Alegre;
MCZ	Museum of Comparative Zoology, Harvard University, Cambridge;
NCSM	North Carolina Museum of Natural Sciences, Raleigh;
NHMUK	Natural History Museum, London;
NMMNH	New Mexico Museum of Natural History and Science, Albuquerque;
NMT	National Museum of Tanzania, Dar es Salaam;
PIN	Paleontological Institute, Russian Academy of Sciences, Moscow;
PVL	Museum of Natural Sciences Miguel Lillo, National University of Tucumán, San Miguel de Tucumán;
PVSJ	Instituto y Museo de Ciencias Naturales, Universidad Nacional de San Juan, San Juan;
QM	Queensland Museum, Brisbane;
RC	Rubidge Collection, Wellwood, Graaff-Reinet;
SAM	Iziko, South African Museum, Cape Town;
SMNS	Staatliches Museum für Naturkunde, Stuttgart;
TTU	Texas Tech University, Lubbock, Texas;
UCMP	University of California Museum of Paleontology, Berkeley, California;
UFRGS	Universidade Federal do Rio Grande do Sul, Porto Alegre;
UMMP	University of Michigan Museum of Paleontology, Ann Arbor, Michigan;
UMZC	University Museum of Zoology, Cambridge;
ZPAL	Institute of Paleobiology, Polish Academy of Sciences, Warsaw.

Other abbreviations

CI	consistency index;
RI	retention index.

MATERIAL AND METHODS

MATERIAL

All the material presented here (Figs 1–16) comes from a single association in Woźniki, Grabowa Formation, Southern Poland. See Sulej *et al.* (2011, 2020) Szulc *et al.* (2015b) and Szulc & Racki (2015) for geological setting and temporal interpretations of the Woźniki assemblage. Since all the remains are considered to belong to a single individual, as suggested by their presence in a single assemblage, congruent size and stage of ossification, and lack of duplicated elements, they are here united by a single prefix (ZPAL V. 34/1/). The numeration of particular elements (after the prefix) follows the numeration of Sulej *et al.* (2011). The material includes:

– ZPAL V. 34/1/1: right frontal, mostly complete, missing the posterodorsal tip of the prefrontal process, anterior tip, and a small part of the medial edge (Fig. 3);

– ZPAL V. 34/1/2: premaxilla, mostly complete, missing right side and the tip of the left side of the nasal process (Fig. 1);

– ZPAL V. 34/1/3: dentaries, missing the ventral left part and the posterior part of the right dorsal ramus (Fig. 4);

- ZPAL V. 34/1/4: fused right surangular (with broken anterior part), prearticular (with broken anterior and ventral part) and articular (complete) (Fig. 6);
- ZPAL V. 34/1/5: right angular, nearly complete (Fig. 5);
- ZPAL V. 34/1/6: right humerus, missing the anterior part of the proximal end (including the deltopectoral crest) and the midshaft (Fig. 13);
- ZPAL V. 34/1/7: right scapula, nearly complete (Fig. 11A–D);
- ZPAL V. 34/1/8: left femur with the proximal part, mid-shaft, and medial condyle preserved (Fig. 16);
- ZPAL V. 34/1/9: left ulna, nearly complete with crushed proximal end (Fig. 14);
- ZPAL V. 34/1/10: right radius, with crushed proximal end and missing the distal end (Fig. 15);
- ZPAL V. 34/1/11, ZPAL V. 34/1/67, ZPAL V. 34/1/68, ZPAL V. 34/1/71: dorsal vertebral centra, mostly complete (Fig. 9K–M);
- ZPAL V. 34/1/12: posterior dorsal vertebra, nearly complete (Fig. 9N–Q);
- ZPAL V. 34/1/13, ZPAL V. 34/1/33, ZPAL V. 34/1/34, ZPAL V. 34/1/35, ZPAL V. 34/1/36: dorsal neural arches, mostly complete (Fig. 9E–J);
- ZPAL V. 34/1/14: cervical neural arch, partial;
- ZPAL V. 34/1/15, ZPAL V. 34/1/16, ZPAL V. 34/1/17, ZPAL V. 34/1/18, ZPAL V. 34/1/21, ZPAL V. 34/1/26, ZPAL V. 34/1/82, ZPAL V. 34/1/84, ZPAL V. 34/1/85, ZPAL V. 34/1/208: left ribs (Fig. 10A, B, E–M, O–Q);
- ZPAL V. 34/1/19, ZPAL V. 34/1/20, ZPAL V. 34/1/23, ZPAL V. 34/1/83: right ribs (Fig. 10C, D, N);
- ZPAL V. 34/1/27: left part of the neural arch of the atlas, complete (Fig. 8A–F);
- ZPAL V. 34/1/30: cervical neural arch, complete (Fig. 8G–J);
- ZPAL V. 34/1/31: anterior dorsal neural arch, complete (Fig. 9A–D);
- ZPAL V. 34/1/42: right nasal, mostly complete with some edge damage (Fig. 2A–D);
- ZPAL V. 34/1/66, ZPAL V. 34/1/70, ZPAL V. 34/1/76, ZPAL V. 34/1/77: cervical vertebral centra, mostly complete (Fig. 8K–P);
- ZPAL V. 34/1/69: right part of the neural arch of the atlas, damaged and missing the dorsal process, and a cervical vertebral centrum;
- ZPAL V. 34/1/74: right clavicle, missing the medial end (Fig. 12E–H);
- ZPAL V. 34/1/75: left clavicle, missing the medial end (Fig. 12A–D);
- ZPAL V. 34/1/80: right lacrimal, nearly complete (Fig. 2E–H);
- ZPAL V. 34/1/81: left angular, missing the anterior and part of the posterior end;
- ZPAL V. 34/1/107: right procoracoid and a small anterior part of the coracoid (Fig. 11E, F).

Despite the specimens coming from a single accumulation and likely belonging to a single individual, their preservation style varies, even along individual elements. Some of the fragments are well-preserved, whereas others show significant crushing and wear. The limb bones, as well as some

skull bones and axial skeleton elements identified as coming from the right side of the body, seem comparatively better preserved and exhibit smooth, beige surfaces with minute detail, whereas the surfaces of the elements coming from the left side in general are more worn and cracked, with a reddish hue, and partially covered by a thin layer of very fine-grained livid-brown crust. Interestingly, their proximal parts are more damaged than the distal. Both phenomena possibly are a result of gradual burial and thus varied availability for scavengers and nonhomogeneous taphonomical conditions along the bones and between the sides of the body. Similar differences are also seen between some of the unpaired axial elements (vertebral arches and centra), possibly because of their varied exposure during burial. Only some elements (mainly ribs and skull) are exceptions from this rule, possibly due to their size, easy disruption postmortem, and/or slightly different taphonomic environment related to the nearby presence of the pulmonary system. The individual shows signs of immaturity, most notably in the rather inconspicuous development of articular structures in long bones, open transcortical canals (Cox 1969; Rothschild & Witzmann 2021; Słowiak *et al.* 2021), and lack of fusion of scapulocoracoid, cranial, and neurocentral sutures.

METHODS

3D imaging

The 3D models of the specimens were prepared using the Shining 3D EinScan Pro 2X 3D scanner fixed on a tripod with EinScan Pro 2X Color Pack (texture scans), EinTurntable (alignment based on features), and EXScan Pro 3.2.0.2 software. The number of turntable steps was varied, chosen depending on the specimen. The models were meshed using the Watertight Model and High Detail presets. The images of the 3D models were captured in MeshLab (Cignoni *et al.* 2008) with enabled Lambertian Radiance Scaling (Vergne *et al.* 2010) to visualize surface details and in orthographic view to remove angular deformations. The 3D models are available for download as Appendix 1.

Anatomical terminology and taxonomy

The review of the literature concerning the postcranial skeleton of dicynodonts revealed rather confused anatomical terminology, particularly when it comes to the anatomical directions. We decided to follow the most common conventions or, in some cases, give both frequently used terms (e.g., the same surface in the humerus is variably called cranial/anterior or dorsal by different researchers, and thus both terms are used here). For the femur, multiple authors give different meanings to the term “greater trochanter” – either referring the whole elongated trochanteric surface running across the lateral surface of the proximal portion of the bone, or any of the ends (frequently elevated into processes) of that surface. For clarity, we decided to use the terms “trochanteric crest” for the whole structure, “greater trochanter” for its proximal end, and “third trochanter” for its distal end. This terminology follows Cruickshank (1965, 1967) and is useful in the light of variable development of the trochanteric crest.

For taxonomic synonymy, we tried to follow the most recent assessments, in which the Paleobiology Database (<https://paleobiodb.org>) and revisions and reviews by Cluver (1971), Renaut & Hancox (2001), Grine *et al.* (2006), Ivakhnenko (2008), Li & Sun (2008), Fröbisch (2009), Camp & Liu (2011), Kammerer *et al.* (2011, 2013) and Kammerer & Ordoñez (2021) were most helpful. Although some historically described taxa are now considered *nomina dubia* (e.g., “*Dicynodon turpior*” (von Huene, 1935) from the Santa Maria Formation of Brazil and numerous dicynodonts from the Donguz and Bukobay formations of Russia), their materials do capture some of the morphological variability of Triassic dicynodonts, and for that reason we include them for comparative purposes.

Phylogenetic analysis

The phylogenetic analysis was performed using the matrix of Kammerer & Ordoñez (2021) with *Lisowicia bojani* Sulej & Niedźwiedzki, 2019 (scorings revised from Sulej & Niedźwiedzki 2019) and *Woznikella triradiata* n. gen., n. sp. added. The matrix consisted of 199 characters (23 continuous, 176 discrete-state characters), and 119 taxa. *Woznikella triradiata* n. gen., n. sp. was scored for three continuous characters (13%) and 55 discrete characters (31.3%), i.e., 29.1% of all characters. For *Lisowicia bojani*, the state of character 35 (marked anterior expansion of preorbital region) was changed from 0 (absent) to unknown, because the preorbital region is not preserved sufficiently; character 38 (snout) was changed from 0 (open to back of the skull) to unknown; character 42 (maxillary alveolar region) was changed from unknown to 0 (short, occupying less than 53% of the ventral length of the bone open to back of the skull); character 44 (maxillary canine) was changed from 2 (present as tusk) to unknown; character 46 (shelf-like area lateral to the maxillary non-caniniform teeth) was changed from 1 (present) to unknown, as for the remaining toothless dicynodonts; character 60 (prefrontal bosses) was changed from 1 (present but separate from nasals) to unknown, since the nasals are not known and only the posterior part of the prefrontal is preserved; character 62 (frontal contribution to the dorsal rim of the orbit) was changed from 1 (thin or absent, if present a thin frontal process extends laterally between the prefrontal and postorbital to reach the orbital margin) to unknown; character 77 (circumpineal ornamentation) was changed from unknown to 1 (no boss, foramen flush with skull surface); character 79 (interparietal) was changed from 1 (makes a small contribution to intertemporal skull roof) to unknown; character 84 (dorsoventral expansion of squamosal posterior to postorbital bar) was changed from 1 (present) to unknown; character 115 (pterygoid dentition) was changed from 1 (absent) to unknown; character 123 (shape of basal tubera) was changed from 2 (strongly rounded, such that anterior and posterior tips of tuber curve towards each other, nearly enclosing the stapedial facet; tuber inflated) to 1 (laterally directed anteroposteriorly elongate with relatively narrow edges); character 127 (stapedial foramen) was changed from unknown to 1 (absent); character 128 (dorsal process of the stapes) was changed from unknown to 0 (present); character 134 (lateral edge of paroccipital process drawn

into sharp posteriorly-directed process that is distinctly offset from the surface of the occipital plate) was changed from 1 (present) to unknown; character 136 (mandibular fenestra) was changed from unknown to 1 (present); character 155 (coronoid bone) was changed from unknown to 1 (absent); character 156 (angular with anterolateral trough for the posterior process of the dentary) was changed from 0 (absent) to 1 (present); character 162 (jaw joint) was changed from 1 (allows parasagittal movement with joint surfaces of quadrate and articular approximately equal) to 2 (allows parasagittal movement with joint surfaces on articular larger than that of quadrate); character 165 (number of sternal bosses) was changed from 1 (4) to 0 (2); character 167 (anterior edge of scapula) changed from 1 (extended laterally to form a strong crest) to 0 (not); character 168 (origin of triceps on posterior surface of scapula) was changed from 0 (relatively low) to 1 (developed into a prominent posterior projection); character 173 (insertion of *m. subcoracoscapularis* on humerus) was changed from 2 (large elongate process) to 0 (rugose area on proximal end of humerus), because the morphology in *Lisowicia bojani* compares much better with, e.g., *Kannemeyeria simocephalus* (Weithofer, 1888) than with cistecephalids; character 175 (anterior and distal edges of deltopectoral crest) was changed from unknown to 1 (very obtuse). All those changes are based on a review of the available material with more careful evaluation of individual character states in comparison with other taxa coded in the matrix.

Characters 80, 83, 101, 162, 172, 173, 188, and 198 were treated as additive (ordered). *Biarmosuchus tener* Chudinov, 1960 was set as the outgroup. The analysis was performed in TNT 1.5 (Goloboff *et al.* 2008; Goloboff & Catalano 2016) using traditional searching (tree bisection-reconnection, 1000 replications, 100 trees saved per replication). To test the impact of *Woznikella triradiata* n. gen., n. sp. and corrected scoring of *Lisowicia bojani* on the topology, the analyses were performed with the former taxon active and inactivated. *Ufudocyclops mukanelai* Kammerer, Viglietti, Hancox, Butler & Choiniere, 2019 was found to be an unstable taxon, causing a polytomy in the Placeriinae King, 1988, and because the subsequently utilized paleobiogeographic analysis methods do not allow polytomies, we repeated the analysis with this species inactivated. This revealed instability of *Eubrachiosaurus browni* Williston, 1904 relative to other taxa in the same branch (see results of the phylogenetic analysis), but the majority rule (50%) consensus allowed creation of a single tree without polytomies, which was used for the paleobiogeographic analysis. The bootstrap values were obtained using 1000 iterations. See Appendices 2–11 for the updated matrix, trees, and the lists of synapomorphies.

Paleobiogeographic analysis

The paleobiogeographic analysis was performed in R 4.0.3 (R Core Team 2020) using the BioGeoBEARS package (Matzke 2013) on the majority rule (50%) consensus tree topology with *Ufudocyclops mukanelai* inactivated. The tree, temporal range, geographic range, and dispersion multiplier files were placed in the R work folder (see Appendices 12–14).

The temporal and geographic occurrences (Tables 1–3) were taken from the primary literature and the Paleobiology Database (<https://paleobiodb.org>). The dicynodont literature (especially older papers) rarely includes detailed data on the stratigraphic origin of the fossils within the profile, the data provided by the Paleobiology Database are usually fairly coarse, most taxa are based on multiple specimens possibly originating from more than one horizon, and biostratigraphic correlations between various localities have limited resolution. Furthermore, the observed FADs and LADs may not indicate the complete duration of taxa (from speciation to extinction), so precise temporal calibration of occurrences was not considered a priority, especially for Permian forms, which are not the main focus of the analysis. Instead, in many cases temporal ranges were given for whole ages/stages based on the most recent International Chronostratigraphic Chart (v. 2021/05) by the International Commission on Stratigraphy (<https://stratigraphy.org>). A notable exception is the Karoo Supergroup, for which detailed biostratigraphy was recently provided in a series of papers (Botha & Smith 2020; Day & Rubidge 2020a, b; Day & Smith 2020; Hancox *et al.* 2020; Smith 2020; Smith *et al.* 2020b; Viglietti 2020; Viglietti *et al.* 2020a, b). Even in this case, however, numerical FAD and LAD values were estimated and must be treated as approximations.

For the analysis, ten regions were demarcated based on the relative positions and geographic connections of the dicynodont-bearing localities in the Permian and Triassic: A) southeastern Africa (Malawi, Mozambique, Namibia, South Africa, Tanzania, Zambia); B) northern Africa (Morocco); C) western Asia (western China and Mongolia, west of the Paleotethys); D) eastern Asia (northeastern China and Laos, east of the Paleotethys); E) North America; F) South America; G) Western and Central Europe; H) Antarctica; I) Russia; and J) South Asia (India). Note that the region names are approximations based on the localization of dicynodont-bearing outcrops and do not necessarily reflect precise geographic extent; e.g., the African regions (A and B) would reasonably include western Asia, which was at the time connected to them. Designation of the areas was performed with two main notions in mind: on one hand, dicynodont-yielding localities are distributed unevenly and separated by large geographic “empty spots”; on the other hand, connection of land masses into Pangea provided extensive opportunities for migration making subdivision of the globe into clearly-demarcated regions difficult. Because of that, particular regions are largely designated in such a way that they represent possible dispersal routes. For example, region B (northern Africa) is conceived as separating region A (southeastern Africa) from region G (Central and Western Europe), whereas regions G (Central and Western Europe) and C (western Asia) are geographic bottlenecks constituting possible routes between neighboring areas. The dispersion multipliers were set to 1 for dispersal between the directly connected areas and to 0.000001 for dispersal between the areas not directly connected, following the convention of Poropat *et al.* (2016). Given the temporal and geographical resolution of the dataset, we decided to use a single dispersion multiplier matrix for the whole analyzed time range (unstrati-

fed analysis). Although available migration routes between the areas of modern-day Europe and North America changed rather dynamically during the Middle and Late Triassic, with shallow epicontinental sea covering much of Central Europe and partitioning the land into islands, at least temporary playas and other ephemeral terrestrial connections (either direct, to the south, or through Greenland, to the north of the basin) were present throughout this time (e.g., McKie & Williams 2009; Torsvik & Cocks 2016). Because Greenland is not recognized as a separate region in our analysis, either way the dispersion multipliers are scored as 1. As a compromise between model complexity and reasonable computing time, maximum range size of six areas was allowed – this constitutes over half of the designated regions and is twice the largest range size observed in the analyzed terminal taxa. The branch lengths for the tree were time calibrated using the script published by Bell & Lloyd (2015). The dataset was tested under DEC, DEC+J, DIVALIKE, DIVALIKE+J, BAYAREALIKE, and BAYAREALIKE+J models (Matzke 2013, 2014).

Aside from the analysis proper, which could only include taxa present on the phylogenetic tree, the occurrences of Triassic dicynodonts, including fragmentary and indeterminate finds, were listed based on the literature (Tables 1–3) and mapped onto paleogeographic maps. The map rasters were exported in Mollweide projection from GPlates 2.2.0 (Müller *et al.* 2018) using the Scotese PALEOMAP PaleoAtlas v. 3 (Scotese 2016; <https://www.earthbyte.org/paleomap-paleoatlas-for-gplates/>). For Triassic paleogeographic maps in a classical form, see Scotese (2001, 2014).

SYSTEMATIC PALEONTOLOGY

Subclass SYNAPSIDA Osborn, 1903

Order THERAPSIDA Broom, 1905

Infra-order DICYNODONTIA Owen, 1860a

Clade KANNEMEYERIIFORMES Maisch, 2001

Woznikella n. gen.

[urn:lsid:zoobank.org:act:39A734F4-1403-43C1-9D99-1DB3F1901478](https://doi.org/10.5852/crpalevol.2023.22.1.1901478)

TYPE SPECIES. — *Woznikella triradiata* n. sp.

Woznikella triradiata n. gen., n. sp.

(Figs 1–16)

[urn:lsid:zoobank.org:act:DACADFD8-C682-4872-82C0-7CB34025868D](https://doi.org/10.5852/crpalevol.2023.22.1.19025868D)

HOLOTYPE. — ZPAL V. 34/1, partial skeleton.

DIAGNOSIS. — A medium-sized stahleckeriid-related dicynodont with triradiate, Y-shaped branching pattern of premaxillary ridges, paired medial ridge on the mental surface of the dentary, slender scapula, weakly-angled scapular spine, well-demarcated acromion process projecting well beyond the border of the scapula, and coracoid foramen completely enclosed by the procoracoid, characterized

by an autapomorphy: acromion directed anterodorsally rather than anteroventrally or anteriorly. Differs from non-kannemeyeriiform dicynodonts and *Dinodontosaurus tener* in presence of a distinct supinator process. Differs from most shansiodontids and stahleckeriids in the gracile scapular blade with significant terminal flaring of the scapula. Differs from more derived stahleckeriines in having a less pronounced supinator process. Differs from *Ischigualastia jensi* Cox, 1962 and *Jachaleria candelariensis* Araujo & Gonzaga, 1980 in scapula not contributing to the coracoid foramen. Differs from *Stahleckeria potens* von Huene, 1935, *Placerias hesternus* Lucas, 1904, *Eubrachiosaurus browni*, and *Zambiasaurus submersus* Cox, 1969 in having a weakly developed scapular spine.

DERIVATIO NOMINIS. — *Woznikella* in reference to the name of the type locality, Woźniki; *triradiata* in reference to the triradiate branching pattern of the premaxillary ridges.

TYPE LOCALITY. — Woźniki, southern Poland.

TYPE HORIZON. — The Patoka Member of the Grabowa Formation, Carnian (Sulej *et al.* 2011, see Szulc *et al.* 2015b for the arguments for the Norian age of the locality; see Discussion for the rationale for its Carnian age).

REFERRED SPECIMEN. — SMNS 91416, a fragmentary mandible from the Carnian of Markt Obernzenn (Bavaria, Germany), Stuttgart Formation (Shilfsandstein).

DISTRIBUTION. — Carnian (and ?Norian) of Poland and Germany.

DESCRIPTION

Skull and mandible

The preserved parts of the skull and mandible (Figs 1–6) lack pronounced rugosities, which may be either taxonomic or related to the young age of the individual. Based on the shape of the beak (both of the premaxilla and dentary) and the width of the preserved skull table elements, at least preorbitally the skull was apparently relatively narrow (Fig. 7). Unlike in, e.g., *Kannemeyeria aganosteus* Kammerer & Ordoñez, 2021, *Kannemeyeria simocephalus*, *Kannemeyeria lophorhinus* Renaut, Damiani, Yates & Hancox, 2003, *Lystrosaurus* spp. (with the possible exception of *L. youngi*), *Rechnisaurus cristarhynchus* Chowdhury, 1970, *Sangusaurus edentatus* Cox, 1969, *Sangusaurus parringtonii* Cruickshank, 1986a, *Shaanbeikanne-meyeria xilouguensis* Cheng, 1980, *Shansiodon wangi* Yeh, 1959, *Shansiodon wuhsiangensis* Yeh, 1959, *Stahleckeria potens*, *Sungeodon kimkraemerae* Maisch & Matzke, 2014, *Tetragonias njalilus* (von Huene, 1942), *Ufudocyclops mukanelai*, *Vinceria andina* Bonaparte, 1969, *Wadiasaurus indicus* Chowdhury, 1970, and *Zambiasaurus submersus* Cox, 1969 there is no conspicuous median ridge on the skull (Weithofer 1888; Broom 1899; Haughton 1915; Pearson 1924a; Case 1934; Yuan & Young 1934b; Young 1935; von Huene 1942; Camp 1956; Yeh 1959; Sun 1964; Cruickshank 1967; Chowdhury 1970; Crozier 1970; Cluver 1971; Kalandadze 1975; Cheng 1980; Cruickshank 1986a; Bandyopadhyay 1989; Pickford 1995; Schwanke-Peruzzo & Araújo-Barbarena 1995; Maisch 2001; Renaut *et al.* 2003; Surkov *et al.* 2005; Vega-Dias *et al.* 2005; Morato 2006; Grine *et al.* 2006; Domnanovich & Marsicano 2012; Angielczyk *et al.* 2014; Maisch & Matzke 2014; Angielczyk *et al.* 2017; Kammerer *et al.* 2019; Kammerer & Ordoñez 2021). Note that the presence and degree of development

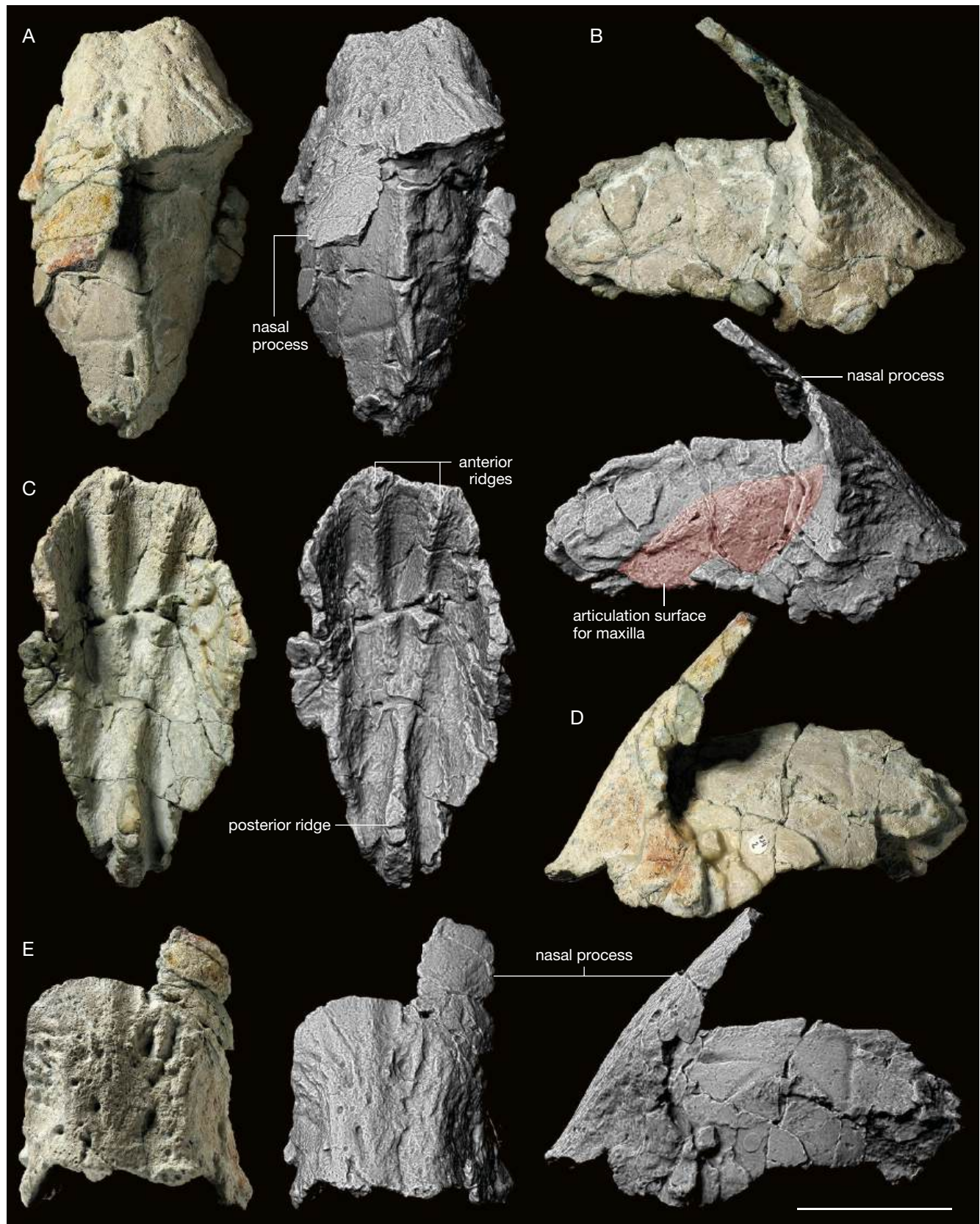


FIG. 1. — *Woznikella triradiata* n. gen., n. sp., ZPAL V. 34/1/2: A-E, premaxillae in dorsal (A), lateral right (B), ventral (C), lateral left (D), and anterior (E) view. Scale bar: 5 cm.

of the median ridge is ontogeny-dependent at least in some dicynodont taxa (e.g., Kammerer & Ordoñez 2021). Comparison of overall proportions of the mandibular bones shows that the mandible of *Woznikella triradiata* n. gen., n. sp. was proportionally significantly longer relative to its height than that of, e.g., *Angonisaurus crickshanki*, *Ischigualastia jensi*, *Lystrosaurus* spp., *Myosaurus gracilis* Haughton, 1917, *Sangusaurus parringtonii*, and *Stahleckeria potens*, and more reminiscent to that of, e.g., *Kannemeyeria simocephalus*, *Sinokannemeyeria* spp., or *Wadiasaurus indicus* (see, e.g., Cox & Li 1983; Pearson 1924a; von Huene 1935, 1936; Young 1935; Broom 1937; Janensch 1952; Camp 1956; Sun 1963, 1964; Cox 1965; Cluver 1971, 1974; Keyser 1974; Cruickshank 1986a; Bandyopadhyay 1988; Renaut 2000; Hancox *et al.* 2013; Angielczyk *et al.* 2017).

Premaxilla

The premaxilla (ZPAL V. 34/1/2; Fig. 1) is fused and well preserved. Only the right side and the tip of the left side of the dorsal process as well as a small fragment of the posteriormost tip are broken. The anterior part is skewed to the left, but it is unclear whether this deformation is taphonomical or if it occurred during the life of the animal. The anterior tip in dorsoventral aspect is blunt (squared off), rather than sharply pointed as in, e.g., *Kannemeyeria lophorhinus*, apparently *Mogbreberia nmachouensis* Dutuit, 1980, *Placerias hesternus*, “*Putillosaurus sennikovi*” Surkov, 2005, and *Ufudocyclops mukanelai* (see Camp & Welles 1956; Cox 1965; Dutuit 1980, 1988; Renaut 2000; Surkov 2005; Angielczyk *et al.* 2014; Kammerer *et al.* 2019). Nonetheless, it appears to be narrower than in *Dinodontosaurus brevirostris* Cox, 1968, *Dinodontosaurus tener* (von Huene, 1935), *Dolichuranus primaevus* Keyser, 1973, *Jachaleria candelariensis*, *Rechnisaurus cristarhynchus*, *Sinokannemeyeria sanchuanheensis* Cheng, 1980, and *Stahleckeria potens*, in which the bone is about as wide as it is long in dorsal view and shows nearly no rostral tapering (Tupi Caldas 1936; Cox 1965, 1968; Chowdhury 1970; Keyser 1973; Araújo & Gonzaga 1980; Cheng 1980; Bandyopadhyay 1989; Maisch 2001; Vega-Dias & Schultz 2004; Vega-Dias *et al.* 2005; Morato 2006; Kammerer & Ordoñez 2021). Its edge and anterodorsal surface are slightly concave medially, so the beak is M-shaped in dorsoventral aspect, similar to *Ischigualastia jensi*, *Jachaleria candelariensis*, *Parakannemeyeria chengi* Liu, 2004, *Parakannemeyeria ningwuensis* Sun, 1963, *Parakannemeyeria youngi* Sun, 1963, *Rhadiodromus mariae* Surkov, 2003, *Uralokannemeyeria vjuschkovi* Danilov, 1971, and *Stahleckeria potens* (see Sun 1963; Cox 1965; Danilov 1971; Araújo & Gonzaga 1980; Maisch 2001; Surkov 2003; Liu 2004; Vega-Dias & Schultz 2004; Kammerer & Ordoñez 2021). In contrast to, e.g., *Dinodontosaurus brevirostris*, *Dinodontosaurus tener*, *Ischigualastia jensi* (pers. obs.: PVSJ 545), *Jachaleria candelariensis*, *Lystrosaurus* spp. (with the possible exception of *L. georgi*, *L. hedini* Young, 1935, and *L. youngi*), *Parakannemeyeria ningwuensis*, and *Sinokannemeyeria yingchiensis* Sun, 1963, there is no pronounced notch in the median part of the tomial edge (unless the tips of the beak of ZPAL V. 34/1/2 are damaged; Yuan & Young 1934b; Young 1935;

Sun 1963, 1964; Cluver 1971; Kalandadze 1975; Araújo & Gonzaga 1980; Vega-Dias & Schultz 2004; Surkov 2005; Morato 2006; Grine *et al.* 2006; Kammerer & Ordoñez 2021).

In lateral view (Fig. 1C), accounting for deformation, the labial (tomial) edge of the premaxilla was apparently directed anteroventrally, roughly perpendicular to the anterodorsally facing surface of the nasal process. This differs from at least some specimens of *Tetragonias njalilus*, in which the labial edge of the beak was set at an obtuse angle to its anteroventrally facing surface and thus the tip of the beak was slightly recessed (Cruickshank 1967; Kammerer & Ordoñez 2021). The lateral surface of the anterior half is coarsely rugose, indicative of a keratinous rhamphotheca (Fig 1B, D, E). The premaxilla forms the anterior edge of the naris. The anterior outline of the narial fossa is straight in the upper part and reaches very close to the ventral edge of the premaxilla, similar to, e.g., *Acratophorus argentinensis* (Bonaparte, 1965), *Kannemeyeria simocephalus*, *Parakannemeyeria dolichocephala* Sun, 1960, *Parakannemeyeria ningwuensis*, *Parakannemeyeria youngi*, “*Putillosaurus sennikovi*”, *Rechnisaurus cristarhynchus*, *Repelinosaurus robustus* Olivier, Battail, Bourquin, Rossignol, Steyer & Jalil, 2019, *Rhadiodromus mariae*, *Rhinodicynodon gracile* Kalandadze, 1970, *Rabidosaurus cristatus* Kalandadze, 1970, the South African *Shansiodon* sp., *Sinokannemeyeria pearsoni* Young, 1937, *Sinokannemeyeria sanchuanheensis*, *Ufudocyclops mukanelai*, *Vinceria andina*, *Wadiasaurus indicus*, and *Xiyukannemeyeria brevirostris* (Sun, 1978) (see Haughton 1915; Pearson 1924a; Case 1934; Watson 1948; Sun 1960, 1963; Cruickshank 1965; Bonaparte 1966a, 1967; Chowdhury 1970; Kalandadze 1970; Cheng 1980; Bandyopadhyay 1988, 1989; Renaut 2000; Renaut & Hancox 2001; Liu & Li 2003; Surkov 2003, 2005; Domnanovich & Marsicano 2012; Hancox *et al.* 2013; Kammerer *et al.* 2019; Olivier *et al.* 2019; Kammerer & Ordoñez 2021). The premaxilla differs dramatically in proportions from the anteroposteriorly short and vertically elongated premaxillae of *Lystrosaurus* spp. (Yuan & Young 1934b; Young 1935; Sun 1964; e.g., Cluver 1971; Colbert 1974; Kalandadze 1975; Surkov *et al.* 2005; Grine *et al.* 2006). On the ventral (palatal) surface of the premaxilla, each of the anteriorly pronounced tips of the beak projects rearward to form a predominantly posteriorly and gently medially directed, rugose ridge (Fig. 1C). Anteriorly, these ridges are separated by the median palatal groove, but merge at approximately 2/3 of the premaxilla's length into a single, higher, posteriorly directed median (posterior) palatal ridge, resulting in a Y-shaped structure, similar to most Triassic dicynodonts with the exception of *Kombuisia frerensis* Hotton, 1974 and *Myosaurus gracilis*, which lack the anterior ridges (Cluver 1974; Hotton 1974; Fröbisch 2007). There are no lateral anterior ridges comparable to those of *Kombuisia frerensis* (see Hotton 1974). The anterior ridges in *Woznikella triradiata* n. gen., n. sp. are more widely separated than in, e.g., *Jachaleria candelariensis* and *Kannemeyeria lophorhinus* (Crozier 1970; Araújo & Gonzaga 1980; Pickford 1995; Renaut 2000; Vega-Dias & Schultz 2004; Angielczyk *et al.* 2014). Unlike in, e.g., *Acratophorus argentinensis*, *Angonisaurus crickshanki* Cox & Li, 1983, *Counillonnia superoculis*

Olivier, Battail, Bourquin, Rossignol, Steyer & Jalil, 2019, “*Cristonasus koltaeviensis*”, *Dolichuranus primaevus*, *Kannemeyeria simocephalus*, *Kannemeyeria lophorhinus*, “*Kannemeyeria*” *latirostris* Crozier, 1970, *Jachaleria candelariensis*, *Parakannemeyeria dolichocephala*, “*Putillosaurus sennikovi*”, *Rechnisaurus cristarhynchus*, *Repelinosaurus robustus*, *Sanguisaurus edentatus*, *Sangusaurus parringtonii*, *Sinokannemeyeria yingchiaoensis*, *Ufudocyclops mukanelai*, *Uralokannemeyeria vjuschkovi*, and *Zambiasaurus submersus*, the ridges diverge anteriorly rather than being parallel (Pearson 1924a; Case 1934; Toerien 1953; Sun 1960, 1963; Bonaparte 1966a; Cox 1969; Chowdhury 1970; Crozier 1970; Danilov 1971; Keyser 1973; Araújo & Gonzaga 1980; Cox & Li 1983; Bandyopadhyay 1989; Pickford 1995; Schwanke-Peruzzo & Araújo-Barbarena 1995; Surkov 1999a; Renaut 2000; Vega-Dias & Schultz 2004; Surkov 2005; Damiani *et al.* 2007; Hancox *et al.* 2013; Angielczyk *et al.* 2014, 2017; Kammerer *et al.* 2019; Olivier *et al.* 2019; Kammerer & Ordoñez 2021). They nearly reach the anterolateral corners of the beak, unlike, e.g., in *Acratophorus argentinensis*, *Dinodontosaurus* spp., *Jachaleria candelariensis*, *Lystrosaurus* spp., *Rechnisaurus cristarhynchus*, *Shaanbeikannemeyeria xilouguensis*, *Stahleckeria potens*, *Vinceria andina*, and *Wadiasaurus indicus*, in which the snout stretches out further laterally (von Huene 1935; Toerien 1953; Cox 1965, 1968; Bonaparte 1966a; Chowdhury 1970; Cluver 1971; Cheng 1980; Araújo & Gonzaga 1980; Bandyopadhyay 1988, 1989; Renaut 2000; Renaut & Hancox 2001; Vega-Dias & Schultz 2004; Morato 2006; Domnanovich & Marsicano 2012; Abdala *et al.* 2013; Kammerer & Ordoñez 2021). The three ridges are continuous with each other and the point of their branching is well demarcated and ventrally convex, in contrast to *Jachaleria candelariensis*, *Kannemeyeria lophorhinus*, *Rabidosaurus cristatus* (pers. obs.), and *Rhinodicyodon gracile*, in which the posterior (median) ridge is flanked by the anterior ones but not connected to them (Crozier 1970; Araújo & Gonzaga 1980; Pickford 1995; Renaut 2000; Vega-Dias & Schultz 2004; Angielczyk *et al.* 2014; Kammerer & Ordoñez 2021) or, e.g., *Acratophorus argentinensis*, *Angonisaurus crickshanki*, *Counillonia superoculis*, *Dolichuranus primaevus*, “*Kannemeyeria*” *latirostris*, *Lystrosaurus* spp., *Parakannemeyeria dolichocephala*, *Placerias hesternus*, *Rechnisaurus cristarhynchus*, *Repelinosaurus robustus*, *Sanguisaurus parringtonii*, *Shaanbeikannemeyeria xilouguensis*, the South African *Shansiodon* sp., *Sinokannemeyeria baidaoyuensis* Liu, 2015, *Ufudocyclops mukanelai*, *Vinceria andina*, *Wadiasaurus indicus*, and *Zambiasaurus submersus*, in which the ridges are separate and the branching point is indistinct (Camp 1956; Camp & Welles 1956; Sun 1960; Cox 1965, 1969; Crozier 1970; Chowdhury 1970; Cluver 1971; Keyser 1973; Cheng 1980; Cox & Li 1983; Bandyopadhyay 1988, 1989; Renaut 2000; Renaut & Hancox 2001; Damiani *et al.* 2007; Domnanovich & Marsicano 2012; Hancox *et al.* 2013; Angielczyk *et al.* 2014, 2017; Liu 2015; Kammerer *et al.* 2019; Olivier *et al.* 2019; Kammerer & Ordoñez 2021). In *Kannemeyeria simocephalus*, both of the latter morphologies can be observed, but the lateral and median palatal ridges never seem to form a well-defined connection (Pearson 1924a; Case 1934;

Toerien 1953; Renaut 2000). This character is usually poorly presented in published figures, but apparently the only Triassic dicynodonts with such a well-defined triradiate branching pattern of the premaxillary ridges comparable to that of *Woznikella triradiata* n. gen., n. sp. Are *Dinodontosaurus brevirostris* and *Dinodontosaurus tener* (see Cox 1965, 1968; Morato 2006; Kammerer & Ordoñez 2021), *Ischigualastia jensi* (see Kammerer & Ordoñez 2021; pers. obs.: PVJ 545), *Kannemeyeria aganosteus* (see Kammerer & Ordoñez 2021), *Rhadiodromus mariae* (see Surkov 2003), *Tetragonias njalilus* (von Huene 1942; Cruickshank 1967; Hancox *et al.* 2013), *Uralokannemeyeria vjuschkovi* (see Danilov 1971), and the specimens illustrated by Camp (1956) as a juvenile *Kannemeyeria* “*vanhoepeni*” and by Cruickshank (1965) as a juvenile *Kannemeyeria* “*latifrons*” Broom 1899. In the latter two cases this is based only on the interpretative drawings – this morphology is not clearly described, and no photographs of these specimens were published, so the accuracy of the drawings cannot be verified. In *Ufudocyclops mukanelai*, the anterior and posterior ridges do not form a connection, but the surface between them is slightly convex (Hancox *et al.* 2013; Kammerer *et al.* 2019). As preserved, the anteriormost parts of these ridges are slightly deeper than the lateral labial edge, and thus visible in lateral view, in contrast to, e.g., *Placerias hesternus* (see Camp & Welles 1956; Cox 1965). The area for the connection with the palatines and vomers is very poorly preserved, so it is not possible to establish the anterior extent of those bones. The dorsal surface of the palatal plate is convex and a single longitudinal ridge spans along its entire midline (Fig. 1A). Large parts of the surfaces on either side of this ridge probably served as facets for the maxillae. These facets are outlined with gentle, anterodorsally aligned, posterodorsally convex grooves, suggesting that the maxillae nearly reached anteriorly the front of the narial fossa, spanning along approximately posterior two thirds of the premaxillae length (Fig. 1B, D). This is relatively further than in, e.g., “*Nasoplanites danilovi*”, *Placerias hesternus*, and “*Putillosaurus sennikovi*”, but comparable to *Kannemeyeria simocephalus* (see Pearson 1924a; Camp & Welles 1956; Surkov 1999a; Renaut 2000; Surkov 2005). Both premaxillae are damaged in a way that obscures the connections with the septomaxillae.

Nasal

The right nasal (ZPAL V. 34/1/42; Fig. 2A-D) is preserved almost completely. It consists of two parts, lateral and dorsal. The bone is slightly deformed due to compaction, which is clearly visible in the anteromedial part, which is concave dorsally (not corresponding with the alignment of the preserved part of the dorsal process of the premaxilla, thus unlikely to represent nasal depressions; compare to, e.g., Chowdhury 1970; Bandyopadhyay 1989; Kammerer & Ordoñez 2021). The deformation also likely affected the angle between the lateral and dorsal plates (Fig. 2B). Unlike in, e.g., “*Planitrostris pechoriensis*” (see Surkov 1999b), the lateral part has a coarsely rugose surface (although the development of the rugosity is mild in comparison with many Kannemeyeriiform taxa) with numerous large vascular openings. It suggests that

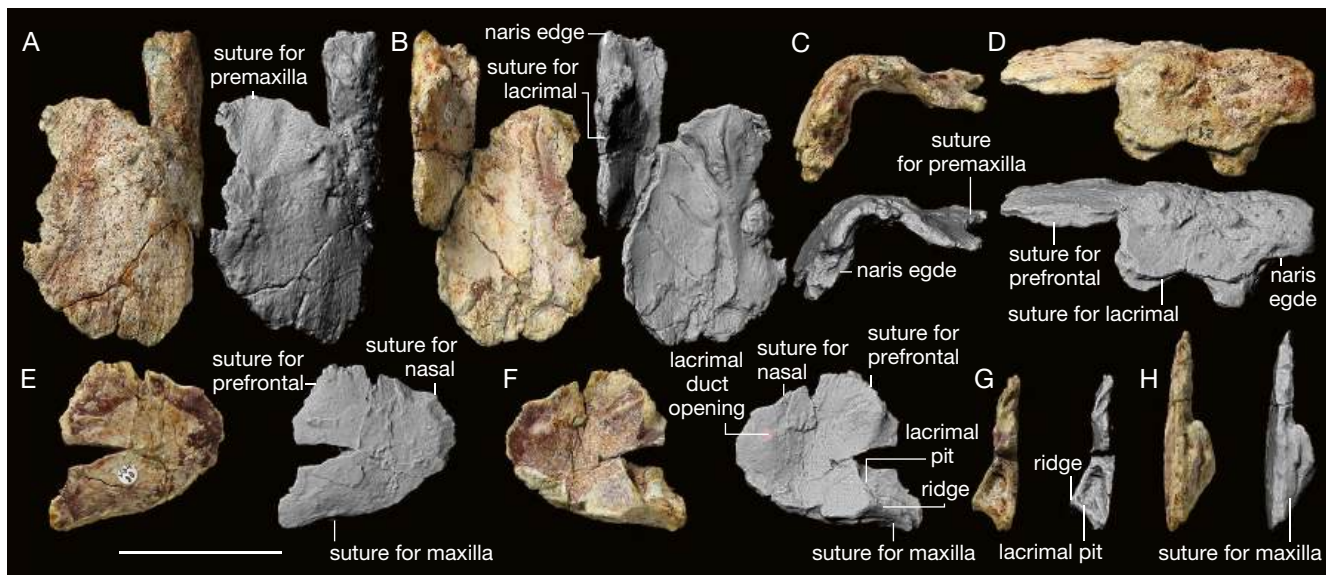


Fig. 2. — *Woznikella triradiata* n. gen., n. sp.: A-D, ZPAL V. 34/1/42, right nasal in dorsal (A), ventral (B), anterior (C), and lateral (D) view; E-H, ZPAL V. 34/1/80, right lacrimal in lateral (E), medial (F), posterior (G), and ventral (H) view. Scale bar: 5 cm.

Woznikella triradiata n. gen., n. sp. had either a sensitive tip of the snout or keratinous covering in that area (e.g., Keyser & Cruickshank 1979; Surkov 2003, 2006; Morato *et al.* 2005; Morato 2006; Benoit *et al.* 2018). The lateral surface of the nasal is roughly even with the lateral edge of the dorsal table and is vertical and mostly flat, without prominent lateral depression (Fig. 2D), unlike in, e.g., some specimens of *Dinodontosaurus brevirostris* and *Dinodontosaurus tener*, *Rhadiodromus klimovi* (Efremov, 1938), *Rhadiodromus mariae*, *Rhinodicyndon gracile*, *Sinokannemeyeria yingchiaoensis*, and *Xiyukannemeyeria brevirostris* (Sun 1963, 1978; Cox 1965, 1968; Vjuschkov 1969; Kalandadze 1970; Surkov 2003; Morato 2006). This may imply the absence of a postnarial depression (although the lack of maxilla makes it uncertain). The ventral edge of the lateral part is sinusoidal. Two ventral processes, which formed the sutural connection with the lacrimal, have distinct ridges on the lateral surfaces. A shallow depression, which is probably the area for the suture with the dorsal process of the premaxilla, is visible on the dorsal surface (Fig. 2A). The edge of this sutural field is directed postero-medially and it spans for about half the length of the dorsal plate of the nasal. Aside from that, there are no pronounced grooves comparable with those described in, e.g., “*Calleonasis furvus*” or “*Elatosaurus facetus*” (see Kalandadze & Sennikov 1985; Surkov 1999a). The contact with the septomaxilla was apparently very small, only at the edge of the naris, due to most of the ventral edge of the nasal being occupied by the lacrimal. The contact with the prefrontal is slightly broken and difficult to interpret, but at least part of the facet for the prefrontal is preserved in the posterior third of the bone. As preserved, the medial portions of the nasals and frontals are separated by a diamond-shaped empty space, which was filled either by a short, pointy median anterior process of the frontal, or by a supernumerary internasal bone (Fig. 7A, B),

as in *Jachaleria* spp. or some individuals of *Lystrosaurus* spp. (Araújo & Gonzaga 1980; Vega-Dias & Schultz 2004; Jasinoski *et al.* 2014; Kammerer & Ordoñez 2021). The nasal roofed the naris, and its anterior edge formed the thick posterodorsal edge of the nostril (Fig. 2B, C), similar to, e.g., *Dolichururus primaevus*, *Acritophorus argentinensis*, *Kannemeyeria lophorhinus*, *Kannemeyeria simocephalus*, *Parakannemeyeria dolichocephala*, *Parakannemeyeria ningwuensis*, *Rabidosaurus cristatus*, the South African *Shansiodon* sp., *Sinokannemeyeria pearsoni*, *Sinokannemeyeria yingchiaoensis*, *Sungeodon kimkraemerae*, *Ufudocyclops mukanelai*, *Uralokannemeyeria vjuschkovi*, and *Vinceria andina* (Pearson 1924a; Case 1934; Sun 1960, 1963; Bonaparte 1966a, 1967, 1969; Kalandadze 1970; Danilov 1971; Keyser 1973; Pickford 1995; Renaut 2000; Maisch 2001; Renaut & Hancox 2001; Damiani *et al.* 2007; Domnanovich & Marsicano 2012; Hancox *et al.* 2013; Maisch & Matzke 2014; Angielczyk *et al.* 2014; Kammerer *et al.* 2019; Kammerer & Ordoñez 2021).

Lacrimal

The right lacrimal (ZPAL V. 34/1/80; Fig. 2E-H)) is almost complete, only a small triangular fragment is missing in the middle of the posterior edge. The bone is subtriangular, approximately as high as it is long, and thus unusually equidimensional compared to other dicynodonts. The lateral surface is flat and the sutural surfaces are prominent (Fig. 2E). The ventral edge is the most massive, with a triangular surface for the contact with the maxilla and, possibly the jugal and/or palatine (Fig. 2H). Unlike, e.g., *Placerias hesternus*, there is no conspicuous jugal process (Camp & Welles 1956). The anteroventral orbit margin is formed by a thin lappet of bone. The suture for the prefrontal is inverted V-shaped. Internally, a ridge is visible in the posterior part of the bone (Fig. 2F). This ridge is most distinctive in the ventral part, where it floors

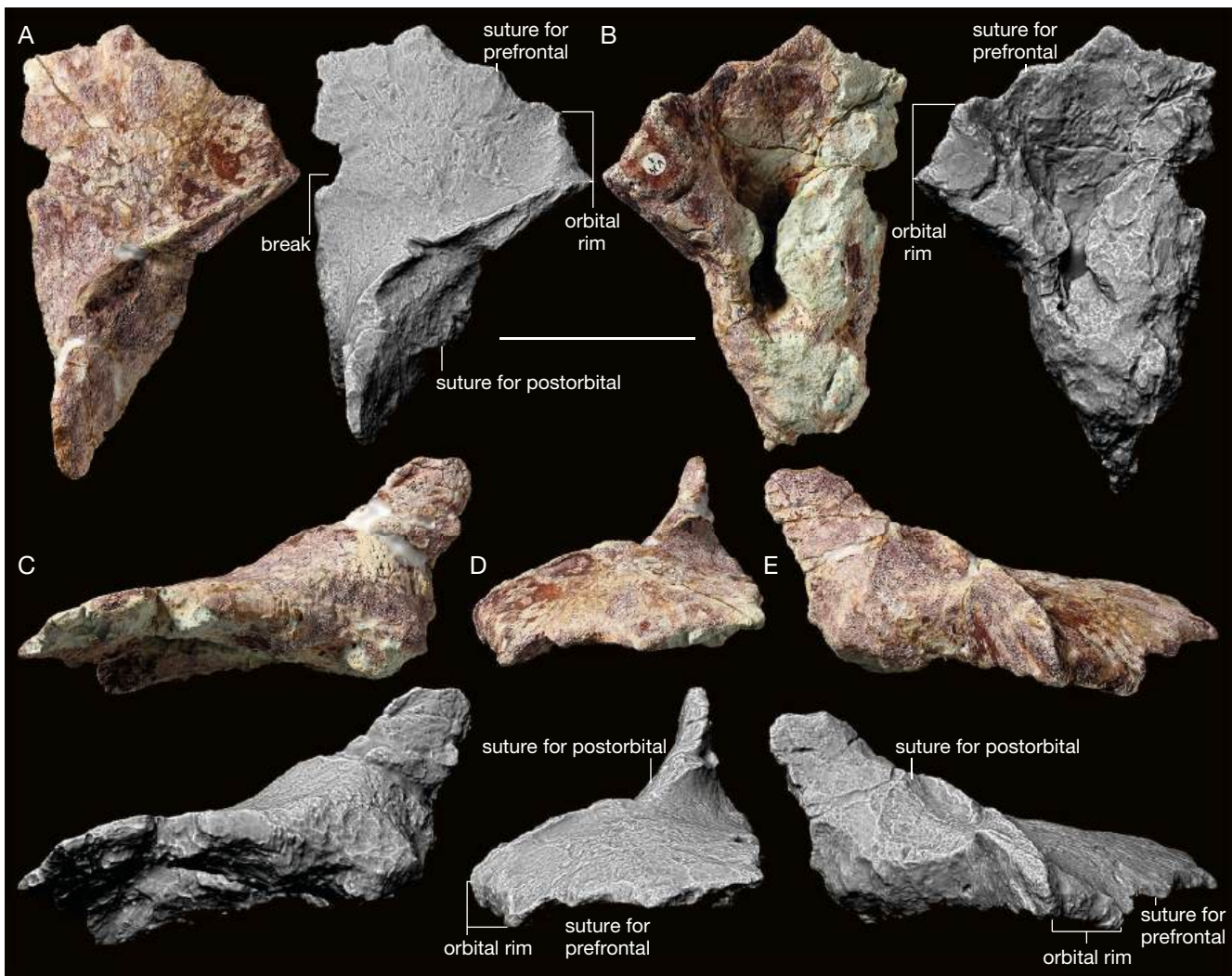


FIG. 3. — *Woznikella triradiata* n. gen., n. sp., ZPAL V. 34/1/1: A-E, right frontal in dorsal (A), ventral (B), medial (C), anterior (D), and lateral (E) view. Scale bar: 5 cm.

and encases anteriorly a pocket-like lacrimal pit, which opens posteriorly as a large lacrimal foramen (Fig. 2G). The ridge continues faintly along the posterior edge towards the dorsal part of the bone. The anterior opening of the lacrimal duct is located on the internal surface, in the anterior part of the bone, and is directed anterodorsally. The specimen articulates well with the preserved nasal (ZPAL V. 34/1/42) and based on that articulation it appears that the lacrimal nearly reached the nostril, preventing or nearly preventing the contact between the nasal and the maxilla – the very posterior edge of the maxilla was formed by another bone, but it is currently impossible to establish whether this was maxilla or septomaxilla (Fig. 7). The anterior extent of the lacrimal, which is usually covered by the more superficial bones, is unknown in many other Triassic dicynodonts, but it is similar to that of *Woznikella triradiata* n. gen., n. sp. at least in *Ischigualastia jensi*, *Jachaleria candelariensis*, *Kannemeyeria simocephalus*, *Parakannemeyeria dolichocephala*, *Parakannemeyeria shenmuensis* Cheng, 1980, *Parakannemeyeria youngi*, *Placerias hesternus*, *Rhadiodromus mariae*, *Shaanbeikannemeyeria xilougouensis*, possibly *Shansiodon*

wangi, the South African *Shansiodon* sp., *Stahleckeria potens*, *Sinokannemeyeria baidaoyuensis*, *Sinokannemeyeria pearsoni*, *Sinokannemeyeria sanchuanheensis*, *Sungeodon kimkraemerae*, and *Vinceria andina*, in which the lacrimal reaches or nearly reaches the nostril (Pearson 1924a; von Huene 1935; Camp 1956; Camp & Welles 1956; Yeh 1959; Sun 1960, 1963; Cox 1965; Bonaparte 1969; Cheng 1980; Aratijo & Gonzaga 1980; Hancox 1998; Renaut 2000; Renaut & Hancox 2001; Surkov 2003; Vega-Dias & Schultz 2004; Domnanovich & Marsicano 2012; Abdala *et al.* 2013; Hancox *et al.* 2013; Maisch & Matzke 2014; Liu 2015; Kammerer & Ordoñez 2021). In contrast to *Kannemeyeria simocephalus*, *Parakannemeyeria youngi* (and, likely, the other species of that genus), *Placerias hesternus*, and *Stahleckeria potens*, however, except for a narrow margin along the dorsoanterior and anterior border, which shows characteristics of a squamous suture, the lacrimal in *Woznikella triradiata* n. gen., n. sp. was almost entirely exposed externally (Pearson 1924a; von Huene 1935; Camp 1956; Sun 1963; Renaut 2000; Maisch 2001; Abdala *et al.* 2013; Kammerer & Ordoñez 2021). In *Dinodontosaurus*

brevirostris and *Dinodontosaurus tener* the morphology of the lacrimal is variable (Cox 1965, 1968; Morato 2006). In the specimens MCZ 1628, MCZ 3454, DGM 309, and the “*Chanaria platyceps*” holotype (UNLaR 14) the lacrimal has a large exposure, unlike in the specimens MCZ 1670 and MCZ 1687 of the same species. However, in MCZ 1628 it is subrectangular and still significantly separated from the nostril, which is located in the anterior third of the narial fossa, whereas in MCZ 3454, DGM 309, and UNLaR 14 it reaches further rostrally (Cox 1965, 1968). In *Dinodontosaurus brevirostris* MCZ 3454 and likely UNLaR 14, as well as in *Dinodontosaurus tener* DGM 309, *Parakannemeyeria youngi*, *Sinokannemeyeria baidaoyuensis*, and *Sinokannemeyeria pearsoni* the lacrimal meets the septomaxilla anteriorly, separating the maxilla from the nasal, but the septomaxilla seems to cover about third of this distance (Sun 1963; Cox 1968; Liu 2015), thus more than in *Woznikella triradiata* n. gen., n. sp. In *Dinodontosaurus tener* specimen DGM 530R the separation is incomplete and the lacrimal is relatively small, probably due to relatively short preorbital length of that skull (Cox 1968). Variable lacrimals, generally large but not separating the nasals from the maxillae, were observed in the series of specimens described by Morato (2006). Some age-related variation was also described in *Kannemeyeria simocephalus* by Renaut (2000), with larger individuals having proportionally smaller exposure of the lacrimal, but in no case was the anterior part of the lacrimal externally exposed *in vivo* in that species. In *Jachaleria candelariensis* the lacrimal, as exposed laterally, is much lower dorsoventrally and more strap-like (Araújo & Gonzaga 1980; Vega-Dias & Schultz 2004). The nasal is also completely or almost completely separated from the maxilla by the lacrimal and septomaxilla in *Lystrosaurus* spp. and the South African *Shansiodon* sp., but due to the shortening of the preorbital part of the skull, the lacrimal remains relatively short (e.g., Sun 1964; Cluver 1971; Li 1988; Hancox *et al.* 2013).

Frontal

The right frontal (ZPAL V. 34/1/1; Fig. 3) is almost complete, only the top of the dorsal (parietal) process, a small fragment of the medial edge, and the anterior tip are broken. The frontal plate is nearly as wide as long and its anterior edge is bowed. The frontal pair thus was fan-shaped in dorsal view and apparently lacked prominent and narrow lateral processes or conspicuous embayments for the nasal or prefrontals, similar to, e.g., *Dolichuranus primaevus*, *Lystrosaurus* spp. (with the exception of *L. curvatus* (Owen, 1876) and *L. hedini*), the South African *Shansiodon* sp., *Sinokannemeyeria sanchuanheensis*, and *Tetragonias njalilus*, but different from, e.g., *Acratophorus argentinensis*, *Dinodontosaurus* spp., *Elephantosaurus jachimovitschi* Vjuschkov, 1969, *Ischigualastria jensi*, *Jachaleria candelariensis*, “*Kannemeyeria*” *latirostris*, *Mogbreberia nmachouensis*, *Parakannemeyeria dolichocephala*, *Parakannemeyeria youngi*, “*Parvobestiola bashkiriensis*”, *Placerias hesternus*, *Rechnisaurus cristarhynchus*, *Rhadiodromus mariae*, *Rhinodicynodon gracile*, *Shaanbeikannemeyeria xilougouensis*, *Sinokannemeyeria yingchiaoensis*, *Stahleckeria potens*, *Ufudocyclops mukanelai*, and *Vinceria andina* (von Huene 1935,

1942; Young 1935; Camp & Welles 1956; Sun 1960, 1963; Cox 1965, 1968; Bonaparte 1966a; Cruickshank 1967; Vjuschkov 1969; Crozier 1970; Kalandadze 1970; Chowdhury 1970; Cluver 1971; Cheng 1980; Araújo & Gonzaga 1980; Dutuit 1988; Bandyopadhyay 1989; Lucas & Harris 1996; Surkov 1999a, 2003; Maisch 2001; Vega-Dias & Schultz 2004; Vega-Dias *et al.* 2005; Morato 2006; Damiani *et al.* 2007; Domnanovich & Marsicano 2012; Abdala *et al.* 2013; Hancox *et al.* 2013; Kammerer 2018; Kammerer *et al.* 2019; Kammerer & Ordoñez 2021). The anterior median process is broken but, considering that the posterior edge of the nasal appears to be complete, it likely either was relatively short and ended in a point, or a supernumerary internasal bone was present, as in *Jachaleria* spp. and some individuals of *Lystrosaurus* spp. (Araújo & Gonzaga 1980; Vega-Dias & Schultz 2004; Jasinoski *et al.* 2014; Kammerer & Ordoñez 2021). It must be noted, however, that the layout of the anterior frontal suture exhibits some variability, even bilaterally within a single individual (e.g., Camp 1956; Cox 1965; Renaut 2000; Kammerer & Ordoñez 2021). The frontal is proportionally much wider than in the narrow-roofed skulls of *Counillonia superoculis*, *Myosaurus gracilis*, *Kombuisia frerensis*, *Kombuisia antarctica* Fröbisch, Angielczyk & Sidor, 2010, and *Repelinosaurus robustus* (see Haughton 1917; Cluver 1974; Hotton 1974; Hammer & Cosgriff 1981; Fröbisch 2007; Olivier *et al.* 2019). It is much longer than the anteroposteriorly shortened (at least, as exposed externally) frontal of *Sangusaurus parringtonii* (see Angielczyk *et al.* 2017; Kammerer & Ordoñez 2021).

The most distinctive feature of the frontal is the strongly elevated dorsal process similar to that of *Kannemeyeria simocephalus* (e.g., Weithofer 1888; Broom 1937; Watson 1948; Kammerer & Ordoñez 2021). On the anterior and lateral surfaces of this process, the area for sutural contact with the postorbital is visible. This area continues throughout the posterodorsal edge of the bone, reaching its lateral edge, where it ends in a point.

The lateral edge of the frontal contributed to the margin of the orbit, and in dorsoventral aspect is slightly oblique to the long axis of the skull (turned anteromedially). The contribution is restricted, similar as in, e.g., *Dolichuranus primaevus* and *Rechnisaurus cristarhynchus*, but larger than in at least some specimens of *Dinodontosaurus* spp., *Ischigualastria jensi*, “*Kannemeyeria*” *latirostris*, *Stahleckeria potens*, and *Uralokannemeyeria vjuschkovi*, and smaller than in most specimens of *Kannemeyeria simocephalus*, *Kombuisia* spp., and *Myosaurus gracilis* (see Haughton 1917; Pearson 1924a; Case 1934; von Huene 1935; Camp 1956; Cox 1965, 1968; Crozier 1970; Danilov 1971; Cluver 1974; Hammer & Cosgriff 1981; Bandyopadhyay 1989; Renaut 2000; Maisch 2001; Vega-Dias *et al.* 2005; Morato 2006; Damiani *et al.* 2007; Fröbisch 2007; Fröbisch *et al.* 2010; Abdala *et al.* 2013; Kammerer & Ordoñez 2021). This differs from *Jachaleria candelariensis*, in which the frontal is excluded from the edge of the orbit by the prefrontal and postorbital (Araújo & Gonzaga 1980; Vega-Dias & Schultz 2004). In anterior view, the part of the skull roof formed by the frontal has its medial part noticeably more elevated dorsally than the lateral one, so this part

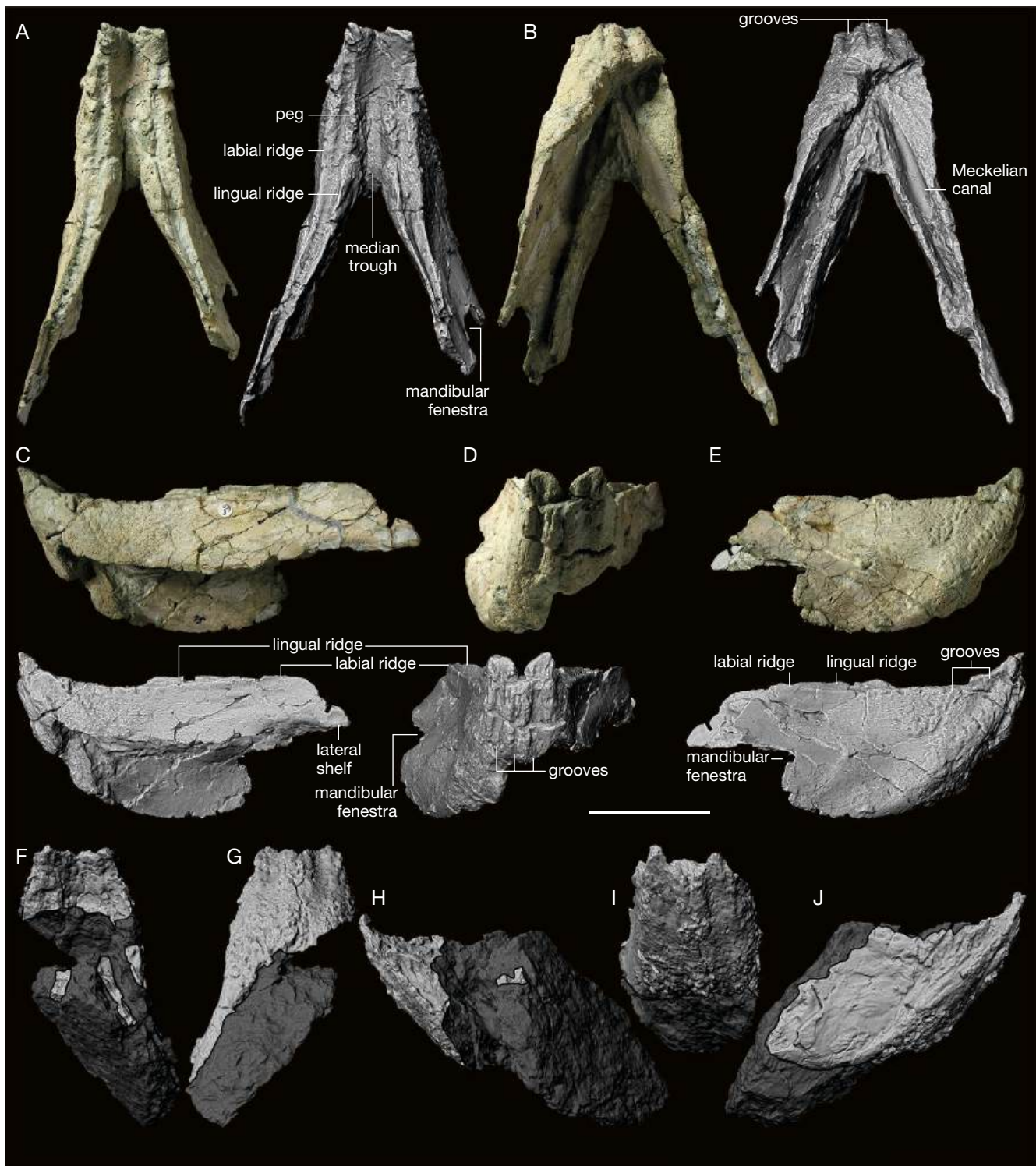


FIG. 4. — *Woznikella triradiata* n. gen., n. sp.: A–E, ZPAL V. 34/1/3: dentaries in dorsal (A), ventral (B), lateral left (C), anterior (D), and lateral right (E) view; F–J, SMNS 91416: dentaries in dorsal (F), ventral (G), lateral left (H), anterior (I), and lateral right (J) view. Scale bar: 5 cm.

of the skull was convex, similar to, e.g., *Ischigualastia jensi* (see Cox 1965; Kammerer & Ordoñez 2021).

The pineal foramen is located in the posteromedial corner of the bone. In that aspect, *Woznikella triradiata* n. gen., n. sp. differs from *Kombuisia frerensis*, in which the pineal foramen is absent (Hotton 1974; Fröbisch 2007). The area

of the suture with the left frontal is damaged, but it appears that the prefrontal bone was absent. The internal side is also poorly preserved, and a large fragment of sediment was left unprepared to avoid destroying the specimen, obscuring most of the internal structures. Still, a deep fissure is visible in the center of the internal surface of the bone.

TABLE 1. — Occurrences of Triassic dicynodonts. Note that the list is not comprehensive and likely numerous other mentions exist, particularly in local, non-English literature. The Country column includes all mentions deemed significant (i.e., not merely listing taxa from original literature, but providing mentions, descriptions, and/or images of new specimens, original data or reinterpretations of morphology, confirming the geographical and/or temporal presence of taxa, confirming or providing novel insights into their validity, or at least presenting them in a novel biostratigraphic context). For simplicity, the Formation column includes only the references providing the most recent and most precise subdivisions either verbatim or in a form unambiguously recognizable without extensive research of local geological literature. The historically used *Lystrosaurus* Cope, 1870a AZ was recently redefined and renamed to *Lystrosaurus declivis* (Owen, 1859) AZ (Botha & Smith 2020). Because of the presence of *Lystrosaurus* spp. also in the underlying *Lystrosaurus maccaigi* (Seeley, 1898)-*Moschorhinus* Broom, 1920 SZ of *Daptocephalus* Hoepen, 1934 AZ (former *Dicynodon* AZ), the meaning of the historical *Lystrosaurus* AZ is somewhat ambiguous and may be dependent on the author (see Table 2). Therefore, the name is used here in parentheses, implying that although in most cases it was probably synonymous with *Lystrosaurus declivis* AZ, it can potentially include the top of the *Daptocephalus* AZ. If the occurrence is not explicitly mentioned in the context of a changed naming scheme, the papers allowing referral (e.g., naming both the old formation and the new formation) are provided. The synonymy of Chinese *Lystrosaurus* spp. follows Camp & Liu (2011). Age includes selected single most recent original study with preference towards radiometric dates, unless those are unavailable, and a sound disagreement exists between several studies. Note that the bottom age (252.24 ± 0.11 Ma) of the *Lystrosaurus declivis* AZ obtained by Gastaldo et al. (2020) is barely about 0.3 Ma older than the currently recognized Triassic/Permian boundary (251.902 ± 0.024 Ma). See Botha et al. (2020) for the entirely Triassic estimation of the age of that assemblage and Botha & Smith (2020) for discussion. Additional noteworthy contributions, not providing precise specific or geographic information include: Broom 1900b; Toerien 1955; Watson 1960; Cruickshank 1964; Anderson & Cruickshank 1978; Kemp 1982; Hotton 1986; King 1990b, 1991; King & Cluver 1991; Smith 1995; King & Jenkins 1997; Cox 1998; Surkov 1998b; Neveling et al. 1999; Smith & Ward 2001; Angelczyk & Kurkin 2003; Ray & Chinsamy 2003; Neveling et al. 2005; Whitney & Sidor 2020; Kammerer 2021; Liu et al. 2021; Whitney et al. 2021. Abbreviations: AZ, assemblage zone; SZ, subzone.

Taxon	Country	Formation	Age
<i>Acratophorus argentinensis</i> (Bonaparte, 1965)	Argentina (Bonaparte 1965, 1966a, 1967, 1970, 1978, 1981; Cruickshank 1970; Keyser & Cruickshank 1979; Brink 1986; King 1988; Renaut 2000; Renaut & Hancox 2001; Domnanovich & Marsicano 2012; Mancuso & Irmis 2019; Ordoñez et al. 2019; Kammerer & Ordoñez 2021; Escobar et al. 2023)	Río Seco de la Quebrada (Domnanovich & Marsicano 2012; Mancuso & Irmis 2019) Quebrada de los Fósiles (Bonaparte 1981; Domnanovich & Marsicano 2012)	Carnian (Ottone et al. 2014)
			?Ladinian-Carnian (Ottone et al. 2014)
<i>Angonisaurus cruckshanki</i> Cox & Li, 1983	Tanzania (Cox & Li 1983; King 1988; Hancox 1998; Surkov & Benton 2004; Kammerer et al. 2017, 2019)	Manda (Cox & Li 1983; King 1988; Hancox 1998; Surkov & Benton 2004; Kammerer et al. 2017, 2019)	Anisian or younger (Wynd et al. 2018)
Anomodontia indet.	Antarctica (Cosgriff et al. 1978) South Africa (Watson 1960)	Lower Fremouw (Cosgriff et al. 1978) <i>Cynognathus</i> AZ (Watson 1960)	Olenekian (Elliot et al. 2017) Anisian-Carnian (Hancox et al. 2020)
	Tanzania (Haughton 1932; Attridge et al. 1964)	Manda (Attridge et al. 1964; Cruickshank 1965)	Anisian or younger (Wynd et al. 2018)
" <i>Azarifeneria barrati</i> " Dutuit, 1989a	Morocco (Dutuit 1989a; Gauffre 1993)	Argana t5 (Dutuit 1989b; Gauffre 1993)	Carnian/?Norian (Kammerer et al. 2012)
" <i>Azarifeneria robustus</i> " Dutuit, 1989b	Morocco (Dutuit 1989b; Gauffre 1993)	Argana t5 (Dutuit 1989b; Gauffre 1993)	Carnian/?Norian (Kammerer et al. 2012)
<i>Counillonia superoculis</i> Olivier, Battail, Bourquin, Rossignol, Steyer & Jalil, 2019	Laos (Olivier et al. 2019)	Purple Claystone (Olivier et al. 2019)	?Late Permian (Liu 2020)/Early Triassic (Olivier et al. 2019)
Dicynodontia indet.	Antarctica (Hammer et al. 2004)	Lashly C (Hammer et al. 2004)	Carnian (Hammer et al. 2004)
	Argentina (Rogers et al. 2001)	Chañares (Rogers et al. 2001)	Late Ladinian-early Carnian (Ezcurra et al. 2017)
	Australia (King 1983, 1988; Thulborn 1983a, b, 1990)	Arcadia (King 1983; Thulborn 1983a, b, 1990)	Early Triassic (Northwood 1997)
	Brazil (von Huene 1935; Holz & Schultz 1998; Da Rosa et al. 2004, 2005; Martinelli et al. 2005, 2017; Pavantino et al. 2020)	Santa Maria <i>Dinodontosaurus</i> AZ (Martinelli et al. 2017; Pavantino et al. 2020)	Ladinian-Carnian (Philipp et al. 2018)/Carnian (Ordoñez et al. 2020)
	Canada (Sues & Olsen 2015)	Wolfville (Sues & Olsen 2015)	Carnian (Sues & Olsen 2015)
	China (Young 1935, 1937, 1939, 1946)	Not given (Young 1935, 1939)	?Late Permian-Induan (Tong et al. 2018)
	India (Bandyopadhyay 1988; Kutty et al. 1988; Kutty & Sengupta 1989; Bandyopadhyay & Ray 2020)	Ermaying (Young 1937) Bhimaram (Kutty et al. 1988; Kutty & Sengupta 1989; Bandyopadhyay & Ray 2020) Lower Maleri (Bandyopadhyay 1988; Kutty & Sengupta 1989)	Anisian (Liu et al. 2017) Late Anisian-Ladinian (Bandyopadhyay & Ray 2020) Carnian (Bandyopadhyay & Ray 2020)
	Japan (Jinnouchi et al. 2018)	Momonoki (Jinnouchi et al. 2018)	Carnian (Jinnouchi et al. 2018)
	Mozambique (Araújo et al. 2020)	Fubué (Araújo et al. 2020)	Early Triassic (Araújo et al. 2020)
	Namibia (Smith & Swart 2002; Abdala & Smith 2009; Abdala et al. 2013)	Omingonde (Smith & Swart 2002; Abdala & Smith 2009; Abdala et al. 2013)	Anisian-Ladinian (Wynd et al. 2018; Zieger et al. 2020)
	Russia (Shishkin et al. 1995; Tverdokhlebov et al. 2002)	Bukobay (Shishkin et al. 1995) Donguz (Shishkin et al. 1995; Tverdokhlebov et al. 2002)	Ladinian (Tverdokhlebov et al. 2020) Anisian (Ivakhnenko 2008)
	South Africa (Nicolas & Rubidge 2010; Bordy et al. 2020)	<i>Cynognathus</i> AZ (Nicolas & Rubidge 2010) Lower Elliott <i>Scalenodontoides</i> AZ (Bordy et al. 2020; Viglietti et al. 2020b)	Anisian-Carnian (Hancox et al. 2020) Norian-Rhaetian (Bordy et al. 2020)

TABLE 1. — Continuation.

Taxon	Country	Formation	Age
	Tanzania (Charig 1956; Nesbitt & Butler 2013; Nesbitt et al. 2013) United States (Sues et al. 2003; Nesbitt et al. 2006)	" <i>Lystrosaurus</i> AZ" (Nicolas & Rubidge 2010) Manda (Charig 1956; Nesbitt & Butler 2013; Nesbitt et al. 2013) Upper Moenkopi (Nesbitt et al. 2006)	Late Permian-Early Triassic (Gastaldo et al. 2020) Anisian or younger (Wynd et al. 2018) Late Anisian (Haque et al. 2021)
	Zambia (Kemp 1975; Peecook et al. 2018; Whitney et al. 2019)	Newark Supergroup, Lithofacies Association II (Sues et al. 2003) Ntawere (Kemp 1975; Peecook et al. 2018)	Late Carnian/early Norian (Sues et al. 2003) Anisian or younger (Wynd et al. 2018)
Dicynodontia indet. (" <i>Astrobrachyops jensei</i> " Colbert & Cosgriff, 1974)	Antarctica (Colbert & Cosgriff 1974; Warren & Marsicano 2000)	Lower Fremouw (Colbert & Cosgriff 1974; Warren & Marsicano 2000)	Olenekian (Elliot et al. 2017)
Dicynodontia indet. ("cf. <i>Dinodontosaurus</i> sp.")	Brazil (Raugust et al. 2013; Martinelli et al. 2017; Schultz et al. 2020)	?Santa Maria <i>Santacruzodon</i> AZ (Raugust et al. 2013; Martinelli et al. 2017; Schultz et al. 2020)	Carnian (Philipp et al. 2018)
Dicynodontia indet. (" <i>Fukangolepis barbosae</i> " Yang, 1978)	China (Yang 1978; Lucas & Hunt 1993b)	Upper Karamay (Yang 1978; Lucas & Hunt 1993b)	Ladinian (Tong et al. 2018)
Dicynodontia indet. (" <i>Dicynodon</i> sp.")	India (Lydekker 1879)	Panchet (Lydekker 1879)	Early Triassic (Prasad & Pundir 2020)
Dicynodontia indet. (" <i>Lystrosaurus</i> sp.")	Tanzania (Boonstra 1953; Cruickshank 1967)	Manda (Cruickshank 1965)	Anisian or younger (Wynd et al. 2018)
Dicynodontia indet. (" <i>Ruhuhungulasaurus croucheri</i> " Larkin, 1994/ "Shansiodon sp.")	Tanzania (Larkin 1994; Surkov & Benton 2004, 2008; Angielczyk et al. 2014; Kammerer et al. 2017)	Manda (Larkin 1994; Surkov & Benton 2004, 2008; Kammerer et al. 2017)	Anisian or younger (Wynd et al. 2018)
Dicynodontia indet. (" <i>Brachybrachium breviceps</i> " Williston, 1904)	United States (Williston 1904; von Huene 1911, 1935; Camp & Welles 1956; King 1988; Huber et al. 1993; Lucas & Hunt 1993a; Long & Murry 1995; Lucas 1998; Lucas & Heckert 2002; Kammerer et al. 2013)	Popo Agie (Williston 1904; von Huene 1911; 1935; Camp & Welles 1956; King 1988; Huber et al. 1993; Lucas & Hunt 1993a; Long & Murry 1995; Lucas 1998; Lucas & Heckert 2002; Kammerer et al. 2013)	Carnian (Hartman et al. 2015)
?Dicynodontia indet. ("aff. <i>Dinodontosaurus</i> sp.")	Germany (Lucas 2007)	Upper Muschelkalk (Lucas 2007)	Anisian/Ladinian (German Stratigraphic Commission 2016)
?Dicynodontia indet. ("cf. <i>Placerias</i> sp.")	France (Broili 1921; Schmidt 1928; von Huene 1935; Camp & Welles 1956; Lucas & Wild 1995; Maisch et al. 2009)	Upper Muschelkalk (Broili 1921; Schmidt 1928; von Huene 1935; Camp & Welles 1956; Lucas & Wild 1995; Maisch et al. 2009)	Anisian/Ladinian (German Stratigraphic Commission 2016)
Dicynodontoida indet.	Australia (Rozefelds et al. 2011)	Upper Parmeer Supergroup (Rozefelds et al. 2011)	Late Permian-Early Triassic (Rozefelds et al. 2011)
Dicynodontoida indet. (" <i>Putillosaurus sennikovi</i> " Surkov, 2005)	Russia (Shishkin et al. 2000; Angielczyk & Kurkin 2003; Surkov 2005; Ivakhnenko 2008)	Donskaya Luka (Surkov 2005; Ivakhnenko 2008)	Olenekian (Ivakhnenko 2008)
<i>Dinodontosaurus breirostris</i> Cox, 1968	Argentina (Cox 1968; Bonaparte 1970, 1978, 1997; Keyser 1974; Keyser & Cruickshank 1979; Brink 1988; King 1988; Morato et al. 2006; Ordoñez et al. 2019; Escobar et al. 2021, 2023; Kammerer & Ordoñez 2021) ?Brazil (Cox 1968; Escobar et al. 2023)	Chañares (Cox 1968; Bonaparte 1970, 1978, 1997; Keyser 1974; Brink 1988; King 1988; Ordoñez et al. 2019; Escobar et al. 2021, 2023; Kammerer & Ordoñez 2021) Santa María (Cox 1968)	Late Ladinian-early Carnian (Ezcurra et al. 2017) Ladinian-Carnian (Philipp et al. 2018)/early Carnian (Ordoñez et al. 2020)
<i>Dinodontosaurus tener</i> (von Huene, 1935)	Brazil (von Huene 1935; Tupi Caldas 1936; Romer 1943; Cox 1965; Bonaparte 1970, 1978; Keyser 1974; Keyser & Cruickshank 1979; Brink 1986, 1988; King 1988; Walter 1989; Lucas & Harris 1996; Lucas 2002; Schwanke & Melo 2002; Vega-Dias et al. 2004; Da Rosa et al. 2004; Morato 2006; Morato et al. 2006, 2008; Langer et al. 2007; Kammerer et al. 2011; de Oliveira Bueno et al. 2011; Abdala et al. 2013; Dassie 2014; Martinelli et al. 2017; Da Silveira 2017; Kammerer 2018; Mancuso & Irmis 2019; Ordoñez et al. 2019, 2020; Schultz et al. 2020; Escobar et al. 2021, 2023; Kammerer & Ordoñez 2021; Knaus et al. 2021; Maisch 2021)	Santa María <i>Dinodontosaurus</i> AZ (Lucas 2002; Langer et al. 2007; de Oliveira Bueno et al. 2011; Abdala et al. 2013; Dassie 2014; Da Silveira 2017; Martinelli et al. 2017; Mancuso & Irmis 2019; Ordoñez et al. 2020; Schultz et al. 2020; Kammerer & Ordoñez 2021; Maisch 2021)	Ladinian-Carnian (Philipp et al. 2018)/ early Carnian (Ordoñez et al. 2020)
<i>Dinodontosaurus</i> sp.	Brazil (Da Rosa et al. 2005; Martinelli et al. 2005, 2016, 2017; Reichel et al. 2009; Mainardes Dutra 2015; Ugalde et al. 2018; Corecco et al. 2020, 2021; Pavantino et al. 2020)	Santa María <i>Dinodontosaurus</i> AZ (Martinelli et al. 2016, 2017; Ugalde et al. 2018; Corecco et al. 2020, 2021; Pavantino et al. 2020)	Ladinian-Carnian (Philipp et al. 2018)/Carnian (Ordoñez et al. 2020)

TABLE 1. — Continuation.

Taxon	Country	Formation	Age
<i>Dinodontosaurus</i> sp. ("Dicynodon turpior") "Dicynodon cf. turpior")	Brazil (von Huene 1935, 1944.; Cox 1965; Bonaparte 1978; Santa Maria <i>Dinodontosaurus</i> AZ (Cox 1965; King 1988; Lucas 1993a; Lucas & Harris 1996; Langer et al. 2007; Kammerer et al. 2011; Kammerer & Ordoñez 2021)	King 1988; Lucas 1993a; Lucas & Harris 1996; Langer et al. 2007; Kammerer et al. 2011; Kammerer & Ordoñez 2021)	Ladinian-Carnian (Philipp et al. 2018)/Carnian (Ordoñez et al. 2020)
cf. <i>Dinodontosaurus</i> sp.	Argentina (Ezcurra et al. 2017)	Chañares <i>Tarjadia</i> AZ (Ezcurra et al. 2017)	Ladinian/Carnian (Ezcurra et al. 2017)
<i>Dolichuranus primaevus</i> Keyser, 1973	Namibia (Keyser 1973; Cooper 1980; Brink 1986; King 1988; Damiani et al. 2007; Govender & Yates 2009)	Omingonde (Keyser 1973, 1974; Cooper 1980; Brink 1986; King 1988; Damiani et al. 2007)	Anisian-Ladinian (Wynd et al. 2018; Zieger et al. 2020)
cf. <i>Dolichuranus primaevus</i> Keyser, 1973	Namibia (Govender & Yates 2009)	Omingonde (Govender & Yates 2009)	Anisian-Ladinian (Wynd et al. 2018; Zieger et al. 2020)
<i>Dolichuranus</i> sp.	Tanzania (Kammerer et al. 2017; Peecook et al. 2018, Smith et al. 2018, Wynd et al. 2018)	Manda (Kammerer et al. 2017, Peecook et al. 2018, Wynd et al. 2018)	Anisian or younger (Wynd et al. 2018)
<i>Elephantosaurus jachimovitschi</i> Vjuschkov, 1969	Russia (Vjuschkov 1969; Keyser & Cruickshank 1979; King 1988; Shishkin et al. 1995; Ivakhnenko et al. 1997; Battail & Surkov 2000; Ivakhnenko 2008; Kammerer et al. 2013)	Bukobay (Shishkin et al. 1995; Ivakhnenko et al. 1997; Battail & Surkov 2000; Ivakhnenko 2008; Kammerer et al. 2013)	Ladinian (Tverdokhlebov et al. 2020)
<i>Eubrachiosaurus browni</i> Williston, 1904	United States (Williston 1904; Cross & Howe 1905; von Huene 1911, 1926a, 1935; Pearson 1924a; Camp & Welles 1956; King 1988; Huber et al. 1993; Long & Murry 1995; Lucas 1998; Lucas & Heckert 2002; Kammerer et al. 2013)	Popo Agie (Williston 1904; von Huene 1911, 1926a, 1935; Camp & Welles 1956; King 1988; Huber et al. 1993; Long & Murry 1995; Lucas 1998; Lucas & Heckert 2002; Kammerer et al. 2013)	Carnian (Hartman et al. 2015)
<i>Ischigualastia jensi</i> Cox, 1962	Argentina (Cox 1962, 1965; Bonaparte 1970, 1978, 1997; Keyser 1974; Keyser & Cruickshank 1979; King 1988; Vega-Dias & Schwanke 2004a; Martínez et al. 2012; Kammerer et al. 2017; Kammerer 2018; Ordoñez et al. 2019; Wynd et al. 2020; Maisch 2021; Kammerer & Ordoñez 2021)	Ischigualasto B1 (Martínez et al. 2012)	Late Carnian (Martínez et al. 2011)
cf. <i>Ischigualastia jensi</i> Cox, 1962	India (Edler 2000)	Pipariya (Edler 2000)	Carnian (Chatterjee et al. 2017)
cf. <i>Ischigualastia</i> sp.	India (Bandyopadhyay 1988; Kutty & Sengupta 1989; Novas et al. 2010; Bandyopadhyay & Ray 2020)	Upper Maleri (Bandyopadhyay 1988; Kutty & Sengupta 1989; Novas et al. 2010; Bandyopadhyay & Ray 2020)	Norian (Bandyopadhyay & Ray 2020)
<i>Jachaleria candelariensis</i> Araújo & Gonzaga, 1980	Brazil (Araújo & Gonzaga 1980; Vega-Dias & Schultz 1999, 2003, 2004, 2007; Schultz & Vega-Dias 2003; Vega-Dias & Schwanke 2004b, 2005; Vega-Dias et al. 2004; Morato et al. 2005; Langer et al. 2007; Francischini Filho 2014; Kammerer 2018; Corecco et al. 2020, 2021; Schultz et al. 2020; Wynd et al. 2020; Maisch 2021)	Caturrita (Lucas 1993a; Schultz & Vega-Dias 2003; Vega-Dias & Schultz 2003, 2007; Vega-Dias & Schwanke 2004b, 2005; Langer et al. 2007; Francischini Filho 2014; Kammerer 2018; Kammerer & Ordoñez 2021; Maisch 2021)	Norian (Langer et al. 2018)
cf. <i>Jachaleria candelariensis</i> Araújo & Gonzaga, 1980	Brazil (Martinelli et al. 2020)	Caturrita (Martinelli et al. 2020)	Norian (Langer et al. 2018)
<i>Jachaleria colorata</i> Bonaparte, 1970	Argentina (Bonaparte 1966b, 1970, 1978, 1997; Keyser 1974; King 1988; Vega-Dias & Schwanke 2004b, 2005; Martínez et al. 2012; Francischini Filho 2014; Kammerer 2018; Ordoñez et al. 2019)	Ischigualasto B3 (Martínez et al. 2012) Lower Los Colorados (Bonaparte 1966a, 1970, 1978; Araújo & Gonzaga 1980; Vega-Dias & Schwanke 2005; Martínez et al. 2012; Francischini Filho 2014; Kammerer 2018)	Norian (Currie et al. 2009) Norian (Currie et al. 2009)
<i>Kannemeyeria agnosteus</i> Kammerer & Ordoñez, 2021	Argentina (Bonaparte 1981; DeFauw 1993; Fröbisch 2009; Kammerer & Ordoñez 2021)	Quebrada de los Fósiles (Bonaparte 1981; DeFauw 1993) Río Seco de la Quebrada (Kammerer & Ordoñez 2021)	?Ladinian-Carnian (Ottone et al. 2014) Carnian (Ottone et al. 2014)
" <i>Kannemeyeria latirostris</i> " Crozier, 1970	Zambia (Brink 1963, 1986; Drysdall & Kitching 1963; Kitching 1963; Crozier 1970; Cruickshank 1970; Keyser & Cruickshank 1979; King 1988; Angielczyk et al. 2014; Peecook et al. 2018)	Ntawere (Brink 1963, 1986; Drysdall & Kitching 1963; Kitching 1963; Crozier 1970; Cruickshank 1970; Keyser & Cruickshank 1979; King 1988; Angielczyk et al. 2014; Peecook et al. 2018)	Anisian or younger (Wynd et al. 2018)
<i>Kannemeyeria lophorhinus</i> Renaut, Damiani, Yates & Hancox, 2003	Namibia (Keyser 1973; Brink 1986; King 1988; Bandyopadhyay 1989; Pickford 1995; Renault 2000; Renault et al. 2003; Govender & Yates 2009)	Omingonde (Keyser 1973; Brink 1986; King 1988; Bandyopadhyay 1989; Pickford 1995; Renault 2000; Renault et al. 2003; Govender & Yates 2009)	Anisian-Ladinian (Wynd et al. 2018; Zieger et al. 2020)
	?Tanzania (Cox 1991; Renault 2000)	Manda (Cox 1991)	Anisian or younger (Wynd et al. 2018)
	Zambia (Brink 1963, 1986; Drysdall & Kitching 1963; Crozier 1970; Keyser & Cruickshank 1979; King 1988; Bandyopadhyay 1989; Renault 2000; Renault et al. 2003; Angielczyk et al. 2014; Peecook et al. 2018)	Ntawere (Brink 1963, 1986; Drysdall & Kitching 1963; Kitching 1963; Crozier 1970; Keyser & Cruickshank 1979; King 1988; Bandyopadhyay 1989; Renault 2000; Renault et al. 2003; Angielczyk et al. 2014; Peecook et al. 2018)	Anisian or younger (Wynd et al. 2018)

TABLE 1. — Continuation.

Taxon	Country	Formation	Age
cf. <i>Kannemeyeria lophorhinus</i>	Namibia (Govender & Yates 2009)	Omingonde (Govender & Yates 2009)	Anisian-Ladinian (Wynd et al. 2018; Zieger et al. 2020)
<i>Kannemeyeria simocephalus</i> (Weithofer, 1888)	South Africa (Weithofer 1888; Broom 1899, 1909, 1913a, 1915, 1923, 1932, 1937; Seeley 1904, 1908; Jaekel 1911; Watson 1912a, 1917, 1948; Haughton 1915, 1917, 1924, 1963; Pearson 1924a, b; von Huene 1925; Case 1934; Courtenay-Latimer 1948; Toerien 1951, 1953, 1955; Haughton & Brink 1954; Camp 1956; Cruickshank 1970, 1975; Anonymous 1972; Keyser 1974; Kitching 1977; Keyser & Cruickshank 1979; Brink 1986; King 1988; Hancox 1998; MacRae 1999; Renault 2000; Nesbitt & Angielczyk 2002; Damiani & Kitching 2003; Neveling 2004; Surkov & Benton 2004; Govender 2005; Ray 2006; Nicolas 2007; Jannah & Rubidge 2007; Damiani 2008; Fröbisch & Reisz 2008; Govender et al. 2008; Botha-Brink & Angielczyk 2010; Nicolas & Rubidge 2010; Kammerer et al. 2011, 2017; Smith et al. 2012, 2020b; Butler et al. 2016; Kammerer 2018; Hancox et al. 2020; Olroyd 2022; Olroyd & Sidor 2022; Viglietti et al. 2022) Tanzania (Haughton 1932; Stockley 1932; Boonstra 1953; Attridge et al. 1964; Cruickshank 1965; Keyser & Cruickshank 1979; Kammerer et al. 2017)	<i>Cynognathus</i> AZ <i>Trirachodon-Kannemeyeria</i> SZ (Hancox et al. 2020; Smith et al. 2020b; Viglietti et al. 2022)	Early Anisian (Hancox et al. 2020)
Kannemeyeriidae indet.	Argentina (Romer 1966; Cox 1968; Ezcurra et al. 2015) China (Sun 1963, 1973; Young 1964; Liu 1973, 2015; Cheng 1980) India (Bandyopadhyay 1988; Mukherjee & Sengupta 1998; Bandyopadhyay & Sengupta 1999; Bandyopadhyay & Ray 2020) Madagascar (Flynn et al. 1999) Russia (Ivakhnenko et al. 1997) South Africa (Warren 1998) United States (Small et al. 2022)	Manda (Stockley 1932; Attridge et al. 1964; Cruickshank 1965; Keyser & Cruickshank 1979; Kammerer et al. 2017) Tarjados Formation (Cox 1968; Ezcurra et al. 2015) Upper Ermaying (Sun 1963; Cheng 1980; Liu 2015) Lower Karamay (Liu 1973; Sun 1973; Liu & Li 2003) Tongchuan I (Liu 2015) Denwa (Bandyopadhyay 1988; Mukherjee & Sengupta 1998; Bandyopadhyay & Sengupta 1999; Bandyopadhyay & Ray 2020) Isalo II (Flynn et al. 1999) Bukobay (Ivakhnenko et al. 1997) <i>Cynognathus</i> AZ (Warren 1998) Tecovas (Small et al. 2022)	Anisian or younger (Wynd et al. 2018) Ladinian (Ezcurra et al. 2017) Anisian (Liu et al. 2017) Anisian (Tong et al. 2018) Anisian (Tong et al. 2018) Anisian or younger (Peacock et al. 2018) Carnian (Flynn et al. 1999) Ladinian (Tverdokhlebov et al. 2020) Anisian-Carnian (Hancox et al. 2020) Norian (Small et al. 2022)
Kannemeyeriiformes indet.	Antarctica (Hammer et al. 1987; Hammer 1990, 1995; Sidor et al. 2014; Smith et al. 2020a) Argentina (Zavattieri & Arcucci 2007; Kammerer & Ordoñez 2021) Kazakhstan (Tverdokhlebov et al. 2020) Russia (Tverdokhlebov et al. 2020) South Africa (Hancox et al. 2013) United States (Nesbitt & Angielczyk 2002; Lehman & Chatterjee 2005; Mueller & Chatterjee 2007; Martz 2008; Martz et al. 2013; Small et al. 2022) Zambia (Angielczyk et al. 2014)	Upper Fremouw (Hammer et al. 1987; Hammer 1990, 1995; Sidor et al. 2014; Smith et al. 2020a) Cerro de las Cabras (Zavattieri & Arcucci 2007; Kammerer & Ordoñez 2021) Inder (Tverdokhlebov et al. 2020) Bukobay (Tverdokhlebov et al. 2020) <i>Cynognathus</i> AZ <i>Cricodon-Ufudocyclops</i> SZ Cooper Canyon (Lehman & Chatterjee 2005; Martz 2008; Martz et al. 2013) Upper Moenkopi (Nesbitt & Angielczyk 2002) Tecovas (Small et al. 2022) Ntawere (Angielczyk et al. 2014)	Late Anisian-Ladinian (Elliot et al. 2017) Late Anisian-early Ladinian (Cariglino et al. 2016) Ladinian (Tverdokhlebov et al. 2020) Ladinian (Tverdokhlebov et al. 2020) Late Anisian-Carnian (Hancox et al. 2020) Norian (Martz et al. 2013) Late Anisian (Haque et al. 2021) Norian (Small et al. 2022) Anisian or younger (Wynd et al. 2018)
Kannemeyeriiformes indet. (" <i>Calleonanus furvus</i> " Kalandadze & Sennikov, 1985)	Russia (Kalandadze & Sennikov 1985; Shishkin et al. 1995; Ivakhnenko et al. 1997; Surkov 1999a, 2003; Battail & Surkov 2000; Ivakhnenko 2008; Kammerer et al. 2013)	Lower Donguz (Surkov 2003)	Anisian (Ivakhnenko 2008)
Kannemeyeriiformes indet. (" <i>Cristonanus koltaeviensis</i> " Surkov, 1999a)	Russia (Surkov 1999a, 2003; Ivakhnenko 2008; Kammerer et al. 2013)	Lower Donguz (Surkov 2003)	Anisian (Ivakhnenko 2008)
Kannemeyeriiformes indet. (" <i>Edaxosaurus edentatus</i> " Kalandadze & Sennikov, 1985)	Russia (Kalandadze & Sennikov 1985; Shishkin et al. 1995; Ivakhnenko et al. 1997; Battail & Surkov 2000; Surkov 2003; Ivakhnenko 2008; Kammerer et al. 2013)	Lower Donguz (Surkov 2003)	Anisian (Ivakhnenko 2008)
Kannemeyeriiformes indet. (" <i>Elatosaurus facetus</i> " Kalandadze & Sennikov, 1985)	Russia (Kalandadze & Sennikov 1985; Shishkin et al. 1995; Ivakhnenko et al. 1997; Surkov 1999a, 2003; Battail & Surkov 2000; Ivakhnenko 2008; Kammerer et al. 2013)	Bukobay (Kalandadze & Sennikov 1985; Shishkin et al. 1995; Ivakhnenko et al. 1997; Battail & Surkov 2000; Ivakhnenko 2008)	Ladinian (Tverdokhlebov et al. 2020)

TABLE 1. — Continuation.

Taxon	Country	Formation	Age
Kannemeyeriiformes indet. (" <i>Nasoplanites danilovi</i> " Surkov, 1999a)	Russia (Surkov 1999a, 2003; Ivakhnenko 2008; Kammerer et al. 2013)	Lower Donguz (Surkov 2003)	Anisian (Ivakhnenko 2008)
Kannemeyeriiformes indet. (" <i>Parvobestiola bashkiriensis</i> " Surkov, 1999a)	Russia (Surkov 1999a, 2003; Ivakhnenko 2008; Kammerer et al. 2013)	Lower Donguz (Surkov 2003)	Anisian (Ivakhnenko 2008)
Kannemeyeriiformes indet. (" <i>Planitorostris pechoriensis</i> " Surkov, 1999b)	Russia (Surkov 1999b; Ivakhnenko 2008; Kammerer et al. 2013)	Bukobay (Surkov 1999b; Shishkin et al. 2000)	Ladinian (Tverdokhlebov et al. 2020)
<i>Kombuisia antarctica</i> Fröbisch, Angielczyk & Sidor, 2010	Antarctica (DeFauw 1989; Fröbisch et al. 2010)	Lower Fremouw (DeFauw 1989; Fröbisch et al. 2010)	Olenekian (Elliot et al. 2017)
<i>Kombuisia frerensis</i> Hotton, 1974	South Africa (Hotton 1974; Keyser 1974; Kitching 1977; Keyser & Cruickshank 1979; Brink 1986; King 1988; Fröbisch 2007; Nicolas & Rubidge 2010; Smith et al. 2020b, 2012; Hancox et al. 2020; Viglietti et al. 2022)	<i>Cynognathus</i> AZ <i>Trirachodon-Kannemeyeria</i> SZ (Hancox et al. 2020; Smith et al. 2020b; Viglietti et al. 2022)	Early Anisian (Hancox et al. 2020)
<i>Lisowicia bojani</i> Sulej & Niedzwiedzki, 2018	Poland (Dzik et al. 2008a, b; Vogel 2008; Sulej & Niedzwiedzki 2009, 2019; Niedzwiedzki et al. 2011; Racki & Lucas 2020; Romano & Manucci 2021)	Grabowa (Szulc et al. 2015b; Racki & Lucas 2020)	Norian/Rhaetian (Kowal-Linka et al. 2019)
cf. <i>Lisowicia bojani</i> Sulej & Niedzwiedzki, 2018	Poland (Budziszewska-Karwowska et al. 2010; Sadlok & Wawrzyniak 2013; Sulej et al. 2019; Racki & Lucas 2020)	Grabowa (Szulc et al. 2015b; Racki & Lucas 2020)	Norian (Szulc et al. 2015b)
<i>Lystrosaurus curvatus</i> (Owen, 1876)	Antarctica (Colbert 1972, 1973, 1974, 1975; Cosgriff & Hammer 1981; Kulik & Sidor 2023) South Africa (Owen 1876; Seeley 1898; Broom 1903, 1907, 1909, 1932, 1940; Van Hoepen 1915, 1916; Haughton 1924; von Huene 1925; Brink 1951, 1986; Haughton & Brink 1954; Barry 1968; Kitching 1968, 1977; Cluver 1971; Colbert 1974, 1975; Keyser & Cruickshank 1979; Cosgriff et al. 1982; DeFauw 1986; King 1988; Surkov & Benton 2004; Ray 2005; Smith & Botha 2005; Grine et al. 2006; Botha & Smith 2006, 2007, 2020; Jasinoski et al. 2009, 2010, 2014; Camp 2010; Kammerer et al. 2011; Jasinoski & Chinsamy-Turan 2012; Smith et al. 2012, 2020b; Smith & Botha-Brink 2014; Botha-Brink et al. 2014, 2016; Rubidge et al. 2016; Viglietti et al. 2016; Botha-Brink 2017; Benoit et al. 2018; Botha 2020; Gastaldo et al. 2020; Modesto 2020; Viglietti 2020; Botha et al. 2020; Liu et al. 2022; Olroyd 2022; Olroyd & Sidor 2022; Viglietti et al. 2022; Kulik & Sidor 2023)	Lower Fremouw (Colbert 1974; Cosgriff & Hammer 1981; Kulik & Sidor 2023) <i>Daptocephalus</i> AZ, <i>Lystrosaurus maccaigi-Moschorhinus</i> SZ (Smith et al. 2020b; Viglietti 2020; Liu et al. 2022; Viglietti et al. 2022) <i>Lystrosaurus declivis</i> AZ (Botha & Smith 2020; Modesto 2020; Smith et al. 2020b; Viglietti 2020; Olroyd 2022; Olroyd & Sidor 2022)	Olenekian (Elliot et al. 2017) Late Permian (Gastaldo et al. 2020) Latest Permian-Early Triassic (Gastaldo et al. 2020)
<i>Lystrosaurus cf. curvatus</i> (Owen, 1876)	India (Gupta & Das 2011; Bandyopadhyay & Ray 2020; Kulik & Sidor 2023) South Africa (Kitching 1977; DeFauw 1986)	Panchet (Gupta & Das 2011; Bandyopadhyay & Ray 2020; Kulik & Sidor 2023) "Lystrosaurus AZ" (Kitching 1977; DeFauw 1986)	Early Triassic (Prasad & Pundir 2020) Late Permian-Early Triassic (Gastaldo et al. 2020)
<i>Lystrosaurus declivis</i> (Owen, 1859)	South Africa (Owen 1859, 1860, 1862, 1876; Broom 1903, 1909, 1915, 1932; Watson 1912b; Van Hoepen 1916; Haughton 1924; von Huene 1925, 1931; Brink 1951, 1986; Haughton & Brink 1954; Toerien 1954; Barry 1968; Kitching 1968, 1977; Cluver 1971; Colbert 1974; Keyser & Cruickshank 1979; Cosgriff et al. 1982; DeFauw 1986; King 1988; Thackeray et al. 1998; Angielczyk 2002; Retallack et al. 2003; Neveling 2004; Smith & Botha 2005; Grine et al. 2006; Botha & Smith 2006, 2007, 2020; Jasinoski et al. 2009, 2014; Camp 2010; Modesto 2010; Botha-Brink & Angielczyk 2010; Kammerer et al. 2011; Viglietti et al. 2013; Botha-Brink et al. 2016; Smith & Botha-Brink 2014; Botha-Brink et al. 2014; Rubidge et al. 2016; Benoit et al. 2018; Thackeray 2018, 2019; Gastaldo et al. 2019, 2020; Botha 2020; Modesto 2020; Smith et al. 2020b; Viglietti 2020; Botha et al. 2020; Olroyd 2022; Olroyd & Sidor 2022; Smith et al. 2022; Viglietti et al. 2022; Kulik & Sidor 2023)	<i>Lystrosaurus declivis</i> AZ (Botha 2020; Botha & Smith 2020; Modesto 2020; Smith et al. 2020b; Viglietti 2020; Olroyd 2022; Smith et al. 2022; Viglietti et al. 2022)	Latest Permian-Early Triassic (Gastaldo et al. 2020)
<i>Lystrosaurus cf. declivis</i> (Owen, 1859)	India (Gupta & Das 2011; Bandyopadhyay & Ray 2020; Kulik & Sidor 2023) South Africa (Broom 1915; von Huene 1931)	Panchet (Gupta & Das 2011; Bandyopadhyay & Ray 2020; Kulik & Sidor 2023) "Lystrosaurus AZ" (Broom 1915)	Early Triassic (Prasad & Pundir 2020) Late Permian-Early Triassic (Gastaldo et al. 2020)
<i>Lystrosaurus georgi</i> Kalandadze, 1975	Russia (Kalandadze 1974, 1975; Colbert 1982; Lozovskii 1983; King 1988; Ochev 1992; Ivakhnenko et al. 1997; Battail & Surkov 2000; Surkov et al. 2005; Ivakhnenko 2008)	Vokhman (Ivakhnenko et al. 1997; Battail & Surkov 2000; Surkov et al. 2005; Ivakhnenko 2008)	Induan (Ivakhnenko 2008)

TABLE 1. — Continuation.

Taxon	Country	Formation	Age
<i>Lystrosaurus hedini</i> Young, 1935	China (Yuan & Young 1934b; Young 1935, 1939, 1946; Brink 1951, 1986, 1988; Liu 1973; Sun 1973; Colbert 1974, 1982; Yuhe 1983; Cheng 1986; King 1988; Li 1988; Upper Guodikeng (Liu et al. 2002; Li & Sun 2008; Lucas 2001; Liu et al. 2002; Li & Sun 2008; Camp 2010; Camp & Liu 2011; Li 2015; Modesto 2020; Kulik & Sidor 2023); Mongolia (Gubin & Sinitza 1993; Kulik & Sidor 2023)	Jiucaiyuan (Yuhe 1983; Li 1988; Lucas 2001; Liu et al. 2002; Li & Sun 2008)	Induan (Tong et al. 2018)
<i>Lystrosaurus cf. hedini</i> Young, 1935	China (Young 1939; Marilao et al. 2020)	Jiucaiyuan (Marilao et al. 2020) Not given (Young 1939)	Induan (Tong et al. 2018) ?Induan (Tong et al. 2018)
<i>Lystrosaurus maccaigi</i> (Seeley, 1898)	Antarctica (Cosgriff & Hammer 1979; Cosgriff et al. 1982; Kulik & Sidor 2023) South Africa (Seeley 1898; Broom 1909, 1932, 1903; Van Hoepen 1915; Haughton 1924; von Huene 1925; Brink 1951; Toerien 1953; Haughton & Brink 1954; Kitching 1968, 1977; Cluver 1971; Colbert 1974; Keyser & Cruickshank 1979; Cosgriff et al. 1982; King 1988; Ray 2005; Smith & Botha 2005; Botha & Smith 2006; Grine et al. 2006; Botha & Smith 2007, 2020; Jasinoski et al. 2010, 2014; Botha-Brink & Angielczyk 2010; Jasinoski & Chinsamy-Turan 2012; Smith & Botha-Brink 2014; Botha-Brink et al. 2014, 2016; Rubidge et al. 2016; Viglietti et al. 2016; Gastaldo et al. 2019, 2020; Botha 2020; Modesto 2020; Smith et al. 2020b; Viglietti 2020; Botha et al. 2020; Liu et al. 2022; Olroyd 2022; Olroyd & Sidor 2022; Viglietti et al. 2022; Kulik & Sidor 2023)	Lower Fremouw (Cosgriff & Hammer 1979; Cosgriff et al. 1982; Kulik & Sidor 2023) <i>Daptocephalus AZ</i> , <i>Lystrosaurus maccaigi-Moschorhinus SZ</i> (Smith et al. 2020b; Viglietti 2020; Liu et al. 2022; Viglietti et al. 2022)	Olenekian (Elliot et al. 2017) Late Permian (Gastaldo et al. 2020)
<i>Lystrosaurus declivis</i>	AZ (Botha 2020; Botha & Smith 2020; Modesto 2020; Smith et al. 2020b; Viglietti 2020; Olroyd 2022; Olroyd & Sidor 2022)	Latest Permian-Early Triassic (Gastaldo et al. 2020)	
<i>Lystrosaurus murrayi</i> (Huxley, 1859)	Antarctica (Colbert 1970a, 1971a, 1972, 1973, 1974, 1975; Cosgriff et al. 1978; Retallack & Hammer 1998; Kulik & Sidor 2023) India (Huxley 1865; Lydekker 1877, 1879, 1889; Cotter 1918; Das Gupta 1922; von Huene 1935; Brink 1951, 1988; Robinson 1958; Tripathi & Puri 1961; Sahani & Tripathi 1962; Tripathi & Satsangi 1963; Colbert 1971a, 1973, 1974; Cosgriff et al. 1982; King 1988; Ray 2005, 2006; Ray et al. 2005, 2009a, b; Kammerer et al. 2011; Bandyopadhyay & Ray 2020; Kulik & Sidor 2023)	Lower Fremouw (Colbert 1974; Cosgriff et al. 1978; Retallack & Hammer 1998)	Olenekian (Elliot et al. 2017)
	South Africa (Huxley 1859; Owen 1860b; Cope 1870a; Seeley 1889; Broom 1902, 1909, 1932, 1941; Van Hoepen 1916; Haughton 1917, 1924; von Huene 1925; Arambourg 1943; Brink 1951, 1986; Janensch 1952; Haughton & Brink 1954; Camp 1956, 2010; Cruickshank 1967; Barry 1968; Kitching 1968, 1977; Cluver 1971; Colbert 1971a, 1974; Aulie 1974; Keyser & Cruickshank 1979; Cosgriff et al. 1982; DeFauw 1986; King 1988; Chinsamy & Rubidge 1993; Thackeray et al. 1998; Ray 2005, 2006; Ray et al. 2005, 2009a; Smith & Botha 2005; Grine et al. 2006; Botha & Smith 2006, 2007, 2020; Jasinoski et al. 2010, 2014; Modesto et al. 2010; Botha-Brink & Angielczyk 2010; Kammerer et al. 2011; Jasinoski & Chinsamy-Turan 2012; Botha-Brink et al. 2016; Smith & Botha-Brink 2014; Botha-Brink et al. 2014; Rubidge et al. 2016; Gastaldo et al. 2017, 2019; Thackeray 2018, 2019; Botha 2020; Modesto 2020; Smith et al. 2020b; Botha et al. 2020; Olroyd 2022; Olroyd & Sidor 2022; Smith et al. 2022; Viglietti et al. 2022; Kulik & Sidor 2023)	Panchet (Huxley 1865; Lydekker 1877, 1879, 1889; Cotter 1918; Das Gupta 1922; von Huene 1935; Robinson 1958; Tripathi & Puri 1961; Sahani & Tripathi 1962; Tripathi & Satsangi 1963; Colbert 1971a, 1974; Cosgriff et al. 1982; Brink 1988; King 1988; Ray 2005, 2006; Ray et al. 2005, 2009a, b; Kammerer et al. 2011; Bandyopadhyay & Ray 2020)	Early Triassic (Prasad & Pundir 2020)
		<i>Lystrosaurus declivis</i> AZ (Botha 2020; Botha & Smith 2020; Modesto 2020; Smith et al. 2020b; Olroyd 2022; Olroyd & Sidor 2022; Smith et al. 2022; Viglietti et al. 2022)	Latest Permian-Early Triassic (Gastaldo et al. 2020)
<i>Lystrosaurus cf. mur-rayi</i> (Huxley, 1859)	South Africa (Broom 1900a, 1915)	?“ <i>Lystrosaurus AZ</i> ” (Broom 1915)	Late Permian-Early Triassic (Gastaldo et al. 2020)
<i>Lystrosaurus youngi</i> Sun, 1964	China (Sun 1964, 1973; Liu 1973; Colbert 1974, 1982; Yuhe 1983; Li 1988; Lucas 2001; Li & Sun 2008; Camp 2010; Camp & Liu 2011; Li 2015; Kulik & Sidor 2023)	Jiucaiyuan (Yuhe 1983; Li 1988; Lucas 2001; Liu et al. 2002; Li & Sun 2008)	Induan (Tong et al. 2018)
<i>Lystrosaurus cf. youngi</i> Sun, 1964	China (Liu et al. 2002; Li 2015)	Upper Guodikeng (Liu et al. 2002)	Induan (Tong et al. 2018)
<i>Lystrosaurus sp. (“Dicy-nodon strigops”</i> Broom, 1913b)	South Africa (Broom 1913b, 1915; Haughton 1917, 1924; von Huene 1925; Brink 1951; Haughton & Brink 1954; Cluver 1971; Colbert 1974; Kammerer et al. 2011)	“ <i>Lystrosaurus AZ</i> ” (Haughton 1917; von Huene 1925; Cluver 1971; Colbert 1974; Kammerer et al. 2011)	Late Permian-Early Triassic (Gastaldo et al. 2020)
<i>Lystrosaurus sp.</i> ("Lystrosaurus weiden-reich" Young, 1939)	China (Young 1939, 1946; Brink 1951; Cluver 1971; Colbert 1974, 1982; King 1988; Li 1988; Lucas 2001; Liu et al. 2002; Li & Sun 2008; Camp & Liu 2011)	Jiucaiyuan (Li 1988; Lucas 2001; Li & Sun 2008)	Induan (Tong et al. 2018)
<i>Lystrosaurus sp.</i>	Antarctica (Colbert 1970a, b, 1971b, 1974; Elliot et al. 1970) Australia (Northwood 1997)	Lower Fremouw (Elliot et al. 1970; Colbert 1974) Arcadia (Northwood 1997)	Olenekian (Elliot et al. 2017) Early Triassic (Northwood 1997)

TABLE 1. — Continuation.

Taxon	Country	Formation	Age
	China (Young 1939, 1946; Liu <i>et al.</i> 2002; Maisch & Matzke 2014; Li 2015; Han <i>et al.</i> 2021; Kulik <i>et al.</i> 2021)	Upper Guodikeng (Liu <i>et al.</i> 2002; Li 2015); Jiucayuan (Maisch & Matzke 2014; Han <i>et al.</i> 2021; Kulik <i>et al.</i> 2021); Not given (Young 1939)	Induan (Tong <i>et al.</i> 2018) Induan (Tong <i>et al.</i> 2018)
	India (Bandyopadhyay & Ray 2020)	Kamthi (Bandyopadhyay & Ray 2020)	?Induan (Tong <i>et al.</i> 2018) Early Triassic (Prasad & Pundir 2020)
	South Africa (Broom 1903, 1908a, b; Watson 1913; Brink 1951; Janensch 1952; Haughton 1963; Crompton & Hotton 1967; Cruickshank 1968; Cluver 1971; DeFauw 1986; Groenewald 1991; Cox 1998; MacRae 1999; Damiani & Welman 2001; Damiani <i>et al.</i> 2003; Neveling 2004; Surkov & Benton 2004; Grine <i>et al.</i> 2006; Jasinoski <i>et al.</i> 2010, 2014; Modesto & Botha-Brink 2010; Jasinoski & Chinsamy-Turan 2012; Angielczyk & Rubidge 2013; Botha-Brink <i>et al.</i> 2014; Gastaldo <i>et al.</i> 2017, 2019; Olivier <i>et al.</i> 2017; Krummeck & Bordy 2018; Whitney <i>et al.</i> 2019; Botha <i>et al.</i> 2020; Knaus <i>et al.</i> 2021; Olroyd 2022; Olroyd & Sidor 2022)	" <i>Lystrosaurus</i> AZ" (Cluver 1971; DeFauw 1986; Groenewald 1991; MacRae 1999; Damiani & Welman 2001; Damiani <i>et al.</i> 2003; Neveling 2004; Surkov & Benton 2004; Grine <i>et al.</i> 2006; Modesto & Botha-Brink 2010; Botha-Brink <i>et al.</i> 2014; Olivier <i>et al.</i> 2017; Gastaldo <i>et al.</i> 2017; Krummeck & Bordy 2018; Whitney <i>et al.</i> 2019; Botha <i>et al.</i> 2020; Knaus <i>et al.</i> 2021) <i>Lystrosaurus declivis</i> AZ (Olroyd 2022; Olroyd & Sidor 2022)	Late Permian-Early Triassic (Gastaldo <i>et al.</i> 2020) Latest Permian-Early Triassic (Gastaldo <i>et al.</i> 2020)
? <i>Lystrosaurus</i> sp. ("Dicynodon seeleyi" Broili, 1908)	South Africa (Broili 1908; Kammerer <i>et al.</i> 2011)	"? <i>Lystrosaurus</i> AZ" (Kammerer <i>et al.</i> 2011)	Late Permian-Early Triassic (Gastaldo <i>et al.</i> 2020)
? <i>Lystrosaurus</i> sp.	China (Yin & Peng 2000) Russia (Ochev 1992; Shishkin <i>et al.</i> 2000)	Shaofanggou (Yin & Peng 2000) Vokhman (Ochev 1992; Shishkin <i>et al.</i> 2000)	Olenekian (Tong <i>et al.</i> 2018) Induan (Ivakhnenko 2008)
cf. <i>Lystrosaurus</i> sp.	Mozambique (Araújo <i>et al.</i> 2020)	Fubué (Araújo <i>et al.</i> 2020)	Early Triassic (Araújo <i>et al.</i> 2020)
<i>Moghreberia nmachouensis</i> Dutuit, 1980	Morocco (Dutuit 1980, 1988; Bandyopadhyay 1988; King 1988; Gauffre 1993; Olivier <i>et al.</i> 2017; Kammerer 2018)	Argana t5 (Dutuit 1988, 1989b; Gauffre 1993)	Carnian/?Norian (Kammerer <i>et al.</i> 2012)
<i>Myosaurus gracilis</i> Haughton, 1917	Antarctica (Cosgriff & Hammer 1979; Hammer & Cosgriff 1981; DeFauw 1989) South Africa (Haughton 1917, 1924; von Huene 1925; Broom 1932; Haughton & Brink 1954; Kitching 1968, 1977; Keyser 1974; Cluver 1974; Keyser & Cruickshank 1979; Hammer & Cosgriff 1981; Brink 1986; King 1988; Botha & Smith 2006; Surkov 2006; Botha & Smith 2020; Nicolas & Rubidge 2010; Smith <i>et al.</i> 2012, 2020b; Benoit <i>et al.</i> 2018; Viglietti <i>et al.</i> 2022)	Lower Fremouw (Cosgriff & Hammer 1979; Hammer & Cosgriff 1981; DeFauw 1989) <i>Lystrosaurus declivis</i> AZ (Botha & Smith 2020; Smith <i>et al.</i> 2020b; Viglietti <i>et al.</i> 2022)	Olenekian (Elliot <i>et al.</i> 2017) Latest Permian-Early Triassic (Gastaldo <i>et al.</i> 2020)
<i>Parakannemeyeria chengi</i> Liu, 2004	China (Liu 2004; Li & Sun 2008; Li 2015)	Lower Karamay (Liu 2004; Li 2015)	Anisian (Tong <i>et al.</i> 2018)
<i>Parakannemeyeria dolichocephala</i> Sun, 1960	China (Sun 1960, 1963; Young 1964; Keyser & Cruickshank 1979; Brink 1986; King 1988; Li & Sun 2008; Li 2015)	Upper Ermaying (Sun 1963; Brink 1986; King 1988; Li & Sun 2008; Li 2015)	Late Anisian (Liu <i>et al.</i> 2017)
<i>Parakannemeyeria ningwuensis</i> Sun, 1963	China (Sun 1963; Young 1964; Keyser & Cruickshank 1979; Cheng 1980; Brink 1988; King 1988; Li & Sun 2008; Li 2015; Liu 2022)	Ermaying (Sun 1963; Cheng 1980; Brink 1988; King 1988; Li & Sun 2008; Li 2015; Liu 2022)	Anisian (Liu <i>et al.</i> 2017)
<i>Parakannemeyeria shemuensis</i> Cheng, 1980	China (Cheng 1980; King 1988; Li & Sun 2008; Li 2015)	Upper Ermaying (Cheng 1980; King 1988; Li & Sun 2008)	Late Anisian (Liu <i>et al.</i> 2017)
<i>Parakannemeyeria youngi</i> Sun, 1963	China (Sun 1963; Young 1963, 1964; Keyser & Cruickshank 1979; Yuhe 1983; Brink 1988; King 1988; Li & Sun 2008; Li 2015)	Upper Ermaying (Sun 1963; Brink 1988; King 1988; Li & Sun 2008; Li 2015)	Late Anisian (Liu <i>et al.</i> 2017)
<i>Parakannemeyeria cf. youngi</i> Sun, 1963	China (Sun 1963; Young 1964)	Upper Ermaying (Sun 1963)	Late Anisian (Liu <i>et al.</i> 2017)
<i>Parakannemeyeria</i> sp.	China (Sun 1963; Young 1964; Cheng 1980; Liu 2015; Liu 2022)	Upper Ermaying (Sun 1963; Cheng 1980) Lower Ermaying (Liu 2022) Tongchuan I (Liu 2015)	Late Anisian (Liu <i>et al.</i> 2017) Early Anisian (Liu <i>et al.</i> 2017) Late Anisian (Tong <i>et al.</i> 2018)
<i>Pentasaurus goggai</i> Kammerer, 2018	South Africa (Kammerer 2018; Viglietti <i>et al.</i> 2020b)	Lower Elliott <i>Scalenodontoides</i> AZ (Viglietti <i>et al.</i> 2020b)	Norian-Rhaetian (Bordy <i>et al.</i> 2020)
<i>Placerias hesternus</i> Lucas, 1904	United States (Lucas 1904; Cross & Howe 1905; Cross 1908; Darton 1910; von Huene 1911, 1926a, 1935, 1936; Broom 1914; Case 1915; Gregory 1917; Pearson 1924a; Camp 1956; Camp & Welles 1956; Cox 1965; Baird & Patterson 1968; Keyser 1974; Keyser & Cruickshank 1979; Rowe 1979; Walter 1985; Brink 1986, 1988; King 1988; Olsen <i>et al.</i> 1989; Huber <i>et al.</i> 1993; Long & Murry 1995; Lucas 1998; Olsen & Huber 1998; Fiorillo <i>et al.</i> 2000; Heckert & Lucas 2003; Green <i>et al.</i> 2010; Parker & Martz 2011; Kammerer <i>et al.</i> 2013; Kammerer 2018; Olroyd 2022; Olroyd & Sidor 2022)	Bluewater Creek (Lucas 1998; Lucas & Heckert 2002; Heckert & Lucas 2003) Cooper Canyon (Lehman & Chatterjee 2005) Pekin (Baird & Patterson 1968; Olsen <i>et al.</i> 1989; Huber <i>et al.</i> 1993; Lucas & Hunt 1993a; Lucas 1998; Olsen & Huber 1998) Petrified Forest (Murry & Long 1989; Long & Murry 1995; Lucas 1998; Fiorillo <i>et al.</i> 2000; Lucas & Heckert 2002; Green <i>et al.</i> 2010)	Norian (Ramezani <i>et al.</i> 2014) Norian (Martz <i>et al.</i> 2013) Carnian (Heckert <i>et al.</i> 2017) Norian (Ramezani <i>et al.</i> 2014)

TABLE 1. — Continuation.

Taxon	Country	Formation	Age
<i>Placerias</i> sp.	United States (Murry & Long 1989; Heckert 1997; Heckert & Lucas 2003)	Bluewater Creek (Heckert 1997; Heckert & Lucas 2003)	Norian (Ramezani et al. 2014)
		Petrified Forest (Murry & Long 1989)	Norian (Ramezani et al. 2014)
? <i>Placerias</i> sp.	United States (Long & Murry 1995; Parker & Martz 2011)	Petrified Forest (Long & Murry 1995; Parker & Martz 2011)	Norian (Ramezani et al. 2014)
<i>Rabidosaurus cristatus</i> Kalanadze, 1970	Russia (Kalandadze 1970; Keyser & Cruickshank 1979; King 1988; Shishkin et al. 1995; Ivakhnenko et al. 1997; Battail & Surkov 2000; Ivakhnenko 2008)	Lower Donguz (Surkov 2003)	Anisian (Ivakhnenko 2008)
<i>Rechnisaurus cristorrhynchus</i> Chowdhury, 1970	India (Jain et al. 1964; Chowdhury 1970; Keyser & Cruickshank 1979; Brink 1986; King 1988; Bandyopadhyay 1989; Bandyopadhyay & Ray 2020)	Yerrapalli (Jain et al. 1964; Chowdhury 1970; Keyser & Cruickshank 1979; Brink 1986; King 1988; Bandyopadhyay 1989; Bandyopadhyay & Ray 2020)	Anisian or younger (Ottone et al. 2014)
	Tanzania (Cox 1991; Renault 2000; Surkov & Benton 2004; Kammerer et al. 2017)	Manda (Cox 1991; Surkov & Benton 2004; Kammerer et al. 2017)	Anisian or younger (Wynd et al. 2018)
<i>Repelinosaurus robustus</i> Olivier, Battail, Bourquin, Rossignol, Steyer & Jalil, 2019	Laos (Olivier et al. 2019)	Purple Claystone (Olivier et al. 2019)	?Late Permian (Liu 2020)/Early Triassic (Olivier et al. 2019)
<i>Rhadiodromus klimovi</i> (Efremov, 1938)	Russia (Efremov 1938, 1940, 1951; Vjuschkov 1969; Kalandadze 1970; King 1988; Shishkin et al. 1995; Ivakhnenko et al. 1997; Battail & Surkov 2000; Ivakhnenko 2008)	Lower Donguz (Surkov 2003)	Anisian (Ivakhnenko 2008)
<i>Rhadiodromus mariae</i> Surkov, 2003	Russia (Surkov 2003; Surkov & Benton 2004; Ivakhnenko 2008)	Upper Donguz (Surkov 2003)	Anisian (Ivakhnenko 2008)
<i>Rhinodicynodon gracile</i> Kalandadze, 1970	Russia (Kalandadze 1970; Keyser & Cruickshank 1979; King 1988; Shishkin et al. 1995; Ivakhnenko et al. 1997; Surkov 1998a, b; Battail & Surkov 2000; Ivakhnenko 2008; Hancox et al. 2013)	Upper Donguz (Surkov 2003)	Anisian (Ivakhnenko 2008)
<i>Sangusaurus edentatus</i> Cox, 1969	Zambia (Cox 1969; King 1988; Angielczyk et al. 2014, 2017; Peecook et al. 2018)	Ntawere (Cox 1969; King 1988; Angielczyk et al. 2014, 2017; Peecook et al. 2018)	Anisian or younger (Wynd et al. 2018)
<i>Sangusaurus parringtonii</i> Cruickshank, 1986a	Tanzania (Cruickshank 1986a, b; Surkov & Benton 2004; Angielczyk et al. 2017; Kammerer et al. 2017)	Manda (Cruickshank 1986a, b; Surkov & Benton 2004; Angielczyk et al. 2017; Kammerer et al. 2017)	Anisian or younger (Wynd et al. 2018)
<i>Sangusaurus</i> sp. ("Ischigualastia sp." / "Stahleckeria potens")	Brazil (Schwanke-Peruzzo 1990; Schwanke-Peruzzo & Araújo-Barbarena 1995; Lucas 2002; Langer et al. 2007; Dassie 2014; Kammerer & Ordoñez 2021)	Santa Maria (Schwanke-Peruzzo 1990; Schwanke-Peruzzo & Araújo-Barbarena 1995; Lucas 2002; Langer et al. 2007; Dassie 2014; Kammerer & Ordoñez 2021)	Ladinian-Carnian (Philipp et al. 2018)/Carnian (Ordoñez et al. 2020)
<i>Shaanbeikannemeyeria xilouguensis</i> Cheng, 1980	China (Cheng 1980; Li 1980; King 1988; Li & Sun 2008; Li 2015; Liu 2022; Escobar et al. 2023)	Lower Ermaying (Cheng 1980; Li 1980; King 1988; Li & Sun 2008; Li 2015; Liu 2022)	Early Anisian (Liu et al. 2017)
<i>Shansiodon wangi</i> Yeh, 1959	China (Yeh 1959; Sun 1963; Young 1964; Keyser & Cruickshank 1979; Cheng 1980; Brink 1988; King 1988; Li & Sun 2008; Kammerer et al. 2013; Li 2015)	Upper Ermaying (Yeh 1959; Brink 1988; King 1988; Li & Sun 2008; Hancox et al. 2013; Li 2015)	Early Anisian (Liu et al. 2017)
<i>Shansiodon wuhsiensis</i> Yeh, 1959	China (Yeh 1959; Keyser & Cruickshank 1979; Brink 1988; King 1988; Li & Sun 2008; Hancox et al. 2013; Li 2015)	Upper Ermaying (Yeh 1959; Brink 1988; King 1988; Li & Sun 2008; Hancox et al. 2013; Li 2015)	Early Anisian (Liu et al. 2017)
<i>Shansiodon</i> sp.	China (Yeh 1959; Sun 1963; Young 1964; Cheng 1980; King 1988)	Upper Ermaying (Yeh 1959; Sun 1963; Cheng 1980; King 1988)	Late Anisian (Liu et al. 2017)
	South Africa (Hancox 1998; Nicolas & Rubidge 2010; Smith et al. 2012, 2020b; Hancox et al. 2013, 2020; Viglietti et al. 2022; Escobar et al. 2023)	Cynognathus AZ Cricodon-Ufudocyclops SZ	Late Anisian-Carnian (Hancox et al. 2020; Smith et al. 2020b; Viglietti et al. 2022)
? <i>Shansiodon</i> sp.	China (Sun 1963; Young 1964)	Upper Ermaying (Sun 1963)	Late Anisian (Liu et al. 2017)
<i>Sinokannemeyeria baidaoysi</i> Liu, 2015	China (Liu 2015)	Tongchuan I (Liu 2015)	Late Anisian (Tong et al. 2018)
<i>Sinokannemeyeria pearsoni</i> Young, 1937	China (Young 1937, 1946, 1964; Sun 1963; Keyser & Cruickshank 1979; Brink 1988; King 1988; Li & Sun 2008; Li 2015)	Upper Ermaying (Sun 1963; Brink 1988; King 1988; Li & Sun 2008; Li 2015)	Late Anisian (Liu et al. 2017)
cf. <i>Sinokannemeyeria pearsoni</i> Young, 1937	China (Sun 1963; Young 1964)	Upper Ermaying (Sun 1963)	Late Anisian (Liu et al. 2017)
<i>Sinokannemeyeria sanhuaneensis</i> Cheng, 1980	China (Cheng 1980; King 1988; Li & Sun 2008; Li 2015)	Upper Ermaying (Cheng 1980; King 1988; Li & Sun 2008; Li 2015)	Late Anisian (Liu et al. 2017)
<i>Sinokannemeyeria yingchiaoensis</i> Sun, 1963	China (Sun 1963; Keyser & Cruickshank 1979; Brink 1988; King 1988; Li & Sun 2008; Li 2015)	Upper Ermaying (Sun 1963; Brink 1988; King 1988; Li & Sun 2008; Li 2015)	Late Anisian (Liu et al. 2017)

TABLE 1. — Continuation.

Taxon	Country	Formation	Age
<i>Sinokannemeyeria</i> sp.	China (Sun 1963; Cheng 1980; King 1988)	Upper Ermaying (Sun 1963; Cheng 1980; King 1988)	Late Anisian (Liu et al. 2017)
<i>Stahleckeria potens</i> von Huene, 1935	Brazil (von Huene 1935, 1936, 1949; Romer & Price 1944; Camp 1956; Bonaparte 1970, 1978; Keyser & Cruickshank 1979; King 1988; Brink 1988; Walter 1989; Lucas 1993a, 2002; Maisch 2001, 2021; Surkov & Benton 2004; Vega-Dias & Schwanke 2004a; Vega-Dias et al. 2005; Langer et al. 2007; Abdala et al. 2013; Vega & Maisch 2014; Dassie 2014; Kammerer et al. 2017; Kammerer 2018; Mancuso & Irmis 2019; Ordoñez et al. 2019; Schultz et al. 2020; Kammerer & Ordoñez 2021) Namibia (Abdala et al. 2013; Mancuso & Irmis 2019; Kammerer & Ordoñez 2021; Maisch 2021; Olroyd 2022; Olroyd & Sidor 2022; Preuschoft et al. 2022)	Santa Maria <i>Dinodontosaurus</i> AZ (Lucas 2002; Langer et al. 2007; Abdala et al. 2013; Dassie 2014; Martinelli et al. 2017; Mancuso & Irmis 2019; Schultz et al. 2020; Maisch 2021)	Ladinian-Carnian (Philipp et al. 2018/Carnian (Ordoñez et al. 2020)
<i>Stahleckeria</i> sp.	Argentina (Mancuso & Irmis 2019; Escobar et al. 2021; Kammerer & Ordoñez 2021)	Chañares <i>Massetognathus-Chanaresuchus</i> AZ (Mancuso & Irmis 2019; Escobar et al. 2021)	Early Carnian (Ezcurra et al. 2017)
Stahleckeriidae indet. (" <i>Angonisaurus</i> sp.")	Antarctica (Sidor et al. 2014; Kammerer et al. 2019)	Upper Fremouw (Sidor et al. 2014; Kammerer et al. 2019)	Late Anisian-Ladinian (Elliot et al. 2017)
Stahleckeriidae indet.	Brazil (Maisch 2021)	Santa Maria <i>Dinodontosaurus</i> AZ (Maisch 2021)	Ladinian-Carnian (Philipp et al. 2018/Carnian (Ordoñez et al. 2020)
	India (Bandyopadhyay 1988; Bandyopadhyay & Sengupta 1999; Bandyopadhyay & Ray 2020)	Denwa (Bandyopadhyay 1988; Bandyopadhyay & Sengupta 1999; Bandyopadhyay & Ray 2020)	Anisian or younger (Peecook et al. 2018)
	South Africa (Watson 1917; Hancox & Rubidge 1994; Govender 2005) Tanzania (Kammerer et al. 2017)	<i>Cynognathus</i> AZ <i>Trirachodon-Kannemeyeria</i> SZ (Govender 2005; Hancox et al. 2020) Manda (Kammerer et al. 2017)	Early Anisian (Hancox et al. 2020) Anisian or younger (Wynd et al. 2018)
Stahleckeriinae indet.	Argentina (Cox 1968; Bonaparte 1997; Escobar et al. 2021) United States (Lucas & Hunt 1993a; Long & Murry 1995; Green et al. 2005; Green 2012; Kammerer et al. 2013)	Chañares <i>Tarjadia</i> AZ (Escobar et al. 2021) Pekin (Green et al. 2005; Green 2012; Kammerer et al. 2013) Santa Rosa (Lucas & Hunt 1993a; Long & Murry 1995; Kammerer et al. 2013)	Ladinian/Carnian (Ezcurra et al. 2017) Carnian (Heckert et al. 2017) Carnian (Hartman et al. 2015)
<i>Sungeodon kimkraemeriae</i> Maisch & Matzke, 2014	China (Maisch & Matzke 2014)	Jiucaiyuan (Maisch & Matzke 2014)	Induan (Tong et al. 2018)
<i>Tetragonias njalilus</i> (von Huene, 1942)	Tanzania (von Huene 1942; Haughton & Brink 1954; Cruickshank 1964, 1967; Bonaparte 1966a; Keyser & Cruickshank 1979; King 1988; Surkov & Benton 2004; Fröbisch 2006; Kammerer et al. 2011, 2017; Hancox et al. 2013; Preuschoft et al. 2022)	Manda (von Huene 1942; Haughton & Brink 1954; Bonaparte 1966b; Cruickshank 1967; Keyser & Cruickshank 1979; King 1988; Surkov & Benton 2004; Fröbisch 2006; Kammerer et al. 2011, 2017; Hancox et al. 2013; Preuschoft et al. 2022)	Anisian or younger (Wynd et al. 2018)
<i>Tetragonias</i> sp.	Argentina (Bonaparte 1981; Domnanovich & Marsicano 2012; Kammerer & Ordoñez 2021)	Quebrada de los Fósiles (Bonaparte 1981; Domnanovich & Marsicano 2012; Kammerer & Ordoñez 2021)	?Ladinian-Carnian (Ottone et al. 2014)
<i>Ufudocyclops mukanelai</i> Kammerer, Viglietti, Hancox, Butler & Choiniere, 2019	South Africa (Hancox & Rubidge 1996; Hancox 1998; Nicolas & Rubidge 2010; Smith et al. 2012, 2020b; Hancox et al. 2013, 2020; Kammerer et al. 2019; Viglietti et al. 2022)	<i>Cynognathus</i> AZ <i>Cricodon-Ufudocyclops</i> SZ (Hancox et al. 2020; Smith et al. 2020b; Viglietti et al. 2022)	Late Anisian-Carnian (Hancox et al. 2020)
<i>Uralokannemeyeria vjuschkovi</i> Danilov, 1971	Russia (Danilov 1971, 1973; Keyser & Cruickshank 1979; King 1988; Shishkin et al. 1995; Ivakhnenko et al. 1997; Battail & Surkov 2000; Surkov & Benton 2004; Ivakhnenko 2008)	Lower Donguz (Surkov 2003)	Anisian (Ivakhnenko 2008)
<i>Vinceria andina</i> Bonaparte, 1969	Argentina (Bonaparte 1969, 1970, 1978; Keyser 1974; Keyser & Cruickshank 1979; King 1988; Domnanovich & Marsicano 2006a, 2012; Hancox et al. 2013; Ordoñez et al. 2019; Kammerer & Ordoñez 2021)	Cerro de las Cabras (Bonaparte 1969; King 1988; Domnanovich & Marsicano 2006a, 2012; Kammerer & Ordoñez 2021)	Late Anisian-early Ladinian (Cariglino et al. 2016)
<i>Wadiasaurus indicus</i> Chowdhury, 1970	India (Jain et al. 1964; Chowdhury 1970; Keyser & Cruickshank 1979; Bandyopadhyay 1988; King 1988; Ray 2006; Ray et al. 2009a, b, 2010; Bandyopadhyay & Ray 2020)	Yerrapalli (Jain et al. 1964; Chowdhury 1970; Keyser & Cruickshank 1979; Bandyopadhyay 1988; King 1988; Ray 2006; Ray et al. 2009a, b, 2010; Bandyopadhyay & Ray 2020)	Anisian or younger (Ottone et al. 2014)
<i>Woznikella triradiata</i> n. gen., n. sp.	Germany (Schoch 2012) Poland (Sulej et al. 2011; Racki & Lucas 2020)	Stuttgart (Schoch 2012) Grabowa (Szulc et al. 2015b; Racki & Lucas 2020)	Carnian (Schoch 2012) Carnian (Sulej et al. 2011)/Norian (Szulc et al. 2015b)
<i>Xiyukannemeyeria brevi-rostris</i> (Sun, 1978)	China (Sun 1978; King 1988; Liu & Li 2003; Li & Sun 2008)	Lower Karamay (Liu & Li 2003)	Anisian (Tong et al. 2018)

TABLE 1. — Continuation.

Taxon	Country	Formation	Age
<i>Zambiasaurus submersus</i> Cox, 1969	Zambia (Attridge <i>et al.</i> 1964; Cox 1969; King 1988; Angielczyk <i>et al.</i> 2014; Kammerer 2018; Peecook <i>et al.</i> 2018; Li 2015)	Ntawere (Attridge <i>et al.</i> 1964; Cox 1969; Keyser & Cruickshank 1979; King 1988; Angielczyk <i>et al.</i> 2014; Kammerer 2018; Peecook <i>et al.</i> 2018; Li 2015)	Anisian or younger (Wynd <i>et al.</i> 2018)

Dentary

The dentaries (ZPAL V. 34/1/3; Fig. 4) are fused together at the symphysis. Each dentary is a massive yet narrow bone with a dorsally projected and dorsolaterally pointed anterodorsal tip, triangular in cross-section. Between the tips there is a narrow notch (Fig. 4D), like in *Angonisaurus cruickshanki* and *Kannemeyeria simocephalus* (see Pearson 1924a; Cox & Li 1983; Renaut 2000; Hancox *et al.* 2013).

In lateral view the dentary is gently hooked (Fig. 4D), similarly to that of *Angonisaurus cruickshanki*, *Dolichurinus primaevus*, *Kannemeyeria simocephalus*, *Kannemeyeria lophorhinus*, “*Kannemeyeria*” *lattrostris*, *Kombuisia frerensis*, *Kombuisia antarctica*, *Lystrosaurus* spp., *Myosaurus gracilis*, *Parakannemeyeria dolichocephala*, *Rhinodicynodon gracile*, *Sangusaurus parringtonii*, *Tetragonias njalilus*, *Wadiasaurus indicus*, and *Xiyukannemeyeria brevirostris* (see Broom 1923, 1937; Pearson 1924a; von Huene 1942; Sun 1960; Cruickshank 1967, 1986a; Crozier 1970; Kalandadze 1970; Cluver 1971, 1974; Keyser 1973; Hotton 1974; Hammer & Cosgriff 1981; Cox & Li 1983; Bandyopadhyay 1988; Renaut 2000; Liu & Li 2003; Damiani *et al.* 2007; Fröbisch 2007; Fröbisch *et al.* 2010; Hancox *et al.* 2013; Angielczyk *et al.* 2014, 2017; Kammerer 2018) and unlike the non-hookeeed or minimally hooked mandibles of, e.g., *Dinodontosaurus* pp., *Ischigualastia jensi*, *Parakannemeyeria ningwuensis*, *Sinokannemeyeria yingchiaensis*, *Stahleckeria potens*, and *Vinceria andina* (see von Huene 1935; Romer & Price 1944; Camp 1956; Sun 1963; Cox 1965, 1968; Lucas 2002; Domnanovich & Marsicano 2012; Abdala *et al.* 2013; Kammerer 2018; Kammerer & Ordoñez 2021; Escobar *et al.* 2023). Unlike in *Dinodontosaurus brevirostris*, the labial (tomial) edge is continuous with the posterior part of the bone and directed either dorsally or (in the anteriormost part) posterodorsally, but never predominantly anterodorsally (Cox 1968; Kammerer & Ordoñez 2021; Escobar *et al.* 2023). The anterior portion of the lateral dentary surface exhibits a coarsely rugose texture indicating the presence of a rhamphotheca-covered beak. The rugosities extend ventrally, towards the mentum, and posteriorly. The posteroventral limit of the rugose area is concave. From the rostral corner of that concavity, rostroradially, crossing the rugose surface towards the dorsal edge of the dentaries, paired, anastomosing vascular grooves are visible. Just anterior to them, shallow, gently expressed lateral grooves similar to those of *Dolichurinus primaevus*, *Kannemeyeria simocephalus*, *Kannemeyeria lophorhinus*, *Parakannemeyeria ningwuensis*, *Sangusaurus parringtonii*, and *Sinokannemeyeria yingchiaensis* span from the lateral surface of each of the tips of the beak posteroventrally towards the ventral edge of the bone (Camp

1956; Sun 1963; Cruickshank 1986a; Renaut 2000; Damiani *et al.* 2007; Angielczyk *et al.* 2017). Like in *Kannemeyeria simocephalus*, *Kannemeyeria lophorhinus*, and *Sangusaurus parringtonii*, the grooves do not follow the ventral curvature of the dentary, but are straight (Camp 1956; Renaut 2000; Angielczyk *et al.* 2017). Paired, more defined grooves coupled with paired ridges are also present laterally on the dentaries of at least the South African *Lystrosaurus* spp. (Cluver 1971). The lateral dentary shelf (Cluver 1971) is not developed, but the lateral surfaces of the posterior part of the dentary above the mandibular fenestra show a laterally symmetrical, rounded, indistinct broadening at the level of the split of the dorsal (tomial), medial (lingual), and lateral (labial) laminae of the dentary ramus, at the roof of the Meckelian canal. This differs significantly from the exceptionally pronounced dentary shelf of *Pentasaurus goggai* Kammerer, 2018 (see Kammerer 2018).

The symphysis in dorsal view is relatively long and narrow but the mandible broadens ventrally (Fig. 4A), similar to the mandibles of, e.g., *Kannemeyeria simocephalus*, *Sinokannemeyeria yingchiaensis*, and *Tetragonias njalilus* (see Pearson 1924a; Sun 1963; Cruickshank 1967). It bears a single wide, deep groove in the junction between the left and right rami, as is typical for dicynodonts. The dorsal surface of each ramus shows two parallel longitudinal ridges separated by a marked groove (posterior dentary sulcus posteriorly and dentary table anteriorly; see discussion in Angielczyk & Rubidge 2013) along its length, with the lingual one higher than the labial around the midlength, and diminishing gradually posteriorly and sharply anteriorly. The anterior end of each lingual ridge is associated with a rounded, mediolaterally compressed peg. Anterior to that peg each lingual ridge continues rostrally, but becomes less prominent and gently diverges laterally, making the median trough slightly wider frontally and eventually ending in the lateral point of the beak. This morphology is different than in *Dinodontosaurus tener* as figured by von Huene (1935) and later by Lucas & Harris (1996), in which the symphyseal part is shorter, the lingual ridges nearly meet anteriorly, and the terminal part of the mandible appears wider and more rounded, but (aside from rostral broadening of the median groove) it is generally similar to that of *Kannemeyeria simocephalus* and *Tetragonias njalilus* (see Pearson 1924a; Cruickshank 1967; Renaut 2000). The lingual ridge in the latter, however, is concave dorsally, lower than the labial, and the anterior pegs appear slightly larger, so they are visible laterally (Cruickshank 1967). Anteroposteriorly short lingual ridges taller than the labial ridges are also present in *Angonisaurus cruickshanki* (“rugosities” of Cox & Li 1983; Hancox *et al.* 2013). In *Stahleckeria potens* the lingual ridge is also taller

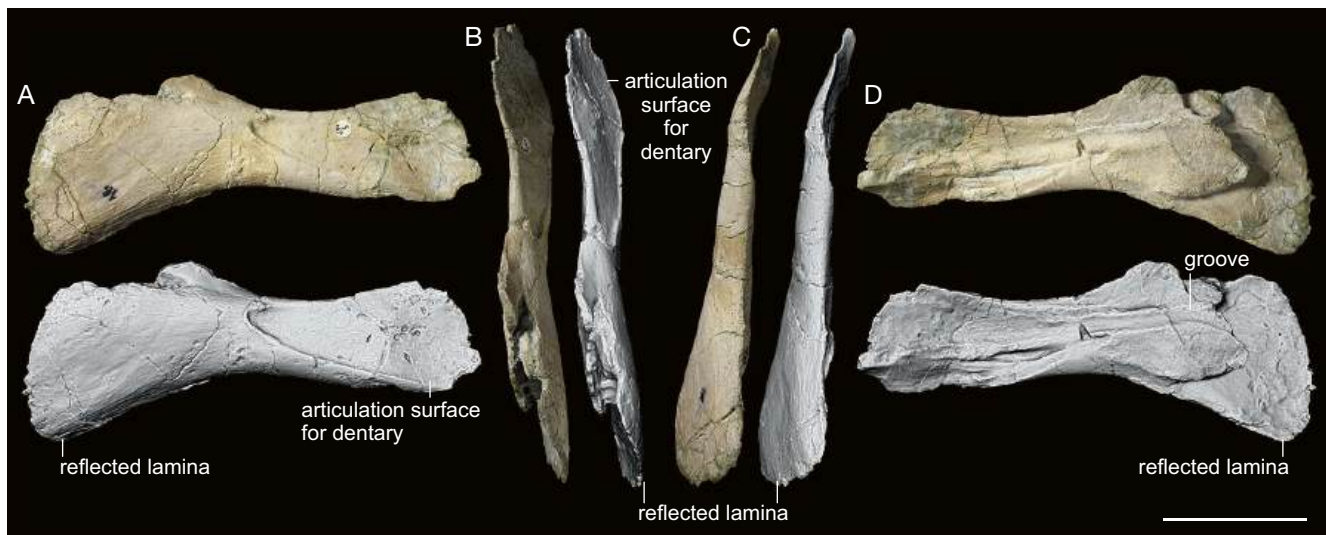


FIG. 5. — *Woznikella triradiata* n. gen., n. sp., ZPAL V. 34/1/5: A–D, right angular in lateral (A), dorsal (B), ventral (C), and medial (D) view. Scale bar: 5 cm.

than the labial (von Huene 1935; Camp 1956; Abdala *et al.* 2013; Kammerer 2018). The morphology of *Woznikella triradiata* n. gen., n. sp. is also different than in *Placerias hesternus* (Camp & Welles 1956; Kammerer 2018; pers. obs.) in which the labial ridge is consistently taller than the lingual and straight. In the latter species the rostral ends of the lingual ridges are visible in lateral view (Camp & Welles 1956), but in *Woznikella triradiata* n. gen., n. sp. they are obscured by the very high dorsal labial edges of the rami. The anatomy of the scoop-shaped dorsal surfaces of the symphyseal areas of *Kombuisia frerensis* and *Myosaurus gracilis* is much simpler and the median groove in these species is wider (Cluver 1974; Hotton 1974; Hammer & Cosgriff 1981; Fröbisch 2007).

In dorsoventral aspect, the dentaries have roughly parallel lateral edges in their anterior part and strongly diverge posteriorly. They are much more slender than the dentaries of *Dolichuranus primaevus*, *Kombuisia* spp., *Lystrosaurus* spp., *Myosaurus gracilis*, *Pentasaurus goggai*, *Shaanbeikannemeyeria xilouguensis*, *Shansiodon wangi*, *Shansiodon wuhsiangensis*, *Sinokannemeyeria baidaoyuensis*, *Vinceria andina*, and *Xiyukannemeyeria brevirostris* (see Young 1935; Yeh 1959; Cluver 1971, 1974; Keyser 1973; Hotton 1974; Li 1980; Hammer & Cosgriff 1981; Liu & Li 2003; Damiani *et al.* 2007; Fröbisch 2007; Fröbisch *et al.* 2010; Domnanovich & Marsicano 2012; Liu 2015; Kammerer 2018).

The ventral part is complete only in the right ramus and the mentum is strongly bowed, more so than in, e.g., *Dinodontosaurus brevirostris* or *Shaanbeikannemeyeria xilouguensis* (Cox 1968; Kammerer & Ordoñez 2021; Liu 2022; Escobar *et al.* 2023). It is, however, strikingly different from the top-heavy, rostrally vertical dentaries of *Sungeodon kimkraemerae* and *Vinceria andina*, in which the rostral and the posteroventral surfaces are set at an acute angle (Domnanovich & Marsicano 2012; Maisch & Matzke 2014). The lateral bone lamella of the dentary in *Woznikella triradiata* n. gen., n. sp. becomes thinner ventrally, forming a large surface for a suture with

the splenial (not preserved) and angular. On the anteroventral (mental) surface of the dentaries two sharply defined, parallel, longitudinal grooves are separated by a wide ridge with a narrow but distinct third groove running medially along the symphysis (Fig. 4B, D). A ridge-like sagittal structure is also present in *Kannemeyeria simocephalus*, *Parakannemeyeria ningwuensis*, *Pentasaurus goggai*, *Placerias hesternus*, *Sinokannemeyeria sanchuaneensis*, *Sungeodon kimkraemerae*, *Tetragonias njalilus*, and *Wadiasaurus indicus* (Camp & Welles 1956; Sun 1963; Cruickshank 1967; Cheng 1980; Bandyopadhyay 1988; Renault 2000; Maisch & Matzke 2014; Kammerer 2018). In *Tetragonias njalilus*, however, it projects its own tip from the anterior edge of the beak (Cruickshank 1967). The tips of the beak bear narrow, longitudinal grooves close to their lateral edges.

The Meckelian canal exposed on the ventral surface of the dorsal part of the disarticulated dentary takes the form of a longitudinal groove which is widest anteriorly and narrows posteriorly (Fig. 4B). This groove ends in a point in contrast to *Placerias hesternus*, in which it forms a vertical edge (Camp & Welles 1956 and pers. obs.). In most dicynodonts at least part of this groove accommodates an anterior process of the surangular.

The posteriormost part of the dentary is formed by a thin blade, which contacted the surangular. Its ventral edge contributed to the mandibular fenestra. Below that, a plate-like process for the angular was present, but only its base is preserved on the right side of ZPAL V. 34/1/3. Given the imprint on the left angular (ZPAL V. 34/1/81), this process was relatively large, about one fourth to one third the length of the dentary, very different than, e.g., the unusually small process of *Dolichuranus primaevus* (see Damiani *et al.* 2007). Unlike *Myosaurus gracilis* and *Tetragonias njalilus*, the dentary was apparently level with the more posterior parts of the mandible, not set at an angle (von Huene 1942; Cruickshank 1967; Cluver 1974).

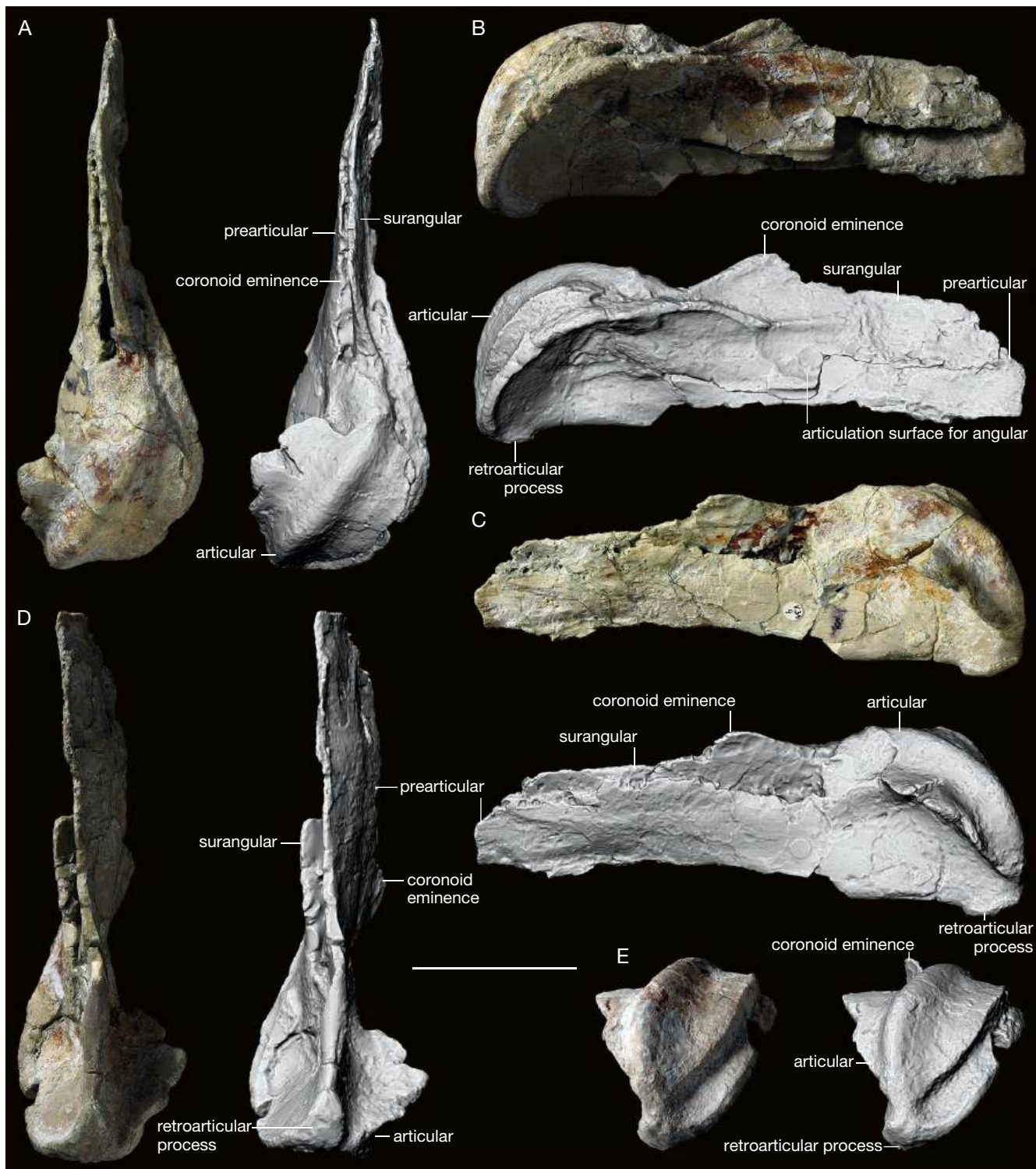


FIG. 6. — *Woznikella triradiata* n. gen., n. sp., ZPAL V. 34/1/4: A-E, right posterior mandibular bone complex in dorsal (A), lateral (B), medial (C), ventral (D), and posterior (E) view. Scale bar: 5 cm.

ZPAL V. 34/1/3 is notably similar to SMNS 91416, the partial mandible from the Stuttgart Formation in Bavaria (Germany) described by Schoch (2012). The similarities include: general shape in lateral view (hooked, with bowed mental surface); presence of a median notch; presence and shape of anterodorsal tips; rugosity of the surface; shape of

the ramphotheca, with distinctly concave posteroventral edge; position and shape of a lateral groove; position and shape of lateral vascular grooves; presence of a symphyseal ridge on the rostroventral (mental) surface of the mandible flanked by lateral grooves and with a sagittal groove (less distinct than in ZPAL V. 34/1/3, possibly due to difference

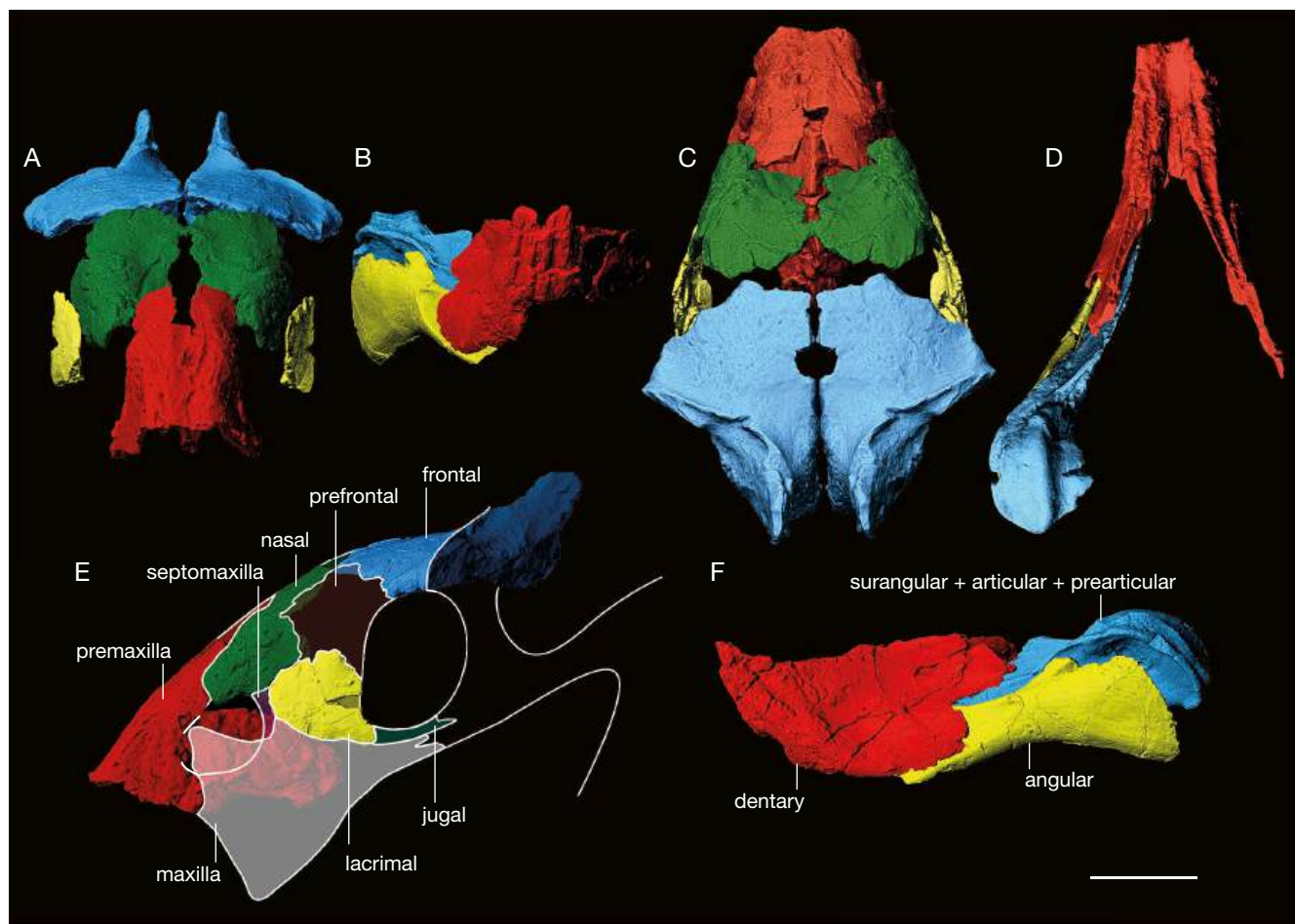


FIG. 7. — *Woznikella triradiata* n. gen., n. sp., ZPAL V. 34/1: A-F, reconstruction of the skull (A, C, E) and mandible (B, D, F) in anterior (A, B), dorsal (C, D), and lateral left (E, F) view. Scale bar: 5 cm.

in ontogenetic age); presence of what appears to be a lingual ridge higher than the labial edge. Based on the published photographs, SMNS 91416 appears to be wider than ZPAL V. 34/1/3, but this, at least to some extent, is caused by the foreshortening due to the perspective and slightly different scale of the panels captioned as the dorsal and ventral view. Because of the morphological similarity, geographical and temporal proximity, and absence of other dicynodonts in the European Carnian, we therefore tentatively refer SMNS 91416 to *Woznikella triradiata* n. gen., n. sp.

Angular

Only the posterior portion of the left angular (ZPAL V. 34/1/81) is preserved, and its posterodorsal edge is incomplete. The right angular (ZPAL V. 34/1/5; Fig. 5) is almost complete. The ventral and dorsal edges are deeply concave in lateromedial aspect. The reflected lamina is very well preserved in ZPAL V. 34/1/5, even though it is a thin plate. Its medial surface is slightly concave, whereas the lateral surface is convex. Medial to the reflected lamina is the main body of the angular, and between the two there is a deep notch, the anterior limit of which is exposed in lateral view. In lateromedial aspect, the main body protrudes dorsally above

the reflected lamina (Fig. 4A, D). Unfortunately, the dorsal edge of the angular is broken in both specimens so its exact height remains unknown – the probable outline of the articular surface on the labial side of the surangular suggests that approximately 5 mm are missing. On the medial surface of the main body a long, shallow groove is visible (Fig. 4D). Its edges are pronounced and mostly parallel in its posterior part, and anteriorly it becomes very wide. It is gently sinuous, with its anterior end turned gently dorsally, the middle part approximately parallel to the long axis of the bone, and the posterior end downturned. In the posterior and middle part, it is situated closer to the dorsal than to the ventral edge of the bone, whereas anteriorly its ventral edge comes closer to the ventral edge of the bone while the dorsal edge diminishes, leaving the groove open dorsally. An additional short ridge is present above the middle part of the groove, close to the half of the angular. These structures probably form the area of connection with the surangular.

A large, clearly demarcated, depressed and mostly flat area for the suture with the dentary is visible on the lateral surface in the anterior part of the angular (Fig. 4A, B). Its posterior end is located around the mid-length of the angular, its dorsal edge quickly merges with the dorsal edge of the angular, and

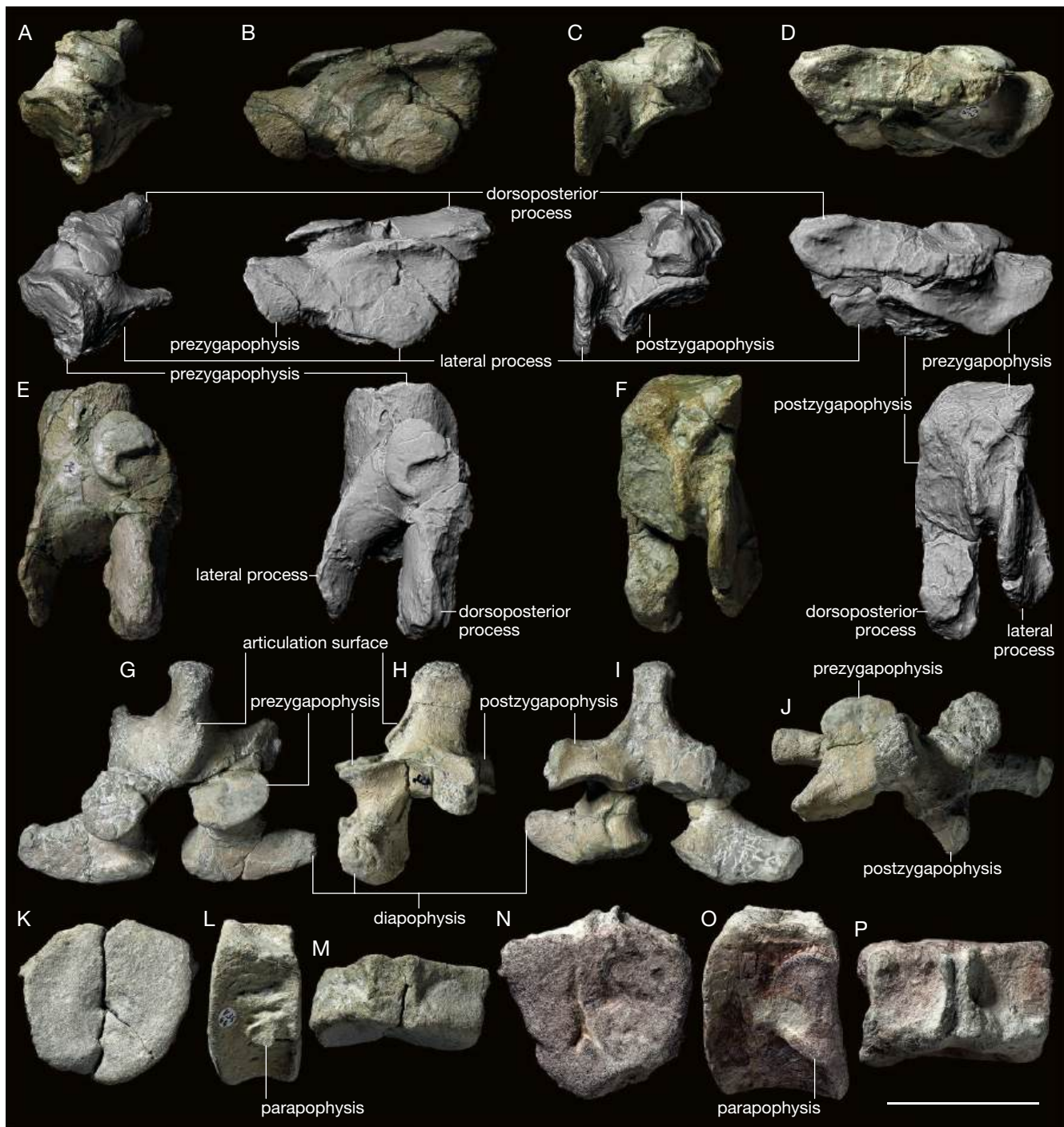


Fig. 8. — *Woznikella triradiata* n. gen., n. sp., cervical vertebrae: A–F, ZPAL V. 34/1/27: left part of the neural arch of the atlas in anterior (A), lateral (B), posterior (C), medial (D), dorsal (E), and ventral (F) view; G–J, ZPAL V. 34/1/30: cervical neural arch in anterior (G), lateral left (H), posterior (I), and dorsal (J) view; K–M, ZPAL V. 34/1/66: cervical vertebral centrum in anterior (K), lateral right (L), and dorsal (M) view; N–P, ZPAL V. 34/1/77: posterior cervical vertebral centrum in anterior (N), lateral right (O), and dorsal (P) view. Scale bar: 5 cm.

its ventral edge is gently bowed, concave dorsally, and reaches the ventral edge of the angular close to its anterior tip.

Surangular

The right surangular is fused with the articular and prearticular (ZPAL V. 34/1/4; Fig. 6). As preserved, its dorsal edge forms a triangular coronoid eminence. The boundary of that structure

is damaged, but what appears to be remnants of its natural edge suggest that the general shape is not significantly altered. The surangular is similar to the homologous bone of, e.g., *Angonisaurus crickshanki* and *Lisowicia bojani* (see Cox & Li 1983; Sulej & Niedźwiedzki 2019). The surangular has a completely flat lingual surface. A distinct ridge on the labial surface begins in front of the coronoid eminence and

posteriorly it continues onto the labial surface of the articular. A narrow ridge and a groove beneath it are close to the ventral edge of the labial side, but the anteroventral part of the bone is broken. This structure was probably the area of contact with the angular.

Preatricular

The right prearticular is fused with the articular and surangular (ZPAL V. 34/1/4; Fig. 6). It is a thin blade of roughly rectangular shape. Its dorsal edge is curved, so the highest point is in the middle of the bone, in front of the coronoid eminence of the surangular.

Articular

The right articular is fused with the surangular and prearticular (ZPAL V. 34/1/4; Fig. 6) and is broadened posterodorsally into a triple-edged condyle. The central ridge is the longest and highest, the inner ridge is the shortest. The retroarticular (digastric) process is very short, as in, e.g., *Ischigulastia jensi*, most *Shaanbeikannemeyeria xilouguensis*, and *Wadiasaurus indicus*, but it is longer than in *Vinceria andina* (see Cox 1965; Bandyopadhyay 1988; Domnanovich & Marsicano 2012; Liu 2022). Note, however, that this character shows some variability, even bilaterally within a single individual (Camp 1956). The fourth, labialmost ridge, which is located outside of the condyle, begins on the surangular like in *Stachleckeria potens* and ends on the retroarticular (digastric) process like in *Kannemeyeria simocephalus* (see Camp 1956).

Vertebral column

All centra and neural arches are preserved separately (Figs 8; 9A-M), with the exception of ZPAL V. 34/1/12, a posterior dorsal vertebra (Fig. 8N-Q). Although the elements were mostly found scattered, their morphology and documented location within the association allow the establishment of their approximate relative positions within the sequence.

Neural arch of the atlas

Both halves of the neural arch of the atlas are preserved. The left part of the atlas neural arch is complete (ZPAL V. 34/1/27; Fig. 8A-F). In lateral view, it is composed of an almost flat lateral process and an elongated posterodorsal process. The posterodorsal process is slightly asymmetric and located entirely to the left of the midline of the neural canal, most likely acting functionally as a postzygapophysis. The postzygapophyseal surface is almost oval with nearly straight medial edge. Above the postzygapophysis, a distinct ridge is present on the dorsomedial side of the process. At the base of the posterodorsal process, a large prezygapophysis is very distinct with a deep notch in its posterior margin. On the anterior portion (main body) there is a flat facet for the exoccipital and a concave, rounded facet for the centrum ventromedially. The lateral process is directed predominantly posterodorsally, its long axis nearly parallel to the posterodorsal process. It is very high and its lateral surface forms a large, oval, flat area, with a gentle but clear, laterally directed lip along its dorsal edge. The overall morphology is nearly identical to that of

the neural arch of the atlas of *Kannemeyeria simocephalus* (see Pearson 1924b; Govender 2005; Govender *et al.* 2008) but more elongated posterodorsally than in *Wadiasarus indicus* (see Bandyopadhyay 1988).

The right part of the atlas neural arch (ZPAL V. 34/1/69) is preserved in the same bone accumulation but has a slightly different state of preservation and shape due to deformation. It is broken into at least three pieces, slightly distorted, and the surface of the bone is reddish and in a bad condition. Both processes, lateral and posterodorsal, are eroded. The lateral process is misshapen and only the base of the dorsal process is preserved. Both modes of preservation are congruent with the state of the rest of the skeleton (see the Material section).

Cervical vertebrae

Five cervical vertebral centra (ZPAL V. 34/1/66, ZPAL V. 34/1/69, ZPAL V. 34/1/70, ZPAL V. 34/1/76, and ZPAL V. 34/1/77; Fig. 8K-P) and three cervical neural arches (ZPAL V. 34/1/14, and ZPAL V. 34/1/30; Fig. 8G-J) are preserved and are mostly complete (ZPAL V. 34/1/14 has its neural process deformed and broken, ZPAL V. 34/1/70 is incomplete laterally on its left side, ZPAL V. 34/1/76 has its posteroventral part broken off). Based on their morphology, the centra can be arranged in a following sequence (anterior to posterior): ZPAL V. 34/1/66, ZPAL V. 34/1/70, ZPAL V. 34/1/69, ZPAL V. 34/1/77, ZPAL V. 34/1/76. The neural arches cannot be attributed to any particular centrum, but ZPAL V. 34/1/14 is larger and has a longer neural process than ZPAL V. 34/1/30, indicating that it is more posterior.

The centra are wide and rounded, subpentagonal in their anteroposterior aspect. Anterior and posterior surfaces are concave (weakly amphicoelous) with pronounced notochordal pits in their centers. The anterior centra are anteroposteriorly short, but gradually increase in length posteriorly, so ZPAL V. 34/1/76 is about double the length of ZPAL V. 34/1/66. The two anteriormost centra (ZPAL V. 34/1/66 and ZPAL V. 34/1/70) have small, knob-like parapophyses located around the mid-height of the centrum (Fig. 8K-M), but the parapophyses of the more posterior centra increase in size and extend further dorsally, in ZPAL V. 34/1/77 and ZPAL V. 34/1/76 reaching around half of the centrum's length and nearly reaching the articular surfaces for the neural arch pedicles (Fig. 8N-P; compare with Camp & Welles 1956; Sun 1963; Bandyopadhyay 1988; Surkov 1998a; Vega-Dias & Schultz 2004). The dorsal surfaces are wide, and the surfaces for articulation with the neural arches change from wider than long in the anterior cervical vertebral centra to almost rectangular in the posterior, and gently slope ventrolaterally. The centra show little to no keeling ventrally. Ventrally and laterally, particularly above the parapophyses, the cortices of the three anteriormost preserved centra are perforated by vascular canals.

The neural arch ZPAL V. 34/1/30 has a very low and anteroposteriorly short neural process, with an additional articulation surface on its anterior edge (Fig. 8G-J). The apex of the neural process is subtriangular in cross-section, with sharpened anterior and posterolateral edges, and the posterior surface

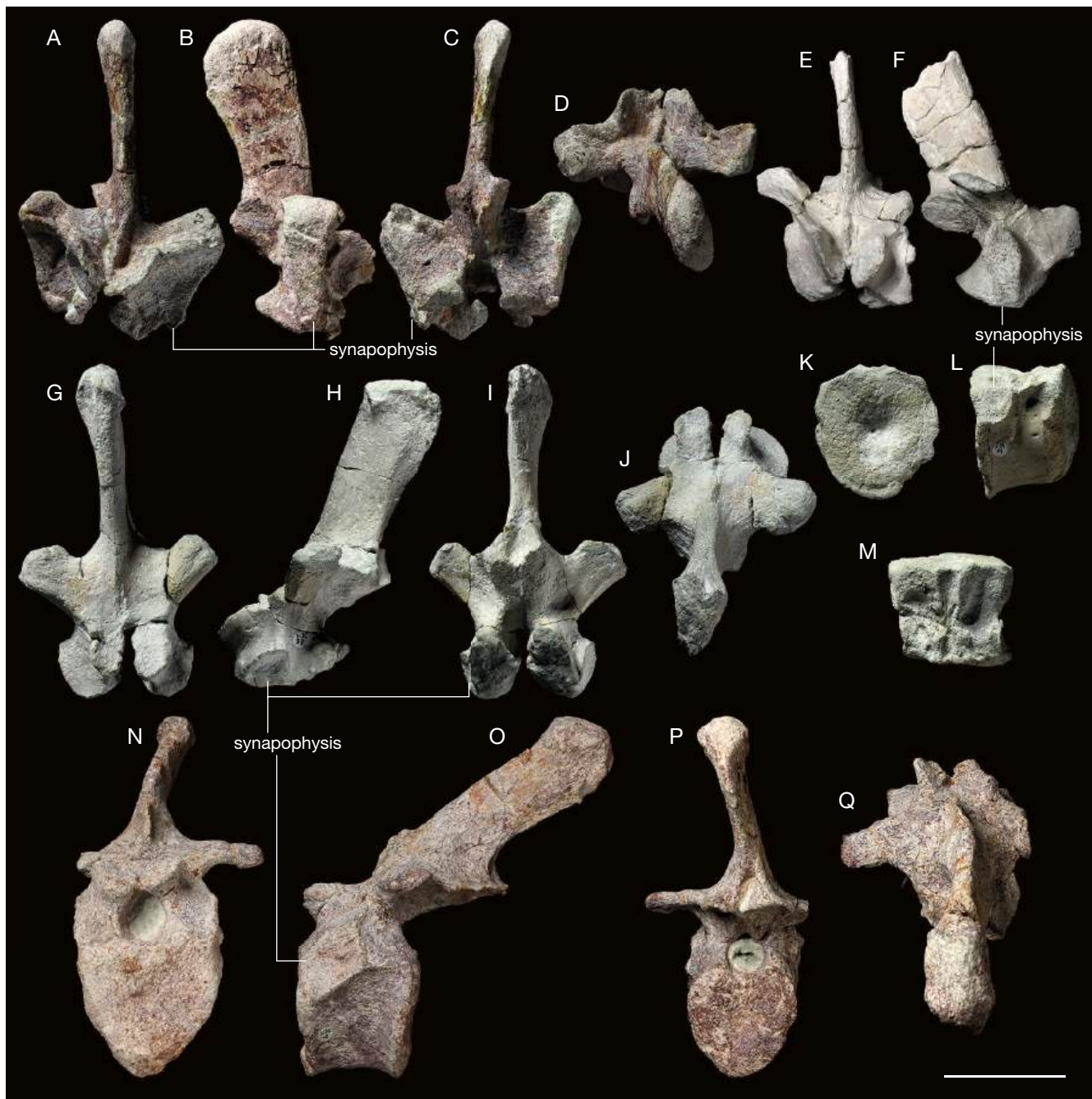


Fig. 9. — *Woznikella triradiata* n. gen., n. sp., dorsal vertebrae: A-D, ZPAL V. 34/1/31: anterior dorsal neural arch in anterior (A), lateral right (B), posterior (C), and dorsal (D) view; E-F, ZPAL V. 34/1/35: middle dorsal neural arch in anterior (E) and lateral right (F) view; G-J, ZPAL V. 34/1/33: more posterior middle dorsal neural arch in anterior (G), lateral left (H), posterior (I), and dorsal (J) view; K-M, ZPAL V. 34/1/11: dorsal vertebral centrum in anterior (K), lateral left (L), and dorsal (M) view; N-Q, ZPAL V. 34/1/12: posterior dorsal vertebra in anterior (N), lateral left (O), posterior (P), and dorsal (Q) view. Scale bar: 5 cm.

is concave. In anteroposterior aspect, the process is slightly expanded laterally near the apex (Fig. 8G, I). In lateral view, the anterior edge of the process is gently concave and slanted posterodorsally, with the posterior edge subvertical (Fig. 8H). There is a narrow, dorsoventrally aligned rugose band on the posterior surface, likely an attachment point for muscles or ligaments (Fig. 8I). The neural process is much higher, although plastically deformed and dorsally incomplete, in ZPAL V. 34/1/14. It is, furthermore, shifted posteriorly, nearly com-

pletely beyond the posterior limit of the transverse processes. The zygapophyses are nearly horizontal. The prezygapophyses are oval, and the postzygapophyses are ovoid (long axes directed posterolaterally) and concave ventrally. In lateral view, the dorsal (non-articular) surfaces of the postzygapophyses of ZPAL V. 34/1/30 are continuous with and parallel to the dorsal (articular) surfaces of the prezygapophyses, and they gently slope anteroventrally. A distinctive vertical ridge is present above each postzygapophysis. In ZPAL V. 34/1/14, the

TABLE 2. — Remains historically considered to belong to post-Permian Dicynodontia or confused with them, but in fact of Permian age and/or not being dicynodonts.

Original description	Country	Comments
" <i>Colossoemys macrococygeana</i> " Rodrigues, 1944; Camp & Welles 1956 1892/“cf. <i>Dicynodon turpior</i> ” von Huene, 1935 unnumbered specimen (von Huene 1944)	Peru (Rodrigues 1892; von Huene 1921, 1944; Camp & Welles 1956)	A bone fragment described as an ilium of a Miocene chelid turtle (one of several syntypes described and figured by Rodrigues 1892; see Ferreira et al. 2006 for more information about the history of the syntype material), later reinterpreted as a partial humerus of a Late Triassic dicynodont (von Huene 1944; Camp & Welles 1956), now lost; probably part of a xenarthran humerus (Price 1956; Paula-Couto 1960; de Lapparent de Broin et al. 1993; Ferreira et al. 2006)
<i>Dapocephalus leoniceps</i> (Owen, 1876) AMNH FARB 5598, RC 96, SAM-PK-7849 (Broom 1921, 1948, Haughton 1924, von Huene 1925, Haughton & Brink 1954, Cruickshank 1967)	South Africa (Owen 1876; Broom 1921, 1948; Haughton 1924; von Huene 1925; Haughton & Brink 1954; Cruickshank 1967; Kitching 1977; Kammerer et al. 2011)	Three skulls originally described as “ <i>Dicynodon osborni</i> ” Broom, 1921, “ <i>Dicynodon leontocephalus</i> ” Broom, 1948, and “ <i>Dicynodon watsoni</i> ” Broom, 1921 (all subsequently synonymized with <i>Dapocephalus leoniceps</i> ; see Kammerer et al. 2011), and originally thought to originate from the Triassic “ <i>Lystrosaurus AZ</i> ” (Broom 1921, 1948; Haughton 1924; von Huene 1925; Haughton & Brink 1954); independently, Cruickshank (1967), citing personal communication with Crompton, noted the presence of <i>Dapocephalus leoniceps</i> in the “ <i>Lystrosaurus AZ</i> ”; most likely, however, all occurrences of <i>Dapocephalus leoniceps</i> are Permian and the confusion arose due to the presence of <i>Lystrosaurus</i> spp. in the latest Permian <i>Lystrosaurus maccaigi-Moschorhinus SZ</i> of the <i>Dapocephalus AZ</i> (Kitching 1977; Kammerer et al. 2011; Viglietti 2020)
“ <i>Dicynodon incisivum</i> ” Repelin, 1923 unnumbered specimen	Laos (Repin 1923; Yuan & Young 1934b; von Huene 1935; Piveteau 1938; Colbert 1982; Brink 1988; King 1988; Battail 2009; Fröbisch 2009; Kammerer et al. 2011)	<i>Nomen dubium</i> , specimen lost; originally believed to be Triassic; probably Permian (Yuan & Young 1934b; Colbert 1982; Battail 2009; Fröbisch 2009; Kammerer et al. 2011)
“ <i>Dicynodon ingens</i> ” Broom, 1908b unnumbered specimens	South Africa (Broom 1908b, 1909; Haughton 1924; Kammerer et al. 2011)	<i>Nomen dubium</i> , several cranial and postcranial specimens, now lost; noted by Broom (1909) as possibly originating from the Triassic “ <i>Lystrosaurus AZ</i> ”; likely Permian (Haughton 1924; Kammerer et al. 2011)
“ <i>Dicynodon rosmarus</i> ” Cope, 1870b unnumbered specimens	United States (Cope 1870a, b, c; von Huene 1926b, 1935; Kammerer et al. 2013)	<i>Nomen dubium</i> , two teeth from the Upper Triassic of the New Oxford Formation described as dicynodont tusks, now lost; probably archosaur teeth, possibly phytosaur (von Huene 1926b; Kammerer et al. 2013)
Dicynodontia indet. QMF990 (former QM F15.990) (Thulborn & Turner 2003)	Australia (Thulborn & Turner 2003; Knutsen & Oerlemans 2020)	Bone fragments, one of which was described as a dicynodont maxilla from the Lower Cretaceous of the Allaru Formation; probably a post-Cretaceous diprotodontid mammal (Knutsen & Oerlemans 2020)
Dicynodontia indet. YPM VPPU 020750 (Baird & Olsen 1983)	Canada (Baird & Olsen 1983; Olsen et al. 1989; Lucas & Hunt 1993a; Nesbitt & Angielczyk 2002; Sues & Olsen 2015)	Weathered skull fragment from the Carnian Wolfville Formation, initially mentioned as an indeterminate dicynodont; reinterpreted as a paracrocodylomorph pseudosuchian by Sues & Olsen (2015)
“aff. <i>Dinodontosaurus</i> sp.” SMNS 56891 (Lucas & Wild 1995)	Germany (Lucas & Wild 1995; Maisch et al. 2009)	Humerus from the Middle Triassic of the Muschelkalk; probably a temnospondyl (Maisch et al. 2009)
<i>Geikia elginensis</i> Newton, 1893 GSM 90998-91015	Scotland (Newton 1893; von Huene 1913; Kammerer et al. 2011)	A series of sandstone fragments with natural molds of a skull, mandible, and limb fragments from the Cuttie's Hillock Sandstone in Scotland, originally considered to be of Triassic age (Judd 1885; Newton 1893); subsequent biostratigraphic correlations suggest a Permian age for that assemblage (e.g., von Huene 1913; Rowe 1980; Kammerer et al. 2011)
<i>Gordonia traquairi</i> Newton, 1893 GSE 11703 and several other specimens	Scotland (Judd 1885; Newton 1893; von Huene 1913; Kammerer et al. 2011)	Several specimens described as <i>Gordonia traquairi</i> Newton, 1893, <i>Gordonia duffiana</i> Newton, 1893, <i>Gordonia huxleyana</i> Newton, 1893, and <i>Gordonia juddiana</i> Newton, 1893, which were later synonymized (King 1988; Kammerer et al. 2011), all coming from the Cuttie's Hillock Sandstone in Scotland, originally considered to be of Triassic age (Judd 1885; Newton 1893); subsequent biostratigraphic correlations suggest a Permian age for that assemblage (e.g., von Huene 1913; Rowe 1980; Kammerer et al. 2011)
<i>Herpetochirus brachycnemus</i> Seeley, 1985 NHMUK R2588	South Africa (Seeley 1895; von Huene 1925; Kammerer 2009)	Fragmentary postcranial skeleton from South Africa, noted by von Huene (1925) as a dicynodont from the Triassic “ <i>Lystrosaurus AZ</i> ”; probably Permian therocephalian (Seeley 1895; Kammerer 2009)

Table 2. — Continuation.

Original description	Country	Comments
" <i>Ischigualastia boreni</i> " Edler, 2000 TTU P-9427	United States (Edler 2000; Nesbitt & Angielczyk 2002; Martz 2008)	Bone fragment from the Norian of the Cooper Canyon Formation, interpreted as a preorbital part of a stahleckeriid skull; its dicynodont affinity was subsequently questioned (Nesbitt & Angielczyk 2002); probably posterior part of a pseudosuchian mandible (Martz 2008)
" <i>Lystrosaurus</i> sp." MCN PV1872 and MCN PV1873 (Schwanke & Kellner 1999; Langer & Lavina 2000)	Brazil (Schwanke & Kellner 1999; Langer & Lavina 2000; Dias-da-Silva et al. 2017)	Two specimens from the Lower Triassic of the Sanga do Cabral Formation, described as lystrosaurid stapes; probably procolophonid sacral ribs (Dias-da-Silva et al. 2017)
<i>Theromus leptotonotus</i> Seeley, 1885 NHMUK R2585, NHMUK R2587	South Africa (Seeley 1895; Watson 1911; von Huene 1925; Kammerer 2009)	Fragmentary postcranial skeleton from South Africa, noted by von Huene (1925) as a dicynodont from the Triassic " <i>Lystrosaurus</i> AZ"; in fact either a therocephalian (Seeley 1895; Watson 1911) or non-dicynodont anomodont (Kammerer 2009), probably Permian (Seeley 1895; Watson 1911)

articular surfaces of both the pre- and postzygapophyses are roughly level with each other, but aligned more ventromedially, and the postzygapophyses are more elongate than in ZPAL V. 34/1/30, with their long axes directed more posteriorly. In both specimens, the prezygapophyses and postzygapophyses are separated mesially along their entire length (the prezygapophyses wider than the postzygapophyses), but in ZPAL V. 34/1/14 the latter are closer to each other than in ZPAL V. 34/1/30. The diapophyses are present beneath the prezygapophyses and are relatively small dorsoventrally, but the transverse processes extend horizontally just above the neurocentral suture, with their ventrolateral surfaces convex (compare with Young 1937; Sun 1963; Cheng 1980; Bandyopadhyay 1988; Vega-Dias & Schultz 2004; Liu 2015).

Dorsal vertebrae

There are six isolated neural arches (ZPAL V. 34/1/13, ZPAL V. 34/1/31, ZPAL V. 34/1/33, ZPAL V. 34/1/34, ZPAL V. 34/1/35, and ZPAL V. 34/1/36; Fig. 9A-J), four isolated vertebral centra (ZPAL V. 34/1/11, ZPAL V. 34/1/67, ZPAL V. 34/1/68, and ZPAL V. 34/1/71; Fig. 9K-M), and a single mostly complete vertebra (ZPAL V. 34/1/12; Fig. 8N-Q) that can be classified as belonging to the dorsal series. Based on recovery documentation, out of the isolated elements, the centrum ZPAL V. 34/1/71 and the neural arch ZPAL V. 34/1/36 were found in near articulation, and ZPAL V. 34/1/34 was found right behind them. The centrum ZPAL V. 34/1/67 was found below the neural arch ZPAL V. 34/1/31. The shapes and sizes of the neurocentral articulation facets as well as the state of preservation suggest that the centra ZPAL V. 34/1/68 and ZPAL V. 34/1/11 (Fig. 9K-M) may belong to the neural arches ZPAL V. 34/1/34 (Fig. 9K-M) and ZPAL V. 34/1/33 (Fig. 9G-J), respectively, and that they come from neighboring segments. Based on those data and gradual changes of morphology, the elements may be hypothesized to form the following relative sequence (anterior to posterior): ZPAL V. 34/1/31, ZPAL V. 34/1/67, ZPAL V. 34/1/35, ZPAL V. 34/1/71 + ZPAL V. 34/1/36, ZPAL V. 34/1/68 + ZPAL V. 34/1/34, ZPAL V. 34/1/11 + ZPAL V. 34/1/33, ZPAL V.

34/1/13, ZPAL V. 34/1/12. However, this sequence should be treated with caution, particularly when it comes to the vertebral centra, due to the lesser number of morphological details observable on them.

The anterior part of the dorsal vertebral column is represented by a single neural arch, ZPAL V. 34/1/31 (Fig. 9A-D). Its anterior position within the dorsal section of the vertebral column is indicated by its extensive, wide synapophyses spanning from the tips of the transverse processes, ventromedially towards the neurocentral suture, and apparently continuing onto the centrum (compare with Pearson 1924b; Young 1937; Sun 1963; Cox 1965; Cruickshank 1967; Bandyopadhyay 1988). The transverse processes are wing-like, massive, and similar to those of the cervical neural arches, but gently raised laterally. Their ventrolateral surfaces are nearly straight, and their edges are angular. The dorsal edges of the transverse processes face anterodorsally and form distinct lateromedial ridges anteriorly and posterodorsally. The synapophyses are wider dorsally than ventrally and skewed posterodorsally in lateral view. In contrast to the cervical neural arches, the prezygapophyses of ZPAL V. 34/1/31 have subrectangular outlines and are aligned dorsolaterally rather than subhorizontally; the angle between their anterior edges is approximately 90° in the medial part, but their lateral parts gently turn dorsally. The postzygapophyses are ovoid, shorter than in the cervical neural arch ZPAL V. 34/1/14, and set at a more acute angle than the prezygapophyses (about 60°). Contralaterally, both the pre- and postzygapophyses are separated only by a narrow notch. The neural process is high and anteroposteriorly long with a rounded and gently anteroposteriorly expanded dorsal end. It is directed gently posteriorly. The neural process apex is fusiform in cross-section and only slightly expanded laterally. At the base of the neural process there is a distinct vertical ridge anteriorly, reaching the notch between the prezygapophyses, and a vertically expanded, rhomboid depression posteriorly, limited by the postzygapophyses ventrolaterally and by low, rounded ridges dorsolaterally. The anterior edge of the base of the neural process reaches anteriorly past the level of the anterior edge of the synapophyses.

ZPAL V. 34/1/35 represents a slightly more posterior neural arch (Fig. 9E, F). In contrast to ZPAL V. 34/1/31, the dorsolaterally directed transverse process in this specimen is free from the synapophysis and is plate-like. Only a low ridge continues from the dorsal end of the synapophysis onto the posteroventral surface of the transverse process. The dorsal extent of the synapophyses is below the dorsolateral edges of the prezygapophyses, which is lower than in ZPAL V. 34/1/31 but higher than in succeeding vertebrae. It is well defined in anteroposterior aspect and clearly separated from the transverse process, as in the remaining, more posterior neural arches. The dorsal part of the synapophysis is rounded and anteroposteriorly wider than the ventral part. The prezygapophyses are set at a more acute angle than in ZPAL V. 34/1/31 (about 60°), the postzygapophyses are set at a greater angle (about 80°) and the dorsal process is directed more posterodorsally. The morphology is reminiscent of that figured and described by Pearson (1924b), Govender (2005), and Govender *et al.* (2008) for the mid-dorsal vertebrae of *Kannemeyeria simocephalus*.

The succeeding neural arches show gradual changes in morphology: 1) the synapophyses recede farther ventrally compared to ZPAL V. 34/1/35 and develop a conspicuous dorsal tip, thus attaining a subtriangular shape with gently bowed anterodorsal and posterodorsal edges; 2) the prezygapophyses and postzygapophyses are ovoid and become more horizontal; 3) the dorsal processes become inclined even more posterodorsally and their bases shift more posteriorly relative to the anterior extent of the synapophyses; 4) the apices of the dorsal processes expand more laterally, particularly in the anterior part, so they become teardrop-shaped in cross-section, and develop subtle medial grooves anteriorly; and 5) the depressions in the posterior bases of the neural processes become deeper and more conspicuous. The posteriormost preserved vertebra, ZPAL V. 34/1/12, presents the most extreme morphology (Fig. 9N-Q). The synapophyses in this specimen are particularly low but anteroposteriorly wide, the prezygapophyses are short but the postzygapophyseal part is extended posteriorly due to the posterior shift of the neural process. The outline of the articular surface of the postzygapophyses, nonetheless, takes up only the posterior half of that area. The transverse processes are more horizontal, both in the lateral and anteroposterior aspect. The posterodorsal alignment of the neural process is particularly pronounced. In lateral view, the process presents subtle sigmoidal curvature, with the mid-section directed more posteriorly than the base and the apex. The base of the process presents a strong ridge, which unlike in ZPAL V. 34/1/31 does not extend to the notch between the prezygapophyses, but ends at the level of the base of the transverse processes. The apex of the neural process is expanded also in the middle part, thus presenting a pentagonal cross-section. The groove in its anterior face is subtle, but more conspicuous than in the preceding neural arches.

The dorsal vertebral centra are weakly amphicoelous with distinct notochordal pits in the anterior and posterior facets, and are ovoid in anterioposterior aspect. They are comparable in length to the posterior cervical vertebral centra but slightly

narrower dorsally, so the facets for the neural arches are longer than wide. Some of them (particularly ZPAL V. 34/1/67 and ZPAL V. 34/1/12) bear a rounded ventral keel. The central parts of synapophyses are located in the anterodorsal corners of the centra. As in the case of their neural parts, they become smaller posteriorly. Most of them present convex posteroventral edges, similar to those in the posterior cervical vertebrae, with the exception of ZPAL V. 34/1/12, in which this edge is straight and the synapophysis has a rhomboid outline.

The observed morphological anteroposterior progression is consistent with the changes observed previously in other Kannemeyeriiformes (compare with Pearson 1924b; Young 1937; Sun 1963; Cruickshank 1967; Bandyopadhyay 1988). It is furthermore consistent with the shape and size of the ribs and their articular regions (see below). According to Vega-Dias *et al.* (2004) the vertebrae of Triassic dicynodonts have no diagnostic value at the family or generic level. However, it must be noted that the relative scarcity of published data on dicynodont vertebrae (in many cases, only selected vertebrae were figured and their precise location within the column was not determined), has made meaningful comparisons difficult, and variation in these elements may be more extensive than currently recognized. In contrast to *Jachaleria candelariensis*, the dorsal vertebral centra of *Woznikella triradiata* n. gen., n. sp. are significantly longer and the transverse processes are more pronounced (Araújo & Gonzaga 1980; Vega-Dias & Schultz 2004; Martinelli *et al.* 2020). They are also narrower relative to height, particularly in the ventral region, than in, e.g., *Dinodontosaurus tener*, *Ischigualastia jensi* (at least for part of the dorsal vertebral column), *Jachaleria colorata* Bonaparte, 1970, *Kannemeyeria simocephalus*, *Lisowicia bojani*, *Pentasaurus goggai*, *Rhinodicynodon gracile*, *Sangusaurus paringtonii*, *Sinokannemeyeria pearsoni*, and *Stahleckeria potens* (see von Huene 1935; Young 1937; Romer & Price 1944; Cox 1965; Araújo & Gonzaga 1980; Surkov 1998a; Vega-Dias & Schultz 2004; Morato 2006; Angielczyk *et al.* 2017; Kammerer 2018; Sulej & Niedzwiedzki 2019; Martinelli *et al.* 2020), being more in line with, e.g., *Parakannemeyeria shenmuensis*, *Placerias hesternus*, *Shansiodon wangi*, *Sinokannemeyeria yingchiaensis*, *Wadiasaurus indicus*, or *Zambiasaurus submersus* (e.g., Camp & Welles 1956; Yeh 1959; Sun 1963; Cox 1969; Cheng 1980; Bandyopadhyay 1988). The shape of the centra, however, aside from taphonomic factors, may potentially be impacted by ontogeny (e.g., von Huene 1935). If the assignment of the neural arches to the vertebral centra is correct, the posterior ends of their pedicels could project posteriorly in the mid-dorsal vertebrae, forming protuberances consistent with the morphology seen in at least some other Kannemeyeriiformes (von Huene 1935; Araújo & Gonzaga 1980; Bandyopadhyay 1988; Vega-Dias & Schultz 2004; Martinelli *et al.* 2020).

Ribs

Ribs are represented by some almost complete specimens and many fragments of varying sizes. Among them several morphotypes may be distinguished, which generally agree with the morphologies presented for *Jachaleria candelariensis*



FIG. 10. — *Woznikella triradiata* n. gen., n. sp., ribs: A, B, ZPAL V. 34/1/82 in anterior (A) and posterior (B) view; C, D, ZPAL V. 39/1/20 in anterior (C) and posterior (D) view; E, F, ZPAL V. 34/1/208 in anterior (E) and posterior (F) view; G, H, ZPAL V. 34/1/17 in anterior (G) and posterior (H) view; I, J, ZPAL V. 34/1/26 in ?anterior (I) and ?posterior (J) view; K-Q, closeups of the articular surfaces: K, ZPAL V. 34/1/16; L, ZPAL V. 34/1/82; M, ZPAL V. 34/1/15; N, ZPAL V. 34/1/20; O, ZPAL V. 34/1/208; P, ZPAL V. 34/1/17; Q, ZPAL V. 34/1/26. Scale bars: A-J, 5 cm; K-N, O-Q, 1 cm.

by Vega-Dias & Schultz (2004), *Kannemeyeria simocephalus* by Pearson (1924b), and *Sinokannemeyeria yingchiaoensis* by Sun (1963), and correspond well with the articulation facets observed on the vertebrae (see above).

ZPAL V. 34/1/26 is a very short (14 cm along the parietal edge), anteroposteriorly flattened rib with a distinct curvature and conspicuous decrease of the visceroparietal width along its length (Fig. 10I, J, Q). The proximal part in anteroposterior aspect is gently flared, slightly sloped anteromedially in proximal view, and exceptionally flat (29 × 8 mm). Unlike the remaining ribs, it does not form a defined articular surface and its edge is uneven, so it is likely that this rib formed a sutural connection with the vertebra rather than a movable articulation. As preserved, the specimen terminates in a blunt 4 × 6 mm large tip. Possibly this is a break, but it seems unlikely that the rib continued much further in life. Given its different morphology, this specimen is tentatively identified as a cervical rib. Ribs with anteroposteriorly narrow and visceroparietally wide shafts are common and attain the largest sizes, possibly coming from the widest, anterior section of the ribcage. The best-preserved specimen in this category is ZPAL V. 34/1/82 (Fig. 10A, B, L). It is a very long rib with a complete head and tubercle, but with a broken distal end. The rib head is set on a short neck and is relatively small compared to the expanded tubercle, the visceroparietal size of which nearly equals the visceroparietal width of the shaft. This amounts to the proximalmost part of the rib being almost two times the size of the shaft visceroparietal width. The articular surface for the diapophysis forms an inverted pear-shape in proximal view and is much larger than the oval surface for the parapophysis. Both facets are separated by a constriction giving the proximal part of the rib an inverted figure 8 shape in articular view. The posterior edges of the articular surfaces protrude in a ridge-like fashion, as does the dorsal edge of the facet for the diapophysis. The specimen is broken in several places and its distal part is crushed and distorted, but it appears to originally have a relatively straight shaft with nearly parallel edges. The specimen ZPAL V. 34/1/16 presents overall the same morphology but the edges of the articular facets also form conspicuous ridges anteriorly (Fig. 10K). The shaft of this specimen is gently sinuous in visceroparietal aspect, but it is not clear whether this waviness was present in vivo, or if it was acquired post-mortem because of distortion. In the specimen ZPAL V. 34/1/83, which represents the same morphotype, the curvature of the shaft is slightly more pronounced, likely as a result of a smaller circumference of the rib cage at its level. In ZPAL V. 34/1/15, the head and tubercle merge in a single, elongated subvertical articular surface (Fig. 10M). More posterior, visceroparietally wide ribs with a smaller single, vertical or nearly vertical articular surface lying in the same plane as the shaft and a curved proximal region (ZPAL V. 34/1/20, ZPAL V. 34/1/21, ZPAL V. 34/1/85) can reach similar visceroparietal width as the previous type, but were likely shorter, considering their curvature. In ZPAL V. 34/1/20 (Fig. 10C, D, N) and ZPAL V. 34/1/85, the articular surface is sinuous in anteroposterior aspect, convex in its ventral

part, and recessed in the dorsal part. In ZPAL V. 34/1/20 it is oblique, directed ventromedially in anteroposterior aspect, and dorsally projected into a small process, whereas in ZPAL V. 34/1/85 the dorsal part is nearly horizontal in anteroposterior aspect. In both specimens, the articular surfaces are slightly sloped anteroventrally in proximal view. The dorsal and ventral parts are continuous but in proximal view there is a very subtle constriction in the middle of the articular surface, giving it a peanut-shaped outline and suggesting that this area is formed by merging of the head and tubercle. In ZPAL V. 34/1/21, the articular surface in proximal view is vertical and convex, inverted comma-shaped, with the thinner end directed posterodorsally and the anterodorsal edge convex. The specimen is visceroparietally narrower than ZPAL V. 34/1/20 and ZPAL V. 34/1/85. In all specimens of this type, the shaft is anteroposteriorly flattened in the proximal part, the anterior and posterior surfaces are gently concave just distal to the curve, and more distally the shaft becomes oval in cross-section and visceroparietally narrower.

The distal (ventral) ends of the ribs belonging to the previous two morphotypes are completely preserved in ZPAL V. 34/1/18 and ZPAL V. 34/1/20. Based on these specimens, it may be established that the oval cross-section, which is present around the midlength of the ribs, becomes flattened again and increases in visceroparietal width distally. The ribs terminate with swollen and rounded ends, ovoid in distal view.

Strongly curved ribs with narrow and long shafts likely come from the posteriormost part of the rib cage. This kind of rib is represented by the specimens ZPAL V. 34/1/17 (Fig. 10G, H, P) and ZPAL V. 34/1/23. The articular surface is only preserved in ZPAL V. 34/1/17. It is horizontal, single, and elongated (the anteroposterior width about twice that of the shaft) with a straight ventral edge and a convex dorsal edge. In dorsoventral aspect, the anteriormost point of the articular surface is protruding. The neck expands dorsally towards a smooth dorsal curve, which constitutes the visceroparietally widest part of the shaft. The shaft just distal to the curve becomes subtriangular in cross-section, with a rounded visceral and posterior edge, an angular anterodorsal edge, and a concave posterovisceral surface, forming along the dorsolateral part of the rib a small, posteriorly directed lappet of bone. More distally, the rib becomes oval in cross-section, with the longer axis directed visceroparietally.

Scapula

The nearly complete, right scapula (ZPAL V. 34/1/7; Fig. 11A–D) only lacks some minor fragments of its ventral and posterior edge and the posterodorsal tip of the blade. It is roughly hourglass-shaped in lateromedial aspect, with the anterior edge more concave than the posterior, and the minimal breadth just below the midlength, above the acromion (Fig. 11A, B). It is gently bowed and twisted in anteroposterior view, with its dorsal and ventral ends turned medially and deflected anteromedially (Fig. 11C, D). The scapular spine is damaged but seems to be only weakly developed and the prespinal surface is flat (Fig. 11C) – in this aspect it differs from dicynodonts such as *Eubrachiosaurus browni*,

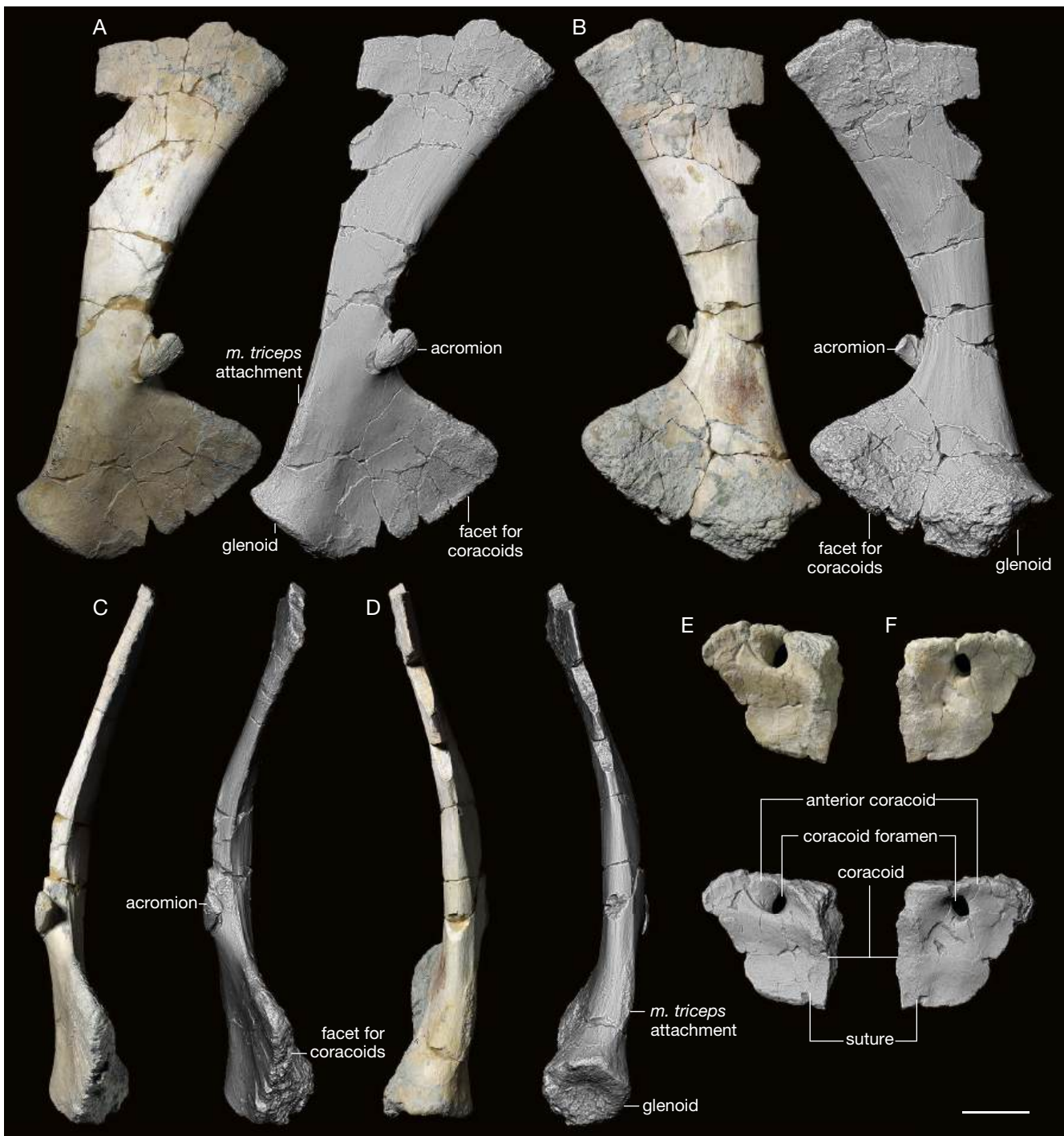


FIG. 11. — *Woznikella triradiata* n. gen., n. sp., scapulocoracoid: A–D, ZPAL V. 34/1/7, right scapula in lateral (A), medial (B), anterior (C), and posterior (D) view; E, F, ZPAL V. 34/1/107, right procoracoid in lateral (E) and medial (F) view. Scale bar: 5 cm.

Placerias hesternus, *Stahleckeria potens*, the indeterminate stahleckeriines (MCZ 3459 and CRILAR-Pv 82) from the Chañares Formation, *Rhinodicynodon gracile*, *Tetragonias njalilus*, or even *Zambiasaurus submersus*, which have a more pronounced spine (von Huene 1935; Romer & Price 1944; Camp & Welles 1956; Cruickshank 1967; Cox 1968, 1969; Surkov 1998a; Kammerer *et al.* 2013; Escobar *et al.* 2021). The acromion is conspicuous, mediolaterally flattened,

hooked medially, protrudes well past the anterior margin of the scapula, and has a blunt, thickened tip forming medially a small tubercle (Fig. 11B) similar to that of *Stahleckeria potens* and *Dinodontosaurus* sp. (“*Dicynodon turpior*”) figured by von Huene (1935). The presence of a well-developed acromion differentiates *Woznikella triradiata* n. gen., n. sp. from cf. *Dolichuranus primaevus* and *Ischigualastia jensi*, which lack this process (Cox 1965; Govender & Yates 2009;



FIG. 12. — *Woznikella triradiata* n. gen., n. sp., clavicles: A-D, ZPAL V. 34/1/75, left clavicle in posterior (A), anteroventral (B), anterodorsal (C), and posterodorsal (D) view; E-H, ZPAL V. 34/1/74, right clavicle in posteroventral (E), anteroventral (F), anterodorsal (G), and posterodorsal (H) view. Scale bar: 5 cm.

Escobar *et al.* 2021). Nonetheless, the acromion is not as large, relative to the rest of the scapula, as in, e.g., *Acratophorus argentinensis*, *Dinodontosaurus tener*, *Dinodontosaurus* sp. (“*Dicynodon turpior*”), *Lystrosaurus* spp., *Rhinodictyonodon gracile*, or *Shansiodon wangi* (see Broom 1908a; von Huene 1935; Young 1935; Yeh 1959; Cox 1965; Bonaparte 1966a; DeFauw 1986; Surkov 1998a; Morato 2006; Ray 2006; Kammerer *et al.* 2013; Escobar *et al.* 2021). Unlike in most Triassic dicynodonts (e.g., Pearson 1924b; von Huene 1935; Broom 1937; Romer & Price 1944; Yeh 1959; Sun 1960, 1963; Bonaparte 1966a; Cruickshank 1967; Colbert 1974; Araújo & Gonzaga 1980; Cox & Li 1983; Bandyopadhyay 1988; Lucas & Harris 1996; Surkov 1998a; Govender 2005; Surkov *et al.* 2005; Ray 2006; Govender *et al.* 2008; Kammerer *et al.* 2013; Escobar *et al.* 2021), it is directed anterodorsally rather than anteriorly, laterally, or antero- or ventrolaterally. The acromion had been broken off during recovery or preparation, causing a wide crack laterally, but its medial and ventral surfaces indicate that the pieces were well fitted together, and that no misalignment occurred. Other than the direction of the acromion, the scapula mostly resembles the narrow and gently flared “kannemeyeriid-like” (*sensu* Kammerer *et al.* 2013; note that the morphologies are not restricted to the clades after which they are named) scapulae of, e.g., *Kannemeyeria simocephalus*, *Parakannemeyeria youngi*, *Rhinodictyonodon gracile*, *Sinokannemeyeria yingchiaoensis*, *Wadiasaurus indicus*, the unnamed stahleckeriid (MCZ 3459) from the Chañares Formation, the morphotype B stahleckeriid of Govender (2005), and possibly *Eubrachiosaurus browni* in its general shape and proportions (Watson 1917; Pearson 1924b; Broom 1937; Sun 1963; Cox 1968; Bandyopadhyay 1988; Surkov 1998a; Govender 2005; Ray 2006; Govender *et al.* 2008; Kammerer *et al.* 2013). Govender (2005) and Govender *et al.* (2008) noted that *Kannemeyeria simocephalus* had relatively wide scapular blade and that the narrow-bladed scapulae previously attributed to that species by Pearson (1924b) differ significantly, resembling more Govender’s (2005) morphotype B stahleckeriid, the scapula of which, however, also fits better the “kannemeyeriid-like type” (*sensu* Kammerer *et al.* (2013)). ZPAL V. 34/1/7 differs from the typical “shansiodontid-” and “stahleckeriid-like” (*sensu* Kammerer *et al.* 2013) scapulae of *Acratophorus argentinensis*.

Dinodontosaurus tener, *Dinodontosaurus* sp. (“*Dicynodon turpior*”), *Ischigualastia jensi*, *Jachaleria candelariensis*, cf. *Kannemeyeria lophorhinus*, *Shansiodon wangi*, *Tetragonias njalilus*, and *Stahleckeria potens*, which are less gracile, have a more expanded scapular blade, and less expanded point of contact with the coracoids (von Huene 1935; Romer & Price 1944; Yeh 1959; Cox 1965; Bonaparte 1966a; Cruickshank 1967; Araújo & Gonzaga 1980; Lucas 2002; Vega-Dias & Schultz 2004; Vega-Dias *et al.* 2005; Morato 2006; Govender & Yates 2009). The scapulae attributed to *Lystrosaurus* spp. show some variability, but generally seem to be stouter as well (e.g., Huxley 1865; Broom 1908a; Young 1935; Colbert 1974; DeFauw 1986; Ray 2006). The scapula of *Zambiasaurus submersus* is similar in its slenderness, but less flared at both ends (Cox 1969; Govender 2005; Kammerer *et al.* 2013), whereas the scapula of *Placerias hesternus* is less constricted (Camp & Welles 1956; Kammerer *et al.* 2013). A lesser degree of flaring around the glenoid area also differentiates it from the scapula of *Angonisaurus cruckshanki* (Cox & Li 1983; Govender 2005). The scapula of *Lisowicia bojani* is less gracile as well, and has a significantly more expanded ventral part (Sulej & Niedźwiedzki 2019). The scapula of *Woznikella triradiata* n. gen., n. sp. is thickest at the glenoid, the articular surface of which in the scapular part is gently concave, rhomboid with rounded corners and set at an angle of ~100° relative to the anteroventral facet for the coracoids. This articular surface is approximately half the length of the gently convex facet for the coracoids. The attachment site for the triceps muscle is present as a rugose field on the posterolateral edge of the scapula above the glenoid (Fig. 11A, D). There is no trace of a *m. teres major* scar (e.g., Vega-Dias & Schultz 2004), but it might have occupied the unpreserved posterior tip of the scapula. Along most of the visceral surface of the scapula, a gentle but clear striation is present but there is no tubercle at the base of the acromion like that described by Govender (2005) and Govender *et al.* (2008) in *Kannemeyeria simocephalus* or *Tetragonias njalilus*. Govender (2005) described a fossa near the same area in her morphotype B stahleckeriid, and a gentle depression seems to be also present at the anteromedially surface of ZPAL V. 34/1/7, right above the acromion, but it is smaller and it is difficult to establish whether the two are homologous.

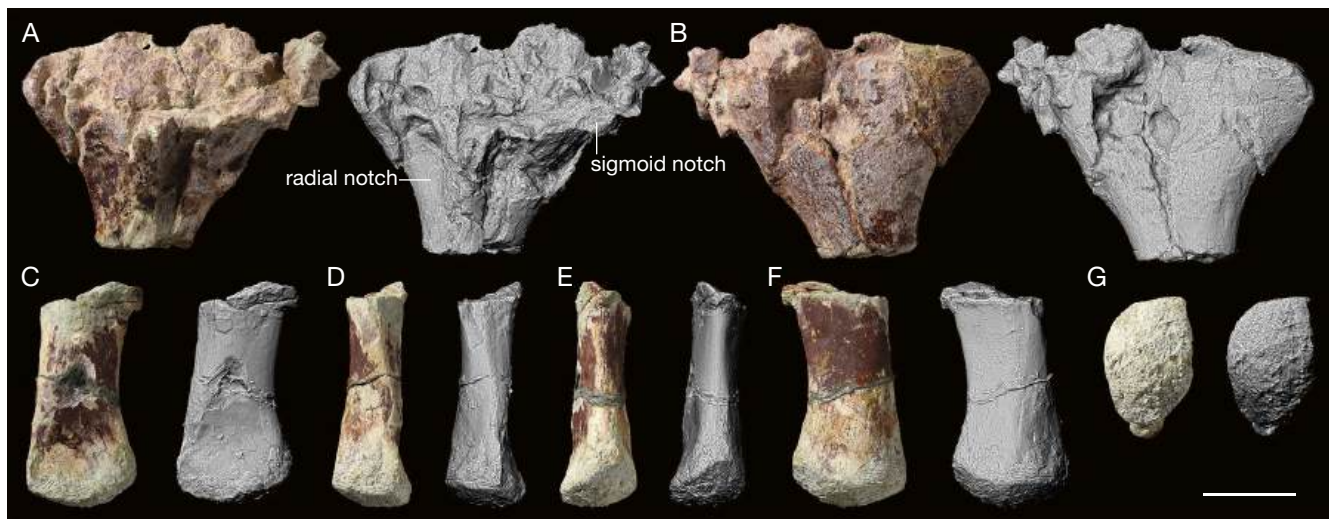


Fig. 13. — *Woznikella triradiata* n. gen., n. sp., ZPAL V. 34/1/9, ?left ulna: A, B, proximal part in dorsal (anterior) (A), and ventral (posterior) (B) view; C–G, distal part in dorsal (anterior) (C), medial (D), lateral (E), ventral (posterior) (F), and distal (G) view. Scale bar: 5 cm.

Procoracoid

The right procoracoid (ZPAL V. 34/1/107; Fig. 11E, F) is preserved almost in its entirety but with its anterior end damaged. The facet for the scapula lacks sutural characteristics and the ventral edge is rounded and porous, but it is unclear whether this state is caused by weathering or if the bone was still finished in cartilage at the time of the animal's death. The posterior suture with the coracoid is nearly straight and closed – it is recognizable as a raised, rugose ridge on both the visceral and external surface of the specimen. The procoracoid foramen is fully enclosed by the procoracoid, although it is very close to the contact with the scapula, especially on the visceral side. As a result, its walls are directed slightly posteroventrally. The procoracoid is very gently sigmoid in anterior view, with its ventral part thin and faintly directed medially. Its external surface is otherwise nearly flat. Viscerally, however, there is a pronounced thickening forming a rounded shelf below the procoracoid foramen and in the posterodorsal part of the bone, behind the foramen and close to the glenoid. There is no indication that the procoracoid itself contributed to the articular surface of the glenoid, unlike, e.g., *Tetragonias njalilus* (see Cruickshank 1967).

Coracoid

Only a minute part of the anterior edge of the right coracoid is preserved connected by a closed, nearly straight suture to the right procoracoid (ZPAL V. 34/1/107; Fig. 11E, F). Nothing can be said about that bone other than that the preserved part thickens dorsally, towards the glenoid area.

Clavicle

Both clavicles are preserved (right ZPAL V. 34/1/74, left ZPAL V. 34/1/75; Fig. 12) but the medial ends of both are broken near the area for contact with the interclavicle. Each clavicle is twisted; the lateral part is vertical while the medial end is horizontal. The lateral part is gently bent posteriorly.

The lateral end with the area of contact with the acromion process of scapula is well preserved and well developed. Its anterior surface is convex, whereas the posterior one is concave in ventral part and its dorsal part forms a massive ridge along the dorsal edge of the lateral half of the bone. The ventral edge of the lateral end forms a ridge along the posterior margin of the rest of the clavicle. Unlike in *Sinokannemeyeria yingchiaoensis*, the clavicles of *Woznikella triradiata* n. gen., n. sp. lack finger-like processes at the scapular ends (Sun 1963). This may be taxonomic or may result from their incomplete ossification due to young ontogenetic age in the individual.

Humerus

The right humerus (ZPAL V. 34/1/6; Fig. 13) is preserved in two parts, lacks the anterior portion of the proximal end and the midshaft, and most of the ventral surfaces of the preserved fragments are heavily damaged. The articular surface of the proximal end is slightly raised and subtriangular in dorsal aspect, but still rather inconspicuous (Fig. 13A, C, F), at least in part due to taphonomic factors, but possibly also due to immature ontogenetic age of the individual – the well-preserved fragments of its surface are porous, indicative of a well-developed cartilaginous finish. As in *Kannemeyeria simocephalus*, its distal corner terminates in a gentle ridge (Govender 2005; Govender et al. 2008). Similarly, the medial process (insertion of *m. subcoracoscapularis*) is short, lacks any rounded tip, lies nearly in line with the posterior (medial) surface of the shaft, and takes form of a relatively short, raised lip, continuous along the proximal and posterior edge of the proximal humeral end, rather than a distinct projection. In that respect, it is similar to, e.g., cf. *Dolichuranus primaevus*, *Lisowicia bojani*, *Parakannemeyeria shenmuensis*, *Parakannemeyeria youngi*, *Sinokannemeyeria yingchiaoensis*, the morphotype B stahleckeriid of Govender (2005), possibly *Eubrachiosaurus browni* and – to some extent – *Angonisaurus cruckshanki*, *Kannemeyeria simocephalus*, and *Sinokannemeyeria pearsoni*, but

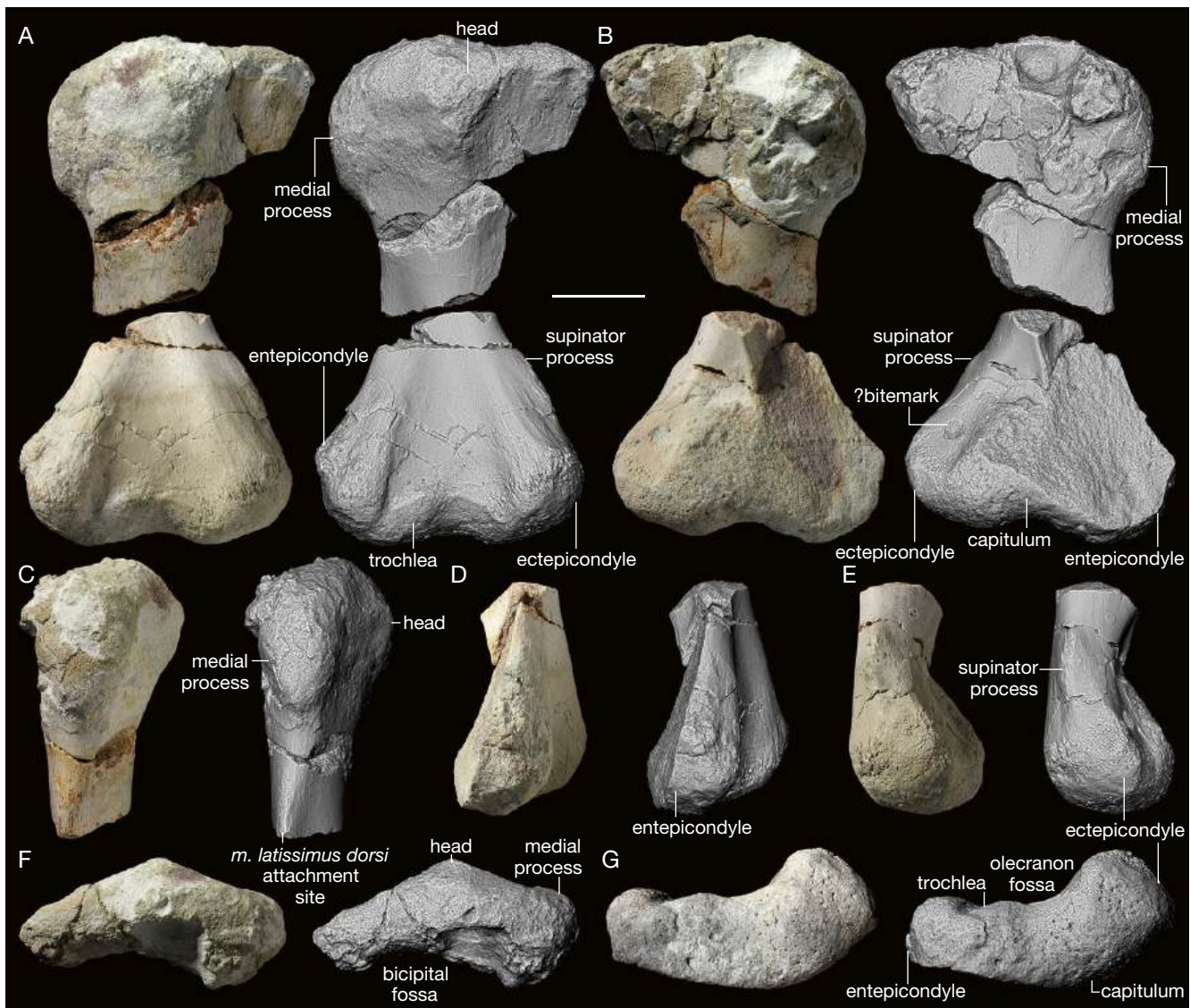


FIG. 14. — *Woznikella triradiata* n. gen., n. sp., ZPAL V. 34/1/6, right humerus: **A**, dorsal view; **B**, ventral view; **C**, proximal part in posterior (medial) view; **D**, **E**, distal part in posterior (medial) (**D**), and anterior (lateral) (**E**) view; **F**, proximal view; **G**, distal view. Scale bar: 5 cm.

different from, e.g., *Dinodontosaurus* sp. ("*Dicynodon turpior*"), *Dinodontosaurus tener*, at least some representatives of *Lystrosaurus* and *Placerias hesternus*, *Shansiodon wangi*, *Stahleckeria potens*, *Wadiasaurus indicus*, *Xiyukannemeyeria brevirostris*, and *Zambiasaurus submersus* (see Williston 1904; Watson 1917; Pearson 1924b; von Huene 1935; Young 1937; Camp & Welles 1956; Yeh 1959; Sun 1963, 1978; Cox 1965, 1969; Cheng 1980; Bandyopadhyay 1988; Lucas & Harris 1996; Lucas 2002; Govender 2005; Ray 2006; Dzik *et al.* 2008a; Govender *et al.* 2008; Govender & Yates 2009; Kammerer *et al.* 2013; Sulej & Niedzwiedzki 2019). A similar morphology is also present in the specimen MCZ 3118 of *Ischigualastia jensi* as pictured by Cox (1965), but the specimen PVL 3807 has a more pronounced rounded medial process (Kammerer *et al.* 2013). The proximal end thickens in that area, but the significant damage of the ventral surface obscures details of the morphology. The deltopectoral crest is not preserved, so its

exact size and shape cannot be determined, but based on the curvature of the proximal edge of the proximal end, at least proximally it did not reach much further anteriorly (laterally) from the proximal condyle than the medial process reaches posteriorly (medially). The bicipital fossa in the preserved part seems to be relatively shallow and gently concave, but the ventral surface is significantly damaged (Fig. 13B, F). The attachment of *m. latissimus dorsi* is inconspicuous, taking form of a rugose, longitudinally extended area (Fig. 13C). The distal end is relatively well preserved in dorsal aspect, presenting a marked smaller entepi- and larger ectepicondyle with rugosities and porous distal surfaces indicative of a cartilaginous cap (Fig. 13A, B, D, E, G). The distal end is slightly narrower than the proximal end. Its outline in this aspect is triangular and its anterior (lateral) and posterior (medial) expansion is relatively gentle and symmetrical, similar to that in *Kanne-meyeria simocephalus*, some specimens of *Lystrosaurus* spp.

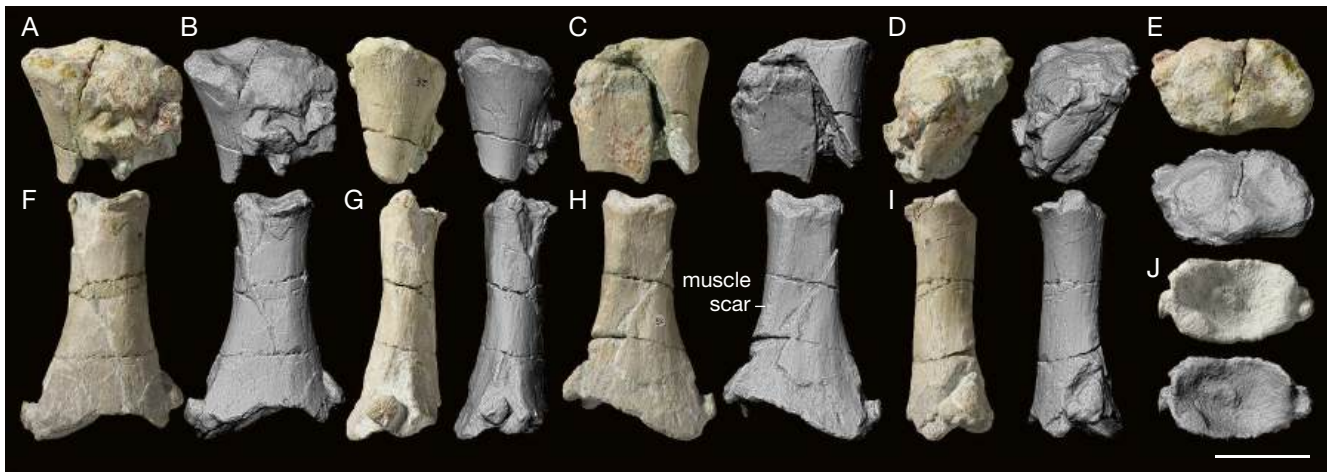


Fig. 15. — *Woznikella triradiata* n. gen., n. sp., ZPAL V. 34/1/10, right radius: A–E, proximal part in dorsal (anterior) (A), lateral (B), ventral (posterior) (C), medial (D), and proximal (E) view; F–J, distal part in dorsal (anterior) (F), lateral (G), ventral (posterior) (H), medial (I), and distal (J) view. Scale bar: 5 cm.

(except *L. georgi*, *L. hedini*, '*Lystrosaurus weidenreichi*' Young, 1939, and some specimens from South Africa and Antarctica; see Young 1935, 1939; Colbert 1974; DeFauw 1986; Surkov *et al.* 2005), and *Zambiasaurus submersus*, but unlike, e.g., cf. *Acratophorus argentinensis*, *Dolichuranus primaevus*, *Dinodontosaurus tener*, *Dinodontosaurus* sp. ("Dicynodon turpior"), *Eubrachiosaurus browni*, *Ischigualastia jensi*, *Parakannemeyeria dolichocephala*, *Parakannemeyeria ningwuensis*, *Pentasaurus goggai*, some (but apparently not all – see Camp & Welles 1956) specimens of *Placerias hesternus*, *Rhinodicynodon gracile*, *Sangusaurus parringtonii*, *Shansiodon wangi*, *Sinokannemeyeria baideroyuensis*, *Sinokannemeyeria pearsoni*, *Sinokannemeyeria sanchuanheensis*, *Sinokannemeyeria yingchiaoensis*, *Stahleckeria potens*, *Wadiasaurus indicus*, or *Xiyukannemeyeria brevirostris* (Williston 1904; Watson 1917; Pearson 1924b; von Huene 1935; Young 1937; Camp 1956; Yeh 1959; Sun 1960, 1963, 1978; Tripathi & Puri 1961; Cox 1965, 1969; Bonaparte 1966a, 1967; Colbert 1974; Cheng 1980; Bandyopadhyay 1988; Lucas & Harris 1996; Lucas 1998, 2002; Surkov 1998a; Surkov *et al.* 2005; Vega-Dias *et al.* 2005; Morato 2006; Ray 2006; Govender *et al.* 2008; Govender & Yates 2009; Kammerer *et al.* 2013; Angielczyk *et al.* 2014, 2017; Liu 2015; Kammerer 2018; Kammerer & Ordoñez 2021). It should be noted, however, that the proportions, symmetry, and shape of the distal humeral end are in Kannemeyeriiformes subject to change during ontogeny and intraspecific variability (Cox 1969; Kammerer *et al.* 2013; Angielczyk *et al.* 2014). The supinator process is easily noticeable, proximodistally elongated and rugose, but rather low (Fig. 13B, E). This morphology differs from non-kannemeyeriiform dicynodonts and *Dinodontosaurus tener* which lack the supinator process (Morato 2006; Kammerer 2018), but also stahleckerines (*Eubrachiosaurus browni*, *Ischigualastia jensi*, *Stahleckeria potens*) and *Lisowicia bojani*, which have a very pronounced, tab-like supinator process (Williston 1904; Cox 1965; Vega-Dias *et al.* 2005; Dzik *et al.* 2008a; Kammerer *et al.* 2013; Kammerer 2018; Sulej & Niedźwiedzki 2019). In that respect, it resembles *Pentasaurus goggai* and *Zambiasaurus submersus* the

most (Cox 1969; Angielczyk *et al.* 2014; Kammerer 2018). The intercondylar groove is well-defined both distally and dorsally. The olecranon fossa is well expressed distally but fades towards the base of the distal end, its broadly concave and its anterior (lateral) and posterior (medial) edges are rounded. The trochlea is readily distinguishable but relatively low and restricted in extent. In ventral aspect, most of the surface except for the anterior (lateral) portion is destroyed. Most of the capitulum and the edges of the entepicondylar foramen are not preserved. Distal to the supinator process, on the ventral surface of the bone, a single, oval puncture is present, likely a bite mark (Fig. 13B). The incompleteness of the bone makes it impossible to establish the exact inclination (angle) between the proximal and distal end, but it seems to have been relatively low.

Ulna

The probable left ulna (ZPAL V. 34/1/9; Fig. 14) is mostly complete (despite the lack of the olecranon process), but its proximal end is severely damaged and distorted, making identification difficult. As preserved, the proximal end is wide, roughly triangular in anteroposterior (dorsoventral) view (Fig. 14A, B). In anterior (dorsal) aspect, a clearly marked radial notch and a gently bowed outline of what seems to be the sigmoid notch are visible (Fig. 14A). Although the lack of olecranon may be an effect of damage or immaturity of the individual, the whole edge of the sigmoid process is sharp, unlike the very rounded edges in the specimens of the (juvenile or worn) holotype of *Shaanbeikannemeyeria "buerdongia"* figured by Li (1980) or juvenile *Stahleckeria potens* figured by Lucas (2002) and Vega-Dias *et al.* (2005). It particularly differs from the ulnae of, e.g., *Ischigualastia jensi*, *Lisowicia bojani*, *Parakannemeyeria youngi*, *Placerias hesternus*, *Shansiodon wangi*, *Sinokannemeyeria yingchiaoensis*, *Stahleckeria potens*, *Wadiasaurus indicus*, and the unidentified kannemeyeriid from the Baidao Yu locality (IVPP V 19365) which have nearly vertical sigmoid notches (von Huene 1935; Romer & Price 1944; Camp & Welles 1956; Yeh 1959; Sun

1963; Cox 1965; Bandyopadhyay 1988; Lucas 1993a; Ray 2006; Liu 2015; Sulej & Niedźwiedzki 2019). Despite the damage, the curvature of the bone is clearly visible, as the proximal end is gently turned and expanded medially. The distal end of the bone is slightly expanded, fusiform in distal view, ends bluntly and is rather featureless (Fig. 14C-G), in a manner resembling, e.g., juvenile *Dinodontosaurus tener*, *Dolichuranus primaevus*, *Jachaleria candelariensis*, *Kannemeyeria simocephalus*, *Lystrosaurus* spp., *Parakannemeyeria youngi*, and *Zambiasaurus submersus* (see Young 1935; Sun 1963; Cox 1969; Colbert 1974; Vega-Dias & Schultz 2004; Govender 2005; Morato 2006; Govender *et al.* 2008; Govender & Yates 2009). Unlike, e.g., *Dinodontosaurus tener* as figured by Cox (1965), it lacks a pronounced medial process for contact with the radius. Right above the distal end, in anterior (dorsal) aspect there is a gentle depression, likely accommodating the distal end of the radius, but possibly exaggerated by crushing (Fig. 14C-E). Despite the crushing, the ulna is significantly more gracile than in the juvenile *Dinodontosaurus tener* figured by Morato (2006), *Lisowicia bojani* figured by Sulej & Niedźwiedzki (2019), and in *Stahleckeria potens* as figured by Lucas (2002) and Vega-Dias *et al.* (2005). The diagnostic value of this character is unclear, however, as the ulna of the latter was described by Vega-Dias *et al.* (2005) as diagenetically swollen.

Radius

The proximal end of the right radius (ZPAL V. 34/1/10. Fig. 15) is crushed, and the proximal part of the shaft and the distal end are missing as well. Despite crushing, the proximal articular surface is subovoid with the lateral portion gently directed ventrally (posteriorly) in a comma-shaped fashion (Fig. 15E). The edge of this portion is gently raised and rounded, surrounding a subtle depression. Medially, this depression is limited by a comparably gentle convexity, comprising most of the articular surface. The raised edges of the lateral portion do not merge smoothly with the convexity, but instead they end medially as low but noticeable bumps, separated from the convexity by shallow fossae. This separation may, however, be an artifact of preservation or preparation, or an effect of incomplete ossification. In the dorsal (anterior) and ventral (posterior) view the edges of the proximal articular surface are sinuous, with the lateral part of the edge higher than the medial part in the anterior (dorsal) view and the medial part of the edge being higher than the lateral part in the posterior (ventral) view. Due to this sinuousness, the articular convexity is exposed in the anterior (dorsal) view (Fig. 15A). This shape may be impacted by crushing, but other dicynodonts (e.g., *Jachaleria candelariensis*) show a similar morphology (e.g., Vega-Dias & Schultz 2004). The shaft is relatively slender and as preserved the bone shows only moderate expansion at each end. Distally, the specimen is slightly flattened anteroposteriorly (dorsoventrally) and ends in a sediment-filled concavity, either as a result of taphonomical processes or incomplete ossification due to immaturity of the individual (Fig. 15J). There is no evidence of pronounced distal expansions, such as in *Stahleckeria potens* or *Dinodontosaurus tener*

radii (Romer & Price 1944; Lucas 2002; Vega-Dias *et al.* 2005; Morato 2006). Along the anterolateral edge of the bone an elongated muscle scar is present, directed slightly proximo-medially. The damage and incompleteness of the specimen preclude observation of further meaningful features. In general outline, the bone resembles the radius of *Dinodontosaurus* sp. ("*Dicynodon turpior*"), *Dinodontosaurus tener*, at least some species of *Lystrosaurus*, *Shaanbeikannemeyeria xilougouensis*, *Sinokannemeyeria baidaoyuensis*, *Sinokannemeyeria yingchiaoensis*, *Xiyukannemeyeria brevirostris*, as well as *Parakannemeyeria* sp., *Jachaleria candelariensis*, or *Wadiasaurus indicus*, but is not as robust as the latter three (von Huene 1935; Young 1935; Sun 1963, 1978; Cox 1965; Colbert 1974; Li 1980; Bandyopadhyay 1988; Lucas & Harris 1996; Vega-Dias & Schultz 2004; Ray 2006; Liu 2015; Liu 2022). It differs from the radii of, e.g., *Ischigualastria jensi*, *Stahleckeria potens*, and *Wadiasaurus indicus*, which are much less gracile (von Huene 1935; Romer & Price 1944; Cox 1965; Lucas 2002; Vega-Dias *et al.* 2005; Ray 2006).

Femur

The left femur (ZPAL V. 34/1/8; Fig. 16) is preserved in three pieces: the proximal end (Fig. 16A-E), part of the shaft (Fig. 16F-I), and the medial condyle (Fig. 16J-M). The articular surface of the proximal head is nearly circular in proximal view (Fig. 16B) and gently turned anteromedially (Fig. 16A), although still directed mostly proximally. Unlike, e.g., *Ischigualastria jensi*, *Placerias hesternus*, *Rhinodicynodon gracile*, *Shansiodon wangi*, or *Sinokannemeyeria pearsoni*, there is no clear neck separating it from the rest of the proximal end (Young 1937; Camp & Welles 1956; Yeh 1959; Cox 1965; Surkov 1998a; Kammerer *et al.* 2013). Still, the proximal end is more geometrically complex than in most Permian dicynodonts and *Lystrosaurus* spp. (e.g., Young 1935; Colbert 1974; Yuhe 1983; DeFauw 1986; Surkov *et al.* 2005; Ray 2006). The greater trochanter is roughly half the size of the articular head, both in the anteroposterior (Fig. 16A, D) and in the proximal aspect (Fig. 16E), but it is clearly demarcated, unlike in e.g., *Dinodontosaurus tener*, *Dolichuranus primaevus*, *Kannemeyeria simocephalus*, the specimen figured by Pearson (1924b) as *K. simocephalus* (but not attributable to that species according to Govender 2005 and Govender & Yates 2009), *Shaanbeikannemeyeria xilougouensis*, or the unnamed stahleckeriids from the Manda Beds (NMT RB463) and the Pekin Formation (NCSM 21719) (Pearson 1924b; Govender 2005; Morato 2006; Govender & Yates 2009; Green 2012; Kammerer *et al.* 2013, 2017; Liu 2022). In proximal aspect it is positioned approximately at the level of the middle of the articular head (Fig. 16E), unlike, e.g., *Dinodontosaurus tener* and *Sangusaurus parringtonii*, in which the greater trochanter is aligned with the posterior limit of the articular head (Morato 2006; Angielczyk *et al.* 2017), but similar to *Lisowicia bojani*, *Tetragonias njalilus*, the unnamed Manda Beds specimens (Cruickshank 1967; Kammerer *et al.* 2017; Sulej & Niedźwiedzki 2019), and *Placerias hesternus* (pers. obs.), although in the latter four the major trochanter is less bulbous. The outline of the proximal end in anteroposterior aspect resembles *Tetragonias njalilus* specimen UMCZ T754

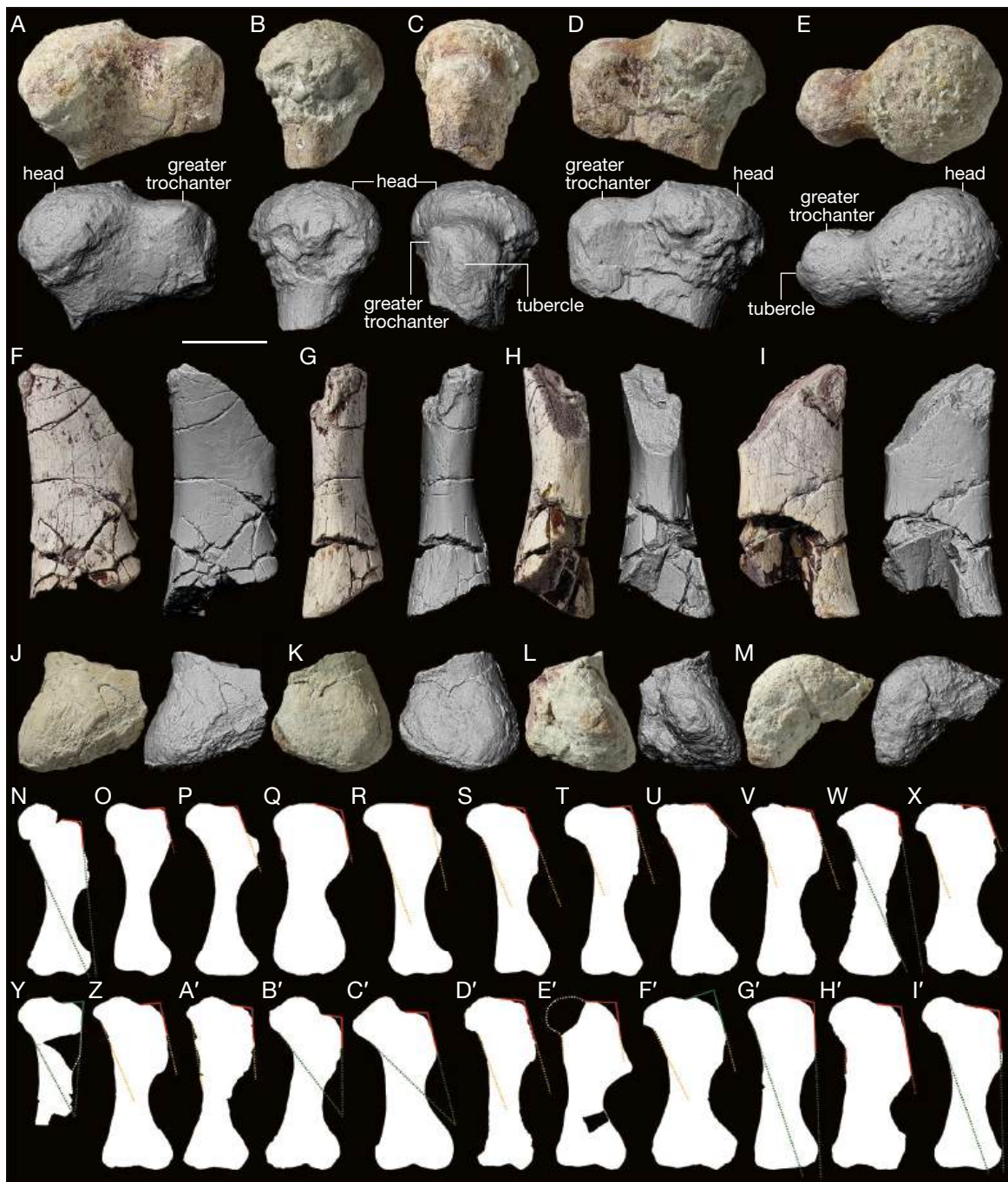


FIG. 16. — Kannemeyeriiform femora: **A–M**, *Woznikella triradiata* n. gen., n. sp., ZPAL V. 34/1/8, left femur: **A–E**, proximal part in anterior (**A**), medial (**B**), lateral (**C**), posterior (**D**), and proximal (**E**) view; **F–I**, shaft in anterior (**F**), medial (**G**), lateral (**H**), and posterior (**I**) view; **J–M**, medial condyle in anterior (**J**), medial (**K**), posterior (**L**), and distal (**M**) view; **N–I'**, outlines of femora (not to scale): **N**, “*Ruhuhuangulasaurus croucheri*” NHMUK R12710 (after Kammerer et al. 2017); **O**, *Rhinodicynodon gracile* Kalandadze, 1970 PIN 1579/50 (after Surkov 1998a); **P**, *Tetragonias njalilis* (von Huene, 1942) GPIT/RE/7110 (after Kammerer et al. 2017); **Q**, *Dinodontosaurus tener* (von Huene, 1935) UFRGS/PV0113T (after Morato 2006); **R**, *Acrapophorus argentinensis* Kammerer & Ordoñez, 2021 PVL 3465 (Bonaparte 1966a); **S**, *Wadiasaurus indicus* Chowdhury, 1970 ISI R172/1 (after Bandyopadhyay 1988); **T**, *Sinokannemeyeria pearsoni* Young, 1937 (number not given, after Young 1937); **U**, *Parakannemeyeria youngi* Sun, 1963 IVPP V 972 (after Sun 1963); **V**, *Shaanbeikannemeyeria xilouguensis* Cheng, 1980 IVPP V 6033 (after Li 1980); **W**, young *Kannemeyeria simocephalus* (Weithofer, 1888) UMZC T757 (after Kammerer et al. 2017); **X**, *Kannemeyeria simocephalus* (Weithofer, 1888) NHMUK R3740 (after Kammerer et al. 2017); **Y**, *Woznikella triradiata* n. gen., n. sp., ZPAL V. 34/1/8; **Z**, *Stahleckeria potens* von Huene, 1935 GPIT unnumbered (after Kammerer et al. 2017); **A'**, *Sangusaurus parringtoni* Cruickshank, 1986a UMZC T1225 (after Kammerer et al. 2017); **B'**, *Ischigualastia jensi* Cox, 1962 PVL 3807 (after Kammerer et al. 2017); **C'**, *Ischigualastia jensi* MCZ 3120 (after Cox 1965); **D'**, stahleckeriid NMT RB463 (after Kammerer et al. 2017); **E'**, stahleckeriid NMMNH P-13001 (after Kammerer et al. 2013); **F'**, morphotype B stahleckeriid BP/1/3518 (after Govender 2005); **G'**, *Zambiasaurus submersus* Cox, 1969 NMNH R9123 (after Angielczyk et al. 2014); **H'**, *Lisowicia bojani* Sulej & Niedzwiedzki, 2019 ZPAL V.33/74 (after Sulej & Niedzwiedzki 2019); **I'**, *Placerias hesternus* Lucas, 1904 UCMP 3294 (after Kammerer et al. 2013). Indicated is an approximate angle between the dorsal (just lateral to the head) and lateral (immediately behind the curve) surfaces of the greater trochanter (green if acute, red if obtuse) as well as the arrangement between the proximal medial (just distal to the head) and lateral edges of the bone: green if clearly converging (tangents meet along or just distal to the bone length, the bone decreases in diameter in its proximal part), orange if subparallel (tangents never meet or meet far beyond the distal end of the bone, the bone keeps roughly constant diameter in its proximal part), red if clearly diverging (tangents never meet, the bone increases in diameter in its proximal part). Scale bar: 5 cm.

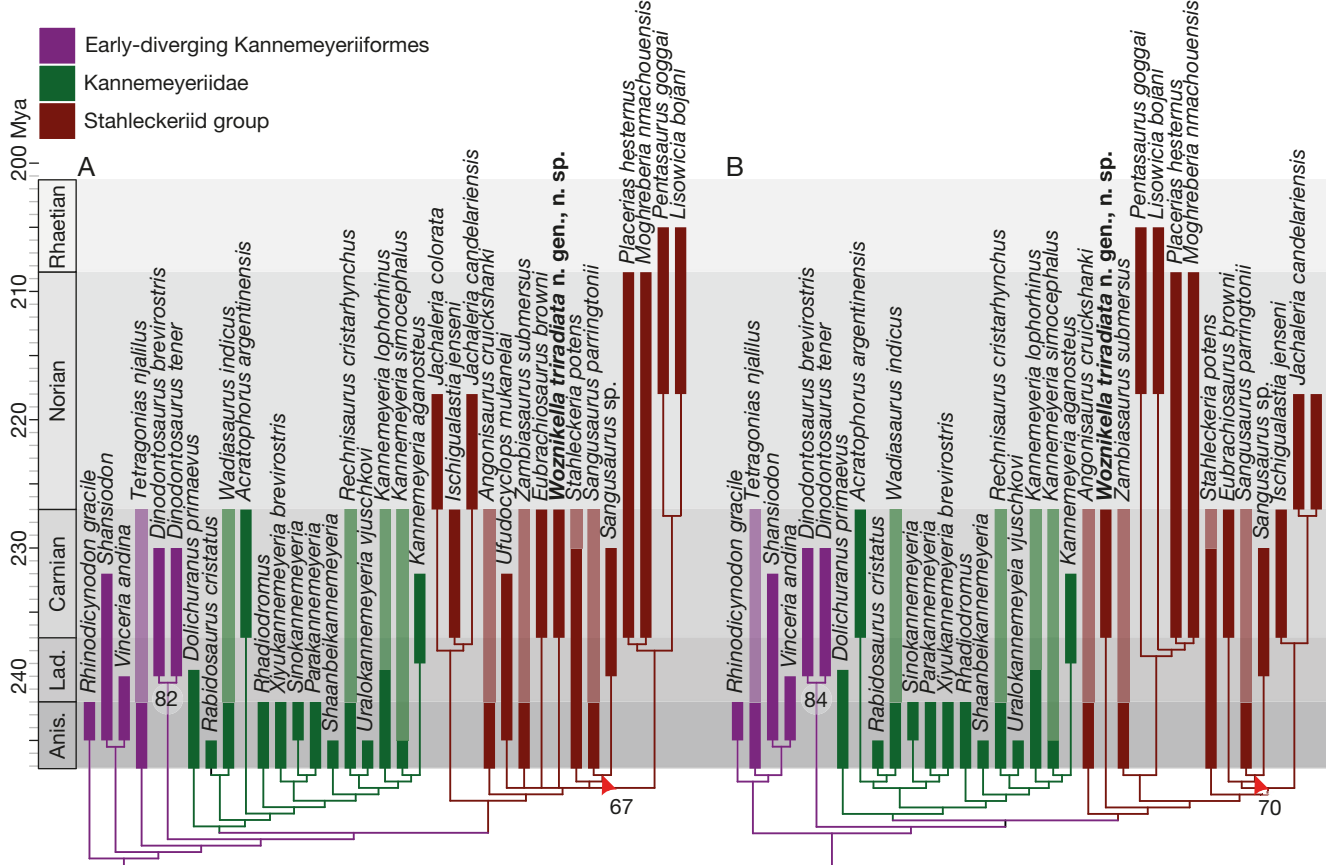


FIG. 17. — Phylogeny of Kannemeyeriformes: **A**, strict consensus tree based on the analysis with all taxa included; **B**, majority rule (50%) consensus tree based on the analysis with *Ufudocyclops mukanelai* Kammerer, Viglietti, Hancox, Butler & Choiniere, 2019 inactivated (the topology used for paleobiogeographic analyses; strict consensus differs only in the presence of an unresolved polytomy of *Eubrachiosaurus browni* Williston, 1904, *Sangusaurus parringtonii* Cruickshank, 1986a, and *Sangusaurus* sp.). Numbers next to nodes indicate bootstrap values above 50. Lighter parts of stratigraphic ranges indicate uncertainty of the ages of the Manda, Ntawere, and Yerrapalli formations (see text for discussion).

figured by Kammerer *et al.* (2013; but much less so the specimen figured by Cruickshank 1967), and the unnamed Manda Beds stahleckeriid (NMT RB463) both in anteroposterior and mediolateral aspects (Kammerer *et al.* 2017). Laterally, the greater trochanter projects a tubercle, narrower than its main body and limited in proximodistal span (Fig. 16C). The third trochanter is not preserved and there is no indication of a pronounced trochanteric crest spanning between the greater and third trochanter, at least in the proximal part of the bone. Unlike most dicynodonts, the mediolateral diameter of the bone starts to clearly decrease just below the tip of the trochanter major (Fig. 16N-I'). This is unlike, e.g., *Dolichurarus primaevis*, *Dinodontosaurus tener*, *Dinodontosaurus* sp. (“*Dicynodon turpior*”), *Lisowicia bojani*, at least some species of *Lystrosaurus*, *Parakannemeyeria youngi*, *Rhinodicyndon gracile*, *Sangusaurus parringtonii*, *Shaanbeikannemeyeria xilouguensis*, *Shansiodon wangi*, *Sinokannemeyeria pearsoni*, *Stahleckeria potens*, *Wadiasaurus indicus*, the unnamed Denwa Formation specimens, the unnamed Pekin Formation specimen (NCSM 21719), the unnamed stahleckeriid from the Santa Rosa Formation (NMMNH P-13001), and the morphotype B stahleckeriid of Govender (2005) but similar to, e.g., young *Kannemeyeria simocephalus* and possibly *Parakannemeyeria dolichocephala* (see

von Huene 1935; Young 1935, 1937; Yeh 1959; Sun 1963; Cox 1965; Li 1980; Yuhe 1983; Cruickshank 1986b; DeFauw 1986; Bandyopadhyay 1988; Lucas & Harris 1996; Surkov 1998a; Bandyopadhyay & Sengupta 1999; Govender 2005; Morato 2006; Ray 2006; Dzik *et al.* 2008a; Govender *et al.* 2008; Govender & Yates 2009; Green 2012; Kammerer *et al.* 2013; Angielczyk *et al.* 2017; Sulej & Niedzwiedzki 2019). A clear trochanteric crest is present in the *Ischigualastia jensi* specimen figured by Cox (1965), but in the specimen PVL 3807 the morphology is more reminiscent of ZPAL V. 34/1/8 (Kammerer *et al.* 2013). Some dicynodonts, such as *Acratophorus argentinensis*, *Placerias hesternus* (pers. obs.), and the Manda Beds stahleckeriid (NMT RB463), exhibit a trochanteric crest that originates proximally wide and inconspicuous in height, but becomes thinner and/or more pronounced distally (Bonaparte 1966a, 1967, Kammerer *et al.* 2017), whereas *Tetragonias njalilus* has a more distinct separation of the major and third trochanter (Fröbisch 2006; Kammerer *et al.* 2017); such morphologies cannot be ruled out for ZPAL V. 34/1/8 due to its incompleteness. Juvenile *Zambiasaurus submersus* has a rather shallow trochanteric crest, but the greater trochanter is apparently narrower and less bulbous than in ZPAL V. 34/1/8 – the morphology in adults is unfortunately unknown (Cox 1969).



FIG. 18. — Paleobiogeographic analysis of dicynodonts. Ancestral states estimated based on BioGeoBEARS analysis (DEC+J). Note that region names are based on the known dicynodont-yielding localities included in the regions and thus do not accurately reflect their potential geographic extent. Triassic taxa indicated in **bold**.

TABLE 3. — Occurrences of Triassic tracks possibly produced by dicynodonts. Note that the list is not comprehensive and likely numerous other mentions exist, particularly in local, non-English literature. The Country column includes all mentions deemed significant (i.e., not merely listing taxa from original literature, but providing mentions, descriptions, and/or images of new specimens, original data or reinterpretations of morphology, confirming the geographical and/or temporal presence of taxa, confirming or providing novel insights into their validity, or at least presenting them in a novel biostratigraphic context). For simplicity, the Formation column includes only the references providing the most recent and most precise subdivisions either verbatim or in a form unambiguously recognizable without extensive research of local geological literature. The historically used *Lystrosaurus* Cope, 1870 AZ was recently redefined and renamed to *Lystrosaurus declivis* Brink, 1951 AZ (Botha & Smith 2020). Because of the presence of *Lystrosaurus* spp. also in the underlying *Lystrosaurus maccaigi* (Seeley, 1898)-*Moschorhinus* Broom, 1920 SZ of *Daptocephalus* Hoepen, 1934 AZ (former Dicynodon AZ), the meaning of the historical *Lystrosaurus* AZ is somewhat ambiguous and may be dependent on the author (see Table 2). Therefore, the name is used here in parentheses, implying that although in most cases it was probably synonymous with *Lystrosaurus declivis* AZ, it can potentially include the top of the *Daptocephalus* AZ. If the occurrence is not explicitly mentioned in the context of a changed naming scheme, the papers allowing referral (e.g., naming both the old formation and the new formation) are provided. Age includes selected single most recent original study with preference towards radiometric dates, unless those are unavailable, and a sound disagreement exists between several studies. Note that the bottom age (252.24 ± 0.11 Ma) of the *Lystrosaurus declivis* AZ obtained by Gastaldo *et al.* (2020) is barely about 0.3 Ma older than the currently recognized Triassic/Permian boundary (251.902 ± 0.024 Ma). See Botha *et al.* (2020) for the entirely Triassic estimation of the age of that assemblage and Botha & Smith (2020) for discussion. Abbreviation: AZ, assemblage zone. At least some *Dicynodontipus* spp. could be produced by cynodonts (e.g. Marchetti *et al.* 2019)

Taxon	Country	Formation	Age
?Dicynodont tracks	Poland (Sulej <i>et al.</i> 2011; Sadlok & Wawrzyniak 2013)	Grabowa (Sadlok & Wawrzyniak 2013; Szulc <i>et al.</i> 2015b; Racki & Lucas 2020)	Carnian (Sulej <i>et al.</i> 2011)/Norian (Szulc <i>et al.</i> 2015b)
" <i>Dicynodontipus</i> " <i>bellambiensis</i> Retallack, 1996	Australia (Retallack 1996; Klein <i>et al.</i> 2015; Francischini <i>et al.</i> 2018; Díaz-Martínez <i>et al.</i> 2019; Klein & Lucas 2021)	Coal Cliff Sandstone (Retallack 1996; Francischini <i>et al.</i> 2018; Díaz-Martínez <i>et al.</i> 2019)	Induan (Retallack 1996)
<i>Dicynodontipus geinitzi</i> (Hornstein, 1876)	England (Demathieu & Haubold 1971; Haubold 1974, 1984) Germany (Hornstein 1876; Rühle von Lilienstern 1944; Demathieu & Haubold 1971; Haubold 1971, 1974, 1984; Demathieu & Fichter 1989; Francischini <i>et al.</i> 2018; Díaz-Martínez <i>et al.</i> 2019; Klein & Lucas 2021)	Helsby Sandstone (Demathieu & Haubold 1971; Pollard 1981) Middle Buntsandstein (Demathieu & Fichter 1989)	Late Olenekian-Anisian (Medici <i>et al.</i> 2019) Early Triassic (German Stratigraphic Commission 2016)
<i>Dicynodontipus</i> isp.	Argentina (Casamiquela 1964, 1975; Haubold 1971, 1974, 1984; Leonardi & Oliveira 1990; Leonardi 1994; Marsicano & Barredo 2004; Melchor & de Valais 2006; Domnanovich & Marsicano 2006b; Calvo 2007; Domnanovich <i>et al.</i> 2008; Francischini <i>et al.</i> 2018; Citton <i>et al.</i> 2018a, b, 2019, 2021; Lagnaoui <i>et al.</i> 2019; Díaz-Martínez <i>et al.</i> 2019; De Valais <i>et al.</i> 2020) Brazil (Francischini <i>et al.</i> 2018; Díaz-Martínez <i>et al.</i> 2019) Catalonia (Valdiserri <i>et al.</i> 2009; Díaz-Martínez <i>et al.</i> 2019) England (Haubold 1971; Pollard 1981; Francischini <i>et al.</i> 2018) Germany (Demathieu & Haubold 1971; Haubold 1984; Klein & Lucas 2018; Díaz-Martínez <i>et al.</i> 2019)	Cerro de Las Cabras (Melchor & de Valais 2006; Francischini <i>et al.</i> 2018; Díaz-Martínez <i>et al.</i> 2019; Lagnaoui <i>et al.</i> 2019) Corral de Piedra (Marsicano & Barredo 2004; Melchor & de Valais 2006; Díaz-Martínez <i>et al.</i> 2019) Sierra de Las Higueras (Leonardi 1994; Melchor & de Valais 2006; Francischini <i>et al.</i> 2018) Los Menudos Complex (Melchor & de Valais 2006; Domnanovich & Marsicano 2006b; Calvo 2007; Domnanovich <i>et al.</i> 2008; Citton <i>et al.</i> 2018a, b, 2019, 2021; Francischini <i>et al.</i> 2018; Díaz-Martínez <i>et al.</i> 2019; De Valais <i>et al.</i> 2020) Pirambója (Francischini <i>et al.</i> 2018; Díaz-Martínez <i>et al.</i> 2019) Lower Buntsandstein (Valdiserri <i>et al.</i> 2009) Helsby Sandstone (Pollard 1981; Francischini <i>et al.</i> 2018) Buntsandstein (Demathieu & Haubold 1971; Haubold 1984) Middle Muschelkalk (Klein & Lucas 2018)	Late Anisian-early Ladinian (Cariglino <i>et al.</i> 2016) Late Carnian (Marsicano & Barredo 2004) Ladinian (Francischini <i>et al.</i> 2018) Late Permian-Early Triassic (Falco 2019) Late Permian-Induan (Francischini <i>et al.</i> 2018) Early Triassic (German Stratigraphic Commission 2016) Late Olenekian-Anisian (Medici <i>et al.</i> 2019) Olenekian-early Anisian (German Stratigraphic Commission 2016) Anisian (German Stratigraphic Commission 2016)
cf. <i>Dicynodontipus</i> isp.	South Africa (Díaz-Martínez <i>et al.</i> 2019; Marchetti <i>et al.</i> 2019; Botha & Smith 2020)	<i>Lystrosaurus declivis</i> AZ (Botha & Smith 2020)	Latest Permian-Early Triassic (Gastaldo <i>et al.</i> 2020)
? <i>Dicynodontipus</i> isp.	Germany (Demathieu & Haubold 1971)	Lower and Middle Buntsandstein (Demathieu & Haubold 1971)	Early Triassic (German Stratigraphic Commission 2016)
<i>Dolomites accordii</i> (Ceoloni, Conti, Mariotti & Nicosia, 1986)	South Africa (Watson 1960; Haubold 1971; Smith & Botha-Brink 2014; Marchetti <i>et al.</i> 2019; Klein & Lucas 2021)	" <i>Lystrosaurus</i> AZ" (Watson 1960; Haubold 1971; Marchetti <i>et al.</i> 2019; Klein & Lucas 2021)	Late Permian-Early Triassic (Gastaldo <i>et al.</i> 2020)

Table 3. — Continuation.

Taxon	Country	Formation	Age
<i>Dolomitipes</i> isp.	South Africa (Smith & Botha-Brink 2014; Marchetti et al. 2019)	" <i>Lystrosaurus</i> AZ" (Marchetti et al. 2019)	Late Permian-Early Triassic (Gastaldo et al. 2020)
?Lystrosaurid tracks	Antarctica (MacDonald et al. 1992)	Middle Fremouw (MacDonald et al. 1992)	Early Anisian (Elliot et al. 2017)
<i>Pentasauropus argentinae</i> Lagnaoui, Melchor, Bellosi, Villegas & Espinoza, 2019	Argentina (Marsicano & Barredo 2004; Porchetti & Nicosia 2007; Citton et al. 2018a; Díaz-Martínez et al. 2019; Lagnaoui et al. 2019; Klein & Lucas 2021)	Cerro de las Cabras (Díaz-Martínez et al. 2019; Lagnaoui et al. 2019)	Late Anisian-early Ladinian (Cariglino et al. 2016)
		Corral de Piedra (Díaz-Martínez et al. 2019; Lagnaoui et al. 2019)	Ladinian (Barredo et al. 2012)
		Los Menudos Complex (Domnanovich et al. 2008; Citton et al. 2018a; Díaz-Martínez et al. 2019; Lagnaoui et al. 2019)	Late Anisian-?Rhaetian (Díaz-Martínez et al. 2019)
<i>Pentasauropus incredibilis</i> Ellenberger, 1972	Lesotho (Ellenberger 1955, 1970, 1972; Ellenberger & Ellenberger 1958, 1960; Ellenberger et al. 1970; Haubold 1971, 1974, 1984; Olsen & Galton 1984; Porchetti & Nicosia 2007; Bordy et al. 2017; Kammerer 2018; Díaz-Martínez et al. 2019; Viglietti 2020; Klein & Lucas 2021)	Lower Elliot <i>Scalenodontoides</i> AZ (Viglietti et al. 2020b)	Norian-Rhaetian (Bordy et al. 2020)
<i>Pentasauropus</i> isp.	Argentina (Domnanovich et al. 2008; Citton et al. 2018a, b, 2019; Díaz-Martínez et al. 2019; Lagnaoui et al. 2019; De Valais et al. 2020)	Los Menudos Complex (Domnanovich et al. 2008; Citton et al. 2018a, b, 2019; Díaz-Martínez et al. 2019; Lagnaoui et al. 2019; De Valais et al. 2020)	Late Anisian-?Rhaetian (Díaz-Martínez et al. 2019)
	United States (Lockley & Hunt 1995; Lockley et al. 1996; Gaston et al. 2003; Hunt & Lucas 2007; Porchetti & Nicosia 2007; Hunt-Foster et al. 2016; Díaz-Martínez et al. 2019)	Rock Point (Lockley et al. 1996; Gaston et al. 2003; Hunt & Lucas 2007; Hunt-Foster et al. 2016; Díaz-Martínez et al. 2019)	Rhaetian (Ramezani et al. 2014)
cf. <i>Pentasauropus</i> isp.	United States (Olsen & Galton 1984; Conrad & Lockley 1986; Porchetti & Nicosia 2007; Díaz-Martínez et al. 2019)	Chinle Group (Conrad & Lockley 1986; Porchetti & Nicosia 2007) Gettysburg (Olsen & Galton 1984; Díaz-Martínez et al. 2019)	Norian-Rhaetian (Ramezani et al. 2014) Norian (Gee & Jasinski 2021)
?Therapsid tracks	Brazil (Leonardi 1994; Francischini et al. 2018) United States (Conrad et al. 1987; Lockley & Hunt 1995; Hunt & Lucas 2007)	Lower Sanga do Cabral (Leonardi 1994) Sloan Canyon (Conrad et al. 1987; Hunt & Lucas 2007)	Early Triassic (Dias-da-Silva et al. 2017) Rhaetian (Hunt & Lucas 2007)
Therapsid tracks	France (Ellenberger 1965; Courel et al. 1968) Italy (Avanzini et al. 2011) Poland (Klein & Niedźwiedzki 2012; Francischini et al. 2018)	Not given (Ellenberger 1965; Courel et al. 1968) Not given (Avanzini et al. 2011) Wióry (Klein & Niedźwiedzki 2012; Francischini et al. 2018)	Triassic (Courel et al. 1968) Anisian (Avanzini et al. 2011) Olenekian (Klein & Niedźwiedzki 2012)
<i>Therapsipus cumminsi</i> Hunt, Santucci, Lockley & Olson, 1993	United States (Hunt et al. 1993; Lockley & Hunt 1995; Nesbitt & Angielczyk 2002; Klein & Lucas 2010, 2021)	Moenkopi Holbrook Member (Hunt et al. 1993; Lockley & Hunt 1995; Nesbitt & Angielczyk 2002; Klein & Lucas 2010, 2021)	Late Anisian (Haque et al. 2021)
<i>Therapsipus</i> isp.	United States (Hunt & Lucas 1993; Lucas et al. 2003; Klein & Lucas 2010)	Moenkopi Anton Chico Member (Hunt & Lucas 1993; Lucas et al. 2003; Klein & Lucas 2010)	Late Anisian (Haque et al. 2021)
cf. <i>Therapsipus</i> isp.	France (Courel et al. 1968; Hunt et al. 1993) Poland (Klein & Niedźwiedzki 2012; Klein & Lucas 2021)	Not given (Courel et al. 1968; Hunt et al. 1993) Wióry (Klein & Niedźwiedzki 2012; Klein & Lucas 2021)	Early Triassic (Courel et al. 1968) Olenekian (Klein & Niedźwiedzki 2012)

The base of the proximal end is flattened anteroposteriorly, as is the preserved part of the shaft (Fig. 16F-I). The mediolateral diameter of these parts is similar, unlike in *Lystrosaurus* spp., *Sangusaurus parringtonii*, *Shansiodon wangi*, or *Wadiasaurus*

indicus in which the femur exhibits a clear constriction along the diaphysis (Young 1935; Yeh 1959; Yuhe 1983; Cruickshank 1986b; DeFauw 1986; Bandyopadhyay 1988; Ray 2006; Angielczyk et al. 2017). The medial condyle of the

TABLE 4. — Notable post-Permian tracks historically misidentified as belonging to ichnotaxa considered to potentially be produced by Dicynodontia.

Original description	Country	Comments
<i>Dicynodontipus prothoriooides</i> Silva, Carvalho, Fernandes, & Fergiolo, 2008 MCN-PIC.007/17-23, MCN-PIC.016/1-21, MCN-PIC.017/1-18, MCN-PIC.018/2-16	Brazil (Silva et al. 2008)	Tracks subsequently reinterpreted as <i>Procolophonichnium</i> spp. by Klein et al. (2015) and indeterminate tetrapods footprints by Klein & Lucas (2021)
“ <i>Dicynodontipus</i> isp.” LAR-Ic 1 and unnumbered specimens (Melchor & de Valais 2006; Melchor et al. 2006)	Argentina (Melchor & de Valais 2006; Melchor et al. 2006)	Melchor et al. (2006) and Melchor & de Valais (2006) noted the presence of <i>Dicynodontipus</i> isp. in the Santo Domingo Formation, which at the time they considered Late Triassic; however, this track-yielding surface of the Santo Domingo Formation was subsequently dated to Late Eocene (Melchor et al. 2013); thus, the tracks may rather belong to mammals (Klein & Lucas 2021)
“cf. <i>Gallegosichnus</i> sp.”/“cf. <i>Dicynodontipus</i> isp.” slab from Locality 2 (Demathieu & Wycisk 1990)	Egypt (Demathieu & Wycisk 1990)	Small tracks from the Turonian (Late Cretaceous) Abu Agag Formation described by Demathieu & Wycisk (1990) as cf. <i>Gallegosichnus</i> sp. – an ichnospecies subsequently synonymized with the ichnospecies <i>Dicynodontopus</i> by Melchor & de Valais (2006); possibly mammal tracks?

distal end (Fig. 16J-M) terminates at a relatively sharp angle in the anterior aspect and is relatively narrow and elongated anteroposteriorly in ventral view (Fig. 16M), similar as in the unnamed Manda Beds stahleckeriid (Kammerer et al. 2017). Its surface is rugose. The preserved fragment indicates a clear separation of the condyles both in the anteroposterior and in the distal aspect.

RESULTS OF THE PHYLOGENETIC ANALYSIS

The analysis including all taxa resulted in six most parsimonious trees (best score 1259.090, CI = 0.223, RI = 0.718). The obtained topology of non-kannemeyeriiform dicynodonts is identical as that recovered by Kammerer & Ordoñez (2021) but some differences appeared within the Kannemeyeriiformes (Fig. 17A). The topology does not include a monophyletic Shansiodontidae, with *Rhinodicynodon gracile*, (*Vinceria andina* + *Shansiodon* spp.), *Tetragonias njalilus*, and *Dindontosaurus* spp. successively occupying the stem of (Kannemeyeriidae + Stahleckeriidae). *Dolichurarus primaevus* is recovered as the basalmost member of the Kannemeyeriidae, followed by (*Wadiasaurus indicus* + *Rabidosaurus cristatus*), *Acratophorus argentinensis*, *Rhadiodromus*, (*Xiyukannemeyeria brevirostris* (*Parakannemeyeria* + *Sinokannemeyeria*)), and the more derived kannemeyeriids as in Kammerer & Ordoñez (2021). Interestingly, a clade (*Jachaleria colorata* + (*Jachaleria candelariensis* + *Ischigualastia jensi*)) is recovered as sister to *Angonisaurus crickshanki* + the remainder of stahleckeriids. The six trees differ in the position of *Ufudocyclops mukanelai* as a sister group to either (*Woznikella triradiata* n. gen., n. sp. + Placeriinae) (tree 1, no synapomorphies), *Woznikella triradiata* n. gen., n. sp. (character 56: nasal bosses present as paired swellings near the dorsal or posterodorsal margin of external nares), Placeriinae (tree 4, no synapomorphies), *Zambiasaurus submersus* (character 132: occipital condyle distinctly tri-radiate in posterior view), Stahleckeriinae Lehman, 1961 (*Jachaleria* spp. and *Ishigualastia jensi* excluded; character 40: notch on dorsal edge of narial opening absent), or *Eubrachiosaurus browni* (tree 5, no synapomorphies). In all the trees, *Woznikella triradiata* n. gen., n. sp. is nested at the base of the Placeriinae,

with (*Lisowicia bojani* + *Pentasaurus goggai*) as a sister group to (*Moghreberia nmachouensis* + *Placerias hesternus*). *Stahleckeria potens* is recovered as a sister group to *Sangusaurus* spp. In the consensus tree, the instability of *Ufudocyclops mukanelai* caused a large polytomy in Stahleckeriidae King, 1988, which made the obtained topology unusable for the paleobiogeographic analysis. For that reason, another analysis with *Ufudocyclops mukanelai* inactivated was performed.

The second analysis resulted in 3 most parsimonious trees (best score 1259.090, CI = 0.224, RI = 0.720). Surprisingly, the removal of *Ufudocyclops mukanelai* impacted the topology of non-kannemeyeriiforms (Fig. 18). The clade of (*Peramodon amalitzkii* (Sushkin, 1926) (*Daptocephalus* spp. (*Turfanodon bogdaensis* (Sun, 1973) + *Dinanomodon gilli* (Broom, 1932)))) is located closer to Kannemeyeriiformes than (*Vivaxosaurus trautscholdi* (Amalitzky, 1922) + *Deletosaurus arefjevi* Kurkin, 2001), outside of a clade containing (*Syops vanhoepeni* (Boonstra, 1938) + *Lystrosaurus* spp.). *Lystrosaurus* spp., instead of forming a single branch of nested species, consists of two sister clades: (*Lystrosaurus murrayi* + *Lystrosaurus declivis*) and (*Lystrosaurus curvatus* (*Lystrosaurus maccaigi* + *Lystrosaurus hedini*)). The grouping of (*Gordonia traquairi* Newton, 1893 + *Jimusaria sinkianensis* (Yuan & Young, 1934a)) is nested closer to Kannemeyeriiformes than the *Syops-Lystrosaurus* clade, outside of (*Eptychognathus bathyrhynchus* (von Huene, 1942) (*Basilodon woodwardi* (Broom, 1921) + *Sintocephalus alticeps* (Broom & Haughton, 1913))), which is the immediate sister group of Kannemeyeriiformes supported by three synapomorphies: characters 3 (relative width of temporal bar at level of postorbital bar versus the relative width at the junction of the intertemporal bar with the occipital plate 0.562), 8 (angle formed by the posterior pterygoid rami 6.900-7.000), and 61 (raised, sometimes rugose, circumorbital rim absent). In our analysis *Basilodon woodwardia*, *Sintocephalus alticeps*, and *Eptychognathus bathyrhynchus* are linked together mostly by continuous characters (2: minimum width of interorbital skull roof relative to basal length of skull 0.212-0.244; 5: relative position of pineal foramen, measured as the ratio of dorsal skull length

posterior to the foramen versus dorsal skull length anterior to the foramen 0.238–0.294; 8: angle formed by the posterior pterygoid rami 6.500; 10: relative area of the internal nares 9.663) and a single discrete synapomorphy (character 116: posterior edges of the interpterygoid vacuity located dorsal to the median pterygoid plate). Furthermore (Fig. 17B; 18), the topology differs in the recovery of monophyletic Shansiodontidae, represented by (*Rhinodicyodon gracile* (*Tetragonias njalilus* (*Vinceria andina* + *Shansiodon* spp.))) nested as a sister clade to (*Dinodontosaurus* spp. (Kannemeyeriidae (*Angonisaurus* *cruickshanki* (*Woznikella triradiata* n. gen., n. sp. + *Stahleckeriidae*))). The Shansiodontidae is supported by characters 5 (relative position of pineal foramen, measured as the ratio of dorsal skull length posterior to the foramen versus dorsal skull length anterior to the foramen 0.435), 14 (ratio of height of dentary ramus to height of dentary symphysis 0.821–0.858), 17 (length of the deltopectoral crest relative to total length of the humerus 0.479–0.481), 106 (2: ectopterygoid absent), and 186 (1: femoral head offset dorsally from dorsal margin). *Dolichuranus primaevis* retains its basalmost position within the monophyletic Kannemeyeriidae, followed by the grouping of ((*Acratophorus argentinensis* (*Wadiasaurus indicus* + *Rabidosaurus cristatus*)) + (*Sinokannemeyeria* (*Parakannemeyeria* + *Xiyukannemeyeria brevirostris*))) outside of *Rhadiodromus*, *Shaanbeikannemeyeria*, and more derived kannemeyeriids. The monophyly of the Kannemeyeriidae is supported by characters 12 (angulation of the occiput relative to the palate, expressed the ratio of dorsal and basal lengths of the skull 1.018), 51 (2: distinct lateral caniniform buttress present with posteroventral furrow), 74 (0: postorbital extend the entire length of intertemporal bar), 123 (2: shape of basal tubera strongly rounded, such that anterior and posterior tips of tuber curve towards each other, nearly enclosing the stapedial facet; tuber inflated), and 134 (1: lateral edge of paroccipital process drawn into sharp posteriorly-directed process that is distinctly offset from the surface of the occipital plate present). Stahleckeriidae includes (*Ischigualastia jensi* + *Jachaleria* spp.). In all three most parsimonious trees, *Woznikella triradiata* n. gen., n. sp. is recovered just outside of the clade (*Placeriinae* + *Stahleckeriinae*), supported by characters 15 (ratio of maximum height of postdentary bones [excluding reflected lamina of angular] to the height of the dentary ramus 0.841–0.897), 66 (1: temporal portion of skull roof angled dorsally with a strong break in slope near its anterior end), and 156 (1: angular with anterolateral trough for the posterior process of the dentary). *Lisowicia bojani* is nested as a sister group to (*Moghreberia nmachouensis* + *Placerias hesternus*) with *Pentasaurus goggai* as outgroup (no synapomorphies). The trees differ in the position of *Eubrachiosaurus browni* as a sister group to either (*Sangusaurus* spp. (*Ischigualastia* + *Jachaleria* spp.)), *Sangusaurus* spp., or *Sangusaurus parringtonii* to the exclusion of *Sangusaurus* sp. This causes a polytomy in the strict consensus tree which is, however, resolved by the majority rule (50%) consensus, resulting in monophyletic *Sangusaurus* spp. sister to *Eubrachiosaurus browni*. Unfortunately, similarly to the phylogenetic results presented in the

previous iterations of the same matrix (e.g., Kammerer *et al.* 2011, 2013, 2019; Olivier *et al.* 2019; Kammerer & Ordoñez 2021), the bootstrap values for most clades remain very low.

A third analysis, excluding *Woznikella triradiata* n. gen., n. sp., was performed to test the impact of corrected scorings of *Lisowicia bojani* and the position of that taxon in the context of the matrix expanded by Kammerer & Ordoñez 2021. The analysis resulted in a single most parsimonious tree (best score 1254.038, CI 0.223, RI 0.719) with topology identical as in Kammerer & Ordoñez (2021) and *Lisowicia bojani* recovered together with *Placerias hesternus* (no synapomorphies).

RESULTS OF THE PALEOBIOGEOGRAPHIC ANALYSIS

DEC+J turned out to be the best suited model for the analyzed dataset (AIC = 527.6) and DIVALIKE and DIVALIKE+J performed the worst (AIC = 903.6 and 884.4, respectively). In all cases the model variants with jump parameter (+J) explained data better than the variants without this parameter (p-values significantly below 0.005). This indicates, given the available fossil record of dicynodonts, that founder-event speciation (J) and subset sympatry (DEC) explain dicynodont paleobiogeography with higher likelihood than widespread vicariance (DIVALIKE) and sympatry (BAYAREALIKE).

According to the DEC+J model (Fig. 18), throughout the Permian and Triassic, southeastern Africa served as a constant hotspot for dicynodont radiation and origin point for dispersion of numerous clades. Virtually all internal divergences in the non-kannemeyeriid part of the tree are estimated to take place in that area. The only exceptions are: two Russian clades, (*Elph borealis* Kurkin, 1999 + *Interpresaurus blomi* Kurkin, 2001) and (*Delectosaurus arefjevi* + *Vivaxosaurus trautscholdi*), the branching of which is estimated to take place in Russia; a short section of the tree at the level of *Taoheidon baizhijun* Liu, 2020 and (*Counillonia superoculis* + *Repelinosaurus robustus*), which shows the highest likelihood for eastern Asia (almost 50%, with more than 33% for southeastern Africa); the *Lystrosaurus* clade, reconstructed ancestral states of both southeastern Africa and Antarctica (probability of over 33%), and (at the branching point of the (*Lystrosaurus declivis* + *Lystrosaurus murrayi*) clade) southeastern Africa, Antarctica, and South Asia (over 50%); and the (*Gordonia traquairi* + *Jimusaria sinkianensis*) clade, with subequal probabilities for Western/Central Europe and western Asia. Similar to non-kannemeyeriiforms, the origins of the Kannemeyeriiformes as well as the Shansiodontidae, Kannemeyeriidae, and Stahleckeriidae are also estimated to take place in southeastern Africa with probability approaching 100%.

Branching points within the Shansiodontidae show minor uncertainty due to the cosmopolitan nature of this small clade, but southeastern Africa is indicated with over 75% probability. The lineage of *Rhinodicyodon gracile* is estimated to migrate individually to Russia. Estimated ancestral states for the (*Shansiodon* + *Vinceria andina*) clade are both southeastern Africa and western Asia (probability nearly 50%; probability of about 33% for southeastern Africa). *Dinodontosaurus* spp. is estimated to migrate to South America as an early offshoot, independently from other South American species.

Southeastern Africa is estimated as the most probable (nearly 50%) ancestral state for the main branch of the Kannemeyeriidae, leading to *Kannemeyeria* spp., but there is some uncertainty, since eastern Asia and Russia are estimated to have probability of about 25% each. This trend continues towards the node of *Rhadiodromus* with more derived kannemeyeriids, the probability for Russia decreasing at the level of *Shaanbeikannemeyeria* branch, and the probability for eastern Asia disappearing in more derived nodes. The lineage of *Kannemeyeria aganosteus* is estimated to migrate independently to South America, and analogous scenario is estimated for the migration of *Uralokannemeyeria vjuschkovi* to Russia. The range of the clade of (*Uralokannemeyeria vjuschkovi* + *Rechnisaurus cristarhynchus*) has, however, about 25% probability of including South Asia (versus nearly 50% of being restricted to southeastern Africa alone). Eastern Asia is estimated as the most probable (about 33%) ancestral state for the node of ((*Sinokannemeyeria* (*Parakannemeyeria* + *Xiyukannemeyeria brevirostris*)) + (*Acratophorus argentinensis* (*Rabidosaurus cristatus* + *Wadiasaurus indicus*))), although comparatively high percentage is also present for Russia (about 25%) and minor signal for other areas. The most probable ancestral state changes to both eastern and western Asia (over 75%) for the node of (*Parakannemeyeria* + *Xiyukannemeyeria brevirostris*). The most probable ancestral states for the nodes at the base and inside of the clade of (*Acratophorus argentinensis* (*Rabidosaurus cristatus* + *Wadiasaurus indicus*)) are estimated for South America (over 33%) and Russia (over 50%), respectively, with the lineage of *Wadiasaurus indicus* migrating independently to South Asia, but the percentages for Russia (about 33%) for the former and South Asia (nearly 50%) for the latter node are comparatively high.

The situation for the Stahleckeriidae is somewhat less ambiguous. Southeastern Africa is the most probable ancestral range for most nodes. *Woznikella triradiata* n. gen., n. sp. is estimated to be an early migrant from Africa, independent from *Lisowicia bojani*. The independent colonization of Europe by these two taxa is shared by all models with high (close to 100%) probability. The node of (*Lisowicia bojani* (*Moghreberia nmachouensis* + *Placerias hesternus*)) is estimated to be Central European (probability about 50%), with the split between the latter two taxa occurring in North America (likewise, about 50%). Still, northern Africa and North America are indicated with the probability of about 25% each for the base of that whole group and the probability for southern Africa for the node of (*Moghreberia nmachouensis* + *Placerias hesternus*) is also nearly 50%. Interestingly, the presence of *Stahleckeria potens* in both South America and Southeastern Africa results in the most probable original range for the whole Stahleckeriinae including both areas (probability about 50% versus about 33% for southeastern Africa alone and less than 25% for South America alone). The remaining nodes within the clade are localized in South America (75% percent; nodes leading to *Sangusaurus parringtonii* have less than 25% for southeastern Africa). *Eubrachiosaurus browni* and *Sangusaurus parringtonii* are thus estimated to migrate independently to their respective areas.

DISCUSSION

GEOGRAPHIC DISTRIBUTION OF TRIASSIC DICYNODONTS

Historical background

Global distribution of Triassic Dicynodontia was one of the most prominently discussed topics in the dicynont-related literature during the second half of the 20th and the 21st century. Usually, these considerations were a mix of biostratigraphic (correlations of dicynodont-bearing formations), paleobiogeographic (routes of colonization), and evolutionary (origin and interrelationships of taxa grouped today into the Kannemeyeriformes) topics, often taking convoluted form. Although intercontinental connections between Triassic dicynodont faunas were known since the late 19th century (Huxley 1865) and von Huene (1935) advocated for a Triassic connection between the South Africa and South America through Antarctica, as well as between North and South America, which would allow spread of similar dicynodont faunas, it was probably Camp (1956) who first presented an in-depth scenario of their dispersal. According to him, the kannemeyeriform line (his “Kannemeyeridae”) originated from a *Kannemeyeria*-like ancestor, possibly resembling *Daptocephalus* spp. or Russian dicynodonts, and migrated through Eurasia, entered North America in the Middle Triassic, and eventually colonized South America. He considered the genus *Kannemeyeria* as the most primitive of his “Kannemeyeridae” and *Sinokannemeyeria* Young, 1937 as more closely related to the New World dicynodonts (genera *Dinodontosaurus*, *Eubrachiosaurus*, *Placerias*, and *Stahleckeria*) than to the African taxa. However, Camp (1956) considered each species derived in its own way, therefore he did not postulate any ancestor-descendant relationships. He rejected the continental drift theory and thus dismissed the possibility of any direct migration from Africa to the Americas. Ironically, in the following years, dicynodonts constituted one of the important links between the South Africa and Antarctica (Elliot *et al.* 1970; Colbert 1971a, 1982; Hammer & Cosgriff 1981; Cosgriff *et al.* 1982; Fröbisch *et al.* 2010), and were considered evidence in support of plate tectonics. Subsequent authors did not share similar reservations concerning taxon dispersal. Sun (1963) considered *Sinokannemeyeria* spp. to be slightly more primitive than *Kannemeyeria*, and the Asian forms overall closely related to both *Kannemeyeria* spp. and *Dinodontosaurus* spp., while *Placerias* was an early divergence and thus evolved independently, implying at least two waves of dicynodont migration to the Americas in the Triassic. Cox (1965) also considered *Sinokannemeyeria* spp. as an ancestor of his Kannemeyeridae (forms with pointed snouts, i.e., *Sinokannemeyeria*, *Parakannemeyeria* Sun, 1960, *Kannemeyeria*, *Ischigualastia*, *Placerias*, and *Barysoma* – the latter now considered a junior synonym of *Stahleckeria*; see Lucas 1993a) and Stahleckeriidae (forms with blunt snouts, i.e., *Stahleckeria* and *Dinodontosaurus*), but he also recognized two more primitive families: the Lystrosauridae (*Lystrosaurus* and ?*Rhadiodromus*) and Shansiodontidae (*Shansiodon* and *Tetragonias*). All four families had basically global distributions. Later, he changed his opinion, stating that *Sinokannemeyeria* is too specialized

to be considered an ancestor due to its elongated preorbital portion of the skull, and deemed interrelationships of Triassic dicynodonts uncertain (Cox 1969).

Cruickshank brought the postulated origin of the Kannemeyeriiformes again to Africa, presenting *Tetragonias njalilus* (considered as closely related to *Shansiodon* spp.) as an intermediate form linking the Lystrosauridae and more derived taxa (Cruickshank 1964, 1967), and *Daptocephalus leoniceps* (Owen, 1876) as an ancestor to all Triassic dicynodonts (Cruickshank 1967). Subsequently (Cruickshank 1970), however, he also changed his opinion, this time proposing *Sinokannemeyeria* spp. as ancestral to all kannemeyeriiforms, *Parakannemeyeria* as possibly ancestral to Stahleckeriidae, *Shansiodon* as ancestral to *Vinceria*, *Tetragonias*, *Kannemeyeria*, and *Wadiasaurus*, and *Ischigualastia*, *Barysoma*, and *Placerias* as a third line descending from *Sinokannemeyeria*. This moved the origin of the whole group to China, with subsequent southwestern migrations. Keyser & Cruickshank (1979) returned the kannemeyeriiform origin to Africa yet again, this time considering Lystrosauridae as too specialized to be ancestral to the kannemeyeriiforms (their “Kannemeyeridae” [sic]), and instead proposing a form similar to *Odontocyclops whaitsi* (Broom, 1913a) as the ultimate ancestor, *Daptocephalus leoniceps* as ancestral to their blunt-snouted “Dinodontosaurinae”, and *Dinanomodon gilli* as ancestral to their pointed-snouted “Kannemeyerinae” [sic], both group of global distribution. A third, completely American subfamily, the “Stahleckerinae” [sic], was considered a derived descendant of either the “Dinodontosaurinae” or “Kannemeyerinae”, and the fourth South American subfamily, the “Jachelerinae” [sic], was considered *incertae sedis*. Additionally, they suggested extensive lists of synonymies, making *Shansiodon* and *Kannemeyeria* globally distributed. This scheme (mainly the polyphyletic origin of the “Kannemeyeridae” *sensu* Keyser & Cruickshank 1979) was partly criticized by Cooper (1980), who proposed even larger lists of global synonymies, an easier subdivision of the kannemeyeriiforms into tusked and tuskless groups (although at the end of the latter branch he placed *Placerias*, which at the time was already known to variably have tusks; Camp & Welles 1956), and *Kannemeyeria* spp. as the ancestor. Cooper’s approach was in turn heavily criticized by Keyser and Cruickshank (Keyser & Cruickshank 1980), who firmly argued that the presence or absence of tusks is totally unacceptable as a basis for Triassic dicynodont systemsatics and that the shape of the snout is a more sound character. However, as noted by King (1988), the wide snout of *Daptocephalus leoniceps* is typical for Permian dicynodonts, not derived (*contra* Keyser & Cruickshank 1979), and thus there was no need for postulating a diphyletic origin of the Triassic taxa.

Cox & Li (1983) further discussed the systemsatics proposed by Keyser & Cruickshank (1979) and reverted the number of postulated kannemeyeriiform families to three (Kannemeyeridae, Stahleckeriidae, and Shansiodontidae, all cosmopolitan), albeit with modifications (e.g., the genera *Sinokannemeyeria* and *Parakannemeyeria* moved to Stahleckeriidae) and a roster of *incertae sedis* taxa, but they provided no paleobiogeographic interpretations. King (1988) discussed the previous schemes

and was the first to perform a cladistic analysis of Triassic dicynodont phylogeny (a followup to the Permian-focused analysis of Cluver & King 1983), with the resulting topology constituting of cosmopolitan clades. According to her, the whole clade now understood as the Kannemeyeriiformes had its origin from one of the species of the genus *Dicynodon*. *Myosaurus gracilis* was classified together with *Myosauroides minnaari* Broom, 1941 in the tribe Myosaurini and *Kombuisia frerensis* in the Family Kingoriidae, unsurprisingly suggesting an African origin for both species phylogenetically separate from the Kannemeyeriiformes (King 1988). The character selection and results of King’s (1988) analysis were subsequently commented on by Cox (1991) and Surkov (2000) suggested worldwide dispersal of kannemeyeriiforms in the Ladinian from a stock of early, less derived forms restricted in the Anisian to the Southern Hemisphere, but from that point onwards, discussions of Triassic dicynodont phylogeny and systematics were mostly apomorphy based, with little attention to paleobiogeographic distribution (see below). An interesting exception is the paper of Angielczyk & Kurkin (2003) who coded the geographic occurrence of (mainly Permian) dicynodonts as a character in the phylogenetic matrix and based on its distribution discussed the possibility of a Laurasian origin of kannemeyeriiforms and equivocal origin of *Lystrosaurus* spp. Although some authors (e.g., Lucas & Wild 1995) postulated synonymies between various taxa (mostly shansiodontids, but also some kannemeyeriids and stahleckeriids), suggesting, e.g., a global distribution of the originally Chinese genus *Shansiodon*, these hypotheses were not broadly accepted (see overviews in Fröbisch 2009; Kammerer *et al.* 2013; Kammerer & Ordoñez 2021). Hancox *et al.* (2013) noted that most of the historically proposed synonymies with other African, Russian, and South American genera are not justified, but they noted that the presence of *Shansiodon sensu stricto* in South Africa is a genuine record. Likewise, the proposed synonymy of Chinese *Lystrosaurus* spp. with South African and Antarctic species (e.g., Colbert 1974; Cosgriff *et al.* 1982) were recently refuted (Camp & Liu 2011; Kulik *et al.* 2021). Maisch & Matzke (2014) described *Sungeodon kimkraemerae* from the Early Triassic of China and postulated that it represents the earliest stahleckeriid, thus moving the origin of that clade to Asia, but according to Kammerer *et al.* (2019) it likely is not a stahleckeriid, and perhaps even not a kannemeyeriiform.

Tracking taxa in time and space

The aim of paleobiogeography is to understand geographic distributions of fossil organisms in the past during a single time slice (horizontal) and their changes over time (vertical). As such, it is afflicted by a number of difficulties regarding the resolution and completeness of the fossil record, stratigraphic correlations between fossil-bearing localities and their dating, taxonomic identification of fossil specimens, etc. King (1990a) discussed some of the problems related to the anomodont diversity studies, which are to a large extent relevant for biogeographic approach as well. She correctly noted that the suprageneric level is not suitable for tracking

diversity changes (over time, as total taxonomic richness, but also across geographic areas) due to varied (dependent on the author or analysis) and unequal inclusivity of families and orders. Conversely, species level was at the time considered unreliable due to obvious oversplitting. The latter problem, fortunately, was mostly solved for dicynodonts due to numerous revisions performed in recent years (e.g., Renaut & Hancox 2001; Grine *et al.* 2006; Fröbisch 2009; Camp & Liu 2011; Kammerer *et al.* 2011, 2013; Kammerer & Ordoñez 2021), therefore a species-level consideration may be performed.

Numerous authors (e.g., King 1990a; Smith 2001; Fröbisch 2008, 2014; Barrett *et al.* 2009; Butler *et al.* 2009, 2011; Benson & Upchurch 2013; Walther & Fröbisch 2013; Gardner *et al.* 2019) noted that the number of species observed in the fossil record may be biased by varied interest of researchers regarding particular groups or time interval, as well as diverse limitations of the geological record (such as the number, area, and availability of rock formations and outcrops representing each interval and/or geographic region, etc.). Out of the latter, the number of fossiliferous formations was frequently proposed as a factor influencing the observed paleodiversity (e.g., Smith 2001; Fröbisch 2008; Barrett *et al.* 2009; Butler *et al.* 2009; Butler *et al.* 2011; Benson & Upchurch 2013). This assumption was, however, criticized by Benton *et al.* (2011) and Benton (2012). Among other arguments, they noted that the formations are often uncomparable when it comes to their extent and content and in some cases the divisions are arbitrary or may be dependent on fossil contents. Furthermore, particularly when only formations yielding a particular higher taxon are considered (e.g., only anomodont-bearing formation for an anomodont diversity study), the correlations result from redundancy – especially in the case of the Permotriassic fossil record, in which many taxa are known from a single formation, when particular formation is selected based on the presence of a taxon, in most cases its addition or removal will automatically cause the change to the taxon count, even in experiments on randomly generated data (Benton *et al.* 2011); this notion is expressly relevant to the Triassic dicynodont fossil record (see below). Benson & Upchurch (2013) addressed this critique and noted, e.g., that formations are usually established based on lithostratigraphy rather than fossils contained. While this is true, the number and definitions of formations or groups may differ depending on the author. A good example is the proposition of Lucas (1993b) who advocated for raising the *Placerias hesternus*-yielding Chinle Formation to the group rank and its members to the formation rank, thus arbitrarily changing the correspondence between the number of formation and dicynodont taxa in the Late Triassic of North America. The varied inclusiveness of formations and lack of strict correspondence between formations and paleohabitats is a particular complication in the case of fully terrestrial animals, the burial of which (usually dependent on fresh water sedimentation) occurred in sedimentation settings different from their habitats. In such cases, the formations most productive in terms of paleobiodiversity may gather animal remains from a mosaic of numerous neighboring paleohabitat types and still retain a

relatively uniform sedimentary (and, thus, lithostratigraphic) character while other formations may only (or mainly) contain pelobiiodiversity from a homogenous environment. Works considering the total number of fossiliferous formations and especially gathering data from various sources in the case of terrestrial settings generally find no correlation between the number of formations and the number of observed taxa (e.g., Benton *et al.* 2011; Mannion *et al.* 2011; Benton 2012; Dunhill *et al.* 2014).

A related but more relevant factor impacting paleobiogeographic analyses is the geographic sampling bias, i.e., the uneven or patchy sampling from various geographic regions and palaeolatitudes over time, potentially creating perceived gaps in the fossil record, artificial record of radiation events, or perceived drastic faunistic overturns (e.g., Benson & Upchurch 2013; Gardner *et al.* 2019). In the Triassic, the fossil record as a whole (not only for dicynodonts, but all animals and plants) is predominantly restricted to coastal and near coastal areas but completely missing intracontinentally – according to the Paleobiology Database (<https://paleobiodb.org>) no Triassic fossiliferous formations are known from most of the areas of the Americas, Africa, Antarctica, and Australia, which at the time were located deep inland; in fact, the same trend of large inland areas devoid of fossils is observed, with varied intensity, throughout most of the Phanerozoic. Many of these areas were located during the Triassic close to the equator, and although to some extent this may represent a genuine record due to the aridity and heat making them inhabitable at least from the Late Permian until the Middle Triassic (Allen *et al.* 2020; Liu *et al.* 2022), we agree with Dunne *et al.* (2021) and Liu *et al.* (2022) who also consider this image to be influenced by a sampling gap. It seems that either locally and temporarily low fossilization potential of the environment, destruction of the fossil record by, e.g., erosion, or inaccessibility of the regions for study due to, e.g., the current presence of tropical forests, deserts, ice caps, or other geographic or political reasons may be at play. While some of these areas certainly were covered by deserts in the past and thus difficult to inhabit, particularly for tetrapods, it seems extremely unlikely that they would be completely uninhabitable and thus barren of animal and plant life for hundreds of millions of years. Additionally, even the areas which preserve the fossil record in some time bins, may lack it in the others, either as a result of not sufficient tempo of sedimentation or increased erosion, e.g., due to the specificity of the habitat or climatic causes. All of this poses a serious difficulty for the reconstruction of animal distribution and migrations: large landmasses that could be inhabited or at least traversed by animals are either inaccessible or lack the fossil record altogether. This may cause lack of significant phylogenetic and/or paleobiogeographic data for some parts of the phylogenetic tree or even erase whole branches, leading to two main problems: 1) errors in the reconstruction of phylogeny due to the lack of pivotal taxa; because the paleobiogeographic analysis used here is based on the phylogenetic topology, this may result in an erroneous paleobiogeographic reconstruction; and 2) missing data about taxon occurrences; this may lead to underestimation of the

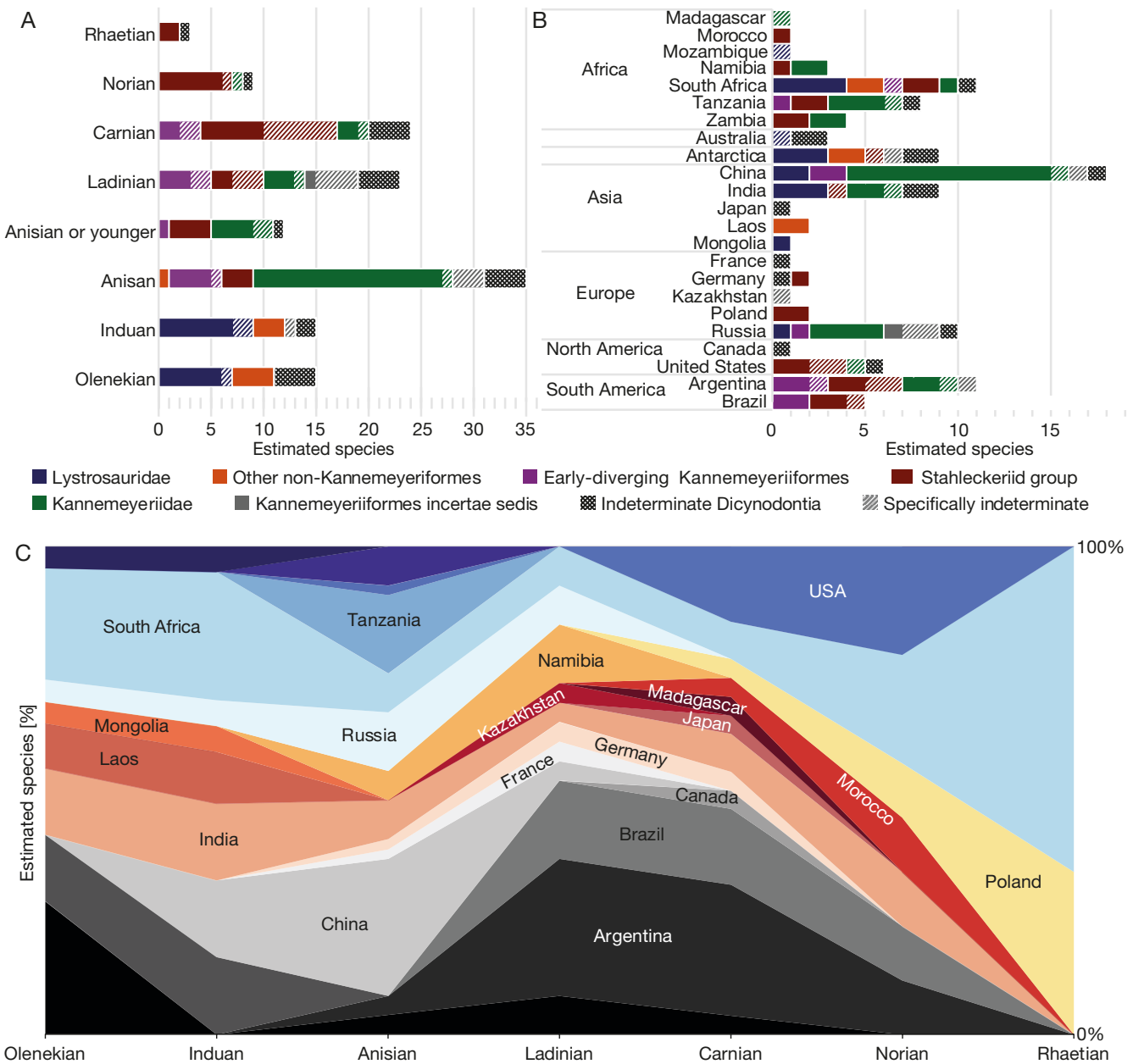


Fig. 19. — Estimated number of Triassic dicynodont species, including named taxa (solid colors in **A** and **B**) and specifically indeterminate finds that may reasonably represent new species based on lack of comparable named forms in the same formations (hatched in **A** and **B**): **A**, estimated number of species by age; **B**, estimated number of species by country across whole Triassic; **C**, per cent contribution of individual countries to estimated species diversity in time. Indeterminate occurrences obviously or likely belonging to known species (e.g., described as "cf." when comparable species were already noted in the same formations or as "sp. indet." but likely representing species already known from the same formations) excluded. "Anisian or younger" in **B** indicates species from formations of uncertain age historically correlated biostratigraphically with South African *Cynognathus* Assemblage Zone (see discussion in the text). For simplicity, these species were counted as Anisian in **C**. Stahleckeriid group includes Stahleckeriidae (Stahleckeriinae + Placeriinae) and taxa more closely related to the Stahleckeriidae than to the Kannemeyeriidae. Occurrences suggested by the ichnological record and ghost lineages not included.

geographic range inhabited by particular taxa or lineages and thus impact the perception of their dispersals. In some cases, particularly in the second instance, the ancestral ranges and migration routes can be interpolated from the existing data, especially that the analysis is performed at a relatively coarse level of geographic resolution.

A new problem is connected with the uncertain ages of the formations traditionally correlated based on biostratigraphy with the *Cynognathus* Assemblage Zone due to its apparently

very long temporal span (Anisian-Carnian; see, e.g., Ottone *et al.* 2014; PeeCook *et al.* 2018; Wynd *et al.* 2018; Hancox *et al.* 2020). Because of these uncertainties, we decided to refrain from using various indices utilized by Fröbisch (Fröbisch 2008), such as exclusion of singletons (taxa confined to a single time interval), different weights given to taxa crossing one (top or bottom) and both boundaries of an interval, and origination and extinction rates, as well as from considering diversity at highly resolved intervals (e.g., 5 Ma or 1 Ma);

in the light of inevitable adjustments to Triassic assemblage correlations in the near future, such indices would quickly become outdated and merely introduce unnecessary information noise into the literature. Their application should be attempted in the future. It must be kept in mind that the attempt made here is a provisional, temporarily low-resolution summary and that future advancements in dating and correlations of dicynodont-bearing strata will allow formulation of a clearer picture.

Another complication is the implied diversity, i.e., the presence of dicynodont taxa unknown from body fossils but suggested by the track record and ghost lineages. These are noted but are not counted towards the estimated numbers of species for several reasons. Firstly, our understanding of the phylogeny of Kannemeyeriiformes is constantly improving and although some aspects are already well established, results of various analyses frequently differ in exact relationships between taxa, even if only in minor details, such as the sequence of divergences between some closely related species. This influences the presence and/or length of ghost lineages. Secondly, although the results of our paleobiogeographic analysis suggest the founder-event speciation as the most probable driving force behind the dicynodont distribution, the possibility of vicariant or anagenetic evolution cannot be excluded, also potentially impacting the ghost lineages observed in the phylogeny. Thirdly, while our analysis provides reconstruction of ancestral ranges for each branch and node, this is done with broad geographic region resolution, not country-level resolution. Furthermore, the current fossil record may not capture full duration of taxa and the exact moment of each divergence can only be speculated upon. Additionally, the current difficulties in dating of dicynodont bearing formations also potentially influence the length and presence of ghost lineages. Therefore, it would be difficult and very speculative to attempt placing each branching event and ghost lineage in space and time and count it as a real entity. Fourthly, the ghost lineages and tracks are difficult to quantify. While each ghost lineage and ichnotaxon can indicate at least a single dicynodont taxon, the ghost lineages may as well indicate a whole lineage with no body fossil record and each ichnotaxon may be produced by more than one dicynodont species. On the other hand, the tracks may as well be left by one of already known species that currently has no body fossil record in a given place or time. Fourthly, in some cases differentiation between the dicynodont or cynodont trackmaker may be difficult (e.g., Marchetti *et al.* 2019). Finally, the track record may capture, e.g., long-distance random exploration, attempts of range expansions, or atypical migration routes of non-native species which did not normally settle in the area (e.g., Arnold *et al.* 2012; van de Kerk *et al.* 2021). This, of course, may also be true for body fossils but, given their relative scarcity, it could be expected that the highest probability of finding numerous skeletal remains of a given species is in the areas in which it was most commonly found in life (i.e., had an established population). According to our data, Triassic dicynodonts did migrate quite intensively, necessarily entering and crossing new areas, but it is unknown whether

(and if so, which of) these migrations were only in passing or associated with establishment of more permanent populations.

Triassic dicynodont diversity and occurrences

Currently (see Table 1), about 38 named genera (not counting the yet not erected separate genus for “*Kannemeyeria*” *latirostris*, and “*Azarifeneria*”, which is possibly congeneric with *Moghreberia*; see Lucas & Wild 1995; Kammerer *et al.* 2013) of Triassic dicynodonts are considered valid, out of which 14 are known from more than one country. There are about 60 valid Triassic species of dicynodonts (not counting the two species of “*Azarifeneria*”, which are in dire need of revision; the taxonomy of Chinese and Russian kannemeyeriiforms was also suggested to need revision, but until a detailed review is performed, we follow here the currently accepted opinions on their validity; see Lucas & Wild 1995; Fröbisch 2009; Kammerer *et al.* 2013; Kammerer *et al.* 2017; Maisch 2021; Liu 2022), out of which about 11 inhabited more than one geographic area corresponding to a modern day country (Cox 1968; Edler 2000; Hancox *et al.* 2013; Kammerer & Ordoñez 2021). Nearly half of these (five species) belong to the genus *Lystrosaurus*, and the rest are restricted to relatively narrow ranges in the southern part of the globe, i.e., the southern part of Africa, Antarctica, India, and South America. This indicates that almost 90% of the currently recognized Middle and Late Triassic species can be considered endemic and the rest occupied relatively small geographical provinces, which is consistent with the previous observations of Fröbisch (2009). To a large extent, this is also true for particular formations, with individual taxa rarely being present in more than one formation (although this obviously depends on local geological history and division schemes, Argentina being the most notable exception). For that reason, it seems very likely that formations yielding thus far only indeterminate finds (e.g., Arcadia, Inder, Isalo II, Maleri, Pipariya, Momonoki) will in the future prove to contain new dicynodont taxa. Twenty-seven valid genera are monotypic. Some cryptic diversity is, however, suggested by indeterminate finds coming from formations otherwise barren in dicynodonts or known to contain named dicynodonts incomparable to the indeterminate finds. Although these finds, due to lack of diagnostic value, are usually not adequate to establish new taxa and many of them are most likely representatives of already known taxa, some seem sufficient to reasonably indicate a greater specific diversity (Figs 19–22).

Although the dicynodonts were very common and diversified during the Permian, at the beginning of the Triassic their diversity suffered a significant decrease (King 1990a, b; Fröbisch 2008, 2014; Ruta *et al.* 2013) – in the Early Triassic (Fig. 20) they were represented only by *Counillonia superoculis* (Laos; please see the Table 1 for references), a group of species belonging to the genus *Lystrosaurus* (Antarctica, Australia, China, India, Mongolia, Russia, and South Africa), *Kombuisia antarctica* (Antarctica), *Myosaurus gracilis* (Antarctica and South Africa), *Repelinosaurus robustus* (Laos), and *Sungeodon kimkraemerae* (China). The Laotian species (*Counillonia superoculis* and *Repelinosaurus robustus*) form a

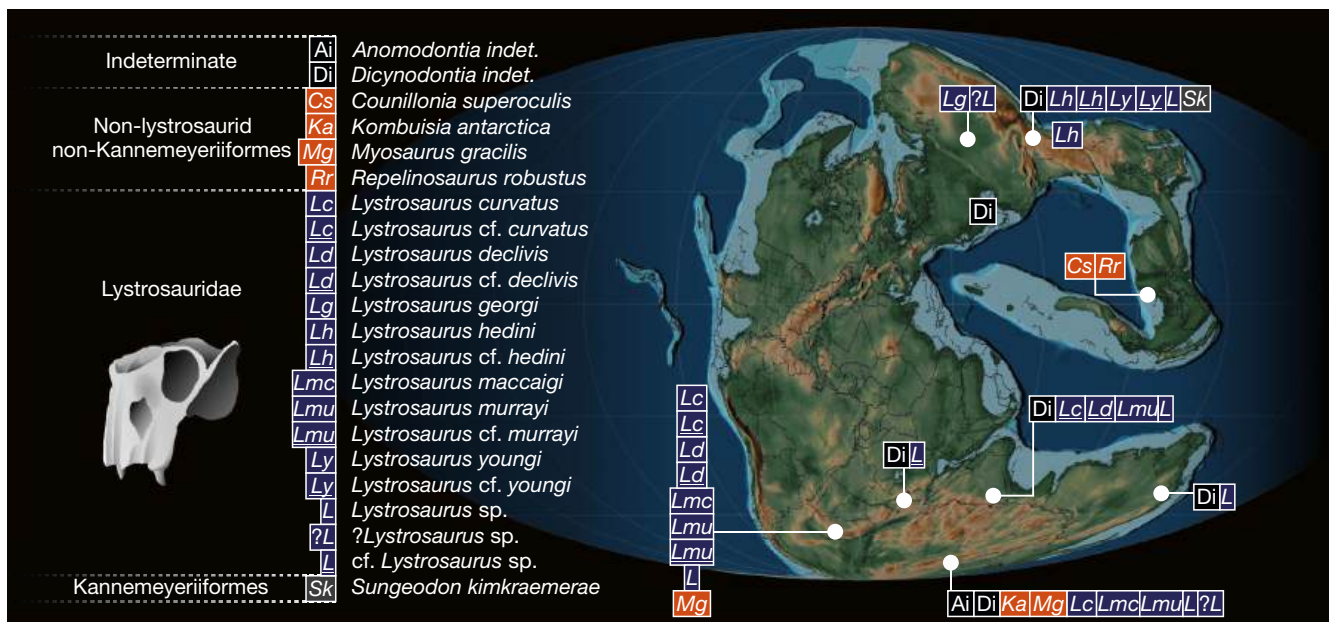


FIG. 20. — Early Triassic distribution of dicynodont finds. Skull of *Lystrosaurus declivis* (Owen, 1859) based on UCMP 42870.

monophyletic clade but their Triassic age was recently questioned by Liu (2020), who suggested that they may rather represent a late Permian fauna. Further studies are needed to resolve that question, the taxa are here provisionally treated as Early Triassic. All these Early Triassic species are nested in the Permian, pre-kannemeyeriform part of the tree and, according to our analysis, are of southeastern African descent, except for *Counillonia superoculis* and *Repelinosaurus robustus*, the origin of which was reconstructed as eastern Asian. Although this could indicate a temporary shift in the location of dicynodont diversity producing hotspot and directions of dicynodont dispersals at that time (see below), this is most probably an artifact caused by the aggregation of two eastern Asian branches (*Taoheidon baizhijuni* and (*Counillonia superoculis* + *Repelinosaurus robustus*)) right next to each other, possibly due to insufficient sampling of that part of the tree or these taxa constituting an Asian clade that is unrecognized in our topology. A monophyletic grouping of these three taxa was recovered in the analyses of Liu (2020) and Angielczyk *et al.* (2021). Recently (during the review of this paper), Angielczyk *et al.* (2021) redescribed the Permian Chinese dicynodont, *Kunpania scopulusa* Sun, 1978, as a very early diverging offshoot of Dicynodontoidea. Because of that and due to the fact that this could potentially provide a new outlook on the biogeographic origin of the dicynodontids and the ancestral range of a significant portion of the tree, we provisionally included that taxon in our phylogenetic matrix; however, we recovered *Kunpania scopulusa* in a less derived position, prior to the divergence of the cryptodonts and dicynodontoids, surrounded by southeastern African taxa, and separated from other Asiatic species (data not shown), thus likely not impacting the paleobiogeographic patterns reconstructed here. Because a more detailed investigation of the potential impact of *Kunpania scopulusa* on the dicynodont phylogeny

and paleobiogeography is beyond the scope of this paper, it will be pursued elsewhere. Even though the Early Triassic dicynodonts had a global distribution, and locally specimen numbers are astoundingly high (thousands of *Lystrosaurus* spp. individuals are housed in various collections; e.g., Nicolas & Rubidge 2010; Smith *et al.* 2012; Botha-Brink *et al.* 2014), the number of known species and, particularly, genera is low, resulting in a fairly homogenous taxonomic composition of Early Triassic dicynodont assemblages. There are 12 valid species and six valid genera of dicynodonts described from the whole Early Triassic, although an indeterminate anomodont significantly larger than *Lystrosaurus* spp. reported from the Olenekian lower Fremouw Formation of Antarctica (Cosgriff *et al.* 1978), up to two indeterminate species from the Upper Parmeer Supergroup and Arcadia Formation of Australia (King 1983; Thulborn 1983a, b, 1990; Rozefelds *et al.* 2011), possibly at least one indeterminate species from Mozambique (although it may potentially represent some known species of the genus *Lystrosaurus*), and a geographically isolated indeterminate dicynodont (“*Putillosaurus sennikovi*”) from the Olenekian Donskaya Luka of Russia may indicate that up to five additional species were present at that time (Fig. 19A). Probable Early Triassic dicynodont tracks (ichno-genera *Dicynodontipus*, *Dolomitipus*, possibly *Therapsipus*, and indeterminate) were described from Australia, Europe (Catalonia, England, France, Germany, Poland), South Africa, and South America (Argentina, Brazil). The worldwide distribution of *Dicynodontipus* spp. generally agrees with the worldwide distribution and restricted diversity of dicynodonts at the time, however, the identification of the trackmaker as a dicynodont is in this case ambiguous and cynodonts are another valid possibility (e.g., Marchetti *et al.* 2019). Presence of some representatives of the lineage leading to Kannemeyeriformes in the Early Triassic, which may or may not be identical with

one or several of fragmentary body fossils or trackmakers, is implied by the ghost lineage based on phylogeny, but these currently lack any confirmed record.

The Middle Triassic fossil record of dicynodonts is rich and diverse (Fig. 21), but due to recent advances in stratigraphy, most notably radioisotope geochronology, understanding of this record is in a process of change. It was the time of appearance of definitive kannemeyeriiforms which, according to our analysis, radiated from an unknown southeastern African lineage but already in the Anisian attained a worldwide distribution. A radiometrically proven Anisian (Liu *et al.* 2017) record of dicynodonts is currently known only from China (Shansiodontidae: *Shansiodon wangi*, *Shan. wuhsiangensis*; Kannemeyeriidae: *Parakannemeyeria chengi*, *Pa. dolichocephala*, *Pa. ningwuensis*, *Pa. shenmuensis*, *Pa. youngi*, *Shaanbeikannemeyeria xilouguensis*, *Sinokannemeyeria baidaoyuensis*, *Si. pearsoni*, *Si. sanchuanheensis*, *Si. yingchiaoensis*, *Xiyukannemeyeria brevirostris*; and some indeterminate specimens) which apparently represent three separate migrations (*Shaanbeikannemeyeria* spp., *Shansiodon* spp., and the remaining taxa) from the southeasetern Africa.

The age of traditionally considered Anisian subzones of the South African Burgersdorp Formation *Cynognathus* Assemblage Zone is currently ambiguous because the base of the *Cynognathus* and *Diademodon*-bearing Río Seco de la Quebrada Formation (Argentina) was recently radiometrically dated to early Carnian (Ottone *et al.* 2014; Peecook *et al.* 2018; Wynd *et al.* 2018). Because of that, the *Trirachodon-Kannemeyeria* and *Cricodon-Ufudocyclops* subzones (former subzones B and C) are currently considered to cover the whole Anisian, Ladinian, and extend into the Carnian (Hancox *et al.* 2020). This is particularly problematic, because the assemblages from Antarctica (Hammer 1995; Sidor *et al.* 2014; Kammerer *et al.* 2019), India (Denwa Formation, Yerrapalli Namibia (Omingonde Formation), Tanzania (Manda Formation), and Zambia (Ntawere Formation) had been biostratigraphically correlated with the *Cynognathus* Assemblage Zone. Ottone *et al.* (2014) noted two possible consequences: either these Antarctic, African, Argentinian, and Indian assemblages are all Carnian, or the biostratigraphic utility of the *Cynognathus* Zone marker taxa is limited due to their unexpectedly long temporal ranges. Although Peecook *et al.* (2018) quite readily accepted the Carnian age for the Ntawere Formation of Zambia, recently obtained detrital zircon age of the upper part of the Omingonde Formation in Namibia (also correlated with the Ntawere Formation; e.g., Peecook *et al.* 2018; Wynd *et al.* 2018) revealed a middle Ladinian age of 240 ± 4 Ma (Zieger *et al.* 2020), and thus more complex temporal relationships. It is uncertain whether (and if so, how far) the lower part of the Omingonde Formation extends into the Anisian.

The South African, Namibian, Tanzanian, and Zambian *Cynognathus* Assemblage Zone-correlated assemblages, due to their proximity and taxonomic similarity, are treated in our paleobiogeographic analysis together as a single region of southeastern Africa. In addition to one non-kannemeyeriiform taxon (*Kombuisia frerensis* from South Africa), they appear to capture the earliest (at least phylogenetically) record

of the split of the Kannemeyeriformes into its three main branches. The first, Shansiodontidae, is represented in this region by *Shansiodon* sp. (Hancox *et al.* 2013; South Africa) and *Tetragonias njalilus* (Tanzania). The second, Kannemeyeriidae, is much more diversified: *Dolichuranus primaevus* (Namibia), *Dolichuranus* sp. (Peecook *et al.* 2018; Wynd *et al.* 2018; Tanzania), *Kannemeyeria lophorhinus* (Namibia and Zambia), *Kannemeyeria simocephalus* (South Africa and Tanzania), “*Kannemeyeria*” *latirostris* (Zambia), and the specimen described by Cox (1991) as *Rechnisaurus cristarhynchus* (Tanzania). Finally, the stahleckeriid group, includes *Angonisaurus crickshanki* (Tanzania), *Sangusaurus edentatus* (Zambia), *Sangusaurus parringtonii* (Tanzania), *Stahleckeria potens* (Namibia), *Ufudocyclops mukanelai* (South Africa), *Zambiasaurus submersus* (Zambia), an unnamed stahleckeriid (Govender 2005; South Africa), and another indeterminate stahleckeriid (Kammerer *et al.* 2017; Tanzania). Unidentified finds consist of a kannemeyeriiform (Hancox *et al.* 2013) and indeterminate remains (Watson 1960; Warren 1998) from South Africa, the latter of which likely belong to some of the mentioned taxa, dicynodont material from Namibia (Abdala *et al.* 2013), indeterminate dicynodonts from Tanzania (e.g., Haughton 1932; Boonstra 1953; Larkin 1994), and an indeterminate dicynodont (Peecook *et al.* 2018) and indeterminate kannemeyeriiform (Angielczyk *et al.* 2014) from Zambia. All named taxa included in our analysis are found to be autochthonic, except for *Sangusaurus parringtoni* which is recovered as a migrant from South America.

The assumed Anisian record from India consists of indeterminate kannemeyeriid and stahleckeriid from the Denwa Formation (Bandyopadhyay 1988; Bandyopadhyay & Sengupta 1999) and Kannemeyeriidae: *Rechnisaurus cristarhynchus* (range extension from southeastern Africa) and *Wadiasaurus indicus* (interestingly, related with *Rabidosaurus cristatus* and possibly representing a migration from Russia).

The Russian strata of the Donguz Horizon, which yielded several species (Shansiodontidae: *Rhinodicynodon gracile*; Kannemeyeriidae: *Rabidosaurus cristatus*, *Rhadiodromus klimovi*, *Rha. mariae*, *Uralokannemeyeria vjuschkovi*) and some very fragmentary and undiagnostic specimens (Kalandadze & Sennikov 1985; Shishkin *et al.* 1995; Surkov 1999a), have not been yet reviewed in light of the new stratigraphic scenario and their Anisian age has not yet been questioned. These Russian kannemeyeriiforms are phylogenetically scattered among the Shansiodontidae and Kannemeyeriidae and appear to represent separate migrations from southeastern Africa and (in the case of *Rabidosaurus cristatus*) South America.

Fragmentary Anisian dicynodont material was also reported from the upper Moenkopi Formation of the United States (Nesbitt & Angielczyk 2002; Nesbitt *et al.* 2006), which is the earliest evidence of dicynodont migration to North America. Because these materials are indeterminate and they predate any record of the group from neighbouring geographic areas (Europe, South America), their relationships and geographic origin remain dubious. Their migration from South America seems a reasonable scenario, since our analysis reconstructed the presence of kannemeyeriiforms in that region as the most

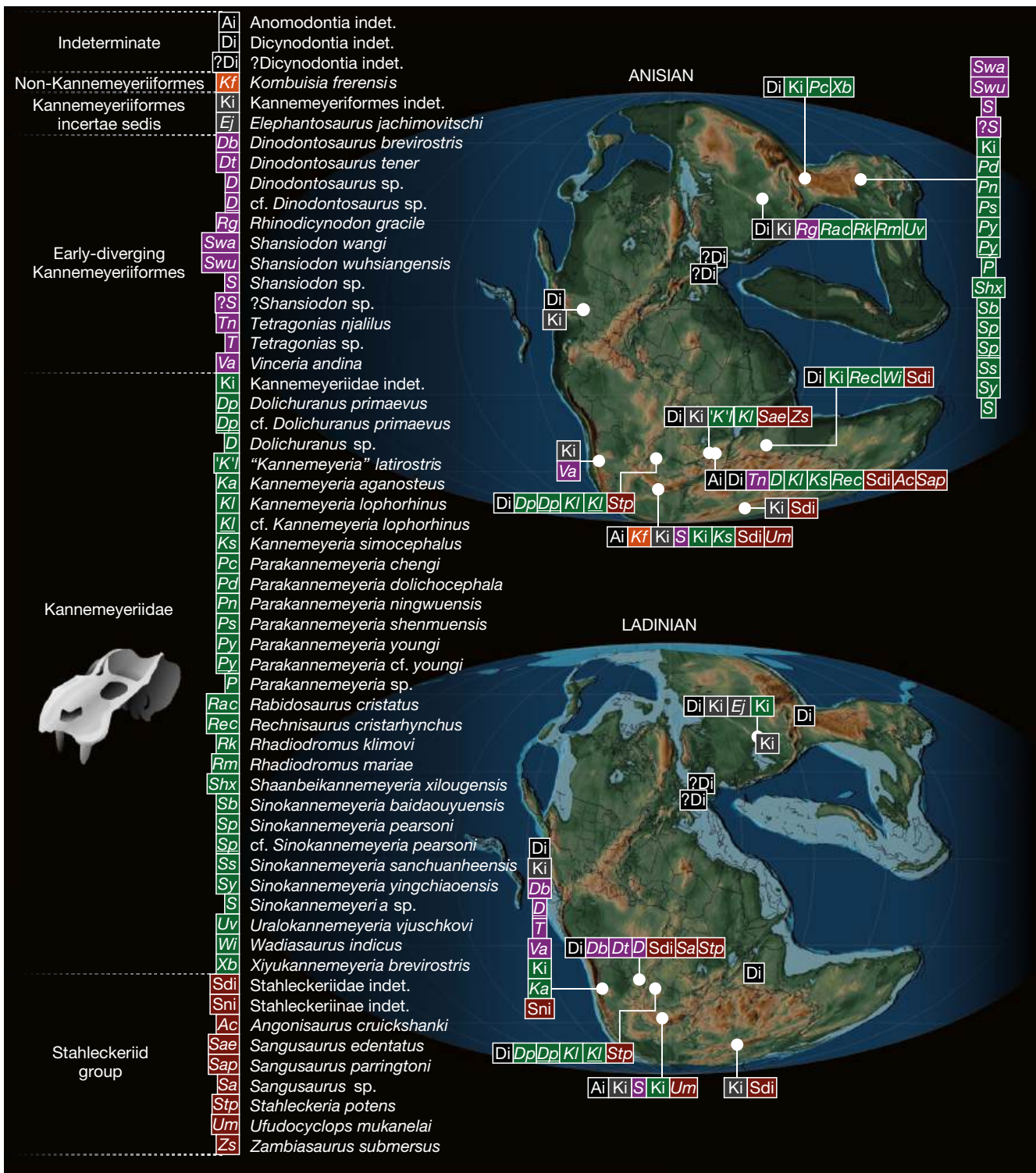


Fig. 21. — Middle Triassic distribution of dicynodont finds. Note that some of the formations traditionally dated to the Anisian may in fact be younger (Ladinian or Carnian; see text for discussion). Stahleckeriid group includes Stahleckeriidae Cox, 1965 (Stahleckeriinae + Placeriinae) and taxa more closely related to the Stahleckeriidae than to the Kannemeyeriidae von Huene, 1948. Skull of *Kannemeyeria simocephalus* (Weithofer, 1888) based on UMMF VP 14530.

probable ancestral state for the basal nodes of the Stahleckerinae and the clade of (*Acratophorus argentinensis* (*Rabidosaurus cristatus* + *Wadiasaurus indicus*)) with their age constrained to be probably no younger than the Anisian by the records

of *Stahleckeria potens* (primary distribution) and *Sangusaurus parringtonii* (secondary migration) in southeastern Africa as well as *Rabidosaurus cristatus* in Russia and *Wadiasaurus indicus* in India. A similar dispersal scenario was proposed by Lagnaoui

et al. (2019) based on the presence of dicynodont footprints around that time in both Argentina and the United States (e.g., Hunt *et al.* 1993; Nesbitt & Angielczyk 2002; Melchor & de Valais 2006); however, their current dating suggest rather a Late Anisian age (Cariglino *et al.* 2016; Díaz-Martínez *et al.* 2019; Haque *et al.* 2021). Possible dicynodont tracks are also known from the Anisian (including early Anisian) of Antarctica and Europe (England, France, Germany, and Italy), but their attribution to dicynodonts is less certain.

From around the Anisian/Ladinian boundary the shansiodont *Vinceria andina* and another, indeterminate kannemeyeriform (Zavattieri & Arcucci 2007; Kammerer & Ordoñez 2021) are known from the Cerro de Las Cabras Formation of Argentina (Cariglino *et al.* 2016) and some fragmentary dicynodont specimens were discovered in India (Kutty *et al.* 1988; Kutty & Sengupta 1989) and Antarctica (Hammer *et al.* 1987; Hammer 1990, 1995; Sidor *et al.* 2014; Kammerer *et al.* 2019; Smith *et al.* 2020a). From that time also are the first body-fossil recorded occurrences of dicynodonts from Western Europe – thus far, only isolated, undiagnostic bones were reported from France (?Dicynodontia indet. – Broili 1921, see discussion in: Camp & Welles 1956; Lucas & Wild 1995; Maisch *et al.* 2009) and Germany (aff. *Dinodontosaurus* sp. – Lucas 2007; note that the humerus previously interpreted by Lucas & Wild 1995 as belonging to aff. *Dinodontosaurus* sp. was subsequently identified as a probable temnospondyl by Maisch *et al.* 2009; the specimen described by Lucas 2007 was thus far not discussed in the literature, but its affinity to the genus *Dinodontosaurus* or even dicynodonts is suspect, therefore it is here regarded as ?Dicynodontia indet.). It remains uncertain from what region these European forms originated, since at the time Europe was a viable dispersal destination from either northeast, west, or south and nothing can be inferred about the phylogenetic affinity of these finds. Nonetheless, it appears that by the end of the Anisian, the Kannemeyeriformes inhabited already all major geographic regions and migrated freely across the Pangea.

Overall, the Anisian record of dicynodonts shows the largest diversity of kannemeyeriids (22 valid species in 11 valid genera + probable separate genus for “*Kannemeyeria latirostris*”), with only a single instance of a non-kannemeyeriid taxon (*Kombuisia frerensis*) and a few occurrences of early-diverging kannemeyeriforms (six species in five genera, traditionally grouped into the Shansiodontidae, globally distributed) and Stahleckeriidae (six species in five genera, all restricted to the Northern Hemisphere). This landscape, however, may be skewed due to the aforementioned problem with dating of the assemblages correlated to the South African *Cynognathus* Assemblage Zone. For example, the maximum age of the dicynodont-bearing strata of the Omingonde Formation, as well as the distribution of particular finds within the profile are currently unknown. Therefore, the times of occurrence of the Namibian Triassic taxa are here provisionally considered to cover parts of the Anisian and Ladinian. Estimated species number, including indeterminate finds reasonably representing new species (i.e., coming from localities and formations otherwise devoid of dicynodonts or representing

taxa otherwise not registered in given formations) in uncontroversial Anisian assemblages (including here the South African *Trirachodon-Kannemeyeria* and the lower part of the *Cricodon-Ufudocyclops* subzones, due to the well-studied biostratigraphy, partial radiometric dating, and continuity of the Karoo Supergroup; e.g., Smith *et al.* 2020b) is about 36, whereas the Anisian or younger assemblages could include up to about 12 species (at least *Kannemeyeria simocephalus* shared with the Karoo; Fig. 19A). Our phylogeny indicates at least eight ghost lineages lasting throughout the Anisian, but this number may not be reliable due to the incertain temporal correlations of the assemblages.

The Ladinian record of dicynodonts (Fig. 21) is very patchy and mostly represented by some very fragmentary and mostly indeterminate specimens from China (Lucas & Hunt 1993b), Kazakhstan (Tverdokhlebov *et al.* 2020), and the Bukobay Horizon of Russia (Kalandadze & Sennikov 1985; Shishkin *et al.* 1995; Ivakhnenko *et al.* 1997; Surkov 1999b), the latter also yielding *Elephantosaurus jachimovitschi*. Due to the poor taxonomic information on these forms, their phylogenetic and geographic origins are obscure but given that they are found in roughly the same geographical regions which were already inhabited in the Anisian (the outcrops of the Inder Formation of Kazakhstan being part of the same paleobiogeographic setting as the Russian Bukobay Formation; Tverdokhlebov *et al.* 2020), they likely are autochthonic. Additionally, the shansiodontid *Tetragonias* sp. (Kammerer & Ordoñez 2021) and the kannemeyeriid *Kannemeyeria aganosteus* have been collected from the Argentinian Quebrada de los Fósiles Formation, which was recently determined mostly Carnian with the Ladinian lower part (Ottone *et al.* 2014). Since these specimens were found in the lower part of that formation (Bonaparte 1981), they are likely Ladinian in age. They are congeneric with the southeastern African *Kannemeyeria simocephalus* and *Tetragonias njalilus* and in our analysis they are reconstructed as migrants from that region. An indeterminate possible kannemeyeriid was reported from the upper part of the Tarjados Formation in Argentina (Romer 1966; Cox 1968; Ezcurra *et al.* 2015), which likely is also Ladinian in age (Marsicano *et al.* 2016; Ezcurra *et al.* 2017).

The Ladinian/Carnian boundary may further be represented by the Brazilian *Dinodontosaurus* Assemblage Zone, the oldest member of the Santa Maria Formation, which yielded *Dinodontosaurus tener*, *Dinodontosaurus* sp. (“*Dicynodon turpior*”), the stahleckeriid *Stahleckeria potens*, and possibly another unrecognized stahleckeriid (Maisch 2021; Kammerer & Ordoñez 2021). These taxa belong to two separate groups which likely independently immigrated from southeastern Africa and mostly remained in South America. Traditionally considered Ladinian based on biostratigraphy (e.g., Lucas & Harris 1996; Fröbisch 2009; Schultz *et al.* 2016; Melo *et al.* 2017), the *Dinodontosaurus* Assemblage Zone was recently suggested to be late Ladinian/early Carnian due to the early and mid-Carnian radiometric ages of, respectively, the overlying *Santacruzodon* (Philipp *et al.* 2018) and *Hyperodapedon* (Langer *et al.* 2018) Assemblage Zones. On the other hand, the validity of the *Santacruzodon* Assemblage Zone

was recently questioned due to its taxonomic similarity with the *Dinodontosaurus* Assemblage Zone (e.g., Martinelli *et al.* 2017; Ordoñez *et al.* 2020) and the *Dinodontosaurus* Assemblage Zone was typically correlated with the radiometrically dated Carnian (Marsicano *et al.* 2016; Ezcurra *et al.* 2017) Chañares Formation, leading some authors to the assumption that both assemblages are roughly coeval and early Carnian (e.g., Melo *et al.* 2017; Ordoñez *et al.* 2020). Kammerer & Ordoñez (2021) noted that the representatives of the genus *Dinodontosaurus* from Argentina and Brazil appear specifically distinct and suggested that this may indicate not only geographical, but also temporal differences between two assemblages. However, they did not address the presence of material from the Santa María Formation (DGM 149R) referred by Cox (1968) to *Dinodontosaurus "platygynathus"* Cox, 1968 (according to Kammerer & Ordoñez 2021, junior synonym of the Argentinian *Dinodontosaurus brevirostris*) and separate from *Dinodontosaurus tener*. Until this attribution is validated or refuted, the relationships between these two assemblages remain uncertain. The Santa María Formation also provided fossils of *Sangusaurus* sp. (Schwanke-Peruzzo 1990; Schwanke-Peruzzo & Araújo-Barbarena 1995; Lucas 2002; Dassie 2014; Kammerer & Ordoñez 2021), as well as an undescribed *Dinodontosaurus*-like dicynodont from the *Santacruzodon* Assemblage Zone (Martinelli *et al.* 2017). Da Rosa *et al.* (2004, 2005) and Martinelli *et al.* (2005) reported the presence of Dicynodontidae indet. from the Santa María formation, but since the representatives of the clade identifiable as the Dicynodontidae (i.e., containing both species of *Dicynodon* but not Lystrosauridae and Kannemeyeriiformes; in our analysis identical with the genus *Dicynodon*) seem to be restricted to the Permian (e.g., Kammerer *et al.* 2011; Kammerer & Ordoñez 2021; this study) and the authors explicitly used this designation in light of no diagnostic characters in the studied material, this should be treated as a lapsus calami and the materials should be referred to Dicynodontia indet.

Overall, the Ladinian, as currently understood, shows a great decrease in the diversity of the Kannemeyeriidae (three valid species in two genera from Argentina and Namibia, and possible additional two species in South Africa and Russia) and extinction of most taxa in the Northern Hemisphere. This results in a larger relative contribution of early-diverging kannemeyeriiforms (Shansiodontidae and *Dinodontosaurus* spp.), although the actual diversity also slightly decreased compared to the Anisian (three valid species in two genera plus two genera with indeterminate species). Likewise, there was a decrease in the number of valid stahleckeriid taxa: two valid species in two genera with another unnamed species in the third genus and possible two additional species in the Antarctica (Sidor *et al.* 2014, aforementioned from the Anisian/Ladinian boundary of the upper Fremouw Formation; Kammerer *et al.* 2019) and Argentina (from the Ladinian/Carnian boundary of the Chañares Formation; Cox 1968; Escobar *et al.* 2021). *Elephantosaurus jachimovitschi* is currently considered *incertae sedis*, therefore it may be part of a representative of either group, most likely aside of Stahleckeriidae (Kammerer *et al.* 2013). “*Fukangolepis barbaros*

Yang, 1978 is a very fragmentary indeterminate dicynodont from the Upper Karamay Formation of China, nonetheless indicative of the presence of that group. Overall, the species number in the currently accepted Ladinian may be estimated to about 23 species (Fig. 19A). As mentioned above, some of the classically considered Anisian, kannemeyeriid-yielding assemblages of southern and eastern Africa and India may in fact represent the Ladinian, thus rendering at least some of the perceived diversity decrease an artifact. The same is true for the five ghost lineages observed throughout the Ladinian in our phylogeny. Interestingly, probable Ladinian dicynodont ichnological record constitutes only of tracks from Argentina and possibly France, which would be consistent with at least some dip in dicynodont diversity around that time.

Carnian finds (Fig. 22) from the Southern Hemisphere include: an indeterminate dicynodont from the Lashly Formation of Antarctica (Hammer *et al.* 2004); *Dinodontosaurus brevirostris*, and an isolated ulna referred to the stahleckeriid *Stahleckeria* sp. (Mancuso & Irmis 2019) from the Chañares Formation (Marsicano *et al.* 2016; Ezcurra *et al.* 2017) of Argentina; the stahleckeriid *Ischigualastia jensei* from the Ischigualasto Formation (Rogers *et al.* 1993; Currie *et al.* 2009; Martínez *et al.* 2011, 2012) of Argentina; the kannemeyeriids *Acratophorus argentinensis* and *Kannemeyeria aganosteus* from the Río Seco de la Quebrada Formation (Ottone *et al.* 2014) of Argentina; and an undescribed kannemeyeriid from Madagascar (Flynn *et al.* 1999). According to our results, in the Carnian the South American dicynodont fauna is autochthonic with no inflow from other regions – the taxa either continue their presence from the Ladinian or belong to sedentary groups reconstructed as ancestrally South American. As mentioned above, the *Cynognathus* Assemblage Zone, Denwa, upper Fremouw, Manda, Ntawere, and Yerrapalli dicynodonts may possibly also be at least partially Carnian.

From the Carnian of the Northern Hemisphere, dicynodonts have been described from a variety of localities. Europe yielded the stahleckeriid-related *Woznikella triradiata* n. gen., n. sp. from the Grabowa Formation (Szulc *et al.* 2015b) of Poland (Sulej *et al.* 2011 and this paper, see Szulc *et al.* 2015b for an alternative view on the age of the Woźniki assemblage) and the Stuttgart Formation of Germany (Schoch 2012). The United States are represented by placeriine stahleckeriids: *Placerias hesternus* from the Pekin Formation (Baird & Patterson 1968; Lucas 1998; Kammerer *et al.* 2013; Heckert *et al.* 2017), *Eubrachiosaurus browni* and its possible synonym, “*Brachybrachium breviceps*” Williston, 1904, from the Popo Agie Formation (Kammerer *et al.* 2013; Hartman *et al.* 2015), and one or two other stahleckeriids (NCSM 21719 from the Pekin Formation (Heckert *et al.* 2017) and NMMNH P-13001 from the Santa Rosa Formation (Hartman *et al.* 2015) – one of them possibly referable to *Eubrachiosaurus browni*; Lucas & Hunt 1993b; Green *et al.* 2005; Green 2012; Kammerer *et al.* 2013). Furthermore, two articulated dicynodont phalanges (possibly *Placerias hesternus*) were reported by Sues *et al.* (2003) from the Lithofacies Association II of the Newark Supergroup, United States, dated to late Carnian/early Norian. Pelvic fragments and a sacrum were reported from the Wolfville Formation of

Canada (Sues & Olsen 2015); The only Late Triassic record of dicynodonts from East Asia is an indeterminate dicynodont from the Momonoki Formation of Japan (Jinnouchi *et al.* 2018). India produced indeterminate dicynodonts from the lower Maleri Formation (Bandyopadhyay 1988; Kutty & Sengupta 1989) and a skull from the Pipariya Formation named by Edler (2000) "*Ischigualastia rama*" (*nomen invalidum*). The characters listed in the diagnosis of the latter species ("The parietal crest is not as high as the parietal crest of *I. jensi*; the posterior process of the postorbital does not come as close to the interparietal as it does in *I. jensi*, and the lacrimal has a more rounded shape along its ventral margin contact with the maxilla than in *I. jensi*") can easily be of taphonomic, sexually dimorphic, or ontogenetic nature (Edler 2000). Thus, the specimen is better tentatively referred to cf. *Ischigualastia jensi* and requires revision and official redescription. The placeriine *Moghreberia nmachouensis*, "*Azarifeneria barrati*" Dutuit, 1989a, and "*Azarifeneria robustus*" Dutuit, 1989b (the latter two now considered *nomina dubia* and possibly synonymous with *Moghreberia nmachouensis*; see discussion in Lucas & Wild 1995; Kammerer *et al.* 2013) from the Argana Formation of Morocco were traditionally considered Carnian, but see Kammerer *et al.* (2012) for a discussion of a possible Norian age of these fossils. The diverse Carnian landscape of dicynodonts from North Hemisphere suggests intensive migrations. According to our results, *Eubrachiosaurus browni* is an offshoot of the South American part of the tree and *Woznikella triradiata* n. gen., n. sp. and the placeriins of the North Hemisphere immigrated from the southeastern Africa. The lineage of *Woznikella triradiata* n. gen., n. sp. diverged early, most probably not later than in the early Anisian, but it has no fossil record before the early Carnian. The Placeriins appear to have migrated through western Europe (node without known record but eventually leading to *Lisowicia bojani*) to North America and later to northern Africa but likewise their record prior to the Carnian is poor. The presence of cf. *Ischigualastia jensi* in India indicates a route of dispersal from South America. Probable dicynodont tracks were found in the Carnian of Argentina and Poland (depending on the age of the Woźniki assemblage). Courel *et al.* (1968) mentioned therapsid tracks from the Keuper of France but did not specify a more exact age; these may, however, be Norian rather than Carnian (Klein & Lucas 2010). Our phylogeny indicates three ghost lineages spanning throughout the Carnian.

The Carnian was a time of kannemeyeriid decrease. Only two named species of two genera of that family (*Acratophorus argentinensis* and *Kannemeyeria aganosteus*) are known from Argentina, and the finds from Madagascar (Flynn *et al.* 1999) may indicate another species. Warren (1998) noted kannemeyeriid specimens from the unspecified portion of the *Cynognathus* Assemblage Zone of South Africa, which potentially may indicate Carnian age (Hancox *et al.* 2020), but it seems reasonable that they come from the pre-Carnian part of that Zone. The same is true for the indeterminate anomodont mentioned by Watson (Watson 1960). Early-diverging kannemeyeriiforms (shansiodontids and *Dinodontosaurus* spp.) are represented by four species (two of them named,

two indeterminate) in three genera and were restricted to the Southern Hemisphere. Stahleckeriid line diversity took a lead, with at least eight valid genera and seven named species ("*Azarifeneria*" spp. treated here as likely synonyms of *Moghreberia nmachouensis*) and possibly up to 13 species if the Indian cf. *Ischigualastia jensi* (Edler 2000) and Argentinian (Cox 1968; Mancuso & Irmis 2019; Escobar *et al.* 2021; Kammerer & Ordoñez 2021) and North American (Lucas & Hunt 1993a; Long & Murry 1995; Green *et al.* 2005; Green 2012; Kammerer *et al.* 2013) Stahleckeriinae prove to be separate species. The total number of Carnian species estimated based on available data is about 24 (Fig. 19A).

Only several certain post-Carnian dicynodonts (Norian, some possibly extending into the earliest Rhaetian, depending on the temporal location of the boundary; see Kowal-Linka *et al.* 2018, 2019) are currently known (Fig. 22). From the Northern Hemisphere these are: an almost complete skeleton of the placeriine *Lisowicia bojani* and fragmentary remains of a similar dicynodont from the Grabowa Formation (Szulc *et al.* 2015b) of Poland (Dzik *et al.* 2008a; Budziszewska-Karwowska *et al.* 2010; Sulej & Niedzwiedzki 2019); some cranial and postcranial elements from the Maleri Formation in India (Kutty & Sengupta 1989); *Placerias hesternus* from the Chinle Group (Olsen *et al.* 2010; Irmis *et al.* 2011; Ramezani *et al.* 2011, 2014) and the Cooper Canyon Formation (Martz *et al.* 2013), a kannemeyeriid and several indeterminate specimens from the Dockum Group (Lehman & Chatterjee 2005; Mueller & Chatterjee 2007; Martz 2008; Martz *et al.* 2013; Small *et al.* 2022) of the United States, and possibly *Moghreberia nmachouensis* from Morocco. The Southern Hemisphere is represented by the South American stahleckeriins, *Jachaleria colorata* from the upper Ischigualasto (Rogers *et al.* 1993; Currie *et al.* 2009; Martínez *et al.* 2011, 2012) and lower Los Colorados (Kent *et al.* 2014) formations of Argentina and *J. candelariensis* from the Caturrita Formation (Santa María Supersequence, *Riograndia* Assemblage Zone) (Langer *et al.* 2018; Martinelli *et al.* 2020) of Brazil, and *Pentasaurus goggai* from the lower Elliott Formation (Fröbisch 2009; Kammerer 2018) of South Africa. Norian and perhaps Rhaetian tracks possibly left by dicynodonts were reported from Argentina, Europe (France, Poland), Lesotho, and United States, generally agreeing with the distribution of body fossils. The reduction of diversity in the Norian was thus significant: seven species in six genera (including the cf. *Ischigualastia* sp. from the Upper Maleri Formation; Bandyopadhyay 1988; Kutty & Sengupta 1989; Novas *et al.* 2010; Bandyopadhyay & Ray 2020), up to ten species if the lower Elliott (Bordy *et al.* 2020) dicynodont represents a new species (Fig. 19A). Interestingly, the Norian marked an apparent end to large scale dicynodont migrations – all taxa are autochthonic and inhabit regions in which the presence of their respective clades was established prior to the Norian (as mentioned above, the lineage of *Lisowicia bojani* has no earlier record but remains in its reconstructed ancestral range). In contrast to the Early Triassic, the global dicynodont population was more partitioned, with individual species occupying restricted geographical areas. The post-Carnian landscape was apparently completely dominated by Stahleck-

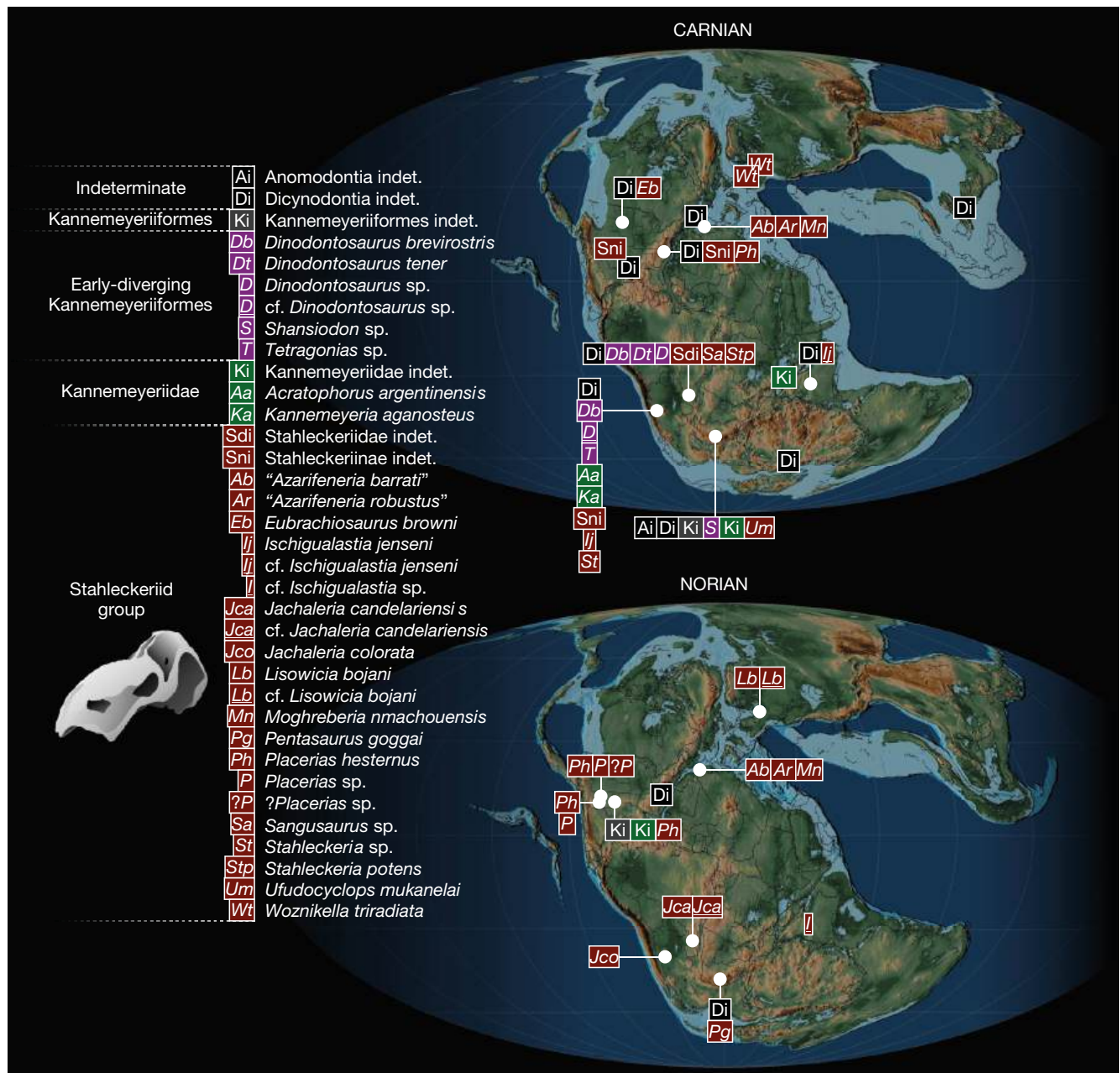


Fig. 22. — Late Triassic distribution of dicynodont finds. Rhaetian not shown, since only the upper temporal ranges of *Lisowicia bojani* Sulej & Niedźwiedzki, 2019 from the Grabowa Formation of Poland and *Pentasaurus goggai* Kammerer, 2018 and Dicynodontia indet. from the *Scalenodontoides* Crompton & Ellenberger, 1957 Assemblage Zone of the Lower Elliott Formation of South Africa may possibly (but not necessarily) extend beyond the Norian. Stahleckeriid group includes Stahleckeriidae Cox, 1965 (Stahleckerinae + Placerinae) and taxa more closely related to the Stahleckeriidae than to the Kannemeyeriidae von Huene, 1948. Skull of *Ischigualastia jensei* Cox, 1962 based on PVSJ 545.

eriidae. Eventually, the dicynodonts went extinct before the Jurassic (Knutsen & Oerlemans 2020).

Based on the data presented above, from the point of dicynodont species richness (Fig. 19B, C), in the Triassic the region of modern-day China was the richest in the world (about 18 species), even though most of that diversity (about 14 species) comes from the Anisian and no Chinese dicynodonts are known after the Ladinian. The Anisian Chinese species number may, however, be overestimated due to likely oversplitting (Fröbisch 2009; Kammerer *et al.* 2017; Maisch

2021). The second place is occupied *ex aequo* by Argentina and South Africa (about 11 species each). Argentina was the main hotspot of dicynodont diversity in the Ladinian and Carnian (about seven species each). South Africa is the only region in the world with a nearly constant record of dicynodonts throughout Permian and Triassic, from Wordian through Norian and possibly Rhaetian, with only minor gaps in the late Olenekian *Langbergia-Garjainia* Subzone of the *Cynognathus* Assemblage Zone and the Carnian/Norian Molteno Formation which is devoid of vertebrate remains

(Hancox *et al.* 2020; Smith *et al.* 2020b; Ellenberger 1970 hinted at the possible presence of *Kannemeyeria* sp.(?) in his zone A/2, lower Molteno *b* of Lesotho, below the *Scalenodonoides* Assemblage Zone, but it appears that this specimen was either misidentified or wrongly attributed stratigraphically, because all newer papers are adamant about the lack of vertebrate fossils in the Molteno Formation – e.g., Anderson & Anderson 1984; Hancox *et al.* 2020; Viglietti *et al.* 2020b). Together with Antarctica, it was also inhabited by the most diverse spectrum of dicynodont clades through the Triassic: three various non-kannemeyeriiform taxa (*Myosaurus gracilis*, *Kombuisia frerensis*, *Lystrosauridae*), shansiodontids, kannemeyeriids, and stahleckeriids (possibly both *Placeriinae* and *Stahleckeriinae*, depending on the exact phylogenetic position of *Ufudocyclops mukanelai*). Russia produces about ten Triassic dicynodont species, Antarctica and India – about nine and are followed by Tanzania with about eight species, the United States with about six species, and Brazil with about five species. The Indian record is also fairly consistent from the Early Triassic to the Norian. Tanzania seemingly experienced a sudden burst of dicynodont diversity in the Anisian (or later, dependent on the dating of the Manda Formation) but has no known Triassic dicynodont finds of earlier or later ages. Each of the other countries was populated by less than five Triassic dicynodont species.

Overall, the distribution of particular clades shows no clear divisions into the Northern and Southern hemispheres. Instead, a sub-longitudinal division seems to be present, with some clades present exclusively in the eastern or in the western/southwestern parts of Pangea. This is the least obvious with the early-diverging Kannemeyeriiformes (Shansiodontidae and *Dinodontosaurus* spp.), which apparently originated in southeastern Africa, but were roughly globally distributed in the Anisian, but in the Ladinian and Carnian resided solely in the southwestern area (modern-day Argentina, Brazil, and South Africa). South America was also the only place of occurrence of *Dinodontosaurus* spp. It seems that stahleckeriids appeared in the Anisian in the southern part of the globe (Vega-Dias *et al.* 2004; Kammerer *et al.* 2017) and with time expanded northward and westward, into Argentina, North America, and Central Europe, but apparently never reached Australia, Russia, and northeastern Asia. Although even quite recently available data suggested that the two subfamilies of the Stahleckeriidae, the *Placeriinae* and *Stahleckeriinae*, in the Late Triassic tended to occur in the Northern and Southern Hemispheres, respectively, newer discoveries indicated that this is not exactly the case, and the paleobiogeographic situation was more complex (e.g., Kammerer *et al.* 2013, 2017, 2019; Kammerer 2018). Representatives of both subfamilies were restricted to the Southern Hemisphere in the Middle Triassic, although the *Placeriinae* were represented at the time only by *Zambiasaurus submersus*. In the Carnian they colonized the Northern Hemisphere. The *Placeriinae* indeed are known from that time only from the Northern Hemisphere, but in the United States they were accompanied by stahleckeriines. In the Norian the situation was reversed: the *Stahleckeriinae* were restricted to South America and India, whereas the Place-

riinae were present in the Northern Hemisphere and in South Africa (*Pentasaurus goggiae*). Conversely, kannemeyeriids, also probably originating in southeastern Africa, but abundant during the Anisian in China, Russia, and southeastern part of Pangea, in the Ladinian and Carnian became restricted to Argentina, South Africa, and Madagascar, but arrived in North America only in the Norian and never in Brazil. Intriguingly, dicynodont dispersal was predominantly directed towards the north and west, with northern groups very rarely migrating southward and taxa leaving southeastern Africa virtually never returning. The only two cases of such a return in our results are *Sangusaurus parringtonii* (immigration from South America, unambiguous in the biogeographic analysis presented above) and the shift in the middle part of the tree, with the whole stem at the level of *Taoheidon baizhijuni* and (*Counillonia superoculis* + *Repelinosaurus robustus*) branches migrating to eastern Asia and then returning. The latter, however, is most probably an artifact (see above).

Interestingly, currently there is no evidence of phylogenetic or paleobiogeographic connections between Central and Eastern Europe (Russia), although the former region could logically serve as a passageway connecting the northeastern and southwestern Pangea. Kammerer (2018) noted that some of the observed patterns of Late Triassic dicynodont distribution, similar to the case of traversodontids (Whiteside *et al.* 2011), could be dictated by the geographic patterns of aridity, due to the physiologically higher demand for water in synapsids caused by their ureotelism, in contrast to the more water efficient uricotelism of sauropsids. A newer study by Dunne *et al.* (2021), on the contrary, noted that Late Triassic synapsids on average preferred lower mean annual precipitation (drier areas) and temperatures but higher seasonal variations in precipitation and temperature than most reptiles and temnospondyls. Unfortunately, dicynodonts were not treated separately in that study. Therefore, it remains uncertain whether they fit within the main bulk of analyzed synapsid taxa or were outliers. Liu *et al.* (2021) suggested that dicynodonts overall preferred local humid environments, but they did not analyze taxa younger than Early Triassic and noted that at least *Lystrosaurus* in the Permian did occur in some arid habitats. Triassic coprolites attributed to dicynodonts indicate that at least some species preferred swampy environments (Hunt *et al.* 1998, 2007; Bajdek *et al.* 2014). It seems that while geographic occurrences of some taxa, most notably the *Placeriinae*, indeed appear to fall in the regions of higher annual precipitation (Kammerer 2018; Dunne *et al.* 2021), the *Stahleckeriinae* are also present in very arid areas (Kammerer *et al.* 2013; Dunne *et al.* 2021). Aside from excretory physiology, this may be also correlated with dietary adaptations within particular clades (e.g., Camp 1956; Cox 1965, 1991; Keyser & Cruickshank 1979; Surkov & Benton 2008), although this explanation alone is likely not exhaustive (Kammerer 2018). It must be, nonetheless, noted that these patterns may be partially influenced by sampling bias. For example, the northern part of South America, southern part of North America, and central Africa are devoid of Triassic dicynodont

fossils, which could be taken as evidence that these regions were avoided by dicynodonts in the early Mesozoic and that there was a strict separation into the Northern Hemisphere and Southern Hemisphere faunas. However, exactly the same pattern is also true for Permian dicynodonts and, in fact, all Permian, Triassic, and even Jurassic vertebrates and other animals and plants (<https://paleobiodb.org>). This sampling bias makes it necessary to exercise caution when considering the results at a finer scale. Missing data may obviously impact the accuracy of the reconstruction and the biogeographic history of some clades is currently unknown. Evaluation of the geographic sampling bias utilizing current methods (e.g., Benton *et al.* 2011; Benson & Upchurch 2013; Dunhill *et al.* 2014; Gardner *et al.* 2019) is beyond the scope of this study but given that Triassic rocks all over the world provide numerous fossil assemblages, in some cases abundant in fossils and capable of preservation of terrestrial animals, such as archosauromorphs or parareptiles, it may be speculated that at least locally and temporally the main factors limiting the fossil record of dicynodonts are true biogeographic and/or ecological factors and not geographic sampling or rock availability bias. Furthermore, it remains to be tested whether the dominance of the southeastern Africa in the ancestral ranges throughout the tree is a true signal or an effect of the unusual completeness and continuity of the fossil record of dicynodonts in South Africa, particularly in the Permian. Our paleobiogeographic data, nonetheless, indicate that throughout the Triassic various dicynodont taxa crossed the equator multiple times. Given the general trend of migration out of the southeastern Africa, as well as the usually more derived phylogenetic positions and later occurrence time of some of the non-southeastern African taxa, it appears likely that this signal is genuine. Additionally, in contrast to the Permian, the diversity of the South African assemblages in the Triassic is more in line with the diversity in other geographic areas (e.g., King 1988; Fröbisch 2009) which may indicate that it is not significantly biased. It seems also realistic that the immediate ancestors of the Kannemeyeriformes of southeastern African descent could in the Early Triassic reside in the equatorial, continental regions of Pangea before they replaced Lystrosauridae at the beginning of the Anisian (Maisch & Matzke 2014). This could explain why, despite multiple decades of Triassic dicynodont studies and relatively good quality of the anomodont fossil record (Walther & Fröbisch 2013), the origin of the Kannemeyeriformes remains enigmatic (Kammerer *et al.* 2013; Maisch & Matzke 2014). Worth noting is also the fact that the currently understood Ladinian-Carnian specific diversity of dicynodonts may be significantly under-represented, since named taxa constitute only slightly over one third (Ladinian) to less than one half (Carnian) of the diversity estimated based on indeterminate finds (Fig. 19A).

AGE OF THE WOŹNIKI ASSEMBLAGE

The ages of Polish Late Triassic vertebrate assemblages, including Woźniki, spark controversy, particularly due to still not understood factors contributing to the very different

specific compositions of individual localities, lack of polytomorphic and/or radiostratigraphic data, and poor specific recognition and/or taxonomic resolution of many potentially biostratigraphically informative invertebrate and vertebrate taxa (Lucas 2015; Czepiński *et al.* 2021). Sulej *et al.* (2011) considered the locality to be of mid-late Carnian age based on the presence of the spinicaudatan *Laxitextella* cf. *Laxitextella laxitexta* (Jones 1890), a member of the genus which, according to Lucas (Lucas 2015), has no Norian records (Olempska 2004; Geyer & Kelber 2018), and unspecified bivalves that they deemed similar to the taxa from Krasiejów (also considered Carnian by them). This interpretation was, however, refuted by Szulc *et al.* (Szulc *et al.* 2015a, b) who noted that the biostratigraphic data available for the locality were poor and that lithostratigraphic sequences that they compared to Krasiejów (considered by them Norian) and the Schilfsandstein were present lower in the same well of the Woźniki K1 borehole (Rubin & Rubin 2009), 2.3 km from the Woźniki outcrop. Based on that, they advocated for a Norian age of the locality. Recently, Racki & Lucas (2020) argued that large terrestrial tetrapods, such as dicynodonts, have a high potential for biostratigraphic correlations. Although this potential is limited by the overall scarcity and incompleteness of large vertebrate taxa in most fossil localities, frequently leading to problems with interpretations of intra- and interspecific variability, and (particularly in the case of dicynodonts) by the high degree of endemism, the presence of material referable to *Woznikella triradiata* n. gen., n. sp. in the lower part of the early Carnian Stuttgart Formation (Schilfsandstein) near Ansbach, Bavaria, southern Germany (Schoch 2012) is an example of such a correlation and the first substantial evidence supporting the Carnian age of the Woźniki assemblage. This may be significant, because such a correlation is independently supported by the fact that the currently recognized temporal range of *Laxitextella laxitexta* also covers the lower part of the Stuttgart Formation and is replaced in the equivalent of the upper Stuttgart Formation in the Ansbach sequence by a different, yet undescribed spinicaudatan species (Geyer & Kelber 2018). Furthermore, both the Woźniki and Ansbach assemblages are nearby parts of the same basin at the time connected by playa (McKie & Williams 2009) and it seems reasonable that no significant barriers prevented exchange of populations, thus requiring a substantial temporal offset between both places. The biostratigraphic data, therefore, suggest an early rather than mid-late Carnian or Norian age for the Woźniki assemblage. This indicates either a more complex paleoenvironmental situation of the Polish Late Triassic with diachronic development of lithostratigraphic features, or a relatively long temporal range and low biostratigraphic utility for the invertebrate and vertebrate taxa used for correlations (Schoch 2012; Geyer & Kelber 2018), although evidence is lacking for the latter hypothesis. More data are needed to establish which approach is more adequate, but it is currently clear that there is a conflict between the lithostratigraphic and biostratigraphic lines of reasoning that cannot be resolved in the case of Polish Late Triassic.

PHYLOGENETIC ANALYSIS

The phylogenetic results obtained herein are in some cases surprising. One of such instances is the relatively derived position of (*Euptychognathus bathyrhynchus* (*Basilodon woodwardi* + *Sintocephalus alticeps*)) right next to the Kannemeyeriiformes in the analysis with *Ufudocyclops mukanelai* excluded. *Basilodon woodwardi* and *Sintocephalus alticeps* are usually recovered close to the base of the Dicynodontoida (e.g., Kammerer *et al.* 2013; 2019; Angielczyk *et al.* 2021) and *Euptychognathus bathyrhynchus* is typically considered either a lystrosaurid (e.g., Kammerer *et al.* 2013; Kammerer & Ordoñez 2021) or an early diverging dicynodontoid (e.g., Kammerer *et al.* 2019; Angielczyk *et al.* 2021). However, a somewhat intermediate position of *Sintocephalus alticeps* and *Euptychognathus bathyrhynchus* in a larger sister group to the Kannemeyeriiformes (also including, e.g., *Lystrosaurus* spp. and *Daptocephalus* spp., consistent with our analysis including all taxa) was obtained by Kammerer (2018) and later also for *Basilodon woodwardi* by Kammerer & Ordoñez (2021). It is probably significant that in our analysis their relationship and derived position is supported by quantitative rather than qualitative characters. According to the tests done by Kammerer *et al.* (2011), continuous characters are useful in resolving dicynodont relationships when used in combination with discrete characters, but on their own do not preserve enough information to provide accurate reconstruction of phylogeny and thus may produce misleading results. Although our dataset includes discrete characters, in the case of the (*Euptychognathus bathyrhynchus* (*Basilodon woodwardi* + *Sintocephalus alticeps*)) clade the continuous characters take precedence and produce a rather unusual result. This topology should be, therefore, taken with caution and validated by future studies.

The observed instability of *Ufudocyclops mukanelai*, its different (less derived) positions in our trees compared with the analyses by Kammerer *et al.* (2019), Kammerer & Ordoñez (2021), and Angielczyk *et al.* (2021), and the discrepancy of the topologies of Kannemeyeriiformes and some non-kannemeyeriiform taxa obtained with and without that species suggest a conflict of phylogenetic signals coming from that taxon and from *Woznikella triradiata* n. gen., n. sp. This is highlighted by the fact that the addition of *Woznikella triradiata* n. gen., n. sp. to the matrix including *Ufudocyclops mukanelai* resulted in a rather unorthodox topology, with *Jachaleria* spp. paraphyletic relative to *Ischigualastia jensi* and located outside of Stahleckeriinae, at the base of Stahleckeriidae. In neither of our trees including *Woznikella triradiata* n. gen., n. sp. did *Ufudocyclops mukanelai* retain its position as a sister group to *Stahleckeria potens*, as was recovered in previous analyses (Kammerer *et al.* 2019; Kammerer & Ordoñez 2021; Angielczyk *et al.* 2021). Notably, in the original description Kammerer *et al.* (2019) admitted that the support for their topology is low, and they suspected *Ufudocyclops mukanelai* of being a basal stahleckeriid based on its broad frontal contribution to the orbital margin and its early time of occurrence. In three out of six topologies recovered by us, the immediate position of *Ufudocyclops mukanelai* was not supported by any synapomorphies, in

two it was supported by the characteristics of the nares (possibly ontogenetically and/or sexually variable due to different development of nasal rugosities or bosses?), and in one by the shape of the occipital condyle (not preserved in *Woznikella triradiata* n. gen., n. sp.). Furthermore, for two of those topologies *Ufudocyclops mukanelai* presented no autapomorphies, while for the remaining four, relatively short lists of autapomorphies (two to four), indicating its overall rather generalized morphology. Interestingly, *Woznikella triradiata* n. gen., n. sp. remained relatively stable regardless of the presence or absence of *Ufudocyclops mukanelai*, occupying positions either just before or just after the divergence of Placeriinae. Conversely, in the analyses with *Woznikella triradiata* n. gen., n. sp. excluded, *Ufudocyclops mukanelai* was stable and constituted the sister group to *Stahleckeria potens* (in accord with previous analyses, e.g., Kammerer *et al.* 2019; Kammerer & Ordoñez 2021; Angielczyk *et al.* 2021). This may result from several factors. Firstly, some taxa pivotal to understanding the evolutionary split between the Shansiodontidae, Kannemeyeriidae, and Stahleckeriidae remain undiscovered, leaving this crucial part of the phylogenetic tree poorly sampled and making interpretations of character polarity and identification of important characters uncertain. Secondly, some possible errors in the scorings of *Ufudocyclops mukanelai* and/or *Woznikella triradiata* n. gen., n. sp. exist that introduce artificial incongruence between them. Certainly, reconsideration of these taxa when new materials become available will be necessary, especially because *Ufudocyclops mukanelai* is currently known exclusively from cranial remains (some associated fragmentary postcranial bones were reported but considered too large compared to the skulls and thus their provenance is dubious; Hancox *et al.* 2013; Kammerer *et al.* 2019) and *Woznikella triradiata* n. gen., n. sp. includes a relatively good sample of postcranial elements but preserves few cranial bones and is represented by an immature individual. Indeed, the postcranial morphology of Triassic dicynodonts may be insufficiently represented in the matrix, and thus further studies should be focused more on that aspect of dicynodont anatomy. This is particularly important in the context of ontogenetic variability, which is still poorly understood. Finally, the matrix still consists of a relatively small number of characters relative to the number of taxa considered. All these factors are reflected in some lability of taxa, instability of clades (particularly the traditionally understood Shansiodontidae and Kannemeyeriidae), and low support values noted in this and previous studies (e.g., Kammerer *et al.* 2011, 2013, 2019; Maisch & Matzke 2014; Olivier *et al.* 2019; Kammerer & Ordoñez 2021). Fortunately, the exclusion of *Ufudocyclops mukanelai* likely did not significantly impact the results of our paleobiogeographic analysis, because in most of our trees and in the previous analyses (Kammerer *et al.* 2019; Kammerer & Ordoñez 2021; Angielczyk *et al.* 2021) that taxon was recovered among other African dicynodonts (the only exception being its position as a side group to *Eubrachiosaurus browni* in one of our trees). The analysis with *Ufudocyclops mukanelai* disabled is, however, one of a few (Maisch 2001;

Kammerer *et al.* 2011, 2013; Kammerer & Smith 2017; Olivier *et al.* 2019) that recovered a monophyletic Shansiodontidae consisting of more than two taxa (Vega-Dias *et al.* 2004; Govender 2005; Surkov & Benton 2008; Maisch & Matzke 2014; Angielczyk & Kammerer 2017; Angielczyk *et al.* 2017) and only the second (after Olivier *et al.* 2019) that at the same time includes a monophyletic Kannemeyeriidae. Although considerable progress in knowledge about Triassic dicynodonts has been made in recent years, particularly when it comes to taxonomy, and although the stability of phylogenetic hypotheses significantly improved in the last decade compared to earlier years (Cox 1965; Cruickshank 1970; Keyser 1974; Keyser & Cruickshank 1979, 1980; Cooper 1980; King 1988; Maisch 2001; Surkov & Benton 2004, 2008; Vega-Dias *et al.* 2004; Govender 2005; Kammerer *et al.* 2011), further work is needed to develop a stable understanding of their phylogeny.

CONCLUSIONS

The new Late Triassic dicynodont taxon from the Carnian of Central Europe, *Woznikella triradiata* n. gen., n. sp., likely represents an early diverging line of the stahleckeriid group and fits into the generally observed paleobiogeographic scenario for Triassic dicynodonts. According to this scenario, the southeastern part of Africa served as a constant origin point for numerous clades migrating westward and northward. Dicynodont clades mostly originated in that region and subsequently inhabited remaining parts of the world. Although the Central European record of dicynodonts is extremely poor, at least two waves migrated there independently from Africa, one represented by *Woznikella triradiata* n. gen., n. sp. and the second represented by *Lisowicia bojani*.

Acknowledgements

We thank, Paul Barrett (Natural History Museum, London), Alessandra D. S. Boos (Universidade Federal do Rio Grande do Sul, Porto Alegre), Gabriela A. Cisterna (Universidad Nacional de La Rioja), Jessica D. Cundiff (MCZ), Zaituna Erasmus (South African Museum, Cape Town), Philipe Havlik (Eberhard Karls Universität Tübingen, Senckenberg Center for Human Evolution and Palaeoenvironment Tübingen), Pat Holroyd (UMMP), Liu Jun (IVPP), Anna Krahl (Eberhard Karls Universität Tübingen), Ricardo Martínez (PVSJ), Pablo Ortiz (PVL), Rainer R. Schoch (SMNS), Dhurjati Sengupta (Indian Statistical Institute, Barrackpore), Andrije G. Sennikov (Paleontological Institute, Russian Academy of Sciences, Moscow), and Bernhard Zipfel (Bernard Price Institute of Palaeontology, University of the Witwatersrand, Johannesburg) for the access to their respective collections. Dawid Drózdź and Justyna Słowiak (ZPAL) are thanked for discussion. Żaneta Bartosińska, Ye-Wei Fang (Hefei University of Technology), Christian Kammerer (North Carolina Museum of Natural Sciences), Max Langer (Universidade de São Paulo), Ewa Uchmańska, and Andrzej S. Wolniewicz

(ZPAL) are thanked for their help providing some of the difficult to access literature. We also thank the two anonymous reviewers, and the associated editor, Hans Sues. Finally, we thank Robert Bronowicz, Grzegorz Niedzwiedzki, Mateusz Tałanda, and all the students who participated in the excavations. The study was supported by the National Science Center, Poland, grant no. 2017/27/B/NZ8/01543.

Authors' contributions

T.S. organized excavations, prepared most of the material and 3D scanned part of the material, performed anatomical identifications, and wrote drafts of the Introduction and anatomical descriptions (axial skeleton, clavicles). T.Sz. reviewed the anatomical and taxonomical literature, compiled the list of occurrences, wrote the manuscript, performed the phylogenetic and biogeographic analyses, 3D scanned and photographed the specimens, and prepared the figures. Both authors designed the study, reviewed scorings for the phylogenetic analysis, and checked the final manuscript.

REFERENCES

- ABDALA F. & SMITH R. M. H. 2009. — A middle Triassic cynodont fauna from Namibia and its implications for the biogeography of Gondwana. *Journal of Vertebrate Paleontology* 29 (3): 837-851. <https://www.jstor.org/stable/20627094>
- ABDALA F., MARSICANO C. A., SMITH R. M. H. & SWART R. 2013. — Strengthening Western Gondwanan correlations: A Brazilian dicynodont (Synapsida, Anomodontia) in the Middle Triassic of Namibia. *Gondwana Research* 23 (3): 1151-1162. <https://doi.org/10.1016/j.gr.2012.07.011>
- ALLEN B. J., WIGNALL P. B., HILL D. J., SAUPE E. E. & DUNHILL A. M. 2020. — The latitudinal diversity gradient of tetrapods across the Permo-Triassic mass extinction and recovery interval: Permo-Triassic tetrapod biogeography. *Proceedings of the Royal Society B* 287 (1929): 20201125. <https://doi.org/10.1098/rspb.2020.1125>
- AMALITZKY V. P. 1922. — Diagnoses of the new forms of vertebrates and plants from the upper Permian on north Dvina. *Bulletin de l'Académie des Sciences de Russie* 16: 329-240.
- ANDERSON J. M. & CRUIKSHANK A. R. I. 1978. — The biostratigraphy of the Permian and the Triassic. Part 5. A review of the classification and distribution of Permo-Triassic tetrapods. *Palaeontologia Africana* 21: 15-44.
- ANDERSON J. M. & ANDERSON H. M. 1984. — The fossil content of the Upper Triassic Molteno Formation, South Africa. *Palaeontologia Africana* 25: 39-59.
- ANGIELCZYK K. D. 2002. — Redescription, phylogenetic position, and stratigraphic significance of the dicynodont genus *Odontocyclops* (Synapsida: Anomodontia). *Journal of Paleontology* 76 (6): 1047-1059. <https://www.jstor.org/stable/1307122>
- ANGIELCZYK K. D. & KURKIN A. A. 2003. — Phylogenetic analysis of Russian Permian dicynodonts (Therapsida: Anomodontia): Implications for Permian biostratigraphy and Pangaea biogeography. *Zoological Journal of the Linnean Society* 139 (2): 157-212. <https://doi.org/10.1046/j.1096-3642.2003.00081.x>
- ANGIELCZYK K. D. & RUBIDGE B. S. 2013. — Skeletal morphology, phylogenetic relationships and stratigraphic range of *Eosimops newtoni* Broom, 1921, a ptylaecephalid dicynodont (Therapsida, Anomodontia) from the middle permian of South Africa. *Journal of Systematic Palaeontology* 11 (2): 191-231. <https://doi.org/10.1080/14772019.2011.623723>

- ANGIELCZYK K. D. & KAMMERER C. F. 2017. — The cranial morphology, phylogenetic position and biogeography of the upper Permian dicynodont *Compsodon helmoedi* van Hoepen (Therapsida, Anomodontia). *Papers in Palaeontology* 3 (4): 513-545. <https://doi.org/10.1002/spp2.1087>
- ANGIELCZYK K. D., STEYER J.-S., SIDOR C. A., SMITH R. M. H., WHATLEY R. L. & TOLAN S. 2014a. — Permian and Triassic dicynodont (Therapsida: Anomodontia) faunas of the Luangwa Basin, Zambia: taxonomic update and implications for dicynodont biogeography and biostratigraphy, in KAMMERER C. F., ANGIELCZYK K. D. & FRÖBISCH J. (eds), *Early evolutionary history of the Synapsida*. Springer, Dordrecht : 93-138. https://doi.org/10.1007/978-94-007-6841-3_7
- ANGIELCZYK K. D., HANCOX P. J. & NABAVIZADEH A. 2017b. — A redescription of the Triassic kannemeyeriform dicynodont *Sangusaurus* (Therapsida, Anomodontia), with an analysis of its feeding system. *Journal of Vertebrate Paleontology* 37 (1): 189-227. <https://doi.org/10.1080/02724634.2017.1395885>
- ANGIELCZYK K. D., LIU J. & YANG W. 2021. — A redescription of *Kunpania scopulusa*, a bidental dicynodont (Therapsida, Anomodontia) from the ?Guadalupian of northwestern China. *Journal of Vertebrate Paleontology* 41 (1): e1922428 <https://doi.org/10.1080/02724634.2021.1922428>
- ANONYMOUS 1972. — A note on the genus *Proplacerias* Cruickshank, 1970. *Palaeontologia Africana* 14: 17.
- ARAMBOURG C. 1943. — Un squelette de *Lystrosaurus* au Muséum National d'Histoire Naturelle. *Bulletin de Mséum National d'Histoire Naturelle* 2: 351-352. <https://www.biodiversitylibrary.org/page/52906703>
- ARAÚJO D. C. & GONZAGA T. D. 1980. — *Uma nova espécie de Jachaleria (Therapsida, Dicynodontia) do Triássico do Brasil*. Actas del Congresso Argentino de Paleontología y Bioestratigrafía y Primer Congreso Latinoamericano de Paleontología, Buenos Aires: 159-174.
- ARAÚJO R., MACUNGO Z., SMITH R. M. H., TOLAN S., ANGIELCZYK K. D., CROWLEY J. L., MILISSE D. & MUGABE J. 2020. — Biostratigraphic refinement of tetrapod-bearing beds from the Metangula Graben (Niassa Province, Mozambique). New radiometric dating and the first Lower Triassic tetrapod fossils from Mozambique. *Palaeontologia Africana* 54: 56-68.
- ARNOLD J., HUMER A., HELTAI M., MURARIU D., SPASSOV N. & HACKLÄNDER K. 2012. — Current status and distribution of golden jackals *Canis aureus* in Europe. *Mammal Review* 42 (1): 1-11. <https://doi.org/10.1111/j.1365-2907.2011.00185.x>
- ATTRIDGE J., BALL H. W., CHARIG A. J. & COX C. B. 1964. — The British Museum (Natural History)-University of London joint palaeontological expedition to northern Rhodesia and Tanganyika, 1963. *Nature* 201: 445-449. <https://doi.org/10.1038/201445a0>
- AULIE R. P. 1974. — The origin of the idea of the mammal-like reptile. III. The Mammal-like reptiles. *American Biology Teacher* 36 (8): 476-511. <https://doi.org/10.2307/4444936>
- AVANZINI M., BERNARDI M. & NICOSIA U. 2011. — The Permo-Triassic tetrapod faunal diversity in the Italian Southern Alps, in DAR I. A. (ed.), *Earth and Environmental Sciences*. InTech, London: 591-608.
- BAIRD D. & OLSEN P. E. 1983. — Late Triassic herpetofauna from the Wolfville Fm. of the Minas Basin (Fundy Basin) Nova Scotia, Can. *Geological Society of America Abstracts with Program* 15 (3): 122.
- BAIRD D. & PATTERSON O. F. 1968. — Dicynodon-archosaur fauna in the Pekin Formation (Upper Triassic) of North Caroline. *The Geological Society of America Special Paper* 115: 11.
- BAJDEK P., OWOCKI K. & NIEDZWIEDZKI G. 2014. — Putative dicynodont coprolites from the Upper Triassic of Poland. *Palaeogeography, Palaeoclimatology, Palaeoecology* 411: 1-17. <https://doi.org/10.1016/j.palaeo.2014.06.013>
- BAJDEK P., SZCZYGIELSKI T., KAPUŚCIŃSKA A. & SULEJ T. 2019. — Bromalites from a turtle-dominated fossil assemblage from the Triassic of Poland. *Palaeogeography, Palaeoclimatology, Palaeoecology* 520: 214-228. <https://doi.org/10.1016/j.palaeo.2019.02.002>
- BANDYOPADHYAY S. 1988. — A kannemeyeriid dicynodont from the Middle Triassic Yerrapalli Formation. *Philosophical Transactions of the Royal Society of London B* 320 (1198): 185-233. <https://doi.org/10.1098/rstb.1988.0072>
- BANDYOPADHYAY S. 1989. — The mammal-like reptile *Rechnisaurus* from the Triassic of India. *Palaeontology* 32: 305-312.
- BANDYOPADHYAY S. & SENGUPTA D. P. 1999. — Middle Triassic vertebrates of India. *Journal of African Earth Sciences* 29 (1): 233-241. [https://doi.org/10.1016/S0899-5362\(99\)00093-7](https://doi.org/10.1016/S0899-5362(99)00093-7)
- BANDYOPADHYAY S. & RAY S. 2020. — Gondwana vertebrate faunas of India: their diversity and intercontinental relationships. *IUGS Episodes* 43 (1): 438-460. <https://doi.org/10.18814/epiiugsg/2020/020028>
- BARREDO S., CHEMALLE F., MARSICANO C., ÁVILA J. N., OTTONE E. G. & RAMOS V. A. 2012. — Tectono-sequence stratigraphy and U-Pb zircon ages of the Rincón Blanco Depocenter, northern Cuyo Rift, Argentina. *Gondwana Research* 21 (2-3): 624-636. <https://doi.org/10.1016/j.gr.2011.05.016>
- BARRETT P. M., MCGOWAN A. J. & PAGE V. 2009. — Dinosaur diversity and the rock record. *Proceedings of the Royal Society B* 276 (1667): 2667-2674. <https://doi.org/10.1098/rspb.2009.0352>
- BARRY T. H. 1968. — Sound conduction in the fossil anomodont *Lystrosaurus*. *Annals of the South African Museum* 50: 275-281. <https://www.biodiversitylibrary.org/part/78189>
- BATTAIL B. 2009. — Late Permian dicynodont fauna from Laos. *Geological Society, London, Special Publications* 315 (1): 33-40. <https://doi.org/10.1144/SP315.4>
- BATTAIL B. & SURKOV M. V. 2000. — Mammal-like reptiles from Russia, in BENTON M. J., SHISHKIN M. A., UNWIN D. M. & KUROCHKIN E. N. (eds), *The Age of Dinosaurs in Russia and Mongolia*. Cambridge University Press, Cambridge: 86-120.
- BELL M. A. & LLOYD G. T. 2015. — Strap: an R package for plotting phylogenies against stratigraphy and assessing their stratigraphic congruence. *Palaeontology* 58 (2): 379-389. <https://doi.org/10.1111/pala.12142>
- BENOIT J., ANGIELCZYK K. D., MIYAMAE J. A., MANGER P., FERNANDEZ V. & RUBIDGE B. S. 2018. — Evolution of facial innervation in anomodont therapsids (Synapsida): Insights from X-ray computerized microtomography. *Journal of Morphology* 279 (5): 673-701. <https://doi.org/10.1002/jmor.20804>
- BENSON R. B. J. & UPCHURCH P. 2013. — Diversity trends in the establishment of terrestrial vertebrate ecosystems: Interactions between spatial and temporal sampling biases. *Geology* 41 (1): 43-46. <https://doi.org/10.1130/G33543.1>
- BENTON M. J. 2012. — No gap in the Middle Permian record of terrestrial vertebrates. *Geology* 40 (4): 339-342. <https://doi.org/10.1130/G32669.1>
- BENTON M. J., DUNHILL A. M., LLOYD G. T. & MARX F. G. 2011. — Assessing the quality of the fossil record: Insights from vertebrates. *Geological Society Special Publication* 358 (1): 63-94. <https://doi.org/10.1144/SP358.6>
- BONAPARTE J. F. 1965. — Sobre nuevos terapsidos Triásicos hallados en el centro de la Provincia de Mendoza, Argentina. *Acta Geologica Lilloana* 8: 91-100.
- BONAPARTE J. F. 1966a. — Una nueva 'fauna' Triásica de Argentina (Therapsida, Cunodontia Dicynodontia) consideraciones filogenéticas y paleobiogeográficas. *Ameghiniana* 4: 243-296.
- BONAPARTE J. F. 1966b. — Chronological survey of the tetrapod-bearing Triassic of Argentina. *Breviora* 251: 1-11. <https://www.biodiversitylibrary.org/part/39581>
- BONAPARTE J. F. 1967. — New vertebrate evidence for a southern transatlantic connexion during the Lower or Middle Triassic. *Palaeontology* 10: 554-463.
- BONAPARTE J. F. 1969. — *Dos nuevas "faunas" de reptiles triásicos de Argentina*. 1st International IUGS Symposium of Gondwana: 283-306.

- BONAPARTE J. F. 1970. — Annotated list of the South American Triassic tetrapods, in *Second Gondwana Symposium Proceedings and Papers*: 665-682.
- BONAPARTE J. F. 1978. — El Mezozoico de América del Sur y sus tetrápodos. *Opera Lilloana* 26: 1-596.
- BONAPARTE J. F. 1981. — Nota sobre una nueva fauna del Triásico inferior del sur de Mendoza, Argentina, correspondiente a la Zona de *Lystrosaurus* (Dicynodontia-Proterosuchia), in *Anais II Congresso Latino-Americano Paleontologia*: 277-288.
- BONAPARTE J. F. 1997. — *El Triásico de San Juan - La Rioja Argentina y sus dinosaurios*. Museo Argentino de Ciencias Naturales, Buenos Aires, 190 p.
- BOONSTRA L. D. 1938. — A report on some Karroo Reptiles from the Luangwa Valley, Northern Rhodesia. *Quarterly Journal of the Geological Society of London* 94: 371-384. <https://doi.org/10.1144/GSL.JGS.1938.094.01-04.14>
- BOONSTRA L. D. 1953. — A report on a collection of fossil reptilian bones from Tanganyika territory. *Annals of the South African Museum* 62: 5-18.
- BORDY E. M., ABRAHAMS M. & SCISCO L. 2017. — The Subeng vertebrate tracks: stratigraphy, sedimentology and a digital archive of a historic Upper Triassic palaeosurface (lower Elliot Formation), Leriche, Lesotho (southern Africa). *Bollettino della Società Paleontologica Italiana* 56: 181-198.
- BORDY E. M., ABRAHAMS M., SHARMAN G. R., VIGLIETTI P. A., BENSON R. B. J., MCPHEE B. W., BARRETT P. M., SCISCO L., CONDON D., MUNDIL R., RADEMAN Z., JINNAH Z. A., CLARK J. M., SUAREZ C. A., CHAPELLE K. E. J. & CHOINIÈRE J. N. 2020. — A chronostratigraphic framework for the upper Stormberg Group: implications for the Triassic-Jurassic boundary in southern Africa. *Earth-Science Reviews* 203: 103120. <https://doi.org/10.1016/j.earscirev.2020.103120>
- BOTHA J. 2020. — The paleobiology and paleoecology of South African *Lystrosaurus*. *PeerJ* 8: e10408. <https://doi.org/10.7717/peerj.10408>
- BOTHA J., HUTTENLOCKER A. K., SMITH R. M. H., PREVEC R., VIGLIETTI P. A. & MODESTO S. P. 2020. — New geochemical and palaeontological data from the Permian-Triassic boundary in the South African Karoo Basin test the synchronicity of terrestrial and marine extinctions. *Palaeogeography, Palaeoclimatology, Palaeoecology* 540: 109467. <https://doi.org/10.1016/j.palaeo.2019.109467>
- BOTHA J. & SMITH R. M. H. 2006. — Rapid vertebrate recuperation in the Karoo Basin of South Africa following the End-Permian extinction. *Journal of African Earth Sciences* 45 (4-5): 502-514. <https://doi.org/10.1016/j.jafrearsci.2006.04.006>
- BOTHA J. & SMITH R. M. H. 2007. — *Lystrosaurus* species composition across the Permo-Triassic boundary in the Karoo Basin of South Africa. *Lethaia* 40 (2): 125-137. <https://doi.org/10.1111/j.1502-3931.2007.00011.x>
- BOTHA-BRINK J. 2017. — Burrowing in *Lystrosaurus*: preadaptation to a postextinction environment? *Journal of Vertebrate Paleontology* 37 (5): e1365080. <https://doi.org/10.1080/02724634.2017.1365080>
- BOTHA-BRINK J. & ANGIELCZYK K. D. 2010. — Do extraordinarily high growth rates in Permo-Triassic dicynodonts (Therapsida, Anomodontia) explain their success before and after the end-Permian extinction? *Zoological Journal of the Linnean Society* 160 (2): 341-365. <https://doi.org/10.1111/j.1096-3642.2009.00601.x>
- BOTHA J. & SMITH R. M. H. 2020. — Biostratigraphy of the *Lystrosaurus declivis* Assemblage Zone (Beaufort Group, Karoo Supergroup), South Africa. *South African Journal of Geology* 123 (2): 207-216. <https://doi.org/10.25131/sajg.123.0015>
- BOTHA-BRINK J., HUTTENLOCKER A. K. & MODESTO S. P. 2014. — Vertebrate paleontology of Nooitgedacht 68: A *Lystrosaurus mackai*-rich Permo-Triassic boundary locality in South Africa, in KAMMERER C. F., ANGIELCZYK K. D. & FRÖBISCH J. (eds), *Early evolutionary history of the Synapsida*. Springer, Dordrecht: 289-304. https://doi.org/10.1007/978-94-007-6841-3_17
- BOTHABRINK J., CODRON D., HUTTENLOCKER A. K., ANGIELCZYK K. D. & RUTA M. 2016. — Breeding young as a survival strategy during Earth's greatest mass extinction. *Scientific Reports* 6: 24053. <https://doi.org/10.1038/srep24053>
- BRINK A. A. 1951. — On the genus *Lystrosaurus* Cope. *Transactions of the Royal Society of South Africa* 33 (1): 107-120. <https://doi.org/10.1080/00359195109519880>
- BRINK A. S. 1963. — Two cynodonts from the Ntawere formation in the Luangwa valley of Northern Rhodesia. *Palaeontologia Africana* 8: 77-96.
- BRINK A. S. 1986. — *Illustrated bibliographical catalogue of the Synapsida. Part I*. Republic of South Africa Department of Mineral and Energy Affairs, Pretoria.
- BRINK A. S. 1988. — *Illustrated bibliographical catalogue of the Synapsida. Part II*. Republic of South Africa Department of Mineral and Energy Affairs, Pretoria.
- BROILI F. 1908. — Ein Dicynodontierrest aus der Karoformation. *Neues Jahrbuch für Mineralogie, Geognosie, Geologie und Petrefaktenkunde* 1: 1-15.
- BROILI F. 1921. — Ein Fund von cf. *Placerias* Lucas in der kontinentalen Trias von Europa. *Zentralblatt für Mineralogie, Geologie und Paläontologie* 1921: 339-343.
- BROOM R. 1899. — On two new species of dicynodonts. *Annals of the South African Museum* 1: 452-456.
- BROOM R. 1900a. — The leg and toe bones of *Ptychosagium*. *Transactions of the South African Philosophical Society* 11 (1): 233-235. <https://doi.org/10.1080/21560382.1900.9525968>
- BROOM R. 1900b. — On the structure of the palate in *Dicynodon*, and its allies. *Transactions of the South African Philosophical Society* 11 (1): 169-176. <https://doi.org/10.1080/21560382.1900.9525963>
- BROOM R. 1902. — The leg and toe bones of *Ptychosagium*. *Transactions of the South African Philosophical Society* 11: 133-235.
- BROOM R. 1903. — On the remains of *Lystrosaurus*, in the Albany Museum. *Records of the Albany Museum* 1: 1-8.
- BROOM R. 1905. — On the use of the term Anomodontia. *Records of the Albany Museum* 1: 266-269.
- BROOM R. 1907. — Reptilian fossil remains from Natal. Part 1. On reptilian remains from the supposed Beaufort Beds of the Umkomazan River in western Natal. *Reports of the Geological Survey of Natal* 3: 93-95.
- BROOM R. 1908a. — III.-On the structure of the shoulder girdle in *Lystrosaurus*. *Annals of the South African Museum* 4: 139-141.
- BROOM R. 1908b. — On two new reptiles from the Karroo Beds of Natal. *Annals of the Natal Government Museum* 1: 167-172.
- BROOM R. 1909. — An attempt to determine the horizons of the fossil vertebrates of the Karroo. *Annals of the South African Museum* 7: 285-289.
- BROOM R. 1913a. — On some new genera and species of dicynodont reptiles, with notes on a few others. *Bulletin of the American Museum of Natural History* 32: 441-457. <https://www.biodiversitylibrary.org/bibliography/89538>
- BROOM R. 1913b. — On four new fossil reptiles from the Beaufort Series, South Africa. *Records of the Albany Museum* 2: 397-401.
- BROOM R. 1914. — Note on the American Triassic genus *Placerias* Lucas. *Bulletin of the Geological Society of America* 25: 141.
- BROOM R. 1915. — Catalogue of types and figured specimens of fossil vertebrates in the American Museum of Natural History. Part II, Permian, Triassic and Jurassic reptiles of South Africa. *Bulletin of the American Museum of Natural History* 25 (2): 105-164. <http://hdl.handle.net/2246/1446>
- BROOM R. 1920. — On some new theropcephalian reptiles from the Karroo Beds of South Africa. *Proceedings of the Zoological Society of London* 1920: 351-354.
- BROOM R. 1921. — On some new genera and species of anomodont reptiles from the Karroo Beds of South Africa. *Proceedings of the Zoological Society of London* 91 (4): 647-674. <https://doi.org/10.1111/j.1096-3642.1921.tb03286.x>

- BROOM R. 1923. — On the structure of the skull in the carnivorous dinocephalian reptiles. *Proceedings of the Zoological Society of London* 93 (4): 661-684. <https://doi.org/10.1111/j.1096-3642.1923.tb02203.x>
- BROOM R. 1932. — *The Mammal-Like Reptiles of South Africa and the Origin Of Mammals*. H. P. & C. Witherby, London, 376 p.
- BROOM R. 1937. — Further contribution to our knowledge of the fossil reptiles of the Karroo. *Proceedings of the Zoological Society of London* B107: 299-318.
- BROOM R. 1940. — On some new genera and species of fossil reptiles from the Karroo Beds of Graaff-Reinet. *Annals of the Transvaal Museum* 20: 157-192.
- BROOM R. 1941. — Some new Karroo reptiles with notes on a few others. *Annals of the Transvaal Museum* 20: 194-213.
- BROOM R. 1948. — Three new species of anomodonts from the Rubidge collection. *Annals of the Transvaal Museum* 21: 246-250.
- BROOM R. & HAUGHTON S. H. 1913. — On two new species of *Dicynodon*. *Annals of the South African Museum* 12: 36-39.
- BUDZISZEWSKA-KARWOWSKA E., BUJOK A. & SADLOK G. 2010. — Bite marks on an Upper Triassic dicynodontid tibia from Zawiercie, Kraków-Częstochowa Upland, southern Poland. *Palaeos* 25: 415-421. <https://doi.org/10.2110/palo.2009.p09-136r>
- BUTLER R. J., BARRETT P. M., NOWBATH S. & UPCHURCH P. 2009. — Estimating the effects of sampling biases on pterosaur diversity patterns: Implications for hypotheses of bird/pterosaur competitive replacement. *Paleobiology* 35 (3): 432-446. <https://doi.org/10.1666/0094-8373-35.3.432>
- BUTLER R. J., BENSON R. B. J., CARRANO M. T., MANNION P. D. & UPCHURCH P. 2011. — Sea level, dinosaur diversity and sampling biases: Investigating the ‘common cause’ hypothesis in the terrestrial realm. *Proceedings of the Royal Society B* 278 (1709): 1165-1170. <https://doi.org/10.1098/rspb.2010.1754>
- BUTLER R. J., EZCURRA M. D., MONTEFELTRO F. C., SAMATHI A. & SOBRAL G. 2016. — A new species of basal rhynchosaur (Diapsida: Archosauromorpha) from the early Middle Triassic of South Africa, and the early evolution of Rhynchosauria. *Zoological Journal of the Linnean Society* 177: 1030. <https://doi.org/10.1111/zoj.12475>
- CALVO J. O. 2007. — Ichnology, in GASPARINI Z., SALGADO L. & CORIA R. A. (eds), *Patagonian Mesozoic Reptiles*. Indiana University Press, Bloomington: 314-334. <https://www.biodiversitylibrary.org/bibliography/53483>
- CAMP C. L. 1956. — Part II. Triassic dicynodonts compared. *Memoirs of the University of California* 13: 305-341.
- CAMP C. L. & WELLES S. P. 1956. — Part I. The North American genus *Placerias*. *Memoirs of the University of California* 13: 255-304.
- CAMP J. A. 2010. — *Morphological variation and disparity in Lystrosaurus (Therapsida: Dicynodontia)*. MSc thesis, University of Iowa, Iowa City, 141 p.
- CAMP J. A. & LIU J. 2011. — The taxonomy and cranial morphology of Chinese Lystrosaurus. *Journal of Vertebrate Paleontology* 31: 82.
- CARIGLINO B., ZAVATTIERI A. M., GUTIÉRREZ P. R. & BALARNO M. L. 2016. — The paleobotanical record of the Triassic Cerro de Las Cabras Formation at its type locality, Potrerillos, Mendoza (Uspallata Group): An historical account and first record of fossil flora. *Ameghiniana* 53 (2): 184-204. <https://doi.org/10.5710/AMGH.17.12.2015.2952>
- CASAMIQUELA R. M. 1964. — *Estudios icnológicos: problemas y métodos de la icnología con aplicación al estudio de pisadas Mesozoicas (Reptilia, Mammalia) de la Patagonia*. Colegio Industrial Pio IX, Buenos Aires, 220 p.
- CASAMIQUELA R. M. 1975. — Nuevo material y reinterpretación de las icnitas mesozoicas (Neotriásicas) de Los Menudos, provincia de Río Negro (Patagonia). *Actas del Primer Congreso Argentino de Paleontología y Bioestratigrafía*: 555-580.
- CASE E. C. 1915. — *The Permo-Carboniferous Red Beds of North America and their vertebrate fauna*. Washington D.C., Carnegie Institution of Washington, 176 p. <https://www.biodiversitylibrary.org/bibliography/57276>
- CASE E. C. 1934. — Description of a skull of *Kannemeyeria erythrea* Haughton. *Contributions from the Museum of Paleontology* 4: 115-127.
- CEOLONI P., CONTI M. A., MARIOTTI N. & NICOSIA U. 1986. — New Late Permian tetrapod footprints from Southern Alps. *Memorie della Società Geologica Italiana* 34: 45-65.
- CHARIG A. J. 1956. — New Triassic archosaur from Tanganyika including *Mandasuchus* and *Teleocrater*. PhD thesis, University of Cambridge, Cambridge, 503 p.
- CHATTERJEE S., SCOTSESE C. R. & BAJPAI S. 2017. — The restless Indian Plate and its epic voyage from Gondwana to Asia: its tectonic, paleoclimatic, and paleobiogeographic evolution. *The Geological Society of America Special Paper* 529: 1-149. <https://doi.org/10.1130/SPE529>
- CHENG Z.-W. 1986. — Permian and Triassic strata and fossil assemblages in the Dalongkou area of Jimusar, Xinjiang: (7) vertebrates. *Geological Memoirs of the People's Republic of China Ministry of Geology and Mineral Resources* 2: 207-218.
- CHINSAMY A. & RUBIDGE B. S. 1993. — Dicynodont (Therapsida) bone histology: phylogenetic and physiological implications. *Palaeontologia Africana* 30: 97-102.
- CHENG Z.-W. 1980. — Vertebrate fossils, in *Mesozoic Stratigraphy and Paleontology of the Shaanxi-Gansu-Ningxia Basin*. Geological Publishing House, Beijing: 115-170. [in Chinese].
- CHOWDHURY T. K. R. 1970. — Two new dicynodonts from the Triassic Yerrapali Formation of Central India. *Palaeontology* 13: 132-144.
- CHUDINOV P. K. 1960. — Upper Permian therapsids from the Ezhovo locality. *Paleontologicheskii Zhurnal* 4: 81-94 [in Russian].
- CIGNONI P., CALLIERI M., CORSINI M., DELLEPIANE M., GANOVELLI F. & RANZUGLIA G. 2008. — *MeshLab: an open-source mesh processing tool*. Sixth Eurographics Italian Chapter Conference: 129-136.
- CITTON P., DÍAZ-MARTÍNEZ I., DE VALAIS S. & CÓNSOLE-GONELLA C. 2018a. — Triassic pentadactyl tracks from the Los Menudos Group (Río Negro province, Patagonia Argentina): possible constraints on the autopodial posture of Gondwanan trackmakers. *PeerJ* 6: e5358. <https://doi.org/10.7717/peerj.5358>
- CITTON P., DÍAZ-MARTÍNEZ I., DE VALAIS S., GONZÁLEZ S. N., GRECO G. A., FALCO J. I. & CÓNSOLE-GONELLA C. 2018b. — New ichnological material from the Vera Formation (Los Menudos Complex, Triassic), Puesto Vera Locality, Río Negro Province, Argentina: A first account. *Reunión de Comunicaciones de la Asociación Paleontológica Argentina, 2018*: R27.
- CITTON P., DÍAZ-MARTÍNEZ I., DE VALAIS S., GONZÁLEZ S. N., GRECO G. A., FALCO J. I. & CÓNSOLE-GONELLA C. 2019. — New ichnological material from the Vera Formation (Los Menudos Complex, Triassic), Puesto Vera locality, Río Negro province, Argentina: a first account. *PE-APA* 18: R27.
- CITTON P., DE VALAIS S., DÍAZ-MARTÍNEZ I., GONZÁLEZ S. N., GRECO G. A., CÓNSOLE-GONELLA C. & LEONARDI G. 2021. — Age-constrained therapsid tracks from a mid-latitude upland (Permian-Triassic transition, Los Menudos Complex, Argentina). *Journal of South American Earth Sciences* 110: 103367. <https://doi.org/10.1016/j.jsames.2021.103367>
- CLUVER M. A. 1971. — The cranial morphology of the dicynodont genus *Lystrosaurus*. *Annals of the South African Museum* 56: 155-247.
- CLUVER M. A. 1974. — The cranial morphology of the Lower Triassic dicynodont *Myosaurus gracilis*. *Annals of the South African Museum* 66: 35-54.
- CLUVER M. A. & KING G. M. 1983. — A reassessment of the relationships of Permian Dicynodontia (Reptilia, Therapsida) and a new classification of dicynodonts. *Annals of the South African Museum* 91: 195-273.
- COLBERT E. H. 1970a. — The fossil tetrapods of Coalsack Bluff. *Antarctic Journal of the United States* 5: 57-61.
- COLBERT E. H. 1970b. — Antarctic Gondwana tetrapods. *Second Gondwana Symposium Proceedings and Papers*: 659-664.

- COLBERT E. H. 1971a. — Tetrapods and continents. *The Quarterly Review of Biology* 46 (3): 250-269. <https://doi.org/10.1086/406898>
- COLBERT E. H. 1971b. — Triassic tetrapods from McGregor Glacier. *Antarctic Journal of the United States* 6: 188-189.
- COLBERT E. H. 1972. — Antarctic Triassic tetrapods in the laboratory. *Antarctic Journal of the United States* 7: 141-142.
- COLBERT E. H. 1973. — Antarctic *Lystrosaurus* defined. *Antarctic Journal of the United States* 8: 273-274.
- COLBERT E. H. 1974. — *Lystrosaurus* from Antarctica. *American Museum Novitates* 2535: 1-44.
- COLBERT E. H. 1975. — Further determinations of antarctic Triassic tetrapods. *Antarctic Journal of the United States* 10: 250-252.
- COLBERT E. H. 1982. — The distribution of *Lystrosaurus* in Pangaea and its implications. *Geobios* 15 (Supplement 1): 375-383. [https://doi.org/10.1016/S0016-6995\(82\)80126-5](https://doi.org/10.1016/S0016-6995(82)80126-5)
- COLBERT E. H. & COSGRIFF J. W. 1974. — Labyrinthodont amphibians from Antarctica. *American Museum Novitates* 2552: 1-30. <https://www.biodiversitylibrary.org/bibliography/91051>
- CONRAD K. L. & LOCKLEY M. G. 1986. — Late Triassic archosaur tracksites from the American southwest. *First International Symposium on Dinosaur Tracks and Traces. Abstracts With Program*: 13.
- CONRAD K., LOCKLEY M. G. & PRINCE N. K. 1987. — Triassic and Jurassic vertebrate-dominated trace fossil assemblages of the Cimarron Valley region: implications for paleoecology and biostratigraphy. *New Mexico Geological Society Guidebook*: 127-138.
- COOPER M. R. 1980. — ‘The origins and classification of Triassic dicynodonts’ by A. W. Keyser and A. R. I. Cruickshank (*Trans. geol. Soc. S. Afr.*, 82 (1), 81-108). Discussion. *Transactions of the Geological Society of South Africa* 83: 107-110.
- COPE E. D. 1870a. — Remarks. *Proceedings of the American Philosophical Society* 11: 419. <https://www.biodiversitylibrary.org/bibliography/109452>
- COPE E. D. 1870b. — Synopsis of the extinct Batrachia, Reptilia and Aves of North America. *Transactions of the American Philosophical Society* 14 (1): 1-252. <https://doi.org/10.2307/1005355>
- COPE E. D. 1870c. — Dicynodont tusks from the Triassic rocks of the Phoenixville tunnel. *Proceedings of the American Philosophical Society* 11: 370.
- CORECCO L., PEREIRA V. P., SOARES M. B. & SCHULTZ C. L. 2020. — Geochemical study of the vertebrate assemblage zones of the Santa Maria Supersequence (Middle to Late Triassic), Paraná Basin, Brazil. *Brazilian Journal of Geology* 50 (4): e20200014. <https://doi.org/10.1590/2317-4889202020200014>
- CORECCO L., PEREIRA V. P., SOARES M. B. & SCHULTZ C. L. 2021. — Geochemical study on fossil vertebrates from some specific Permian and Triassic beds of the Paraná Basin (Brazil): a preliminary approach. *Journal of South American Earth Sciences* 110: 103362. <https://doi.org/10.1016/j.jsames.2021.103362>
- COSGRIFF J. W. & HAMMER W. R. 1979. — New species of Dicynodontia from the Fremouw Formation. *Antarctic Journal of the United States* 14: 30-32.
- COSGRIFF J. W. & HAMMER W. R. 1981. — New skull of *Lystrosaurus curvatus* from the Fremouw Formation. *Antarctic Journal of the United States* 16: 52-53.
- COSGRIFF J. W., HAMMER W. R., ZAWISKIE J. M. & KEMP N. R. 1978. — New Triassic vertebrates from the Fremouw Formation of the Queen Maud Mountains. *Antarctic Journal of the United States* 13: 23-24.
- COSGRIFF J. W., HAMMER W. R. & RYAN W. J. 1982. — The Pangaeian reptile, *Lystrosaurus maccaigi*, in the Lower Triassic of Antarctica. *Journal of Paleontology* 56 (2): 371-385. <https://www.jstor.org/stable/1304463>
- COTTER G. DE P. 1918. — A revised classification of the Gondwana system. *Records of the Geological Survey of India* 48: 23-33.
- COUREL L., DEMATHIEU G. R. & BUFFARD R. 1968. — Empreintes de pas de Vertébrés et stratigraphie du Trias. *Bulletin de la Société Géologique de France* 7 (3): 275-281. <https://doi.org/10.2113/gssfbull.S7-X.3.275>
- COURTENAY-LATIMER M. 1948. — *Kannemeyeria wilsoni* Broom; how it came to the East London Museum, *in* du Toit A. L. (ed.) *Special Publications of the Royal Society of South Africa. The Robert Broom Commemorative Volume*. Royal Society of South Africa, Cape Town: 107-109.
- COX C. B. 1962. — Preliminary diagnosis of *Ischigualastia*, a new genus of dicynodont from Argentina. *Breviora* 156: 8-9.
- COX C. B. 1965. — New Triassic dicynodonts from South America, their origins and relationships. *Philosophical Transactions of the Royal Society of London B* 248 (753): 457-514. <https://doi.org/10.1098/rstb.1965.0005>
- COX C. B. 1968. — The Chañares (Argentina) Triassic reptile fauna. IV. The dicynodont fauna. *Breviora* 295: 1-27.
- COX C. B. 1969. — Two new dicynodonts from the Triassic Ntawere Formation, Zambia. *Bulletin of the British Museum (Natural History), Geology* 17 (6): 255-294. <https://doi.org/10.5962/p.313836>
- COX C. B. 1991. — The Pangaea dicynodont *Rechnisaurus* and the comparative biostratigraphy of Triassic dicynodont faunas. *Palaeontology* 34: 767-784.
- COX C. B. 1998. — The jaw function and adaptive radiation of the dicynodont mammal-like reptiles of the Karoo basin of South Africa. *Zoological Journal of the Linnean Society* 122 (1-2): 349-384. <https://doi.org/10.1111/j.1096-3642.1998.tb02534.x>
- COX C. B. & LI J. L. 1983. — A new genus of Triassic dicynodont from East Africa and its classification. *Palaeontology* 26: 389-406.
- CROMPTON A. W. & HOTTON N. 1967. — Functional morphology of the masticatory apparatus of two dicynodonts (Reptilia, Therapsida). *Postilla* 109: 1-51.
- CROSS W. 1908. — The Triassic portion of the Shinarump Group, Powell. *The Journal of Geology* 16 (2): 97-123. <https://doi.org/10.1086/621501>
- CROSS W. & HOWE E. 1905. — Red Beds of southwestern Colorado and their correlation. *Bulletin of the Geological Society of America* 16 (1): 447-498. <https://doi.org/10.1130/GSAB-16-447>
- CROZIER E. A. 1970. — Preliminary report on two Triassic dicynodonts from Zambia. *Palaeontologia Africana* 13: 39-45.
- CRUICKSHANK A. R. I. 1964. — Origin of the Triassic dicynodonts (Reptilia: Synapsida). *Nature* 201: 733. <https://doi.org/10.1038/201733a0>
- CRUICKSHANK A. R. I. 1965. — On a specimen of the anomodont reptile *Kannemeyeria latifrons* (Broom) from the Manda Formation of Tanganyika, Tanzania. *Proceedings of the Linnean Society of London* 176 (2): 149-157. <https://doi.org/10.1111/j.1095-8312.1965.tb00941.x>
- CRUICKSHANK A. R. I. 1967. — A new dicynodont genus from the Manda Formation of Tanzania (Tanganyika). *Journal of Zoology* 153 (2): 163-208. <https://doi.org/10.1111/j.1469-7998.1967.tb04059.x>
- CRUICKSHANK A. R. I. 1968. — A comparison of the palates of Permian and Triassic dicynodonts. *Palaeontologia Africana* 11: 23-31.
- CRUICKSHANK A. R. I. 1970. — Taxonomy of the Triassic anomodont genus *Kannemeyeria*. *Palaeontologia Africana* 13: 47-55.
- CRUICKSHANK A. R. I. 1975. — The skeleton of the Triassic anomodont *Kannemeyeria wilsoni* Broom. *Palaeontologia Africana* 18: 137-142.
- CRUICKSHANK A. R. I. 1986a. — Biostratigraphy and classification of a new Triassic dicynodont from east Africa. *Modern Geology* 10: 121-131.
- CRUICKSHANK A. R. I. 1986b. — Archosaur predation on an East African Middle Triassic dicynodont. *Palaeontology* 29 (2): 415-422.
- CURRIE B. S., COLOMBI C. E., TABOR N. J., SHIPMAN T. C. & MONTAÑEZ I. P. 2009. — Stratigraphy and architecture of the Upper Triassic Ischigualasto Formation, Ischigualasto Provincial Park, San Juan, Argentina. *Journal of South American Earth Sciences* 27 (1): 74-87. <https://doi.org/10.1016/j.jsames.2008.10.004>

- CZĘPIŃSKI Ł., DRÓZDZ D., SZCZYGIELSKI T., TALANDA M., PAWLAK W., LEWCZUK A., RYTEL A. & SULEJ T. 2021. — An Upper Triassic terrestrial vertebrate assemblage from the forgotten Kocury locality in southern Poland with a new aetosaur taxon. *Journal of Vertebrate Paleontology* 41 (1): e1898977. <https://doi.org/10.1080/02724634.2021.1898977>
- DAMIANI R. J. 2008. — A giant skull of the temnospondyl *Xenosuchus africanus* from the Middle Triassic of South Africa and its ontogenetic implications. *Acta Palaeontologica Polonica* 53 (1): 75-84. <https://doi.org/10.4202/app.2008.0104>
- DAMIANI R. J. & KITCHING J. W. 2003. — A new brachyopid temnospondyl from the *Cynognathus* Assemblage Zone, upper Beaufort Group, South Africa. *Journal of Vertebrate Paleontology* 23 (1): 67-78. [https://doi.org/10.1671/0272-4634\(2003\)23\[67:ANBTFT\]2.0.CO;2](https://doi.org/10.1671/0272-4634(2003)23[67:ANBTFT]2.0.CO;2)
- DAMIANI R. J. & WELMAN J. 2001. — A long-snouted trematosaurid amphibian from the Early Triassic of South Africa. *South African Journal of Science* 97: 318-320.
- DAMIANI R. J., NEVELING J., MODESTO S. P. & YATES A. M. 2003. — Barendskraal, a diverse amniote locality from the *Lystrosaurus* Assemblage Zone, Early Triassic of South Africa. *Palaeontologia Africana* 39: 53-62.
- DAMIANI R. J., VASCONCELOS C., RENAUT A. J., HANCOX P. J. & YATES A. M. 2007. — *Dolichuranus primaevus* (Therapsida: Anomodontia) from the Middle Triassic of Namibia and its phylogenetic relationships. *Palaeontology* 50 (6): 1531-1546. <https://doi.org/10.1111/j.1475-4983.2007.00727.x>
- DARTON N. H. 1910. — *A reconnaissance of parts of northwestern New Mexico and northern Arizona*. Government Printing Office, Washington, 88 p.
- DANILOV A. I. 1971. — A new dicynodont from the Middle Triassic of Southern Cisuralia. *Paleontologicheskii Zhurnal* 1971: 132-135 [in Russian].
- DANILOV A. I. 1973. — Remains of the postcranial skeleton of *Uralokannemeyeria* (Dicynodontia). *Paleontological Journal* 7: 244-247.
- DASSIE E. C. G. 2014. — *Tetrápodas triásicos brasileiros: uma investigação envolvendo banco de dados e análise de cluster*. MSc thesis, Universidade de São Paulo, Ribeirão Preto, 108 p.
- DAY M. O. & RUBIDGE B. S. 2020a. — Biostratigraphy of the *Eodicyndodon* Assemblage Zone (Beaufort Group, Karoo Supergroup), South Africa. *South African Journal of Geology* 123 (2): 141-148. <https://doi.org/10.25131/sajg.123.0010>
- DAY M. O. & RUBIDGE B. S. 2020b. — Biostratigraphy of the *Tapinocephalus* Assemblage Zone (Beaufort Group, Karoo Supergroup), South Africa. *South African Journal of Geology* 123 (2): 149-164. <https://doi.org/10.25131/sajg.123.0012>
- DAY M. O. & SMITH R. M. H. 2020. — Biostratigraphy of the *Endothiodon* Assemblage Zone (Beaufort Group, Karoo Supergroup), South Africa. *South African Journal of Geology* 123 (2): 165-180. <https://doi.org/10.25131/sajg.123.0011>
- DEFAUW S. L. 1986. — *The appendicular skeleton of African dicynodonts*. PhD thesis, Wayne State University, Detroit, Michigan, 284 p.
- DEFAUW S. L. 1989. — Patterns of evolution in the Dicynodontia, with special reference to austral taxa. *Geological Society Special Publication* 47 (1): 63-84. <https://doi.org/10.1144/GSL.SP.1989.047.01.06>
- DEFAUW S. L. 1993. — The Pangean dicynodont *Rechnisaurus* from the Triassic of Argentina. *New Mexico Museum of Natural History and Science Bulletin* 3: 101-105.
- DEMATHIEU G. & HAUBOLD H. 1971. — Stratigraphische Aussagen der Tetrapodenfährten aus der terrestrischen Trias Europas. *Geologie* 21: 802-836.
- DEMATHIEU G. R. & FICHTER J. 1989. — Die Karlshafener Fährten im Naturkundemuseum der Stadt Kassel. Ihre Beschreibung und Bedeutung. *Philippia* 6: 111-154.
- DEMATHIEU G. R. & WYCISK P. 1990. — Tetrapod trackways from Southern Egypt and Northern Sudan. *Journal of African Earth Sciences* 10 (3): 435-443. [https://doi.org/10.1016/0899-5362\(90\)90096-W](https://doi.org/10.1016/0899-5362(90)90096-W)
- DEUTSCHE STRATIGRAPHISCHE KOMMISSION 2005. — Stratigraphie von Deutschland IV – Keuper. *Courier Forschungsinstitut Senckenberg* 253: 1-296.
- DIAS-DA-SILVA S., PINHEIRO F. L., DA ROSA Á. A. S., MARTINELLI A. G., SCHULTZ C. L., SILVA-NEVES E. & MODESTO S. P. 2017. — Biostratigraphic reappraisal of the Lower Triassic Sanga do Cabral Supersequence from South America, with a description of new material attributable to the parareptile genus *Procolophon*. *Journal of South American Earth Sciences* 79: 281-296. <https://doi.org/10.1016/j.jsames.2017.07.012>
- DÍAZ-MARTÍNEZ I., CITTON P., DE VALAIS S., CÓNSOLE-GONELLA C. & GONZÁLEZ S. N. 2019. — Late Permian-Early Jurassic vertebrate tracks from Patagonia: Biochronological inferences and relationships with southern African realms. *Journal of African Earth Sciences* 160: 103619. <https://doi.org/10.1016/j.jafrearsci.2019.103619>
- DOMNANOVICH N. S. & MARSICANO C. A. 2006a. — Revision of the basal Triassic dicynodont *Vinceria andina* Bonaparte (Therapsida, Dicynodontia) of Argentina. *Ameghiniana* 43: 35R.
- DOMNANOVICH N. S. & MARSICANO C. A. 2006b. — Tetrapod footprints from the Triassic of Patagonia: Reappraisal of the evidence. *Ameghiniana* 43 (1): 55-70. <https://www.ameghiniana.org.ar/index.php/ameghiniana/article/view/738>
- DOMNANOVICH N. S. & MARSICANO C. A. 2012. — The Triassic dicynodont *Vinceria* (Therapsida, Anomodontia) from Argentina and a discussion on basal Kannemeyeriiformes. *Geobios* 45 (2): 173-186. <https://doi.org/10.1016/j.geobios.2011.03.003>
- DOMNANOVICH N. S., TOMASSINI R., MANERA DE BIANCO T. & DALPONTE M. 2008. — Nuevos aportes al conocimiento de la icnofauna de tetrápodos del Triásico Superior de Los Menucos (Complejo Los Menucos), provincia de Río Negro, Argentina. *Ameghiniana* 45: 211-224.
- DUNHILL A. M., BENTON M. J., TWITCHETT R. J. & NEWELL A. J. 2014. — Testing the fossil record: Sampling proxies and scaling in the British Triassic-Jurassic. *Palaeogeography, Palaeoclimatology, Palaeoecology* 404: 1-11. <https://doi.org/10.1016/j.palaeo.2014.03.026>
- DUNNE E. M., FARNSWORTH A., GREENE S. E., LUNT D. J. & BUTLER R. J. 2021. — Climatic drivers of latitudinal variation in Late Triassic tetrapod diversity. *Palaeontology* 64 (1): 101-117. <https://doi.org/10.1111/pala.12514>
- DUTUIT J.-M. 1980. — Principaux caractères d'un genre de Dicynodont du Trias marocain. *Comptes Rendus de l'Académie des Sciences D* 290: 655-658.
- DUTUIT J.-M. 1988. — Ostéologie crânienne et ses enseignements apports géologique et paléocologique de *Moghreria nmachouensis*, dicynodonte (Reptilia, Therapsida) du Trias supérieur marocain. *Bulletin du Muséum National d'Histoire Naturelle* 10: 227-285.
- DUTUIT J.-M. 1989a. — *Azarifeneria barrati*, un deuxième genre de dicynodonte du Trias supérieur marocain. *Comptes Rendus de l'Académie des Sciences II* 309: 303-306.
- DUTUIT J.-M. 1989b. — Confirmation des affinités entre Trias supérieurs marocain et sud-américain: découverte d'un troisième dicynodonte (Reptilia, Therapsida), *Azarifeneria robustus*, n. sp., de la formation d'Argana (Atlas occidental). *Comptes Rendus de l'Académie des Sciences II* 309: 1267-1270.
- DRYSDALE A. R. & KITCHING J. W. 1963. — A re-examination of the Karroo succession and fossil localities of part of the upper Luangwa Valley. *Geological Survey of Northern Rhodesia Memoir* 1: 1-62.
- DZIK J., NIEDZWIEDZKI G. & SULEJ T. 2008b. — Zaskakujące uwieńczenie ery gadów ssakoształtnych. *Ewolucja* 3: 2-21.
- DZIK J. 2001. — A new *Paleorhinus* fauna in the early Late Triassic of Poland. *Journal of Vertebrate Paleontology* 21 (3): 625-627. [https://doi.org/10.1671/0272-4634\(2001\)021\[0625:ANPFIT\]2.0.CO;2](https://doi.org/10.1671/0272-4634(2001)021[0625:ANPFIT]2.0.CO;2)

- DZIK J., SULEJ T. & NIEDZWIEDZKI G. 2008a. — A dicynodont-theropod association in the latest Triassic of Poland. *Acta Palaeontologica Polonica* 53 (4): 733–738. <https://doi.org/10.4202/app.2008.0415>
- EDLER A. L. 2000. — Late Triassic dicynodonts: their anatomy, relationships, and paleobiogeography. MSc thesis, Texas Tech University, Lubbock, Texas, 105 p.
- EFREMOV J. A. 1938. — The recovery of a Triassic anomodont in the Orenburg province. *Doklady Akademii Nauk SSSR* 20: 227–229 [in Russian].
- EFREMOV J. A. 1940. — Preliminary description of the new Permian and Triassic Tetrapoda from USSR. *Trudy Paleontologicheskogo Instituta Akademii Nauk SSSR* 10: 1–140.
- EFREMOV J. A. 1951. — On the structure of the knee joint in higher dicynodonts. *Doklady Akademii Nauk SSSR* 77: 483–485.
- ELLENBERGER P. 1970. — Les niveaux paléontologiques de première apparition des mammifères primoridiaux en Afrique du Sud et leur ichnologie. *Establishement de zones stratigraphiques détaillées dans le Stormberg du Lesotho (Afrique du Sud) (Trias Supérieur à Jurassique. Second Symposium on Gondwana Stratigraphy and Paleontology, International Union of Geological Sciences. Council for Scientific and Industrial Research, Pretoria: 343–370.*
- ELLENBERGER F. & ELLENBERGER P. 1958. — Principaux types de pistes de Vertébrés dans les couches du Stormberg au Basutoland (Afrique du Sud) (Note préliminaire). *Compte rendu sommaire des séances de la Société Géologique de France* 1958: 65–67.
- ELLENBERGER F. & ELLENBERGER P. 1960. — Sur une nouvelle dalle à pistes de Vertébrés, découverte au Basutoland (Afrique du Sud). *Compte Rendus de la Société Géologique de France* 1960: 236–238.
- ELLENBERGER F., ELLENBERGER P. & GINSBURG L. 1970. — Les Dinosaures du Trias et du Lias en France et en Afrique du Sud, d'après les pistes qu'ils ont laissées. *Bulletin de la Société Géologique de France* 7: 151–159. <https://doi.org/10.2113/gssgbull.S7-XII.1.151>
- ELLENBERGER P. 1955. — Note préliminaire sur les pistes et les restes osseux de Vertébrés du Basutoland (Afrique du Sud). *Comptes Rendus Hebdomadaires des Séances de l'Académie des Sciences, Paris* 240: 889–891.
- ELLENBERGER P. 1965. — Découverte de pistes de Vertébrés dans le Permien, le Trias et le Lias inférieur, aux abords de Toulon (Var) et d'Anduze (Gard). *Comptes Rendus de l'Académie des Sciences à Paris* 260: 5856–5859.
- ELLENBERGER P. 1972. — Contribution à la classification des Pistes de Vertébrés du Trias. Les types du Stormberg d'Afrique du Sud (I). *Palaeovertebrata* 1972: 1–152.
- ELLIOT D. H., COLBERT E. H., BREED W. J., JENSEN J. A. & POWELL J. S. 1970. — Triassic tetrapods from Antarctica: evidence for continental drift. *Science* 169: 1197–1201. <https://doi.org/10.1126/science.169.3951.1197>
- ELLIOT D. H., FANNING C. M., ISBELL J. L. & HULETT S. R. W. 2017. — The Permo-Triassic Gondwana sequence, central Transantarctic Mountains, Antarctica: Zircon geochronology, provenance, and basin evolution. *Geosphere* 13 (1): 155–178. <https://doi.org/10.1130/GES01345.1>
- ESCOBAR J. A., MARTINELLI A. G., EZCURRA M. D., FIORELLI L. E. & DESOJO J. B. 2021. — A new stahleckeriid dicynodont record from the late Ladinian-?early Carnian levels of the Chañares Formation (Ischigualasto-Villa Unión Basin) of northwestern Argentina. *Journal of South American Earth Sciences* 109: 103275. <https://doi.org/10.1016/j.jsames.2021.103275>
- ESCOBAR J., MARTINELLI A., EZCURRA M., FIORELLI L., VON BACZKO B., NOVAS F. & DESOJO J. 2023. — A reassessment of the mandibular anatomy of *Dinodontosaurus brevirostris* (Synapsida, Dicynodontia) from the Ladinian-early Carnian Chañares Formation (northwestern Argentina), and its taxonomic and phylogenetic significance. *Ameghiniana* 62 (2): 178–201. <https://doi.org/10.5710/amgh.24.10.2022.3532>
- EZCURRA M. D., FIORELLI L. E., MARTINELLI A. G., ROCHER S., VON BACZKO M. B., EZPELETA M., TABORDA J. R. A., HECHENLEITNER E. M., TROTTEYN M. J. & DESOJO J. B. 2017. — Deep faunistic turnovers preceded the rise of dinosaurs in southwestern Pangaea. *Nature Ecology & Evolution* 1: 1477–1483. <https://doi.org/10.1038/s41559-017-0305-5>
- EZCURRA M. D., MARTINELLI A. G., FIORELLI L. E., DA ROSA Á. A. S. & DESOJO J. B. 2015. — Archosauromorph Remains from the Tarjados Formation (Early-Middle Triassic, NW Argentina). *Ameghiniana* 52 (5): 475–486. <https://doi.org/10.5710/AMGH.12.05.2015.2907>
- FALCO J. I. 2019. — *Estratigrafía y evolución magmática del Grupo Los Menudos (Tríásico), Provincia de Río Negro, Argentina*. PhD thesis, Universidad Nacional del Sur, Bahía Blanca, 249 p.
- FERREIRA G. S., RINCÓN A. D., SOLÓRZANO A. & LANGER M. C. 2006. — Review of the fossil matamata turtles: earliest well-dated record and hypotheses on the origin of their present geographical distribution. *Science of Nature* 103: 28. <https://doi.org/10.1007/s00114-016-1355-2>
- FIORILLO A. R., PADIAN K. & MUSIKASINTHORN C. 2000. — Taphonomy and depositional setting of the *Placerias* Quarry (Chinle Formation: Late Triassic, Arizona). *Palaios* 15 (5): 373–386. <https://doi.org/bfwrwj>
- FLYNN J. J., PARRISH J. M., RAKOTOSAMIMANANA B., SIMPSON W. F., WHATLEY R. L. & WYSS A. R. 1999. — A Triassic fauna from Madagascar, including early dinosaurs. *Science* 286 (5440): 763–765. <https://doi.org/10.1126/science.286.5440.763>
- FRANCISCHINI FILHO H. R. 2014. — *Paleobiología de Jachaleria candelariensis Araújo & Gonzaga, 1980 e comentários sobre a termoregulação em dicynodontia*. MSc thesis, Universidade federal do Rio Grande do Sul, Porto Alegre, 135 p.
- FRANCISCHINI H., DENTZIEN-DIAS P., LUCAS S. G. & SCHULTZ C. L. 2018. — Tetrapod tracks in Permo-Triassic eolian beds of southern Brazil (Paraná Basin). *PeerJ* 6: e4764. <https://doi.org/10.7717/peerj.4764>
- FRÖBISCH J. 2009. — Composition and similarity of global anomodont-bearing tetrapod faunas. *Earth-Science Reviews* 95 (3–4): 119–157. <https://doi.org/10.1016/j.earscirev.2009.04.001>
- FRÖBISCH J. 2006. — Locomotion in derived dicynodonts (Synapsida, Anomodontia): a functional analysis of the pelvic girdle and hind limb of *Tetragonias njalilus*. *Canadian Journal of Earth Sciences* 43 (9): 1297–1308. <https://doi.org/10.1139/e06-031>
- FRÖBISCH J. 2007. — The cranial anatomy of *Kombuisia frerensis* Hotton (Synapsida, Dicynodontia) and a new phylogeny of anomodont therapsids. *Zoological Journal of the Linnean Society* 150 (1): 117–144. <https://doi.org/10.1111/j.1096-3642.2007.00285.x>
- FRÖBISCH J. 2008. — Global taxonomic diversity of anomodonts (Tetrapoda, Therapsida) and the terrestrial rock record across the Permian-Triassic boundary. *PLoS ONE* 3: e3733. <https://doi.org/10.1371/journal.pone.0003733>
- FRÖBISCH J. 2009. — Composition and similarity of global anomodont-bearing tetrapod faunas. *Earth-Science Reviews* 95 (3–4): 119–157. <https://doi.org/10.1016/j.earscirev.2009.04.001>
- FRÖBISCH J. 2014. — Synapsid diversity and the rock record in the Permian-Triassic Beaufort Group (Karoo Supergroup), South Africa, in KAMMERER C. F., ANGIELCZYK K. D. & FRÖBISCH J. (eds), *Early Evolutionary History of the Synapsida*. Springer, Dordrecht: 305–319. https://doi.org/10.1007/978-94-007-6841-3_18
- FRÖBISCH J. & REISZ R. R. 2008. — A new species of *Emydops* (Synapsida, Anomodontia) and a discussion of dental variability and pathology in dicynodonts. *Journal of Vertebrate Paleontology* 28 (3): 770–787. <https://doi.org/dfqsqc>
- FRÖBISCH J., ANGIELCZYK K. D. & SIDOR C. A. 2010. — The Triassic dicynodont *Kombuisia* (Synapsida, Anomodontia) from Antarctica, a refuge from the terrestrial Permian-Triassic mass extinction. *Naturwissenschaften* 97: 187–196. <https://doi.org/10.1007/s00114-009-0626-6>

- GARDNER J. D., SURYA K. & ORGAN C. L. 2019. — Early tetrapodomorph biogeography: Controlling for fossil record bias in macroevolutionary analyses. *Comptes Rendus Palevol* 18 (7): 699-709. <https://doi.org/10.1016/j.crpv.2019.10.008>
- GASTALDO R. A., KAMO S. L., NEVELING J., GEISSMAN J. W., LOOY C. V. & MARTINI A. M. 2020. — The base of the *Lystrosaurus* Assemblage Zone, Karoo Basin, predates the end-Permian marine extinction. *Nature Communications* 11: 1428. <https://doi.org/10.1038/s41467-020-15243-7>
- GASTALDO R. A., NEVELING J., GEISSMAN J. W. & LOOY C. V. 2019. — Testing the *Daptocephalus* and *Lystrosaurus* Assemblage Zones in a lithostratigraphic, magnetostratigraphic, and palynological framework in the Free State, South Africa. *Palaios* 34 (11): 542-561. <https://doi.org/10.2110/palo.2019.019>
- GASTALDO R. A., NEVELING J., LOOY C. V., BAMFORD M. K., KAMO S. L. & GEISSMAN J. W. 2017. — Paleontology of the Blaauwwater 67 and 65 farms, South Africa: testing the *Daptocephalus/Lystrosaurus* biozone boundary in a stratigraphic framework. *Palaios* 32 (6): 349-366. <https://doi.org/10.2110/palo.2016.106>
- GASTON R., LOCKLEY M. G., LUCAS S. G. & HUNT A. P. 2003. — *Grallator*-dominated fossil footprint assemblages and associated enigmatic footprints from the Chinle group (Upper Triassic), Gateway Area, Colorado. *Ichnos* 10 (2-4): 153-163. <https://doi.org/10.1080/10420940390256258>
- GAUFFRE F.-X. 1993. — The prosauropod dinosaur *Azendohsaurus laaroussi* from the Upper Triassic of Morocco. *Palaeontology* 36: 897-908. <https://www.biodiversitylibrary.org/part/174152>
- GEE B. M. & JASINSKI S. E. 2021. — Description of the metoposaurid *Anaschisma browni* from the New Oxford Formation of Pennsylvania. *Journal of Paleontology* 95 (5): 1061-1078. <https://doi.org/10.1017/jpa.2021.30>
- GERMAN STRATIGRAPHIC COMMISSION 2016. — *Stratigraphic table of Germany 2016*. German Research Centre for Geosciences, Postdam.
- GEYER G. & KELBER K.-P. 2018. — Spinicaudata (“Conchostraca,” Crustacea) from the Middle Keuper (Upper Triassic) of the southern Germanic Basin, with a review of Carnian–Norian taxa and suggested biozones. *PalZ* 92: 1-34. <https://doi.org/10.1007/s12542-017-0363-7>
- GIERLIŃSKI G. D. 2009. — *A preliminary report on new dinosaur tracks in the Triassic, Jurassic and Cretaceous of Poland*. Actas de las IV Jornadas Internacionales sobre Paleontología de Dinosaurios y su Entorno, Salas de los Infantes, Burgos: 75-90.
- GOLOBOFF P. A. & CATALANO S. A. 2016. — TNT version 1.5, including a full implementation of phylogenetic morphometrics. *Cladistics* 32 (3): 221-238. <https://doi.org/10.1111/cla.12160>
- GOLOBOFF P. A., FARRIS S. & NIXON K. 2008. — TNT, a free programm for phylogenetic analysis. *Cladistics* 24 (5): 774-786. <https://doi.org/10.1111/j.1096-0031.2008.00217.x>
- GOVENDER R. 2005. — *Morphological and Functional Analysis of the Postcranial Anatomy of Two Dicynodont Morphotypes from the Cynognathus Assemblage Zone of South Africa Nad their Taxonomic Implications*. PhD thesis, University of the Witwatersrand, Johannesburg, 179 p.
- GOVENDER R. & YATES A. M. 2009. — Dicynodont postcrania from the Triassic of Namibia and their implication for the systematics of Kannemeyeriform dicynodonts. *Palaeontologia Africana* 44: 41-57.
- GOVENDER R., HANCOX P. J. & YATES A. M. 2008. — Re-evaluation of the postcranial skeleton of the Triassic dicynodont *Kannemeyeria simocephalus* from the *Cynognathus* Assemblage Zone (Subzone B) of South Africa. *Palaeontologia Africana* 43: 19-37.
- GREEN J. L. 2012. — Bone and dental histology of Late Triassic dicynodonts from North America, in CHINSAMY-TURAN A. (ed.), *Forerunners of Mammals: Radiation, Histology, Biology*. Indiana University Press, Bloomington: 178-196.
- GREEN J., SCHNEIDER V. P., SCHWEITZER M. H. & CLARKE J. A. 2005. — New evidence for non-*Placerias* dicynodonts in the Late Triassic (Carnian-Norian) of North America. *Journal of Vertebrate Paleontology* 25 (3): 65A-66A. <https://doi.org/10.1080/02781800512335367>
- GREEN J. L., SCHWEITZER M. H. & LAMM E. T. 2010. — Limb bone histology and growth in *Placerias hesternus* (Therapsida: Anomodontia) from the Upper Triassic of North America. *Palaeontology* 53 (2): 347-364. <https://doi.org/10.1111/j.1475-4983.2010.00944.x>
- GREGORY H. E. 1917. — *Geology of the Navajo Country. A Reconnaissance of Parts of Arizona, New Mexico, and Utah*. Government Printing Office, Washington, 161 p.
- GRINE F. E., FORSTER C. A., CLUVER M. A. & GEORGI J. A. 2006. — Cranial variability, ontogeny, and taxonomy of *Lystrosaurus* from the Karoo Basin of South Africa, in GAUDIN T. J., BLOB R. W. & WIBLE J. R. (eds), *Amniote Paleobiology. Perspectives on the Evolution of Mammals, Birds, and Reptiles*. University of Chicago Press, Chicago: 432-503.
- GROENEWALD G. H. 1991. — Burrow casts from the *Lystrosaurus-Procolophon* Assemblage-zone, Karoo Sequence, South Africa. *Koedoe* 34 (1): 13-22. <https://doi.org/10.4102/koedoe.v34i1.409>
- GUBIN Y. M. & SINITZA S. M. 1993. — Triassic terrestrial tetrapods of Mongolia and the geological structure of the Sain-Sar-Bulak locality. *New Mexico Museum of Natural History and Science Bulletin* 3: 169-170.
- HAMMER W. R. 1990. — Triassic terrestrial vertebrate faunas of Antarctica, in TAYLOR T. N. & TAYLOR E. L. (eds), *Antarctic Paleobiology. Its Role in the Reconstruction of Gondwana*. Springer, New York; Berlin; Heidelberg; London; Paris; Tokyo; Hong Kong: 42-50.
- HAMMER W. R. 1995. — New therapsids from the Upper Fremouw Formation (Triassic) of Antarctica. *Journal of Vertebrate Paleontology* 15 (1): 105-112. <https://doi.org/10.1080/02724634.1995.10011210>
- HAMMER W. R. & COSGRIFF J. W. 1981. — *Myosaurus gracilis*, an anomodont reptile from the Lower Triassic of Antarctica and South Africa. *Journal of Paleontology* 55 (2): 410-424. <https://www.jstor.org/stable/1304227>
- HAMMER W. R., RYAN W. J. & DEFAUW S. L. 1987. — Comments on the vertebrate fauna from the Fremouw Formation (Triassic), Beardmore Glacier region Antarctica. *Antarctic Journal of the United States* 22: 32-33.
- HAMMER W. R., COLLINSON J. W., ASKIN R. A. & HICKERSON W. J. 2004. — The first Upper Triassic vertebrate locality in Antarctica. *Gondwana Research* 7 (1): 199-204. [https://doi.org/10.1016/S1342-937X\(05\)70319-1](https://doi.org/10.1016/S1342-937X(05)70319-1)
- HAN F., ZHAO Q. & LIU J. 2021. — Preliminary bone histological analysis of *Lystrosaurus* (Therapsida: Dicynodontia) from the Lower Triassic of North China, and its implication for lifestyle and environments after the end-Permian extinction. *PLoS ONE* 16: e0248681. <https://doi.org/10.1371/journal.pone.0248681>
- HANCOX P. J. 1998. — *A Stratigraphic, Sedimentological and Palaeoenvironmental Synthesis of the Beaufort-Molteno Contact, in the Karoo Basin*. PhD thesis, University of the Witwatersrand, Johannesburg, 381 p.
- HANCOX P. J. & RUBIDGE B. S. 1994. — A new dicynodont therapsid from South Africa: implications for the biostratigraphy of the Upper Beaufort (*Cynognathus* Assemblage Zone). *South African Journal of Science* 90: 98-99.
- HANCOX P. J. & RUBIDGE B. S. 1996. — The first specimen of the Mid-Triassic dicynodont *Angonisaurus* from the Karoo of South Africa: implications for the dating and biostratigraphy of the

- Cynognathus* Assemblage Zone, upper Beaufort Group. *South African Journal of Science* 92: 391-392.
- HANCOX P. J., ANGIELCZYK K. D. & RUBIDGE B. S. 2013. — *Angonisaurus* and *Shansiodon*, dicynodonts (Therapsida, Anomodontia) from subzone C of the *Cynognathus* Assemblage Zone (Middle Triassic) of South Africa. *Journal of Vertebrate Paleontology* 33: 655-676. <https://doi.org/10.1080/02724634.2013.723551>
- HANCOX P. J., NEVELING J. & RUBIDGE B. S. 2020. — Biostratigraphy of the *Cynognathus* Assemblage Zone (Beaufort Group, Karoo Supergroup), South Africa. *South African Journal of Geology* 123 (3): 217-238. <https://doi.org/10.25131/sajg.123.0016>
- HAQUE Z., GEISSMAN J. W., IRMIS R. B., OLSEN P. E., LEPRE C., BUHEDMA H., MUNDIL R., PARKER W. G., RASMUSSEN C. & GEHRELS G. E. 2021. — Magnetostratigraphy of the Triassic Moenkopi Formation from the continuous cores recovered in Colorado Plateau Coring Project Phase 1 (CPCP-1), Petrified Forest National Park, Arizona, USA: Correlation of the Early to Middle Triassic strata and biota in Colorado Plateau and its environs. *Journal of Geophysical Research: Solid Earth* 126 (9): 1-28. <https://doi.org/10.1029/2021JB021899>
- HARTMAN S. A., LOVELACE D. M. & STOCKER M. R. 2015. — Stratigraphic and chronologic relationships of the Popo Agie Formation, upper Chugwater Group. *Geological Society of America Abstracts with Program*: 36.
- HAUBOLD H. 1971. — *Encyclopedia of paleoherpetology. Part 18. Ichnia Amphibiorum et Reptiliorum fossilium*. Gustav Fischer Verlag, Stuttgart and Portland, 124 p.
- HAUBOLD H. 1974. — *Die fossilen Saurierfährten*. A. Ziemsen Verlag, Wittenberg Lutherstadt, 168 p.
- HAUBOLD H. 1984. — *Saurierfährten*. A. Ziemsen Verlag, Lutherstadt, 231 p.
- HAUGHTON S. H. 1915. — On a skull of the genus *Kannemeyeria*. *Annals of the South African Museum* 8: 91-97.
- HAUGHTON S. H. 1917. — Investigations in South African fossil reptiles and Amphibia (part 10). Descriptive catalogue of the Anomodontia, with especial reference to the examples in the South African Museum (part 1). *Annals of the South African Museum* 12: 127-174.
- HAUGHTON S. H. 1924. — A bibliographic list of pre-Stormberg Karroo Reptilia, with a table of horizons. *Transactions of the Royal Society of South Africa* 12 (1): 51-104. <https://doi.org/10.1080/00359192409519299>
- HAUGHTON S. H. 1932. — On a collection of Karroo vertebrates from Tanganyika territory. *Quarterly Journal of the Geological Society* 88: 634-671. <https://doi.org/10.1144/GSL.JGS.1932.088.01-04.22>
- HAUGHTON S. H. 1963. — Note on the distribution of fossil Reptilia of Karroo age. *Palaeontologia Africana* 8: 1-11.
- HAUGHTON S. H. & BRINK A. S. 1954. — A bibliographic list of Reptilia from the Karroo beds of Africa. *Palaeontologia Africana* 2: 1-171.
- HECKERT A. B. 1997. — The tetrapod fauna of the Upper Triassic lower Chinle Group (Adamonian: latest Carnian) of the Zuni Mountains, west-central New Mexico. *New Mexico Museum of Natural History and Science Bulletin* 11: 29-39.
- HECKERT A. B. & LUCAS S. G. 2003. — Stratigraphy and paleontology of the lower Chinle Group (Adamonian: latest Carnian) in the vicinity of St. Johns, Arizona. *New Mexico Geological Society Guidebook* 54: 281-288.
- HECKERT A. B., FRASER N. C. & SCHNEIDER V. P. 2017. — A new species of *Coahomasuchus* (Archosauria, Aetosauria) from the Upper Triassic Pekin Formation, Deep River Basin, North Carolina. *Journal of Paleontology* 91 (1): 162-178. <https://doi.org/10.1017/jpa.2016.130>
- VAN HOEPEN E. C. N. 1915. — Contributions to the knowledge of the reptiles of the Karroo Formation. 3. The skull and other remains of *Lystrosaurus putterelli*, n. sp.. *Annals of the Transvaal Museum* 5: 70-82. <https://www.biodiversitylibrary.org/part/352216>
- VAN HOEPEN E. C. N. 1916. — Preliminary description of some new Lystrosaurini. *Annals of the Transvaal Museum* 5: 214-216.
- HOLZ M. & SCHULTZ C. L. 1998. — Taphonomy of the south Brazilian Triassic herpetofauna: fossilization mode and implications for morphological studies. *Lethaia* 31 (4): 335-345. <https://doi.org/10.1111/j.1502-3931.1998.tb00523.x>
- HORNSTEIN F. F. 1876. — Mittheilungen an Professor H. B. Geinitz. *Neues Jahrbuch für Mineralogie, Geologie und Paläontologie* 1876: 932-924.
- HOTTON N. 1974. — A new dicynodont (Reptilia, Therapsida) from *Cynognathus* zone deposits of South Africa. *Annals of the South African Museum* 64: 157-165.
- HOTTON N. 1986. — Dicynodonts and their role as primary consumers, in HOTTON N., MACLEAN P. D., ROTH J. J. & ROTH E. C. (eds), *The Ecology and Biology of Mammal-Like Reptiles*. Smithsonian Institution Press, Washington D.C.; London: 71-82.
- HUBER P., LUCAS S. G. & HUNT A. P. 1993. — Revised age and correlation of the Upper Triassic Chatham Group (Deep River Basin, Newark Supergroup), North Carolina. *Southeastern Geology* 33: 171-193.
- VON HUENE F. 1911. — Ueber *Erythrosuchus*, verterer der neuen Reptil-Ordnung Pelycosimia. *Geologische und Paläontologische Abhandlungen* 10: 1-60.
- VON HUENE F. 1913. — Über die Reptilführenden Sandsteine bei Elgin. *Zentralblatt für Mineralogie, Geologie und Paläontologie* 1913: 617-623.
- VON HUENE F. 1925. — Die südafrikanische Karroo-Formation als geologisches und faunistisches Lebensbild. *Fortschritte der Geologie und Paläontologie* 12: 1-124.
- VON HUENE F. 1926a. — Notes on the age of the continental Triassic beds in North America, with remarks on some fossil vertebrates. *Proceedings of the U. S. National Museum* 69: 1-10.
- VON HUENE F. 1926b. — Gondwana-Reptiliens in Südamerika. *Palaeontologia Hungarica* 2: 1-108.
- VON HUENE F. 1931. — Beitrag zur Kenntnis der Fauna der südafrikanischen Karrooformation. *Geologische und Paläontologische Abhandlungen* 18: 157-227.
- VON HUENE F. 1935. — Lieferung 1. Anomodontia. In: *Die Fossilien Reptilien des Südamerikanischen Gondwanalandes. Ergebnisse der Sauriergrabungen in Südbrasiliens 1928/29*. C. H. Beck'sche Verlagsbuchhandlung, Munich: 1-82.
- VON HUENE F. 1936. — Ein *Stahleckeria*-Schädel. *Zentralblatt für Mineralogie, Geologie und Paläontologie B. Geologie und Paläontologie* 11: 507-509.
- VON HUENE F. 1942. — Die Anomodontier des Ruhuhu-Gebietes in der Tübinger Sammlung. *Palaeontographica A* 94: 154-184.
- VON HUENE F. 1944. — Ein Anomodontier-Fund am oberen Amazonas. *Neues Jahrbuch für Geologie und Paläontologie - Monatshefte* 10: 260-265.
- VON HUENE F. 1948. — Short review of the lower tetrapods, in DU TOIT A. L. (ed.), *Special Publication of the Royal Society of South Africa: Robert Broom Commemorative Volume*. Royal Society of South Africa, Cape Town: 65-106.
- VON HUENE F. 1949. — Der Stapes und ein problematischer Knochen von *Stahleckeria*. *Neues Jahrbuch für Geologie und Paläontologie - Monatshefte* 1949: 344-347.
- HUNT A. P. & LUCAS S. G. 1993. — Tetrapod footprints from the Middle Triassic Moenkopi Formation, west-central New Mexico. *New Mexico Museum of Natural History and Science Bulletin* 3: G20-G23.
- HUNT A. P. & LUCAS S. G. 2007. — Late Triassic tetrapod tracks of western North America. *New Mexico Museum of Natural History and Science Bulletin* 40: 215-230.
- HUNT A. P., LUCAS S. G. & LOCKLEY M. G. 1998. — Taxonomy and stratigraphic and facies significance of vertebrate coprolites of the Upper Triassic Chinle Group, western United States. *Ichnos* 5 (3): 225-234. <https://doi.org/10.1080/10420949809386419>

- HUNT A. P., SANTUCCI V. L., LOCKLEY M. G. & OLSON T. J. 1993. — Dicynodont trackways from the Holbrook Member of the Moenkopi Formation (Middle Triassic: Anisian), Arizona, USA. *New Mexico Museum of Natural History and Science Bulletin* 3: 213-218.
- HUNT A. P., LUCAS S. G., SPIELMANN J. A. & LERNER A. J. 2007. — A review of vertebrate coprolites of the Triassic with descriptions of new Mesozoic ichnotaxa. *New Mexico Museum of Natural History and Science Bulletin* 41: 88-107.
- HUNT-FOSTER R. K., LOCKLEY M. G., MILNER A. R. C., FOSTER J. R., MATTHEWS N. A., BREITHAUPT B. H. & SMITH J. A. 2016. — Tracking dinosaurs in BLM Canyon Country, Utah. *Geology of the Intermountain West* 3: 67-100. <https://doi.org/10.31711/giw.v3.pp67-100>
- HUXLEY T. H. 1859. — On a new species of *Dicynodon* (*D. murayi*) from near Colesberg, South Africa. *Quarterly Journal of the Geological Society of London* 8: 207-208.
- HUXLEY T. H. 1865. — *On a Collection of Vertebrate Fossils from the Panchet Rocks, Raniganj, Bengal*. Trübner, Calcutta, 27 p.
- IRMIS R. B., MUNDIL R., MARTZ J. W. & PARKER W. G. 2011. — High-resolution U-Pb ages from the Upper Triassic Chinle Formation (New Mexico, USA) support a diachronous rise of dinosaurs. *Earth and Planetary Science Letters* 309 (258-267): 258-267. <https://doi.org/10.1016/j.epsl.2011.07.015>
- IVAKHNENKO M. F. 2008. — Subclass Theromorpha, in IVAKHNENKO M. F. & KUROCHKIN E. N. (eds), *Fossil Vertebrates of Russia and Neighbouring Countries. Fossil Reptiles and Birds Part I*. GEOS, Moscow: 101-183 [in Russian].
- IVAKHNENKO M. F., GOLUBEV V. K., GUBIN Y. M., KALANDADZE N. N., NOVIKOV I. V., SENNIKOV A. G. & RAUTIAN A. S. 1997. — *Permian and Triassic Tetrapods of Eastern Europe*. GEOS, Moscow, 216 p.
- JAEKEL O. 1911. — *Die Wirbeltiere. Eine Übersicht über die fossilen und lebenden Formen*. Verlag von Gebrüder Borntraeger, Berlin, 252 p. <https://doi.org/10.5962/bhl.title.119340>
- JAIN S. L., ROBINSON P. L. & CHOWDHURY T. K. R. 1964. — A new vertebrate fauna from the Triassic of the Deccan, India. *Quarterly Journal of the Geological Society* 120: 115-124. <https://doi.org/10.1144/gsjgs.120.1.0115>
- JANENSCH W. 1952. — Über den Unterkiefer der Therapsiden. *Paläontologische Zeitschrift* 26: 229-247. <https://doi.org/10.1007/BF03041734>
- JASINOSKI S. C. & CHINSAMY-TURAN A. 2012. — Biological inferences of the cranial microstructure of the dicynodonts *Oudenodon* and *Lystrosaurus*, in CHINSAMY-TURAN A. (ed.), *Forerunners of Mammals: Radiation, Histology, Biology*. Indiana University Press, Bloomington & Indianapolis: 149-176.
- JASINOSKI S. C., RAYFIELD E. J. & CHINSAMY A. 2009. — Comparative feeding biomechanics of *Lystrosaurus* and the generalized dicynodont *Oudenodon*. *Anatomical Record* 292: 862-874. <https://doi.org/10.1002/ar.20906>
- JASINOSKI S. C., RAYFIELD E. J. & CHINSAMY A. 2010. — Functional implications of dicynodont cranial suture morphology. *Journal of Morphology* 271 (6): 705-728. <https://doi.org/10.1002/jmor.10828>
- JASINOSKI S. C., CLUVER M. A., CHINSAMY A. & REDDY B. D. 2014. — Anatomical plasticity in the snout of *Lystrosaurus*, in KAMMERER C. F., ANGIELCZYK K. D. & FRÖBISCH J. (eds), *Early Evolutionary History of the Synapsida*. Springer, Dordrecht: 139-149.
- JINNAH Z. A. & RUBIDGE B. S. 2007. — A double-tusked dicynodont and its biostratigraphic significance. *South African Journal of Science* 103: 51-53.
- JINNOUCHI K., KUSUHASHI N., LIU J., TAKAHASHI F., SHINODA K. & HASEGAWA Y. 2018. — Dicynodont fossils from the Upper Triassic Momonoki Formation, Mine Group, Yamaguchi, Japan, in *The Palaeontological Society of Japan, 167th Regular Meeting Abstracts with Programs*: 42.
- JONES T. R. 1890. — I.-On some fossil Estheriae. *Geological Magazine* 7 (9): 385-390. <https://doi.org/10.1017/S0016756800188028>
- JUDD J. W. 1885. — The presence of the remains of *Dicynodon* in the triassic sandstone of Elgin. *Nature* 32: 573. <https://doi.org/10.1038/032573a0>
- KALANDADZE N. N. 1970. — New Triassic kannemeyeriids from Southern Cisuralia, in FLEROV K. K. (ed.), *Materials on the Evolution of Terrestrial Vertebrates*. Nauka, Moscow: 51-57 [in Russian].
- KALANDADZE N. N. 1974. — The first lystrosaur from the territory of Laurasia. *Priroda* 8: 109-110 [in Russian].
- KALANDADZE N. N. 1975. — The first lystrosaur find from the territory of the European part of the USSR. *Palaeontologicheskiy Zhurnal* 4: 140-142.
- KALANDADZE N. N. & SENNIKOV A. G. 1985. — New reptiles from the Middle Triassic of the Cis-Urals. *Paleontological Journal* 1985: 77-84.
- KAMMERER C. F. 2009. — *Cranial disparity in the non-mammalian Synapsida*. PhD thesis, University of Chicago, Chicago, 633 p.
- KAMMERER C. F. 2018. — The first skeletal evidence of a dicynodont from the lower Elliot Formation of South Africa. *Palaeontologia Africana* 52: 102-128.
- KAMMERER C. F. 2021. — Elevated cranial sutural complexity in burrowing dicynodonts. *Frontiers in Ecology and Evolution* 9: 674151. <https://doi.org/10.3389/fevo.2021.674151>
- KAMMERER C. F. & SMITH R. M. H. 2017. — An early geikiid dicynodont from the *Tropidostoma* Assemblage Zone (late Permian) of South Africa. *PeerJ* 5: e2913. <https://doi.org/10.7717/peerj.2913>
- KAMMERER C. F., ANGIELCZYK K. D. & FRÖBISCH J. 2011. — A comprehensive taxonomic revision of *Dicynodon* (Therapsida, Anomodontia) and its implications for dicynodont phylogeny, biogeography, and biostratigraphy. *Journal of Vertebrate Paleontology* 31 (Supplement 1): 1-158. <https://doi.org/10.1080/02724634.2011.627074>
- KAMMERER C. F., NESBITT S. J. & SHUBIN N. H. 2012. — The first silesaurid dinosauriform from the Late Triassic of Morocco. *Acta Palaeontologica Polonica* 57 (2): 277-284. <https://doi.org/10.4202/app.2011.0015>
- KAMMERER C. F., FRÖBISCH J. & ANGIELCZYK K. D. 2013. — On the validity and phylogenetic position of *Eubrachiosaurus browni*, a kannemeyeriiform dicynodont (Anomodontia) from Triassic North America. *PLoS ONE* 8: e64203. <https://doi.org/10.1371/journal.pone.0064203>
- KAMMERER C. F., ANGIELCZYK K. D. & NESBITT S. J. 2017. — Novel hind limb morphology in a kannemeyeriiform dicynodont from the Manda Beds (Songea Group, Ruhuhu Basin) of Tanzania. *Journal of Vertebrate Paleontology* 37 (Supplement 1): 178-188. <https://doi.org/10.1080/02724634.2017.1309422>
- KAMMERER C. F., VIGLIETTI P. A., HANCOX P. J., BUTLER R. J. & CHOINIÈRE J. N. 2019. — A new kannemeyeriiform dicynodont (*Ufudocyclops mukanelai*, gen. et sp. nov.) from Subzone C of the *Cynognathus* Assemblage Zone, Triassic of South Africa, with implications for biostratigraphic correlation with other African Triassic Faunas. *Journal of Vertebrate Paleontology* 39 (2): e1596921. <https://doi.org/10.1080/02724634.2019.1596921>
- KAMMERER C. F. & ORDOÑEZ M. DE LOS A. 2021. — Dicynodonts (Therapsida: Anomodontia) of South America. *Journal of South American Earth Sciences* 108: 103171. <https://doi.org/10.1016/j.jsames.2021.103171>
- KEMP T. S. 1975. — Vertebrate localities in the Karroo System of the Luangwa Valley, Zambia. *Nature* 254: 415-416. <https://doi.org/10.1038/254415a0>
- KEMP T. S. 1982. — *Mammal-Like Reptiles and the Origin of Mammals*. Academic Press, London, New York, Paris, San Diego, San Francisco, São Paulo, Sydney, Tokyo, Toronto, 363 p.
- KENT D. V., SANTI MALNIS P., COLOMBI C. E., ALCOBER O. A. & MARTINEZ R. N. 2014. — Age constraints on the dispersal of dinosaurs in the Late Triassic from magnetochronology of the Los Colorados Formation (Argentina). *Proceedings of the National Academy of Sciences* 111 (22): 7958-7963. <https://doi.org/10.1073/pnas.1402369111>

- VAN DE KERK M., LARSEN R. T., OLSON D. D., HERSEY K. R. & MCMILLAN B. R. 2021. — Variation in movement patterns of mule deer: Have we oversimplified migration? *Movement Ecology* 9 (44): 1-12. <https://doi.org/10.1186/s40462-021-00281-7>
- KEYSER A. W. 1973. — A new Triassic vertebrate fauna from South West Africa. *Palaeontologia Africana* 16: 1-15.
- KEYSER A. W. 1974. — Evolutionary trends in Triassic dicynodontia (Reptilia Therapsida). *Palaeontologia Africana* 17: 57-68.
- KEYSER A. W. & CRUICKSHANK A. R. I. 1979. — The origins and classification of Triassic dicynodonts. *Transactions of the Geological Society of South Africa* 82: 81-108.
- KEYSER A. W. & CRUICKSHANK A. R. I. 1980. — Author's reply to discussion. Reply to M.R. Cooper. *Transactions of the Geological Society of South Africa* 83: 110-111.
- KING G. M. 1983. — First mammal-like reptile from Australia. *Nature* 306: 209. <https://doi.org/10.1038/306209a0>
- KING G. M. 1988. — *Encyclopedia of paleoherpetology. Part 17 C. Anomodontia*. Gustav Fischer Verlag, Stuttgart; New York: 174 p.
- KING G. 1990a. — Dicynodonts and the end Permian event. *Palaeontology Africana* 27: 31-39.
- KING G. M. 1990b. — *The dicynodonts. A study in palaeobiology*. Chapman & Hall, London; New York: 233 p.
- KING G. M. 1991. — The aquatic *Lystrosaurus*: a palaeontological myth. *Historical Biology* 4 (3-4): 285-321. <https://doi.org/10.1080/08912969009386547>
- KING G. M. & CLUVER M. A. 1991. — The aquatic *Lystrosaurus*: an alternative lifestyle. *Historical Biology* 4 (3-4): 323-341. <https://doi.org/10.1080/08912969009386548>
- KING G. M. & JENKINS I. 1997. — The dicynodont *Lystrosaurus* from the Upper Permian of Zambia: evolutionary and stratigraphical implications. *Palaeontology* 40: 149-156. <https://www.biodiversitylibrary.org/part/174341>
- KITCHING J. W. 1963. — The fossil localities and mammal-like reptiles of the upper Luangwa valley, Northern Rhodesia. *South African Journal of Science* 59: 259-264.
- KITCHING J. W. 1968. — On the *Lystrosaurus* zone and its fauna with special reference to some immature Lystrosauridae. *Palaeontology Africana* 11: 61-76.
- KITCHING J. W. 1977. — The distribution of the Karroo vertebrate fauna. *Bernard Price Institute for Palaeontological Research Memoir* 1: 1-131.
- KLEIN H. & LUCAS S. G. 2010. — Review of the tetrapod ichnofauna of the Moenkopi Formation/Group (Early-Middle Triassic) of the American Southwest. *New Mexico Museum of Natural History and Science Bulletin* 50: 1-67.
- KLEIN H. & LUCAS S. G. 2018. — Diverse Middle Triassic tetrapod footprint assemblage from the Muschelkalk of Germany. *Ichnos* 25 (2-3): 162-176. <https://doi.org/10.1080/10420940.2017.1337632>
- KLEIN H. & LUCAS S. G. 2021. — The Triassic tetrapod footprint record. *New Mexico Museum of Natural History and Science Bulletin* 83: 1-194.
- KLEIN H., LUCAS S. G. & VOIGT S. 2015. — Revision of the ?Permian-Triassic tetrapod ichnogenus *Procolophonichnium* Nopcsa 1923 with description of the new ichnospecies *P. lockleyi*. *Ichnos* 22 (3-4): 155-176. <https://doi.org/10.1080/10420940.2015.1063490>
- KLEIN H. & NIEDZWIEDZKI G. 2012. — Revision of the Lower Triassic tetrapod ichnofauna from Wióry, Holy Cross Mountains, Poland. *New Mexico Museum of Natural History and Science Bulletin* 56: 1-62.
- KNAUS P. L., VAN HETEREN A. H., LUNGUS J. K. & SANDER P. M. 2021. — High blood flow into the femur indicates elevated aerobic capacity in synapsids since the Synapsida-Sauropsida split. *Frontiers in Ecology and Evolution* 9: 751238. <https://doi.org/10.3389/fevo.2021.751238>
- KNUTSEN E. M. & OERLEMANS E. 2020. — The last dicynodont? Re-assessing the taxonomic and temporal relationships of a contentious Australian fossil. *Gondwana Research* 77: 184-203. <https://doi.org/10.1016/j.gr.2019.07.011>
- KOWAL-LINKA M., KRZEMIŃSKA E. & CZUPYT Z. 2018. — Najmłodsze detrytyczne cirkony z utwórów triasów z Lipie Śląskiego (Lisowice) koło Lublińca a wiek lisowickiego poziomu kościonośnego, in *Polska Konferencja Sedymentologiczna POKOS 7. Materiały konferencyjne* p. 77.
- KOWAL-LINKA M., KRZEMIŃSKA E. & CZUPYT Z. 2019. — The youngest detrital zircons from the Upper Triassic Lipie Śląskie (Lisowice) continental deposits (Poland): Implications for the maximum depositional age of the Lisowice bone-bearing horizon. *Palaeogeography, Palaeoclimatology, Palaeoecology* 514: 487-501. <https://doi.org/10.1016/j.palaeo.2018.11.012>
- KRUMMECK W. D. & BORDY E. M. 2018. — *Reniformichnus kati-katii* (new ichnogenus and ichnospecies): continental vertebrate burrows from the Lower Triassic, main Karoo Basin, South Africa. *Ichnos* 25 (2-3): 138-149. <https://doi.org/10.1080/10420940.2017.1292909>
- KULIK Z. T. & SIDOR C. A. 2023. — A test of Bergmann's rule in the Early Triassic: latitude, body size, and sampling in *Lystrosaurus*. *Paleobiology* 49 (1): 53-67. <https://doi.org/10.1017/pab.2022.25>
- KUTTY T. S. & SENGUPTA D. P. 1989. — The Late Triassic formations of the Pranhita Godavari Valley and their faunal succession – a reappraisal. *Indian Journal of Earth Sciences* 16: 189-206.
- KULIK Z. T., LUNGUS J. K., ANGIELCZYK K. D. & SIDOR C. A. 2021. — Living fast in the Triassic: New data on life history in *Lystrosaurus* (Therapsida: Dicynodontia) from Northeastern Pangea. *PLoS ONE* 16: e0259369. <https://doi.org/10.1371/journal.pone.0259369>
- KURKIN A. A. 1999. — New dicynodont from Little Northern Dvina River excavations. *Paleontological Journal* 1999: 87-92.
- KURKIN A. A. 2001. — New late Permian dicynodonts from the Vyazniki assemblage of terrestrial tetrapods of eastern Europe. *Paleontological Journal* 35: 53-59.
- KUTTY T. S. & SENGUPTA D. P. 1989. — The Late Triassic formations of the Pranhita Godavari Valley and their faunal succession – a reappraisal. *Indian Journal of Earth Sciences* 16: 189-206.
- KUTTY T. S., JAIN S. L. & CHOWDHURY T. K. R. 1988. — Gondwana sequence of the northern Pranhita-Godavari Valley: its stratigraphy and vertebrate faunas. *The Palaeobotanist* 36: 214-229. <https://doi.org/10.54991/jop.1987.1582>
- LAGNAOUI A., MELCHOR R. N., BELLOSI E. S., VILLEGRAS P. M., ESPINOZA N. & UMAZANO A. M. 2019. — Middle Triassic *Pentasauropus*-dominated ichnofauna from western Gondwana: Ichnotaxonomy, palaeoenvironment, biostratigraphy and palaeobiogeography. *Palaeogeography, Palaeoclimatology, Palaeoecology* 524: 41-61. <https://doi.org/10.1016/j.palaeo.2019.03.020>
- LANGER M. C. & LAVINA E. L. 2000. — Os amniotas do neopermiano e eotriássico da Bacia do Paraná-Repteis e 'Repteis Mamaliformes', in HOLZ M. & DE ROS L. F. (eds), *Paleontologia do Rio Grande do Sul*. Universidade Federal do Rio Grande do Sul: 210-235.
- LANGER M. C., RIBEIRO A. M., SCHULTZ C. L. & FERIGOLO J. 2007. — The continental tetrapod-bearing Triassic of South Brazil. *New Mexico Museum of Natural History and Science Bulletin* 41: 201-218.
- LANGER M. C., RAMEZANI J. & DA ROSA Á. A. S. 2018. — U-Pb age constraints on dinosaur rise from south Brazil. *Gondwana Research* 57: 133-140. <https://doi.org/10.1016/j.gr.2018.01.005>
- DE LAPPARENT DE BROIN F., BOCCVENTIN J. & NEGRI F. R. 1993. — Gigantic turtles (Pleurodira, Podocnemididae) from the late Miocene-early Pliocene of south western Amazon. *Bulletin de l'Institut Français des Études Andines* 22: 657-670.
- LARKIN N. 1994. — *Description of a New Triassic Dicynodont from the Manda Formation of Tanzania*. MSc thesis, University College London, London, 104 p.
- LEHMAN, J.-P. 1961. — Dicynodontia, in PIVETEAU J.-P. (ed.), *Tratit de Paléontologie, VI, Mammifères, Vol 1.: Origine Reptiliennne Evolution*. Masson et Cie, Paris: 287-351.

- LEHMAN T. M. & CHATTERJEE S. 2005. — Depositional setting and vertebrate biostratigraphy of the Triassic Dockum Group of Texas. *Journal of Earth System Science* 114: 235-351. <https://doi.org/10.1007/BF02702953>
- LEONARDI G. 1994. — *Annotated Atlas of South America Tetrapod Footprints (Devonian to Holocene) with an Appendix on Mexico and Central America*. Companhia de Pesquisa de Recursos Minerais, Brasília, 247 p.
- LEONARDI G. & OLIVEIRA F. H. DE 1990. — A revision of the Triassic and Jurassic tetrapod footprints of Argentina and a new approach on the age and meaning of the Botucatu Formation footprints (Brazil). *Revista Brasileira de Geociências* 20: 216-229. <https://doi.org/10.25249/0375-7536.1990216229>
- LI J. 1980. — *Kannemeyeria* fossil from Inner Mongolia. *Vertebrata PalAsiatica* 18: 94-99.
- LI J. 1988. — *Lystrosaurus* of Xinjiang, China. *Vertebrata PalAsiatica* 10: 241-249.
- LI J. 2015. — Suborder Anomodontia, in LI J. & LIU J. (eds.), *Palaeovertebrata Sinica. Volume III. Basal Synapsids and Mammals. Fascicle 1 (Serial no. 14). Basal Synapsids*. Science Press, Beijing: 25-63.
- LIU H. 1973. — The fossil-bearing beds of Taoshuyantze, Turfan Basin, Sinkiang. *Memoirs of the Institute of Vertebrate Paleontology and Paleoanthropology, Academia Sinica* 10: 1-5.
- LIU J. 2004. — *Parakannemeyeria chengi* sp. nov. from Kelmayi Formation of Jimusar, Xinjiang. *Vertebrata PalAsiatica* 42: 77-80.
- LIU J. 2015. — New discoveries from the *Sinokannemeyeria-Shansisuchus* Assemblage Zone: 1. Kannemeyeriformes from Shanxi, China. *Vertebrata PalAsiatica* 53: 16-28.
- LIU J. 2020. — *Taoheidon baizhijuni*, gen. et sp. nov. (Anomodontia, Dicynodontida), from the upper Permian Sunjiagou Formation of China and its implications. *Journal of Vertebrate Paleontology* 40 (1): e1762088. <https://doi.org/10.1080/02724634.2020.1762088>
- LIU J. 2022. — On kannemeyeriform dicynodonts from the *Shaanbeikannemeyeria* Assemblage Zone of the Ordos Basin, China. *Vertebrata PalAsiatica* 60 (3): 212-248.
- LIU J. & LI J.-L. 2003. — A new material of kannemeyerid from Xinjiang and the restudy of *Parakannemeyeria brevirostris*. *Vertebrata PalAsiatica* 41: 147-156.
- LI J. & SUN A. 2008. — Subclass Synapsida, in LI J., WU X. & ZHANG F. (eds), *The Chinese fossil reptiles and their kin*. Science Press, Beijing: 379-417.
- LIU J., LI J.-L. & CHENG Z.-W. 2002. — The *Lystrosaurus* fossils from Xinjiang and their bearing on the terrestrial Permian-Triassic boundary. *Vertebrata PalAsiatica* 40: 267-275.
- LIU J., RAMEZANI J., LI L., SHANG Q.-H., XU G.-H., WANG Y.-Y. & YANG J.-S. 2017. — High-precision temporal calibration of Middle Triassic vertebrate biostratigraphy: U-Pb zircon constraints for the *Sinokannemeyeria* Fauna and *Yonghesuchus*. *Vertebrata PalAsiatica* 55: 1-9.
- LIU J., ANGIELCZYK K. D. & ABDALA F. 2021. — Permo-Triassic tetrapods and their climate implications. *Global and Planetary Change* 205: 103618. <https://doi.org/10.1016/j.gloplacha.2021.103618>
- LIU J., ABDALA F., ANGIELCZYK K. D. & SIDOR C. A. 2022. — Tetrapod turnover during the Permo-Triassic transition explained by temperature change. *Earth-Science Reviews* 224: 103886. <https://doi.org/10.1016/j.earscirev.2021.103886>
- LOCKLEY M. G. & HUNT A. P. 1995. — *Dinosaur tracks and other fossil footprints of the Western United States*. Columbia University Press, New York, 338 p.
- LOCKLEY M. G., HUNT A. P., GASTON R. & KIRKLAND J. I. 1996. — A trackway bonanza with mammal footprints from the Late Triassic of Colorado. *Journal of Vertebrate Paleontology* 16 (1): 49A. <https://doi.org/10.1080/02724634.1996.10011283>
- LONG R. A. & MURRAY P. A. 1995. — Late Triassic (Carnian and Norian) tetrapods from the southwestern United States. *New Mexico Museum of Natural History and Science Bulletin* 4: 1-254.
- LOZOVS'KII V. R. 1983. — Age of the *Lystrosaurus* beds in the Moscow syneclyse. *Doklady Akademii Nauk SSSR* 272: 1433-1437 [in Russian].
- LUCAS F. A. 1904. — A new batrachian and a new reptile from the Trias of Arizona. *Proceedings of the United States National Museum* 27 (1353): 193-195. <https://doi.org/10.5479/si.00963801.27-1353.193>
- LUCAS S. G. 1993a. — *Barysoma lenzii* (Synapsida: Dicynodontia) from the Middle Triassic of Brazil, a synonym of *Stahleckeria potens*. *Journal of Paleontology* 67 (2): 318-321. <https://doi.org/10.1017/S0022336000032285>
- LUCAS S. G. 1993b. — The Chinle Group: revised stratigraphy and biochronology of Upper Triassic Nonmarine strata in the western United States. *Museum of Northern Arizona Bulletin* 59: 27-50.
- LUCAS S. G. 1998. — *Placerias* (Reptilia, Dicynodontia) from the Upper Triassic of the Newark Supergroup, North Carolina, USA, and its biochronological significance. *Neues Jahrbuch für Geologie und Paläontologie - Monatshefte* 1998 (7): 432-448. <https://doi.org/10.1127/njgp/1998/1998/432>
- LUCAS S. G. 2001. — *Chinese fossil vertebrates*. Columbia University Press, New York, 375 p.
- LUCAS S. G. 2002. — A new dicynodont from the Triassic of Brazil and the tetrapod biochronology of the Brazilian Triassic. *New Mexico Museum of Natural History and Science Bulletin* 21: 131-141.
- LUCAS S. G. 2007. — Another dicynodont from the Triassic Muschelkalk of Germany and its biochronological significance. *New Mexico Museum of Natural History and Science Bulletin* 41: 219-221.
- LUCAS S. G. 2015. — Age and correlation of Late Triassic tetrapods from southern Poland. *Annales Societatis Geologorum Poloniae* 85 (4): 627-635. <https://doi.org/10.14241/asgp.2015.024>
- LUCAS S. G. & HUNT A. P. 1993a. — A dicynodont from the Upper Triassic of New Mexico and its biochronologic significance. *New Mexico Museum of Natural History and Science Bulletin* 3: 321-325.
- LUCAS S. G. & HUNT A. P. 1993b. — *Fukangolepis* Yang, 1978 from the Triassic of China is not an aetosaur. *Journal of Vertebrate Paleontology* 13 (1): 145-147. <https://doi.org/10.1080/02724634.1993.10011493>
- LUCAS S. G. & WILD R. 1995. — A Middle Triassic dicynodont from Germany and the biochronology of Triassic dicynodonts. *Stuttgarter Beiträge zur Naturkunde B* 220: 1-16.
- LUCAS S. G. & HARRIS S. K. 1996. — Taxonomic and biochronological significance of specimens of the Triassic dicynodont *Dinodonto-saurus* Romer 1943 in the Tübingen collection. *Paläontologische Zeitschrift* 70: 603-622. <https://doi.org/10.1007/BF02988096>
- LUCAS S. G. & HECKERT A. B. 2002. — Skull of the dicynodont *Placerias* from the Upper Triassic of Arizona. *New Mexico Museum of Natural History and Science Bulletin* 21: 127-130.
- LUCAS S. G., HECKERT A. B. & HUNT A. P. 2003. — Tetrapod footprints from the Middle Triassic (Perovkan-early Anisian) Moenkopi Formation, west-central New Mexico. *New Mexico Geological Society 54th Annual Fall Field Conference Guidebook*: 241-244.
- LYDEKKER R. 1877. — Notices of new and other vertebrate from Indian Tertiary and Secondary Rocks. *Records of the Geological Survey of India* 10: 30-43.
- LYDEKKER R. 1879. — Indian Pretertiary Vertebrata. Fossil Reptilia and Batrachia. *Palaeontologia Indica* 1: 1-36.
- LYDEKKER R. 1889. — On the pectoral and pelvic girdles and skull of the Indian dicynodonts. *Records of the Geological Survey of India* 23: 17-20.
- MACDONALD D. I. M., ISBELL J. L. & HAMMER W. R. 1992. — Vertebrate trackways from the Triassic Fremouw Formation, Queen Alexandra Range, Antarctica. *Antarctic Journal of the United States* 26: 20-22.
- MACRAE C. 1999. — *Life etched in stone. Fossils of South Africa*. Geological Society of South Africa, Johannesburg, 305 p.

- MAINARDES DUTRA B. A. 2015. — *Therapsida, Dicynodontia: aspectos gerais e registros brasileiros*. B.Sc. thesis, Universidade Federal do Paraná, Curitiba, 41 p.
- MAISCH M. W. 2001. — Observations on Karoo and Gondwana vertebrates. Part 2: A new skull-reconstruction of *Stableckeria potens* von Huene, 1935 (Dicynodontia, Middle Triassic) and a reconsideration of kannemeyeriiform phylogeny. *Neues Jahrbuch für Geologie und Paläontologie - Abhandlungen* 220 (1): 127-152. <https://doi.org/10.1127/njgp/220/2001/127>
- MAISCH M. W. 2021. — An unusual historic dicynodont specimen (Therapsida: Dicynodontia) from the *Dinodontosaurus* Assemblage Zone of the Santa Maria Formation (Middle Triassic) of Rio Grande do Sul, Brazil. *PalZ* 95: 129-144. <https://doi.org/10.1007/s12542-020-00525-8>
- MAISCH M. W. & MATZKE A. T. 2014. — *Sungeodon kimkraemerae* n. gen. n. sp., the oldest kannemeyeriiform (Therapsida, Dicynodontia) and its implications for the early diversification of large herbivores after the P/T boundary. *Neues Jahrbuch für Geologie und Paläontologie - Abhandlungen* 272 (1): 1-12. <https://doi.org/10.1127/0077-7749/2014/0394>
- MAISCH M. W., VEGA C. S. & SCHOCH R. R. 2009. — No dicynodont in the Keuper - a reconsideration of the occurrence of aff. *Dinodontosaurus* in the Middle Triassic of Southern Germany. *Palaeodiversity* 2: 271-278.
- MANCUSO A. C. & IRMIS R. B. 2019. — The large-bodied dicynodont *Stableckeria* (Synapsida, Anomodontia) from the Upper Triassic (Carnian) Chañares Formation (Argentina); new data for Triassic Gondwanan biogeography. *Ameghiniana* 57 (1): 45-57. <https://doi.org/10.5710/AMGH.20.12.2019.3302>
- MANNION P. D., UPCHURCH P., CARRANO M. T. & BARRETT P. M. 2011. — Testing the effect of the rock record on diversity: A multidisciplinary approach to elucidating the generic richness of sauropodomorph dinosaurs through time. *Biological Reviews* 86 (1): 157-181. <https://doi.org/10.1111/j.1469-185X.2010.00139.x>
- MARCHETTI L., KLEIN H., BUCHWITZ M., RONCHI A., SMITH R. M. H., DE KLERK W. J., SCISCO L. & GROENEWALD G. H. 2019. — Permian-Triassic vertebrate footprints from South Africa: Ichnotaxonomy, producers and biostratigraphy through two major faunal crises. *Gondwana Research* 72: 139-168. <https://doi.org/10.1016/j.gr.2019.03.009>
- MARILAO L. M., KULIK Z. T. & SIDOR C. A. 2020. — Histology of the preparietal: a neomorphic cranial element in dicynodont therapsids. *Journal of Vertebrate Paleontology* 40 (2): e1770775. <https://doi.org/10.1080/02724634.2020.1770775>
- MARSICANO C. A. & BARREDO S. P. 2004. — A Triassic tetrapod footprint assemblage from southern South America: Palaeobiogeographical and evolutionary implications. *Palaeogeography, Palaeoclimatology, Palaeoecology* 203 (3-4): 313-335. [https://doi.org/10.1016/S0031-0182\(03\)00689-8](https://doi.org/10.1016/S0031-0182(03)00689-8)
- MARSICANO C. A., IRMIS R. B., MANCUSO A. C., MUNDIL R. & CHEMALLE F. 2016. — The precise temporal calibration of dinosaur origins. *Proceedings of the National Academy of Sciences* 113 (3): 509-513. <https://doi.org/10.1073/pnas.1512541112>
- MARTINELLI G., DA ROSA Á. A. S. & REGINATO P. A. R. 2005. — Estudo quantitativo e qualitativo da assembléia fossilífera do sítio Linha Várzea, Paraíso do Sul, RS. *Boletim da Sociedade Brasileira de Paleontologia* 49: 51.
- MARTINELLI A. G., KAMMERER C. F., MELO T. P., PAES NETO V. D., RIBEIRO A. M., DA ROSA Á. A. S., SCHULTZ C. L. & SOARES M. B. 2017. — The African cynodont *Aleodon* (Cynodontia, Probainognathia) in the Triassic of southern Brazil and its biostratigraphic significance. *PLoS ONE* 12: e0177948. <https://doi.org/10.1371/journal.pone.0177948>
- MARTINELLI A. G., SOARES M. B. & SCHWANKE C. 2016. — Two new cynodonts (Therapsida) from the middle-early Late Triassic of Brazil and comments on South American probainognathians. *PLoS ONE* 11: e0162945. <https://doi.org/10.1371/journal.pone.0162945>
- MARTINELLI A. G., ESCOBAR J. A., FRANCISCHINI H., KERBER L., MÜLLER R. T., RUPERT R., SCHULTZ C. L. & DA ROSA Á. A. S. 2020. — New record of a stableckeriid dicynodont (Therapsida, Dicynodontia) from the Late Triassic of southern Brazil and biostratigraphic remarks on the *Riograndia* Assemblage Zone. *Historical Biology* 33 (11): 1-10. <https://doi.org/10.1080/08912963.2020.1850715>
- MARTINEZ R. N., SERENO P. C., ALCOBER O. A., COLOMBI C. E., RENNE P. R., MONTAÑEZ I. P. & CURRIE B. S. 2011. — A basal dinosaur from the dawn of the dinosaur era in southwestern Pangaea. *Science* 331 (6014): 206-210. <https://doi.org/10.1126/science.1198467>
- MARTÍNEZ R. N., APALDETTI C., ALCOBER O. A., COLOMBI C. E., SERENO P. C., FERNANDEZ E., MALNIS P. S., CORREA G. A. & ABELIN D. 2012. — Vertebrate succession in the Ischigualasto Formation. *Journal of Vertebrate Paleontology* 32 (Supplement 1): 10-30. <https://doi.org/10.1080/02724634.2013.818546>
- MARTZ J. W. 2008. — *Lithostratigraphy, Chemostratigraphy, and Vertebrate Biostratigraphy of the Dockum Group (Upper Triassic), of Southern Garza County, West Texas*. PhD thesis, Texas Tech University, Lubbock, Texas, 504 p.
- MARTZ J. W., MUELLER B., NESBITT S. J., STOCKER M. R., PARKER W. G., ATANASSOV M., FRASER N. C., WEINBAUM J. C. & LEHANE J. R. 2013. — A taxonomic and biostratigraphic re-evaluation of the Post Quarry vertebrate assemblage from the Cooper Canyon Formation (Dockum Group, Upper Triassic) of southern Garza County, western Texas. *Earth and Environmental Science Transactions of the Royal Society of Edinburgh* 103 (3-4): 339-364. <https://doi.org/10.1017/S1755691013000376>
- MARZOLA M., MATEUS O., MILAN J. & CLEMENSEN L. B. 2018. — A review of palaeozoic and mesozoic tetrapods from Greenland. *Bulletin of the Geological Society of Denmark* 66: 21-46. <https://doi.org/10.37570/bgsd-2018-66-02>
- MATZKE N. J. 2013. — Probabilistic historical biogeography: new models for founder-event speciation, imperfect detection, and fossils allow improved accuracy and model-testing. *Frontiers of Biogeography* 5: 242-248. <https://doi.org/10.21425/F55419694>
- MATZKE N. J. 2014. — Model selection in historical biogeography reveals that founder-event speciation is a crucial process in island clades. *Systematic Biology* 63 (6): 951-970. <https://doi.org/10.1093/sysbio/syu056>
- MCKIE T. & WILLIAMS B. 2009. — Triassic palaeogeography and fluvial dispersal across the northwest European basins. *Geological Journal* 44 (6): 711-741. <https://doi.org/10.1002/gj.1201>
- MEDICI G., WEST L. J., MOUNTNEY N. P. & WELCH M. 2019. — Permeability of rock discontinuities and faults in the Triassic Sherwood Sandstone Group (UK): insights for management of fluvio-aeolian aquifers worldwide. *Hydrogeology Journal* 27: 2835-2855. <https://doi.org/10.1007/s10040-019-02035-7>
- MELCHOR R. N. & DE VALAIS S. 2006. — A review of Triassic tetrapod track assemblages from Argentina. *Palaeontology* 49 (2): 355-379. <https://doi.org/10.1111/j.1475-4983.2006.00538.x>
- MELCHOR R. N., BEDATOU E., DE VALAIS S. & GENISE J. F. 2006. — Lithofacies distribution of invertebrate and vertebrate trace-fossil assemblages in an Early Mesozoic ephemeral fluvio-lacustrine system from Argentina: Implications for the Scyenia ichnofacies. *Palaeogeography, Palaeoclimatology, Palaeoecology* 239 (3-4): 253-285. <https://doi.org/10.1016/j.palaeo.2006.01.011>
- MELCHOR R. N., BUCHWALDT R. & BOWRING S. 2013. — A Late Eocene date for Late Triassic bird tracks. *Nature* 495: E1-E2. <https://doi.org/10.1038/nature11931>
- MELO T. P., MARTINELLI A. G. & SOARES M. B. 2017. — A new gomphodont cynodont (Traversodontidae) from the Middle-Late Triassic *Dinodontosaurus* Assemblage Zone of the Santa Maria Supersequence, Brazil. *Palaeontology* 60 (4): 571-582. <https://doi.org/10.1111/pala.12302>

- MODESTO S. P. 2020. — The disaster taxon *Lystrosaurus*: a paleontological myth. *Frontiers in Earth Science* 8: 610463. <https://doi.org/10.3389/feart.2020.610463>
- MODESTO S. P. & BOTHA-BRINK J. 2010. — A burrow cast with *Lystrosaurus* skeletal remains from the Lower Triassic of South Africa. *Palaios* 25 (4): 274–281. <https://doi.org/10.2110/palo.2009.p09-077r>
- MODESTO S. P., SCOTT D. M., BOTHA-BRINK J. & REISZ R. R. 2010. — A new and unusual procolophonid parareptile from the Lower Triassic Katberg Formation of South Africa. *Journal of Vertebrate Paleontology* 30 (3): 715–723. <https://doi.org/10.1080/02724631003758003>
- MORATO L. 2006. — *Dinodontosaurus (Synapsida, Dicynodontia): reconstituições morfológicas e aspectos biomecânicos*. MSc thesis, Universidade Federal do Rio Grande do Sul, Porto Alegre, 158 p.
- MORATO L., SCHULTZ C. L. & VEGA-DIAS C. S. 2005a. — Ornamentações faciais em dicinodontes de grande porte do Triássico do Rio Grande do Sul. *Boletim da Sociedade Brasileira de Paleontologia* 49: 51–52.
- MORATO L., SCHULTZ C. L. & VEGA-DIAS C. S. 2005b. — Retrodeformação do crânio de *Jachaleria candelariensis* (Synapsida: Dicynodontia) do Neotriássico do sul do Brasil: uso de metodologias e considerações preliminares. *Boletim da Sociedade Brasileira de Paleontologia* 49: 52.
- MORATO L., SCHULTZ C. L., VEGA-DIAS C. S., DA SILVA F. P. & KINDLEIN W. 2008. — Discussing a myth: biomechanical comparisons between *Dinodontosaurus* (Synapsida, Dicynodontia) and extinct ground sloths. *Arquivos do Museu Nacional, Rio de Janeiro* 66: 145–154.
- MORATO L., VEGA-DIAS C. S. & SCHULTZ C. L. 2006. — Taxonomic revision of *Dinodontosaurus* Romer, 1943 (Therapsida, Dicynodontia). *Ameghiniana* 43: 46R.
- MUELLER B. & CHATTERJEE S. 2007. — Dicynodonts (Synapsida: Therapsida) from the Late Triassic Dockum Group of Texas. *Journal of Vertebrate Paleontology* 27 (1): 121A. <https://doi.org/bg89h9>
- MÜLLER R. D., CANNON J., QIN X., WATSON R. J., GURNIS M., WILLIAMS S., PFAFFELMOSER T., SETON M., RUSSELL S. H. J. & ZAHIROVIC S. 2018. — GPlates: Building a virtual Earth through deep time. *Geochemistry, Geophysics, Geosystems* 19 (7): 2243–2261. <https://doi.org/10.1029/2018GC007584>
- MUKHERJEE R. N. & SENGUPTA D. P. 1998. — New capitosaurid amphibians from the Triassic Denwa Formation of the Satpura Gondwana Basin, central India. *Alcheringa* 22 (4): 317–327. <https://doi.org/10.1080/03115519808619330>
- MURRY P. A. & LONG R. A. 1989. — Geology and paleontology of the Chinle Formation, Petrified Forest National Park and vicinity, Arizona and a discussion of vertebrate fossils of the southwestern Upper Triassic, in LUCAS S. G. & HUNT A. P. (eds), *Dawn of the Age of Dinosaurs in the American Southwest*. New Mexico Museum of Natural History, Albuquerque: 29–64.
- NESBITT S. J. & ANGIELCZYK K. D. 2002. — New evidence of large dicynodonts in the upper Moenkopi Formation (Middle Triassic) of northern Arizona. *PaleoBios* 22: 10–17.
- NESBITT S. J. & BUTLER R. J. 2013. — Redescription of the archosaur *Parringtonia gracilis* from the Middle Triassic Manda beds of Tanzania, and the antiquity of Erpetosuchidae. *Geological Magazine* 150 (2): 225–238. <https://doi.org/10.1017/S0016756812000362>
- NESBITT S. J., LUCAS S. G. & SCHOCH R. R. 2006. — A new, large archosauriform from the Anton Chico Member of the upper Moenkopi Formation (Middle Triassic), east-central New Mexico, USA. *Neues Jahrbuch für Geologie und Paläontologie - Abhandlungen* 239 (2): 289–311. <https://doi.org/10.1127/njpa/239/2006/289>
- NESBITT S. J., BUTLER R. J. & GOWER D. J. 2013. — A new archosauriform (Reptilia: Diapsida) from the Manda Beds (Middle Triassic) of Southwestern Tanzania. *PLoS ONE* 8: e72753. <https://doi.org/10.1371/journal.pone.0072753>
- NEVELING J. 2004. — Stratigraphic and sedimentological investigation of the contact between the *Lystrosaurus* and the *Cynognathus* Assemblage Zones (Beaufort Group; Karoo Supergroup). *Council for Geoscience Bulletin* 137: 1–165.
- NEVELING J., HANCOX P. J. & RUBIDGE B. S. 2005. — Biostratigraphy of the lower Burgersdorp Formation (Beaufort Group; Karoo Supergroup) of South Africa – implications for the stratigraphic ranges of early Triassic tetrapods. *Palaeontologia Africana* 41: 81–87.
- NEVELING J., RUBIDGE B. S. & HANCOX P. J. 1999. — A lower *Cynognathus* Assemblage Zone fossil from the Katberg Formation (Beaufort group, South Africa). *South African Journal of Science* 95: 555–556.
- NEWTON E. T. 1893. — VII. On some new reptiles from the Elgin Sandstones. *Philosophical Transactions of the Royal Society of London B* 184: 431–503. <https://doi.org/10.1098/rstb.1893.0007>
- NICOLAS M. V. M. 2007. — *Tetrapod Biodiversity through the Permo-Triassic Beaufort Group (Karoo Supergroup) of South Africa*. PhD thesis, University of the Witwatersrand, Johannesburg, 312 p.
- NICOLAS M. & RUBIDGE B. S. 2010. — Changes in Permo-Triassic terrestrial tetrapod ecological representation in the Beaufort Group (Karoo Supergroup) of South Africa. *Lethaia* 43 (1): 45–59. <https://doi.org/10.1111/j.1502-3931.2009.00171.x>
- NIEDZWIEDZKI G. 2011. — A Late Triassic dinosaur-dominated ichnofauna from the Tomanová Formation of the Tatra Mountains, Central Europe. *Acta Palaeontologica Polonica* 56 (2): 291–300. <https://doi.org/10.4202/app.2010.0027>
- NIEDZWIEDZKI G., GORZELAK P. & SULEJ T. 2011. — Bite traces on dicynodont bones and the early evolution of large terrestrial predators. *Lethaia* 44 (1): 87–92. <https://doi.org/10.1111/j.1502-3931.2010.00227.x>
- NORTHWOOD C. 1997. — *Palaeontological interpretations of the Early Triassic Arcadia Formation, Queensland*. PhD thesis, La Trobe University, Melbourne, 479 p.
- NOVAS F. E., EZCURRA M. D., CHATTERJEE S. & KUTTY T. S. 2010. — New dinosaur species from the Upper Triassic Upper Maleri and Lower Dharmaram formations of Central India. *Earth and Environmental Science Transactions of the Royal Society of Edinburgh* 101 (3–4): 333–349. <https://doi.org/10.1017/S175569101020093>
- OCHEV V. G. 1992. — On the second unquestionable find of an anomodontian the Lower Triassic of East Europe. *Izvestiya Vysshikh Uchebnykh Zavedenii (Geologiya i Razvedka)* 1992: 132–133.
- OLEMPSKA E. 2004. — Late Triassic spinicaudatan crustaceans from southwestern Poland. *Acta Palaeontologica Polonica* 49: 429–442.
- DE OLIVEIRA BUENO A., CISNEROS J. C. & SCHULTZ C. L. 2011. — Evidence of gregarious and burrowing habits in *Dinodontosaurus turpior* (Therapsida, Dicynodontia) from the Triassic Santa Maria Formation of Rio Grande do Sul, Brazil. *Ameghiniana* 48: R39.
- OLIVIER C., HOUSSAYE A., JALIL N.-E. & CUBO J. 2017. — First palaeohistological inference of resting metabolic rate in an extinct synapsid, *Moghareira nmachouensis* (Therapsida: Anomodontia). *Biological Journal of the Linnean Society* 121 (2): 409–419. <https://doi.org/10.1093/biolinnean/blw044>
- OLIVIER C., BATTAIL B., BOURQUIN S., ROSSIGNOL C., STEYER J.-S. & JALIL N.-E. 2019. — New dicynodonts (Therapsida, Anomodontia) from near the Permo-Triassic boundary of Laos: implications for dicynodont survivorship across the Permo-Triassic mass extinction and the paleobiogeography of Southeast Asian blocks. *Journal of Vertebrate Paleontology* 39 (2): e1584745. <https://doi.org/10.1080/02724634.2019.1584745>
- OLROYD S. L. 2022. — *The function of the reflected lamina in therapsids and the origin of the mammalian middle ear*. PhD thesis, University of Washington, Seattle, 150 p.
- OLROYD S. L. & SIDOR C. A. 2022. — Nomenclature, comparative anatomy, and evolution of the reflected lamina of the angular in non-mammalian synapsids. *Journal of Vertebrate Paleontology* 42 (1): e2101923. <https://doi.org/10.1080/02724634.2022.2101923>

- OLSEN P. E. & GALTON P. M. 1984. — A review of the reptile and amphibian assemblages from the Stormberg of Southern Africa with special emphasis on the footprints and the age of the Stormberg. *Palaeontology Africana* 25: 87-110.
- OLSEN P. E. & HUBER P. 1998. — The oldest Late Triassic footprint assemblage from North America (Pekin Formation, Deep River Basin, North Carolina, USA). *Southeastern Geology* 38: 77-90.
- OLSEN P. E., SCHLISCHÉ R. W. & GORE P. J. W. (eds) 1989. — *Tectonic, Depositional, and Paleoenvironmental History of Early Mesozoic Rift Basins, Eastern North America. Gulf, North Carolina, USA to Parrsboro, Nova Scotia, Canada. July 20-30, 1989. Field Trip Guidebook T351*. American Geophysical Union, Washington D.C.
- OLSEN P. E., KENT D. V. & WHITESIDE J. H. 2010. — Implications of the Newark Supergroup-based astrochronology and geomagnetic polarity time scale (Newark-APTS) for the tempo and mode of the early diversification of the Dinosauria. *Earth and Environmental Science Transactions of the Royal Society of Edinburgh* 101 (3-4): 201-229. <https://doi.org/10.1017/S1755691011020032>
- ORDÓÑEZ M. DE LOS A., CASSINI G. H., VIZCAÍNO S. F. & MARCICANO C. A. 2019. — A geometric morphometric approach to the analysis of skull shape in Triassic dicynodonts (Therapsida, Anomodontia) from South America. *Journal of Morphology* 280 (12): 1808-1820. <https://doi.org/10.1002/jmor.21066>
- ORDÓÑEZ M. DE LOS A., MARCICANO C. A. & MANCUSO A. C. 2020. — New specimen of *Dinodontosaurus* (Therapsida, Anomodontia) from west-central Argentina (Chañares Formation) and a reassessment of the Triassic *Dinodontosaurus* Assemblage Zone of southern South America. *Journal of South American Earth Sciences* 100: 102597. <https://doi.org/10.1016/j.jsames.2020.102597>
- OSBORN H. F. 1903. On the primary division of the Reptilia into two sub-classes, Synapsida and Diapsida. *Science* 17 (424): 275-276. <https://doi.org/10.1126/science.17.424.275.c>
- OTTONE E. G., MONTI M., MARCICANO C. A., DE LA FUENTE M. S., NAIPAUER M., ARMSTRONG R. & MANCUSO A. C. 2014. — Age constraints for the Triassic Puesto Viejo Group (San Rafael depocenter, Argentina): SHRIMP U-Pb zircon dating and correlations across southern Gondwana. *Journal of American Earth Sciences* 56: 186-199.
- OWEN R. 1859. — On some reptilian remains from South Africa. *The Edinburgh New Philosophical Journal* 10: 289-291.
- OWEN R. 1860a. — On the orders of fossil and recent Reptilia, and their distribution in time. *Report of the Twenty-Ninth Meeting of the British Association for the Advancement of Science* 1859: 153-166.
- OWEN R. 1860b. — On some reptilian fossils from South Africa. *Quarterly Journal of the Geological Society of London* 16: 49-63. <https://doi.org/10.1144/GSL.JGS.1860.016.01-02.07>
- OWEN R. 1862. — (I.) On the dicynodont reptilia, with a description of some fossil remains brought by H. R. H. Prince Alfred from South Africa, November 1860. *Philosophical Transactions of the Royal Society* 152: 455-467. <https://doi.org/10.1098/rstl.1862.0024>
- OWEN R. 1876. — *Descriptive and Illustrated Catalogue of the Fossil Reptilia of South Africa in the Collection of the British Museum*. Taylor & Francis, London, 88 p.
- PARKER W. G. & MARTZ J. W. 2011. — The Late Triassic (Norian) Adamanian-Revueltian tetrapod faunal transition in the Chinle Formation of Petrified Forest National Park, Arizona. *Earth and Environmental Science Transactions of the Royal Society of Edinburgh* 101 (3-4): 231-260. <https://doi.org/10.1017/S1755691011020020>
- PAULA-COUTO C. 1960. — Uma preguiça terrestre da região do Alto Amazonas, Colômbia. *Boletim do Museu Nacional (Nova Série, Geologia)* 31: 1-9.
- PAVANTINO A. E. B., DA ROSA Á. A. S., MÜLLER R. T., ROBERTO-DA-SILVA L., RIBEIRO A. M., MARTINELLI A. G. & DIAS-DA-SILVA S. 2020. — Bortolin site, a new fossiliferous locality in the Triassic (Ladinian/Carnian) of Southern Brazil. *Revista Brasileira de Paleontologia* 23: 123-137. <https://doi.org/10.4072/rbp.2020.2.04>
- PEARSON H. S. 1924a. — The skull of the dicynodont reptile *Kannemeyeria*. *Proceedings of the Zoological Society of London* 94 (3): 793-826. <https://doi.org/10.1111/j.1096-3642.1924.tb03316.x>
- PEARSON H. S. 1924b. — A dicynodont reptile reconstructed. *Proceedings of the Zoological Society of London* 94 (3): 827-855. <https://doi.org/10.1111/j.1096-3642.1924.tb03317.x>
- PEECOOK B. R., STEYER J.-S., TABOR N. J. & SMITH R. M. H. 2018. — Updated geology and vertebrate paleontology of the Triassic Ntawere Formation of northeastern Zambia, with special emphasis on the archosauromorphs. *Journal of Vertebrate Paleontology* 37 (Supplement 1): 8-38. <https://doi.org/10.1080/02724634.2017.1410484>
- PHILIPP R. P., SHULTZ C. L., KLOSS H. P., HORN B. L. D., SOARES M. B. & BASEI M. A. S. 2018. — Middle Triassic SW Gondwana paleogeography and sedimentary dispersal revealed by integration of stratigraphy and U-Pb zircon analysis: The Santa Cruz Sequence, Paraná Basin, Brazil. *Journal of South American Earth Sciences* 88: 216-237. <https://doi.org/10.1016/j.jsames.2018.08.018>
- PICKFORD M. 1995. — Karoo Supergroup palaeontology of Namibia and brief description of a thecodont from Omingonde. *Palaeontology Africana* 32: 51-66.
- PIVETEAU J. 1938. — Un théraspidé d'Indochine. Remarques sur la notion de continent de Gondwana. *Annales de Paléontologie (Vertébrés)* 27: 139-152.
- POLLARD J. E. 1981. — A comparison between the Triassic tracefossils of Cheshire and South Germany. *Palaeontology* 24: 555-588.
- PORCHETTI S. D. O. & NICOSIA U. 2007. — Re-examination of some large early mesozoic tetrapod footprints from the African collection of Paul Ellenberger. *Ichnos* 14 (3-4): 219-245. <https://doi.org/10.1080/10420940601049990>
- POROPAT S. F., MANNION P. D., UPCHURCH P., HOCKNULL S. A., KEAR B. P., KUNDRÁT M., TISCHLER T. R., SLOAN T., SINAPIUS G. H. K., ELLIOTT J. A. & ELLIOTT D. A. 2016. — New Australian sauropods shed light on Cretaceous dinosaur palaeobiogeography. *Scientific Reports* 6: 34467. <https://doi.org/10.1038/srep34467>
- PRASAD B. & PUNDIR B. S. 2020. — Gondwana biostratigraphy and geology of West Bengal Basin, and its correlation with adjoining Gondwana basins of India and western Bangladesh. *Journal of Earth System Science* 129: 22. <https://doi.org/10.1007/s12040-019-1287-2>
- PREUSCHOFT H., KRAHL A. & WERNEBURG I. 2022. — From sprawling to parasagittal locomotion in Therapsida: a preliminary study of historically collected museum specimens. *Vertebrate Zoology* 72: 907-936. <https://doi.org/10.3897/vz.72.e85989>
- PRICE I. L. 1956. — Sobre a suposta presença de um anomodontídeo triássico no alto rio Amazonas. *Notas Preliminares e Estudos* 93: 1-10.
- R CORE TEAM 2020. — *R: A language and environment for statistical computing*. R Foundation for Statistical Computing, Vienna.
- RACKI G. & LUCAS S. G. 2020. — Timing of dicynodont extinction in light of an unusual Late Triassic Polish fauna and Cuvier's approach to extinction. *Historical Biology* 32 (4): 451-461. <https://doi.org/10.1080/08912963.2018.1499734>
- RAMEZANI J., HOKE G. D., FASTOVSKY D. E., BOWRING S. A., THERRIEN F., DWORKIN S. I., ATCHLEY S. C. & NORDT L. C. 2011. — High-precision U-Pb zircon geochronology of the Late Triassic Chinle Formation, Petrified Forest National Park (Arizona, USA): temporal constraints on the early evolution of dinosaurs. *Geological Society of America Bulletin* 123 (11-12): 2142-2159. <https://doi.org/10.1130/B30433.1>
- RAMEZANI J., FASTOVSKY D. E. & BOWRING S. A. 2014. — Revised chronostratigraphy of the Lower Chinle Formation strata in Arizona and New Mexico (USA): high-precision U-Pb geochronological constraints on the Late Triassic evolution of dinosaurs. *American Journal of Science* 314 (6): 981-1008. <https://doi.org/10.2475/06.2014.01>

- RAUGUST T., LACERDA M. & SCHULTZ C. L. 2013. — The first occurrence of *Chanaresuchus bonapartei* (Archosauriformes, Proterochampsia) of the Middle Triassic of Brazil from the *Santacruzodon* Assemblage Zone, Santa Maria Formation (Paraná Basin). *Geological Society, London, Special Publications* 379 (1): 303-318. <https://doi.org/10.1144/SP379.22>
- RAY S. 2005. — *Lystrosaurus* (Therapsida, Dicynodontia) from India: taxonomy, relative growth and cranial dimorphism. *Journal of Systematic Palaeontology* 3 (2): 203-221. <https://doi.org/10.1017/S1477201905001574>
- RAY S. 2006. — Functional and evolutionary aspects of the postcranial anatomy of dicynodonts. *Palaeontology* 49 (6): 1263-1286. <https://doi.org/10.1111/j.1475-4983.2006.00597.x>
- RAY S. & CHINSAMY A. 2003. — Functional aspects of the postcranial anatomy of the Permian dicynodont *Diictodon* and their ecological implications. *Palaeontology* 46 (1): 151-183. <https://doi.org/10.1111/1475-4983.00292>
- RAY S., CHINSAMY A. & BANDYOPADHYAY S. 2005. — *Lystrosaurus murrayi* (Therapsida, Dicynodontia): Bone histology, growth and lifestyle adaptations. *Palaeontology* 48 (6): 1169-1185. <https://doi.org/10.1111/j.1475-4983.2005.00513.x>
- RAY S., BANDYOPADHYAY S. & BHAWAL D. 2009a. — Growth patterns as deduced from bone microstructure of some selected neotherapsids with special emphasis on dicynodonts: phylogenetic implications. *Palaeoworld* 18 (1): 53-66. <https://doi.org/10.1016/j.palwor.2008.09.001>
- RAY S., MUKHERJEE D. & BANDYOPADHYAY S. 2009b. — Growth patterns of fossil vertebrates as deduced from bone microstructure: case studies from India. *Journal of Biosciences* 34: 661-672. <https://doi.org/10.1007/s12038-009-0055-x>
- RAY S., BANDYOPADHYAY S. & APPANA R. 2010. — Bone histology of a kannemeyeriid dicynodont *Wadiasaurus*: palaeobiological implications, in BANDYOPADHYAY S. (ed.), *New Aspects of Mesozoic Biodiversity*. Springer, Berlin, Heidelberg, Dordrecht, London, New York: 73-89.
- REICHEL M., SCHULTZ C. L. & SOARES M. B. 2009. — A new traversodontid cynodont (Therapsida, Rucynodontia) from the Middle Triassic Santa Maria formation of Rio Grande Do Sul, Brazil. *Palaeontology* 52 (1): 229-250. <https://doi.org/10.1111/j.1475-4983.2008.00824.x>
- RENAUT A. J. 2000. — *A re-evaluation of the cranial morphology and taxonomy of the Triassic dicynodont genus Kannemeyeria*. PhD thesis, University of the Witwatersrand, Johannesburg, 197 p.
- RENAUT A. J. & HANCOX P. J. 2001. — Cranial description and taxonomic re-evaluation of *Kannemeyeria argentinensis* (Therapsida: Dicynodontia). *Palaeontologia Africana* 37: 81-91.
- RENAUT A. J., DAMIANI R. J., YATES A. M. & HANCOX P. J. 2003. — A taxonomic note concerning a dicynodont (Synapsida: Anomodontia) from the Middle Triassic of East Africa. *Palaeontologia Africana* 39: 93-94.
- REPELIN J. 1923. — Sur un fragment de crâne de *Dicynodon* recueilli par H. Counillon dans les environs de Luang-Prabang (Haut-Laos). *Bulletin du Service géologique de l'Indochine* 12: 1-8.
- RETALLACK G. J. 1996. — Early Triassic therapsid footprints from the Sydney Basin, Australia. *Alcheringa* 20 (4): 301-314. <https://doi.org/10.1080/03115519608619473>
- RETALLACK G. J. & HAMMER W. R. 1998. — Palaeoenvironment of the Triassic therapsid *Lystrosaurus* in the central Transantarctic Mountains, Antarctica. *Antarctic Journal of the United States* 31: 33-35.
- RETALLACK G. J., SMITH R. M. H. & WARD P. D. 2003. — Vertebrate extinction across Permian-Triassic boundary in Karoo Basin, South Africa. *Geological Society of America Bulletin* 115 (9): 1133-1152. <https://doi.org/10.1130/B25215.1>
- ROBINSON P. L. 1958. — Some new vertebrate fossils from the Panchet Series of west Bengal. *Nature* 182: 1722-1723. <https://doi.org/10.1038/1821722a0>
- RODRIGUES J. B. 1892. — Les reptiles fossiles de la vallée de l'Amazone. *Velliosia* 2: 41-56.
- ROGERS R. R., SWISHER C. C., SERENO P. C., MONETTA A. M., FORSTER C. A. & MARTÍNEZ R. N. 1993. — The Ischigualasto tetrapod assemblage (Late Triassic, Argentina) and 40Ar/39Ar dating of dinosaur origins. *Science* 260 (5109): 794-797. <https://doi.org/10.1126/science.260.5109.794>
- ROMANO M. & MANUCCI F. 2021. — Resizing *Lisowicia bojani*: volumetric body mass estimate and 3D reconstruction of the giant Late Triassic dicynodont. *Historical Biology* 33 (4): 474-479. <https://doi.org/10.1080/08912963.2019.1631819>
- ROGERS R. R., ARCUCCI A. B., ABDALA F., SERENO P. C., FORSTER C. A. & MAY C. L. 2001. — Paleoenvironment and taphonomy of the Chañares Formation tetrapod assemblage (Middle Triassic), Northwestern Argentina: spectacular preservation in volcanogenic concretions. *Palaios* 16 (5): 461-481. <https://doi.org/fqms4d>
- ROMERA S. 1943. — Recent mounts of fossil reptiles and amphibians in the Museum of Comparative Zoölogy. *Bulletin of the Museum of Comparative Zoölogy* 92: 331-336.
- ROMER A. S. 1966. — The Chañares (Argentina) Triassic reptile fauna. I. Introduction. *Breviora* 247: 1-14.
- ROMER A. S. & PRICE L. I. 1944. — *Stableckeria lenzii*, a giant Triassic Brazilian dicynodont. *Bulletin of the Museum of Comparative Zoölogy* 93: 463-491.
- RUBIDGE B. S., DAY M. O., BARBOLINI N., HANCOX P. J., CHOINIERE J. N., BAMFORD M. K., VIGLIETTI P. A., MCPHEE B. W. & JIRAH S. 2016. — Advances in nonmarine Karoo biostratigraphy: significance for understanding basin development, in Linol B. & de Wit M. J. (eds), *Origin and Evolution of the Cape Mountains and Karoo Basin*. Springer International Publishing: 141-149. https://doi.org/10.1007/978-3-319-40859-0_14
- RÜHLE VON LILIENSTERN H. 1944. — Eine Dicynodontierfährte aus dem Chirotheriumsandstein von Hessberg bei Hildburghausen. *Paläontologische Zeitschrift* 23: 368-387. <https://doi.org/10.1007/BF03160445>
- RUTA M., ANGIELCZYK K. D., FRÖBISCH J. & BENTON M. J. 2013. — Decoupling of morphological disparity and taxic diversity during the adaptive radiation of anomodont therapsids. *Proceedings of the Royal Society B* 280 (1768): 20131071. <https://doi.org/10.1098/rspb.2013.1071>
- DA ROSA Á. A. S., SCHWANKE C., CISNEROS J. C., WITECK NETO L., AURÉLIO P. L. P. & POITEVIN M. 2004. — Sítio Cortado - uma nova assembleia fossilífera do Triássico médio do sul do Brasil. *Revista Brasileira de Paleontologia* 7 (2): 289-300. <https://doi.org/10.4072/rbp.2004.2.24>
- DA ROSA Á. A. S., SCHWANKE C., AURÉLIO P. L. P., POITEVIN M. & WITECK NETO L. 2005. — Sítio Linha Várzea – uma nova assembleia fossilífera do Triássico Médio do Sul do Brasil. *Geociências* 24: 115-129.
- ROTHSCHILD B. M. & WITZMANN F. 2021. — Identification of growth cessation in dinosaurs based on microscopy of long bone articular surfaces: preliminary results. *Alcheringa: An Australasian Journal of Palaeontology* 45 (2): 260-273. <https://doi.org/10.1080/03115518.2021.1921273>
- ROWE T. 1980. — The morphology, affinities, and age of the dicynodont reptile *Geikia elginensis*, in JACOBS L. L. (ed.), *Aspects of vertebrate history. Essays in honor of Edwin Harris Colbert*. Museum of Mpryjern Arizona Press, Flagstaff: 269-294. <https://doi.org/10.1111/j.1096-3642.1924.tb03317.x>
- ROWE T. B. 1979. — *Placerias*: an unusual reptile from the Chinle Formation. *Plateau* 51: 30-32.
- ROZEFELDS A. C., WARREN A., WHITFIELD A. & BULL S. 2011. — New evidence of large Permo-Triassic dicynodonts (Synapsida) from Australia. *Journal of Vertebrate Paleontology* 31 (5): 1158-1162. <https://doi.org/10.1080/02724634.2011.595858>
- RUBIN H. & RUBIN K. 2009. — Hydrogeochemistry of the Upper Triassic formations in the Woźniki area (borehole K-1). *Buletyn Państwowego Instytutu Geologicznego* 436 (2): 429-436.

- SADŁOK G. & WAWRZYNIAK Z. 2013. — Upper Triassic vertebrate tracks from Kraków-Częstochowa Upland, Southern Poland. *Annales Societatis Geologorum Poloniae* 83 (2): 105-111.
- SAHANI M. R. & TRIPATHI C. 1962. — Vertebrate laboratory. *Records of the Geological Survey of India* 90: 170-171.
- SCHMIDT M. 1928. — *Die Lebenwelt unserer Trias*. Hohenlohesche Buchhandlung Ferdinand Rau, Ohringen: 461 p.
- SCHOCH R. R. 2012. — A dicynodont mandible from the Triassic of Germany forms the first evidence of large herbivores in the Central European Carnian. *Neues Jahrbuch für Geologie und Paläontologie - Abhandlungen* 263 (2): 119-123. <https://doi.org/10.1127/0077-7749/2012/0216>
- SCHULTZ C. L. & VEGA-DIAS C. S. 2003. — Evidences of predation or scavenging in a dicynodont scapula from the Upper Triassic of South Brazil. *Ameghiniana* 40: 71R.
- SCHULTZ C. L., LANGER M. C. & MONTEFELTRO F. C. 2016. — A new rhynchosaur from south Brazil (Santa Maria Formation) and rhynchosaur diversity patterns across the Middle-Late Triassic boundary. *Palaontologische Zeitschrift* 90: 593-609. <https://doi.org/10.1007/s12542-016-0307-7>
- SCHULTZ C. L., MARTINELLI A. G., SOARES M. B., PINHEIRO F. L., KERBER L., HORN B. L. D., PRETTO F. A., MÜLLER R. T. & MELO T. P. 2020. — Triassic faunal successions of the Paraná Basin, southern Brazil. *Journal of South American Earth Sciences* 104: 102846. <https://doi.org/10.1016/j.jsames.2020.102846>
- SCHWANKE-PERUZZO C. 1990. — *A presença do gênero Ischigualastia Cox, 1962 (Reptilia, Synapsida, Therapsida, Anomodontia, Dicynodontia) na Formação Santa Maria, Rio Grande Do Sul, Brasil*. MSc thesis, Universidade Federal do Rio Grande do Sul, Porto Alegre, 186 p.
- SCHWANKE-PERUZZO C. & ARAÚJO-BARBARENA D. C. 1995. — Sobre a ocorrência do gênero *Ischigualastia* Cox, 1962 na Formação Santa Maria, Triássico do Rio Grande do Sul. *Anais da Academia Brasileira de Ciências* 67: 175-181.
- SCHWANKE C. & KELLNER A. W. A. 1999. — Sobre o primeiro registro de Synapsida no Triássico basal do Brasil. *XVI Congresso Brasileiro de Paleontologia, boletim de resumos*: 101.
- SCHWANKE C. & MELO D. J. DE 2002. — Descrição craniana preliminar de um espécime juvenil de dicinodonte (Therapsida, Anomodontia, Dicynodontia) do Triássico do Rio Grande do Sul, Brasil – Uma discussão acerca da validade do gênero *Chanaria* Cox, 1968. *Arquivos do Museu Nacional, Rio de Janeiro* 60: 177-182.
- SCOTese C. R. 2001. — *Atlas of Earth history*. PALEOMAP Project, Arlington.
- SCOTese C. R. 2014. — *Atlas of Triassic paleogeographic maps, maps 43-48 from Volume 3 of the PALEOMAP Atlas for ArcGIS (Jurassic and Triassic), Mollweide projection*. PALEOMAP Project, Evanston, IL.
- SCOTese C. R. 2016. — *PALEOMAP PaleoAtlas for GPlates and the PaleoData Plotter Program*. PALEOMAP Project. Available at the following address: <http://www.scotese.com>
- SEELEY H. G. 1889. — VI. Researches on the structure, organization, and classification of the fossil Reptilia. VI. On the anomodont Reptilia and their allies. *Philosophical Transactions of the Royal Society of London B* 180: 215-296. <https://doi.org/10.1098/rstb.1889.0006>
- SEELEY H. G. 1895. — III. Researches on the structure, organization, and classification of the fossil Reptilia.-Part IX., Section 6. Associated remains of two small skeletons from Klipfontein, Fraserburg. *Philosophical Transactions of the Royal Society B* 186: 149-162. <https://www.biodiversitylibrary.org/bibliography/132212>
- SEELEY H. G. 1898. — XXVII.-On the skull of *Mochlorhinus platyceps*, from Bethulie, Orange Free State, preserved in the Albany Museum, Grahamstown. *Annals and Magazine of Natural History; Zoology, Botany, and Geology* 1: 164-176.
- SEELEY H. G. 1904. — XLIII.-On a new type of reptilian tooth (*Ptychocynodon*) from the upper Karoo Beds near Burghersdorp, Cape Colony. *Annals and Magazine of Natural History* 14 (82): 290-293. <https://doi.org/10.1080/03745480409443010>
- SEELEY H. G. 1908. — 7. On a fossil reptile with a trunk from the upper Karroo Rocks of Cape Colony. *Report of the British Association for the Advancement of Science* 1908: 713. <https://www.biodiversitylibrary.org/bibliography/136426>
- SHISHKIN M. A., OCHEV V. G., TVERDOKHLEBOV V. P., VERGAY I. F., GOMAN'KOV A. V., KALANDADZE N. N., LEONOVA E. M., LOPATO A. Y., MAKAROVA I. S., MINIKH M. G., MOLOSTOVSKII E. M., NOVIKOV I. V. & SENNIKOV A. G. 1995. — *Biostratigraphy of the Triassic of Southern Cis-Urals*. Nauka, Moscow, 205 p.
- SHISHKIN M. A., OCHEV V. G., LOZOVSKII V. R. & NOVIKOV I. V. 2000. — Tetrapod biostratigraphy of the Triassic of Eastern Europe, in BENTON M. J., SHISHKIN M. A., UNWIN D. M. & KUROCHKIN E. N. (eds), *The age of dinosaurs in Russia and Mongolia*. Cambridge University Press, Cambridge: 120-139.
- SIDOR C. A., SMITH R. M. H., HUTTENLOCKER A. K. & PEACOCK B. R. 2014. — New Middle Triassic tetrapods from the upper Fremou Formation of Antarctica and their depositional setting. *Journal of Vertebrate Paleontology* 34 (4): 793-801. <https://doi.org/10.1080/02724634.2014.837472>
- SILVA R. C. DA, CARVALHO I. DE S., FERNANDES A. C. S. & FERIGOLO J. 2008. — Pegadas teromorfóides do Triássico Superior (Formação Santa Maria) do Sul do Brasil. *Revista Brasileira de Geociências* 38: 98-113. <https://doi.org/10.25249/0375-7536.200838198113>
- DA SILVEIRA L. 2017. — *Alometria ontogenética no gênero Dindontosaurus Romer, 1943 (Therapsida, Anomodontia) do Triássico Sul-Brasileiro*. B.Sc. thesis, Universidade Federal do Rio Grande do Sul, Porto Alegre, 63 p.
- SKAWIŃSKI T., ZIEGLER M., CZEPIŃSKI Ł., SZERMAŃSKI M., TAŁANDA M., SURMIK D. & NIEDZWIEDZKI G. 2016. — A re-evaluation of the historical ‘dinosaur’ remains from the Middle-Upper Triassic of Poland. *Historical Biology* 2963 (4): 1-31. <https://doi.org/10.1080/08912963.2016.1188385>
- SŁOWIAK J., SZCZYGIELSKI T., ROTHSCHILD B. M. & SURMIK D. 2021. — Dinosaur senescence: a hadrosauroid with age-related diseases brings a new perspective of “old” dinosaurs. *Scientific Reports* 11: 11947. <https://doi.org/10.1038/s41598-021-91366-1>
- SMALL B. J., HUTTENLOCKER A., MUELLER B., KENDRA D., & CHATTERJEE S. 2022. A new Late Triassic (Norian) dicynodont from the Tecovas Formation (Dockum Group) of Texas, U.S.A. reveals hidden dicynodont diversity and abundance in Laurasia. *Society of Vertebrate Paleontology 82nd Annual Meeting Program Guide*: 308-309.
- SMITH R. M. H. 1995. — Changing fluvial environments across the Permian-Triassic boundary in the Karoo Basin, South Africa and possible causes of tetrapod extinctions. *Palaeogeography, Palaeoclimatology, Palaeoecology* 117 (1-2): 81-104. [https://doi.org/10.1016/0031-0182\(94\)00119-S](https://doi.org/10.1016/0031-0182(94)00119-S)
- SMITH A. B. 2001. — Large-scale heterogeneity of the fossil record: Implications for phanerozoic biodiversity studies. *Philosophical Transactions of the Royal Society of London B* 356 (1407): 351-367. <https://doi.org/10.1098/rstb.2000.0768>
- SMITH R. M. H. 2020. — Biostratigraphy of the *Cistecephalus* Assemblage Zone (Beaufort Group, Karoo Supergroup), South Africa. *South African Journal of Geology* 123 (2): 181-190. <https://doi.org/10.25131/sajg.123.0013>
- SMITH R. M. H. & BOTHA J. 2005. — The recovery of terrestrial vertebrate diversity in the South African Karoo Basin after the end-Permian extinction. *Comptes Rendus Pelevol* 4 (6-7): 623-636. <https://doi.org/10.1016/j.crpv.2005.07.005>
- SMITH R. M. H. & BOTHA-BRINK J. 2014. — Anatomy of a mass extinction: Sedimentological and taphonomic evidence for drought-induced die-offs at the Permo-Triassic boundary in the main Karoo Basin, South Africa. *Palaeogeography, Palaeoclimatology, Palaeoecology* 396: 99-118. <https://doi.org/10.1016/j.palaeo.2014.01.002>

- SMITH R. M. H. & SWART R. 2002. — Changing fluvial environments and vertebrate taphonomy in response to climatic drying in a mid-Triassic rift valley fill: The Omingonde formation (Karoo supergroup) of central Namibia. *Palaios* 17 (3): 249-267. <https://doi.org/10.1080/08831340212000001>
- SMITH R. M. H. & WARD P. D. 2001. — Pattern of vertebrate extinctions across an event bed at the Permian-Triassic boundary in the Karoo Basin of South Africa. *Geology* 29 (12): 1147-1150. [https://doi.org/10.1130/0091-7613\(2001\)029<1147:POTVEB>2.0.CO;2](https://doi.org/10.1130/0091-7613(2001)029<1147:POTVEB>2.0.CO;2)
- SMITH R. M. H., RUBIDGE B. S. & VAN DER WALT M. 2012. — Therapsid biodiversity patterns and paleoenvironments of the Karoo Basin, South Africa, in CHINSAMY-TURAN A. (ed.), *Forerunners of mammals: radiation, histology, biology*. Indiana University Press, Bloomington: 30-62.
- SMITH R. M. H., SIDOR C. A., ANGIELCZYK K. D., NESBITT S. J. & TABOR N. J. 2018. — Taphonomy and paleoenvironments of the Middle Triassic bone accumulations in the Lifua Member of the Manda Beds, Songea Group (Ruhuhu Basin), Tanzania. *Journal of Vertebrate Paleontology* 37 (Sup. 1): 65-79. <https://doi.org/10.1080/02724634.2017.1415915>
- SMITH N. D., MAKOVICKY P. J., SIDOR C. A. & HAMMER W. R. 2020a. — A kannemeyeriform (Synapsida: Dicynodontia) occipital plate from the Middle Triassic upper Fremouw Formation of Antarctica. *Journal of Vertebrate Paleontology* 40 (5): e1829634.
- SMITH R. M. H., RUBIDGE B. S., DAY M. O. & BOTHA J. 2020b. — Introduction to the tetrapod biozonation of the Karoo Supergroup. *South African Journal of Geology* 123 (2): 131-140. <https://doi.org/10.25131/sajg.123.0009>
- SMITH R. M. H., BOTHA J. & VIGLIETTI P. A. 2022. — Taphonomy of drought afflicted tetrapods in the Early Triassic Karoo Basin, South Africa. *Palaeogeography, Palaeoclimatology, Palaeoecology* 604: 111207. <https://doi.org/10.1016/j.palaeo.2022.111207>
- STOCKLEY G. M. 1932. — The geology of the Ruhuhu coalfields, Tanganyika territory. *Quarterly Journal of the Geological Society* 88: 610-622. <https://doi.org/10.1144/GSL.JGS.1932.088.01-04.20>
- SUES H.-D. & OLSEN P. E. 2015. — Stratigraphic and temporal context and faunal diversity of Permian-Jurassic continental tetrapod assemblages from the Fundy rift basin, eastern Canada. *Atlantic Geology* 51: 139-205. <https://doi.org/10.4138/atgeol.2015.006>
- SUES H.-D., OLSEN P. E., CARTER J. G. & SCOTT D. M. 2003. — A new crocodylomorph archosaur from the Upper Triassic of North Carolina. *Journal of Vertebrate Paleontology* 23 (2): 329-343. [https://doi.org/10.1671/0272-4634\(2003\)023\[0329:ANCRAFT\]2.0.CO;2](https://doi.org/10.1671/0272-4634(2003)023[0329:ANCRAFT]2.0.CO;2)
- SULEJ T. & NIEDZWIEDZKI G. 2019. — An elephant-sized Late Triassic synapsid with erect limbs. *Science* 363 (6422): 78-80. <https://doi.org/10.1126/science.aal4853>
- SULEJ T., BRONOWICZ R., TAŁANDA M. & NIEDZWIEDZKI G. 2011. — A new dicynodont-archosaur assemblage from the Late Triassic (Carnian) of Poland. *Earth and Environmental Science Transactions of the Royal Society of Edinburgh* 101 (3-4): 261-269. <https://doi.org/10.1017/S1755691011020123>
- SULEJ T., NIEDZWIEDZKI G. & BRONOWICZ R. 2012. — A new Late Triassic vertebrate fauna from Poland with turtles, aetosaurs, and coelophysoid dinosaurs. *Journal of Vertebrate Paleontology* 32 (5): 1033-1041. <https://doi.org/10.1080/02724634.2012.694384>
- SULEJ T., NIEDZWIEDZKI G. & SZCZYGIELSKI T. 2019. — Późnotriasowe dicynodonty ze Śląska, in XXIV Konferencja Naukowa Sekcji Paleontologicznej Polskiego Towarzystwa Geologicznego. Wrocław: 79.
- SULEJ T., NIEDZWIEDZKI G., TAŁANDA M., DRÓŻDŻ D. & HARA E. 2020. — A new early Late Triassic non-mammaliaform eucynodont from Poland. *Historical Biology* 32 (1): 80-92. <https://doi.org/10.1080/08912963.2018.1471477>
- SUN A. 1960. — On a new genus of kannemeyerids from Ningwu, Shansi. *Vertebrata PalAsiatica* 4: 67-81.
- SUN A. 1963. — *The Chinese kannemeyerids*. Science Press, Beijing, 109 p.
- SUN A. 1964. — Preliminary report on a new species of *Lystrosaurus* of Sinkiang. *Vertebrata PalAsiatica* 8: 216-217.
- SUN A. 1973. — Permo-Triassic dicynodonts from Turfan, Sinkiang. *Memoirs of the Institute of Vertebrate Paleontology and Paleoanthropology, Academia Sinica* 10: 53-68.
- SUN A. 1978a. — Two new genera of Dicynodontidae. *Memoirs of the Institute of Vertebrate Paleontology and Paleoanthropology, Academia Sinica* 13: 19-25 [in Chinese].
- SUN A. 1978b. — On occurrence of *Parakannemeyeria* in Sinkiang. *Memoirs of the Institute of Vertebrate Paleontology and Paleoanthropology, Academia Sinica* 13: 47-55 [in Chinese].
- SURKOV M. V. 1998a. — The postcranial skeleton of Rhinodicyodon gracile Kalandadze, 1970 (Dicynodontia). *Paleontologicheski Zhurnal* 32: 78-86.
- SURKOV M. V. 1998b. — Morphological features of the postcranial skeleton in anomodonts reflecting the evolutionary development of the group. *Paleontological Journal* 6: 74-77.
- SURKOV M. V. 1999a. — New data on Middle Triassic anomodonts from the southern Fore-Urals. *Paleontological Journal* 33: 302-307.
- SURKOV M. V. 1999b. — A new Middle Triassic kannemeyerin from the Pechora district. *Paleontological Journal* 33: 420-421.
- SURKOV M. V. 2000. — On the historical biogeography of Middle Triassic anomodonts. *Paleontological Journal* 34: 79-83.
- SURKOV M. V. 2003. — A new anomodont (Therapsida) from the Middle Triassic of the southern Fore-Urals. *Paleontological Journal* 37: 425-431.
- SURKOV M. V. 2005. — The first dicynodont from the terminal Lower Triassic of European Russia, with special reference to the evolution of the masticatory apparatus of these therapsids. *Paleontological Journal* 39: 72-78.
- SURKOV M. V. 2006. — The first evidence of tactile sensor zones among dicynodonts (Therapsida). *Izvestiya of Saratov University* 6: 91-95.
- SURKOV M. V. & BENTON M. J. 2004. — The basicranium of dicynodonts (Synapsida) and its use in phylogenetic analysis. *Palaeontology* 47 (3): 619-638. <https://doi.org/10.1111/j.0031-0239.2004.00382.x>
- SURKOV M. V. & BENTON M. J. 2008. — Head kinematics and feeding adaptations of the Permian and Triassic dicynodonts. *Journal of Vertebrate Paleontology* 28 (4): 1120-1129. <https://doi.org/10.1671/0272-4634-28.4.1120>
- SURKOV M. V., KALANDADZE N. N. & BENTON M. J. 2005. — *Lystrosaurus georgii*, a dicynodont from the Lower Triassic of Russia. *Journal of Vertebrate Paleontology* 25 (2): 402-413. [https://doi.org/10.1671/0272-4634\(2005\)025\[0402:LGADFT\]2.0.CO;2](https://doi.org/10.1671/0272-4634(2005)025[0402:LGADFT]2.0.CO;2)
- SUSHKIN P. P. 1926. — Notes on the pre-Jurassic Tetrapoda from Russia. I. *Dicynodon amalitzkii*, n. sp. *Palaeontologia Hungarica* 1: 323-327.
- SZULC J. & RACKI G. 2015. — Grabowa Formation – the basic lithostratigraphic unit of the Upper Silesian Keuper. *Przeglad Geologiczny* 63: 103-113.
- SZULC J., GRADZIŃSKI M., LEWANDOWSKA A. & HEUNISCH C. 2006. — The Upper Triassic crenogenic limestones in Upper Silesia (southern Poland) and their paleoenvironmental context. *Geological Society of America Special Papers* 416: 133-151. [https://doi.org/10.1130/2006.2416\(09\)](https://doi.org/10.1130/2006.2416(09))
- SZULC J., RACKI G. & JEWUŁA K. 2015a. — Key aspects of the stratigraphy of the Upper Silesian Middle Keuper, southern Poland. *Annales Societatis Geologorum Poloniae* 85: 557-586.
- SZULC J., RACKI G., JEWUŁA K. & ŚRODON J. 2015b. — How many Upper Triassic bone-bearing levels are there in Upper Silesia (southern Poland)? A critical overview of stratigraphy and facies. *Annales Societatis Geologorum Poloniae* 85: 587-626.
- THACKERAY J. F. 2018. — Do specimens attributed to *Lystrosaurus murrayi* and *L. declivis* (Triassic Therapsida) represent one species? *South African Journal of Science* 114: #a0258.

- THACKERAY J. F. 2019. — Alpha and sigma taxonomy of *Lystrosaurus murrayi* and *L. declivis*, Triassic dicynodonts (Therapsida) from the Karoo Basin, South Africa. *South African Journal of Science* 115: #a0296.
- THACKERAY J. F., DURAND J. F. & MEYER L. 1998. — Morphometric analysis of South African dicynodonts attributed to *Lystrosaurus murrayi* (Huxley, 1859) and *L. declivis* (Owen, 1860): probabilities of conspecificity. *Annals of the Transvaal Museum* 36: 413–420.
- THULBORN R. A. 1983a. — A mammal-like reptile from Australia. *Nature* 303: 330–331. <https://doi.org/10.1038/303330a0>
- THULBORN R. A. 1983b. — Thulborn replies. *Nature* 306: 209. <https://doi.org/10.1038/306209b0>
- THULBORN R. A. 1990. — Mammal-like reptiles of Australia. *Memoirs of the Queensland Museum* 28: 169.
- THULBORN T. & TURNER S. 2003. — The last dicynodont: an Australian Cretaceous relict. *Proceedings of the Royal Society B* 270: 985–993. <https://doi.org/10.1098/rspb.2002.2296>
- TOERIEN M. J. 1951. — Notes on the genus *Kannemeyeria*. *South African Journal of Science* 47: 279–282.
- TOERIEN M. J. 1953. — The evolution of the palate in South African Anomodontia and its classificatory significance. *Palaeontology Africana* 1: 49–117.
- TOERIEN M. J. 1954. — CXIII.-*Lystrosaurus primitivus*, sp. nov., and the origin of the genus *Lystrosaurus*. *Annals and Magazine of Natural History* 7: 934–938. <https://doi.org/10.1080/00222935408651814>
- TOERIEN M. J. 1955. — Convergent trends in Anomodontia. *Evolution* 9 (2): 152–156. <https://doi.org/10.2307/2405586>
- TONG J., CHU D., LIANG L., SHU W., SONG H., SONG T., SONG H. & WU Y. 2018. — Triassic integrative stratigraphy and timescale of China. *Science China Earth Sciences* 61.
- TORSVIK T. H. & COCKS R. M. 2016. — *Earth History and Palaeogeography*. Cambridge University Press, Cambridge, 317 p. <https://doi.org/10.1017/9781316225523>
- TRIPATHI C. & PURI S. N. 1961. — On the remains of *Lystrosaurus* from the Panchets of the Raniganj coalfield. *Records of the Geological Survey of India* 89: 407–426.
- TRIPATHI C. & SATSANGI P. P. 1963. — *Lystrosaurus* fauna of the Panchet Series of the Raniganj coalfield. *Memoirs of the Geological Survey of India, Palaeontology Indica* 37.
- TUPI CALDAS J. 1936. — Paleontologia do Rio-Grande-do Sul o fóssil de São-Pedro. *Revista Instituto Historico e Geográfico do Rio-Grande-do-Sul* 16: 243–249.
- TVERDOKHLEBOV V. P., TVERDOKHLEBOVA G. I., SURKOV M. V. & BENTON M. J. 2002. — Tetrapod localities from the Triassic of the SE of European Russia. *Earth-Science Reviews* 60 (1–2): 1–66. [https://doi.org/10.1016/S0012-8252\(02\)00076-4](https://doi.org/10.1016/S0012-8252(02)00076-4)
- TVERDOKHLEBOV V. P., SENNIKOV A. G., NOVIKOV I. V. & ILYINA N. V. 2020. — The youngest Triassic land vertebrate assemblage of Russia: composition and dating. *Paleontological Journal* 54: 297–310. <https://doi.org/10.1134/S0031030120030156>
- UGALDE G. D., MÜLLER R. T., ARAÚJO-JÚNIOR H. I. DE, DIAS-DA-SILVA S. & PINHEIRO F. L. 2018. — A peculiar bonebed reinforces gregarious behaviour for the Triassic dicynodont *Dinodontosaurus*. *Historical Biology* 32 (6): 764–772. <https://doi.org/10.1080/08912963.2018.1533960>
- DE VALAIS S., DÍAZ-MARTINEZ I., CITTON P. & CÓNSOLE-GONELLA C. 2020. — Vertebrate tracks of the Río Negro province, Patagonia, Argentina: Stratigraphy, palaeobiology and environmental contexts. *Revista de la Asociación Geológica Argentina* 77: 402–426.
- VALDISERRI D., FORTUNY J. & GALOBART À. 2009. — New insight on old material: Triassic tetrapods footprints in Catalonia (NE Iberian Peninsula). *Tenth International Symposium on Mesozoic Terrestrial Ecosystems and Biota*: 163.
- VEGA C. S. & MAISCH M. W. 2014. — Pathological features in Upper Permian and Middle Triassic dicynodonts (Synapsida, Therapsida), in KAMMERER C. F., ANGIELCZYK K. D. & FRÖBISCH J. (eds), *Early evolutionary history of the Synapsida*. Springer, Dordrecht: 151–161.
- VEGA-DIAS C. S. & SCHULTZ C. L. 1999. — Materiais pós-cranianos de *Jachaleria Araújo* & Gonzaga, 1980 (Therapsida, Dicynodontia) no Triássico Superior do Rio Grande do Sul, Brasil. *XVI Congresso Brasileiro de Paleontologia, boletim de resumos*: 122.
- VEGA-DIAS C. S. & SCHULTZ C. L. 2003. — A paleopathology in *Jachaleria candelariensis* Araújo and Gonzaga 1980 (Synapsida, Dicynodontia) from the Upper Triassic of Southern Brazil. *Ameghiniana* 40: 74R.
- VEGA-DIAS C. S. & SCHULTZ C. L. 2004. — Postcranial material of *Jachaleria candelariensis* Araújo and Gonzaga 1980 (Therapsida, Dicynodontia), Upper Triassic of Rio Grande do Sul. *PaleoBios* 24: 7–31.
- VEGA-DIAS C. S. & SCHULTZ C. L. 2007. — Evidence of archosauriform feeding on dicynodonts in the Late Triassic of southern Brazil. *PaleoBios* 27: 62–67.
- VEGA-DIAS C. S. & SCHWANKE C. 2004a. — Reevaluating the link of *Stahleckeria* von Huene to *Ischigualastia* Cox, two Middle/Late Triassic tuskless dicynodonts of South America. *Ameghiniana* 41: 65R–66R.
- VEGA-DIAS C. S. & SCHWANKE C. 2004b. — Verifying the validity of *Jachaleria* Bonaparte (Therapsida, Dicynodontia). *Ameghiniana* 41: 66R.
- VEGA-DIAS C. S. & SCHWANKE C. 2005. — Verifying the validity of *Jachaleria* genus (Therapsida, Dicynodontia). *Boletim da Sociedade Brasileira de Paleontologia* 49: 52–53.
- VEGA-DIAS C., MAISCH M. W. & SCHULTZ C. L. 2004. — A new phylogenetic analysis of Triassic dicynodonts (Therapsida) and the systematic position of *Jachaleria candelariensis* from the Upper Triassic of Brazil. *Neues Jahrbuch für Geologie und Paläontologie - Abhandlungen* 231 (2): 145–166. <https://doi.org/10.1127/njgp/231/2004/145>
- VEGA-DIAS C. S., MAISCH M. W. & SCHWANKE C. 2005. — The taxonomic status of *Stahleckeria impotens* (Therapsida, Dicynodontia): redescription and discussion of its phylogenetic position. *Revista Brasileira de Paleontologia* 8: 221–228.
- VERGNE R., PACANOWSKI R., BARLA P., GRANIER X. & SCHLICK C. 2010. — Radiance scaling for versatile surface enhancement, in *Proceedings of the 2010 ACM SIGGRAPH symposium on Interactive 3D Graphics and Games*: 143–150.
- VIGLIETTI P. A. 2020. — Biostratigraphy of the *Daptocephalus* Assemblage Zone (Beaufort Group, Karoo Supergroup), South Africa. *South African Journal of Geology* 123 (2): 191–206. <https://doi.org/10.25131/sajg.123.0014>
- VIGLIETTI P. A., SMITH R. M. H. & COMPTON J. 2013. — Origin and palaeoenvironmental significance of *Lystrosaurus* bonebeds in the earliest Triassic Karoo Basin, South Africa. *Palaeogeography, Palaeoclimatology, Palaeoecology* 392: 9–21. <https://doi.org/10.1016/j.palaeo.2013.08.015>
- VIGLIETTI P. A., SMITH R. M. H., ANGIELCZYK K. D., KAMMERER C. F., FRÖBISCH J. & RUBIDGE B. S. 2016. — The *Daptocephalus* Assemblage Zone (Lopingian), South Africa: A proposed biostratigraphy based on a new compilation of stratigraphic ranges. *Journal of African Earth Sciences* 113: 153–164. <https://doi.org/10.1016/j.jafrearsci.2015.10.011>
- VIGLIETTI P. A., MCPHEE B. W., BORDY E. M., SCISCIO L., BARRETT P. M., BENSON R. B. J., WILLS S., CHAPELLE K. E. J., DOLLMAN K. N., MDEKAZI C. & CHOINIERE J. N. 2020a. — Biostratigraphy of the *Massospondylus* Assemblage Zone (Stormberg Group, Karoo Supergroup), South Africa. *South African Journal of Geology* 123 (2): 249–262. <https://doi.org/10.25131/sajg.123.0018>
- VIGLIETTI P. A., MCPHEE B. W., BORDY E. M., SCISCIO L., BARRETT P. M., BENSON R. B. J., WILLS S., TOLCHARD F. & CHOINIERE J. N. 2020b. — Biostratigraphy of the *Scalenodonoides* Assemblage Zone (Stormberg Group, Karoo Supergroup), South Africa. *South African Journal of Geology* 123 (2): 239–248. <https://doi.org/10.25131/sajg.123.0017>

- VIGLIETTI P. A., ROJAS A., ROSVALL M., KLIMES B. & ANGIELCZYK K. D. 2022. — Network-based biostratigraphy for the late Permian to mid-Triassic Beaufort Group Karoo. *Palaeontology* 65 (5): e12622. <https://doi.org/10.1111/pala.12622>
- VJUSCHKOV B. P. 1969. — New dicynodonts from the Triassic of the southern Fore-Urals. *Paleontological Journal* 1969: 99-106.
- VOGEL G. 2008. — Giant mammal cousin rivaled early dinosaurs. *Science* 362 (6417): 879. <https://doi.org/10.1126/science.362.6417.879>
- WALTER L. R. 1985. — The formation of secondary centers of ossification in kannemeyeriid dicynodonts. *Journal of Paleontology* 59: 1486-1488.
- WALTER L. R. 1989. — The limb posture of kannemeyeriid dicynodonts: functional and ecological considerations, in Padian K. (ed.), *The Beginning of the Age of Dinosaurs. Faunal Change Across the Triassic-Jurassic Boundary*. Cambridge University Press, Cambridge: 89-97.
- WALTHER M. & FRÖBISCH J. 2013. — The quality of the fossil record of anomodonts (Synapsida, Therapsida). *Comptes Rendus Palevol* 12 (7-8): 495-504. <https://doi.org/10.1016/j.crpv.2013.07.007>
- WARREN A. 1998. — *Laidleria* uncovered: a redescription of *Laidleria gracilis* Kitching (1957), a temnospondyl from the Cynognathus Zone of South Africa. *Zoological Journal of the Linnean Society* 122 (1-2): 167-185. <https://doi.org/10.1111/j.1096-3642.1998.tb02528.x>
- WARREN A. & MARSICANO C. 2000. — A phylogeny of the Brachyopidea (Temnospondyli, Stereospondyli). *Journal of Vertebrate Paleontology* 20 (3): 462-483. <https://doi.org/bfbtwf>
- WATSON D. M. S. 1911. — XL.— The skull of *Diademodon*, with notes on those of some other cynodonts. *Annals and Magazine of Natural History* 8 (45): 293-330. <https://doi.org/10.1080/00222931108693034>
- WATSON D. M. S. 1912a. — LXVII.-On some reptilian lower jaws. *Journal of Natural History* 10 (60): 573-587. <https://doi.org/10.1080/00222931208693273>
- WATSON D. M. S. 1912b. — The skeleton of *Lystrosaurus*. *Records of the Albany Museum* 2: 287-295.
- WATSON D. M. S. 1913. — The limbs of *Lystrosaurus*. *Geological Magazine* 10 (6): 256-258. <https://doi.org/10.1017/S0016756800126445>
- WATSON D. M. S. 1917. — The evolution of the tetrapod shoulder girdle and fore-limb. *Journal of Anatomy* 52: 1-63.
- WATSON D. M. S. 1948. — *Dicynodon* and its allies. *Proceedings of the Zoological Society of London* 118: 823-877.
- WATSON D. M. S. 1960. — The anomodont skeleton. *Transactions of the Zoological Society of London* 29 (3): 131-209. <https://doi.org/10.1111/jzo.1960.29.3.131>
- WEITHOFER A. 1888. — Ueber einen neuen Dicynodonten (*Dicynodon simocephalus*) aus der Karrooformation Sudafrikas. *Annalen des K. K. Naturhistorischen Hofmuseum* 3: 1-5.
- WHITESIDE J. H., GROGAN D. S., OLSEN P. E. & KENT D. V. 2011. — Climatically driven biogeographic provinces of Late Triassic tropical Pangea. *Proceedings of the National Academy of Sciences of the United States of America* 108 (22): 8972-8977. <https://doi.org/10.1073/pnas.1102473108>
- WHITNEY M. R., ANGIELCZYK K. D., PEECOOK B. R. & SIDOR C. A. 2021. — The evolution of the synapsid tusk: Insights from dicynodont therapsid tusk histology. *Proceedings of the Royal Society B* 288: 20211670. <https://doi.org/10.1098/rspb.2021.1670>
- WHITNEY M. R. & SIDOR C. A. 2020. — Evidence of torpor in the tusks of *Lystrosaurus* from the Early Triassic of Antarctica. *Communications Biology* 3: 471. <https://doi.org/10.1038/s42003-020-01207-6>
- WHITNEY M. R., TSE Y. T. & SIDOR C. A. 2019. — Histological evidence of trauma in tusks of southern African dicynodonts. *Palaeontologia Africana* 53: 75-80.
- WILLISTON S. W. 1904. — Notice of some new reptiles from the Upper Trias of Wyoming. *The Journal of Geology* 12 (8): 688-697. <https://doi.org/10.1086/621190>
- WYND B. M., PEECOOK B. R., WHITNEY M. R. & SIDOR C. A. 2018. — The first occurrence of *Cynognathus crateronotus* (Cynodontia: Cynognathia) in Tanzania and Zambia, with implications for the age and biostratigraphic correlation of Triassic strata in southern Pangea. *Journal of Vertebrate Paleontology* 37 (Supplement 1): 228-239. <https://doi.org/10.1080/02724634.2017.1421548>
- WYND B. M., MARTÍNEZ R. N., COLOMBI C. & ALCOBER O. 2020. — A review of vertebrate beak morphologies in the Triassic; a framework to characterize an enigmatic beak from the Ischigualasto Formation, San Juan, Argentina. *Ameghiniana* 57 (4): 370-387. <https://doi.org/10.5710/AMGH.13.05.2020.3313>
- YANG C. 1978. — A Late Triassic vertebrate fauna from Fukang, Sinkiang. *Memoirs of the Institute of Vertebrate Paleontology and Paleoanthropology, Academia Sinica* 13: 60-67 [in Chinese].
- YEH H.-K. 1959. — New dicynodont from *Sinokannemeyeria*-fauna from Shansi. *Vertebrata PalAsiatica* 3: 187-204.
- YIN H. & PENG Y. 2000. — The Triassic of China and its inter-regional correlation, in YIN H., DICKINS J. M., SHI G. R. & TONG J. (eds), *Persian-Triassic evolution of Tethys and western Circum-Pacific*. Elsevier Science, Amsterdam, Lausanne, New York, Oxford, Shannon, Singapore, Tokyo: 197-219.
- YOUNG C. C. 1935. — On two skeletons of Dicynodontia from Sinkiang. *Bulletin of the Geological Survey of China* 14 (4): 483-517. <https://doi.org/10.1111/j.1755-6724.1935.mp14004003.x>
- YOUNG C. C. 1937. — On the Triassic dicynodonts from Shansi. *Acta Geologica Sinica* 17 (3-4): 393-412. <https://doi.org/10.1111/j.1755-6724.1937.mp173-4011.x>
- YOUNG C. C. 1939. — Additional Dicynodontia remains from Sinkiang. *Bulletin of the Geological Society of China* 19 (2): 111-139. <https://doi.org/10.1111/j.1755-6724.1939.mp19002001.x>
- YOUNG C. C. 1946. — The Triassic vertebrate remains of China. *American Museum Novitates* 1324: 1-14. <https://www.biodiversitylibrary.org/bibliography/90614>
- YOUNG C. C. 1963. — Note on the labyrinthodonts of the Sino-kannemeyerian fauna in Shansi. *Vertebrata PalAsiatica* 7: 331-341.
- YOUNG C. C. 1964. — The pseudosuchians in China. *Palaeontologia Sinica C* 19: 1-205.
- YUAN P. L. & YOUNG C. C. 1934a. — On the discovery of a new *Dicynodon* in Sinkiang. *Bulletin of the geological Society of China* 13 (1): 563-574. <https://doi.org/10.1111/j.1755-6724.1934.mp13001028.x>
- YUAN P. L. & YOUNG C. C. 1934b. — On the occurrence of *Lystrosaurus* in Sinkiang. *Bulletin of the Geological Society of China* 13 (1): 575-580. <https://doi.org/10.1111/j.1755-6724.1934.mp13001029.x>
- YUHE L. 1983. — Restoration of pelvic muscles of *Lystrosaurus*. *Vertebrata PalAsiatica* 21: 328-340.
- ZAVATTIERI A. M. & ARCUCCI A. B. 2007. — Edad y posición estratigráfica de los tetrápodos del cerro Bayo de Potrerillos (Triásico), Mendoza, Argentina. *Ameghiniana* 44 (1): 133-142.
- ZIEGER J., HARAZIM S., HOFMANN M., GÄRTNER A., GERDES A., MARKO L. & LINNEMANN U. 2020. — Mesozoic deposits of SW Gondwana (Namibia): unravelling Gondwanan sedimentary dispersion drivers by detrital zircon. *International Journal of Earth Sciences* 109: 1683-1704. <https://doi.org/10.1007/s00531-020-01864-2>

Submitted on 6 October 2021;
accepted on 22 February 2022;
published on 16 May 2023.

APPENDICES

APPENDIX 1. — The 3D models: https://doi.org/10.5852/cr-palevol2023v22a16_s1

APPENDIX 2. — Character list taken from Kammerer & Ordoñez 2021. Dicynodonts (Therapsida: Anomodontia) of South America.

Continuous characters

1. Length of preorbital region of skull relative to basal length of skull.
2. Relative length of premaxillary secondary palate.
3. Minimum width of interorbital skull roof relative to basal length of skull.
4. Relative width of temporal bar at level of postorbital bar versus the relative width at the junction of the intertemporal bar with the occipital plate.
5. Length of temporal fenestra relative to basal length of skull.
6. Relative position of pineal foramen, measured as the ratio of dorsal skull length posterior to the foramen versus dorsal skull length anterior to the foramen.
7. Height of anterior pterygoid keel in lateral view relative height of non-keel ramus.
8. Width of median pterygoid plate relative to basal skull length.
9. Angle formed by the posterior pterygoid rami.
10. Length of interpterygoid vacuity relative to basal length of skull.
11. Relative area of the internal nares.
12. Angle between ascending and zygomatic processes of the squamosal.
13. Angulation of the occiput relative to the palate, expressed the ratio of dorsal and basal lengths of the skull.
14. Ratio of height to length of mandibular fenestra in lateral view.
15. Ratio of height of dentary ramus to height of dentary symphysis.
16. Ratio of maximum height of postdentary bones (excluding reflected lamina of angular) to the height of the dentary ramus.
17. Ratio of minimum width of the scapula to maximum width of dorsal end of scapula.
18. Length of the deltopectoral crest relative to total length of the humerus.
19. Maximum width of the distal end of the radius relative to the maximum length of the radius.
20. Ratio of posterior iliac process length to acetabulum diameter.
21. Ratio of anterior iliac process Length to acetabulum diameter.
22. Length of trochanteric crest on femur relative to length of femur.
23. Breadth of scapula measured as ratio of maximal proximal width of scapula versus length of scapula (measured from dorsal edge of glenoid to proximal tip).

Discrete characters

24. Premaxillae unfused (0) or fused (1).
25. Paired anterior ridges on palatal surface of premaxilla absent (0), present and converge posteriorly (1), or present and do not converge (2).
26. Lateral anterior palatal ridges absent (0) or present (1).
27. Rounded depression on anterior palatal surface of premaxilla: absent (0); present (1).
28. Posterior median ridge on palatal surface of premaxilla absent (0), present with a flattened, expanded anterior area (1), or present without a flattened, expanded anterior area (2).
29. Palatal surface of premaxilla with well-defined depressions with curved sides lateral to median ridge (if present) (0), with distinct accessory ridges lateral to medial ridge (1), or relatively flat with poorly defined or no depressions present (2).
30. Palatal surface of premaxilla with antero-posterior vascular groove lateral to median ridge (if present) absent (0); present (1).
31. Location of premaxillary teeth lateral (0), medial (1) or absent (2).
32. Posterior exposure of the premaxilla on the palate: absent (0), present (1).
33. Posterior process of the premaxilla with a non-bifurcated posterior tip (0) or with a bifurcated posterior tip (1).
34. Palatine shelf ventral to internal naris: absent (0), present (1).
35. Anterior tip of snout rounded (0), squared off (1), or with a deep central invagination, giving the snout a “hare-lip” appearance in anterior view (2).
36. Marked anterior expansion of preorbital region absent (0) or present (1).
37. Snout roughly parallel to long axis of skull (0) or strongly angled ventrally (1).
38. Height of canine-bearing portion of maxilla: relatively short (0); extremely deep, with long caniniform process, but with equally long premaxilla resulting in an overall tall snout (1); extremely long caniniform process offset from rest of snout (2).
39. Snout open to back of the skull (0) or anterior margin of orbit extended posteromedially to partly close off the snout from the rest of the skull (1).
40. Septomaxilla posterodorsal spur present and widely separates nasal and maxilla (0), spur present but does not separate maxilla and nasal (i.e., nasal-maxilla suture present and well defined in this region) (1), septomaxilla spur absent (2).
41. Notch on dorsal edge of narial opening absent (0) or present (1).
42. Postnarial excavation absent (0), present, relatively small, and rounded posteriorly (1), or present, very large, and elongate (2).
43. Maxillary alveolar region short, occupying less than 53% of the ventral length of the bone (0) or tooth bearing region long, occupying 72% or more of the ventral length of the bone (1).
44. Palatal surface of premaxilla exposed in lateral view (1) or not exposed in lateral view (0).
45. Maxillary canine present as large member of tooth series (0), absent (1), or present as tusk (2).
46. Maxillary non-caniniform teeth located near lateral margin of maxilla (0), located more medially, (1), or absent (2).
47. Shelf-like area lateral to the maxillary non-caniniform teeth absent (0) or present (1).
48. Fine serrations on maxillary teeth present (0), serrations absent (1), or coarse serrations present (2).
49. Sutural contact of maxilla and prefrontal present (0) or absent (1).
50. Caniniform process absent (0) or present (1).
51. Caniniform depression: has the form of an embayment bounded by a ridge medially of palatal rim anterior to caniniform process or tusk (1), has the form of a notch in palatal rim anterior to caniniform process (2), or absent (0).
52. Distinct lateral caniniform buttress absent (0), present (1), or present with posteroventral furrow (2).
53. Keel-like extension of the palatal rim posterior to the caniniform process absent (0) or present (1).
54. Postcaniniform crest absent (0) or present (1).

APPENDIX 2. — Continuation.

55. Ventral edge of the caniniform process or dorsal edge of the erupted portion of the canine tusk anterior (0) to, or at the same level to slightly posterior to (1) the anterior orbital margin.
56. Nasals with a long median suture that separates the premaxilla from the frontals (0) or with a short median suture and frontals and premaxilla in close proximity (1).
57. Nasal bosses absent (0), present as a median swelling with a continuous posterior margin (1), present as paired swellings near the dorsal or posterodorsal margin of external nares (2), present as paired swellings that meet in the midline to form a swollen anterodorsal surface on the snout (3).
58. Naso-frontal suture relatively straight, interdigitated, or gently bowed (0), with a distinct anterior process (1), or with a distinct posterior process (2).
59. Transverse crest approximately at level of naso-frontal suture absent (0); present and straightly transverse to curved with posterior convexity (1); present and strongly curved with posterior concavity (2).
60. Lacrimal does not contact septomaxilla (0) or does contact septomaxilla (1).
61. Prefrontal bosses absent (0), present but separate from nasals (1), or present and confluent with nasal bosses (2).
62. Raised, sometimes rugose, circumorbital rim absent (0) or present (1).
63. Frontal contribution to the dorsal rim of the orbit: broad, frontal forms a major part of the orbital rim (0); thin or absent, if present a thin frontal process extends laterally between the prefrontal and postorbital to reach the orbital margin (1).
64. Postfrontal bone present on dorsal surface of skull (0) or absent (1).
65. Postorbital bar without (0) or with thickenings and rugosities (1).
66. Mediolateral flattening and anteroposterior expansion of postorbital bar for most or all of its length absent (0) or present (1).
67. Temporal portion of skull roof relatively straight, without a strong break in slope (0), or temporal portion of skull roof angled dorsally with a strong break in slope near its anterior end (1).
68. Preparietal bone absent (0), present and flush with skull roof (1), present and depressed (2).
69. Lateral ridges bounding preparietal absent (0) or present (1).
70. Parietals' contribution to skull table transversely as broad as long (0), longer anteroposteriorly than broad (1), or shorter anteroposteriorly than broad (2).
71. Parietal posterolateral process slender and elongate (0), or short (1).
72. Parietals well exposed on the skull roof and relatively flat (0), parietals exposed in midline groove or channel (1), dorsal parietal exposure narrow and crest-like (2).
73. Postparietal bulges outwards as ovoid swellings at posterior end of sagittal crest: no (0); yes (1).
74. Orientation of the temporal portion of the postorbital: relatively flat, so that most of the exterior surface of the bone faces dorsally (0), close to vertical, so that most of the exterior surface of the bone faces laterally (1), or bi-planar, with approximately equally-sized dorsal and lateral surfaces that are close to perpendicular (2).
75. Postorbitals extend the entire length of intertemporal bar (0) or do not extend the entire length of intertemporal bar, such that the posterior portion of the bar is formed only by the parietals (1).
76. Fossa on the ventral surface of the intertemporal bar formed by the postorbital and parietal large (0), reduced (1), or absent (2).
77. Pineal foramen present (0); absent (1).
78. Circumpineal ornamentation: chimney-like boss (0); no boss, foramen flush with skull surface (1); dome- or collar-like boss, rugosity present (2); boss present with incomplete border, more strongly developed on lateral edges of pineal foramen (3).
79. Orientation of pineal foramen: exits perpendicular to long axis of intertemporal bar (0); angled anterior to perpendicular relative to long axis of intertemporal bar (1).
80. Interparietal does not contribute to intertemporal skull roof (0), makes a small contribution to intertemporal skull roof (1), or makes a large contribution to intertemporal skull roof (2).
81. Squamosal without (0) or with (1) a small or (2) large lateral fossa for the origin of the lateral branch of the M. adductor mandibulae externus. ORDERED.
82. Distinct dorsolateral notch in squamosal below zygomatic arch in posterior view absent (0) or present (1).
83. Squamosal posteroventral process short such that there is relatively extensive exposure of quadrate and quadratojugal in posterior view and the quadrate foramen (if present) is visible in posterior view (0) or long such that nearly all of the quadrate and quadratojugal are covered by the squamosal in posterior view and the quadrate foramen (if present) is not visible in posterior view (1).
84. Zygomatic portion of the squamosal without folded edge (0), out-turned to downturned (1) (*Oudenodon*, *Odontocylops*, etc.), or folded-over (2) (*Pelanomodon*, *Geikia*). ORDERED.
85. Dorsoventral expansion of squamosal posterior to postorbital bar: (0) absent (1) present.
86. Zygomatic process of squamosal parasagittally deep (0), narrow and rod-like (1), or transversely expanded (2).
87. Oblique ridge on lateral side of zygomatic arch giving triangular cross-section and overhanging a weak groove present (1) or absent (0).
88. Squamosal zygomatic process narrowly based and in line with occipital condyle (0) or widely based and flares posteriorly beyond occipital condyle (1).
89. Sutural contact of squamosal and maxilla absent (0) or present (1).
90. Squamosal separated by tabular bone from supraoccipital (0) or contacts supraoccipital (1).
91. Suborbital boss on jugal absent (0) or present (1).
92. Quadratojugal narrow and rod-like (0) or plate-like distally (1).
93. Quadrate with a dorsal lobe that has a convex, rounded anterior edge that rests against quadrate ramus of pterygoid (0) or with a dorsal lobe that is developed into a distinct process that extends anteriorly along the quadrate ramus of the pterygoid and is triangular to sub-triangular in shape (1).
94. Vomers unfused (0) or fused (1).
95. Mid-ventral plate of vomers with an expanded, oval-shaped area posterior to junction with premaxilla (0) or without a notable expanded area posterior to junction with premaxilla (1).
96. Mid-ventral plate of vomers relatively wide in ventral view (0), more narrow and blade-like in ventral view (1).
97. Trough on mid-ventral plate of vomers (i.e., ventral surface concave ventrally with raised edges): present (0) or absent (1).
98. Palatine dentition present (0) or absent (1).
99. Bone texture of the palatine: primarily smooth, without evidence of keratinized covering (0); relatively smooth but with fine pitting and texturing suggestive of a keratinized covering (1); rugose and textured (2).
100. Position of palatine: raised, central palatine boss present (0); entire palatine flush with surrounding palatal elements (1); raised posterior section with anterior section that is flush with the secondary palate (2).
101. Paired fossae on palatine surface absent (0); present (1).

APPENDIX 2. — Continuation.

102. Palatine widest at its approximate midpoint of length (0), widens posteriorly (1), width relatively constant for entire length (2), widens anteriorly forming a palatine pad (3). ORDERED.
103. Foramen on the palatal surface of the palatine absent (0) or present (1).
104. Lateral palatal foramen absent (0), present at level of the anterior, expanded palatal exposure of the palatines (1), present posterior and dorsal to the level of the anterior, expanded palatal exposure of the palatines (2).
105. Sutural contact of palatine and premaxilla absent (0) or present (1).
106. Labial fossa surrounded by maxilla, jugal, and palatine absent (0) or present (1).
107. Ectopterygoid extends further posteriorly than palatine in palatal aspect (0), or does not extend further posteriorly than palatine in palatal aspect (1), or absent (2).
108. Ectopterygoid dentition absent (0) or present (1).
109. Pterygoids contact anteriorly (0) or separated by vomers (1).
110. Transverse flange of pterygoid projects laterally, free of posterior ramus (0), projects laterally, bound by posterior ramus (1) does not project laterally (2).
111. Anterior pterygoid keel: absent (0); present (1).
112. Anterior pterygoid keel extending for most of the length of anterior ramus of pterygoid (0); anterior pterygoid keel restricted to the anterior tip of the anterior ramus of the pterygoid (1).
113. Contact of pterygoid and maxilla absent (0) or present (1).
114. Converging ventral ridges on posterior portion of anterior pterygoid rami absent (0) or present (1).
115. Ventral surface of the median pterygoid plate depressed (0), smooth and flat (1), with a thin median ridge (2), with a wide, boss-like median ridge (3), or with a low rugose median swelling (4), or with a conical ventral projection (5), or with thin paired ridges that are contiguous with the edges of the interpterygoid vacuity (6).
116. Pterygoid dentition present, conical (0); absent (1); present, bucco-lingually expanded.
117. Posterior edges of the interpterygoid vacuity located dorsal to the median pterygoid plate (0) or extended ventrally such that they are flush with the median pterygoid plate (1).
118. Development of the pila antotica as a rod-like process on the anterior edge of the periotic with a corresponding notch for the trigeminal never posterior to it (0), or pronounced pila antotica absent and trigeminal notch is a horizontal hollow in the anterior edge of the periotic (1).
119. Contact between periotic and parietal absent (0) or present (1).
120. Parasphenoid excluded from (0) or reaches (1) interpterygoid vacuity.
121. Basisphenoid contribution to the basisphenoid-basioccipital tubera slopes anterodorsally at a shallow angle, forming elongate ridges on the basicranium that are close to the same height as the tubera for most of their length (0), slopes anterodorsally at a steeper angle such that the parabasisphenoid contribution is still somewhat ridge-like but the portion of the ridge on the anterior surface of the tuber is more vertically-oriented (1), or is nearly vertical, forming very weak ridges if any (2).
122. Stapedial facet of basisphenoid-basioccipital tuber exposed laterally (0), exposed ventrolaterally (1), or exposed ventrolaterally and open distally (2).
123. Exposure of internal carotid between mid-pterygoid plate and parasphenoid: directed laterally (0); directed medially (1).
124. Shape of basal tubera: bifurcating and posteriorly-directed (0); laterally directed anteroposteriorly elongate with relatively narrow edges (1); strongly rounded, such that anterior and posterior tips of tuber curve towards each other, nearly enclosing the stapedial facet; tuber inflated (2); elongate, nearly quadrangular, with tubera extremely close together (3).
125. Margin of fenestra ovalis formed predominantly by parabasisphenoid, with little or no contribution from basioccipital (0), formed by approximately equal portions of parabasisphenoid and basioccipital (1), or formed predominantly by basioccipital, with little or no contribution by parabasisphenoid (2).
126. Intertuberal ridge absent (0) or present (1).
127. Dorsal process on anterior end of epitygoid footplate absent (0) or present (1).
128. Stapedial foramen present (0) or absent (1).
129. Dorsal process of the stapes present (0) or absent (1).
130. Tabular contacts opisthotic (0) or separated from opisthotic by squamosal (1).
131. Prootic bearing rectangular alar process that forms a plate raised above surface of temporal fenestra wall, in front of fossa: absent (0) present (1).
132. Exoccipital and basioccipital contributions to the occipital condyle distinct (0) or co-ossified into a single unit (1).
133. Occipital condyle round to subspherical in posterior view (0) or distinctly tri-radiate (1) in posterior view.
134. Circular central depression or fossa on the occipital condyle between the exoccipitals and basioccipital present (0) or absent (1).
135. Lateral edge of paroccipital process drawn into sharp posteriorly-directed process that is distinctly offset from the surface of the occipital plate: absent (0) present (1).
136. Floccular fossa present (0) or absent (1).
137. Mandibular fenestra absent (0), present (1), or present but occluded by a thin sheet of the dentary (2).
138. Jaw ramus straight in dorsal view, without strong lateral bends (0), or bends strongly laterally (1) posterior to symphysis.
139. Dentaries sutured (0) or fused (1) at symphysis.
140. Teeth present on dorsal surface of dentaries (0), medially displaced, sometimes on a swelling or shelf (1), or absent (2).
141. Fine serrations on dentary teeth present (0), serrations absent (1), or coarse serrations present (2).
142. Denticulated cingulum on dentary teeth absent (0) or present (1).
143. Anteriormost dentary tooth: not distinct from rest of tooth row (0); massively enlarged and incisiform (1).
144. Jaw symphysis terminates in dorsal platform bearing the incisors and canine elevated above level of posterior dentary ramus (0); Symphyseal region of lower jaw smoothly rounded and at same level as rest of dentary ramus in lateral view (1), with an upturned beak that is raised above the level of the dorsal surface of the jaw rami and has a scooped-out depression on its posterior surface (2), drawn into a sharp, spiky beak (3), or shovel-shaped beak with a rounded or squared-off edge and a weak depression on its posterior surface (4).
145. Curved ridge that follows the profile of the symphysis present on the edge between the anterior and lateral surfaces of the dentary absent (0) or present (1).
146. Boss present on ventral surface of anterior dentary ramus. absent (0) present (1).
147. Dentary table absent (0) or present (1).
148. Posterior dentary sulcus absent (0), present but does not extend past dentary teeth (if present) (1), present and extends past dentary teeth (if present), but is relatively wide and shallow (2), or present, extends past dentary teeth (if present) and is narrower and deeper (3).
149. Tall, dorsally-convex cutting blade on medial edge of dorsal surface of dentary absent (0) or present (1).
150. Lateral dentary shelf absent (0), present but relatively small (1), present and well developed (2).
151. Anterodorsal edge of lateral dentary shelf relatively flat (0), with a groove (1), or developed into a rounded swelling (2).

APPENDIX 2. — Continuation.

- 152. Lateral dentary shelf relatively thick, with distinct dorsal and ventral surfaces above the mandibular fenestra (0) or a thin ventrolaterally-directed sheet that forms the dorsal margin of the mandibular fenestra (1).
- 153. Splenial symphysis unfused (0) or fused (1).
- 154. Splenial contribution to dentary symphysis: anterior process on splenial present in ventral view (0) or absent (1).
- 155. Exposed contribution of the angular to the symphysis: absent (0) present (1).
- 156. Coronoid bone present (0), or absent (1).
- 157. Angular with anterolateral trough for the posterior process of the dentary absent (0) or present (1).
- 158. Reflected lamina: (0) reflected lamina large, rounded, unornamented; (1) with perpendicular ridges; (2) with reticulate ridges; (3) triradiate, with distinct groove-ridge-groove morphology dorsoventrally arrayed along lamina; (4) small, tab-like (more elongate than rounded), unornamented (5); large, rounded, but with only a central groove bisecting the lamina.
- 159. Reflected lamina of angular closely approaches or touches articular (0) or widely separated from articular (1).
- 160. Prearticular with (0) or without (1) lateral exposure posteriorly.
- 161. Articular distinct (0) or at least partially fused to prearticular (1).
- 162. Surangular vertical lamina present and lateral to articular (0) or absent (1).
- 163. Jaw joint allows strictly orthal closure (0); allows parasagittal movement with joint surfaces of quadrate and articular approximately equal (1); allows parasagittal movement with joint surfaces on articular large than that of quadrate (2). ORDERED.
- 164. Enlarged dentary caniniform present (0) or absent (1).
- 165. Number of sacral vertebrae three (0), four (1), five (2), or six or more (3).
- 166. Number of sternal bosses: 2 (0), 4(1).
- 167. Cleithrum absent (0) or present (1).
- 168. Anterior edge of scapula extended laterally to form a strong crest (1) or not (0).
- 169. Origin of triceps on posterior surface of scapula relatively low (0) or developed into a prominent posterior projection (1).
- 170. Acromion process: absent or very small (0) or present and well defined (1).
- 171. Procoracoid foramen or notch entirely contained within the procoracoid (0) or formed by contributions of the procoracoid and scapula in lateral view (1).
- 172. Procoracoid does not participate in formation of glenoid (0) or participates in formation of glenoid (1).
- 173. Proximal articular surface of humerus formed by a slightly convex area on proximal surface of the bone without much expansion onto the dorsal surface (0), somewhat expanded with some encroachment onto the dorsal surface (1), or strongly developed and set off from rest of humerus by a weak neck (2). ORDERED.
- 174. Insertion of *M. subcoracoscapularis* on humerus a rounded, rugose area on proximal end of humerus (0), short, pinna-like process (1); large elongate process (2). ORDERED.
- 175. Insertion of *M. latissimus dorsi* at rugose tuberosity on the posteroventral surface of humerus (0) or extended into a dorsoventrally flattened pinna-like process (1).
- 176. Anterior and distal edges of deltopectoral crest close to perpendicular (0) or very obtuse (1).
- 177. Ectepicondylar foramen on humerus present (0) or absent (1).
- 178. Radial and ulnar condyle continuous (0) or well ossified and separate (1) on ventral surface of humerus.
- 179. Ulna with small olecranon process that does not extend far past the articular surface for the humerus (0), or with a large olecranon process that extends well past the articular surface for the humerus (1).
- 180. Distal carpal 5: present as a distinct element (0), not present as a distinct element (1).
- 181. Manual digit III, shape of second phalanx: short (disc-like) (0), absent (1).
- 182. Manual digit IV, phalangeal number: 5 (0), or 3 (1).
- 183. Dorsal edge of ilium: unnotched (0) or notched (1).
- 184. Pubic plate is significantly expanded anteroposteriorly, such that its length is comparable to that of ischium (0) or anteroposteriorly short, so that it is much shorter than ischium (1).
- 185. Pubic plate is significantly expanded ventrally such that it is nearly the same height as ischium (0) or reduced ventrally such that it is shorter than ischium (1).
- 186. Distinct cranial process on anterior end of pubis absent (0) or present (1).
- 187. Femoral head continuous with the dorsal margin of femur (0) or offset dorsally from dorsal margin (1).
- 188. Proximal articular surface of the femur present as a weak swelling that is mostly limited to the proximal surface of the bone (0) or present as a more rounded, hemispherical swelling that has some encroachment on the anterior surface of the femur (1).
- 189. Insertion of *M. iliofemoralis* present as a low rugosity on the dorsolateral portion of the femur (0), developed into a distinct crest that extends down part of the lateral surface of the femur (1) or a lateral crest that is split into a distinct first trochanter and third trochanter (2). ORDERED.
- 190. Pedal digit III, shape of second phalanx: short (disc-like) (0), absent (1).
- 191. Pedal digit IV, phalangeal number: 5 (0), 4 (1), or 3 (2).
- 192. Pedal digit IV, shape of second and third phalanges: long (0), short (1).
- 193. Pedal digit V, shape of second phalanx: short (0), absent (1).
- 194. Greatly enlarged vascular channels present (1) or absent (0).
- 195. Anterior face of dentary symphysis: unornamented (0), with median ridge (1).
- 196. Supinator process above ectepicondyle of humerus absent (0), present (1).
- 197. Morphology of supinator process: low, broadly separated from the shaft (0), tall and subvertical, with dorsal margin close to base of shaft (1), discrete, tab-like process occupying restricted portion of anterior face of distal humerus (2).
- 198. Angulation of subtemporal zygoma: horizontal to low-angle, such that dorsal margin of squamosal is ventral to skull roof in lateral view (0), steeply-angled, such that dorsal margin of squamosal is at the level of or dorsal to the skull roof in lateral view (1).
- 199. Median snout ridge: absent (0), restricted to premaxilla (1), present on premaxilla and nasal (2), present on premaxilla, nasal, and terminates in transversely-expanded boss on frontal (3). ORDERED.

APPENDIX 3. — Strict consensus tree, all taxa enabled, node numbers. https://doi.org/10.5852/cr-palevol2023v22a16_s2

APPENDIX 4. — Strict consensus tree, all taxa enabled, bootstrap supports. https://doi.org/10.5852/cr-palevol2023v22a16_s3

APPENDIX 5. — List of synapomorphies, all taxa, strict consensus.

Biarmosuchus tener
No autapomorphies

Hipposaurus boonstrai
Char. 8: 5.800 → 3.500
Char. 12: 1.060 → 1.070
Char. 15: 1.870 → 2.630
Char. 73: 2 → 0
Char. 95: 0 → 1
Char. 114: 2 → 0
Char. 166: 0 → 1
Char. 184: 1 → 0
Char. 191: 1 → 0

Archaeosyodon praeventor
Char. 141: 0 → 1

Titanophoneus potens
Char. 0: 0.509-0.547 → 0.758
Char. 4: 0.272-0.305 → 0.227
Char. 5: 0.072-0.104 → 0.051
Char. 12: 1.020-1.060 → 1.160
Char. 16: 0.545-0.558 → 0.500
Char. 17: 0.299-0.329 → 0.292
Char. 18: 0.149-0.200 → 0.274
Char. 22: 0.257-0.342 → 0.343
Char. 64: 0 → 1
Char. 73: 1 → 0
Char. 155: 0 → 1
Char. 185: 0 → 1

Gorgonops torvus
Char. 0: 0.509-0.547 → 0.504
Char. 2: 0.261-0.263 → 0.290
Char. 3: 0.842 → 1.150
Char. 8: 5.800-6.200 → 8.500
Char. 12: 1.020-1.060 → 0.977
Char. 62: 0 → 1
Char. 77: 0 → 2
Char. 158: 0 → 1
Char. 183: 0 → 1
Char. 186: 0 → 1
Char. 187: 0 → 1
Char. 188: 0 → 1

Lycosuchus vanderrieti
Char. 5: 0.218 → 0.303
Char. 8: 5.800-6.200 → 7.700
Char. 16: 0.545 → 0.500
Char. 17: 0.309-0.329 → 0.333
Char. 18: 0.200 → 0.294
Char. 22: 0.342 → 0.400
Char. 46: 0 → 1
Char. 57: 0 → 2
Char. 119: 0 → 1

Glanosuchus macrops
Char. 2: 0.244-0.261 → 0.145
Char. 3: 0.333 → 0.250
Char. 4: 0.352 → 0.367
Char. 8: 5.800-6.200 → 5.300
Char. 9: 0.090-0.094 → 0.050
Char. 15: 1.710-1.870 → 2.120
Char. 66: 0 → 1

Biseridens qilianicus
Char. 65: 0 → 1
Char. 90: 0 → 1
Char. 113: 1 → 0
Char. 159: 0 → 1

Anomocephalus africanus
No autapomorphies

Tiarajudens eccentricus
Char. 44: 1 → 0

Otsheria netzvetajevi
Char. 1: 5.364 → 5.425
Char. 2: 0.205-0.228 → 0.231
Char. 4: 0.407 → 0.512
Char. 5: 0.102-0.105 → 0.108
Char. 7: 0.198 → 0.181
Char. 10: 10.905 → 10.950
Char. 11: 15.400 → 15.500
Char. 12: 0.902 → 0.860
Char. 33: 1 → 0
Char. 101: 12 → 0

Ulemica
Char. 0: 0.381 → 0.470
Char. 2: 0.205-0.228 → 0.125
Char. 7: 0.198 → 0.216
Char. 8: 5.000-5.300 → 4.900
Char. 12: 0.902 → 1.098
Char. 44: 1 → 0
Char. 61: 0 → 1
Char. 124: 0 → 1

Suminia getmanovi
Char. 0: 0.339-0.381 → 0.336
Char. 1: 5.325-5.364 → 4.879
Char. 4: 0.272-0.305 → 0.230
Char. 14: 0.920-0.956 → 0.899
Char. 47: 1 → 2
Char. 57: 0 → 1
Char. 80: 01 → 2
Char. 103: 0 → 2
Char. 140: 1 → 2
Char. 162: 1 → 2

Patranomodon nyaphulii
Char. 0: 0.339 → 0.290
Char. 5: 0.094-0.105 → 0.076
Char. 7: 0.198 → 0.202
Char. 9: 0.090-0.094 → 0.043
Char. 10: 10.455-10.905 → 11.029
Char. 11: 11.600-12.000 → 13.700
Char. 12: 0.847-0.871 → 0.744
Char. 13: 0.355-0.395 → 0.476
Char. 14: 0.920-0.956 → 1.250
Char. 87: 1 → 0
Char. 105: 0 → 1
Char. 122: 0 → 1

Galeops whaitsi
Char. 2: 0.195-0.228 → 0.180
Char. 7: 0.140 → 0.136
Char. 8: 5.600-6.000 → 4.100
Char. 13: 0.355-0.395 → 0.489
Char. 16: 0.545-0.558 → 0.646
Char. 17: 0.396-0.401 → 0.356
Char. 92: 0 → 1
Char. 119: 0 → 1
Char. 121: 0 → 1
Char. 153: 0 → 1
Char. 168: 0 → 1

Galepus jouberti
Char. 3: 0.914 → 0.855
Char. 170: 0 → 1

Galechirus scholtzi
Char. 15: 0.968 → 0.700

Eodicyndon oelofseni
Char. 0: 0.339 → 0.351
Char. 3: 0.914 → 0.968
Char. 87: 1 → 0

Eodicyndon oosthuizeni
Char. 2: 0.195-0.228 → 0.234
Char. 6: 2.470 → 2.501
Char. 8: 6.600-8.100 → 8.200
Char. 11: 10.600-11.200 → 9.000
Char. 14: 0.708-0.723 → 0.698
Char. 15: 0.968 → 1.061
Char. 16: 0.487-0.558 → 0.446
Char. 17: 0.437-0.486 → 0.509
Char. 19: 0.301-0.553 → 0.300
Char. 22: 0.315-0.366 → 0.475
Char. 127: 1 → 0
Char. 177: 0 → 1
Char. 193: 0 → 1

APPENDIX 5. — Continuation.

Colobodectes cluveri

Char. 0: 0.231-0.237 → 0.203
 Char. 5: 0.222-0.257 → 0.269
 Char. 7: 0.140 → 0.142
 Char. 9: 0.182-0.199 → 0.206
 Char. 12: 0.850-0.871 → 0.948
 Char. 63: 0 → 1
 Char. 73: 1 → 0
 Char. 96: 0 → 1

Lanthanostegus mohoui

Char. 3: 0.795-0.908 → 0.661
 Char. 65: 0 → 1
 Char. 77: 1 → 2
 Char. 85: 2 → 0
 Char. 111: 0 → 1

Eosimops newtoni

Char. 0: 0.231-0.237 → 0.186
 Char. 1: 5.863 → 5.890
 Char. 2: 0.197 → 0.243
 Char. 9: 0.182-0.199 → 0.172
 Char. 10: 9.417 → 9.402
 Char. 11: 10.600-11.200 → 11.300
 Char. 12: 0.850 → 0.831
 Char. 13: 0.253-0.257 → 0.402
 Char. 14: 0.723-0.742 → 0.803
 Char. 16: 0.487-0.558 → 0.633
 Char. 22: 0.315-0.366 → 0.444
 Char. 65: 0 → 1
 Char. 114: 2 → 3
 Char. 122: 1 → 0
 Char. 143: 2 → 4
 Char. 146: 1 → 0
 Char. 177: 0 → 1

Diictodon feliceps

Char. 0: 0.238 → 0.247
 Char. 1: 5.810-5.863 → 5.925
 Char. 2: 0.195-0.197 → 0.223
 Char. 3: 0.795-0.864 → 0.640
 Char. 5: 0.228-0.257 → 0.273
 Char. 6: 1.751-2.013 → 1.702
 Char. 7: 0.123-0.126 → 0.135
 Char. 8: 8.100 → 8.000
 Char. 9: 0.182-0.199 → 0.214
 Char. 11: 10.600-11.200 → 11.900
 Char. 45: 1 → 2
 Char. 94: 0 → 1
 Char. 95: 0 → 1
 Char. 96: 0 → 1
 Char. 124: 1 → 2
 Char. 139: 1 → 2

Robertia broomiana

Char. 3: 0.795 → 0.721
 Char. 4: 0.541 → 0.555
 Char. 5: 0.257 → 0.259
 Char. 6: 1.751-2.013 → 1.681
 Char. 7: 0.123-0.126 → 0.108
 Char. 8: 8.100 → 8.600
 Char. 11: 10.600-11.200 → 9.800
 Char. 13: 0.253-0.257 → 0.132
 Char. 14: 0.723-0.742 → 0.711
 Char. 15: 0.901-0.904 → 0.868
 Char. 17: 0.466-0.486 → 0.502
 Char. 18: 0.260 → 0.227
 Char. 22: 0.315-0.366 → 0.309

Prosictodon dubei

Char. 1: 5.810-5.863 → 5.807
 Char. 2: 0.195-0.197 → 0.171
 Char. 4: 0.534-0.541 → 0.548
 Char. 6: 1.751-2.013 → 2.469
 Char. 7: 0.123-0.126 → 0.098
 Char. 9: 0.182-0.199 → 0.131
 Char. 10: 9.418-9.687 → 9.780
 Char. 11: 10.600-11.200 → 9.300
 Char. 14: 0.742 → 0.834
 Char. 15: 0.901 → 0.637

Abajudon kaayai

Char. 1: 5.396 → 5.215
 Char. 3: 0.867-0.906 → 1.030
 Char. 4: 0.515-0.541 → 0.412
 Char. 6: 1.548-1.565 → 2.844
 Char. 7: 0.118-0.126 → 0.146
 Char. 14: 0.798-0.859 → 0.898
 Char. 15: 0.924-0.938 → 1.016
 Char. 29: 1 → 0
 Char. 70: 1 → 0
 Char. 104: 1 → 0
 Char. 117: 0 → 1
 Char. 122: 1 → 0
 Char. 146: 1 → 0
 Char. 150: 0 → 1

Niassodon mfumukasi

Char. 12: 0.850-0.871 → 0.697
 Char. 19: 0.301 → 0.214
 Char. 44: 2 → 1
 Char. 54: 0 → 1
 Char. 67: 1 → 2
 Char. 68: 0 → 1
 Char. 69: 1 → 2
 Char. 73: 1 → 2
 Char. 81: 1 → 0
 Char. 102: 0 → 1
 Char. 111: 0 → 1
 Char. 164: 2 → 1

Brachyprosopus broomi

Char. 5: 0.222-0.257 → 0.338
 Char. 7: 0.123-0.126 → 0.129
 Char. 8: 8.100-8.400 → 6.800
 Char. 12: 0.850-0.871 → 0.898
 Char. 13: 0.208-0.257 → 0.132
 Char. 14: 0.723 → 0.715
 Char. 15: 0.924-0.928 → 0.824
 Char. 16: 0.554-0.594 → 0.612
 Char. 25: 0 → 1
 Char. 34: 0 → 1
 Char. 46: 0 → 1
 Char. 77: 1 → 2
 Char. 93: 1 → 0
 Char. 116: 0 → 1

Endothiodon tolani

Char. 5: 0.126-0.257 → 0.025
 Char. 7: 0.111 → 0.109
 Char. 8: 8.400-9.400 → 10.600
 Char. 14: 0.798 → 0.723
 Char. 94: 0 → 1

Endothiodon bathystoma

Char. 0: 0.328 → 0.335
 Char. 3: 0.396 → 0.268
 Char. 5: 0.126-0.257 → 0.400
 Char. 6: 1.505 → 1.457
 Char. 8: 8.400-9.400 → 8.100
 Char. 12: 0.902-0.907 → 0.988
 Char. 13: 0.319 → 0.373
 Char. 15: 0.825 → 0.730
 Char. 38: 1 → 0
 Char. 44: 2 → 1
 Char. 60: 0 → 1
 Char. 66: 0 → 1
 Char. 68: 0 → 1
 Char. 110: 1 → 0

Pristerodon mackayi

Char. 0: 0.231-0.237 → 0.225
 Char. 1: 5.810-5.863 → 5.874
 Char. 2: 0.190-0.197 → 0.184
 Char. 3: 0.867-0.998 → 1.026
 Char. 4: 0.520-0.541 → 0.582
 Char. 8: 8.100-8.400 → 10.000
 Char. 9: 0.182-0.199 → 0.206
 Char. 12: 0.850-0.871 → 0.813
 Char. 17: 0.437-0.486 → 0.430
 Char. 19: 0.301-0.454 → 0.275
 Char. 22: 0.315-0.366 → 0.275
 Char. 79: 0 → 1
 Char. 167: 0 → 1

APPENDIX 5. — Continuation.

Emydops

Char. 1: 5.874 → 5.872
 Char. 2: 0.207 → 0.204
 Char. 10: 9.740-9.775 → 9.667
 Char. 11: 10.600-11.000 → 9.300
 Char. 38: 1 → 0
 Char. 81: 1 → 0
 Char. 128: 1 → 0

Compsodon helmoedi

Char. 0: 0.220 → 0.196
 Char. 3: 0.906 → 1.066
 Char. 4: 0.473-0.537 → 0.431

Char. 6: 1.646 → 1.710
 Char. 7: 0.118 → 0.082
 Char. 8: 9.800 → 10.300
 Char. 9: 0.176 → 0.220
 Char. 10: 9.740-9.775 → 9.858
 Char. 12: 0.840 → 0.817
 Char. 41: 0 → 1
 Char. 61: 0 → 1
 Char. 67: 1 → 2
 Char. 68: 0 → 1
 Char. 70: 1 → 0
 Char. 71: 0 → 1
 Char. 77: 1 → 3
 Char. 102: 0 → 1
 Char. 115: 1 → 0
 Char. 120: 0 → 1
 Char. 131: 1 → 0

Digalodon rubidgei

Char. 0: 0.269-0.281 → 0.354
 Char. 1: 5.948-5.950 → 6.155
 Char. 7: 0.118-0.123 → 0.134
 Char. 24: 0 → 2
 Char. 48: 1 → 0
 Char. 77: 1 → 3
 Char. 79: 0 → 1

Illiptosaurus imperforatus

Char. 2: 0.202-0.240 → 0.198
 Char. 4: 0.473-0.483 → 0.407
 Char. 15: 0.924 → 0.667
 Char. 137: 0 → 1

Rastodon procurvidens

Char. 0: 0.231-0.279 → 0.197
 Char. 2: 0.207-0.232 → 0.199
 Char. 4: 0.541-0.544 → 0.558
 Char. 5: 0.260-0.281 → 0.298
 Char. 8: 8.250-8.333 → 6.600
 Char. 9: 0.121-0.132 → 0.105
 Char. 12: 0.850-0.871 → 0.798
 Char. 13: 0.212-0.240 → 0.100
 Char. 14: 0.723-0.730 → 0.623
 Char. 15: 0.766-0.819 → 0.667
 Char. 136: 1 → 2

Dicynodontoides

Char. 6: 1.500-1.565 → 1.492
 Char. 7: 0.116 → 0.085
 Char. 10: 9.775 → 9.814
 Char. 12: 0.853-0.871 → 0.887
 Char. 26: 0 → 1
 Char. 44: 1 → 2

Kombuisia frerensis

Char. 0: 0.269 → 0.193
 Char. 1: 5.950 → 5.976
 Char. 3: 0.764 → 0.400
 Char. 4: 0.539 → 0.555
 Char. 6: 1.500-1.565 → 1.589
 Char. 7: 0.116 → 0.195
 Char. 10: 9.775 → 9.645
 Char. 12: 0.853-0.871 → 0.746
 Char. 14: 0.726 → 0.684
 Char. 48: 1 → 0
 Char. 54: 0 → 1
 Char. 74: 0 → 1
 Char. 131: 1 → 0
 Char. 146: 0 → 1
 Char. 150: 1 → 0
 Char. 160: 1 → 0

Myosaurus gracilis

Char. 0: 0.269-0.279 → 0.260
 Char. 1: 5.948-5.950 → 5.902
 Char. 6: 1.500-1.565 → 1.590
 Char. 7: 0.116 → 0.085
 Char. 9: 0.181 → 0.208
 Char. 11: 10.600-11.000 → 9.600
 Char. 14: 0.726-0.750 → 0.958
 Char. 15: 0.924-0.928 → 0.942
 Char. 16: 0.485-0.554 → 0.586
 Char. 22: 0.353-0.359 → 0.208
 Char. 25: 1 → 0
 Char. 28: 0 → 1
 Char. 54: 0 → 1
 Char. 57: 0 → 2
 Char. 98: 1 → 0
 Char. 174: 0 → 1
 Char. 175: 0 → 1

Kembawacela kitchingi

Char. 0: 0.308-0.311 → 0.372
 Char. 3: 1.319-1.404 → 1.487
 Char. 6: 1.490-1.500 → 1.455
 Char. 12: 0.872 → 0.969
 Char. 13: 0.380 → 0.415
 Char. 15: 0.914-0.964 → 0.990
 Char. 28: 0 → 2
 Char. 44: 1 → 2
 Char. 96: 1 → 0
 Char. 134: 0 → 1
 Char. 159: 1 → 0

Cistecephalus microrhinus

Char. 1: 5.948-5.950 → 6.056
 Char. 4: 0.421-0.483 → 0.509
 Char. 11: 10.600-11.000 → 10.200
 Char. 14: 0.726-0.730 → 0.687
 Char. 17: 0.419 → 0.403
 Char. 22: 0.353-0.359 → 0.324
 Char. 61: 0 → 1
 Char. 174: 0 → 1

Sauroscoptor tharavati

Char. 12: 0.872 → 0.912
 Char. 13: 0.380 → 0.564
 Char. 15: 0.789-0.928 → 0.714

Cistecephalooides boonstrai

Char. 1: 5.948-5.950 → 6.047
 Char. 2: 0.330-0.383 → 0.425
 Char. 7: 0.135 → 0.194
 Char. 10: 10.119-10.173 → 10.305
 Char. 11: 10.600-11.650 → 12.500
 Char. 12: 0.836 → 0.632
 Char. 62: 0 → 1
 Char. 88: 1 → 0
 Char. 127: 0 → 1

Kawingasaurus fossilis

Char. 1: 5.948-5.950 → 5.933
 Char. 4: 0.357-0.372 → 0.340
 Char. 11: 10.600-11.650 → 10.000
 Char. 13: 0.346 → 0.286
 Char. 56: 1 → 0
 Char. 57: 0 → 2
 Char. 76: 0 → 1
 Char. 130: 1 → 0
 Char. 137: 1 → 0
 Char. 147: 2 → 0
 Char. 149: 2 → 1
 Char. 150: 1 → 0

APPENDIX 5. — Continuation.

Daqingshanodon limbus

Char. 2: 0.220-0.232 → 0.260
 Char. 3: 0.672-0.892 → 0.619
 Char. 4: 0.541-0.544 → 0.442
 Char. 5: 0.203 → 0.180
 Char. 7: 0.083 → 0.080
 Char. 12: 0.831 → 0.808
 Char. 63: 0 → 1
 Char. 77: 1 → 3

Keyseria benjamini

Char. 1: 6.112 → 6.155
 Char. 2: 0.220-0.232 → 0.159
 Char. 3: 0.672-0.892 → 1.034
 Char. 4: 0.541-0.544 → 0.605
 Char. 6: 1.528 → 1.600
 Char. 11: 10.300 → 9.000
 Char. 54: 0 → 1
 Char. 71: 1 → 0
 Char. 113: 1 → 0

Rhachiocephalus magnus

Char. 0: 0.320 → 0.329
 Char. 4: 0.566 → 0.598
 Char. 8: 8.100-8.333 → 8.800
 Char. 9: 0.132-0.141 → 0.143
 Char. 10: 9.219-9.740 → 9.170
 Char. 11: 12.300 → 12.800
 Char. 12: 0.936 → 1.010
 Char. 15: 0.752 → 0.777
 Char. 79: 1 → 0
 Char. 83: 1 → 0
 Char. 150: 2 → 0
 Char. 151: 1 → 0
 Char. 168: 0 → 1

Kitchinganomodon crassus

Char. 1: 6.094 → 6.137
 Char. 2: 0.271 → 0.318
 Char. 3: 0.738 → 0.708
 Char. 5: 0.606 → 0.752
 Char. 6: 1.480 → 1.556
 Char. 7: 0.094-0.098 → 0.108
 Char. 8: 8.100-8.333 → 7.400
 Char. 9: 0.132-0.141 → 0.070
 Char. 10: 9.219-9.740 → 9.747
 Char. 11: 12.300 → 11.100
 Char. 13: 0.167 → 0.165
 Char. 14: 0.838 → 0.843
 Char. 17: 0.491-0.506 → 0.466
 Char. 95: 1 → 0
 Char. 114: 2 → 3

Oudenodon bainii

Char. 0: 0.284-0.320 → 0.281
 Char. 2: 0.183-0.197 → 0.173
 Char. 4: 0.565-0.566 → 0.609
 Char. 7: 0.094-0.098 → 0.092
 Char. 11: 12.300 → 11.300
 Char. 12: 0.875-0.882 → 0.864
 Char. 13: 0.212-0.237 → 0.264
 Char. 16: 0.531-0.550 → 0.570
 Char. 20: 1.033-1.130 → 0.765
 Char. 194: 0 → 1

Tropidostoma dubium

Char. 1: 6.054-6.058 → 5.989
 Char. 3: 0.844 → 0.899
 Char. 8: 8.100-8.333 → 8.800
 Char. 10: 9.219-9.740 → 9.106
 Char. 15: 0.745-0.752 → 0.766
 Char. 19: 0.514 → 0.474
 Char. 20: 1.033-1.130 → 1.368
 Char. 22: 0.391 → 0.378
 Char. 95: 1 → 0
 Char. 96: 1 → 0

Australobarbarus

Char. 0: 0.284-0.320 → 0.333
 Char. 3: 0.844 → 0.697
 Char. 4: 0.565 → 0.561
 Char. 5: 0.277 → 0.298
 Char. 6: 1.436 → 1.324
 Char. 7: 0.098 → 0.101
 Char. 8: 8.100-8.333 → 6.100
 Char. 9: 0.140-0.141 → 0.160
 Char. 10: 9.219-9.740 → 9.822
 Char. 11: 12.400 → 13.350
 Char. 13: 0.212-0.237 → 0.193
 Char. 14: 0.758 → 0.624
 Char. 15: 0.745-0.752 → 0.694
 Char. 16: 0.531 → 0.466
 Char. 17: 0.491-0.503 → 0.485
 Char. 19: 0.514 → 0.848
 Char. 21: 0.345 → 0.333
 Char. 104: 1 → 0
 Char. 112: 0 → 1

Syops vanhoopeni

Char. 3: 0.562-0.563 → 0.484
 Char. 27: 2 → 1
 Char. 53: 0 → 1
 Char. 99: 1 → 2
 Char. 126: 1 → 0
 Char. 131: 1 → 0
 Char. 144: 1 → 0
 Char. 154: 1 → 0
 Char. 198: 1 → 2

Odontocyclops whaitsi

Char. 0: 0.289-0.320 → 0.376
 Char. 3: 0.844-0.892 → 0.988
 Char. 6: 1.458-1.480 → 1.448
 Char. 7: 0.094-0.098 → 0.092
 Char. 8: 8.250-8.333 → 10.100
 Char. 9: 0.132-0.141 → 0.131
 Char. 15: 0.745-0.752 → 0.731
 Char. 16: 0.550 → 0.551
 Char. 18: 0.366 → 0.427
 Char. 19: 0.514 → 0.435
 Char. 21: 0.353-0.395 → 0.426
 Char. 60: 0 → 2
 Char. 68: 0 → 1

Idelesaurus tataricus

Char. 0: 0.289-0.320 → 0.367
 Char. 1: 6.003-6.066 → 5.967
 Char. 2: 0.220-0.232 → 0.175
 Char. 3: 0.844-0.892 → 1.022
 Char. 4: 0.534-0.544 → 0.500
 Char. 5: 0.213-0.232 → 0.174
 Char. 9: 0.132-0.141 → 0.173
 Char. 10: 9.740-9.851 → 10.118
 Char. 12: 0.910-0.929 → 0.969
 Char. 57: 0 → 1
 Char. 60: 0 → 1
 Char. 68: 0 → 1
 Char. 96: 1 → 0
 Char. 120: 1 → 0
 Char. 131: 1 → 0

Bulbasaurus phylloxyron

Char. 0: 0.289-0.300 → 0.284
 Char. 3: 0.844-0.892 → 0.562
 Char. 5: 0.213-0.232 → 0.233
 Char. 6: 1.425-1.468 → 1.362
 Char. 8: 8.250-8.720 → 10.333
 Char. 9: 0.122-0.141 → 0.052
 Char. 11: 13.500 → 14.780
 Char. 14: 0.693-0.749 → 0.643
 Char. 53: 1 → 0
 Char. 59: 1 → 0

Aulacephalodon bainii

Char. 2: 0.305 → 0.323
 Char. 5: 0.213-0.232 → 0.204
 Char. 7: 0.107-0.112 → 0.117
 Char. 8: 8.250-8.720 → 6.800
 Char. 13: 0.204-0.205 → 0.172
 Char. 144: 1 → 0
 Char. 153: 0 → 1

APPENDIX 5. — Continuation.

Pelanomodon moschops
 Char. 1: 6.049-6.089 → 6.093
 Char. 3: 0.892-0.908 → 0.912
 Char. 4: 0.534-0.583 → 0.584
 Char. 8: 8.720 → 9.400
 Char. 9: 0.141 → 0.155
 Char. 11: 13.100-13.500 → 12.300
 Char. 15: 0.764-0.785 → 0.742

Geikia locusticeps
 Char. 0: 0.289-0.300 → 0.256
 Char. 2: 0.305 → 0.278
 Char. 4: 0.529 → 0.514
 Char. 6: 1.429-1.468 → 1.627
 Char. 11: 13.100-13.500 → 13.900
 Char. 12: 0.801-0.822 → 0.756
 Char. 81: 1 → 0
 Char. 150: 2 → 0

Geikia elginensis
 Char. 0: 0.289-0.300 → 0.366
 Char. 2: 0.305 → 0.521
 Char. 3: 0.892-0.908 → 0.846
 Char. 12: 0.801-0.822 → 0.829
 Char. 13: 0.205 → 0.212
 Char. 14: 0.818-0.856 → 0.900
 Char. 15: 0.848 → 0.987
 Char. 54: 0 → 1
 Char. 55: 0 → 1
 Char. 118: 0 → 1
 Char. 137: 1 → 0

Elph borealis
 No autapomorphies

Interpresosaurus blomi
 Char. 73: 0 → 1

Katumbia parringtoni
 Char. 0: 0.240-0.279 → 0.196
 Char. 1: 5.927 → 5.868
 Char. 3: 0.640 → 0.527
 Char. 5: 0.290 → 0.347
 Char. 8: 8.900 → 9.300
 Char. 11: 13.000 → 14.400
 Char. 14: 0.781 → 0.833
 Char. 51: 1 → 0
 Char. 68: 0 → 1
 Char. 112: 0 → 1
 Char. 125: 0 → 1
 Char. 131: 1 → 0

Delectosaurus arefjevi
 Char. 1: 5.937-6.019 → 5.861
 Char. 2: 0.253 → 0.258
 Char. 3: 0.685 → 0.702
 Char. 7: 0.116-0.117 → 0.119
 Char. 9: 0.121 → 0.130
 Char. 11: 13.900 → 14.700
 Char. 40: 0 → 1
 Char. 120: 2 → 1
 Char. 131: 1 → 0
 Char. 135: 1 → 0

Dicynodon lacerticeps
 Char. 0: 0.308 → 0.324
 Char. 11: 12.000 → 11.900
 Char. 13: 0.219-0.240 → 0.241
 Char. 112: 1 → 0

Dicynodon angielczyki
 Char. 3: 0.607 → 0.524
 Char. 4: 0.546 → 0.569
 Char. 6: 1.443-1.485 → 1.351
 Char. 7: 0.116-0.117 → 0.105
 Char. 8: 7.700 → 7.560
 Char. 9: 0.121 → 0.114
 Char. 10: 9.869 → 9.950
 Char. 14: 0.749 → 0.808
 Char. 150: 2 → 0

Daptocephalus huenei
 Char. 3: 0.562-0.563 → 0.564
 Char. 6: 1.338-1.347 → 1.250
 Char. 7: 0.118 → 0.123
 Char. 9: 0.111 → 0.117
 Char. 12: 0.858-0.895 → 1.024

Daptocephalus leoniceps
 Char. 0: 0.292 → 0.268
 Char. 2: 0.230 → 0.237
 Char. 3: 0.562-0.563 → 0.539
 Char. 5: 0.414 → 0.437
 Char. 6: 1.338-1.347 → 1.500
 Char. 10: 9.680 → 9.378
 Char. 17: 0.543 → 0.545

Dinanomodon gilli
 Char. 3: 0.562-0.563 → 0.480
 Char. 5: 0.405-0.414 → 0.522
 Char. 12: 0.895 → 1.047
 Char. 54: 1 → 0

Peramodon amalitzkii
 Char. 0: 0.292-0.315 → 0.272
 Char. 11: 9.900-10.250 → 9.500
 Char. 13: 0.186-0.238 → 0.167
 Char. 14: 0.763 → 0.676
 Char. 15: 0.724-0.750 → 0.680
 Char. 60: 1 → 0

Taoheodon baizhijuni
 Char. 1: 5.927-5.982 → 6.100
 Char. 6: 1.443-1.485 → 1.180
 Char. 7: 0.112-0.117 → 0.110
 Char. 9: 0.121-0.132 → 0.105
 Char. 10: 9.740-9.775 → 9.640
 Char. 13: 0.219-0.240 → 0.285
 Char. 41: 0 → 1
 Char. 55: 0 → 1
 Char. 63: 0 → 1
 Char. 110: 1 → 0
 Char. 132: 1 → 0
 Char. 133: 0 → 1

Counillonia superoculis
 Char. 4: 0.408 → 0.276
 Char. 5: 0.260-0.281 → 0.134
 Char. 11: 12.000 → 9.616
 Char. 57: 0 → 2

Repelinosaurus robustus
 Char. 0: 0.240-0.297 → 0.200
 Char. 11: 12.000 → 14.698
 Char. 12: 0.876 → 0.829
 Char. 34: 0 → 1
 Char. 54: 0 → 1

Vivaxosaurus trautscholdi
 Char. 0: 0.369 → 0.380
 Char. 2: 0.253 → 0.230
 Char. 4: 0.546 → 0.481
 Char. 5: 0.334 → 0.285
 Char. 6: 1.618 → 1.824
 Char. 8: 7.800 → 7.900
 Char. 10: 9.798 → 10.203
 Char. 12: 0.985 → 1.041
 Char. 41: 0 → 1
 Char. 55: 0 → 1
 Char. 61: 1 → 0
 Char. 71: 2 → 1
 Char. 95: 1 → 0
 Char. 96: 1 → 0

APPENDIX 5. — Continuation.

<i>Jimusaria sinkianensis</i>	<i>Euptychognathus bathyrhynchus</i>	<i>Lystrosaurus declivis</i>
Char. 2: 0.253 → 0.278	Char. 0: 0.304-0.315 → 0.336	Char. 0: 0.315 → 0.347
Char. 4: 0.546-0.604 → 0.767	Char. 2: 0.224-0.253 → 0.130	Char. 1: 6.003-6.005 → 5.954
Char. 5: 0.334-0.343 → 0.464	Char. 4: 0.523-0.553 → 0.560	Char. 5: 0.119 → 0.112
Char. 7: 0.116-0.117 → 0.089	Char. 7: 0.116-0.118 → 0.091	Char. 6: 1.664-2.001 → 2.141
Char. 11: 10.100-10.250 → 8.900	Char. 9: 0.097-0.100 → 0.084	Char. 8: 8.400 → 8.800
Char. 12: 0.926-0.985 → 0.992	Char. 10: 9.680-9.798 → 9.663	Char. 16: 0.473 → 0.418
Char. 13: 0.219-0.240 → 0.251	Char. 12: 0.816-0.874 → 0.792	Char. 17: 0.460-0.485 → 0.458
Char. 15: 0.731-0.754 → 0.699	Char. 15: 0.734-0.754 → 0.815	Char. 20: 1.455 → 1.300
Char. 51: 1 → 2	Char. 56: 2 → 0	
Char. 79: 0 → 1	Char. 67: 2 → 1	
Char. 112: 1 → 0	Char. 116: 1 → 0	
<i>Sintocephalus alticeps</i>	<i>Lystrosaurus hedini</i>	<i>Lystrosaurus murrayi</i>
Char. 0: 0.315 → 0.354	Char. 0: 0.315 → 0.320	Char. 0: 0.304-0.315 → 0.288
Char. 1: 5.994 → 5.969	Char. 1: 6.072 → 6.111	Char. 2: 0.383-0.424 → 0.427
Char. 3: 0.562-0.563 → 0.516	Char. 5: 0.119 → 0.146	Char. 3: 0.689-0.705 → 0.726
Char. 10: 9.599 → 9.399	Char. 6: 1.664-1.764 → 1.471	Char. 7: 0.157-0.162 → 0.175
Char. 11: 9.900-10.250 → 9.600	Char. 7: 0.165 → 0.174	Char. 9: 0.097-0.100 → 0.101
Char. 12: 0.839-0.895 → 1.022	Char. 8: 8.400 → 9.200	Char. 10: 10.145-10.309 → 10.358
Char. 56: 2 → 0	Char. 9: 0.086-0.097 → 0.079	Char. 11: 10.100-10.250 → 11.700
Char. 61: 1 → 0	Char. 11: 10.900 → 11.400	Char. 13: 0.294-0.315 → 0.316
Char. 67: 2 → 1	Char. 12: 0.805 → 0.673	Char. 14: 0.763-0.790 → 0.793
<i>Basilodon woodwardi</i>	Char. 14: 0.711 → 0.691	Char. 19: 0.750-0.787 → 0.843
Char. 2: 0.224-0.244 → 0.212	Char. 15: 0.706-0.711 → 0.781	Char. 21: 0.352 → 0.392
Char. 3: 0.562-0.563 → 0.722	Char. 54: 1 → 0	Char. 22: 0.494-0.545 → 0.605
Char. 4: 0.522 → 0.497	Char. 57: 1 → 0	Char. 135: 1 → 0
Char. 5: 0.294 → 0.225	Char. 61: 1 → 0	
Char. 6: 1.338 → 1.305	Char. 67: 2 → 1	
Char. 7: 0.124 → 0.128	Char. 104: 0 → 1	
Char. 8: 6.500 → 5.700		
Char. 9: 0.132 → 0.139		
Char. 11: 9.900-10.250 → 12.600		
Char. 12: 0.839-0.895 → 0.814		
Char. 99: 1 → 2		
<i>Turfanodon bogdaensis</i>	<i>Lystrosaurus maccagii</i>	<i>Shansiodon</i>
Char. 3: 0.562-0.563 → 0.588	Char. 0: 0.315 → 0.274	Char. 0: 0.267 → 0.265
Char. 6: 1.338-1.347 → 1.327	Char. 2: 0.383-0.414 → 0.347	Char. 3: 0.201 → 0.163
Char. 11: 9.900-10.250 → 10.300	Char. 3: 0.689-0.705 → 0.656	Char. 5: 0.466 → 0.633
Char. 61: 1 → 0	Char. 4: 0.413 → 0.325	Char. 8: 7.000 → 7.200
Char. 79: 0 → 1	Char. 5: 0.119 → 0.108	Char. 12: 0.983-1.004 → 1.129
Char. 106: 1 → 2	Char. 9: 0.086-0.097 → 0.123	Char. 67: 1 → 2
<i>Gordonia traquairi</i>	Char. 10: 10.145-10.203 → 10.022	
Char. 0: 0.304-0.307 → 0.252	Char. 13: 0.294-0.315 → 0.354	
Char. 2: 0.224-0.253 → 0.139	Char. 55: 0 → 1	
Char. 5: 0.334-0.343 → 0.309	Char. 56: 2 → 0	
Char. 13: 0.219-0.240 → 0.188		
Char. 15: 0.734-0.754 → 0.773		
Char. 16: 0.476-0.490 → 0.543		
Char. 18: 0.317-0.348 → 0.144		
Char. 22: 0.491-0.494 → 0.476		
	<i>Lystrosaurus curvatus</i>	<i>Tetragonias njalilus</i>
	Char. 8: 8.400 → 7.400	Char. 1: 6.064-6.099 → 5.912
	Char. 11: 9.700-10.250 → 8.600	Char. 4: 0.523-0.538 → 0.574
	Char. 12: 0.816-0.874 → 0.906	Char. 8: 6.900-7.000 → 6.800
	Char. 13: 0.294-0.315 → 0.289	Char. 14: 0.821 → 0.858
	Char. 15: 0.706-0.711 → 0.643	Char. 18: 0.361 → 0.300
	Char. 21: 0.347-0.352 → 0.313	Char. 21: 0.310-0.352 → 0.304
		<i>Vinceria andina</i>
		Char. 4: 0.523-0.538 → 0.490
		Char. 7: 0.130 → 0.137
		Char. 9: 0.100 → 0.153
		Char. 10: 9.780-10.009 → 10.552
		Char. 11: 11.200 → 11.300
		Char. 51: 1 → 2
		Char. 86: 1 → 0

APPENDIX 5. — Continuation.

Rhinodicynodon gracile

Char. 1: 6.064-6.099 → 6.213
 Char. 6: 1.443-1.485 → 1.568
 Char. 7: 0.116-0.118 → 0.100
 Char. 10: 9.680-9.798 → 9.174
 Char. 14: 0.821 → 0.875
 Char. 17: 0.479-0.481 → 0.354
 Char. 22: 0.491-0.494 → 0.383
 Char. 57: 0 → 1
 Char. 131: 1 → 0

Acratophorus argentinensis

Char. 0: 0.376-0.423 → 0.329
 Char. 2: 0.403-0.413 → 0.445
 Char. 3: 0.285-0.293 → 0.205
 Char. 4: 0.515-0.574 → 0.666
 Char. 6: 1.468-1.505 → 1.872
 Char. 7: 0.122-0.143 → 0.120
 Char. 8: 6.900-7.000 → 6.655
 Char. 9: 0.088-0.091 → 0.094
 Char. 11: 10.000-10.600 → 8.055
 Char. 14: 0.734-0.786 → 0.716
 Char. 16: 0.442-0.494 → 0.345
 Char. 17: 0.519-0.520 → 0.468
 Char. 18: 0.450 → 0.292
 Char. 22: 0.411-0.526 → 0.574
 Char. 61: 0 → 1
 Char. 111: 0 → 1
 Char. 158: 1 → 0
 Char. 194: 1 → 0

Kannemeyeria simocephalus

Char. 43: 1 → 0

Kannemeyeria aganosteus

No autapomorphies

Kannemeyeria lophorhinus

Char. 0: 0.421 → 0.361
 Char. 1: 6.121 → 6.286
 Char. 3: 0.460-0.526 → 0.663
 Char. 6: 1.468-1.505 → 2.051
 Char. 8: 9.800-9.900 → 10.800
 Char. 13: 0.179 → 0.077
 Char. 15: 0.668-0.686 → 0.542
 Char. 60: 1 → 2
 Char. 67: 2 → 1
 Char. 131: 1 → 0
 Char. 158: 1 → 0
 Char. 160: 1 → 0

Dolichuranus primaevus

Char. 0: 0.376-0.378 → 0.356
 Char. 1: 6.104-6.105 → 6.079
 Char. 4: 0.515-0.518 → 0.484
 Char. 5: 0.446-0.476 → 0.400
 Char. 6: 1.414-1.431 → 1.339
 Char. 8: 6.900-7.000 → 8.700
 Char. 10: 10.155-10.206 → 10.672
 Char. 11: 10.000-10.400 → 9.700
 Char. 13: 0.202-0.205 → 0.192
 Char. 15: 0.705-0.766 → 0.542
 Char. 57: 1 → 0
 Char. 106: 2 → 1
 Char. 114: 1 → 6
 Char. 126: 1 → 0
 Char. 169: 1 → 0
 Char. 186: 1 → 0

Sinokannemeyeria

Char. 2: 0.409-0.413 → 0.478
 Char. 3: 0.460 → 0.543
 Char. 5: 0.195 → 0.175
 Char. 8: 7.500 → 5.900
 Char. 9: 0.102 → 0.109
 Char. 10: 10.027-10.206 → 10.469
 Char. 14: 0.734-0.786 → 0.549
 Char. 15: 0.515 → 0.385
 Char. 17: 0.519-0.520 → 0.489
 Char. 18: 0.478 → 0.556
 Char. 20: 1.206-1.239 → 1.187
 Char. 21: 0.411 → 0.408
 Char. 34: 1 → 0
 Char. 40: 0 → 1
 Char. 92: 0 → 1
 Char. 178: 0 → 1

Parakannemeyeria

Char. 1: 6.140-6.203 → 6.280
 Char. 2: 0.409-0.413 → 0.377
 Char. 3: 0.460 → 0.359
 Char. 4: 0.382 → 0.354
 Char. 7: 0.147-0.161 → 0.122
 Char. 10: 10.027-10.206 → 9.688
 Char. 13: 0.202-0.243 → 0.166
 Char. 14: 0.734-0.786 → 0.790
 Char. 19: 0.458 → 0.443
 Char. 20: 1.206-1.239 → 1.465
 Char. 22: 0.405 → 0.294
 Char. 43: 0 → 1
 Char. 114: 2 → 1
 Char. 164: 2 → 3
 Char. 173: 1 → 0

Xiyukannemeyeria brevirostris

Char. 0: 0.420-0.455 → 0.286
 Char. 7: 0.147-0.161 → 0.169
 Char. 8: 7.500-7.800 → 8.500
 Char. 9: 0.088-0.091 → 0.086
 Char. 11: 10.800-11.300 → 8.900
 Char. 12: 0.918-0.920 → 0.795
 Char. 13: 0.202-0.243 → 0.320
 Char. 54: 0 → 1
 Char. 131: 1 → 0

Rabidosaurus cristatus

Char. 0: 0.423 → 0.464
 Char. 3: 0.285-0.293 → 0.268
 Char. 4: 0.515-0.574 → 0.607
 Char. 81: 0 → 1

Rhadiodromus

Char. 0: 0.420-0.490 → 0.509
 Char. 10: 10.027-10.206 → 10.023
 Char. 18: 0.450-0.478 → 0.604
 Char. 67: 2 → 1
 Char. 68: 0 → 1
 Char. 106: 2 → 1
 Char. 117: 0 → 1
 Char. 132: 0 → 1

Wadiasaurus indicus

Char. 3: 0.285-0.293 → 0.539
 Char. 4: 0.515-0.574 → 0.506
 Char. 64: 1 → 0

Shaanbeikannemeyeria

Char. 0: 0.421-0.490 → 0.527
 Char. 2: 0.409-0.413 → 0.513
 Char. 3: 0.460-0.526 → 0.886
 Char. 5: 0.254-0.318 → 0.414
 Char. 9: 0.088-0.091 → 0.176
 Char. 10: 10.432-10.478 → 10.642
 Char. 12: 1.147-1.154 → 1.432
 Char. 17: 0.558 → 0.580
 Char. 67: 2 → 1
 Char. 144: 1 → 0

Rechnisaurus cristarhynchus

Char. 0: 0.490 → 0.510
 Char. 2: 0.409-0.413 → 0.436
 Char. 3: 0.460-0.526 → 0.154
 Char. 5: 0.233 → 0.211
 Char. 7: 0.147 → 0.140
 Char. 64: 1 → 0

APPENDIX 5. — Continuation.

Uralokannemeyeria vjuschkovi
Char. 2: 0.409-0.413 → 0.407

Angonisaurus cruckshanki
Char. 0: 0.376-0.378 → 0.339
Char. 1: 6.104-6.177 → 6.301
Char. 2: 0.461-0.468 → 0.514
Char. 3: 0.450-0.618 → 0.667
Char. 4: 0.515-0.518 → 0.572
Char. 5: 0.446-0.499 → 0.600
Char. 6: 1.414-1.431 → 1.491
Char. 7: 0.156 → 0.190
Char. 13: 0.202-0.205 → 0.143
Char. 14: 0.814-0.822 → 0.785
Char. 20: 1.789 → 2.541
Char. 41: 1 → 0
Char. 196: 0 → 1

Ufudocyclops mukanelai
Char. 11: 10.000-10.400 → 10.900
Char. 56: 3 → 2
Char. 66: 1 → 0
Char. 72: 0 → 1
Char. 103: 1 → 2
Char. 111: 0 → 1

Zambiasaurus submersus
Char. 17: 0.524-0.530 → 0.498
Char. 21: 0.417-0.433 → 0.401
Char. 43: 1 → 0
Char. 51: 1 → 0
Char. 168: 0 → 1
Char. 175: 0 → 1
Char. 178: 1 → 0
Char. 196: 0 → 1

Placerias hesternus
Char. 50: 0 → 1
Char. 67: 2 → 1
Char. 198: 0 → 1

Moghreberia nmachouensis
Char. 51: 0 → 2
Char. 158: 1 → 0

Pentasaurus goggiae
No autapomorphies

Stahleckeria potens
Char. 0: 0.411 → 0.438
Char. 1: 6.104-6.177 → 5.992
Char. 2: 0.461 → 0.445
Char. 3: 0.618 → 0.726
Char. 5: 0.332-0.368 → 0.288
Char. 7: 0.156 → 0.183
Char. 9: 0.060-0.084 → 0.052
Char. 11: 9.200 → 8.700
Char. 12: 0.983-1.012 → 0.953
Char. 14: 0.832 → 0.856
Char. 19: 0.592 → 0.391
Char. 20: 1.944 → 2.217
Char. 21: 0.433 → 0.434
Char. 28: 2 → 0
Char. 41: 1 → 2
Char. 106: 2 → 1
Char. 111: 0 → 1

Sangusaurus parringtonii
No autapomorphies

Sangusaurus sp.
Char. 43: 1 → 0

Eubrachiosaurus browni
Char. 17: 0.524-0.530 → 0.538

Ischigualastia jensi
Char. 0: 0.392 → 0.482
Char. 5: 0.499 → 0.528
Char. 6: 1.414-1.431 → 1.390
Char. 10: 10.155-10.206 → 10.023
Char. 12: 1.004-1.012 → 1.032
Char. 14: 0.822 → 0.912
Char. 15: 0.766 → 0.841
Char. 16: 0.427 → 0.419
Char. 18: 0.529 → 0.561
Char. 21: 0.417-0.433 → 0.412
Char. 41: 1 → 2
Char. 54: 1 → 0
Char. 66: 0 → 1
Char. 114: 1 → 5
Char. 167: 0 → 1
Char. 198: 0 → 1

Jachaleria candelariensis
Char. 1: 6.104-6.139 → 6.078
Char. 3: 0.285-0.331 → 0.199
Char. 4: 0.479 → 0.379
Char. 7: 0.151-0.156 → 0.161
Char. 8: 5.700 → 4.000
Char. 10: 10.155-10.206 → 10.269
Char. 12: 1.004-1.012 → 0.766
Char. 20: 0.818 → 0.808
Char. 21: 0.417-0.433 → 0.434
Char. 22: 0.526 → 0.667
Char. 59: 0 → 1
Char. 67: 1 → 2
Char. 168: 0 → 1

Jachaleria colorata
Char. 110: 1 → 0

Dinodontosaurus brevirostris
Char. 0: 0.376-0.378 → 0.321
Char. 3: 0.240-0.293 → 0.314
Char. 6: 1.414-1.431 → 2.180
Char. 7: 0.135-0.143 → 0.176
Char. 8: 7.300 → 9.106
Char. 9: 0.085-0.088 → 0.107
Char. 11: 10.000-10.400 → 9.690

Dinodontosaurus tener
Char. 0: 0.376-0.378 → 0.398
Char. 2: 0.354-0.388 → 0.347
Char. 4: 0.515-0.518 → 0.461
Char. 5: 0.354 → 0.328
Char. 9: 0.085-0.088 → 0.074
Char. 11: 10.000-10.400 → 10.900
Char. 12: 1.004-1.010 → 0.926

Lisowicia bojani
Char. 75: 1 → 2

Woznikella triradiata
Char. 15: 0.897 → 0.930
Char. 16: 0.442 → 0.362
Char. 22: 0.457-0.526 → 0.371
Char. 24: 2 → 1
Char. 56: 3 → 2
Char. 59: 0 → 1
Char. 167: 1 → 0

Node 120
No synapomorphies

APPENDIX 5. — Continuation.

Node 121	Node 130	Node 137
Char. 14: 0.855 → 0.920	Char. 31: 0 → 1	Char. 0: 0.339 → 0.322
Char. 47: 0 → 1	Char. 33: 0 → 1	Char. 3: 0.914 → 0.908
Char. 140: 0 → 1	Char. 44: 0 → 1	Char. 4: 0.435 → 0.518
Node 122	Char. 61: 1 → 0	Char. 11: 11.600-12.000 → 10.600-11.200
Char. 14: 0.595-0.718 → 0.855	Char. 97: 0 → 1	Char. 13: 0.259 → 0.253-0.257
Char. 15: 1.710-1.870 → 1.620	Char. 106: 0 → 1	Char. 30: 0 → 2
Char. 61: 0 → 1	Char. 115: 0 → 1	Char. 44: 1 → 2
Char. 132: 0 → 1	Char. 129: 0 → 1	Char. 49: 0 → 1
Node 123	Char. 136: 0 → 1	Char. 81: 0 → 1
Char. 73: 2 → 1	Char. 163: 0 → 1	Char. 146: 0 → 1
Char. 93: 1 → 0	Node 131	Node 138
Char. 94: 0 → 1	Char. 4: 0.272-0.305 → 0.407	Char. 0: 0.322 → 0.231-0.237
Char. 101: 0 → 1	Char. 11: 11.600-12.000 → 15.400	Char. 1: 5.555 → 5.714
Char. 181: 0 → 1	Char. 113: 1 → 0	Char. 4: 0.518 → 0.520
Char. 189: 0 → 1	Char. 131: 0 → 1	Char. 5: 0.111 → 0.222-0.257
Node 124	Node 132	Char. 6: 2.470 → 2.070-2.434
Char. 0: 0.606 → 0.509-0.547	Char. 8: 5.600-6.000 → 5.000-5.300	Char. 10: 10.385-10.457 → 10.177
Char. 4: 0.190 → 0.272-0.305	Char. 93: 0 → 1	Char. 24: 0 → 1
Char. 5: 0.046 → 0.072	Char. 99: 0 → 1	Char. 69: 0 → 1
Char. 17: 0.367 → 0.329	Char. 104: 0 → 1	Char. 124: 0 → 1
Char. 96: 1 → 0	Char. 119: 0 → 1	Node 139
Char. 176: 1 → 0	Char. 141: 0 → 1	Char. 48: 0 → 1
Char. 177: 1 → 0	Char. 142: 0 → 1	Char. 61: 0 → 1
Node 125	Char. 149: 0 → 1	Node 140
Char. 3: 0.700-0.842 → 0.333	Node 133	Char. 10: 9.418-9.687 → 9.417
Char. 4: 0.272-0.305 → 0.352	Char. 39: 1 → 2	Char. 77: 1 → 2
Char. 5: 0.072-0.104 → 0.218	Node 134	Node 141
Char. 71: 0 → 2	Char. 14: 0.865 → 0.831	Char. 15: 0.924-0.928 → 0.901-0.904
Char. 74: 0 → 1	Char. 156: 0 → 1	Char. 25: 0 → 1
Char. 77: 0 → 1	Char. 175: 1 → 0	Char. 32: 0 → 1
Char. 97: 0 → 1	Char. 176: 0 → 1	Char. 50: 0 → 2
Char. 102: 0 → 1	Node 135	Char. 54: 0 → 1
Char. 153: 0 → 1	Char. 14: 0.920-0.956 → 0.865	Char. 148: 0 → 1
Char. 159: 0 → 1	Char. 15: 1.059 → 0.968	Char. 170: 0 → 1
Node 126	Char. 56: 0 → 1	Char. 176: 1 → 0
Char. 29: 0 → 1	Node 136	Node 142
Char. 143: 0 → 1	Char. 4: 0.327 → 0.435	Char. 6: 2.070-2.434 → 1.751-2.013
Node 127	Char. 13: 0.355-0.395 → 0.259	Char. 45: 0 → 1
Char. 91: 0 → 1	Char. 14: 0.831 → 0.708-0.723	Char. 93: 0 → 1
Char. 107: 0 → 1	Char. 82: 0 → 1	Char. 114: 3 → 2
Char. 115: 1 → 2	Char. 85: 1 → 2	Char. 122: 0 → 1
Node 128	Char. 99: 0 → 1	Node 143
Char. 17: 0.351 → 0.396	Char. 101: 1 → 3	Char. 0: 0.231-0.237 → 0.238
Node 129	Char. 108: 0 → 1	Char. 12: 0.850-0.871 → 0.881
Char. 17: 0.299-0.329 → 0.351	Char. 109: 0 → 2	Char. 71: 0 → 2
	Char. 114: 0 → 3	Char. 73: 1 → 0
	Char. 116: 1 → 0	
	Char. 143: 1 → 2	
	Char. 161: 0 → 1	
	Char. 162: 1 → 2	

APPENDIX 5. — Continuation.

Node 144	Node 149	Node 154
Char. 11: 9.500 → 8.000	Char. 0: 0.279 → 0.328	Char. 2: 0.275 → 0.202-0.240
Char. 12: 0.850-0.871 → 0.902-0.907	Char. 3: 0.867-0.906 → 0.396	Char. 3: 0.899-1.032 → 0.840
Char. 13: 0.290 → 0.302	Char. 6: 1.548-1.565 → 1.505	Char. 136: 1 → 2
Char. 27: 2 → 0	Char. 7: 0.118-0.126 → 0.111	
Char. 46: 0 → 1	Char. 13: 0.302 → 0.319	Node 155
Char. 49: 1 → 0	Char. 15: 0.924-0.938 → 0.825	Char. 7: 0.117-0.123 → 0.116
Char. 63: 0 → 1	Char. 34: 0 → 2	Char. 88: 1 → 0
Char. 143: 4 → 3	Char. 41: 0 → 1	Char. 144: 0 → 1
Char. 145: 0 → 1	Char. 47: 1 → 2	Char. 147: 2 → 0
	Char. 48: 1 → 0	Char. 170: 0 → 1
	Char. 71: 0 → 1	
Node 145	Char. 75: 0 → 1	Node 156
Char. 11: 10.600-11.000 → 9.500	Char. 77: 1 → 2	Char. 44: 2 → 1
Char. 14: 0.723-0.730 → 0.798-0.859	Char. 90: 0 → 1	
Char. 30: 2 → 1	Char. 114: 2 → 3	Node 157
Char. 100: 0 → 1	Char. 198: 0 → 2	Char. 3: 0.867-0.906 → 0.742
Node 146		Char. 5: 0.166-0.257 → 0.260-0.281
Char. 2: 0.190-0.197 → 0.207-0.232	Node 150	Char. 9: 0.150-0.173 → 0.121-0.132
Char. 6: 1.751-1.847 → 1.548-1.565	Char. 0: 0.231-0.279 → 0.220	Char. 11: 10.600-11.000 → 12.000
Char. 10: 9.687 → 9.694	Char. 6: 1.548-1.565 → 1.646	Char. 15: 0.924-0.928 → 0.766-0.819
Char. 27: 1 → 2	Char. 8: 9.550-9.600 → 9.800	
Char. 61: 1 → 0	Char. 12: 0.850-0.871 → 0.840	Node 158
Char. 118: 1 → 0	Char. 27: 2 → 1	Char. 3: 0.840 → 0.764
Char. 143: 2 → 4	Char. 45: 2 → 0	Char. 4: 0.473-0.483 → 0.539
Node 147	Char. 54: 0 → 1	Char. 67: 1 → 2
Char. 9: 0.182-0.199 → 0.150-0.173	Char. 113: 1 → 0	Char. 71: 0 → 2
Char. 24: 1 → 0	Char. 134: 0 → 1	
Char. 38: 0 → 1	Node 151	Node 159
Char. 130: 0 → 1	Char. 8: 8.250-8.400 → 9.550-9.600	Char. 0: 0.279-0.281 → 0.308-0.311
Char. 187: 0 → 1	Char. 13: 0.212-0.290 → 0.293-0.348	Char. 2: 0.289-0.298 → 0.330-0.383
Node 148	Char. 25: 0 → 1	Char. 4: 0.421-0.483 → 0.357-0.372
Char. 28: 0 → 2	Char. 28: 2 → 0	Char. 5: 0.048-0.088 → 0.042
Char. 52: 0 → 1	Char. 146: 1 → 0	Char. 7: 0.117-0.123 → 0.132
Char. 124: 1 → 2	Char. 150: 0 → 1	Char. 8: 9.550-9.600 → 10.550
Char. 140: 1 → 2	Char. 164: 2 → 0	Char. 10: 9.965 → 10.119-10.173
Char. 164: 0 → 2	Char. 166: 0 → 1	Char. 124: 2 → 1
	Char. 176: 1 → 0	
Node 152		Node 160
Char. 1: 5.810-5.863 → 5.874-5.950	Node 153	Char. 41: 0 → 1
Char. 10: 9.694 → 9.740-9.775	Char. 2: 0.207-0.232 → 0.275-0.294	Char. 79: 0 → 1
Char. 45: 1 → 2	Char. 5: 0.166-0.187 → 0.139	
Char. 94: 0 → 1	Char. 63: 0 → 1	Node 161
Char. 95: 0 → 1	Char. 73: 01 → 2	Char. 3: 0.899-1.032 → 1.139-1.339
		Char. 5: 0.108-0.139 → 0.048-0.088
		Char. 12: 0.853-0.871 → 0.872
		Char. 13: 0.348 → 0.380
		Char. 67: 1 → 0
		Char. 87: 1 → 0
		Char. 137: 0 → 1

APPENDIX 5. — Continuation.

Node 162
 Char. 7: 0.132 → 0.135
 Char. 12: 0.872 → 0.836
 Char. 13: 0.380 → 0.346
 Char. 25: 1 → 0
 Char. 48: 1 → 0
 Char. 110: 1 → 0

Node 163
 Char. 1: 6.003-6.066 → 6.112
 Char. 5: 0.213-0.232 → 0.203
 Char. 6: 1.489-1.515 → 1.528
 Char. 7: 0.094-0.107 → 0.083
 Char. 11: 12.000-12.300 → 10.300
 Char. 12: 0.910-0.914 → 0.831

Node 164
 Char. 1: 5.927-5.982 → 6.003-6.066
 Char. 5: 0.260-0.281 → 0.213-0.232
 Char. 7: 0.112-0.117 → 0.094-0.107
 Char. 53: 0 → 1
 Char. 56: 1 → 2

Node 165
 Char. 99: 1 → 2
 Char. 120: 0 → 1
 Char. 149: 2 → 1

Node 166
 Char. 7: 0.118-0.123 → 0.112-0.117
 Char. 12: 0.850-0.871 → 0.910
 Char. 38: 1 → 0
 Char. 51: 0 → 1
 Char. 52: 1 → 0
 Char. 71: 0 → 1
 Char. 130: 1 → 0
 Char. 137: 0 → 1
 Char. 143: 4 → 2
 Char. 144: 0 → 1
 Char. 150: 0 → 2
 Char. 151: 0 → 1

Node 167
 Char. 1: 6.054-6.066 → 6.094
 Char. 2: 0.220-0.232 → 0.271
 Char. 3: 0.844 → 0.738
 Char. 5: 0.271-0.277 → 0.606
 Char. 12: 0.910-0.929 → 0.936
 Char. 13: 0.212-0.213 → 0.167
 Char. 14: 0.787-0.798 → 0.838
 Char. 51: 1 → 0
 Char. 60: 0 → 1
 Char. 64: 0 → 1
 Char. 71: 1 → 2
 Char. 78: 0 → 1
 Char. 92: 0 → 1

Node 168
 Char. 4: 0.551 → 0.565-0.566
 Char. 5: 0.232 → 0.271-0.277
 Char. 22: 0.491 → 0.391-0.411
 Char. 198: 0 → 1

Node 169
 Char. 4: 0.541-0.544 → 0.551
 Char. 14: 0.693-0.749 → 0.787
 Char. 15: 0.764-0.785 → 0.745-0.752
 Char. 18: 0.348 → 0.366
 Char. 79: 0 → 1
 Char. 144: 1 → 0

Node 170
 Char. 0: 0.244-0.282 → 0.289-0.320
 Char. 34: 0 → 1
 Char. 59: 0 → 1
 Char. 83: 0 → 1

Node 171
 Char. 2: 0.220-0.232 → 0.183-0.197
 Char. 12: 0.910-0.929 → 0.875-0.882
 Char. 57: 0 → 1
 Char. 61: 0 → 1
 Char. 193: 1 → 0

Node 172
 Char. 6: 1.458 → 1.436
 Char. 11: 12.300 → 12.400
 Char. 14: 0.787-0.798 → 0.758
 Char. 21: 0.353 → 0.345
 Char. 45: 2 → 1
 Char. 139: 2 → 1
 Char. 195: 1 → 0

Node 173
 Char. 198: 0 → 1

Node 174
 Char. 67: 1 → 2
 Char. 164: 2 → 3
 Char. 175: 0 → 1

Node 175
 Char. 3: 0.650 → 0.562-0.563
 Char. 18: 0.317-0.348 → 0.361
 Char. 60: 0 → 1
 Char. 194: 0 → 1

Node 176
 Char. 3: 0.672 → 0.650
 Char. 12: 0.926-0.985 → 0.924
 Char. 54: 0 → 1
 Char. 56: 1 → 2

Node 177
 Char. 8: 7.700-7.800 → 7.200
 Char. 9: 0.121 → 0.098-0.100
 Char. 11: 12.000 → 10.100-10.250
 Char. 67: 2 → 1

Node 178
 Char. 15: 0.766 → 0.731-0.754
 Char. 60: 1 → 0
 Char. 73: 0 → 1

Node 179
 Char. 0: 0.240-0.297 → 0.307-0.308
 Char. 4: 0.541-0.544 → 0.546
 Char. 5: 0.260-0.281 → 0.334-0.343
 Char. 8: 8.250-8.333 → 7.700-7.800
 Char. 12: 0.910 → 0.926-0.965
 Char. 61: 0 → 1
 Char. 71: 1 → 2
 Char. 75: 0 → 1
 Char. 125: 0 → 1

Node 180
 Char. 2: 0.237 → 0.253
 Char. 67: 1 → 2
 Char. 112: 0 → 1
 Char. 120: 0 → 2

Node 181
 Char. 2: 0.220-0.232 → 0.237
 Char. 6: 1.489-1.515 → 1.443-1.485
 Char. 60: 0 → 1
 Char. 105: 0 → 1
 Char. 116: 0 → 1
 Char. 154: 0 → 1

Node 182
 Char. 11: 12.300 → 13.500
 Char. 13: 0.212-0.213 → 0.204-0.205
 Char. 95: 1 → 0

Node 183
 Char. 2: 0.220-0.232 → 0.250
 Char. 12: 0.910-0.929 → 0.887
 Char. 58: 0 → 1
 Char. 63: 0 → 1
 Char. 64: 0 → 1
 Char. 73: 0 → 1
 Char. 194: 0 → 1

APPENDIX 5. — Continuation.

Node 184	Node 192	Node 201
Char. 2: 0.250 → 0.305	Char. 4: 0.553 → 0.567-0.569	Char. 4: 0.466 → 0.415-0.417
Char. 10: 9.740-9.851 → 9.480	Char. 5: 0.369 → 0.405-0.414	Char. 5: 0.143 → 0.119
Char. 12: 0.887 → 0.822	Char. 40: 0 → 1	Char. 15: 0.734-0.754 → 0.711
Char. 14: 0.693-0.749 → 0.760		Char. 18: 0.441 → 0.465-0.478
Char. 35: 0 → 1		Char. 57: 0 → 1
Char. 60: 0 → 2		Char. 126: 1 → 0
Node 185	Node 193	Node 202
Char. 7: 0.107-0.112 → 0.104	Char. 5: 0.334-0.343 → 0.369	Char. 2: 0.224-0.253 → 0.383-0.424
Char. 10: 9.480 → 9.414	Char. 41: 0 → 1	Char. 3: 0.562-0.563 → 0.689-0.705
Char. 14: 0.760 → 0.818-0.856	Char. 56: 2 → 1	Char. 4: 0.523-0.553 → 0.466
Char. 44: 2 → 1		Char. 5: 0.238 → 0.143
Char. 68: 0 → 1		Char. 6: 1.559 → 1.664-2.001
Char. 83: 1 → 2		Char. 7: 0.116-0.118 → 0.157-0.162
Char. 95: 0 → 1		Char. 8: 6.500-7.000 → 8.400
Node 186	Node 194	Char. 10: 9.680-9.798 → 10.145-10.309
Char. 4: 0.534-0.583 → 0.529	Char. 6: 1.443-1.485 → 1.338-1.347	Char. 35: 0 → 1
Char. 15: 0.764-0.785 → 0.848	Char. 9: 0.098-0.100 → 0.107-0.111	Char. 64: 0 → 1
Char. 61: 0 → 1	Char. 120: 2 → 1	Char. 71: 2 → 0
Char. 73: 1 → 0		Char. 104: 1 → 0
Node 187	Node 195	Node 203
Char. 56: 1 → 0	Char. 55: 0 → 1	Char. 0: 0.304-0.307 → 0.267
Node 188	Char. 111: 0 → 1	Char. 5: 0.446 → 0.466
Char. 3: 0.672-0.742 → 0.640		Char. 11: 10.100-10.400 → 11.200
Char. 5: 0.260-0.281 → 0.290		Char. 125: 1 → 0
Char. 8: 8.250-8.333 → 8.900		
Char. 11: 12.000-12.300 → 13.000		
Char. 14: 0.723-0.749 → 0.781		
Char. 41: 0 → 1		
Char. 54: 0 → 1		
Char. 61: 0 → 1		
Char. 71: 1 → 2		
Char. 153: 0 → 1		
Node 189	Node 197	Node 204
Char. 0: 0.307-0.308 → 0.369	Char. 1: 6.003-6.028 → 5.994	Char. 2: 0.253 → 0.327-0.352
Char. 6: 1.443-1.485 → 1.618	Char. 4: 0.523-0.553 → 0.522	Char. 3: 0.500 → 0.201-0.293
Char. 11: 12.000 → 13.900	Char. 5: 0.334-0.343 → 0.294	Char. 5: 0.435 → 0.446
Char. 57: 0 → 1	Char. 7: 0.116-0.118 → 0.124	Char. 6: 1.443-1.485 → 1.414-1.431
Node 190	Char. 9: 0.107-0.111 → 0.132	Char. 7: 0.116-0.118 → 0.125-0.130
Char. 3: 0.672-0.685 → 0.607	Char. 10: 9.680-9.751 → 9.599	Char. 12: 0.879-0.924 → 0.983-1.004
Char. 5: 0.334-0.343 → 0.359	Char. 51: 1 → 0	Char. 22: 0.491-0.494 → 0.596
Char. 10: 9.740-9.798 → 9.869	Char. 54: 1 → 0	Char. 79: 0 → 1
Char. 116: 1 → 0	Char. 71: 2 → 1	Char. 173: 0 → 1
Char. 153: 0 → 1	Char. 79: 0 → 1	
Node 191	Char. 116: 1 → 0	
Char. 114: 2 → 1		
Char. 133: 0 → 1		
Node 192	Node 198	Node 205
Char. 4: 0.553 → 0.567-0.569	Char. 5: 0.334-0.343 → 0.238	Char. 1: 6.003-6.028 → 6.064-6.099
Char. 5: 0.369 → 0.405-0.414	Char. 36: 0 → 1	Char. 3: 0.562-0.563 → 0.500
Char. 40: 0 → 1	Char. 37: 0 → 1	Char. 5: 0.334-0.343 → 0.435
Node 193		Char. 14: 0.763-0.790 → 0.821
Char. 5: 0.334-0.343 → 0.369		Char. 63: 0 → 1
Char. 41: 0 → 1		Char. 74: 0 → 1
Char. 56: 2 → 1		Char. 75: 1 → 2
Node 194		Char. 81: 1 → 0
Char. 6: 1.443-1.485 → 1.338-1.347		Char. 86: 0 → 1
Char. 9: 0.098-0.100 → 0.107-0.111		Char. 106: 1 → 2
Char. 120: 2 → 1		Char. 186: 0 → 1
Node 195		Char. 195: 0 → 1
Char. 55: 0 → 1		
Char. 111: 0 → 1		
Node 196		
Char. 4: 0.541-0.544 → 0.408		
Char. 12: 0.910 → 0.876		
Char. 113: 1 → 0		
Char. 131: 1 → 0		
Node 197		
Char. 1: 6.003-6.028 → 5.994		
Char. 4: 0.523-0.553 → 0.522		
Char. 5: 0.334-0.343 → 0.294		
Char. 7: 0.116-0.118 → 0.124		
Char. 9: 0.107-0.111 → 0.132		
Char. 10: 9.680-9.751 → 9.599		
Char. 51: 1 → 0		
Char. 54: 1 → 0		
Char. 71: 2 → 1		
Char. 79: 0 → 1		
Char. 116: 1 → 0		
Node 198		
Char. 5: 0.334-0.343 → 0.238		
Char. 36: 0 → 1		
Char. 37: 0 → 1		
Node 199		
Char. 1: 6.005 → 6.072		
Char. 4: 0.415-0.417 → 0.413		
Char. 7: 0.162 → 0.165		
Char. 11: 9.700-10.250 → 10.900		
Char. 12: 0.816-0.874 → 0.805		
Char. 14: 0.757-0.767 → 0.711		
Char. 113: 1 → 0		
Char. 114: 2 → 4		
Node 200		
Char. 175: 1 → 0		
Char. 187: 1 → 0		
Char. 198: 1 → 0		

APPENDIX 5. — Continuation.

Node 206	Node 212	Node 221
Char. 0: 0.304-0.307 → 0.376-0.378	Char. 61: 0 → 1	Char. 5: 0.254-0.318 → 0.233
Char. 2: 0.327-0.352 → 0.354		Char. 71: 2 → 1
Char. 9: 0.098-0.100 → 0.088		
Char. 13: 0.219-0.240 → 0.205	Node 213	Node 222
Char. 16: 0.476-0.490 → 0.447	Char. 9: 0.088-0.091 → 0.086	Char. 2: 0.393-0.423 → 0.461-0.468
Char. 149: 2 → 1	Char. 34: 1 → 0	Char. 3: 0.285-0.331 → 0.450-0.618
	Char. 40: 0 → 1	Char. 67: 1 → 0
Node 207	Char. 72: 0 → 1	Char. 71: 2 → 0
Char. 2: 0.392 → 0.403-0.413	Char. 114: 2 → 1	Char. 75: 2 → 1
Char. 104: 0 → 1		Char. 104: 0 → 1
Char. 114: 1 → 2	Node 214	Char. 164: 2 → 3
Char. 178: 1 → 0	Char. 8: 7.800 → 9.800-9.900	
	Char. 11: 11.300 → 11.900	
Node 208	Char. 43: 0 → 1	Node 223
Char. 12: 1.018 → 1.031-1.052		Char. 2: 0.392 → 0.393-0.423
Char. 66: 0 → 1	Node 215	Char. 7: 0.143 → 0.151-0.156
Char. 67: 1 → 2	Char. 10: 10.027-10.206 → 10.432-	Char. 9: 0.085-0.088 → 0.064-0.084
Char. 174: 0 → 1	10.478	Char. 17: 0.519-0.520 → 0.524-
	Char. 12: 1.031-1.085 → 1.147-	0.530
Node 209	1.154	Char. 18: 0.450 → 0.499-0.522
Char. 12: 1.004-1.012 → 1.018	Char. 17: 0.519-0.520 → 0.558	Char. 43: 0 → 1
Char. 51: 1 → 2	Char. 198: 0 → 2	Char. 44: 2 → 1
Char. 54: 1 → 0		Char. 157: 5 → 0
Char. 74: 1 → 0	Node 216	Char. 197: 0 → 1
Char. 123: 1 → 2	Char. 3: 0.285-0.293 → 0.460	
Char. 134: 0 → 1	Char. 4: 0.515-0.574 → 0.500	Node 224
	Char. 7: 0.122-0.143 → 0.147-0.157	Char. 5: 0.446-0.499 → 0.332-0.368
Node 210	Char. 8: 6.900-7.000 → 7.500-7.800	Char. 6: 1.414-1.431 → 1.409
Char. 2: 0.354-0.388 → 0.392		Char. 8: 5.900-7.000 → 9.310
Char. 17: 0.507 → 0.519-0.520	Node 217	Char. 15: 0.722-0.766 → 0.897
Char. 18: 0.423 → 0.450	Char. 5: 0.446-0.476 → 0.254-0.318	Char. 54: 1 → 0
Char. 21: 0.310-0.352 → 0.417-0.425	Char. 11: 10.000-10.600 → 10.800	Char. 66: 0 → 1
Char. 22: 0.596 → 0.457-0.526	Char. 40: 1 → 0	Char. 117: 0 → 1
Char. 64: 0 → 1		Char. 156: 0 → 1
Char. 86: 1 → 0	Node 218	Char. 167: 0 → 1
Char. 125: 1 → 0	Char. 4: 0.433 → 0.382	
	Char. 5: 0.230 → 0.195	Node 225
Node 211	Char. 9: 0.088-0.091 → 0.102	No synapomorphies
Char. 1: 6.064-6.099 → 6.104	Char. 15: 0.668 → 0.515	
Char. 4: 0.523-0.538 → 0.515-0.518		Node 226
Char. 7: 0.125-0.130 → 0.135-0.143	Node 219	Char. 37: 0 → 2
Char. 10: 10.009 → 10.155	Char. 4: 0.500 → 0.433	Char. 51: 1 → 0
Char. 17: 0.481 → 0.507	Char. 5: 0.254-0.318 → 0.230	Char. 67: 0 → 2
Char. 18: 0.361 → 0.423	Char. 12: 1.031-1.085 → 0.918-0.920	Char. 133: 0 → 1
Char. 19: 0.675 → 0.652	Char. 41: 1 → 2	Char. 144: 1 → 0
Char. 41: 0 → 1	Char. 59: 0 → 1	Char. 168: 0 → 1
Char. 56: 2 → 3	Char. 75: 2 → 1	Char. 196: 0 → 1
Char. 57: 0 → 1		
Char. 114: 2 → 1	Node 220	Node 227
Char. 132: 1 → 0	Char. 71: 2 → 0	No synapomorphies
Char. 174: 1 → 0		

APPENDIX 5. — Continuation.

Node 228	Node 229	Node 232
Char. 0: 0.376-0.378 → 0.411	Char. 60: 1 → 2	Char. 5: 0.446 → 0.354
Char. 11: 10.000-10.400 → 9.200	Char. 67: 0 → 1	Char. 8: 6.900-7.000 → 7.300
Char. 19: 0.647-0.652 → 0.592	Char. 198: 0 → 3	Char. 67: 1 → 2
Char. 20: 1.789 → 1.944		Char. 103: 1 → 0
Char. 62: 0 → 1	Node 230	Char. 106: 2 → 1
Char. 74: 1 → 0	Char. 87: 1 → 0	
Char. 125: 0 → 1		
Char. 158: 1 → 0	Node 231	
Char. 194: 1 → 0	Char. 62: 0 → 1	
	Char. 92: 0 → 1	
	Char. 123: 1 → 3	
	Char. 194: 1 → 0	

APPENDIX 6. — *Ufudocyclops mukanelai* Kammerer, Viglietti, Hancox, Butler & Choiniere, 2019 inactivated, strict consensus tree, node numbers. https://doi.org/10.5852/cr-palevol2023v22a16_s4

APPENDIX 7. — Strict consensus tree, *Ufudocyclops mukanelai* Kammerer, Viglietti, Hancox, Butler & Choiniere, 2019 inactivated, bootstrap supports. https://doi.org/10.5852/cr-palevol2023v22a16_s5

APPENDIX 8. — List of synapomorphies, *Ufudocyclops mukanelai* Kammerer, Viglietti, Hancox, Butler & Choiniere, 2019 inactivated, strict consensus.

<i>Biarmosuchus tener</i>	<i>Glanosuchus macrops</i>	<i>Patranomodon nyaphulii</i>
No autapomorphies	Char. 2: 0.244-0.261 → 0.145	Char. 0: 0.339 → 0.290
<i>Hipposaurus boonstrai</i>	Char. 3: 0.333 → 0.250	Char. 5: 0.094-0.105 → 0.076
Char. 8: 5.800 → 3.500	Char. 4: 0.352 → 0.367	Char. 7: 0.198 → 0.202
Char. 12: 1.060 → 1.070	Char. 8: 5.800-6.200 → 5.300	Char. 9: 0.090-0.094 → 0.043
Char. 15: 1.870 → 2.630	Char. 9: 0.090-0.094 → 0.050	Char. 10: 10.455-10.905 → 11.029
Char. 73: 2 → 0	Char. 15: 1.710-1.870 → 2.120	Char. 11: 11.600-12.000 → 13.700
Char. 95: 0 → 1	Char. 66: 0 → 1	Char. 12: 0.847-0.871 → 0.744
Char. 114: 2 → 0	<i>Biseridens qilianicus</i>	Char. 13: 0.355-0.395 → 0.476
Char. 166: 0 → 1	Char. 65: 0 → 1	Char. 14: 0.920-0.956 → 1.250
Char. 184: 1 → 0	Char. 90: 0 → 1	Char. 87: 1 → 0
Char. 191: 1 → 0	Char. 113: 1 → 0	Char. 105: 0 → 1
<i>Archaeosyodon praeventor</i>	Char. 159: 0 → 1	Char. 122: 0 → 1
Char. 141: 0 → 1	<i>Anomocephalus africanus</i>	<i>Galeops whaitsi</i>
<i>Titanophoneus potens</i>	No autapomorphies	Char. 2: 0.195-0.228 → 0.180
Char. 0: 0.509-0.547 → 0.758	<i>Tiarajudens eccentricus</i>	Char. 7: 0.140 → 0.136
Char. 4: 0.272-0.305 → 0.227	Char. 44: 1 → 0	Char. 8: 5.600-6.000 → 4.100
Char. 5: 0.072-0.104 → 0.051	<i>Otsheria netzvetajevi</i>	Char. 13: 0.355-0.395 → 0.489
Char. 12: 1.020-1.060 → 1.160	Char. 1: 5.364 → 5.425	Char. 16: 0.545-0.558 → 0.646
Char. 16: 0.545-0.558 → 0.500	Char. 2: 0.205-0.228 → 0.231	Char. 17: 0.396-0.401 → 0.356
Char. 17: 0.299-0.329 → 0.292	Char. 4: 0.407 → 0.512	Char. 92: 0 → 1
Char. 18: 0.149-0.200 → 0.274	Char. 5: 0.102-0.105 → 0.108	Char. 119: 0 → 1
Char. 22: 0.257-0.342 → 0.343	Char. 7: 0.198 → 0.181	Char. 121: 0 → 1
Char. 64: 0 → 1	Char. 10: 10.905 → 10.950	Char. 153: 0 → 1
Char. 73: 1 → 0	Char. 11: 15.400 → 15.500	Char. 168: 0 → 1
Char. 155: 0 → 1	Char. 12: 0.902 → 0.860	<i>Galepus jouberti</i>
Char. 185: 0 → 1	Char. 33: 1 → 0	Char. 3: 0.914 → 0.855
<i>Gorgonops torvus</i>	Char. 101: 12 → 0	Char. 170: 0 → 1
Char. 0: 0.509-0.547 → 0.504	<i>Ulemica</i>	<i>Galechirus scholtzi</i>
Char. 2: 0.261-0.263 → 0.290	Char. 0: 0.381 → 0.470	Char. 15: 0.968 → 0.700
Char. 3: 0.842 → 1.150	Char. 2: 0.205-0.228 → 0.125	<i>Eodicynodon oelofseni</i>
Char. 8: 5.800-6.200 → 8.500	Char. 7: 0.198 → 0.216	Char. 0: 0.339 → 0.351
Char. 12: 1.020-1.060 → 0.977	Char. 8: 5.000-5.300 → 4.900	Char. 3: 0.914 → 0.968
Char. 62: 0 → 1	Char. 12: 0.902 → 1.098	Char. 87: 1 → 0
Char. 77: 0 → 2	Char. 44: 1 → 0	<i>Eodicynodon oosthuizeni</i>
Char. 158: 0 → 1	Char. 61: 0 → 1	Char. 2: 0.195-0.228 → 0.234
Char. 183: 0 → 1	Char. 124: 0 → 1	Char. 6: 2.470 → 2.501
Char. 186: 0 → 1	<i>Suminia getmanovi</i>	Char. 8: 6.600-8.100 → 8.200
Char. 187: 0 → 1	Char. 0: 0.339-0.381 → 0.336	Char. 11: 10.600-11.200 → 9.000
Char. 188: 0 → 1	Char. 1: 5.325-5.364 → 4.879	Char. 14: 0.708-0.723 → 0.698
<i>Lycosuchus vanderrieti</i>	Char. 4: 0.272-0.305 → 0.230	Char. 15: 0.968 → 1.061
Char. 5: 0.218 → 0.303	Char. 14: 0.920-0.956 → 0.899	Char. 16: 0.487-0.558 → 0.446
Char. 8: 5.800-6.200 → 7.700	Char. 47: 1 → 2	Char. 17: 0.437-0.486 → 0.509
Char. 16: 0.545 → 0.500	Char. 57: 0 → 1	Char. 19: 0.301-0.553 → 0.300
Char. 17: 0.309-0.329 → 0.333	Char. 80: 01 → 2	Char. 22: 0.315-0.366 → 0.475
Char. 18: 0.200 → 0.294	Char. 103: 0 → 2	Char. 127: 1 → 0
Char. 22: 0.342 → 0.400	Char. 140: 1 → 2	Char. 177: 0 → 1
Char. 46: 0 → 1	Char. 162: 1 → 2	Char. 193: 0 → 1
Char. 57: 0 → 2		
Char. 119: 0 → 1		

APPENDIX 8. — Continuation.

Colobodectes cluveri

Char. 0: 0.231-0.237 → 0.203
 Char. 5: 0.222-0.257 → 0.269
 Char. 7: 0.140 → 0.142
 Char. 9: 0.182-0.199 → 0.206
 Char. 12: 0.850-0.871 → 0.948
 Char. 63: 0 → 1
 Char. 73: 1 → 0
 Char. 96: 0 → 1

Lanthanostegus mohoui

Char. 3: 0.795-0.908 → 0.661
 Char. 65: 0 → 1
 Char. 77: 1 → 2
 Char. 85: 2 → 0
 Char. 111: 0 → 1

Eosimops newtoni

Char. 0: 0.231-0.237 → 0.186
 Char. 1: 5.863 → 5.890
 Char. 2: 0.197 → 0.243
 Char. 9: 0.182-0.199 → 0.172
 Char. 10: 9.417 → 9.402
 Char. 11: 10.600-11.200 → 11.300
 Char. 12: 0.850 → 0.831
 Char. 13: 0.253-0.257 → 0.402
 Char. 14: 0.723-0.742 → 0.803
 Char. 16: 0.487-0.558 → 0.633
 Char. 22: 0.315-0.366 → 0.444
 Char. 65: 0 → 1
 Char. 114: 2 → 3
 Char. 122: 1 → 0
 Char. 143: 2 → 4
 Char. 146: 1 → 0
 Char. 177: 0 → 1

Diictodon feliceps

Char. 0: 0.238 → 0.247
 Char. 1: 5.810-5.863 → 5.925
 Char. 2: 0.195-0.197 → 0.223
 Char. 3: 0.795-0.864 → 0.640
 Char. 5: 0.228-0.257 → 0.273
 Char. 6: 1.751-2.013 → 1.702
 Char. 7: 0.123-0.126 → 0.135
 Char. 8: 8.100 → 8.000
 Char. 9: 0.182-0.199 → 0.214
 Char. 11: 10.600-11.200 → 11.900
 Char. 45: 1 → 2
 Char. 94: 0 → 1
 Char. 95: 0 → 1
 Char. 96: 0 → 1
 Char. 124: 1 → 2
 Char. 139: 1 → 2

Robertia broomiana

Char. 3: 0.795 → 0.721
 Char. 4: 0.541 → 0.555
 Char. 5: 0.257 → 0.259
 Char. 6: 1.751-2.013 → 1.681
 Char. 7: 0.123-0.126 → 0.108
 Char. 8: 8.100 → 8.600
 Char. 11: 10.600-11.200 → 9.800
 Char. 13: 0.253-0.257 → 0.132
 Char. 14: 0.723-0.742 → 0.711
 Char. 15: 0.901-0.904 → 0.868
 Char. 17: 0.466-0.486 → 0.502
 Char. 18: 0.260 → 0.227
 Char. 22: 0.315-0.366 → 0.309

Prosictodon dubei

Char. 1: 5.810-5.863 → 5.807
 Char. 2: 0.195-0.197 → 0.171
 Char. 4: 0.534-0.541 → 0.548
 Char. 6: 1.751-2.013 → 2.469
 Char. 7: 0.123-0.126 → 0.098
 Char. 9: 0.182-0.199 → 0.131
 Char. 10: 9.418-9.687 → 9.780
 Char. 11: 10.600-11.200 → 9.300
 Char. 14: 0.742 → 0.834
 Char. 15: 0.901 → 0.637

Abajudon kaayai

Char. 1: 5.396 → 5.215
 Char. 3: 0.867-0.906 → 1.030
 Char. 4: 0.515-0.541 → 0.412
 Char. 6: 1.548-1.565 → 2.844
 Char. 7: 0.118-0.126 → 0.146
 Char. 14: 0.798-0.859 → 0.898
 Char. 15: 0.924-0.938 → 1.016
 Char. 29: 1 → 0
 Char. 70: 1 → 0
 Char. 104: 1 → 0
 Char. 117: 0 → 1
 Char. 122: 1 → 0
 Char. 146: 1 → 0
 Char. 150: 0 → 1

Niassodon mfumukasi

Char. 12: 0.850-0.871 → 0.697
 Char. 19: 0.301 → 0.214
 Char. 44: 2 → 1
 Char. 54: 0 → 1
 Char. 67: 1 → 2
 Char. 68: 0 → 1
 Char. 69: 1 → 2
 Char. 73: 1 → 2
 Char. 81: 1 → 0
 Char. 102: 0 → 1
 Char. 111: 0 → 1
 Char. 164: 2 → 1

Brachyprosopus broomi

Char. 5: 0.222-0.257 → 0.338
 Char. 7: 0.123-0.126 → 0.129
 Char. 8: 8.100-8.400 → 6.800
 Char. 12: 0.850-0.871 → 0.898
 Char. 13: 0.208-0.257 → 0.132
 Char. 14: 0.723 → 0.715
 Char. 15: 0.924-0.928 → 0.824
 Char. 16: 0.554-0.594 → 0.612
 Char. 25: 0 → 1
 Char. 34: 0 → 1
 Char. 46: 0 → 1
 Char. 77: 1 → 2
 Char. 93: 1 → 0
 Char. 116: 0 → 1

Endothiodon tolani

Char. 5: 0.126-0.257 → 0.025
 Char. 7: 0.111 → 0.109
 Char. 8: 8.400-9.400 → 10.600
 Char. 14: 0.798 → 0.723
 Char. 94: 0 → 1

Endothiodon bathystoma

Char. 0: 0.328 → 0.335
 Char. 3: 0.396 → 0.268
 Char. 5: 0.126-0.257 → 0.400
 Char. 6: 1.505 → 1.457
 Char. 8: 8.400-9.400 → 8.100
 Char. 12: 0.902-0.907 → 0.988
 Char. 13: 0.319 → 0.373
 Char. 15: 0.825 → 0.730
 Char. 38: 1 → 0
 Char. 44: 2 → 1
 Char. 60: 0 → 1
 Char. 66: 0 → 1
 Char. 68: 0 → 1
 Char. 110: 1 → 0

Pristerodon mackayi

Char. 0: 0.231-0.237 → 0.225
 Char. 1: 5.810-5.863 → 5.874
 Char. 2: 0.190-0.197 → 0.184
 Char. 3: 0.867-0.998 → 1.026
 Char. 4: 0.520-0.541 → 0.582
 Char. 8: 8.100-8.400 → 10.000
 Char. 9: 0.182-0.199 → 0.206
 Char. 12: 0.850-0.871 → 0.813
 Char. 17: 0.437-0.486 → 0.430
 Char. 19: 0.301-0.454 → 0.275
 Char. 22: 0.315-0.366 → 0.275
 Char. 79: 0 → 1
 Char. 167: 0 → 1

APPENDIX 8. — Continuation.

Emydops

Char. 1: 5.874 → 5.872
 Char. 2: 0.207 → 0.204
 Char. 10: 9.740-9.775 → 9.667
 Char. 11: 10.600-11.000 → 9.300
 Char. 38: 1 → 0
 Char. 81: 1 → 0
 Char. 128: 1 → 0

Compsodon helmoedi

Char. 0: 0.220 → 0.196
 Char. 3: 0.906 → 1.066
 Char. 4: 0.473-0.537 → 0.431

Char. 6: 1.646 → 1.710
 Char. 7: 0.118 → 0.082
 Char. 8: 9.800 → 10.300
 Char. 9: 0.176 → 0.220
 Char. 10: 9.740-9.775 → 9.858
 Char. 12: 0.840 → 0.817
 Char. 41: 0 → 1
 Char. 61: 0 → 1
 Char. 67: 1 → 2
 Char. 68: 0 → 1
 Char. 70: 1 → 0
 Char. 71: 0 → 1
 Char. 77: 1 → 3
 Char. 102: 0 → 1
 Char. 115: 1 → 0
 Char. 120: 0 → 1
 Char. 131: 1 → 0

Digalodon rubidgei

Char. 0: 0.269-0.281 → 0.354
 Char. 1: 5.948-5.950 → 6.155
 Char. 7: 0.118-0.123 → 0.134
 Char. 24: 0 → 2
 Char. 48: 1 → 0
 Char. 77: 1 → 3
 Char. 79: 0 → 1

Illiptosaurus imperforatus

Char. 2: 0.202-0.240 → 0.198
 Char. 4: 0.473-0.483 → 0.407
 Char. 15: 0.924 → 0.667
 Char. 137: 0 → 1

Rastodon procurvidens

Char. 0: 0.231-0.279 → 0.197
 Char. 2: 0.207-0.232 → 0.199
 Char. 4: 0.541-0.544 → 0.558
 Char. 5: 0.260-0.281 → 0.298
 Char. 8: 8.250-8.333 → 6.600
 Char. 9: 0.121-0.132 → 0.105
 Char. 12: 0.850-0.871 → 0.798
 Char. 13: 0.212-0.219 → 0.100
 Char. 14: 0.723-0.730 → 0.623
 Char. 15: 0.766-0.819 → 0.667
 Char. 136: 1 → 2

Dicynodontoides

Char. 6: 1.500-1.565 → 1.492
 Char. 7: 0.116 → 0.085
 Char. 10: 9.775 → 9.814
 Char. 12: 0.853-0.871 → 0.887
 Char. 26: 0 → 1
 Char. 44: 1 → 2

Kombuisia frerensis

Char. 0: 0.269 → 0.193
 Char. 1: 5.950 → 5.976
 Char. 3: 0.764 → 0.400
 Char. 4: 0.539 → 0.555
 Char. 6: 1.500-1.565 → 1.589
 Char. 7: 0.116 → 0.195
 Char. 10: 9.775 → 9.645
 Char. 12: 0.853-0.871 → 0.746
 Char. 14: 0.726 → 0.684
 Char. 48: 1 → 0
 Char. 54: 0 → 1
 Char. 74: 0 → 1
 Char. 131: 1 → 0
 Char. 146: 0 → 1
 Char. 150: 1 → 0
 Char. 160: 1 → 0

Myosaurus gracilis

Char. 0: 0.269-0.279 → 0.260
 Char. 1: 5.948-5.950 → 5.902
 Char. 6: 1.500-1.565 → 1.590
 Char. 7: 0.116 → 0.085
 Char. 9: 0.181 → 0.208
 Char. 11: 10.600-11.000 → 9.600
 Char. 14: 0.726-0.750 → 0.958
 Char. 15: 0.924-0.928 → 0.942
 Char. 16: 0.485-0.554 → 0.586
 Char. 22: 0.353-0.359 → 0.208
 Char. 25: 1 → 0
 Char. 28: 0 → 1
 Char. 54: 0 → 1
 Char. 57: 0 → 2
 Char. 98: 1 → 0
 Char. 174: 0 → 1
 Char. 175: 0 → 1

Kembawacela kitchingi

Char. 0: 0.308-0.311 → 0.372
 Char. 3: 1.319-1.404 → 1.487
 Char. 6: 1.490-1.500 → 1.455
 Char. 12: 0.872 → 0.969
 Char. 13: 0.380 → 0.415
 Char. 15: 0.914-0.964 → 0.990
 Char. 28: 0 → 2
 Char. 44: 1 → 2
 Char. 96: 1 → 0
 Char. 134: 0 → 1
 Char. 159: 1 → 0

Cistecephalus microrhinus

Char. 1: 5.948-5.950 → 6.056
 Char. 4: 0.421-0.483 → 0.509
 Char. 11: 10.600-11.000 → 10.200
 Char. 14: 0.726-0.730 → 0.687
 Char. 17: 0.419 → 0.403
 Char. 22: 0.353-0.359 → 0.324
 Char. 61: 0 → 1
 Char. 174: 0 → 1

Sauroscoptor tharavati

Char. 12: 0.872 → 0.912
 Char. 13: 0.380 → 0.564
 Char. 15: 0.789-0.928 → 0.714

Cistecephaloïdes boonstrai

Char. 1: 5.948-5.950 → 6.047
 Char. 2: 0.330-0.383 → 0.425
 Char. 7: 0.135 → 0.194
 Char. 10: 10.119-10.173 → 10.305
 Char. 11: 10.600-11.650 → 12.500
 Char. 12: 0.836 → 0.632
 Char. 62: 0 → 1
 Char. 88: 1 → 0
 Char. 127: 0 → 1

Kawingasaurus fossilis

Char. 1: 5.948-5.950 → 5.933
 Char. 4: 0.357-0.372 → 0.340
 Char. 11: 10.600-11.650 → 10.000
 Char. 13: 0.346 → 0.286
 Char. 56: 1 → 0
 Char. 57: 0 → 2
 Char. 76: 0 → 1
 Char. 130: 1 → 0
 Char. 137: 1 → 0
 Char. 147: 2 → 0
 Char. 149: 2 → 1
 Char. 150: 1 → 0

APPENDIX 8. — Continuation.

Daqingshanodon limbus

Char. 2: 0.220-0.232 → 0.260
 Char. 3: 0.640-0.892 → 0.619
 Char. 4: 0.541-0.544 → 0.442
 Char. 5: 0.203 → 0.180
 Char. 7: 0.083 → 0.080
 Char. 12: 0.831 → 0.808
 Char. 63: 0 → 1
 Char. 77: 1 → 3

Keyseria benjamini

Char. 1: 6.112 → 6.155
 Char. 2: 0.220-0.232 → 0.159
 Char. 3: 0.640-0.892 → 1.034
 Char. 4: 0.541-0.544 → 0.605
 Char. 6: 1.528 → 1.600
 Char. 11: 10.300 → 9.000
 Char. 54: 0 → 1
 Char. 71: 1 → 0
 Char. 113: 1 → 0

Rhachiocephalus magnus

Char. 0: 0.320 → 0.329
 Char. 4: 0.566 → 0.598
 Char. 8: 8.100-8.333 → 8.800
 Char. 9: 0.132-0.141 → 0.143
 Char. 10: 9.219-9.740 → 9.170
 Char. 11: 12.300 → 12.800
 Char. 12: 0.936 → 1.010
 Char. 15: 0.752 → 0.777
 Char. 79: 1 → 0
 Char. 83: 1 → 0
 Char. 150: 2 → 0
 Char. 151: 1 → 0
 Char. 168: 0 → 1

Kitchinganomodon crassus

Char. 1: 6.094 → 6.137
 Char. 2: 0.271 → 0.318
 Char. 3: 0.738 → 0.708
 Char. 5: 0.606 → 0.752
 Char. 6: 1.480 → 1.556
 Char. 7: 0.094-0.098 → 0.108
 Char. 8: 8.100-8.333 → 7.400
 Char. 9: 0.132-0.141 → 0.070
 Char. 10: 9.219-9.740 → 9.747
 Char. 11: 12.300 → 11.100
 Char. 13: 0.167 → 0.165
 Char. 14: 0.838 → 0.843
 Char. 17: 0.491-0.506 → 0.466
 Char. 95: 1 → 0
 Char. 114: 2 → 3

Oudenodon bainii

Char. 0: 0.284-0.320 → 0.281
 Char. 2: 0.183-0.197 → 0.173
 Char. 4: 0.565-0.566 → 0.609
 Char. 7: 0.094-0.098 → 0.092
 Char. 11: 12.300 → 11.300
 Char. 12: 0.875-0.882 → 0.864
 Char. 13: 0.212-0.237 → 0.264
 Char. 16: 0.531-0.550 → 0.570
 Char. 20: 1.033-1.130 → 0.765
 Char. 194: 0 → 1

Tropidostoma dubium

Char. 1: 6.054-6.058 → 5.989
 Char. 3: 0.844 → 0.899
 Char. 8: 8.100-8.333 → 8.800
 Char. 10: 9.219-9.740 → 9.106
 Char. 15: 0.745-0.752 → 0.766
 Char. 19: 0.514 → 0.474
 Char. 20: 1.033-1.130 → 1.368
 Char. 22: 0.391 → 0.378
 Char. 95: 1 → 0
 Char. 96: 1 → 0

Australobarbarus

Char. 0: 0.284-0.320 → 0.333
 Char. 3: 0.844 → 0.697
 Char. 4: 0.565 → 0.561
 Char. 5: 0.277 → 0.298
 Char. 6: 1.436 → 1.324
 Char. 7: 0.098 → 0.101
 Char. 8: 8.100-8.333 → 6.100
 Char. 9: 0.140-0.141 → 0.160
 Char. 10: 9.219-9.740 → 9.822
 Char. 11: 12.400 → 13.350
 Char. 13: 0.212-0.237 → 0.193
 Char. 14: 0.758 → 0.624
 Char. 15: 0.745-0.752 → 0.694
 Char. 16: 0.531 → 0.466
 Char. 17: 0.491-0.503 → 0.485
 Char. 19: 0.514 → 0.848
 Char. 21: 0.345 → 0.333
 Char. 104: 1 → 0
 Char. 112: 0 → 1

Syops vanhoopeni

Char. 3: 0.563-0.650 → 0.484
 Char. 27: 2 → 1
 Char. 53: 0 → 1
 Char. 57: 1 → 0
 Char. 99: 1 → 2
 Char. 144: 1 → 0
 Char. 154: 1 → 0
 Char. 198: 01 → 2

Odontocyclops whaitsi

Char. 0: 0.289-0.320 → 0.376
 Char. 3: 0.844-0.892 → 0.988
 Char. 6: 1.458-1.480 → 1.448
 Char. 7: 0.094-0.098 → 0.092
 Char. 8: 8.250-8.333 → 10.100
 Char. 9: 0.132-0.141 → 0.131
 Char. 15: 0.745-0.752 → 0.731
 Char. 16: 0.550 → 0.551
 Char. 18: 0.366 → 0.427
 Char. 19: 0.514 → 0.435
 Char. 21: 0.353-0.395 → 0.426
 Char. 60: 0 → 2
 Char. 68: 0 → 1

Idelesaurus tataricus

Char. 0: 0.289-0.320 → 0.367
 Char. 1: 6.003-6.066 → 5.967
 Char. 2: 0.220-0.232 → 0.175
 Char. 3: 0.844-0.892 → 1.022
 Char. 4: 0.534-0.544 → 0.500
 Char. 5: 0.213-0.232 → 0.174
 Char. 9: 0.132-0.141 → 0.173
 Char. 10: 9.740-9.851 → 10.118
 Char. 12: 0.910-0.929 → 0.969
 Char. 57: 0 → 1
 Char. 60: 0 → 1
 Char. 68: 0 → 1
 Char. 96: 1 → 0
 Char. 120: 1 → 0
 Char. 131: 1 → 0

Bulbasaurus phylloxyron

Char. 0: 0.289-0.300 → 0.284
 Char. 3: 0.844-0.892 → 0.562
 Char. 5: 0.213-0.232 → 0.233
 Char. 6: 1.425-1.468 → 1.362
 Char. 8: 8.250-8.720 → 10.333
 Char. 9: 0.122-0.141 → 0.052
 Char. 11: 13.500 → 14.780
 Char. 14: 0.693-0.749 → 0.643
 Char. 53: 1 → 0
 Char. 59: 1 → 0

Aulacephalodon bainii

Char. 2: 0.305 → 0.323
 Char. 5: 0.213-0.232 → 0.204
 Char. 7: 0.107-0.112 → 0.117
 Char. 8: 8.250-8.720 → 6.800
 Char. 13: 0.204-0.205 → 0.172
 Char. 144: 1 → 0

APPENDIX 8. — Continuation.

<i>Pelanomodon moschops</i>	<i>Delectosaurus arefjevi</i>	<i>Peramodon amalitzkii</i>
Char. 1: 6.049-6.089 → 6.093	Char. 1: 5.937-6.019 → 5.861	Char. 0: 0.292-0.315 → 0.272
Char. 3: 0.892-0.908 → 0.912	Char. 2: 0.253 → 0.258	Char. 11: 9.900-10.100 → 9.500
Char. 4: 0.534-0.583 → 0.584	Char. 3: 0.685 → 0.702	Char. 12: 0.895-0.924 → 0.839
Char. 8: 8.720 → 9.400	Char. 7: 0.117-0.118 → 0.119	Char. 13: 0.186-0.219 → 0.167
Char. 9: 0.141 → 0.155	Char. 9: 0.121 → 0.130	Char. 14: 0.723-0.763 → 0.676
Char. 11: 13.100-13.500 → 12.300	Char. 11: 13.900 → 14.700	Char. 15: 0.724-0.731 → 0.680
Char. 15: 0.764-0.785 → 0.742	Char. 40: 0 → 1	Char. 60: 1 → 0
<i>Geikia locusticeps</i>	Char. 120: 2 → 1	<i>Taoheodon baizhijuni</i>
Char. 0: 0.289-0.300 → 0.256	Char. 131: 1 → 0	Char. 1: 5.927-5.982 → 6.100
Char. 2: 0.305 → 0.278	Char. 135: 1 → 0	Char. 6: 1.443-1.485 → 1.180
Char. 4: 0.529 → 0.514	<i>Dicynodon lacerticeps</i>	Char. 7: 0.112-0.118 → 0.110
Char. 6: 1.429-1.468 → 1.627	Char. 0: 0.308-0.315 → 0.324	Char. 9: 0.121-0.132 → 0.105
Char. 11: 13.100-13.500 → 13.900	Char. 11: 12.000 → 11.900	Char. 10: 9.740-9.775 → 9.640
Char. 12: 0.801-0.822 → 0.756	Char. 13: 0.219 → 0.241	Char. 13: 0.212-0.219 → 0.285
Char. 81: 1 → 0	Char. 112: 1 → 0	Char. 41: 0 → 1
Char. 150: 2 → 0	<i>Dicynodon angielczyki</i>	Char. 55: 0 → 1
<i>Geikia elginensis</i>	Char. 3: 0.607 → 0.524	Char. 63: 0 → 1
Char. 0: 0.289-0.300 → 0.366	Char. 4: 0.546 → 0.569	Char. 110: 1 → 0
Char. 2: 0.305 → 0.521	Char. 6: 1.443-1.485 → 1.351	Char. 132: 1 → 0
Char. 3: 0.892-0.908 → 0.846	Char. 7: 0.117 → 0.105	Char. 133: 0 → 1
Char. 12: 0.801-0.822 → 0.829	Char. 8: 7.700 → 7.560	<i>Counillonia superoculis</i>
Char. 13: 0.205 → 0.212	Char. 9: 0.121 → 0.114	Char. 4: 0.408 → 0.276
Char. 14: 0.818-0.856 → 0.900	Char. 10: 9.869 → 9.950	Char. 5: 0.260-0.281 → 0.134
Char. 15: 0.848 → 0.987	Char. 12: 0.926 → 0.965	Char. 11: 12.000 → 9.616
Char. 54: 0 → 1	Char. 14: 0.749 → 0.808	Char. 57: 0 → 2
Char. 55: 0 → 1	Char. 150: 2 → 0	<i>Repelinosaurus robustus</i>
Char. 118: 0 → 1	<i>Daptocephalus huenei</i>	Char. 0: 0.240-0.297 → 0.200
Char. 137: 1 → 0	Char. 6: 1.347-1.485 → 1.250	Char. 11: 12.000 → 14.698
<i>Elph borealis</i>	Char. 7: 0.118 → 0.123	Char. 12: 0.876 → 0.829
No autapomorphies	Char. 9: 0.111 → 0.117	Char. 34: 0 → 1
<i>Interpresaurus blomi</i>	Char. 12: 0.895-0.924 → 1.024	Char. 54: 0 → 1
Char. 73: 0 → 1	<i>Daptocephalus leoniceps</i>	<i>Vivaxosaurus trautscholdi</i>
<i>Katumbia parringtoni</i>	Char. 0: 0.292 → 0.268	Char. 0: 0.369 → 0.380
Char. 0: 0.240-0.279 → 0.196	Char. 2: 0.230 → 0.237	Char. 2: 0.253 → 0.230
Char. 1: 5.927 → 5.868	Char. 3: 0.563-0.564 → 0.539	Char. 4: 0.541-0.546 → 0.481
Char. 3: 0.640 → 0.527	Char. 5: 0.414 → 0.437	Char. 5: 0.334 → 0.285
Char. 5: 0.290 → 0.347	Char. 6: 1.347-1.485 → 1.500	Char. 6: 1.618 → 1.824
Char. 8: 8.900 → 9.300	Char. 10: 9.680 → 9.378	Char. 7: 0.117-0.118 → 0.116
Char. 11: 13.000 → 14.400	Char. 12: 0.895-0.924 → 0.858	Char. 8: 7.800 → 7.900
Char. 14: 0.781 → 0.833	Char. 17: 0.543 → 0.545	Char. 10: 9.798-9.869 → 10.203
Char. 51: 1 → 0	<i>Dinanomodon gilli</i>	Char. 12: 0.985 → 1.041
Char. 68: 0 → 1	Char. 3: 0.563-0.564 → 0.480	Char. 41: 0 → 1
Char. 112: 0 → 1	Char. 5: 0.405-0.414 → 0.522	Char. 55: 0 → 1
Char. 125: 0 → 1	Char. 12: 0.895-0.924 → 1.047	Char. 61: 1 → 0
Char. 131: 1 → 0	Char. 54: 1 → 0	Char. 71: 2 → 1
		Char. 95: 1 → 0
		Char. 96: 1 → 0

APPENDIX 8. — Continuation.

Jimusaria sinkianensis
 Char. 3: 0.650 → 0.672
 Char. 4: 0.604 → 0.767
 Char. 5: 0.334-0.343 → 0.464
 Char. 12: 0.924 → 0.992
 Char. 13: 0.203-0.240 → 0.251
 Char. 15: 0.724-0.734 → 0.699
 Char. 51: 1 → 2
 Char. 54: 1 → 0
 Char. 56: 2 → 1
 Char. 112: 1 → 0

Sintocephalus alticeps
 Char. 0: 0.315-0.336 → 0.354
 Char. 1: 5.994 → 5.969
 Char. 3: 0.562 → 0.516
 Char. 10: 9.599 → 9.399
 Char. 11: 10.000-10.250 → 9.600
 Char. 12: 0.814-0.924 → 1.022
 Char. 34: 1 → 0

Basilodon woodwardi
 Char. 3: 0.562 → 0.722
 Char. 4: 0.522 → 0.497
 Char. 5: 0.238-0.294 → 0.225
 Char. 6: 1.338 → 1.305
 Char. 7: 0.124 → 0.128
 Char. 8: 6.500 → 5.700
 Char. 9: 0.132 → 0.139
 Char. 11: 10.000-10.250 → 12.600
 Char. 57: 1 → 0
 Char. 61: 0 → 1
 Char. 67: 1 → 2
 Char. 99: 1 → 2

Turfanodon bogdaensis
 Char. 3: 0.563-0.564 → 0.588
 Char. 6: 1.347 → 1.327
 Char. 11: 9.900-10.100 → 10.300
 Char. 61: 1 → 0
 Char. 79: 0 → 1
 Char. 106: 1 → 2

Gordonia traquairi
 Char. 0: 0.307 → 0.252
 Char. 2: 0.253-0.278 → 0.139
 Char. 5: 0.334-0.343 → 0.309
 Char. 13: 0.203-0.240 → 0.188
 Char. 15: 0.724-0.734 → 0.773
 Char. 34: 1 → 0

Euptychognathus bathyrhynchus
 Char. 2: 0.212-0.244 → 0.130
 Char. 4: 0.523-0.546 → 0.560
 Char. 6: 1.443-1.485 → 1.559
 Char. 7: 0.117-0.124 → 0.091
 Char. 9: 0.088-0.098 → 0.084
 Char. 12: 0.814-0.924 → 0.792
 Char. 36: 0 → 1
 Char. 37: 0 → 1
 Char. 58: 0 → 1
 Char. 198: 0 → 1

Lystrosaurus hedini
 Char. 0: 0.308-0.315 → 0.320
 Char. 1: 6.072 → 6.111
 Char. 2: 0.383 → 0.414
 Char. 3: 0.689 → 0.705
 Char. 5: 0.119-0.143 → 0.146
 Char. 6: 1.664 → 1.471
 Char. 7: 0.165 → 0.174
 Char. 8: 8.400 → 9.200
 Char. 9: 0.086-0.098 → 0.079
 Char. 10: 10.145 → 10.203
 Char. 11: 10.900 → 11.400
 Char. 12: 0.805 → 0.673
 Char. 14: 0.711 → 0.691
 Char. 15: 0.706-0.731 → 0.781
 Char. 54: 1 → 0
 Char. 57: 1 → 0
 Char. 61: 1 → 0
 Char. 67: 2 → 1
 Char. 104: 0 → 1

Lystrosaurus maccaigi
 Char. 0: 0.308-0.315 → 0.274
 Char. 2: 0.383 → 0.347
 Char. 3: 0.689 → 0.656
 Char. 4: 0.413 → 0.325
 Char. 5: 0.119-0.143 → 0.108
 Char. 6: 1.664 → 1.764
 Char. 9: 0.086-0.098 → 0.123
 Char. 10: 10.145 → 10.022
 Char. 13: 0.294 → 0.354
 Char. 55: 0 → 1
 Char. 56: 2 → 0

Lystrosaurus curvatus
 Char. 8: 7.800-8.400 → 7.400
 Char. 11: 9.900-10.100 → 8.600
 Char. 15: 0.706-0.731 → 0.643
 Char. 21: 0.352 → 0.313

Lystrosaurus declivis
 Char. 0: 0.308-0.315 → 0.347
 Char. 1: 6.003 → 5.954
 Char. 4: 0.417-0.466 → 0.415
 Char. 5: 0.119-0.143 → 0.112
 Char. 6: 2.001 → 2.141
 Char. 8: 8.400 → 8.800
 Char. 11: 9.900-10.100 → 9.700
 Char. 16: 0.473 → 0.418
 Char. 17: 0.460 → 0.458
 Char. 18: 0.441-0.465 → 0.478
 Char. 20: 1.455 → 1.300
 Char. 21: 0.352 → 0.347

Lystrosaurus murrayi
 Char. 0: 0.308-0.315 → 0.288
 Char. 2: 0.424 → 0.427
 Char. 3: 0.705 → 0.726
 Char. 7: 0.157-0.162 → 0.175
 Char. 9: 0.097-0.098 → 0.101
 Char. 10: 10.309 → 10.358
 Char. 11: 9.900-10.100 → 11.700
 Char. 12: 0.874 → 0.816
 Char. 13: 0.315 → 0.316
 Char. 14: 0.757-0.767 → 0.793
 Char. 15: 0.711-0.731 → 0.754
 Char. 16: 0.473 → 0.478
 Char. 19: 0.750-0.787 → 0.843
 Char. 21: 0.352 → 0.392
 Char. 22: 0.545 → 0.605
 Char. 57: 1 → 0
 Char. 61: 1 → 0
 Char. 126: 0 → 1
 Char. 135: 1 → 0

Shansiodon
 Char. 0: 0.267 → 0.265
 Char. 3: 0.201 → 0.163
 Char. 5: 0.466 → 0.633
 Char. 8: 7.000 → 7.200
 Char. 10: 9.798-10.009 → 9.780
 Char. 12: 0.983-1.004 → 1.129
 Char. 61: 0 → 1
 Char. 67: 1 → 2

Tetragonias njalilus
 Char. 0: 0.304-0.336 → 0.378
 Char. 1: 6.064-6.099 → 5.912
 Char. 2: 0.327-0.352 → 0.354
 Char. 4: 0.523-0.538 → 0.574
 Char. 8: 6.900-7.000 → 6.800
 Char. 16: 0.473-0.490 → 0.447
 Char. 20: 1.484-1.789 → 1.852
 Char. 21: 0.352 → 0.304
 Char. 149: 2 → 1

APPENDIX 8. — Continuation.

Vinceria andina

Char. 4: 0.523-0.538 → 0.490
 Char. 7: 0.130 → 0.137
 Char. 9: 0.100 → 0.153
 Char. 10: 9.798-10.009 → 10.552
 Char. 11: 11.200 → 11.300
 Char. 51: 1 → 2
 Char. 86: 1 → 0

Rhinodicyodon gracile

Char. 1: 6.064-6.104 → 6.213
 Char. 6: 1.443-1.485 → 1.568
 Char. 7: 0.117-0.125 → 0.100
 Char. 10: 9.798-10.009 → 9.174
 Char. 12: 0.895-1.004 → 0.879
 Char. 14: 0.821-0.858 → 0.875
 Char. 17: 0.479-0.481 → 0.354
 Char. 22: 0.476-0.494 → 0.383
 Char. 61: 0 → 1
 Char. 79: 1 → 0
 Char. 131: 1 → 0

Acratophorus argentinensis

Char. 0: 0.420 → 0.329
 Char. 2: 0.403-0.413 → 0.445
 Char. 3: 0.268-0.460 → 0.205
 Char. 4: 0.506-0.607 → 0.666
 Char. 7: 0.143-0.161 → 0.120
 Char. 11: 10.000-10.600 → 8.055
 Char. 14: 0.756-0.786 → 0.716
 Char. 16: 0.467-0.494 → 0.345
 Char. 17: 0.519-0.520 → 0.468
 Char. 18: 0.450 → 0.292
 Char. 19: 0.562-0.652 → 0.706
 Char. 20: 1.239 → 1.206
 Char. 21: 0.417 → 0.424
 Char. 22: 0.405-0.411 → 0.574
 Char. 61: 0 → 1
 Char. 111: 0 → 1
 Char. 158: 1 → 0
 Char. 194: 1 → 0

Kannemeyeria simocephalus

Char. 43: 1 → 0

Kannemeyeria aganosteus

No autapomorphies

Kannemeyeria lophorhinus

Char. 0: 0.421 → 0.361
 Char. 1: 6.121 → 6.286
 Char. 3: 0.293-0.526 → 0.663
 Char. 6: 1.461-1.505 → 2.051
 Char. 7: 0.147 → 0.149
 Char. 8: 9.800-9.900 → 10.800
 Char. 13: 0.179 → 0.077
 Char. 60: 1 → 2
 Char. 131: 1 → 0
 Char. 158: 1 → 0
 Char. 160: 1 → 0

Dolichuranus primaevus

Char. 1: 6.104-6.105 → 6.079
 Char. 4: 0.500-0.518 → 0.484
 Char. 5: 0.354-0.368 → 0.400
 Char. 6: 1.443-1.485 → 1.339
 Char. 8: 6.900-7.000 → 8.700
 Char. 10: 10.206-10.469 → 10.672
 Char. 11: 10.000-10.100 → 9.700
 Char. 57: 1 → 0
 Char. 72: 0 → 1
 Char. 104: 1 → 0
 Char. 126: 1 → 0
 Char. 169: 1 → 0

Sinokannemeyeria

Char. 2: 0.403-0.413 → 0.478
 Char. 3: 0.359-0.460 → 0.543
 Char. 5: 0.195-0.230 → 0.175
 Char. 8: 6.655-7.000 → 5.900
 Char. 9: 0.094-0.102 → 0.109
 Char. 14: 0.756-0.786 → 0.549
 Char. 15: 0.515-0.668 → 0.385
 Char. 17: 0.519-0.520 → 0.489
 Char. 18: 0.478 → 0.556
 Char. 20: 1.239-1.381 → 1.187
 Char. 21: 0.411 → 0.408
 Char. 92: 0 → 1

Parakannemeyeria

Char. 0: 0.420 → 0.455
 Char. 1: 6.203 → 6.280
 Char. 2: 0.403-0.413 → 0.377
 Char. 4: 0.382-0.433 → 0.354
 Char. 7: 0.143-0.161 → 0.122
 Char. 10: 10.027 → 9.688
 Char. 11: 10.000-10.600 → 12.300
 Char. 13: 0.243 → 0.166
 Char. 43: 0 → 1
 Char. 114: 2 → 1
 Char. 173: 1 → 0

Xiyukannemeyeria brevirostris

Char. 0: 0.420 → 0.286
 Char. 7: 0.143-0.161 → 0.169
 Char. 8: 7.500 → 8.500
 Char. 9: 0.094-0.102 → 0.086
 Char. 11: 10.000-10.600 → 8.900
 Char. 12: 0.918-0.920 → 0.795
 Char. 13: 0.243 → 0.320
 Char. 54: 0 → 1
 Char. 131: 1 → 0

Rabidosaurus cristatus

Char. 0: 0.423 → 0.464
 Char. 81: 0 → 1

Rhadiodromus

Char. 1: 6.104-6.105 → 6.144
 Char. 3: 0.293-0.460 → 0.285
 Char. 4: 0.500-0.518 → 0.574
 Char. 5: 0.318-0.368 → 0.254
 Char. 7: 0.143-0.147 → 0.122
 Char. 10: 10.206-10.469 → 10.023
 Char. 18: 0.450-0.478 → 0.604
 Char. 68: 0 → 1
 Char. 132: 0 → 1

Wadiasaurus indicus

Char. 3: 0.268-0.460 → 0.539
 Char. 64: 1 → 0

Shaanbeikannemeyeria

Char. 0: 0.490-0.509 → 0.527
 Char. 2: 0.409 → 0.513
 Char. 3: 0.293-0.526 → 0.886
 Char. 5: 0.318-0.368 → 0.414
 Char. 7: 0.147 → 0.157
 Char. 9: 0.088-0.091 → 0.176
 Char. 10: 10.432-10.478 → 10.642
 Char. 12: 1.147-1.154 → 1.432
 Char. 14: 0.756-0.786 → 0.734
 Char. 17: 0.558 → 0.580
 Char. 86: 0 → 1
 Char. 144: 1 → 0

Rechnisaurus cristarhynchus

Char. 0: 0.490-0.509 → 0.510
 Char. 2: 0.409 → 0.436
 Char. 3: 0.293-0.526 → 0.154
 Char. 5: 0.233 → 0.211
 Char. 7: 0.147 → 0.140
 Char. 64: 1 → 0

Uralokannemeyeria vjuschkovi

Char. 2: 0.409 → 0.407

APPENDIX 8. — Continuation.

<i>Angonisaurus cruickshanki</i>	Char. 101: 0 → 3	<i>Stahleckeria potens</i>
Char. 1: 6.104-6.139 → 6.301	Char. 103: 0 → 2	Char. 0: 0.411 → 0.438
Char. 2: 0.445 → 0.514	Char. 104: 0 → 1	Char. 1: 6.104-6.139 → 5.992
Char. 4: 0.500-0.518 → 0.572	Char. 105: 0 → 1	Char. 3: 0.618-0.667 → 0.726
Char. 5: 0.354-0.368 → 0.600	Char. 106: 0 → 2	Char. 5: 0.354-0.368 → 0.288
Char. 6: 1.443-1.485 → 1.491	Char. 108: 0 → 1	Char. 8: 5.900-7.000 → 11.100
Char. 7: 0.151-0.183 → 0.190	Char. 109: 0 → 2	Char. 9: 0.060-0.084 → 0.052
Char. 13: 0.192-0.202 → 0.143	Char. 110: 0 → 1	Char. 10: 10.206-10.269 → 10.284
Char. 20: 1.484-1.789 → 2.541	Char. 112: 0 → 1	Char. 11: 9.200 → 8.700
Char. 132: 0 → 1	Char. 113: 1 → 0	Char. 12: 1.012 → 0.953
Char. 196: 0 → 1	Char. 114: 2 → 1	Char. 14: 0.832 → 0.856
	Char. 115: 0 → 1	Char. 19: 0.592 → 0.391
	Char. 122: 0 → 1	Char. 20: 1.789 → 2.217
<i>Ufudocyclops mukanelai</i>	Char. 123: 0 → 1	Char. 21: 0.433 → 0.434
Char. 0: 0.693 → 0.376	Char. 129: 0 → 1	Char. 28: 2 → 0
Char. 2: 0.261 → 0.468	Char. 131: 0 → 1	Char. 111: 0 → 1
Char. 4: 0.148 → 0.515	Char. 136: 0 → 1	Char. 174: 0 → 1
Char. 5: 0.029 → 0.332	Char. 137: 0 → 1	
Char. 8: 5.800 → 9.310	Char. 138: 0 → 1	<i>Sangusaurus parringtonii</i>
Char. 12: 1.060 → 0.983	Char. 139: 0 → 2	Char. 1: 6.104-6.139 → 6.177
Char. 23: 0 → 1	Char. 144: 0 → 1	Char. 2: 0.445 → 0.461
Char. 24: 0 → 2	Char. 146: 0 → 1	Char. 6: 1.390-1.431 → 1.129
Char. 27: 0 → 2	Char. 147: 0 → 3	Char. 7: 0.151-0.161 → 0.144
Char. 30: 0 → 2	Char. 149: 0 → 1	Char. 9: 0.064-0.084 → 0.091
Char. 31: 0 → 1	Char. 152: 0 → 1	Char. 12: 1.012-1.032 → 1.061
Char. 33: 0 → 1	Char. 160: 0 → 1	Char. 20: 1.789 → 1.944
Char. 39: 0 → 2	Char. 162: 0 → 2	Char. 39: 2 → 0
Char. 41: 0 → 1	Char. 163: 0 → 1	Char. 48: 1 → 0
Char. 42: 1 → 0	Char. 197: 0 → 1	Char. 130: 0 → 1
Char. 44: 0 → 1		
Char. 45: 0 → 2	<i>Zambiasaurus submersus</i>	<i>Sangusaurus</i> sp.
Char. 48: 0 → 1	Char. 21: 0.416-0.433 → 0.401	Char. 43: 1 → 0
Char. 49: 0 → 1	Char. 132: 0 → 1	
Char. 56: 0 → 2	Char. 175: 0 → 1	<i>Eubrachiosaurus browni</i>
Char. 60: 0 → 1	Char. 178: 1 → 0	No autapomorphies
Char. 63: 0 → 1		
Char. 64: 0 → 1	<i>Placerias hesternus</i>	<i>Ischigualastia jensi</i>
Char. 69: 2 → 1	Char. 50: 0 → 1	Char. 0: 0.411 → 0.482
Char. 70: 0 → 1	Char. 67: 2 → 1	Char. 5: 0.499 → 0.528
Char. 72: 0 → 1	Char. 198: 0 → 1	Char. 10: 10.206-10.269 → 10.023
Char. 73: 2 → 1		Char. 14: 0.832 → 0.912
Char. 74: 0 → 1	<i>Moghreberia nmachouensis</i>	Char. 16: 0.427 → 0.419
Char. 75: 0 → 1	Char. 51: 0 → 2	Char. 18: 0.529 → 0.561
Char. 77: 0 → 1	Char. 158: 1 → 0	Char. 21: 0.433 → 0.412
Char. 79: 0 → 2		Char. 41: 1 → 2
Char. 80: 0 → 2	<i>Pentasaurus goggai</i>	Char. 114: 1 → 5
Char. 82: 0 → 1	Char. 150: 2 → 0	
Char. 85: 0 → 2		<i>Jachaleria candelariensis</i>
Char. 88: 0 → 1		Char. 67: 1 → 2
Char. 89: 0 → 1		
Char. 91: 0 → 1		<i>Jachaleria colorata</i>
Char. 94: 0 → 1		Char. 87: 0 → 1
Char. 95: 0 → 1		Char. 110: 1 → 0
Char. 97: 0 → 1		
Char. 98: 0 → 2		
Char. 99: 0 → 1		

APPENDIX 8. — Continuation.

<i>Dinodontosaurus brevirostris</i>	Node 124	Node 132
Char. 6: 1.443-1.485 → 2.180	Char. 0: 0.606 → 0.509-0.547	Char. 8: 5.600-6.000 → 5.000-5.300
Char. 7: 0.135-0.147 → 0.176	Char. 4: 0.190 → 0.272-0.305	Char. 93: 0 → 1
Char. 8: 7.300 → 9.106	Char. 5: 0.046 → 0.072	Char. 99: 0 → 1
Char. 9: 0.085-0.098 → 0.107	Char. 17: 0.367 → 0.329	Char. 104: 0 → 1
Char. 11: 10.000-10.100 → 9.690	Char. 96: 1 → 0	Char. 119: 0 → 1
<i>Dinodontosaurus tener</i>	Char. 176: 1 → 0	Char. 141: 0 → 1
Char. 0: 0.321-0.356 → 0.398	Char. 177: 1 → 0	Char. 142: 0 → 1
Char. 3: 0.314 → 0.240	Node 125	Char. 149: 0 → 1
Char. 4: 0.500-0.518 → 0.461	Char. 3: 0.700-0.842 → 0.333	Node 133
Char. 5: 0.354 → 0.328	Char. 4: 0.272-0.305 → 0.352	Char. 39: 1 → 2
Char. 6: 1.443-1.485 → 1.414	Char. 5: 0.072-0.104 → 0.218	Node 134
Char. 9: 0.085-0.098 → 0.074	Char. 71: 0 → 2	Char. 14: 0.865 → 0.831
Char. 11: 10.000-10.100 → 10.900	Char. 74: 0 → 1	Char. 156: 0 → 1
<i>Lisowicia bojani</i>	Char. 77: 0 → 1	Char. 175: 1 → 0
Char. 17: 0.498-0.524 → 0.576	Char. 97: 0 → 1	Char. 176: 0 → 1
Char. 65: 0 → 1	Char. 102: 0 → 1	Node 135
Char. 75: 1 → 2	Char. 153: 0 → 1	Char. 14: 0.920-0.956 → 0.865
Char. 121: 2 → 1	Char. 159: 0 → 1	Char. 15: 1.059 → 0.968
Char. 128: 1 → 0	Node 126	Char. 56: 0 → 1
Char. 167: 1 → 0	Char. 29: 0 → 1	Node 136
Char. 169: 1 → 0	Char. 143: 0 → 1	Char. 4: 0.327 → 0.435
Char. 183: 1 → 0	Node 127	Char. 13: 0.355-0.395 → 0.259
Char. 184: 1 → 0	Char. 91: 0 → 1	Char. 14: 0.831 → 0.708-0.723
<i>Woznikella triradiata</i>	Char. 107: 0 → 1	Char. 82: 0 → 1
Char. 15: 0.841-0.897 → 0.930	Char. 115: 1 → 2	Char. 85: 1 → 2
Char. 16: 0.442-0.490 → 0.362	Node 128	Char. 99: 0 → 1
Char. 22: 0.411-0.457 → 0.371	Char. 17: 0.351 → 0.396	Char. 101: 1 → 3
Char. 24: 2 → 1	Node 129	Char. 108: 0 → 1
Char. 56: 3 → 2	Char. 17: 0.299-0.329 → 0.351	Char. 109: 0 → 2
Char. 59: 0 → 1	Node 130	Char. 114: 0 → 3
Node 120	Char. 31: 0 → 1	Char. 116: 1 → 0
No synapomorphies	Char. 33: 0 → 1	Char. 143: 1 → 2
Node 121	Char. 44: 0 → 1	Char. 161: 0 → 1
Char. 14: 0.855 → 0.920	Char. 61: 1 → 0	Char. 162: 1 → 2
Char. 47: 0 → 1	Char. 97: 0 → 1	Node 137
Char. 140: 0 → 1	Char. 106: 0 → 1	Char. 0: 0.339 → 0.322
Node 122	Char. 115: 0 → 1	Char. 3: 0.914 → 0.908
Char. 14: 0.595-0.718 → 0.855	Char. 129: 0 → 1	Char. 4: 0.435 → 0.518
Char. 15: 1.710-1.870 → 1.620	Char. 136: 0 → 1	Char. 11: 11.600-12.000 → 10.600-11.200
Char. 61: 0 → 1	Char. 163: 0 → 1	Char. 13: 0.259 → 0.253-0.257
Char. 132: 0 → 1	Node 131	Char. 30: 0 → 2
Node 123	Char. 4: 0.272-0.305 → 0.407	Char. 44: 1 → 2
Char. 73: 2 → 1	Char. 11: 11.600-12.000 → 15.400	Char. 49: 0 → 1
Char. 93: 1 → 0	Char. 113: 1 → 0	Char. 81: 0 → 1
Char. 94: 0 → 1	Char. 131: 0 → 1	Char. 146: 0 → 1
Char. 101: 0 → 1		
Char. 181: 0 → 1		
Char. 189: 0 → 1		

APPENDIX 8. — Continuation.

Node 138
 Char. 0: 0.322 → 0.231-0.237
 Char. 1: 5.555 → 5.714
 Char. 4: 0.518 → 0.520
 Char. 5: 0.111 → 0.222-0.257
 Char. 6: 2.470 → 2.070-2.434
 Char. 10: 10.385-10.457 → 10.177
 Char. 24: 0 → 1
 Char. 69: 0 → 1
 Char. 124: 0 → 1

Node 139
 Char. 48: 0 → 1
 Char. 61: 0 → 1

Node 140
 Char. 10: 9.418-9.687 → 9.417
 Char. 77: 1 → 2

Node 141
 Char. 15: 0.924-0.928 → 0.901-0.904
 Char. 25: 0 → 1
 Char. 32: 0 → 1
 Char. 50: 0 → 2
 Char. 54: 0 → 1
 Char. 148: 0 → 1
 Char. 170: 0 → 1
 Char. 176: 1 → 0

Node 142
 Char. 6: 2.070-2.434 → 1.751-2.013
 Char. 45: 0 → 1
 Char. 93: 0 → 1
 Char. 114: 3 → 2
 Char. 122: 0 → 1

Node 143
 Char. 0: 0.231-0.237 → 0.238
 Char. 12: 0.850-0.871 → 0.881
 Char. 71: 0 → 2
 Char. 73: 1 → 0

Node 144
 Char. 11: 9.500 → 8.000
 Char. 12: 0.850-0.871 → 0.902-0.907
 Char. 13: 0.290 → 0.302
 Char. 27: 2 → 0
 Char. 46: 0 → 1
 Char. 49: 1 → 0
 Char. 63: 0 → 1
 Char. 143: 4 → 3
 Char. 145: 0 → 1

Node 145
 Char. 11: 10.600-11.000 → 9.500
 Char. 14: 0.723-0.730 → 0.798-0.859
 Char. 30: 2 → 1
 Char. 100: 0 → 1

Node 146
 Char. 2: 0.190-0.197 → 0.207-0.232
 Char. 6: 1.751-1.847 → 1.548-1.565
 Char. 10: 9.687 → 9.694
 Char. 27: 1 → 2
 Char. 61: 1 → 0
 Char. 118: 1 → 0
 Char. 143: 2 → 4

Node 147
 Char. 9: 0.182-0.199 → 0.150-0.173
 Char. 24: 1 → 0
 Char. 38: 0 → 1
 Char. 130: 0 → 1
 Char. 187: 0 → 1

Node 148
 Char. 28: 0 → 2
 Char. 52: 0 → 1
 Char. 124: 1 → 2
 Char. 140: 1 → 2
 Char. 164: 0 → 2

Node 149
 Char. 0: 0.279 → 0.328
 Char. 3: 0.867-0.906 → 0.396
 Char. 6: 1.548-1.565 → 1.505
 Char. 7: 0.118-0.126 → 0.111
 Char. 13: 0.302 → 0.319
 Char. 15: 0.924-0.938 → 0.825
 Char. 34: 0 → 2
 Char. 41: 0 → 1
 Char. 47: 1 → 2
 Char. 48: 1 → 0
 Char. 71: 0 → 1
 Char. 75: 0 → 1
 Char. 77: 1 → 2
 Char. 90: 0 → 1
 Char. 114: 2 → 3
 Char. 198: 0 → 2

Node 150
 Char. 0: 0.231-0.279 → 0.220
 Char. 6: 1.548-1.565 → 1.646
 Char. 8: 9.550-9.600 → 9.800
 Char. 12: 0.850-0.871 → 0.840
 Char. 27: 2 → 1
 Char. 45: 2 → 0
 Char. 54: 0 → 1
 Char. 113: 1 → 0
 Char. 134: 0 → 1

Node 151
 Char. 8: 8.250-8.400 → 9.550-9.600
 Char. 13: 0.212-0.290 → 0.293-0.348
 Char. 25: 0 → 1
 Char. 28: 2 → 0
 Char. 146: 1 → 0
 Char. 150: 0 → 1
 Char. 164: 2 → 0
 Char. 166: 0 → 1
 Char. 176: 1 → 0

Node 152
 Char. 1: 5.810-5.863 → 5.874-5.950
 Char. 10: 9.694 → 9.740-9.775
 Char. 45: 1 → 2
 Char. 94: 0 → 1
 Char. 95: 0 → 1

Node 153
 Char. 2: 0.207-0.232 → 0.275-0.294
 Char. 5: 0.166-0.187 → 0.139
 Char. 63: 0 → 1
 Char. 73: 01 → 2

Node 154
 Char. 2: 0.275 → 0.202-0.240
 Char. 3: 0.899-1.032 → 0.840
 Char. 136: 1 → 2

Node 155
 Char. 7: 0.117-0.123 → 0.116
 Char. 88: 1 → 0
 Char. 144: 0 → 1
 Char. 147: 2 → 0
 Char. 170: 0 → 1

Node 156
 Char. 44: 2 → 1

APPENDIX 8. — Continuation.

Node 157	Node 164	Node 170
Char. 3: 0.867-0.906 → 0.742	Char. 1: 5.927-5.982 → 6.003-6.066	Char. 0: 0.244-0.282 → 0.289-0.320
Char. 5: 0.166-0.257 → 0.260-0.281	Char. 5: 0.260-0.281 → 0.213-0.232	Char. 34: 0 → 1
Char. 9: 0.150-0.173 → 0.121-0.132	Char. 7: 0.112-0.118 → 0.094-0.107	Char. 59: 0 → 1
Char. 11: 10.600-11.000 → 12.000	Char. 53: 0 → 1	Char. 83: 0 → 1
Char. 15: 0.924-0.928 → 0.766-0.819	Char. 56: 1 → 2	
Node 158	Node 165	Node 171
Char. 3: 0.840 → 0.764	Char. 99: 1 → 2	Char. 2: 0.220-0.232 → 0.183-0.197
Char. 4: 0.473-0.483 → 0.539	Char. 120: 0 → 1	Char. 12: 0.910-0.929 → 0.875-0.882
Char. 67: 1 → 2	Char. 149: 2 → 1	Char. 57: 0 → 1
Char. 71: 0 → 2		Char. 61: 0 → 1
Node 159	Node 166	Char. 193: 1 → 0
Char. 0: 0.279-0.281 → 0.308-0.311	Char. 12: 0.850-0.871 → 0.910	
Char. 2: 0.289-0.298 → 0.330-0.383	Char. 38: 1 → 0	Node 172
Char. 4: 0.421-0.483 → 0.357-0.372	Char. 51: 0 → 1	Char. 6: 1.458 → 1.436
Char. 5: 0.048-0.088 → 0.042	Char. 52: 1 → 0	Char. 11: 12.300 → 12.400
Char. 7: 0.117-0.123 → 0.132	Char. 71: 0 → 1	Char. 14: 0.787-0.798 → 0.758
Char. 8: 9.550-9.600 → 10.550	Char. 130: 1 → 0	Char. 21: 0.353 → 0.345
Char. 10: 9.965 → 10.119-10.173	Char. 137: 0 → 1	Char. 45: 2 → 1
Char. 124: 2 → 1	Char. 143: 4 → 2	Char. 139: 2 → 1
Node 160	Char. 144: 0 → 1	Char. 195: 1 → 0
Char. 41: 0 → 1	Char. 150: 0 → 2	
Char. 79: 0 → 1	Char. 151: 0 → 1	Node 173
Node 161	Node 167	Char. 59: 0 → 1
Char. 3: 0.899-1.032 → 1.139-1.339	Char. 1: 6.054-6.066 → 6.094	Char. 126: 1 → 0
Char. 5: 0.108-0.139 → 0.048-0.088	Char. 2: 0.220-0.232 → 0.271	
Char. 12: 0.853-0.871 → 0.872	Char. 3: 0.844 → 0.738	Node 174
Char. 13: 0.348 → 0.380	Char. 5: 0.271-0.277 → 0.606	Char. 9: 0.107-0.111 → 0.097-0.098
Char. 67: 1 → 0	Char. 12: 0.910-0.929 → 0.936	Char. 17: 0.518-0.543 → 0.490
Char. 87: 1 → 0	Char. 13: 0.212-0.213 → 0.167	Char. 34: 0 → 1
Char. 137: 0 → 1	Char. 14: 0.787-0.798 → 0.838	Char. 56: 1 → 2
Node 162	Char. 51: 1 → 0	
Char. 7: 0.132 → 0.135	Char. 60: 0 → 1	Node 175
Char. 12: 0.872 → 0.836	Char. 64: 0 → 1	Char. 9: 0.121 → 0.107-0.111
Char. 13: 0.380 → 0.346	Char. 71: 1 → 2	Char. 11: 12.000 → 9.900-10.100
Char. 25: 1 → 0	Char. 78: 0 → 1	Char. 54: 0 → 1
Char. 48: 1 → 0	Char. 92: 0 → 1	Char. 194: 0 → 1
Char. 110: 1 → 0		
Node 163	Node 168	Node 176
Char. 1: 6.003-6.066 → 6.112	Char. 4: 0.551 → 0.565-0.566	Char. 15: 0.766 → 0.731
Char. 5: 0.213-0.232 → 0.203	Char. 5: 0.232 → 0.271-0.277	Char. 16: 0.476 → 0.463-0.473
Char. 6: 1.489-1.515 → 1.528	Char. 17: 0.518 → 0.491-0.506	Char. 57: 0 → 1
Char. 7: 0.094-0.107 → 0.083	Char. 22: 0.491 → 0.391-0.411	Char. 73: 0 → 1
Char. 11: 12.000-12.300 → 10.300	Char. 198: 0 → 1	
Char. 12: 0.910-0.914 → 0.831		Node 177

APPENDIX 8. — Continuation.

Node 178 Char. 2: 0.237 → 0.253 Char. 67: 1 → 2 Char. 112: 0 → 1 Char. 120: 0 → 2	Node 186 Char. 5: 0.260-0.281 → 0.290 Char. 8: 8.250-8.333 → 8.900 Char. 11: 12.000-12.300 → 13.000 Char. 14: 0.723-0.749 → 0.781 Char. 41: 0 → 1 Char. 54: 0 → 1 Char. 61: 0 → 1 Char. 71: 1 → 2	Node 195 Char. 8: 7.800 → 7.200 Char. 67: 2 → 1 Char. 79: 0 → 1
Node 179 Char. 2: 0.220-0.232 → 0.237 Char. 6: 1.489-1.515 → 1.443-1.485 Char. 60: 0 → 1 Char. 105: 0 → 1 Char. 116: 0 → 1 Char. 154: 0 → 1	Node 187 Char. 0: 0.308-0.315 → 0.369 Char. 6: 1.443-1.485 → 1.618 Char. 11: 12.000 → 13.900 Char. 12: 0.910-0.926 → 0.985 Char. 60: 1 → 0	Node 196 Char. 1: 6.005-6.028 → 5.994 Char. 4: 0.523-0.546 → 0.522 Char. 6: 1.443-1.485 → 1.338 Char. 9: 0.088-0.098 → 0.132 Char. 10: 9.663 → 9.599 Char. 51: 1 → 0 Char. 54: 1 → 0 Char. 71: 2 → 1
Node 180 Char. 11: 12.300 → 13.500 Char. 13: 0.212-0.213 → 0.204-0.205 Char. 95: 1 → 0	Node 188 Char. 5: 0.334-0.343 → 0.359 Char. 8: 7.800 → 7.700 Char. 116: 1 → 0	Node 197 Char. 2: 0.253-0.278 → 0.212-0.244 Char. 5: 0.334-0.343 → 0.238-0.294 Char. 8: 6.900-7.000 → 6.500 Char. 10: 9.798-10.009 → 9.663 Char. 116: 1 → 0
Node 181 Char. 2: 0.220-0.232 → 0.250 Char. 12: 0.910-0.929 → 0.887 Char. 58: 0 → 1 Char. 63: 0 → 1 Char. 64: 0 → 1 Char. 73: 0 → 1 Char. 194: 0 → 1	Node 189 Char. 10: 9.751 → 9.680 Char. 114: 2 → 1 Char. 133: 0 → 1	Node 198 Char. 3: 0.563-0.650 → 0.562 Char. 8: 7.200 → 6.900-7.000 Char. 61: 1 → 0
Node 182 Char. 2: 0.250 → 0.305 Char. 10: 9.740-9.851 → 9.480 Char. 12: 0.887 → 0.822 Char. 14: 0.693-0.749 → 0.760 Char. 35: 0 → 1 Char. 60: 0 → 2	Node 190 Char. 4: 0.553 → 0.567-0.569 Char. 5: 0.369 → 0.405-0.414 Char. 40: 0 → 1	Node 199 Char. 1: 6.005-6.028 → 6.072 Char. 4: 0.417 → 0.413 Char. 7: 0.162 → 0.165 Char. 11: 9.900-10.100 → 10.900 Char. 12: 0.874-0.906 → 0.805 Char. 14: 0.757-0.767 → 0.711 Char. 113: 1 → 0 Char. 114: 2 → 4
Node 183 Char. 7: 0.107-0.112 → 0.104 Char. 10: 9.480 → 9.414 Char. 14: 0.760 → 0.818-0.856 Char. 44: 2 → 1 Char. 68: 0 → 1 Char. 83: 1 → 2 Char. 95: 0 → 1	Node 192 Char. 55: 0 → 1 Char. 111: 0 → 1	Node 200 Char. 187: 1 → 0
Node 184 Char. 4: 0.534-0.583 → 0.529 Char. 15: 0.764-0.785 → 0.848 Char. 61: 0 → 1 Char. 73: 1 → 0	Node 193 Char. 4: 0.541-0.544 → 0.408 Char. 12: 0.910 → 0.876 Char. 113: 1 → 0 Char. 131: 1 → 0	Node 201 Char. 3: 0.563-0.650 → 0.689 Char. 5: 0.334-0.343 → 0.119-0.143 Char. 35: 0 → 1 Char. 36: 0 → 1 Char. 37: 0 → 1 Char. 71: 2 → 0 Char. 104: 1 → 0 Char. 106: 1 → 2
Node 185 Char. 56: 1 → 0	Node 194 Char. 0: 0.308-0.315 → 0.307 Char. 4: 0.523-0.546 → 0.604 Char. 60: 1 → 0 Char. 194: 1 → 0	

APPENDIX 8. — Continuation.

Node 202	Node 209	Node 216
Char. 1: 6.005-6.028 → 6.003	Char. 0: 0.356 → 0.420	Char. 8: 6.900-7.000 → 7.800
Char. 2: 0.383 → 0.424	Char. 66: 0 → 1	Char. 11: 10.800 → 11.300
Char. 3: 0.689 → 0.705	Char. 174: 0 → 1	Char. 12: 1.085 → 1.147-1.154
Char. 6: 1.664 → 2.001		Char. 198: 0 → 2
Char. 10: 10.145 → 10.309	Node 210	Node 217
Char. 13: 0.289-0.294 → 0.315	Char. 12: 1.012 → 1.018	Char. 0: 0.420 → 0.490-0.509
Char. 17: 0.485-0.490 → 0.460	Char. 51: 1 → 2	Char. 11: 10.000-10.600 → 10.800
Char. 20: 1.484 → 1.455	Char. 74: 1 → 0	Char. 12: 1.018-1.031 → 1.085
Char. 22: 0.489-0.494 → 0.545	Char. 123: 1 → 2	
Char. 58: 0 → 2	Char. 134: 0 → 1	Node 218
Node 203	Node 211	Char. 1: 6.105 → 6.140
Char. 0: 0.304-0.336 → 0.267	Char. 2: 0.347-0.388 → 0.392-0.409	Char. 4: 0.500-0.518 → 0.382-0.433
Char. 5: 0.446 → 0.466	Char. 10: 10.155 → 10.206-10.269	Char. 5: 0.318-0.368 → 0.195-0.230
Char. 7: 0.125 → 0.130	Char. 12: 0.926-1.010 → 1.012	Char. 12: 1.018-1.031 → 0.918-0.920
Char. 9: 0.088-0.098 → 0.100	Char. 17: 0.507 → 0.519-0.520	Char. 19: 0.562-0.652 → 0.458
Char. 11: 10.400 → 11.200	Char. 18: 0.423 → 0.450-0.478	Char. 21: 0.416-0.417 → 0.411
Char. 125: 1 → 0	Char. 21: 0.352 → 0.416-0.425	Char. 37: 0 → 2
Node 204	Char. 22: 0.476-0.494 → 0.411-0.457	Char. 41: 1 → 2
Char. 3: 0.314-0.500 → 0.201	Char. 64: 0 → 1	Char. 86: 0 → 1
Char. 5: 0.435 → 0.446	Char. 125: 1 → 0	Node 219
Char. 11: 10.100 → 10.400	Node 212	Char. 1: 6.140 → 6.203
Char. 15: 0.734 → 0.796	Char. 4: 0.523-0.538 → 0.500-0.518	Char. 8: 6.655-7.000 → 7.500
Char. 22: 0.476-0.494 → 0.596	Char. 7: 0.117-0.125 → 0.135-0.147	Char. 10: 10.206-10.469 → 10.027
Char. 57: 1 → 0	Char. 10: 9.798-10.009 → 10.155	
Node 205	Char. 13: 0.203-0.240 → 0.202	Node 220
Char. 5: 0.354-0.368 → 0.435	Char. 15: 0.724-0.734 → 0.653-0.722	Char. 0: 0.420 → 0.423
Char. 14: 0.790-0.814 → 0.821-0.858	Char. 17: 0.490 → 0.507	Char. 71: 2 → 0
Char. 17: 0.490 → 0.479-0.481	Char. 18: 0.348-0.361 → 0.423	
Char. 106: 1 → 2	Char. 56: 2 → 3	Node 221
Char. 186: 0 → 1	Char. 132: 1 → 0	Char. 5: 0.318-0.368 → 0.233
Node 206	Char. 149: 2 → 1	Char. 71: 2 → 1
Char. 1: 6.005-6.028 → 6.064-6.104	Char. 174: 1 → 0	
Char. 3: 0.562 → 0.314-0.500	Char. 178: 0 → 1	Node 222
Char. 5: 0.334-0.343 → 0.354-0.368	Node 213	Char. 2: 0.392-0.409 → 0.445
Char. 63: 0 → 1	Char. 61: 0 → 1	Char. 3: 0.314-0.500 → 0.618-0.667
Char. 74: 0 → 1	Node 214	Char. 7: 0.143-0.147 → 0.151-0.183
Char. 75: 1 → 2	Char. 0: 0.490-0.509 → 0.421	Char. 9: 0.085-0.091 → 0.060-0.084
Char. 81: 1 → 0	Char. 1: 6.069-6.105 → 6.121	Char. 43: 0 → 1
Char. 113: 1 → 0	Char. 9: 0.088-0.091 → 0.086	Char. 44: 2 → 1
Node 207	Char. 34: 1 → 0	Char. 67: 1 → 0
Char. 5: 0.318-0.368 → 0.476	Char. 40: 0 → 1	Char. 71: 2 → 0
Char. 15: 0.542-0.686 → 0.705	Char. 72: 0 → 1	Char. 75: 2 → 1
Char. 186: 0 → 1	Char. 106: 1 → 2	Char. 157: 5 → 0
Node 208	Char. 114: 2 → 1	Char. 197: 0 → 1
Char. 9: 0.088-0.091 → 0.094	Node 215	
Char. 13: 0.192-0.202 → 0.243	Char. 8: 7.800 → 9.800-9.900	Node 223
Char. 67: 1 → 2	Char. 11: 11.300 → 11.900	Char. 43: 1 → 0
Char. 106: 1 → 2	Char. 43: 0 → 1	Char. 51: 1 → 0
		Char. 168: 0 → 1
		Char. 196: 0 → 1

APPENDIX 8. — Continuation.

Node 224	Node 229	Node 231
Char. 167: 0 → 1	Char. 17: 0.519-0.524 → 0.530	Char. 2: 0.445 → 0.423
Node 225	Char. 19: 0.647-0.652 → 0.592	Char. 3: 0.618 → 0.331
Char. 15: 0.722 → 0.841-0.897	Char. 22: 0.457 → 0.526-0.565	Char. 5: 0.368 → 0.499
Char. 66: 0 → 1	Char. 62: 0 → 1	Char. 20: 1.789 → 0.818
Char. 156: 0 → 1	Char. 158: 1 → 0	Char. 123: 1 → 3
Node 226	Char. 165: 0 → 1	Char. 164: 3 → 2
No synapomorphies	Char. 194: 1 → 0	Char. 169: 1 → 0
Node 227	Node 230	Node 232
No synapomorphies	Char. 17: 0.530 → 0.538	Char. 54: 0 → 1
Node 228	Char. 67: 0 → 1	Node 233
Char. 67: 0 → 2	Char. 75: 1 → 2	Char. 8: 6.900-7.000 → 7.300
	Char. 87: 1 → 0	Char. 67: 1 → 2
	Char. 106: 1 → 2	Char. 103: 1 → 0
	Char. 198: 0 → 123	Char. 104: 1 → 0

APPENDIX 9. — *Ufudocyclops mukanelai* Kammerer, Viglietti, Hancox, Butler & Choiniere, 2019 inactivated, majority rule (50%) consensus tree. Majority rule (50%) consensus, *Ufudocyclops mukanelai* inactivated, node numbers. https://doi.org/10.5852/cr-palevol2023v22a16_s6

APPENDIX 10. — Majority rule (50%) consensus tree, *Ufudocyclops mukanelai* Kammerer, Viglietti, Hancox, Butler & Choiniere, 2019 inactivated, bootstrap supports. https://doi.org/10.5852/cr-palevol2023v22a16_s7

APPENDIX 11. — List of synapomorphies, *Ufudocyclops mukanelai* Kammerer, Viglietti, Hancox, Butler & Choiniere, 2019 inactivated, majority rule (50%) consensus.

<i>Biarmosuchus tener</i>	<i>Glanosuchus macrops</i>	<i>Patranomodon nyaphulii</i>
No autapomorphies	Char. 2: 0.244-0.261 → 0.145 Char. 3: 0.333 → 0.250 Char. 4: 0.352 → 0.367 Char. 8: 5.800-6.200 → 5.300 Char. 9: 0.090-0.094 → 0.050 Char. 10: 10.455-10.905 → 11.029 Char. 11: 11.600-12.000 → 13.700 Char. 12: 0.847-0.871 → 0.744 Char. 13: 0.355-0.395 → 0.476 Char. 14: 0.920-0.956 → 1.250 Char. 15: 1.870 → 2.630 Char. 66: 0 → 1	Char. 0: 0.339 → 0.290 Char. 5: 0.094-0.105 → 0.076 Char. 7: 0.198 → 0.202 Char. 9: 0.090-0.094 → 0.043 Char. 10: 10.455-10.905 → 11.029 Char. 11: 11.600-12.000 → 13.700 Char. 12: 0.847-0.871 → 0.744 Char. 13: 0.355-0.395 → 0.476 Char. 14: 0.920-0.956 → 1.250 Char. 15: 1.870 → 2.630 Char. 66: 0 → 1
<i>Hipposaurus boonstrai</i>	<i>Biseridens qilianicus</i>	<i>Galeops whaitsi</i>
Char. 8: 5.800 → 3.500 Char. 12: 1.060 → 1.070 Char. 15: 1.870 → 2.630 Char. 73: 2 → 0 Char. 95: 0 → 1 Char. 114: 2 → 0 Char. 166: 0 → 1 Char. 184: 1 → 0 Char. 191: 1 → 0	Char. 65: 0 → 1 Char. 90: 0 → 1 Char. 113: 1 → 0 Char. 159: 0 → 1	Char. 2: 0.195-0.228 → 0.180 Char. 7: 0.140 → 0.136 Char. 8: 5.600-6.000 → 4.100 Char. 13: 0.355-0.395 → 0.489 Char. 16: 0.545-0.558 → 0.646 Char. 17: 0.396-0.401 → 0.356 Char. 92: 0 → 1 Char. 119: 0 → 1 Char. 121: 0 → 1 Char. 153: 0 → 1 Char. 168: 0 → 1
<i>Archaeosyodon praeventor</i>	<i>Anomocephalus africanus</i>	<i>Galepus jouberti</i>
Char. 141: 0 → 1	No autapomorphies	Char. 3: 0.914 → 0.855 Char. 170: 0 → 1
<i>Titanophoneus potens</i>	<i>Tiarajudens eccentricus</i>	<i>Galechirus scholtzi</i>
Char. 0: 0.509-0.547 → 0.758 Char. 4: 0.272-0.305 → 0.227 Char. 5: 0.072-0.104 → 0.051 Char. 12: 1.020-1.060 → 1.160 Char. 16: 0.545-0.558 → 0.500 Char. 17: 0.299-0.329 → 0.292 Char. 18: 0.149-0.200 → 0.274 Char. 22: 0.257-0.342 → 0.343 Char. 64: 0 → 1 Char. 73: 1 → 0 Char. 155: 0 → 1 Char. 185: 0 → 1	Char. 44: 1 → 0	Char. 15: 0.968 → 0.700
<i>Gorgonops torvus</i>	<i>Otsheria netzvetajevi</i>	<i>Eodicyodon oelofseni</i>
Char. 0: 0.509-0.547 → 0.504 Char. 2: 0.261-0.263 → 0.290 Char. 3: 0.842 → 1.150 Char. 8: 5.800-6.200 → 8.500 Char. 12: 1.020-1.060 → 0.977 Char. 62: 0 → 1 Char. 77: 0 → 2 Char. 158: 0 → 1 Char. 183: 0 → 1 Char. 186: 0 → 1 Char. 187: 0 → 1 Char. 188: 0 → 1	Char. 1: 5.364 → 5.425 Char. 2: 0.205-0.228 → 0.231 Char. 4: 0.407 → 0.512 Char. 5: 0.102-0.105 → 0.108 Char. 7: 0.198 → 0.181 Char. 10: 10.905 → 10.950 Char. 11: 15.400 → 15.500 Char. 12: 0.902 → 0.860 Char. 33: 1 → 0 Char. 101: 12 → 0	Char. 0: 0.381 → 0.470 Char. 2: 0.205-0.228 → 0.125 Char. 7: 0.198 → 0.216 Char. 8: 5.000-5.300 → 4.900 Char. 12: 0.902 → 1.098 Char. 44: 1 → 0 Char. 61: 0 → 1 Char. 124: 0 → 1
<i>Lycosuchus vanderrieti</i>	<i>Suminia getmanovi</i>	<i>Eodicyodon oosthuizeni</i>
Char. 5: 0.218 → 0.303 Char. 8: 5.800-6.200 → 7.700 Char. 16: 0.545 → 0.500 Char. 17: 0.309-0.329 → 0.333 Char. 18: 0.200 → 0.294 Char. 22: 0.342 → 0.400 Char. 46: 0 → 1 Char. 57: 0 → 2 Char. 119: 0 → 1	Char. 0: 0.339-0.381 → 0.336 Char. 1: 5.325-5.364 → 4.879 Char. 4: 0.272-0.305 → 0.230 Char. 14: 0.920-0.956 → 0.899 Char. 47: 1 → 2 Char. 57: 0 → 1 Char. 80: 01 → 2 Char. 103: 0 → 2 Char. 140: 1 → 2 Char. 162: 1 → 2	Char. 2: 0.195-0.228 → 0.234 Char. 6: 2.470 → 2.501 Char. 8: 6.600-8.100 → 8.200 Char. 11: 10.600-11.200 → 9.000 Char. 14: 0.708-0.723 → 0.698 Char. 15: 0.968 → 1.061 Char. 16: 0.487-0.558 → 0.446 Char. 17: 0.437-0.486 → 0.509 Char. 19: 0.301-0.553 → 0.300 Char. 22: 0.315-0.366 → 0.475 Char. 127: 1 → 0 Char. 177: 0 → 1 Char. 193: 0 → 1

APPENDIX 11. — Continuation.

Colobodectes cluveri

Char. 0: 0.231-0.237 → 0.203
 Char. 5: 0.222-0.257 → 0.269
 Char. 7: 0.140 → 0.142
 Char. 9: 0.182-0.199 → 0.206
 Char. 12: 0.850-0.871 → 0.948
 Char. 63: 0 → 1
 Char. 73: 1 → 0
 Char. 96: 0 → 1

Lanthanostegus mohoui

Char. 3: 0.795-0.908 → 0.661
 Char. 65: 0 → 1
 Char. 77: 1 → 2
 Char. 85: 2 → 0
 Char. 111: 0 → 1

Eosimops newtoni

Char. 0: 0.231-0.237 → 0.186
 Char. 1: 5.863 → 5.890
 Char. 2: 0.197 → 0.243
 Char. 9: 0.182-0.199 → 0.172
 Char. 10: 9.417 → 9.402
 Char. 11: 10.600-11.200 → 11.300
 Char. 12: 0.850 → 0.831
 Char. 13: 0.253-0.257 → 0.402
 Char. 14: 0.723-0.742 → 0.803
 Char. 16: 0.487-0.558 → 0.633
 Char. 22: 0.315-0.366 → 0.444
 Char. 65: 0 → 1
 Char. 114: 2 → 3
 Char. 122: 1 → 0
 Char. 143: 2 → 4
 Char. 146: 1 → 0
 Char. 177: 0 → 1

Diictodon feliceps

Char. 0: 0.238 → 0.247
 Char. 1: 5.810-5.863 → 5.925
 Char. 2: 0.195-0.197 → 0.223
 Char. 3: 0.795-0.864 → 0.640
 Char. 5: 0.228-0.257 → 0.273
 Char. 6: 1.751-2.013 → 1.702
 Char. 7: 0.123-0.126 → 0.135
 Char. 8: 8.100 → 8.000
 Char. 9: 0.182-0.199 → 0.214
 Char. 11: 10.600-11.200 → 11.900
 Char. 45: 1 → 2
 Char. 94: 0 → 1
 Char. 95: 0 → 1
 Char. 96: 0 → 1
 Char. 124: 1 → 2
 Char. 139: 1 → 2

Robertia broomiana

Char. 3: 0.795 → 0.721
 Char. 4: 0.541 → 0.555
 Char. 5: 0.257 → 0.259
 Char. 6: 1.751-2.013 → 1.681
 Char. 7: 0.123-0.126 → 0.108
 Char. 8: 8.100 → 8.600
 Char. 11: 10.600-11.200 → 9.800
 Char. 13: 0.253-0.257 → 0.132
 Char. 14: 0.723-0.742 → 0.711
 Char. 15: 0.901-0.904 → 0.868
 Char. 17: 0.466-0.486 → 0.502
 Char. 18: 0.260 → 0.227
 Char. 22: 0.315-0.366 → 0.309

Prosictodon dubei

Char. 1: 5.810-5.863 → 5.807
 Char. 2: 0.195-0.197 → 0.171
 Char. 4: 0.534-0.541 → 0.548
 Char. 6: 1.751-2.013 → 2.469
 Char. 7: 0.123-0.126 → 0.098
 Char. 9: 0.182-0.199 → 0.131
 Char. 10: 9.418-9.687 → 9.780
 Char. 11: 10.600-11.200 → 9.300
 Char. 14: 0.742 → 0.834
 Char. 15: 0.901 → 0.637

Abajudon kaayai

Char. 1: 5.396 → 5.215
 Char. 3: 0.867-0.906 → 1.030
 Char. 4: 0.515-0.541 → 0.412
 Char. 6: 1.548-1.565 → 2.844
 Char. 7: 0.118-0.126 → 0.146
 Char. 14: 0.798-0.859 → 0.898
 Char. 15: 0.924-0.938 → 1.016
 Char. 29: 1 → 0
 Char. 70: 1 → 0
 Char. 104: 1 → 0
 Char. 117: 0 → 1
 Char. 122: 1 → 0
 Char. 146: 1 → 0
 Char. 150: 0 → 1

Niassodon mfumukasi

Char. 12: 0.850-0.871 → 0.697
 Char. 19: 0.301 → 0.214
 Char. 44: 2 → 1
 Char. 54: 0 → 1
 Char. 67: 1 → 2
 Char. 68: 0 → 1
 Char. 69: 1 → 2
 Char. 73: 1 → 2
 Char. 81: 1 → 0
 Char. 102: 0 → 1
 Char. 111: 0 → 1
 Char. 164: 2 → 1

Brachyprosopus broomi

Char. 5: 0.222-0.257 → 0.338
 Char. 7: 0.123-0.126 → 0.129
 Char. 8: 8.100-8.400 → 6.800
 Char. 12: 0.850-0.871 → 0.898
 Char. 13: 0.208-0.257 → 0.132
 Char. 14: 0.723 → 0.715
 Char. 15: 0.924-0.928 → 0.824
 Char. 16: 0.554-0.594 → 0.612
 Char. 25: 0 → 1
 Char. 34: 0 → 1
 Char. 46: 0 → 1
 Char. 77: 1 → 2
 Char. 93: 1 → 0
 Char. 116: 0 → 1

Endothiodon tolani

Char. 5: 0.126-0.257 → 0.025
 Char. 7: 0.111 → 0.109
 Char. 8: 8.400-9.400 → 10.600
 Char. 14: 0.798 → 0.723
 Char. 94: 0 → 1

Endothiodon bathystoma

Char. 0: 0.328 → 0.335
 Char. 3: 0.396 → 0.268
 Char. 5: 0.126-0.257 → 0.400
 Char. 6: 1.505 → 1.457
 Char. 8: 8.400-9.400 → 8.100
 Char. 12: 0.902-0.907 → 0.988
 Char. 13: 0.319 → 0.373
 Char. 15: 0.825 → 0.730
 Char. 38: 1 → 0
 Char. 44: 2 → 1
 Char. 60: 0 → 1
 Char. 66: 0 → 1
 Char. 68: 0 → 1
 Char. 110: 1 → 0

Pristerodon mackayi

Char. 0: 0.231-0.237 → 0.225
 Char. 1: 5.810-5.863 → 5.874
 Char. 2: 0.190-0.197 → 0.184
 Char. 3: 0.867-0.998 → 1.026
 Char. 4: 0.520-0.541 → 0.582
 Char. 8: 8.100-8.400 → 10.000
 Char. 9: 0.182-0.199 → 0.206
 Char. 12: 0.850-0.871 → 0.813
 Char. 17: 0.437-0.486 → 0.430
 Char. 19: 0.301-0.454 → 0.275
 Char. 22: 0.315-0.366 → 0.275
 Char. 79: 0 → 1
 Char. 167: 0 → 1

APPENDIX 11. — Continuation.

Emydops

Char. 1: 5.874 → 5.872
 Char. 2: 0.207 → 0.204
 Char. 10: 9.740-9.775 → 9.667
 Char. 11: 10.600-11.000 → 9.300
 Char. 38: 1 → 0
 Char. 81: 1 → 0
 Char. 128: 1 → 0

Compsodon helmoedi

Char. 0: 0.220 → 0.196
 Char. 3: 0.906 → 1.066
 Char. 4: 0.473-0.537 → 0.431
 Char. 6: 1.646 → 1.710
 Char. 7: 0.118 → 0.082
 Char. 8: 9.800 → 10.300
 Char. 9: 0.176 → 0.220
 Char. 10: 9.740-9.775 → 9.858
 Char. 12: 0.840 → 0.817
 Char. 41: 0 → 1
 Char. 61: 0 → 1
 Char. 67: 1 → 2
 Char. 68: 0 → 1
 Char. 70: 1 → 0
 Char. 71: 0 → 1
 Char. 77: 1 → 3
 Char. 102: 0 → 1
 Char. 115: 1 → 0
 Char. 120: 0 → 1
 Char. 131: 1 → 0

Digalodon rubidgei

Char. 0: 0.269-0.281 → 0.354
 Char. 1: 5.948-5.950 → 6.155
 Char. 7: 0.118-0.123 → 0.134
 Char. 24: 0 → 2
 Char. 48: 1 → 0
 Char. 77: 1 → 3
 Char. 79: 0 → 1

Illiptosaurus imperforatus

Char. 2: 0.202-0.240 → 0.198
 Char. 4: 0.473-0.483 → 0.407
 Char. 15: 0.924 → 0.667
 Char. 137: 0 → 1

Rastodon procurvidens

Char. 0: 0.231-0.279 → 0.197
 Char. 2: 0.207-0.232 → 0.199
 Char. 4: 0.541-0.544 → 0.558
 Char. 5: 0.260-0.281 → 0.298
 Char. 8: 8.250-8.333 → 6.600
 Char. 9: 0.121-0.132 → 0.105
 Char. 12: 0.850-0.871 → 0.798
 Char. 13: 0.212-0.219 → 0.100
 Char. 14: 0.723-0.730 → 0.623
 Char. 15: 0.766-0.819 → 0.667
 Char. 136: 1 → 2

Dicynodontoides

Char. 6: 1.500-1.565 → 1.492
 Char. 7: 0.116 → 0.085
 Char. 10: 9.775 → 9.814
 Char. 12: 0.853-0.871 → 0.887
 Char. 26: 0 → 1
 Char. 44: 1 → 2

Kombuisia frerensis

Char. 0: 0.269 → 0.193
 Char. 1: 5.950 → 5.976
 Char. 3: 0.764 → 0.400
 Char. 4: 0.539 → 0.555
 Char. 6: 1.500-1.565 → 1.589
 Char. 7: 0.116 → 0.195
 Char. 10: 9.775 → 9.645
 Char. 12: 0.853-0.871 → 0.746
 Char. 14: 0.726 → 0.684
 Char. 48: 1 → 0
 Char. 54: 0 → 1
 Char. 74: 0 → 1
 Char. 131: 1 → 0
 Char. 146: 0 → 1
 Char. 150: 1 → 0
 Char. 160: 1 → 0

Myosaurus gracilis

Char. 0: 0.269-0.279 → 0.260
 Char. 1: 5.948-5.950 → 5.902
 Char. 6: 1.500-1.565 → 1.590
 Char. 7: 0.116 → 0.085
 Char. 9: 0.181 → 0.208
 Char. 11: 10.600-11.000 → 9.600
 Char. 14: 0.726-0.750 → 0.958
 Char. 15: 0.924-0.928 → 0.942
 Char. 16: 0.485-0.554 → 0.586
 Char. 22: 0.353-0.359 → 0.208
 Char. 25: 1 → 0
 Char. 28: 0 → 1
 Char. 54: 0 → 1
 Char. 57: 0 → 2
 Char. 98: 1 → 0
 Char. 174: 0 → 1
 Char. 175: 0 → 1

Kembawacela kitchingi

Char. 0: 0.308-0.311 → 0.372
 Char. 3: 1.319-1.404 → 1.487
 Char. 6: 1.490-1.500 → 1.455
 Char. 12: 0.872 → 0.969
 Char. 13: 0.380 → 0.415
 Char. 15: 0.914-0.964 → 0.990
 Char. 28: 0 → 2
 Char. 44: 1 → 2
 Char. 96: 1 → 0
 Char. 134: 0 → 1
 Char. 159: 1 → 0

Cistecephalus microrhinus

Char. 1: 5.948-5.950 → 6.056
 Char. 4: 0.421-0.483 → 0.509
 Char. 11: 10.600-11.000 → 10.200
 Char. 14: 0.726-0.730 → 0.687
 Char. 17: 0.419 → 0.403
 Char. 22: 0.353-0.359 → 0.324
 Char. 61: 0 → 1
 Char. 174: 0 → 1

Sauropsraptor tharavati

Char. 12: 0.872 → 0.912
 Char. 13: 0.380 → 0.564
 Char. 15: 0.789-0.928 → 0.714

Cistecephalooides boonstrai

Char. 1: 5.948-5.950 → 6.047
 Char. 2: 0.330-0.383 → 0.425
 Char. 7: 0.135 → 0.194
 Char. 10: 10.119-10.173 → 10.305
 Char. 11: 10.600-11.650 → 12.500
 Char. 12: 0.836 → 0.632
 Char. 62: 0 → 1
 Char. 88: 1 → 0
 Char. 127: 0 → 1

Kawingasaurus fossilis

Char. 1: 5.948-5.950 → 5.933
 Char. 4: 0.357-0.372 → 0.340
 Char. 11: 10.600-11.650 → 10.000
 Char. 13: 0.346 → 0.286
 Char. 56: 1 → 0
 Char. 57: 0 → 2
 Char. 76: 0 → 1
 Char. 130: 1 → 0
 Char. 137: 1 → 0
 Char. 147: 2 → 0
 Char. 149: 2 → 1
 Char. 150: 1 → 0

APPENDIX 11. — Continuation.

Daqingshanodon limbus

Char. 2: 0.220-0.232 → 0.260
 Char. 3: 0.640-0.892 → 0.619
 Char. 4: 0.541-0.544 → 0.442
 Char. 5: 0.203 → 0.180
 Char. 7: 0.083 → 0.080
 Char. 12: 0.831 → 0.808
 Char. 63: 0 → 1
 Char. 77: 1 → 3

Keyseria benjamini

Char. 1: 6.112 → 6.155
 Char. 2: 0.220-0.232 → 0.159
 Char. 3: 0.640-0.892 → 1.034
 Char. 4: 0.541-0.544 → 0.605
 Char. 6: 1.528 → 1.600
 Char. 11: 10.300 → 9.000
 Char. 54: 0 → 1
 Char. 71: 1 → 0
 Char. 113: 1 → 0

Rhachiocephalus magnus

Char. 0: 0.320 → 0.329
 Char. 4: 0.566 → 0.598
 Char. 8: 8.100-8.333 → 8.800
 Char. 9: 0.132-0.141 → 0.143
 Char. 10: 9.219-9.740 → 9.170
 Char. 11: 12.300 → 12.800
 Char. 12: 0.936 → 1.010
 Char. 15: 0.752 → 0.777
 Char. 79: 1 → 0
 Char. 83: 1 → 0
 Char. 150: 2 → 0
 Char. 151: 1 → 0
 Char. 168: 0 → 1

Kitchinganomodon crassus

Char. 1: 6.094 → 6.137
 Char. 2: 0.271 → 0.318
 Char. 3: 0.738 → 0.708
 Char. 5: 0.606 → 0.752
 Char. 6: 1.480 → 1.556
 Char. 7: 0.094-0.098 → 0.108
 Char. 8: 8.100-8.333 → 7.400
 Char. 9: 0.132-0.141 → 0.070
 Char. 10: 9.219-9.740 → 9.747
 Char. 11: 12.300 → 11.100
 Char. 13: 0.167 → 0.165
 Char. 14: 0.838 → 0.843
 Char. 17: 0.491-0.506 → 0.466
 Char. 95: 1 → 0
 Char. 114: 2 → 3

Oudenodon bainii

Char. 0: 0.284-0.320 → 0.281
 Char. 2: 0.183-0.197 → 0.173
 Char. 4: 0.565-0.566 → 0.609
 Char. 7: 0.094-0.098 → 0.092
 Char. 11: 12.300 → 11.300
 Char. 12: 0.875-0.882 → 0.864
 Char. 13: 0.212-0.237 → 0.264
 Char. 16: 0.531-0.550 → 0.570
 Char. 20: 1.033-1.130 → 0.765
 Char. 194: 0 → 1

Tropidostoma dubium

Char. 1: 6.054-6.058 → 5.989
 Char. 3: 0.844 → 0.899
 Char. 8: 8.100-8.333 → 8.800
 Char. 10: 9.219-9.740 → 9.106
 Char. 15: 0.745-0.752 → 0.766
 Char. 19: 0.514 → 0.474
 Char. 20: 1.033-1.130 → 1.368
 Char. 22: 0.391 → 0.378
 Char. 95: 1 → 0
 Char. 96: 1 → 0

Australobarbarus

Char. 0: 0.284-0.320 → 0.333
 Char. 3: 0.844 → 0.697
 Char. 4: 0.565 → 0.561
 Char. 5: 0.277 → 0.298
 Char. 6: 1.436 → 1.324
 Char. 7: 0.098 → 0.101
 Char. 8: 8.100-8.333 → 6.100
 Char. 9: 0.140-0.141 → 0.160
 Char. 10: 9.219-9.740 → 9.822
 Char. 11: 12.400 → 13.350
 Char. 13: 0.212-0.237 → 0.193
 Char. 14: 0.758 → 0.624
 Char. 15: 0.745-0.752 → 0.694
 Char. 16: 0.531 → 0.466
 Char. 17: 0.491-0.503 → 0.485
 Char. 19: 0.514 → 0.848
 Char. 21: 0.345 → 0.333
 Char. 104: 1 → 0
 Char. 112: 0 → 1

Syops vanhoopeni

Char. 3: 0.563-0.650 → 0.484
 Char. 27: 2 → 1
 Char. 53: 0 → 1
 Char. 57: 1 → 0
 Char. 99: 1 → 2
 Char. 144: 1 → 0
 Char. 154: 1 → 0
 Char. 198: 01 → 2

Odontocyclops whaitsi

Char. 0: 0.289-0.320 → 0.376
 Char. 3: 0.844-0.892 → 0.988
 Char. 6: 1.458-1.480 → 1.448
 Char. 7: 0.094-0.098 → 0.092
 Char. 8: 8.250-8.333 → 10.100
 Char. 9: 0.132-0.141 → 0.131
 Char. 15: 0.745-0.752 → 0.731
 Char. 16: 0.550 → 0.551
 Char. 18: 0.366 → 0.427
 Char. 19: 0.514 → 0.435
 Char. 21: 0.353-0.395 → 0.426
 Char. 60: 0 → 2
 Char. 68: 0 → 1

Idelesaurus tataricus

Char. 0: 0.289-0.320 → 0.367
 Char. 1: 6.003-6.066 → 5.967
 Char. 2: 0.220-0.232 → 0.175
 Char. 3: 0.844-0.892 → 1.022
 Char. 4: 0.534-0.544 → 0.500
 Char. 5: 0.213-0.232 → 0.174
 Char. 9: 0.132-0.141 → 0.173
 Char. 10: 9.740-9.851 → 10.118
 Char. 12: 0.910-0.929 → 0.969
 Char. 57: 0 → 1
 Char. 60: 0 → 1
 Char. 68: 0 → 1
 Char. 96: 1 → 0
 Char. 120: 1 → 0
 Char. 131: 1 → 0

Bulbasaurus phylloxyron

Char. 0: 0.289-0.300 → 0.284
 Char. 3: 0.844-0.892 → 0.562
 Char. 5: 0.213-0.232 → 0.233
 Char. 6: 1.425-1.468 → 1.362
 Char. 8: 8.250-8.720 → 10.333
 Char. 9: 0.122-0.141 → 0.052
 Char. 11: 13.500 → 14.780
 Char. 14: 0.693-0.749 → 0.643
 Char. 53: 1 → 0
 Char. 59: 1 → 0

Aulacephalodon bainii

Char. 2: 0.305 → 0.323
 Char. 5: 0.213-0.232 → 0.204
 Char. 7: 0.107-0.112 → 0.117
 Char. 8: 8.250-8.720 → 6.800
 Char. 13: 0.204-0.205 → 0.172
 Char. 144: 1 → 0

APPENDIX 11. — Continuation.

Pelanomodon moschops
 Char. 1: 6.049-6.089 → 6.093
 Char. 3: 0.892-0.908 → 0.912
 Char. 4: 0.534-0.583 → 0.584
 Char. 8: 8.720 → 9.400
 Char. 9: 0.141 → 0.155
 Char. 11: 13.100-13.500 → 12.300
 Char. 15: 0.764-0.785 → 0.742

Geikia locusticeps
 Char. 0: 0.289-0.300 → 0.256
 Char. 2: 0.305 → 0.278
 Char. 4: 0.529 → 0.514
 Char. 6: 1.429-1.468 → 1.627
 Char. 11: 13.100-13.500 → 13.900
 Char. 12: 0.801-0.822 → 0.756
 Char. 81: 1 → 0
 Char. 150: 2 → 0

Geikia elginensis
 Char. 0: 0.289-0.300 → 0.366
 Char. 2: 0.305 → 0.521
 Char. 3: 0.892-0.908 → 0.846
 Char. 12: 0.801-0.822 → 0.829
 Char. 13: 0.205 → 0.212
 Char. 14: 0.818-0.856 → 0.900
 Char. 15: 0.848 → 0.987
 Char. 54: 0 → 1
 Char. 55: 0 → 1
 Char. 118: 0 → 1
 Char. 137: 1 → 0

Elph borealis
 No autapomorphies

Interpresosaurus blomi
 Char. 73: 0 → 1

Katumbia parringtoni
 Char. 0: 0.240-0.279 → 0.196
 Char. 1: 5.927 → 5.868
 Char. 3: 0.640 → 0.527
 Char. 5: 0.290 → 0.347
 Char. 8: 8.900 → 9.300
 Char. 11: 13.000 → 14.400
 Char. 14: 0.781 → 0.833
 Char. 51: 1 → 0
 Char. 68: 0 → 1
 Char. 112: 0 → 1
 Char. 125: 0 → 1
 Char. 131: 1 → 0

Delectosaurus arefjevi
 Char. 1: 5.937-6.019 → 5.861
 Char. 2: 0.253 → 0.258
 Char. 3: 0.685 → 0.702
 Char. 7: 0.117-0.118 → 0.119
 Char. 9: 0.121 → 0.130
 Char. 11: 13.900 → 14.700
 Char. 40: 0 → 1
 Char. 120: 2 → 1
 Char. 131: 1 → 0
 Char. 135: 1 → 0

Dicynodon lacerticeps
 Char. 0: 0.308-0.315 → 0.324
 Char. 11: 12.000 → 11.900
 Char. 13: 0.219 → 0.241
 Char. 112: 1 → 0

Dicynodon angielczyki
 Char. 3: 0.607 → 0.524
 Char. 4: 0.546 → 0.569
 Char. 6: 1.443-1.485 → 1.351
 Char. 7: 0.117 → 0.105
 Char. 8: 7.700 → 7.560
 Char. 9: 0.121 → 0.114
 Char. 10: 9.869 → 9.950
 Char. 12: 0.926 → 0.965
 Char. 14: 0.749 → 0.808
 Char. 150: 2 → 0

Daptocephalus huenei
 Char. 6: 1.347-1.485 → 1.250
 Char. 7: 0.118 → 0.123
 Char. 9: 0.111 → 0.117
 Char. 12: 0.895-0.924 → 1.024

Daptocephalus leoniceps
 Char. 0: 0.292 → 0.268
 Char. 2: 0.230 → 0.237
 Char. 3: 0.563-0.564 → 0.539
 Char. 5: 0.414 → 0.437
 Char. 6: 1.347-1.485 → 1.500
 Char. 10: 9.680 → 9.378
 Char. 12: 0.895-0.924 → 0.858
 Char. 17: 0.543 → 0.545

Dinanomodon gilli
 Char. 3: 0.563-0.564 → 0.480
 Char. 5: 0.405-0.414 → 0.522
 Char. 12: 0.895-0.924 → 1.047
 Char. 54: 1 → 0

Peramodon amalitzkii
 Char. 0: 0.292-0.315 → 0.272
 Char. 11: 9.900-10.100 → 9.500
 Char. 12: 0.895-0.924 → 0.839
 Char. 13: 0.186-0.219 → 0.167
 Char. 14: 0.723-0.763 → 0.676
 Char. 15: 0.724-0.731 → 0.680
 Char. 60: 1 → 0

Taoheodon baizhijuni
 Char. 1: 5.927-5.982 → 6.100
 Char. 6: 1.443-1.485 → 1.180
 Char. 7: 0.112-0.118 → 0.110
 Char. 9: 0.121-0.132 → 0.105
 Char. 10: 9.740-9.775 → 9.640
 Char. 13: 0.212-0.219 → 0.285
 Char. 41: 0 → 1
 Char. 55: 0 → 1
 Char. 63: 0 → 1
 Char. 110: 1 → 0
 Char. 132: 1 → 0
 Char. 133: 0 → 1

Counillonia superoculis
 Char. 4: 0.408 → 0.276
 Char. 5: 0.260-0.281 → 0.134
 Char. 11: 12.000 → 9.616
 Char. 57: 0 → 2

Repelinosaurus robustus
 Char. 0: 0.240-0.297 → 0.200
 Char. 11: 12.000 → 14.698
 Char. 12: 0.876 → 0.829
 Char. 34: 0 → 1
 Char. 54: 0 → 1

Vivaxosaurus trautscholdi
 Char. 0: 0.369 → 0.380
 Char. 2: 0.253 → 0.230
 Char. 4: 0.541-0.546 → 0.481
 Char. 5: 0.334 → 0.285
 Char. 6: 1.618 → 1.824
 Char. 7: 0.117-0.118 → 0.116
 Char. 8: 7.800 → 7.900
 Char. 10: 9.798-9.869 → 10.203
 Char. 12: 0.985 → 1.041
 Char. 41: 0 → 1
 Char. 55: 0 → 1
 Char. 61: 1 → 0
 Char. 71: 2 → 1
 Char. 95: 1 → 0
 Char. 96: 1 → 0

APPENDIX 11. — Continuation.

Jimusaria sinkianensis
 Char. 3: 0.650 → 0.672
 Char. 4: 0.604 → 0.767
 Char. 5: 0.334-0.343 → 0.464
 Char. 12: 0.924 → 0.992
 Char. 13: 0.203-0.240 → 0.251
 Char. 15: 0.724-0.734 → 0.699
 Char. 51: 1 → 2
 Char. 54: 1 → 0
 Char. 56: 2 → 1
 Char. 112: 1 → 0

Sintocephalus alticeps
 Char. 0: 0.315-0.336 → 0.354
 Char. 1: 5.994 → 5.969
 Char. 3: 0.562 → 0.516
 Char. 10: 9.599 → 9.399
 Char. 11: 10.000-10.250 → 9.600
 Char. 12: 0.814-0.924 → 1.022
 Char. 34: 1 → 0

Basilodon woodwardi
 Char. 3: 0.562 → 0.722
 Char. 4: 0.522 → 0.497
 Char. 5: 0.238-0.294 → 0.225
 Char. 6: 1.338 → 1.305
 Char. 7: 0.124 → 0.128
 Char. 8: 6.500 → 5.700
 Char. 9: 0.132 → 0.139
 Char. 11: 10.000-10.250 → 12.600
 Char. 57: 1 → 0
 Char. 61: 0 → 1
 Char. 67: 1 → 2
 Char. 99: 1 → 2

Turfanodon bogdaensis
 Char. 3: 0.563-0.564 → 0.588
 Char. 6: 1.347 → 1.327
 Char. 11: 9.900-10.100 → 10.300
 Char. 61: 1 → 0
 Char. 79: 0 → 1
 Char. 106: 1 → 2

Gordonia traquairi
 Char. 0: 0.307 → 0.252
 Char. 2: 0.253-0.278 → 0.139
 Char. 5: 0.334-0.343 → 0.309
 Char. 13: 0.203-0.240 → 0.188
 Char. 15: 0.724-0.734 → 0.773
 Char. 34: 1 → 0

Euptychognathus bathyrhynchus
 Char. 2: 0.212-0.244 → 0.130
 Char. 4: 0.523-0.546 → 0.560
 Char. 6: 1.443-1.485 → 1.559
 Char. 7: 0.117-0.124 → 0.091
 Char. 9: 0.088-0.098 → 0.084
 Char. 12: 0.814-0.924 → 0.792
 Char. 36: 0 → 1
 Char. 37: 0 → 1
 Char. 58: 0 → 1
 Char. 198: 0 → 1

Lystrosaurus hedini
 Char. 0: 0.308-0.315 → 0.320
 Char. 1: 6.072 → 6.111
 Char. 2: 0.383 → 0.414
 Char. 3: 0.689 → 0.705
 Char. 5: 0.119-0.143 → 0.146
 Char. 6: 1.664 → 1.471
 Char. 7: 0.165 → 0.174
 Char. 8: 8.400 → 9.200
 Char. 9: 0.086-0.098 → 0.079
 Char. 10: 10.145 → 10.203
 Char. 11: 10.900 → 11.400
 Char. 12: 0.805 → 0.673
 Char. 14: 0.711 → 0.691
 Char. 15: 0.706-0.731 → 0.781
 Char. 54: 1 → 0
 Char. 57: 1 → 0
 Char. 61: 1 → 0
 Char. 67: 2 → 1
 Char. 104: 0 → 1

Lystrosaurus maccaigi
 Char. 0: 0.308-0.315 → 0.274
 Char. 2: 0.383 → 0.347
 Char. 3: 0.689 → 0.656
 Char. 4: 0.413 → 0.325
 Char. 5: 0.119-0.143 → 0.108
 Char. 6: 1.664 → 1.764
 Char. 9: 0.086-0.098 → 0.123
 Char. 10: 10.145 → 10.022
 Char. 13: 0.294 → 0.354
 Char. 55: 0 → 1
 Char. 56: 2 → 0

Lystrosaurus curvatus
 Char. 8: 7.800-8.400 → 7.400
 Char. 11: 9.900-10.100 → 8.600
 Char. 15: 0.706-0.731 → 0.643
 Char. 21: 0.352 → 0.313

Lystrosaurus declivis
 Char. 0: 0.308-0.315 → 0.347
 Char. 1: 6.003 → 5.954
 Char. 4: 0.417-0.466 → 0.415
 Char. 5: 0.119-0.143 → 0.112
 Char. 6: 2.001 → 2.141
 Char. 8: 8.400 → 8.800
 Char. 11: 9.900-10.100 → 9.700
 Char. 16: 0.473 → 0.418
 Char. 17: 0.460 → 0.458
 Char. 18: 0.441-0.465 → 0.478
 Char. 20: 1.455 → 1.300
 Char. 21: 0.352 → 0.347

Lystrosaurus murrayi
 Char. 0: 0.308-0.315 → 0.288
 Char. 2: 0.424 → 0.427
 Char. 3: 0.705 → 0.726
 Char. 7: 0.157-0.162 → 0.175
 Char. 9: 0.097-0.098 → 0.101
 Char. 10: 10.309 → 10.358
 Char. 11: 9.900-10.100 → 11.700
 Char. 12: 0.874 → 0.816
 Char. 13: 0.315 → 0.316
 Char. 14: 0.757-0.767 → 0.793
 Char. 15: 0.711-0.731 → 0.754
 Char. 16: 0.473 → 0.478
 Char. 19: 0.750-0.787 → 0.843
 Char. 21: 0.352 → 0.392
 Char. 22: 0.545 → 0.605
 Char. 57: 1 → 0
 Char. 61: 1 → 0
 Char. 126: 0 → 1
 Char. 135: 1 → 0

Shansiodon
 Char. 0: 0.267 → 0.265
 Char. 3: 0.201 → 0.163
 Char. 5: 0.466 → 0.633
 Char. 8: 7.000 → 7.200
 Char. 10: 9.798-10.009 → 9.780
 Char. 12: 0.983-1.004 → 1.129
 Char. 61: 0 → 1
 Char. 67: 1 → 2

Tetragonias njalilus
 Char. 0: 0.304-0.336 → 0.378
 Char. 1: 6.064-6.099 → 5.912
 Char. 2: 0.327-0.352 → 0.354
 Char. 4: 0.523-0.538 → 0.574
 Char. 8: 6.900-7.000 → 6.800
 Char. 16: 0.473-0.490 → 0.447
 Char. 20: 1.484-1.789 → 1.852
 Char. 21: 0.352 → 0.304
 Char. 149: 2 → 1

APPENDIX 11. — Continuation.

Vinceria andina

Char. 4: 0.523-0.538 → 0.490
 Char. 7: 0.130 → 0.137
 Char. 9: 0.100 → 0.153
 Char. 10: 9.798-10.009 → 10.552
 Char. 11: 11.200 → 11.300
 Char. 51: 1 → 2
 Char. 86: 1 → 0

Rhinodicyodon gracile

Char. 1: 6.064-6.104 → 6.213
 Char. 6: 1.443-1.485 → 1.568
 Char. 7: 0.117-0.125 → 0.100
 Char. 10: 9.798-10.009 → 9.174
 Char. 12: 0.895-1.004 → 0.879
 Char. 14: 0.821-0.858 → 0.875
 Char. 17: 0.479-0.481 → 0.354
 Char. 22: 0.476-0.494 → 0.383
 Char. 61: 0 → 1
 Char. 79: 1 → 0
 Char. 131: 1 → 0

Acratophorus argentinensis

Char. 0: 0.420 → 0.329
 Char. 2: 0.403-0.413 → 0.445
 Char. 3: 0.268-0.460 → 0.205
 Char. 4: 0.506-0.607 → 0.666
 Char. 7: 0.143-0.161 → 0.120
 Char. 11: 10.000-10.600 → 8.055
 Char. 14: 0.756-0.786 → 0.716
 Char. 16: 0.467-0.494 → 0.345
 Char. 17: 0.519-0.520 → 0.468
 Char. 18: 0.450 → 0.292
 Char. 19: 0.562-0.652 → 0.706
 Char. 20: 1.239 → 1.206
 Char. 21: 0.417 → 0.424
 Char. 22: 0.405-0.411 → 0.574
 Char. 61: 0 → 1
 Char. 111: 0 → 1
 Char. 158: 1 → 0
 Char. 194: 1 → 0

Kannemeyeria simocephalus

Char. 43: 1 → 0

Kannemeyeria aganosteus

No autapomorphies

Kannemeyeria lophorhinus

Char. 0: 0.421 → 0.361
 Char. 1: 6.121 → 6.286
 Char. 3: 0.293-0.526 → 0.663
 Char. 6: 1.461-1.505 → 2.051
 Char. 7: 0.147 → 0.149
 Char. 8: 9.800-9.900 → 10.800
 Char. 13: 0.179 → 0.077
 Char. 60: 1 → 2
 Char. 131: 1 → 0
 Char. 158: 1 → 0
 Char. 160: 1 → 0

Dolichuranus primaevus

Char. 1: 6.104-6.105 → 6.079
 Char. 4: 0.500-0.518 → 0.484
 Char. 5: 0.354-0.368 → 0.400
 Char. 6: 1.443-1.485 → 1.339
 Char. 8: 6.900-7.000 → 8.700
 Char. 10: 10.206-10.469 → 10.672
 Char. 11: 10.000-10.100 → 9.700
 Char. 57: 1 → 0
 Char. 72: 0 → 1
 Char. 104: 1 → 0
 Char. 126: 1 → 0
 Char. 169: 1 → 0

Sinokannemeyeria

Char. 2: 0.403-0.413 → 0.478
 Char. 3: 0.359-0.460 → 0.543
 Char. 5: 0.195-0.230 → 0.175
 Char. 8: 6.655-7.000 → 5.900
 Char. 9: 0.094-0.102 → 0.109
 Char. 14: 0.756-0.786 → 0.549
 Char. 15: 0.515-0.668 → 0.385
 Char. 17: 0.519-0.520 → 0.489
 Char. 18: 0.478 → 0.556
 Char. 20: 1.239-1.381 → 1.187
 Char. 21: 0.411 → 0.408
 Char. 92: 0 → 1

Parakannemeyeria

Char. 0: 0.420 → 0.455
 Char. 1: 6.203 → 6.280
 Char. 2: 0.403-0.413 → 0.377
 Char. 4: 0.382-0.433 → 0.354
 Char. 7: 0.143-0.161 → 0.122
 Char. 10: 10.027 → 9.688
 Char. 11: 10.000-10.600 → 12.300
 Char. 13: 0.243 → 0.166
 Char. 43: 0 → 1
 Char. 114: 2 → 1
 Char. 173: 1 → 0

Xiyukannemeyeria brevirostris

Char. 0: 0.420 → 0.286
 Char. 7: 0.143-0.161 → 0.169
 Char. 8: 7.500 → 8.500
 Char. 9: 0.094-0.102 → 0.086
 Char. 11: 10.000-10.600 → 8.900
 Char. 12: 0.918-0.920 → 0.795
 Char. 13: 0.243 → 0.320
 Char. 54: 0 → 1
 Char. 131: 1 → 0

Rabidosaurus cristatus

Char. 0: 0.423 → 0.464
 Char. 81: 0 → 1

Rhadiodromus

Char. 1: 6.104-6.105 → 6.144
 Char. 3: 0.293-0.460 → 0.285
 Char. 4: 0.500-0.518 → 0.574
 Char. 5: 0.318-0.368 → 0.254
 Char. 7: 0.143-0.147 → 0.122
 Char. 10: 10.206-10.469 → 10.023
 Char. 18: 0.450-0.478 → 0.604
 Char. 68: 0 → 1
 Char. 132: 0 → 1

Wadiasaurus indicus

Char. 3: 0.268-0.460 → 0.539
 Char. 64: 1 → 0

Shaanbeikannemeyeria

Char. 0: 0.490-0.509 → 0.527
 Char. 2: 0.409 → 0.513
 Char. 3: 0.293-0.526 → 0.886
 Char. 5: 0.318-0.368 → 0.414
 Char. 7: 0.147 → 0.157
 Char. 9: 0.088-0.091 → 0.176
 Char. 10: 10.432-10.478 → 10.642
 Char. 12: 1.147-1.154 → 1.432
 Char. 14: 0.756-0.786 → 0.734
 Char. 17: 0.558 → 0.580
 Char. 86: 0 → 1
 Char. 144: 1 → 0

Rechnisaurus cristarhynchus

Char. 0: 0.490-0.509 → 0.510
 Char. 2: 0.409 → 0.436
 Char. 3: 0.293-0.526 → 0.154
 Char. 5: 0.233 → 0.211
 Char. 7: 0.147 → 0.140
 Char. 64: 1 → 0

Uralokannemeyeria vjuschkovi

Char. 2: 0.409 → 0.407

APPENDIX 11. — Continuation.

<i>Angonisaurus cruickshanki</i>	Char. 95: 0 → 1	<i>Stahleckeria potens</i>
Char. 1: 6.104-6.139 → 6.301	Char. 97: 0 → 1	Char. 0: 0.411 → 0.438
Char. 2: 0.445 → 0.514	Char. 98: 0 → 2	Char. 1: 6.104-6.139 → 5.992
Char. 4: 0.500-0.518 → 0.572	Char. 99: 0 → 1	Char. 3: 0.618-0.667 → 0.726
Char. 5: 0.354-0.368 → 0.600	Char. 101: 0 → 3	Char. 5: 0.354-0.368 → 0.288
Char. 6: 1.443-1.485 → 1.491	Char. 103: 0 → 2	Char. 8: 5.900-7.000 → 11.100
Char. 7: 0.151-0.183 → 0.190	Char. 104: 0 → 1	Char. 9: 0.060-0.084 → 0.052
Char. 13: 0.192-0.202 → 0.143	Char. 105: 0 → 1	Char. 10: 10.206-10.269 → 10.284
Char. 20: 1.484-1.789 → 2.541	Char. 106: 0 → 2	Char. 11: 9.200 → 8.700
Char. 132: 0 → 1	Char. 108: 0 → 1	Char. 12: 1.012 → 0.953
Char. 196: 0 → 1	Char. 109: 0 → 2	Char. 14: 0.832 → 0.856
	Char. 110: 0 → 1	Char. 19: 0.592 → 0.391
	Char. 112: 0 → 1	Char. 20: 1.484-1.789 → 2.217
<i>Ufudocyclops mukanelai</i>	Char. 113: 1 → 0	Char. 21: 0.433 → 0.434
Char. 0: 0.693 → 0.376	Char. 114: 2 → 1	Char. 28: 2 → 0
Char. 2: 0.261 → 0.468	Char. 115: 0 → 1	Char. 111: 0 → 1
Char. 4: 0.148 → 0.515	Char. 122: 0 → 1	Char. 174: 0 → 1
Char. 5: 0.029 → 0.332	Char. 123: 0 → 1	
Char. 8: 5.800 → 9.310	Char. 129: 0 → 1	<i>Sangusaurus parringtonii</i>
Char. 12: 1.060 → 0.983	Char. 131: 0 → 1	No autapomorphies
Char. 23: 0 → 1	Char. 136: 0 → 1	
Char. 24: 0 → 2	Char. 137: 0 → 1	<i>Sangusaurus</i> sp.
Char. 27: 0 → 2	Char. 138: 0 → 1	Char. 43: 1 → 0
Char. 30: 0 → 2	Char. 139: 0 → 2	
Char. 31: 0 → 1	Char. 144: 0 → 1	<i>Eubrachiosaurus browni</i>
Char. 33: 0 → 1	Char. 146: 0 → 1	No autapomorphies
Char. 39: 0 → 2	Char. 147: 0 → 3	
Char. 41: 0 → 1	Char. 149: 0 → 1	<i>Ischigualastia jensi</i>
Char. 42: 1 → 0	Char. 152: 0 → 1	Char. 0: 0.411 → 0.482
Char. 44: 0 → 1	Char. 160: 0 → 1	Char. 5: 0.499 → 0.528
Char. 45: 0 → 2	Char. 162: 0 → 2	Char. 10: 10.206-10.269 → 10.023
Char. 48: 0 → 1	Char. 163: 0 → 1	Char. 14: 0.832 → 0.912
Char. 49: 0 → 1	Char. 197: 0 → 1	Char. 16: 0.427 → 0.419
Char. 56: 0 → 2		Char. 18: 0.529 → 0.561
Char. 60: 0 → 1	<i>Zambiasaurus submersus</i>	Char. 21: 0.433 → 0.412
Char. 63: 0 → 1	Char. 21: 0.416-0.433 → 0.401	Char. 114: 1 → 5
Char. 64: 0 → 1	Char. 132: 0 → 1	
Char. 69: 2 → 1	Char. 175: 0 → 1	<i>Jachaleria candelariensis</i>
Char. 70: 0 → 1	Char. 178: 1 → 0	Char. 67: 1 → 2
Char. 72: 0 → 1		
Char. 73: 2 → 1	<i>Placerias hesternus</i>	<i>Jachaleria colorata</i>
Char. 74: 0 → 1	Char. 50: 0 → 1	Char. 87: 0 → 1
Char. 75: 0 → 1	Char. 67: 2 → 1	Char. 110: 1 → 0
Char. 77: 0 → 1	Char. 198: 0 → 1	
Char. 79: 0 → 2		<i>Dinodontosaurus brevirostris</i>
Char. 80: 0 → 2	<i>Moghreberia nmachouensis</i>	Char. 6: 1.443-1.485 → 2.180
Char. 82: 0 → 1	Char. 51: 0 → 2	Char. 7: 0.135-0.147 → 0.176
Char. 85: 0 → 2	Char. 158: 1 → 0	Char. 8: 7.300 → 9.106
Char. 88: 0 → 1		Char. 9: 0.085-0.098 → 0.107
Char. 89: 0 → 1	<i>Pentasaurus goggai</i>	Char. 11: 10.000-10.100 → 9.690
Char. 91: 0 → 1	Char. 150: 2 → 0	
Char. 94: 0 → 1		

APPENDIX 11. — Continuation.

<i>Dinodontosaurus tener</i>	Node 124	Node 132
Char. 0: 0.321-0.356 → 0.398	Char. 0: 0.606 → 0.509-0.547	Char. 8: 5.600-6.000 → 5.000-5.300
Char. 3: 0.314 → 0.240	Char. 4: 0.190 → 0.272-0.305	Char. 93: 0 → 1
Char. 4: 0.500-0.518 → 0.461	Char. 5: 0.046 → 0.072	Char. 99: 0 → 1
Char. 5: 0.354 → 0.328	Char. 17: 0.367 → 0.329	Char. 104: 0 → 1
Char. 6: 1.443-1.485 → 1.414	Char. 96: 1 → 0	Char. 119: 0 → 1
Char. 9: 0.085-0.098 → 0.074	Char. 176: 1 → 0	Char. 141: 0 → 1
Char. 11: 10.000-10.100 → 10.900	Char. 177: 1 → 0	Char. 142: 0 → 1
<i>Lisowicia bojani</i>	Node 125	Char. 149: 0 → 1
Char. 17: 0.498-0.524 → 0.576	Char. 3: 0.700-0.842 → 0.333	Node 133
Char. 65: 0 → 1	Char. 4: 0.272-0.305 → 0.352	Char. 39: 1 → 2
Char. 75: 1 → 2	Char. 5: 0.072-0.104 → 0.218	
Char. 121: 2 → 1	Char. 71: 0 → 2	Node 134
Char. 128: 1 → 0	Char. 74: 0 → 1	Char. 14: 0.865 → 0.831
Char. 167: 1 → 0	Char. 77: 0 → 1	Char. 156: 0 → 1
Char. 169: 1 → 0	Char. 97: 0 → 1	Char. 175: 1 → 0
Char. 183: 1 → 0	Char. 102: 0 → 1	Char. 176: 0 → 1
Char. 184: 1 → 0	Char. 153: 0 → 1	
	Char. 159: 0 → 1	Node 135
<i>Woznikella triradiata</i>	Node 126	Char. 14: 0.920-0.956 → 0.865
Char. 15: 0.841-0.897 → 0.930	Char. 29: 0 → 1	Char. 15: 1.059 → 0.968
Char. 16: 0.442-0.490 → 0.362	Char. 143: 0 → 1	Char. 56: 0 → 1
Char. 22: 0.411-0.457 → 0.371		
Char. 24: 2 → 1	Node 127	Node 136
Char. 56: 3 → 2	Char. 91: 0 → 1	Char. 4: 0.327 → 0.435
Char. 59: 0 → 1	Char. 107: 0 → 1	Char. 13: 0.355-0.395 → 0.259
	Char. 115: 1 → 2	Char. 14: 0.831 → 0.708-0.723
Node 120		Char. 82: 0 → 1
No synapomorphies	Node 128	Char. 85: 1 → 2
	Char. 17: 0.351 → 0.396	Char. 99: 0 → 1
Node 121		Char. 101: 1 → 3
Char. 14: 0.855 → 0.920	Node 129	Char. 108: 0 → 1
Char. 47: 0 → 1	Char. 17: 0.299-0.329 → 0.351	Char. 109: 0 → 2
Char. 140: 0 → 1		Char. 114: 0 → 3
	Node 130	Char. 116: 1 → 0
Node 122	Char. 31: 0 → 1	Char. 143: 1 → 2
Char. 14: 0.595-0.718 → 0.855	Char. 33: 0 → 1	Char. 161: 0 → 1
Char. 15: 1.710-1.870 → 1.620	Char. 44: 0 → 1	Char. 162: 1 → 2
Char. 61: 0 → 1	Char. 61: 1 → 0	
Char. 132: 0 → 1	Char. 97: 0 → 1	Node 137
	Char. 106: 0 → 1	Char. 0: 0.339 → 0.322
Node 123	Char. 115: 0 → 1	Char. 3: 0.914 → 0.908
Char. 73: 2 → 1	Char. 129: 0 → 1	Char. 4: 0.435 → 0.518
Char. 93: 1 → 0	Char. 136: 0 → 1	Char. 11: 11.600-12.000 → 10.600-11.200
Char. 94: 0 → 1	Char. 163: 0 → 1	Char. 13: 0.259 → 0.253-0.257
Char. 101: 0 → 1		Char. 30: 0 → 2
Char. 181: 0 → 1	Node 131	Char. 44: 1 → 2
Char. 189: 0 → 1	Char. 4: 0.272-0.305 → 0.407	Char. 49: 0 → 1
	Char. 11: 11.600-12.000 → 15.400	Char. 81: 0 → 1
	Char. 113: 1 → 0	Char. 146: 0 → 1
	Char. 131: 0 → 1	

APPENDIX 11. — Continuation.

Node 138	Node 145	Node 151
Char. 0: 0.322 → 0.231-0.237	Char. 11: 10.600-11.000 → 9.500	Char. 8: 8.250-8.400 → 9.550-9.600
Char. 1: 5.555 → 5.714	Char. 14: 0.723-0.730 → 0.798-0.859	Char. 13: 0.212-0.290 → 0.293-0.348
Char. 4: 0.518 → 0.520	Char. 30: 2 → 1	Char. 25: 0 → 1
Char. 5: 0.111 → 0.222-0.257	Char. 100: 0 → 1	Char. 28: 2 → 0
Char. 6: 2.470 → 2.070-2.434	Node 146	Char. 146: 1 → 0
Char. 10: 10.385-10.457 → 10.177	Char. 2: 0.190-0.197 → 0.207-0.232	Char. 150: 0 → 1
Char. 24: 0 → 1	Char. 6: 1.751-1.847 → 1.548-1.565	Char. 164: 2 → 0
Char. 69: 0 → 1	Char. 10: 9.687 → 9.694	Char. 166: 0 → 1
Char. 124: 0 → 1	Char. 27: 1 → 2	Char. 176: 1 → 0
Node 139	Char. 61: 1 → 0	Node 152
Char. 48: 0 → 1	Char. 118: 1 → 0	Char. 1: 5.810-5.863 → 5.874-5.950
Char. 61: 0 → 1	Char. 143: 2 → 4	Char. 10: 9.694 → 9.740-9.775
Node 140	Node 147	Char. 45: 1 → 2
Char. 10: 9.418-9.687 → 9.417	Char. 9: 0.182-0.199 → 0.150-0.173	Char. 94: 0 → 1
Char. 77: 1 → 2	Char. 24: 1 → 0	Char. 95: 0 → 1
Node 141	Char. 38: 0 → 1	Node 153
Char. 15: 0.924-0.928 → 0.901-0.904	Char. 130: 0 → 1	Char. 2: 0.207-0.232 → 0.275-0.294
Char. 25: 0 → 1	Char. 187: 0 → 1	Char. 5: 0.166-0.187 → 0.139
Char. 32: 0 → 1	Node 148	Char. 63: 0 → 1
Char. 50: 0 → 2	Char. 28: 0 → 2	Char. 73: 01 → 2
Char. 54: 0 → 1	Char. 52: 0 → 1	Node 154
Char. 148: 0 → 1	Char. 124: 1 → 2	Char. 2: 0.275 → 0.202-0.240
Char. 170: 0 → 1	Char. 140: 1 → 2	Char. 3: 0.899-1.032 → 0.840
Char. 176: 1 → 0	Char. 164: 0 → 2	Char. 136: 1 → 2
Node 142	Node 149	Node 155
Char. 6: 2.070-2.434 → 1.751-2.013	Char. 0: 0.279 → 0.328	Char. 7: 0.117-0.123 → 0.116
Char. 45: 0 → 1	Char. 3: 0.867-0.906 → 0.396	Char. 88: 1 → 0
Char. 93: 0 → 1	Char. 6: 1.548-1.565 → 1.505	Char. 144: 0 → 1
Char. 114: 3 → 2	Char. 7: 0.118-0.126 → 0.111	Char. 147: 2 → 0
Char. 122: 0 → 1	Char. 13: 0.302 → 0.319	Char. 170: 0 → 1
Node 143	Char. 15: 0.924-0.938 → 0.825	Node 156
Char. 0: 0.231-0.237 → 0.238	Char. 34: 0 → 2	Char. 44: 2 → 1
Char. 12: 0.850-0.871 → 0.881	Char. 41: 0 → 1	Node 157
Char. 71: 0 → 2	Char. 47: 1 → 2	Char. 3: 0.867-0.906 → 0.742
Char. 73: 1 → 0	Char. 48: 1 → 0	Char. 5: 0.166-0.257 → 0.260-0.281
Node 144	Char. 71: 0 → 1	Char. 9: 0.150-0.173 → 0.121-0.132
Char. 11: 9.500 → 8.000	Char. 75: 0 → 1	Char. 11: 10.600-11.000 → 12.000
Char. 12: 0.850-0.871 → 0.902-0.907	Char. 77: 1 → 2	Char. 15: 0.924-0.928 → 0.766-0.819
Char. 13: 0.290 → 0.302	Char. 90: 0 → 1	Node 158
Char. 27: 2 → 0	Char. 114: 2 → 3	Char. 3: 0.840 → 0.764
Char. 46: 0 → 1	Char. 198: 0 → 2	Char. 4: 0.473-0.483 → 0.539
Char. 49: 1 → 0	Node 150	Char. 67: 1 → 2
Char. 63: 0 → 1	Char. 0: 0.231-0.279 → 0.220	Char. 71: 0 → 2
Char. 143: 4 → 3	Char. 6: 1.548-1.565 → 1.646	
Char. 145: 0 → 1	Char. 8: 9.550-9.600 → 9.800	
	Char. 12: 0.850-0.871 → 0.840	
	Char. 27: 2 → 1	
	Char. 45: 2 → 0	
	Char. 54: 0 → 1	
	Char. 113: 1 → 0	
	Char. 134: 0 → 1	

APPENDIX 11. — Continuation.

Node 159	Node 167	Node 161
Char. 0: 0.279-0.281 → 0.308-0.311	Char. 1: 6.054-6.066 → 6.094	Char. 3: 0.899-1.032 → 1.139-1.339
Char. 2: 0.289-0.298 → 0.330-0.383	Char. 2: 0.220-0.232 → 0.271	Char. 5: 0.108-0.139 → 0.048-0.088
Char. 4: 0.421-0.483 → 0.357-0.372	Char. 3: 0.844 → 0.738	Char. 12: 0.853-0.871 → 0.872
Char. 5: 0.048-0.088 → 0.042	Char. 5: 0.271-0.277 → 0.606	Char. 13: 0.348 → 0.380
Char. 7: 0.117-0.123 → 0.132	Char. 12: 0.910-0.929 → 0.936	Char. 67: 1 → 0
Char. 8: 9.550-9.600 → 10.550	Char. 13: 0.212-0.213 → 0.167	Char. 87: 1 → 0
Char. 10: 9.965 → 10.119-10.173	Char. 14: 0.787-0.798 → 0.838	Char. 137: 0 → 1
Char. 124: 2 → 1	Char. 51: 1 → 0	Char. 45: 2 → 1
Node 162	Char. 60: 0 → 1	Char. 139: 2 → 1
Char. 7: 0.132 → 0.135	Char. 64: 0 → 1	Char. 195: 1 → 0
Char. 12: 0.872 → 0.836	Char. 71: 1 → 2	Node 173
Char. 13: 0.380 → 0.346	Char. 78: 0 → 1	Char. 59: 0 → 1
Char. 25: 1 → 0	Char. 92: 0 → 1	Char. 126: 1 → 0
Char. 48: 1 → 0	Node 168	Node 174
Char. 110: 1 → 0	Char. 4: 0.551 → 0.565-0.566	Char. 9: 0.107-0.111 → 0.097-0.098
Node 163	Char. 5: 0.232 → 0.271-0.277	Char. 17: 0.518 → 0.491-0.506
Char. 1: 6.003-6.066 → 6.112	Char. 17: 0.518 → 0.491-0.506	Char. 22: 0.491 → 0.391-0.411
Char. 5: 0.213-0.232 → 0.203	Char. 198: 0 → 1	Char. 34: 0 → 1
Char. 6: 1.489-1.515 → 1.528	Node 169	Char. 56: 1 → 2
Char. 7: 0.094-0.107 → 0.083	Char. 4: 0.541-0.544 → 0.551	Node 175
Char. 11: 12.000-12.300 → 10.300	Char. 14: 0.693-0.749 → 0.787	Char. 9: 0.121 → 0.107-0.111
Char. 12: 0.910-0.914 → 0.831	Char. 15: 0.764-0.785 → 0.745-0.752	Char. 11: 12.000 → 9.900-10.100
Node 164	Char. 18: 0.348-0.361 → 0.366	Char. 54: 0 → 1
Char. 1: 5.927-5.982 → 6.003-6.066	Char. 79: 0 → 1	Char. 194: 0 → 1
Char. 5: 0.260-0.281 → 0.213-0.232	Char. 144: 1 → 0	Node 176
Char. 7: 0.112-0.118 → 0.094-0.107	Node 170	Char. 15: 0.766 → 0.731
Char. 53: 0 → 1	Char. 0: 0.244-0.282 → 0.289-0.320	Char. 16: 0.476 → 0.463-0.473
Char. 56: 1 → 2	Char. 34: 0 → 1	Char. 57: 0 → 1
Node 165	Char. 59: 0 → 1	Char. 73: 0 → 1
Char. 99: 1 → 2	Char. 83: 0 → 1	Node 177
Char. 120: 0 → 1	Node 171	Char. 0: 0.240-0.297 → 0.308-0.315
Char. 149: 2 → 1	Char. 2: 0.220-0.232 → 0.183-0.197	Char. 5: 0.260-0.281 → 0.334-0.343
Node 166	Char. 12: 0.910-0.929 → 0.875-0.882	Char. 8: 8.250-8.333 → 7.800
Char. 12: 0.850-0.871 → 0.910	Char. 57: 0 → 1	Char. 61: 0 → 1
Char. 38: 1 → 0	Char. 61: 0 → 1	Char. 71: 1 → 2
Char. 51: 0 → 1	Char. 193: 1 → 0	Char. 75: 0 → 1
Char. 52: 1 → 0	Node 172	Char. 125: 0 → 1
Char. 71: 0 → 1	Char. 6: 1.458 → 1.436	Node 178
Char. 130: 1 → 0	Char. 11: 12.300 → 12.400	Char. 2: 0.237 → 0.253
Char. 137: 0 → 1	Char. 14: 0.787-0.798 → 0.758	Char. 67: 1 → 2
Char. 143: 4 → 2	Char. 21: 0.353 → 0.345	Char. 112: 0 → 1
Char. 144: 0 → 1	Node 160	Char. 120: 0 → 2
Char. 150: 0 → 2	Char. 41: 0 → 1	Node 179
Char. 151: 0 → 1	Char. 79: 0 → 1	Char. 2: 0.220-0.232 → 0.237
		Char. 6: 1.489-1.515 → 1.443-1.485
		Char. 60: 0 → 1
		Char. 105: 0 → 1
		Char. 116: 0 → 1
		Char. 154: 0 → 1

APPENDIX 11. — Continuation.

Node 180
 Char. 11: 12.300 → 13.500
 Char. 13: 0.212-0.213 → 0.204-0.205
 Char. 95: 1 → 0

Node 181
 Char. 2: 0.220-0.232 → 0.250
 Char. 12: 0.910-0.929 → 0.887
 Char. 58: 0 → 1
 Char. 63: 0 → 1
 Char. 64: 0 → 1
 Char. 73: 0 → 1
 Char. 194: 0 → 1

Node 182
 Char. 2: 0.250 → 0.305
 Char. 10: 9.740-9.851 → 9.480
 Char. 12: 0.887 → 0.822
 Char. 14: 0.693-0.749 → 0.760
 Char. 35: 0 → 1
 Char. 60: 0 → 2

Node 183
 Char. 7: 0.107-0.112 → 0.104
 Char. 10: 9.480 → 9.414
 Char. 14: 0.760 → 0.818-0.856
 Char. 44: 2 → 1
 Char. 68: 0 → 1
 Char. 83: 1 → 2
 Char. 95: 0 → 1

Node 184
 Char. 4: 0.534-0.583 → 0.529
 Char. 15: 0.764-0.785 → 0.848
 Char. 61: 0 → 1
 Char. 73: 1 → 0

Node 185
 Char. 56: 1 → 0

Node 186
 Char. 5: 0.260-0.281 → 0.290
 Char. 8: 8.250-8.333 → 8.900
 Char. 11: 12.000-12.300 → 13.000
 Char. 14: 0.723-0.749 → 0.781
 Char. 41: 0 → 1
 Char. 54: 0 → 1
 Char. 61: 0 → 1
 Char. 71: 1 → 2

Node 187
 Char. 0: 0.308-0.315 → 0.369
 Char. 6: 1.443-1.485 → 1.618
 Char. 11: 12.000 → 13.900
 Char. 12: 0.910-0.926 → 0.985
 Char. 60: 1 → 0

Node 188
 Char. 5: 0.334-0.343 → 0.359
 Char. 8: 7.800 → 7.700
 Char. 116: 1 → 0

Node 189
 Char. 10: 9.751 → 9.680
 Char. 114: 2 → 1
 Char. 133: 0 → 1

Node 190
 Char. 4: 0.553 → 0.567-0.569
 Char. 5: 0.369 → 0.405-0.414
 Char. 40: 0 → 1

Node 191
 Char. 2: 0.253 → 0.224-0.230
 Char. 4: 0.541-0.546 → 0.553
 Char. 5: 0.334-0.343 → 0.369
 Char. 41: 0 → 1

Node 192
 Char. 55: 0 → 1
 Char. 111: 0 → 1

Node 193
 Char. 4: 0.541-0.544 → 0.408
 Char. 12: 0.910 → 0.876
 Char. 113: 1 → 0
 Char. 131: 1 → 0

Node 194
 Char. 0: 0.308-0.315 → 0.307
 Char. 4: 0.523-0.546 → 0.604
 Char. 60: 1 → 0
 Char. 194: 1 → 0

Node 195
 Char. 8: 7.800 → 7.200
 Char. 67: 2 → 1
 Char. 79: 0 → 1

Node 196
 Char. 1: 6.005-6.028 → 5.994
 Char. 4: 0.523-0.546 → 0.522
 Char. 6: 1.443-1.485 → 1.338
 Char. 9: 0.088-0.098 → 0.132
 Char. 10: 9.663 → 9.599
 Char. 51: 1 → 0
 Char. 54: 1 → 0
 Char. 71: 2 → 1

Node 197
 Char. 2: 0.253-0.278 → 0.212-0.244
 Char. 5: 0.334-0.343 → 0.238-0.294
 Char. 8: 6.900-7.000 → 6.500
 Char. 10: 9.798-10.009 → 9.663
 Char. 116: 1 → 0

Node 198
 Char. 3: 0.563-0.650 → 0.562
 Char. 8: 7.200 → 6.900-7.000
 Char. 61: 1 → 0

Node 199
 Char. 1: 6.005-6.028 → 6.072
 Char. 4: 0.417 → 0.413
 Char. 7: 0.162 → 0.165
 Char. 11: 9.900-10.100 → 10.900
 Char. 12: 0.874-0.906 → 0.805
 Char. 14: 0.757-0.767 → 0.711
 Char. 113: 1 → 0
 Char. 114: 2 → 4

Node 200
 Char. 187: 1 → 0

Node 201
 Char. 3: 0.563-0.650 → 0.689
 Char. 5: 0.334-0.343 → 0.119-0.143
 Char. 35: 0 → 1
 Char. 36: 0 → 1
 Char. 37: 0 → 1
 Char. 71: 2 → 0
 Char. 104: 1 → 0
 Char. 106: 1 → 2

Node 202
 Char. 1: 6.005-6.028 → 6.003
 Char. 2: 0.383 → 0.424
 Char. 3: 0.689 → 0.705
 Char. 6: 1.664 → 2.001
 Char. 10: 10.145 → 10.309
 Char. 13: 0.289-0.294 → 0.315
 Char. 17: 0.485-0.490 → 0.460
 Char. 20: 1.484 → 1.455
 Char. 22: 0.489-0.494 → 0.545
 Char. 58: 0 → 2

Node 203
 Char. 0: 0.304-0.336 → 0.267
 Char. 5: 0.446 → 0.466
 Char. 7: 0.125 → 0.130
 Char. 9: 0.088-0.098 → 0.100
 Char. 11: 10.400 → 11.200
 Char. 125: 1 → 0

APPENDIX 11. — Continuation.

Node 204	Node 211	Node 218
Char. 3: 0.314-0.500 → 0.201	Char. 2: 0.347-0.388 → 0.392-0.409	Char. 1: 6.105 → 6.140
Char. 5: 0.435 → 0.446	Char. 10: 10.155 → 10.206-10.269	Char. 4: 0.500-0.518 → 0.382-0.433
Char. 11: 10.100 → 10.400	Char. 12: 0.926-1.010 → 1.012	Char. 5: 0.318-0.368 → 0.195-0.230
Char. 15: 0.734 → 0.796	Char. 17: 0.507 → 0.519-0.520	Char. 12: 1.018-1.031 → 0.918-0.920
Char. 22: 0.476-0.494 → 0.596	Char. 18: 0.423 → 0.450-0.478	Char. 19: 0.562-0.652 → 0.458
Char. 57: 1 → 0	Char. 21: 0.352 → 0.416-0.425	Char. 21: 0.416-0.417 → 0.411
Node 205	Char. 22: 0.476-0.494 → 0.411-0.457	Char. 37: 0 → 2
Char. 5: 0.354-0.368 → 0.435	Char. 40: 0 → 1	Char. 41: 1 → 2
Char. 14: 0.790-0.814 → 0.821-0.858	Char. 64: 0 → 1	Char. 86: 0 → 1
Char. 17: 0.490 → 0.479-0.481	Char. 125: 1 → 0	Node 219
Char. 106: 1 → 2	Node 212	Char. 1: 6.140 → 6.203
Char. 186: 0 → 1	Char. 4: 0.523-0.538 → 0.500-0.518	Char. 8: 6.655-7.000 → 7.500
Node 206	Char. 7: 0.117-0.125 → 0.135-0.147	Char. 10: 10.206-10.469 → 10.027
Char. 1: 6.005-6.028 → 6.064-6.104	Char. 10: 9.798-10.009 → 10.155	Char. 40: 1 → 0
Char. 3: 0.562 → 0.314-0.500	Char. 13: 0.203-0.240 → 0.202	Node 220
Char. 5: 0.334-0.343 → 0.354-0.368	Char. 15: 0.724-0.734 → 0.653-0.722	Char. 0: 0.420 → 0.423
Char. 63: 0 → 1	Char. 17: 0.490 → 0.507	Char. 71: 2 → 0
Char. 74: 0 → 1	Char. 18: 0.348-0.361 → 0.423	Node 221
Char. 75: 1 → 2	Char. 56: 2 → 3	Char. 5: 0.318-0.368 → 0.233
Char. 81: 1 → 0	Char. 132: 1 → 0	Char. 71: 2 → 1
Char. 113: 1 → 0	Char. 149: 2 → 1	Node 222
Node 207	Char. 174: 1 → 0	Char. 2: 0.392-0.409 → 0.445
Char. 5: 0.318-0.368 → 0.476	Char. 178: 0 → 1	Char. 3: 0.314-0.500 → 0.618-0.667
Char. 15: 0.542-0.686 → 0.705	Node 213	Char. 7: 0.143-0.147 → 0.151-0.183
Char. 186: 0 → 1	Char. 61: 0 → 1	Char. 9: 0.085-0.091 → 0.060-0.084
Node 208	Node 214	Char. 43: 0 → 1
Char. 9: 0.088-0.091 → 0.094	Char. 0: 0.490-0.509 → 0.421	Char. 44: 2 → 1
Char. 13: 0.192-0.202 → 0.243	Char. 1: 6.069-6.105 → 6.121	Char. 67: 1 → 0
Char. 67: 1 → 2	Char. 9: 0.088-0.091 → 0.086	Char. 71: 2 → 0
Char. 106: 1 → 2	Char. 34: 1 → 0	Char. 75: 2 → 1
Node 209	Char. 40: 0 → 1	Char. 157: 5 → 0
Char. 0: 0.356 → 0.420	Char. 72: 0 → 1	Char. 197: 0 → 1
Char. 66: 0 → 1	Char. 106: 1 → 2	Node 223
Char. 174: 0 → 1	Char. 114: 2 → 1	Char. 43: 1 → 0
Node 210	Node 215	Char. 51: 1 → 0
Char. 12: 1.012 → 1.018	Char. 8: 7.800 → 9.800-9.900	Char. 168: 0 → 1
Char. 51: 1 → 2	Char. 11: 11.300 → 11.900	Char. 196: 0 → 1
Char. 74: 1 → 0	Char. 43: 0 → 1	Node 224
Char. 123: 1 → 2	Node 216	Char. 167: 0 → 1
Char. 134: 0 → 1	Char. 8: 6.900-7.000 → 7.800	Node 225
	Char. 11: 10.800 → 11.300	Char. 15: 0.722 → 0.841-0.897
	Char. 12: 1.085 → 1.147-1.154	Char. 66: 0 → 1
	Char. 198: 0 → 2	Char. 156: 0 → 1
	Node 217	Node 226
	Char. 0: 0.420 → 0.490-0.509	No synapomorphies
	Char. 11: 10.000-10.600 → 10.800	
	Char. 12: 1.018-1.031 → 1.085	
	Char. 40: 1 → 0	

APPENDIX 11. — Continuation.

Node 227 No synapomorphies	Node 231 No synapomorphies	Node 234 Char. 54: 0 → 1
Node 228 Char. 67: 0 → 2	Node 232 Char. 17: 0.530 → 0.538 Char. 67: 0 → 1 Char. 75: 1 → 2 Char. 87: 1 → 0 Char. 106: 1 → 2	Node 235 Char. 8: 6.900-7.000 → 7.300 Char. 67: 1 → 2 Char. 103: 1 → 0 Char. 104: 1 → 0
Node 229 Char. 17: 0.519-0.524 → 0.530 Char. 19: 0.647-0.652 → 0.592 Char. 22: 0.457 → 0.526-0.565 Char. 62: 0 → 1 Char. 158: 1 → 0 Char. 165: 0 → 1 Char. 194: 1 → 0	Node 233 Char. 2: 0.445 → 0.423 Char. 3: 0.618 → 0.331 Char. 5: 0.368 → 0.499 Char. 20: 1.484-1.789 → 0.818	
Node 230 No synapomorphies	Char. 123: 1 → 3 Char. 164: 3 → 2 Char. 169: 1 → 0	

APPENDIX 12. — Paleobiogeographic analysis results. Log of likelihood, higher is better (**LnL**), number of free parameters, free parameter values (d, e, j), Akaike Information Criterion, lower is better (**AIC**), and AIC weights for individual models. The best model for the analyzed dataset indicated in **green**, the worst indicated in **red**.

	LnL	Free parameters	d	e	j	AIC	AIC weight
DEC	-433.4	2	0.036	0.061	0	870.8	3.0e-75
DEC+J	-260.8	3	0.0024	1.0e-12	0.027	527.6	1
DIVALIKE	-449.8	2	0.047	0.061	0	903.6	2.2e-82
DIVALIKE+J	-439.2	3	0.024	0.023	0.098	884.4	3.2e-78
BAYAREALIKE	-387.4	2	0.018	0.15	0	778.8	2.9e-55
BAYAREALIKE+J	-353.6	3	0.0089	0.080	0.052	713.3	4.8e-41

APPENDIX 13. — Pairwise comparisons of nested model variants: likelihood ratio test (**LRT**) and relative probabilities.

alt	DEC+J	DIVALIKE+J	BAYAREALIKE+J
null	DEC	DIVALIKE	BAYAREALIKE
LnLalt	-260.8	-439.2	-353.6
LnLnull	-433.4	-449.8	-387.4
DFalt	3	3	3
DFnull	2	2	2
DF	1	1	1
Dstatistic	345.2	21.15	67.49
pval	4.7e-77	4.2e-06	2.1e-16
test	chi-squared	chi-squared	chi-squared
tail	one-tailed	one-tailed	one-tailed
AIC1	527.6	884.4	713.3
AIC2	870.8	903.6	778.8
AICwt1	1	1.00	1.00
AICwt2	3.0e-75	6.9e-05	6.0e-15
AICweight_ratio_model1	3.32e+74	14391	1.66e+14
AICweight_ratio_model2	3.0e-75	6.9e-05	6.0e-15

APPENDIX 14. — Data for paleobiogeographic analysis and results. https://doi.org/10.5852/cr-palevol2023v22a16_s8